ЖУРНАЛ
ЭКСПЕРИМЕНТАЛЬНОЙ И ТЕОРЕТИЧЕСКОЙ
ФИЗИКИ
Zhurnal Éksperimental'noĭ i Teoreticheskoĭ Fiziki

SOVIET PHYSICS
JETP

VOL. 14, NO. 1 JANUARY, 1962

A Translation
of the
Journal of Experimental and Theoretical Physics
of the
Academy of Sciences of the USSR

(Russian Original Vol. 41, No. 1, July, 1961)

Published by the
AMERICAN INSTITUTE OF PHYSICS
INCORPORATED

SOVIET PHYSICS
JETP

A translation of the Journal of Experimental and Theoretical Physics of the USSR.

A publication of the

AMERICAN INSTITUTE OF PHYSICS

SOVIET PHYSICS—JETP is a monthly journal published by the American Institute of Physics and contains a complete translation of the JOURNAL OF EXPERIMENTAL AND THEORETICAL PHYSICS of the U.S.S.R. Academy of Sciences.

This translating and publishing project was undertaken by the institute in the conviction that dissemination of the results of researches everywhere in the world is invaluable to the advancement of science. The NATIONAL SCIENCE FOUNDATION of the United States has encouraged the project initially and is supporting it in large part by a grant.

The American Institute of Physics and its translators propose to translate faithfully all the material appearing in the original articles. The views expressed in the translations are therefore those of the original authors, and not those of the translators nor of the American Institute of Physics.

Volume 1 of SOVIET PHYSICS—JETP corresponds to Russian Volume 28 (1955). Two volumes are published annually, each of six issues. Each volume contains the translation of one volume of the JOURNAL OF EXPERIMENTAL AND THEORETICAL PHYSICS.

Beginning with Vol. 9 (36), the transliteration of the names of Russian authors follows British Standard 2979, which is being adopted by a large number of scientific journals in the United States. The Library of Congress transliteration is followed in the earlier volumes.

Subscription Prices

Per Year (12 issues), starting with Vol. 13, No. 1

General:
United States and Canada $75.00
Elsewhere 79.00

Libraries of non-profit degree-granting Institutions:
United States and Canada $50.00
Elsewhere 54.00

Single Copies ..... $ 8.00

Subscriptions should be addressed to the American Institute of Physics, 335 East 45th Street, New York 17, New York.

SOVIET PHYSICS, JETP is published monthly by the American Institute of Physics, Inc. Second Class postage paid at New York, N. Y. and Ann Arbor, Michigan.

SOVIET PHYSICS

JETP

A translation of the Zhurnal Éksperimental'noĭ i Teoreticheskoĭ Fiziki.

Vol. 14, No. 1, pp 1-223 (Russ. orig. Vol. 41. No. 1, pp 3-308, July, 1961) January, 1962

SECONDARY ION EMISSION FROM METALS INDUCED BY 10 — 100 kev IONS

B. V. PANIN

Submitted to JETP editor September 29, 1960

J. Exptl. Theoret. Phys. (U.S.S.R.) 41, 3-10 (July, 1961)

Secondary ion emission from Mo, Zr, and graphite bombarded with H_1^+, H_2^+, H_3^+, He^+, C^+, N^+, Cl^+, Ar^+, and Mo^+ ions was studied to determine the mechanism of interactions between medium-energy (10 — 100 kev) atomic particles and solids. The dependences of ion-ion emission coefficients on the nature of the primary ions, and on their initial velocity and charge were investigated.

THE study of the mechanism of interactions between atoms or ions with intermediate energies (10 — 100 kev) and solids has acquired increasing importance in recent years, because of the continually expanding utilization of fast ions in widely diversified fields of science and technology. Information is obtained by studying the secondary ion emission induced when solids are bombarded with ions or atoms. This field is very well covered by reviews such as [1] and a number of theories describing ion bombardment processes have recently been proposed.[2-6] The testing of these theoreies requires new experimental investigations, since conflicting data are often found in the literature. Even relatively recent publications are either inadequate methodologically or discuss narrowly limited special cases.

The shortcomings of these investigations include a) uncontrolled composition and energy of the bombarding particles (as in measurements in connection with a glow discharge); b) insufficiently thorough cleaning of the working surfaces of target (adsorption from the ambient, nonvolatile impurities that can be formed during the production and treatment of the target material or during its thermal conditioning in the measuring apparatus or under ion bombardment); and c) systematic errors in measuring particle emission from the target surface, resulting often from lack of knowledge regarding the mass, charge, and energy distributions of the particles. The present investigation of some characteristics of ion-ion emission excludes some of these defects, while reducing considerably the influence that the other defects have on the results.

APPARATUS AND EXPERIMENTAL TECHNIQUE

The mass monochromator represented in Fig. 1 was used to produce ions of rigorously defined masses and energies. Different isotopes from H_1^+ to Mo^+ with energies ranging from 5 to 120 kev bombarded 2×5 mm^2 targets; the resolving power was $m/\Delta m \approx 200$. The ion current density at the target was $10^{-8} - 10^{-3}$ amp/cm^2. Ion energies were determined from the accelerating potential difference (with 0.01% stabilization) between the electrodes of the ion source. The ion energy spread at the target was under 1%.

Target contamination by atoms from the surrounding space was reduced by lowering residual gas pressure in the chamber of the target 16, and by using hot targets (above 1000° C). A differential pumping system (a series of oil diffusion pumps with "non-leaking" liquid nitrogen traps) and the copper shell 12 at liquid nitrogen temperature reduced the residual gas pressure in the working chamber to $(2 - 3) \times 10^{-8}$ mm Hg.

Metal targets in the form of $30 \times 12 \times 0.2$ mm ribbons and graphite targets 0.4 — 0.5 mm thick

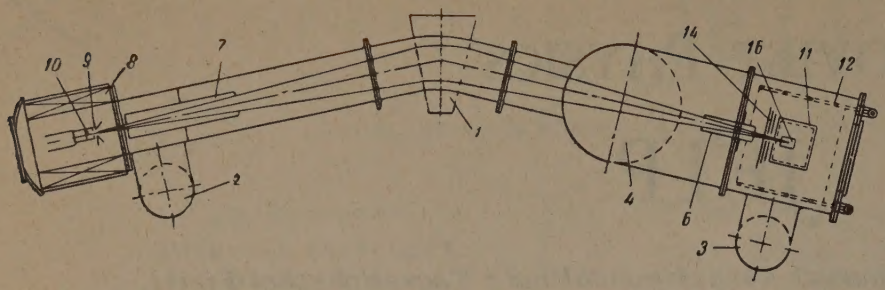

FIG. 1. Diagram of apparatus. 1 – electromagnet; 2, 3, 4 – diffusion pumps; 6, 7 – tubular diaphragms; 8 – solenoid of ion source; 9 – accelerating electrode; 10 – gas-discharge unit of ion source; 11 – secondary-ion collector; 12 – enclosing shell cooled by liquid nitrogen; 14 – three-electrode diaphragm; 16 – target.

were heated by emission from a tungsten-ribbon heater located directly behind the target.

Figure 2 shows the method used to measure ion-ion emission coefficients. A beam of ions with a specified mass and charge was directed at the target 1 through an aperture in the three-electrode diaphragm 11. A 3 × 3 mm aperture for the purpose of defining the ion-beam cross section was cut in the first electrode, a plate of the same material as the target. This protected the target surface from contamination by foreign atoms produced through sputtering of the edges of the first diaphragm.

The apertures in the second and third electrodes were somewhat larger, so that their edges were not bombarded by ions. These electrodes prevented secondary electrons and ions formed at the edge of the first diaphragm from entering the target-to-collector system. A 400-volt potential was applied to all three electrodes, with alternating signs in a sequence depending on the charge sign of the secondary ion under investigation. The secondary-ion collector was a rectangular chamber surrounding the target 1.

For the purpose of excluding errors in current measurements resulting from tertiary electrons formed on the collector walls, a molybdenum grid was installed on the inner walls of the collector and was given a 150-volt negative potential with respect to the latter. During the measurements of the coefficient δ^+ the potential difference between the target and collector was maintained at −400 v, which when added to the grid potential provided a −550-volt stopping potential for negative secondary ions.

Analysis of the secondary-ion energy spectra revealed the existence of a considerable number of negative secondary ions with energies above 550 ev. The error thus introduced in the measurement of positive secondary-ion currents was estimated from the secondary-ion energy spectra. In bombardments with ions of atoms (Ar) possessing no electron affinity, attenuation of the positive secondary-ion current cannot exceed 2%. For bombardments with O^+ and C^+ this error increases somewhat; for H^+ the error reaches 20%.

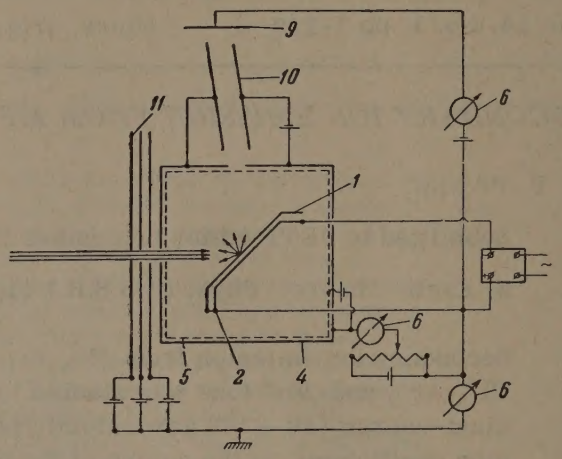

FIG. 2. Experimental arrangement for measuring ion-ion emission coefficients $\delta^{\pm}$. 1 – target; 2 – heater; 4 – ion collector; 5 – grid; 6 – microammeters; 9 – electron collector; 10 – deflecting system; 11 – three-electrode diaphragm.

The value obtained for δ^+ was also affected by the escape of fast ions of both signs from the measuring system. It follows from geometrical considerations that this error cannot exceed ±1% of the true value of δ^+; this error has therefore been neglected. Random errors measured from the spread of the measurements did not exceed ±5% in any instance. All currents were measured with M-95 microammeters having a maximum sensitivity of 2×10^{-9} amp per scale division.

Figure 3 shows three additional electrodes (9 and 10), which were used to determine the negative component δ^- of secondary-ion emission. If the current received by the collector is to consist only of negative secondary ions, it is insufficient to hold positive ions at the target. The negative ions must also be separated from the simultaneous flux of secondary electrons, which is at least ten times greater than the ion flux. For this purpose the entire measuring setup was placed in a magnetic field whose lines of force proceeded from the target 1 through an opening in the collector 4, between the electrodes 10, and through the electrode 9. Consequently, all electrons leaving

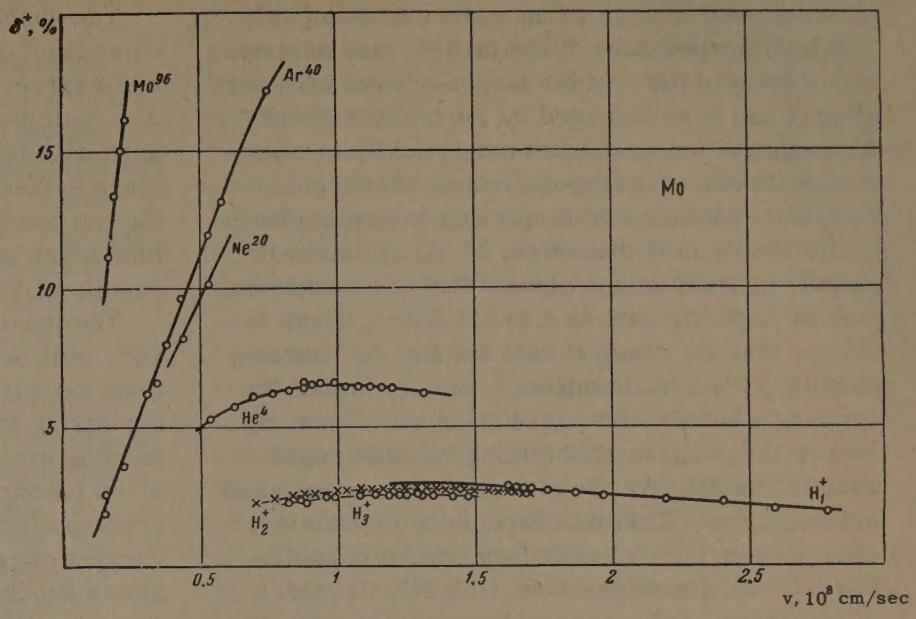

FIG. 3. Ion-ion emission coefficient δ^+ for Mo target vs velocity v of bombarding Mo^+, Ar^+, Ne^+, He^+, H_3^+, H_2^+, and H_1^+ ions. For H_3^+, $\frac{1}{3}\delta$ is given; for H_2^+, $\frac{1}{2}\delta$ is given.

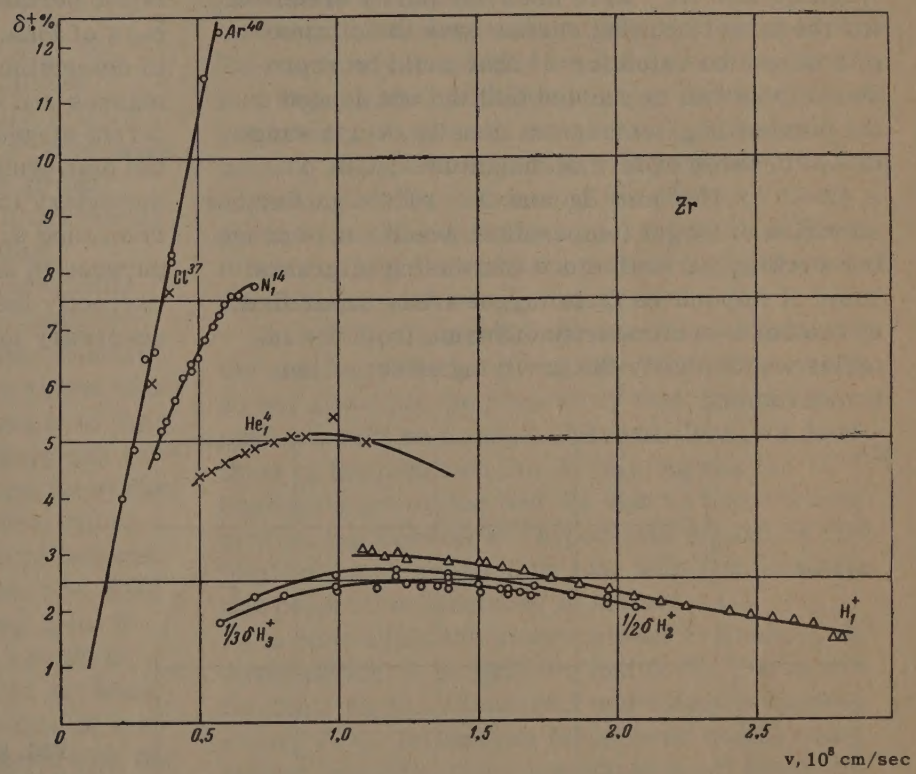

FIG. 4. Ion-ion emission coefficient δ^+ for Zr target vs velocity v of bombarding Ar^+, Cl^+, N^+, He^+, H_3^+, H_2^+, and H_1^+ ions.

the target moved to the electrode 9 along helical trajectories even in relatively weak fields (not stronger than 1000 oe).

A few very slow negative secondary ions that accompanied electrons passing through the collector aperture were returned to the collector circuit by the electric field between the electrodes 10. Unfortunately, our apparatus did not permit the use of potentials large enough to prevent the return of slow negative secondary ions to the target by the action of the magnetic field, or to stop a large group of fast positive ions that reached the collector along with the negative ions. Our values of the negative ion-ion emission coefficient δ^- are therefore only estimates.

It must be noted that even prolonged thermal conditioning in a high vacuum does not rid the target of nonvolatile impurities. As a second stage of purification preceding all measurements, the working surfaces of targets were bombarded with $\sim 500\ \mu a/cm^2$ of Ar^+ ions at 30 — 40 kev. Nonvolatile carbides, silicides, nitrides, and oxides of the different target elements were thus removed from the surface by means of cathode sputtering. The high-temperature targets did not retain deeply penetrating Ar atoms as impurities. (The same

effect is used in separating noble gas isotopes.) The high temperature of the targets also assisted restoration of the regular target-crystal structure after it had been damaged by ion bombardment. Although the ion beam acts catalytically in chemical reactions on a target surface, the targets were not contaminated in our experiments. Early in the 1950's I. M. Samoĭlov, V. G. Tel'kovskii and the present author showed that the formation rate of impurity film on a molybdenum target is slower than its removal rate for the Ar^+ current density $j > 0.1$ milliamp/cm^2 with the initial energy $E_0 = 30$ kev and pressure $p < 10^{-6}$ mm Hg.

For the purpose of obtaining reliable reproducible results, Ar^+ bombardment preceded each measurement. This was especially important when measuring the secondary emission coefficient δ^+ for active gas ions (O^+, N^+, Cl^+ etc.). When 30-kev Ar^+ were used our purity criterion for the target working surface was the attainment of a minimum value for δ^+ that could be reproduced from run to run and that did not depend on the bombarding-ion current density over a range of two to three orders of magnitude (with $p \leq (2-3) \times 10^{-7}$ mm Hg and $T = 1000°$ C). Further elevation of target temperature would not improve the working surface, since increasing migration rates of impurities from target areas unpurified by the beam and impurity diffusion from the interior would nullify the purifying effect of ion bombardment.

The absolute values of the ion-ion emission coefficient obtained in different runs did not always agree even after careful target preparation. The ionic purification technique enabled us to compare data from different runs. The results for any given series were expressed in relative units with the ion-ion emission coefficient for 30-kev Ar^+ ions taken as unity. Smooth curves then fitted the results of many runs with greatly reduced spread.

The ion-ion emission coefficient of either sign ($\delta^\pm$) will be understood to mean the ratio of the total ion current of the given sign leaving the target during ion bombardment to the current of bombarding ions. Figures 3 to 5 show the coefficients δ^+ as functions of primary ion velocity. Our measured coefficients thus take into account both the current of reflected ions and the current of ionized atoms knocked out of the target surface. Our definition pertains to ion currents rather than to numbers of ions, since it is a very complicated problem to determine the numbers of ions with different masses and overlapping energy spectra and in different stages of ionization. For the same reason the distinguishing of reflected ions from all other secondary ions according to their energies, as in reference 9, for example, does not achieve its purpose in most instances; it does not represent correctly the true ratio between the numbers of secondary ions formed in different ways.

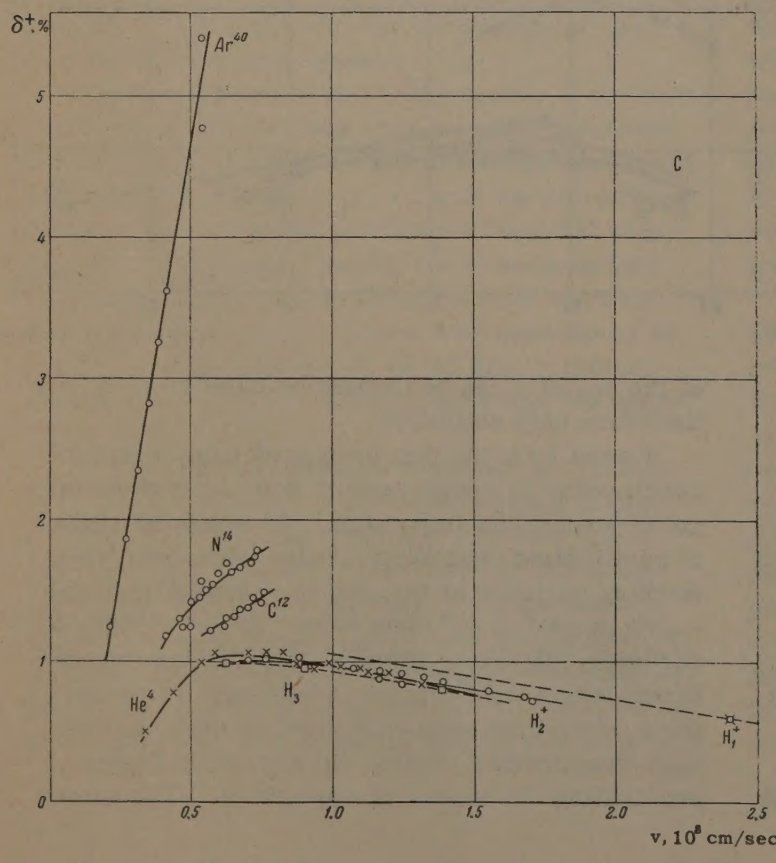

FIG. 5. Ion-ion emission coefficient $\delta^+(v_0)$ for graphite target bombarded with Ar^+, N^+, C^+, H_1^+, H_2^+, and H_3^+ ions. For H_3^+, $\frac{1}{3}\delta$ is given; for H_2^+, $\frac{1}{2}\delta$ is given.

RESULTS

Before the measurements of δ^+ were begun, a special experimental run investigated the dependence of secondary-ion emission on the gas pressure around the target, on target temperature, and on the primary ion current density. It was found that at pressures below $2-3\times10^{-7}$ mm and at 1300°K, δ^+ for pure Mo and Zr targets is independent of the incident ion current density. All curves in Figs. 3—5 were obtained under these conditions.

The most complete studies were carried out for secondary ion emission from Mo (containing 0.008% Fe and 0.007% Al), Zr (obtained by the iodide decomposition process), and graphite (EG-14) bombarded with H_1^+, H_2^+, H_3^+, He^+, C^+, N^+, O^+, Cl^+, Ar^+, and Mo^+. Even a slightly increased impurity content in the Mo target resulted in an appreciable increase of δ^+.

In Figs. 3, 4, and 5 the curves of $\delta^+(v_0)$ for all targets are similar. This applies also to copper and molten tin, the data for which are not presented here. It is noteworthy that δ^+ increases proportionately to the velocity of heavy primary ions from 10^7 to 10^8 cm/sec, and that it decreases smoothly at higher velocities of light ions.

Figures 3, 4, and 5 show that with increasing mass of the incident ion secondary-ion emission grows rapidly regardless of whether the bombarding ions are heavier or lighter than the target ions. Secondly, δ^+ also increases with the mass of the target ions. It is found that the secondary-ion currents produced by bombardment with the molecular ions H_2^+ and H_3^+ are almost two and three times greater, respectively, than the secondary-ion current produced by H_1^+ with the same velocity. This agrees well with the hypothesis of many investigators that molecular ions dissociate into their atomic components upon striking a solid surface. In this case the somewhat smaller number of secondary ions produced per atom, compared with the results from bombardment with the corresponding monatomic ions, suggests that a small fraction of molecular ions are reflected without dissociating. This difference could be attributed to a possible difference between the secondary emission coefficients for ions and neutral atoms. However, a special experimental run showed that in our energy range the emission coefficient does not depend on the unneutralized charge of bombarding particles. This effect results from the completely determinate statistically averaged equilibrium charge distribution in a beam of particles with like velocities, traversing even a small number of atomic layers in a target. Both of our conclusions are in accord with the analogous characteristics of secondary-electron emission under ion bombardment.[8]

More detailed measurements of $\delta^+(v_0)$ for protons sometimes reveal a fine structure. The smoothness of the $\delta^+(v_0)$ curve for Mo is broken by a sharp decline of ion emission at H_1^+ velocities around 1.4×10^8, 1.7×10^8, and 2.8×10^8 cm/sec. In all instances the half-width of the minimum was not greater than 0.5 kev.

The measurements indicated that $\delta^-(v_0)$ varies in the same way as $\delta^+(v_0)$, and that the respective absolute values are of the same order of magnitude. The curves for $\delta^-(v_0)$ are not given here because of their low accuracy. The resemblance between $\delta^-(v_0)$ and $\delta^+(v_0)$ suggests that $\delta^0(v_0)$ will vary in a similar manner. (Some ions can be reflected in the neutralized state.)

We can therefore assume identical mechanisms for secondary-ion emission and cathode sputtering in a high vacuum with bombarding currents that do not greatly elevate the temperature of the entire target. The relative numbers of particles can vary depending on the amount and character of metal surface contamination and the probabilities for the formation and neutralization of all kinds of emitted particles in each energy interval.

It is difficult to compare our present data with the existing theories of cathode sputtering, which do not allow for the possibility that sputtering products will be ionized. Nevertheless, the positions of the peaks on the $\delta^+(v_0)$ curves for H_1^+ bombardment of Mo and Zr can be regarded as confirming Keywell's[2] hypothesis regarding the interaction of bombarding ions with lattice atoms and conduction electrons in metals.

In conclusion the author wishes to thank L. A. Artsimovich, I. N. Golovin, and G. Ya. Shchepkin for their continued interest and valuable discussions, V. G. Tel'kovskii for several useful comments, and laboratory assistants A. A. Borisov and Yu. E. Pavlov for assistance with the apparatus.

[1] H. Massey and E. Burhop, Electronic and Ionic Impact Phenomena, Clarendon Press, Oxford, 1952.

[2] F. Keywell, Phys. Rev. **97**, 1611 (1955).

[3] D. E. Harrison, Phys. Rev. **102**, 1473 (1956).

[4] D. T. Goldman and A. Simon, Phys. Rev. **111**, 383 (1958).

[5] O. von Roos, Z. Physik **147**, 184 (1957).

[6] K. Thommen, Z. Physik **151**, 144 (1958).

[7] Craston, Hancox, Robson, Kaufman, Miles, Ware, and Wesson, Proc. 2nd International Con-

ference on the Peaceful Uses of Atomic Energy, Geneva, 1958, vol. 32, p. 414.

[8] V. G. Tel'kovskii, Doklady Akad. Nauk SSSR **108**, 446 (1956), Soviet Phys.-Doklady **1**, 334 (1957).

[9] Fogel', Slabospitskii, and Rastrepin, J. Tech. Phys. (U.S.S.R.) **30**, 63 (1960), Soviet Phys.-Tech. Phys. **5**, 58 (1960).

[10] F. Seitz and D. Turnbull, editors, Solid State Physics, Academic Press, Inc., New York, 1958.

[11] R. L. Hines and R. Arndt, Phys. Rev. **119**, 623 (1960).

Translated by I. Emin
1

TERNARY FISSION OF URANIUM INDUCED BY FAST NEUTRONS

N. A. PERFILOV, Z. I. SOLOV'EVA, and R. A. FILOV

Radium Institute, Academy of Sciences, U.S.S.R.

Submitted to JETP editor December 12, 1960

J. Exptl. Theoret. Phys. (U.S.S.R.) 41, 11-12 (July, 1961)

Ternary fission of U^{238} induced by 14-Mev neutrons is investigated. The fission characteristics are compared with ternary fission of U^{235} induced by thermal neutrons.

DURING the study of fission of uranium induced by 14-Mev neutrons, it was observed that in some cases the uranium undergoes fission with the emission of a third charged particle, an α particle.[1] This phenomenon has been widely studied earlier in the case of fission of U^{235}, Pu^{239}, and U^{233} induced by thermal neutrons,[2] and was also observed in the fission of U^{238} induced by 2.5-Mev neutrons.[3] Comparison of the characteristics of complex fission at different excitation energies is of considerable interest, but the results obtained from the small number of cases observed[1] allows one only to establish the fact that such a reaction occurs with an approximate probability of 1: (1000 – 1300) with respect to the number of binary fissions. In the present article, we shall discuss more fully the characteristics of the process.

The experiment was carried out by the emulsion method under the same conditions as before.[1] To eliminate background due to a random superposition of α-particle tracks from the natural activity of uranium, we recorded only cases in which the α-particle range was at least 30 μ in the emulsion.

A total of 231 α particles from complex fission was recorded. The ratio of the number of complex fissions to the number of binary fissions was 1:1250. Owing to the fact that we recorded only those events in which the range of the α-particle track in the emulsion pellicle was greater than 30 μ, we introduced an appropriate correction, from which it followed that the probability of complex fission should be taken as $1:(1050 \pm 100)$.

The cited error includes the statistical error and systematic error due to the fact that part of the cases of ternary fission cannot be separated from the random superposition of binary fissions with α particles from nuclear reactions occurring in the emulsion.

To construct the energy spectrum of the α particles from complex fission, we made use of 158 particles which stopped in the emulsion. After introducing the geometrical corrections for the escape of particles from the emulsion, we plotted the spectrum by the method of Ferreira and Waloschek.[4] The spectrum is shown in Fig. 1. Also shown in this figure is the α-particle spectrum from ternary fission of U^{235} induced by thermal neutrons, obtained by the photographic emulsion method of Titterton.[5]

The size of the asymmetry in ternary fission which, in our case, can be characterized by the ratio of the ranges of the two fragments R_l/R_h, is shown in Fig. 2. The corresponding curve is also given for the complex fission of U^{235} induced by thermal neutrons obtained earlier by Solov'eva from 650 cases. The angular distribution of the α particles relative to the fission fragments does not differ from that obtained previously.[1]

There is quite good agreement between the characteristics of complex fission of U^{238} induced by 14-Mev neutrons and of U^{235} induced by thermal neutrons.

The decreased probability of ternary fission of U^{238} induced by 14-Mev neutrons indicates, perhaps, that the emission of α particles during fission takes place only after the nuclear excitation is reduced by the evaporation of one or two

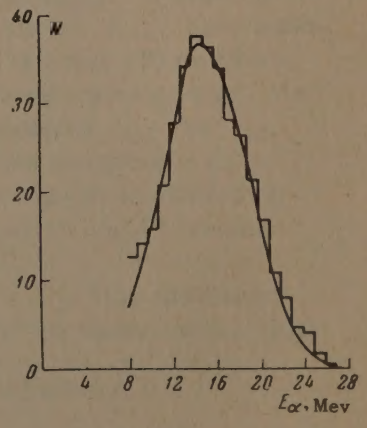

FIG. 1. Energy spectrum of alpha particles from ternary fission of U^{238} by 14-Mev neutrons. Solid curve – spectrum of alpha particles from ternary fission of U^{235} by thermal neutrons.

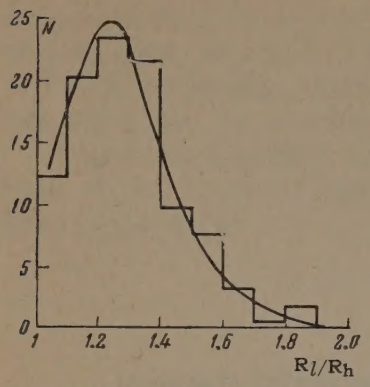

Fig. 2. Distribution of ternary-fission events by asymmetry of fission fragments. Solid curve – analogous data for U^{235} fission by thermal neutrons (R_l and R_h are the ranges of the light and heavy fragments).

neutrons. This considerably complicates the process, since different nuclei undergo fission with different excitation energies.

[1] N. A. Perfilov and Z. I. Solov'eva, Atomnaya energiya (Atomic Energy) 5, 175 (1958).

[2] Perfilov, Romanov, and Solov'eva, Usp. Fiz. Nauk 71, 471 (1960), Soviet Phys.-Uspekhi 3, 542 (1961).

[3] Z. I. Solov'eva, Atomnaya energiya (Atomic Energy) 8, 137 (1960).

[4] E. P. Ferreira and P. J. Waloschek, Proceedings of the International Conference on the Peaceful Uses of Atomic Energy, Geneva, 1955, vol. 14.

[5] E. W. Titterton, Phys. Rev. 83, 673 (1951).

Translated by E. Marquit
2

NUCLEAR-ACTIVE PARTICLES IN ATMOSPHERIC SHOWERS

J. S. BABECKI, Z. A. BUJA, N. L. GRIGOROV, E. S. LOSKIEWICZ, E. I. MASSALSKI, A. A. OLES, V. Ya. SHESTOPEROV, and S. FISCHER

Institute of Nuclear Physics, Moscow State University

Submitted to JETP editor December 20, 1960

J. Exptl. Theoret. Phys. (U.S.S.R.) **41**, 13-21 (July, 1961)

Extensive and "young" air showers were studied at sea level with an array of 128 ionization chambers covering an area of 10 m^2. The energy of the nuclear-active particles near the axes of the extensive showers was found to be less than 50 percent of the energy of the electron-photon component. The mean inelasticity coefficient of the nuclear-active particles of the extensive showers exceeds 0.6 — 0.75. There is practically no nuclear-active component in a large fraction of the "young" atmospheric showers.

INTRODUCTION

THE opinion that the extensive air shower (EAS) is an electronic cascade in equilibrium with a nuclear avalanche, which in turn serves so to speak as a base for the shower,[1] has for a long time been regarded as suitably founded and not subject to doubt.

Many recent investigations, however, have shown, on the one hand, that the arguments used to prove the important role played by the nuclear-active component in the development of the EAS deep in the atmosphere is not unequivocal.[2] Models have been proposed, on the other hand, by which all the average characteristics of the EAS are explained without stipulating that the nuclear-active particles play a decisive role in the development of the EAS.[3]

It seems to us, in this connection, that the question of the characteristics of the elementary processes that underlie the formation of EAS has now again become timely. It is possible that a study of the nuclear-active particles in an EAS will help answer this important question. We deemed it advisable, therefore, with an aim toward obtaining information on nuclear-active particles in air showers, to carry out a suitable reduction of the experimental data obtained with the apparatus[4] used to study ionization bursts at sea level.

The apparatus used to carry out this research was described elsewhere.[4] The same reference contains data on the threshold for the registration of ionization with chambers in various rows, and on the system used to trigger the signal control in the case of registration of an air shower.

1. NUCLEAR-ACTIVE PARTICLES IN EXTENSIVE AIR SHOWERS

In the case when an EAS strikes the array, the summary ionization in chamber rows III and IV (see[4], Fig. 1) served as an indication of the energy $E_{e\text{-}ph}$ of the electron-photon component of the EAS striking the array. If nuclear-active particles were simultaneously incident on the array from the EAS, they interacted with the graphite block in the array and transferred part of their energy to the π^0 mesons. The energy transferred to the π^0 mesons was determined from the summary ionization in chamber rows I or II.

If we measure the ionization J_{max} produced by all the particles of the electron-photon cascade during the maximum of its development, then the energy of the cascade is $E = kJ_{max}$, where k is practically constant.

In the real conditions of our array, when the ionization was determined only at two cascade-development depths (in rows III and IV or I and II), it was impossible to locate the maximum of the shower or to determine J_{max}. In order to minimize the error, we took for J_{max} each time the ionization in that pair of rows (III or IV and I or II), in which the ionization was greater. We shall henceforth use the notation $J_{1,2}$ and $J_{3,4}$, bearing in mind that we took the greater of the two possible values of the overall ionization obtained from rows I and II or III and IV, respectively.

If it is true that $J_{max} = J_{1,2}$ (for the lower rows) or $J_{max} = J_{3,4}$ (for the upper rows), then

$$E_{e\text{-}ph} = kJ_{3,4} \text{ and } E_{\pi^0} = kJ_{1,2},$$

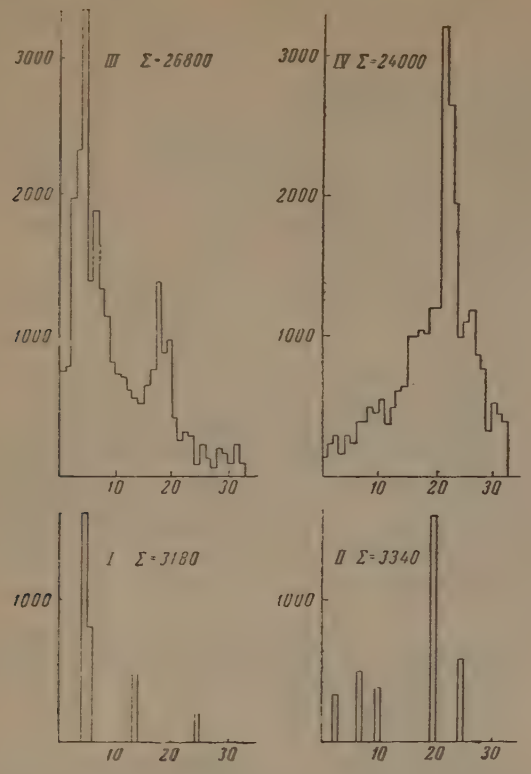

FIG. 1. Example of distribution of ionization over chambers of rows III and IV in the case when the axis of the EAS goes through the array. Abscissas—number of the chambers in a given row; ordinates—ionization in a given chamber, expressed in terms of relativistic particles passing through the the central chord. The lower part of the figure shows the distribution of the ionization, due to nuclear-active particles, in rows I and II.

i.e.,

$$E_{\pi^0}/E_{e\text{-ph}} = J_{1,2}/J_{3,4}.$$

It must be noted that the determination of the absolute value of $E_{e\text{-ph}}$ or of E_{π^0} from the measured values of $J_{3,4}$ or $J_{1,2}$ is subject to considerable errors, since the coefficient k depends on corrections for the transition effect, on constructive features of the chambers, and on the spatial and angular distributions of the particles, factors that do not lend themselves to accurate evaluation. This coefficient does not enter into the ratio $E_{\pi^0}/E_{e\text{-ph}}$ (if the chambers of the upper and lower rows are identical, as was the case in our array); it is therefore methodologically more correct to measure this ratio rather than $E_{e\text{-ph}}$ and E_{π^0} separately. Thus, the ratio of the summary ionization (summed over the row), measured by the lower rows of chambers, to the ionization measured in the upper rows of the chamber, will yield the energy transferred by the π^0 mesons to the nuclear-active particles of the EAS, referred to the energy of the electron-photon component of the EAS at the shower location where the nuclear active particles were located.

Since we did not use any special systems to determine the position of the shower axis in the registration of the EAS, the average $\overline{(J_{1,2}/J_{3,4})}$ is essentially equal to the ratio $\overline{(E_{\pi^0}/E_{e\text{-ph}})}$, averaged over showers with different numbers of particles (of different "powers") and over different portions of the shower. In those cases when the distribution of the ionization over the chambers of rows III and IV had a maximum at the central part of the layout and decreased monotonically towards the edges in both rows, III and IV, we assumed that the shower axis passed through the array.

An example of one such case is shown in Fig. 1. When the ionization distribution had no maximum or when the ionization increased monotonically from one edge of the array to the opposite one, or finally, when the ionization had a maximum in one row in the central part of the array, while the other row had no maximum, it was assumed in all these cases that the shower axis did not pass through the array.

We have singled out from among all EAS registered by the array those cases for which $J_{3,4} \geq 1.2 \times 10^4$ relativistic particles, i.e., cases for which $E_{e\text{-ph}} \gtrsim 2 \times 10^{12}$ ev. During the 1842 hours that the array was in operation, 284 EAS with $J_{3,4} \geq 1.2 \times 10^4$ were registered. The distribution of the number of cases of incidence of the axes of EAS of various "powers" is listed in Table I.

Table I

Size of registered EAS	Number of showers with axis over array	Number of showers with axis outside array
$1.2 \cdot 10^4 \leqslant J_{3,4} < 2{,}4 \cdot 10^4$	68±8	83±9
$2.4 \cdot 10^4 \leqslant J_{3,4} < 6 \cdot 10^4$	47±7	54±7.7
$6 \cdot 10^4 \leqslant J_{3,4} < 1.2 \cdot 10^5$	13±3.6	11±3.3

As can be seen from Table I, the EAS axis passes through the array in approximately 50 percent of the cases. In those cases when the axis passes outside the array, the EAS region registered is close to the shower axis. Consequently the ratio $\overline{E_{\pi^0}/E_{e\text{-ph}}}$ pertains to the central regions of the EAS.

Starting from the frequency of the registered EAS and from the energy of the electron-photon component of the showers ($J_{3,4} \geq 1.2 \times 10^4$ corresponds to $E_{e\text{-ph}} \gtrsim 2 \times 10^{12}$ ev), we can conclude that by picking out the showers with $J_{3,4} \geq 1.2 \times 10^4$ we automatically pick out the EAS with $\gtrsim 10^5$ particles. The average for these showers is $\overline{(J_{1,2}/J_{3,4})} = 0.130 \pm 0.047$. The distribution of the

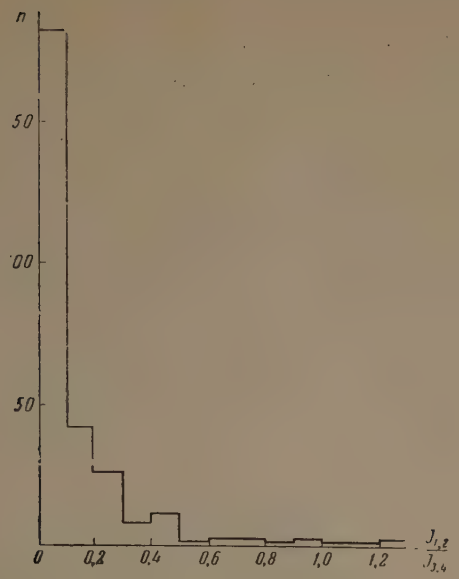

FIG. 2. Distribution of EAS based on the ratio $J_{1,2}/J_{3,4}$, (abscissas). The ordinates represent the number of showers with given ratio $J_{1,2}/J_{3,4}$.

values of $J_{1,2}/J_{3,4}$ over all 284 showers is shown in Fig. 2.

For the showers whose axes passed through the array, we obtained $\overline{(J_{1,2}/J_{3,4})} = 0.128 \pm 0.036$. The distribution of the ratios $J_{1,2}/J_{3,4}$ does not differ in this case from the one shown in Fig. 2.

In order for $\overline{(J_{1,2}/J_{3,4})}$ to be equal to $\overline{(E_{\pi^0}/E_{e\text{-}ph})}$ it is necessary that rows I and II of the array, which are under graphite, register only the electron-photon component generated by the nuclear-active particles in the array. However, because the EAS have a definite angular distribution, part of the electron-photon component of the air shower will pass through the side surfaces of the graphite absorber, multiply in the lead, and simulate the nuclear component in the EAS. This effect will cause the summary ionization recorded in all EAS in the outermost chambers of rows I and II to be greater than that recorded in the central chambers of the array.

In order to estimate the contribution of the electron-photon component of the EAS to the ionization registered by the chambers under the graphite layer, we plotted the distribution, over the chambers of row I, of the summary ionization registered in all 284 EAS.

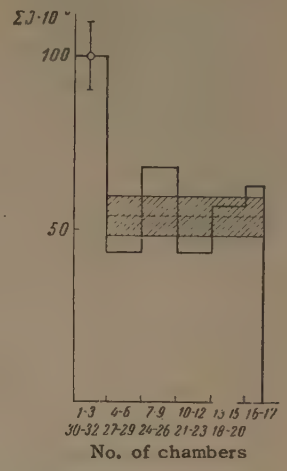

FIG. 3. Distribution of ionization over the chambers of the first row in all the registered EAS. Abscissas—number of chambers connected in one group; ordinates—values of the summary ionization registered by the given group of chambers in all the showers. The width of the shaded region is equal to twice the mean-square error.

To increase the accuracy we interconnected the chambers in groups of three, and additionally interconnected the groups that were symmetrical about the vertical plane passing through the center of the array. The result was the summary-ionization distribution shown in Fig. 3. This distribution shows that the three outermost chambers, taken together, registered in all the EAS an ionization 1.86 ± 0.26 times greater than registered on the average by the like three-chamber groups remote from the edge of the array. Assuming that the ionization produced in the chambers by the nuclear-active particles is independent of the location of the chamber in the array, we deduce from Fig. 3 that the electron-photon component of the EAS increases the ionization in row I by $30 \pm 7.5\%$. Therefore $\overline{(E_{\pi^0}/E_{e\text{-}ph})} = (0.130 \pm 0.047) \times (0.70 \pm 0.075) = 0.091 \pm 0.031$.

The nuclear-active particles can leave through the side surfaces of the array and thereby reduce E_{π^0}. By taking account of the angular distribution of the EAS, we can calculate the magnitude of this effect. It decreases E_{π^0} by 6 percent. We therefore have finally $E_{\pi^0}/E_{e\text{-}ph} = 0.097 \pm 0.036$.

Since the lateral distribution of the energy flux of the nuclear-active component is not broader than the lateral distribution of the energy flux of the electron-photon component of the shower, the average $\overline{(E_{\pi^0}/E_{e\text{-}ph})}$ over the entire shower will not exceed 0.097 ± 0.036.

A characteristic feature is that the value of $\overline{(E_{\pi^0}/E_{e\text{-}ph})}$ is determined to a considerable degree by a small number of showers having a

Table II

Size of shower $J_{3,4}$	Shower axes over array $\overline{(J_{1,2}/J_{3,4})}$	Shower axes outside array $\overline{(J_{1,2}/J_{3,4})}$	Average value of $J_{1,2}/J_{3,4}$ for given group of showers
$1.2 \cdot 10^4$—$2.4 \cdot 10^4$	0.062±0.011	0.092±0.023	0.078±0.014
$2.4 \cdot 10^4$—$6 \cdot 10^4$	0.202±0.046	0.182±0.041	0.191±0.031
$6 \cdot 10^4$—$1.2 \cdot 10^5$	—	—	0.178±0.068
$>1.2 \cdot 10^5$	—	—	0.150±0.046

nuclear-active component of anomalously high energy. As can be seen from Fig. 2, $E_{\pi^0}/E_{e\text{-}ph} < 0.10$ in 65 percent of the registered EAS.

It should be noted that, within the limits of experimental error, we observed no relation between the ratio $\overline{(J_{1,2}/J_{3,4})}$ and the value of $J_{3,4}$, except in the smallest of the registered showers.

The value of $\overline{(J_{1,2}/J_{3,4})}$ for different shower groups is listed in Table II.

It is possible that the low value of $\overline{(J_{1,2}/J_{3,4})}$ for showers with $J_{3,4} < 2.4 \times 10^4$ was due to the apparatus effect, since the ionization chambers in the lower rows (I and II) had an ionization-registration threshold of 200 — 300 relativistic particles. If this is so, it is more correct to take for the average $\overline{(J_{1,2}/J_{3,4})}$ the value corresponding to showers with $J_{3,4} \geq 2.4 \times 10^4$, namely 0.186 ± 0.027. Consequently, taking the foregoing corrections into account, we have in this case $\overline{(E_{\pi^0}/E_{e\text{-}ph})} = (0.186 \pm 0.027) \times (0.70 \pm 0.075) \times 1.06 = 0.138 \pm 0.024$.

2. "YOUNG" AIR SHOWERS

a) Intensity and spectrum of "young" air showers. In 1900 hours of operation, the array registered 52 "young" atmospheric showers (YAS),[3] which produced in rows III and IV an ionization $J_{3,4} \geq 1.2 \times 10^4$ relativistic particles. We classified showers as "young" if the bursts in rows III and IV were such that ≥ 60% of all the ionization was produced in four or less chambers, i.e., in a circle of radius ~ 20 cm. Cases when the chamber with maximum ionization was on the edge of the array were excluded. This caused the area of the array effective in the registration of the "young" showers to decrease from 10 to 8 m^2. With account of this correction, the intensity of the YAS is $(0.95 \pm 0.13) \times 10^{-10}$ cm^{-2} sec^{-1}.

The requirement $J_{3,4} \geq 1.2 \times 10^4$ is tantamount to stating that the energy of the electron-photon cascade in the YAS be not less than 2×10^{12} ev. In all the YAS, the summary ionization in the third row of chambers was 1.5 or 2 times greater than the summary ionization in the fourth row. It follows therefore that YAS are highly collimated streams of the electron-photon component contained in the high-energy photons and electrons.

It is easy to show that the main part of the bursts in rows III and IV, which we attribute to the incidence of a narrow electron-photon shower from the air onto the array, cannot be simulated by electromagnetic interactions of high-energy muons in the lead absorbers of the array.

In fact, the number of bursts due to muons in the third row of chambers should not exceed the number of bursts registered by the second row. The intensity of single bursts in the second row, with $J_2 \geq 1.2 \times 10^4$ (the muons cannot produce structural bursts) is 2×10^{-11} cm^{-2} sec^{-1}. It is obvious that not all single bursts are produced by muons. Some are produced also by single nuclear-active particles. But if all the single bursts in the second row are attributed to electromagnetic muon interactions, even then their fraction in the "young" air showers will be merely 20 percent.

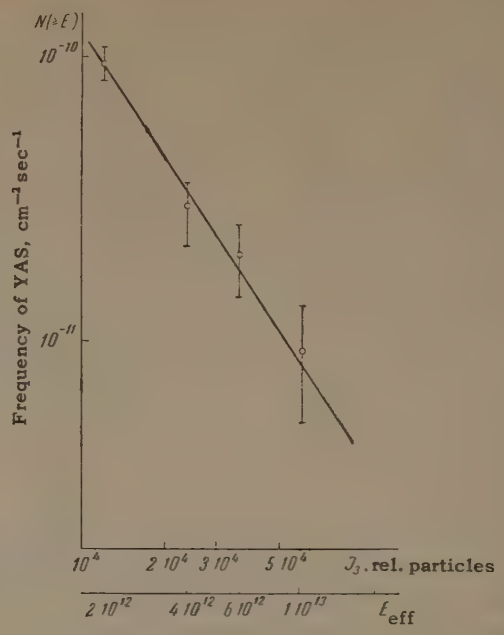

FIG. 4. Integral energy spectrum of YAS. Abscissas—summary ionization in the third row of chambers, produced by the YAS (the second scale shows the energy of the electron-photon component of the YAS). Ordinates—number of showers with $E_{e\text{-}ph}$ (or J_3) greater than a given value.

We have determined the energy of the electron-photon component of the YAS from the summary ionization in the third row of chambers.

Figure 4 shows the integral distribution of YAS relative to the value of J_3 (or $E_{e\text{-}ph}$, the energy of the electron-photon component of the YAS). This distribution can be approximated by a power law of the type $N(\geq J_3) = AJ_3^{-\gamma}$, where $\gamma = 1.5 \pm 0.4$.

As can be seen from Fig. 4, several YAS with energy $E_{e\text{-}ph} \geq 10^{13}$ ev were recorded during the time of operation. Were the young electron-photon showers of such high energy to move further through the atmosphere (had they been observed not at sea level, but some 3000 — 4000 m above sea level), they would develop into a cascade with ~ 10^4 particles at the maximum, i.e., they would develop into an ordinary extensive air shower.

Thus, "young" air showers are the forerunners of extensive air showers with at least $N \sim 10^4$ particles.

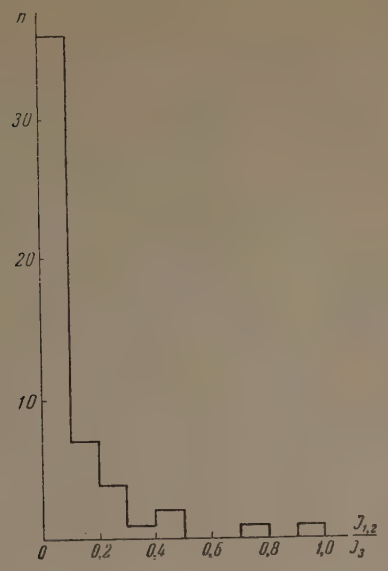

FIG. 5. Distribution of value of $J_{1,2}/J_3$ in "young" showers. Abscissas–$J_{1,2}/J_3$, ordinates–number of YAS with given value of $J_{1,2}/J_3$.

b) Nuclear-active particles in "young" air showers. The role of nuclear-active particles in the development of extensive air showers deep in the atmosphere is difficult to assay, for a number of reasons. First, the point where the EAS is registered is separated from the point where the shower is produced by a considerable layer of atmosphere, in which the nuclear-active particles can, in principle, expend the greater part of their energy on the formation of the electron-photon component of the EAS. The low energy of the EAS nuclear-active component, found at the observation level of a large fraction of the showers (see Fig. 2) cannot serve as a decisive argument against attributing a decisive role to the nuclear-active particles in the development of the EAS. Second, the appreciable development of the nuclear cascade within the layer of the atmosphere causes only a part of the nuclear-active particles contained in a given air shower to fall on an array of limited area. The natural fluctuations in the number and energy of the nuclear-active particles in a shower of given number of particles will become aggravated by fluctuations due to the small dimensions of the array used to register the nuclear-active particles. The most direct answer to this question could therefore be obtained by studying the nuclear-active particles in the acts of generation of extensive air showers.

Inasmuch as "young" air showers are cases wherein the electron-photon component is generated directly above the array (calculations show that at sea level the effective layer within which YAS with $E_{e\text{-}ph} \approx 10^{12}$ ev are produced is three cascade units thick), the majority of the secondary nuclear-active particles generated in the same act in which the electron-photon component of the YAS was generated should strike an array of the size we used. Since YAS involve cases wherein the energy transferred to the electron-photon component is large enough for an extensive air shower to develop upon passage of this component through the atmosphere, a study of the nuclear-active component in YAS can help answer the question raised above.

We therefore examined, in 52 incidences of YAS with $E_{e\text{-}ph} \geq 2 \times 10^{12}$ ev, the ratio $J_{1,2}/J_3 = E_{\pi^0}/E_{YAS}$, which characterizes the energy transferred by the neutral pions to the nuclear-active particles of the YAS in 60 g/cm^2 of graphite, referred to the energy of the electron-photon component of the YAS. The distribution of $J_{1,2}/J_3$ is shown in Fig. 5.

This distribution calls for two clarifications. First, the interval $0 \leq J_{1,2}/J_{3,4} \leq 0.1$ contains 24 cases when $J_{1,2} = 0$. Second, a structural burst was observed in an overwhelming number of cases when $J_{1,2} \neq 0$ ($\sim 70\%$), demonstrating the presence of several nuclear-active particles in the YAS. We can therefore state that the cases $J_{1,2} = 0$ signify a practically total lack of nuclear-active component in a "young" air shower.

The mean value $\overline{(J_{1,2}/J_{3,4})}$ in all 52 YAS was 0.11 ± 0.03, i.e., its value is practically the same in YAS as in EAS with $J_3 \geq 1.2 \times 10^4$. It is curious that the distribution of the ratios $J_{1,2}/J_3$ is practically the same in YAS as in EAS.

3. DISCUSSION OF RESULTS

The question of the fraction of the energy of nuclear-active particles in EAS is of great interest because of the role that nuclear-active particles play in the development of EAS deep in the atmosphere. The energy of the nuclear-active particles contained in an EAS is usually (see, e.g.,[5]) estimated by measuring the energy transferred to the neutral pions in a thick layer of light matter, and the mean summary energy $\bar{E}_{n\text{-}a}$ of the nuclear-active particles in the EAS is determined by assigning an arbitrary mean inelasticity coefficient $\bar{K} \sim 0.3$ to these nuclear-active particles. Whereas an inelasticity coefficient $\bar{K} \sim 3$ can be justified in the case of nucleons, (a low inelasticity coefficient was in fact obtained[6] for nucleons in the energy region $\sim 10^{10}$ ev), this is not the case for the nuclear-active particles of an EAS. In fact, if it assumed that the electron-photon component of the shower deep in the atmosphere (in particular, at sea

level) is in equilibrium with the nuclear component and if it is assumed that the nucleons and mesons have different mean inelasticity coefficients, $\bar{K}_n$ and $\bar{K}_\pi$ respectively, then the change in the summary energy flux due to the nucleon and pion components in the shower can be described by the following equations (neglecting the decay of the $\pi^\pm$ mesons):

$$dE_n/dX = -\bar{K}_n E_n(X)/L; \quad (1)$$

$$dE_\pi/dX = -\bar{K}_\pi E_\pi(X)/3L + 2\bar{K}_n E_n(X)\,3L, \quad (2)$$

where $E_n(X)$ and $E_\pi(X)$ is the summary energy of the nucleon and meson components at a depth X g/cm^2 from the top of the atmosphere.

From these equations it follows that:

a) If $\bar{K}_n = 1/3$ and $\bar{K}_\pi = 1$, then for a depth 1000 g/cm^2 and an interaction range L = 70 g/cm^2 the nucleon energy flux will amount to 25 percent of the total energy flux of all the nuclear-active particles. The contribution to the electron-photon component of an EAS in a thin layer of the atmosphere, made by the nucleon component, will be one-ninth the contribution of the $\pi^\pm$ mesons, i.e., the effective value of $\bar{K}$ will be close to 1.

b) If $\bar{K}_n = \bar{K}_\pi = 1/3$, then the nucleon energy flux at a depth 1000 g/cm^2 will in this case be merely 5 percent of the total energy flux of the nuclear-active shower component. This case, however, is apparently impossible, for it corresponds to too small an absorption coefficient for the nuclear-active component, $\mu_{n\text{-}a} = (630\ \text{g/cm}^2)^{-1}$. This absorption coefficient does not correspond to the mean absorption coefficient of the particles in the shower, $\mu_N = (200\ \text{g/cm}^2)^{-1}$. Consequently, an effective value $\bar{K} \approx 0.3$ can hardly be assumed for the nuclear-active particles with any justification.

It seems to us that a more logical way to determine the energy of the nuclear-active particles in the EAS will be one in which the inelasticity coefficient K is not stipulated a priori.

From our data we can estimate the mean fraction of the energy of the nuclear-active component of an EAS in the following fashion:

We know that the mean fraction of particles absorbed in a shower (averaged over different showers with a given number of particles) has a value $\mu_N = (200\ \text{g/cm}^2)^{-1}$ and is practically independent of the "power" of the shower N.

If the independence of μ_N of the depth of the level of observation of the EAS in the atmosphere is attributed to the role of the nuclear-active component, then the absorption of the energy flux of this component will be determined by the range $\Lambda = 1/\mu_N = 200\ \text{g/cm}^2$.

The fact that μ_N is independent of the number of particles N over a wide range of values of N indicates that the $\pi^\pm$-meson decay plays an insignificant role in the dissipation of the energy of the nuclear-active component of the EAS in the atmosphere. Consequently, the value of Λ is determined by the singularities of the nuclear-interaction processes, and primarily by the transfer of energy to the neutral pions. Neglecting the decay of the $\pi^\pm$ mesons, we can easily relate the energy $E_{\pi^0 C}(X)$, transferred to the neutral pions in a layer of graphite X g/cm^2 thick, to the energy flux $E^0_{n\text{-}a}$ of the nuclear-active component of the EAS.

We denote by $E_C(X)$ and $E_a(X)$ the energy fluxes of the nuclear active components under a layer of graphite and air of thickness X, respectively. Then

$$E_{\pi^0 C}(X) = E^0_{n\text{-}a} - E_C(X) = E^0_{n\text{-}a} - E_a(X)$$
$$= E^0_{n\text{-}a} - E^0_{n\text{-}a}\, e^{-X/\Lambda} = E^0_{n\text{-}a}\left(1 - e^{-X/\Lambda}\right); \quad (3)$$

on the other hand, we can readily ascertain that under the same assumptions

$$E_{\pi^0 C}(X) = \frac{\bar{\alpha}_{\pi^0}}{L}\int_0^X E_C(X)\,dX = \frac{\bar{\alpha}_{\pi^0}}{L}\int_0^X E_a(X)\,dX$$
$$= \frac{\bar{\alpha}_{\pi^0}\Lambda}{L}\left(1 - e^{-X/\Lambda}\right). \quad (4)$$

Here $\overline{\alpha_{\pi^0}}$ is the mean fraction of energy transferred to the neutral pions by the nuclear-active particles of the EAS in one interaction. Comparing (3) and (4), we can readily note that $\overline{\alpha_{\pi^0}} = L/\Lambda$.

If we take for L and Λ the customary values L = 70 g/cm^2 and Λ = 200 g/cm^2, we obtain $\overline{\alpha_{\pi^0}} \approx 1/3$, i.e., the effective inelasticity coefficient for nuclear-active particles of an EAS is $\bar{K} = 3\overline{\alpha_{\pi^0}} \approx 1$.

The ratio of the energy transferred to the neutral pions in a given layer of graphite to the energy of the electron-photon component of the EAS, $E_{e\text{-}ph}$, is

$$E_{\pi^0 C}(X)/E_{e\text{-}ph} = (E^0_{n\text{-}a}/E_{e\text{-}ph})\,(1 - e^{-X/\Lambda}). \quad (5)$$

According to our data, we have for 60 g/cm^2 of graphite

$$\overline{E_{\pi^0 C}\,(60\ \text{g/cm}^2)/E_{e\text{-}ph}} = 0.10 \pm 0.036$$

and if Λ = 200 g/cm^2, then $E_{n\text{-}a}/E_{e\text{-}ph} = 0.40 \pm 0.14$.

On the other hand if we assume, with account of the remarks made earlier, that

$$\overline{[E_{\pi^0 C}\,(60\ \text{g/cm}^2)/E_{e\text{-}ph}]} = 0.138 \pm 0.024,$$

then

$$\overline{E_{n\text{-}a}/E_{e\text{-}ph}} = 0.53 \pm 0.09.$$

The foregoing estimate of the ratio of the energy of the nuclear-active particles to the energy of the electron-photon component of the shower yields a value some 2 — 2.5 times smaller than previously obtained by some workers,[5] who assumed an inelasticity coefficient ~ 0.3 for the nuclear active particles in the EAS.

This discrepancy signifies that the true inelasticity coefficient of the nuclear-active particles in an EAS is not 0.3, but at least 2.5 or 2 times greater, i.e., $\bar{K} \cong 0.75 - 0.6$.

[1] Dobrotin, Zatsepin, Rozental', Sarycheva, Khristiansen, and Éĭdus, Usp. Fiz. Nauk **49**, 185 (1953); O. I. Dovzhenko and S. I. Nikol'skii, DAN SSSR **102**, 241 (1955); V. V. Guzhavin and G. T. Zatsepin, JETP **32**, 365 (1957), Soviet Phys. JETP **5**, 312 (1957).

[2] N. L. Grigorov and V. Ya. Shestoperov, JETP **34**, 1539 (1958), Soviet Phys. JETP **7**, 1061 (1958).

[3] N. L. Grigorov and V. Ya. Shestoperov, JETP **37**, 1147 (1959), Soviet Phys. JETP **10**, 816 (1960).

[4] Babecki, Buja, Grigorov, Loskiewicz, Massalskii, Oles, and Shestoperov, JETP **40**, 1551 (1961), Soviet Phys. JETP **13**, 1089 (1961).

[5] Abrosimov, Dmitriev, Kulikov, Massalskii, Solov'ev, and Khristiansen, JETP **36**, 751 (1959), Soviet Phys. JETP **9**, 528 (1959).

[6] N. L. Grigorov, Usp. Fiz. Nauk **58**, 599 (1956).

Translated by J. G. Adashko
3

MEAN ENERGY OF THE Y^{90} *BETA SPECTRUM*

E. I. BIRYUKOV, B. S. KUZNETSOV, and N. S. SHIMANSKAYA

Radium Institute, Academy of Sciences, U.S.S.R.

Submitted to JETP editor December 26, 1960

J. Exptl. Theoret. Phys. (U.S.S.R.) **41**, 22-23 (July, 1961)

The mean energy of the Y^{90} beta-ray spectrum was measured calorimetrically and the value 933 ± 18 kev obtained.

VARIOUS methods may be employed for an experimental determination of the average energy of the beta spectrum, $\bar{E}_\beta$. The calorimetric method, however, is at the present time the simplest and the most accurate. We measured calorimetrically the mean energy of the beta spectrum of Y^{90}, which is one of the isotopes most frequently used in radiometry and biology. The procedure was similar to that employed previously.[1]

The Y^{90} source was obtained by irradiating in a reactor 1 — 1.5 g of yttrium oxide. The initial activity was usually on the order of 300 — 500 mC. The heating effect was measured using a double static calorimeter with a sensitivity of $\sim 2.5 \times 10^{-5}$ watt/mm. Measurements were made with four different Y^{90} sources. For each of these, calorimetric measurements lasted from three to seven days. The individual experimental points fell properly on straight lines which correspond to a decay with a 64.9 hour period. This is consistent with recent data on the half-life of Y^{90} (64.8 ± 0.2 hours)[2] and is evidence of the purity of the sources; this was also controlled by measurements on a scintillation gamma spectrometer. Corrections were introduced into the calorimetric measurement results for the energy of internal bremsstrahlung of the Y^{90} absorbed in the calorimeter, and for the thermal inertia of the latter.[3]

After the calorimetric measurements, all of the active yttrium was dissolved in weak nitric acid and the absolute activity of a known aliquot of the solution was measured by a 4π counter.

The mean energy of the Y^{90} beta-ray spectrum obtained when the results for all four sources were averaged was 933 ± 18 kev. The noticeable discrepancy between this value and the quantity $\bar{E}_\beta(Y^{90}) = 895 \pm 35$ kev obtained by Caswell[4] using an extrapolation chamber may, it seems, be explained by the reduced value of ionization energy ϵ ($\epsilon = 32.5$ ev) adopted by that author. If we recompute Caswell's results using the value of ϵ currently applied ($\epsilon = 34.0$ ev),[5] we obtain the value 936 ± 35 kev, which agrees well with our measurements. Values of $\bar{E}_\beta$ which we calculated on the basis of the shape of Y^{90} beta spectra measured on the magnetic spectrograph by Yuasa[6] and Braden[7] equal, respectively, 900 and 925 kev with an error of about 5%.

The mean energy of the Y^{90} beta spectrum can also be compared with theoretical values of $\bar{E}_\beta$ for the unique, first-forbidden beta-transition ($n = 1$, $\Delta J = 2$, the wave function changes sign) with an energy of 2275 kev. Our experimental value is closest to the value of $\bar{E}_\beta$ computed using the form factors $S = (W_0 - W)^2 L_0 + 9L_1$[8] ($\bar{E}_\beta = 928.8$ kev) and $S = (W^2 - 1) + \lambda(p) \times (W_0 - W)^2$[9] ($\bar{E}_\beta = 929.2$ kev). The form factor $S = (W^2 - 1) + (W_0 - W)^2$,[10] which does not take into account the influence of the Coulomb field of the nucleus on the emitted electron, yields a somewhat higher value: $\bar{E}_\beta = 942.6$ kev.

The authors thank Yu. S. Martynov for his participation in the measurements.

[1] N. S. Shimanskaya, JETP **31**, 393 (1956), Soviet Phys. JETP **4**, 355 (1957).

[2] G. Herrmann and F. Strassmann, Z. Naturforsch. **11a**, 946 (1956).

[3] N. S. Shimanskaya, Trudy, Radium Inst. **9**, 126 (1959).

[4] R. Caswell, Phys. Rev. **86**, 82 (1952).

[5] J. Boag, Paper at the Symposium on the Methodology of Measurements of Ionizing Radiations, Rome, 1958.

[6] Yuasa, Laberrigue-Frolow, and Feuvrais, Comp. rend. **242**, 2129 (1956).

[7] Braden, Slack, and Shull, Phys. Rev. **75**, 1964 (1949).

[8] K. Siegbahn, Beta- and Gamma-Ray Spectroscopy, Amsterdam, 1955, Russ. Transl. Fizmatgiz 1959, p. 283.

[9] Laslett, Jensen, and Paskin, Phys. Rev. 79, 412 (1950).

[10] E. J. Konopinski and G. E. Uhlenbeck, Phys. Rev. 60, 308 (1941).

Translated by Mrs. Jack D. Ullman
4

ANGULAR DISTRIBUTION OF 14-Mev NEUTRONS INELASTICALLY SCATTERED ON CARBON, NITROGEN AND SULFUR

V. V. BOBYR', L. Ya. GRONA, and V. I. STRIZHAK

Physics Institute, Academy of Sciences, Ukrainian S.S.R.

Submitted to JETP editor January 9, 1961

J. Exptl. Theoret. Phys. (U.S.S.R.) **41**, 24-25 (July, 1961)

The angular distributions of neutrons inelastically scattered on C, N and S nuclei with excitation of the first excited states of these nuclei are measured. The results are in agreement with calculations according to the direct interaction model.

EXPERIMENTS on angular distributions for inelastically scattered nucleons are of considerable interest in that they clarify the mechanism of reactions. Thus, the first qualitative studies of the angular distributions of inelastically scattered 14-Mev neutrons [1] were not consistent with the compound nucleus theory. The direct interaction model was in considerably better agreement with these experiments.

Experiments involving inelastic scattering for individual nuclear excited states are especially interesting, since the results can be directly compared with various theories.

In the present work a measurement was made of the angular distribution of inelastically scattered 14-Mev neutrons with excitation of the first excited states of the C^{12}, N^{14}, and S^{32} nuclei.

The neutron source was the reaction $T(d,n)He^4$, which was produced in the low-voltage accelerator of the Physics Institute of the Ukrainian S.S.R. Academy of Sciences. The measurements were made in an annular geometry. The scatterers were in the form of toruses of diameter 200 and 330 mm and cross-section diameter of 30 mm. For the measurements on nitrogen, a thin-walled copper container was employed whose double walls permitted the use of liquid nitrogen as the scatterer. A scintillation spectrometer consisting of a photomultiplier (FÉU-14-A), a stilbene crystal, and a 100-channel pulse-height analyzer (AI-100-1) was used to detect the neutrons. The spectrometer had an energy resolution of 3%. A scintillation counter was also used for monitoring.

In the experiment the spectra of scattered neutrons, of the background, and of the incident neutrons were measured for each angle.

The ratio between the intensity of inelastically scattered neutrons for the first excited level to the intensity of the incident neutron beam was determined by analyzing the quantity

$$S_m = \left(\sum_{i=m}^{M} N_{\mathrm{s}i} - N_{\mathrm{b}i}\right) \Big/ \sum_{i=m}^{M} N_{\mathrm{inc}\,i},$$

where N_{si}, N_{bi} and $N_{inc\,i}$ are, respectively, the number of counts in the j-th channel when measuring scattered neutrons, background neutrons, and the incident beam; M is the number of channels registering the spectrum. Corrections were introduced into S for the energy and angular sensitivity of the detector and for attenuation of the neutron beam in the scatterer. The adjusted spectrum of S values allows us to determine the interaction cross section for groups of inelastically scattered neutrons separated by 1 Mev energy intervals. The energy of the levels is in good agreement with the results of other authors. [2]

The graphs represent the results of measuring the inelastic scattering cross section in which the first excited levels of C^{12}, N^{14}, and S^{32} nuclei have

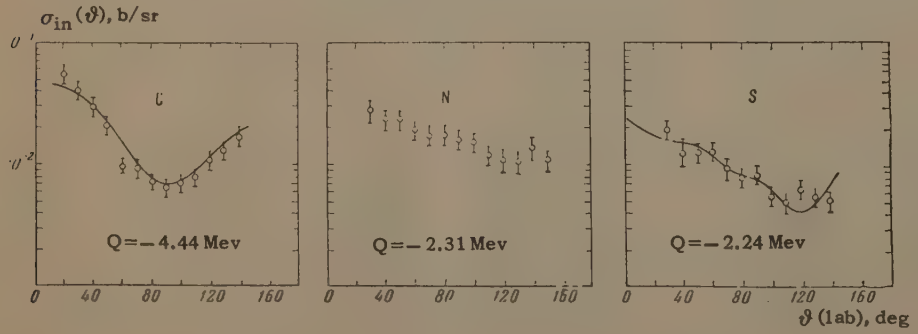

Angular distribution of inelastically scattered neutrons with excitation of the first excited state of the C^{12}, N^{14}, and S^{32} nuclei respectively. The solid curve represents a calculation from direct interaction theory.

been excited. The results for carbon agree well with those of Anderson et al.[3] The measurements on nitrogen and sulfur are performed for the first time.

The angular distributions measured for carbon and sulfur were compared with calculations performed on the basis of direct interaction theory by Glendenning.[4] In the case of sulfur, the comparison was made with calculations for a nucleus with atomic weight of ~30 and the same first excited state characteristics as sulfur.

The large cross section for forward scattering and the good agreement with theoretical curves computed on the basis of the direct-interaction hypothesis allow us to conclude that the excitation of the first levels of these nuclei by 14-Mev neutrons is due to a direct interaction process.

[1] L. Rosen and L. Stewart, Phys. Rev. 99, 1052 (1955).

[2] B. S. Dzhelepov and L. K. Peker, Skhemy raspada radioaktivnykh yader (Decay Schemes of Radioactive Nuclei), AN UkrSSR, 1958.

[3] Anderson, Gardner, McClure, Nakada, and Wong, Phys. Rev. 111, 572 (1958).

[4] N. K. Glendenning, Phys. Rev. 114, 1297 (1959).

Translated by Mrs. Jack D. Ullman
5

ELECTRON LOSS AND CAPTURE BY 200 — 1500 kev HELIUM IONS IN VARIOUS GASES

L. I. PIVOVAR, V. M. TUBAEV, and M. T. NOVIKOV

Khar'kov Physico-Technical Institute, Academy of Sciences, Ukrainian S.S.R.

Submitted to JETP editor February 7, 1961

J. Exptl. Theoret. Phys. (U.S.S.R.) **41**, 26-31 (July, 1961)

The cross sections for electron loss σ_{12} and electron capture σ_{10} by singly charged helium ions in single collisions in gases have been measured. The relative amounts of He^0, He^+, and He^{2+} ions in beams of equilibrium composition traversing the gases have also been measured. The cross section for electron capture by doubly charged helium ions σ_{21} and the cross section for electron loss by helium atoms σ_{01} are estimated from the ratios of these components. The gas targets consisted of helium, nitrogen, argon, and krypton. The measurements were performed for ion energies between 200 and 1500 kev.

1. INTRODUCTION

A number of studies have been devoted to charge-exchange processes involving helium atoms and ions in collisions with gas molecules. A summary of the basic experimental results is given in the review article of Allison.[1] This review article gives the results of experimental investigations on the loss and capture of electrons by helium ions and atoms in collisions with molecules of H_2, N_2, O_2, He, Ne, Ar, Kr, and Xe in the 0.2 — 200 kev interval and with molecules of H_2, He, and air up to an energy of 450 kev. The article also gives separate data for the charge exchange of α particles in air obtained at high energies by Rutherford.

Extension of the investigations in the direction of higher energies is of interest from the viewpoint of further development of the theory of atomic collisions.

In the present article, we describe the results of measurements of the effective cross section for the loss and capture of an electron by helium ions and also the results of measurements of collisions between helium particle beams of equilibrium composition and H_2 and N_2 molecules and He, Ar, and Kr atoms in the 200 — 1500 kev interval.

2. APPARATUS AND EXPERIMENTAL METHOD

In this experiment, we used the arrangement employed by us earlier[2] for the measurement of the cross sections for the dissociation of molecular ions of hydrogen. The method of measurement was basically the same.

The primary beam of single charged helium ions produced by an electrostatic accelerator was separated by a mass monochromator and passed through the collision chamber. The He^+ and He^{2+} components which were formed were separated by an electrostatic analyzer and entered Faraday cups. The currents were measured by ÉMU-3 vacuum-tube electrometers. The intensity of the beam of neutral He^0 particles was recorded with a detector which measured the secondary electron emission current arising from the bombardment of copper foil by the fast helium atoms.

The basic design of this detector is the same as that described by Stier, Barnett, and Evans.[3] The detector was calibrated with an auxiliary detector consisting of a thin copper foil and a copper-constantan thermocouple mounted at the center of the foil (on the rear side). This foil too was bombarded by the He^0 beam. Since the difference in temperature at the ends of the thermocouple did not exceed 0.1° C during the measurements, the thermal emf was proportional to the intensity of the beam of particles bombarding the foil. The size of the secondary electron emission current was measured with an ÉMU-3 vacuum-tube electrometer.

The beam component currents were measured simultaneously, which made it possible to decrease the error caused by oscillations in the primary ion beam intensity. The measurements of the cross sections for electron capture σ_{10} and electron loss σ_{12} by singly charged helium ions were made by the mass-spectrographic method.

The cross sections were calculated from the formulas

$$\sigma_{10} = \left\{ d\left[\frac{N^0}{N^0 + N^+ + N^{2+}} - \left(\frac{N^0}{N^+}\right)_b \right] / d(nL) \right\}_{nL \to 0}, \quad (1)$$

$$\sigma_{12} = \left\{ d\left[\frac{N^{2+}}{N^0 + N^+ + N^{2+}} - \left(\frac{N^{2+}}{N^+}\right)_b \right] / d(nL) \right\}_{nL \to 0}, \quad (2)$$

where N^0, N^+, and N^{2+} are the amounts of neutral atoms, singly charged ions, and doubly charged ions of helium in the beam traversing the collision chamber; n is the concentration of the gas atoms in the chamber; L is the effective length of the chamber; the subscript b indicates background. For each case, we plotted the ratio of the number of secondary particles to the number of primary particles as a function of nL. We determined the cross sections σ_{10} and σ_{12} from the linear part of these curves.

In all cases, we checked the influence of the difference in the scattering of secondary and primary beam particles by means of diaphragms at the exit channel of the collision chamber. Under the geometrical conditions of our experiment (beam diameter 2 mm and channel diameter 6.5 mm), the scattering had no influence on the size of the measured cross sections, within the limits of experimental error. The cross sections σ_{10} and σ_{12} were calculated as the mean of two or three independent measurements. The random errors of measurement did not exceed ±12% for the cross sections σ_{12} and ±18% for the cross sections σ_{10}. The primary ion beam energy was determined to an accuracy of ±2%.

For the measurements of the equilibrium components of the beam, entrance and exit channels, each of diameter 2.5 mm and length 80 mm, were mounted in the collision chamber, which had an over-all length of 400 mm. The beam entered the collision chamber through a diaphragm 1.6 mm in diameter mounted in front of the entrance channel. The large diffusion resistances of the channels made it possible to use target thicknesses of about $(3-5) \times 10^{17}$ molecules per cm^2. At each value of the primary ion beam energy, a check was made to establish whether the charge distribution of the beam had attained a stationary value. To do this, we investigated the dependence of the size of the He^0, He^+, and He^{2+} components of the beam on the gas pressure in the collision chamber close to the equilibrium composition.

In the ion energy region studied by us, we could neglect the influence of the process of formation of negative helium ions[4] and assume that the above-mentioned three components were present in the 200 to 500—700 kev energy interval and that effectively only two components, He^+ and He^{2+}, were present in the 500—700 to 1500 kev interval, since at 500—700 kev the He^0 is already present in the beam in quantities no greater than 6% of the total number of particles, and its content drops very quickly with an increase in energy. If we also neglect the influence of the two-electron loss and capture processes, then we can estimate the electron capture cross section σ_{21} and electron loss cross section σ_{01} from the following relations:[1]

$$\sigma_{21} = \sigma_{12} F_{1\infty}/F_{2\infty}, \qquad \sigma_{01} = \sigma_{10} F_{1\infty}/F_{0\infty}, \quad (3)$$

where σ_{12} and σ_{10} are the cross sections for electron loss and capture by singly charged helium ions; $F_{0\infty}$, $F_{1\infty}$, and $F_{2\infty}$ are the relative contents of the He^0, He^+, and He^{2+} components in a beam of equilibrium composition.

In order to check whether differences in the scattering of the beam components affect their size, we changed the collision chamber channels. It turned out that, when the 6.5-mm diam channels were replaced by 2.5-mm diam channels, the ratios of the beam components remained unchanged within the limits of experimental error. The random errors in the measurement of the equilibrium composition were about ±5% for the $F_{1\infty}$ and $F_{2\infty}$ components and ±11% for the $F_{0\infty}$ component.

3. RESULTS OF MEASUREMENTS AND DISCUSSION

In this experiment, we measured the cross sections for electron capture and loss by singly charged helium ions in collisions with H_2, N_2 molecules and He, Ar, and Kr atoms. We used the following gases as targets: hydrogen admitted through a palladium filter, helium with impurities not exceeding 0.1%, nitrogen with 0.03% impurities, and argon and krypton with 0.1% impurities.

The results of the measurements of equilibrium compositions in the helium beam are shown in the table. The equilibrium components of the helium beam in some gases have been measured and calculated by other authors in the 8- to 450-kev interval. The data of the present experiment are in satisfactory agreement with the data calculated by Allison[1] for hydrogen, helium, and air and with the measurements of Snitzer[5] in argon. At 200 kev, our data fit together with the data of Barnett and Stier[6] for hydrogen, helium, nitrogen, and argon.

Owing to the small cross sections for electron capture by He^+ and He^{2+} ions, the neutral component of the beam $F_{0\infty}$ did not attain equilibrium for the target thicknesses used at energies above 800—1000 kev (above 600 kev in the case of hydrogen and above 900 kev for the $F_{1\infty}$ component).

Energy, kev	$F_{0\infty}$	$F_{1\infty}$	$F_{2\infty}$	$F_{0\infty}$	$F_{1\infty}$	$F_{2\infty}$	$F_{0\infty}$	$F_{1\infty}$	$F_{2\infty}$
	Hydrogen			Helium			Nitrogen		
200	0.43	0.556	0.014	0.495	0.485	0.02	0.335	0.628	0.037
300	0.24	0.696	0.064	0.307	0.637	0.056	0.23	0.66	0.11
400	0.128	0.712	0.16	0.204	0.666	0.13	0.13	0.685	0.185
500	0.07	0.67	0.26	0.125	0.67	0.205	0.086	0.63	0.284
600	0.045	0.57	0.385	0.08	0.63	0.29	0.05	0.55	0.4
700	(0.02)	0.43	0.55	0.06	0.58	0.36	0.03	0.47	0.5
800	(0.010)	0.35	0.64	0.045	0.525	0.43	0.02	0.41	0.57
900	(0.006)	0.264	0.73	(0.03)	0.47	0.5	0.012	0.35	0.64
1000	(0.004)	(0.22)	0.776	(0.02)	0.42	0.56	0.008	0.3	0.700
1100	(0.0025)	(0.17)	0.828	(0.013)	0.37	0.617	(0.006)	0.224	0.77
1200	(0.0015)	(0.125)	0.874	(0.01)	0.31	0.68	(0.0037)	0.19	0.806
1300	(0.0012)	(0.105)	0.894	(0.007)	0.26	0.733	(0.003)	0.165	0.832
1400	(0.001)	(0.09)	0.909	(0.005)	0.215	0.78	(0.002)	0.145	0.853
1500	—	(0.07)	0.93	(0.0035)	0.187	0.81	—	0.123	0.877
	Argon			Krypton					
200	0.36	0.615	0.025	0.5	0.49	0.01			
300	0.19	0.72	0.09	0.258	0.697	0.045			
400	0.102	0.7	0.198	0.170	0.725	0.105			
500	0.056	0.604	0.34	0.09	0.68	0.23			
600	0.03	0.48	0.49	0.05	0.55	0.4			
700	0.017	0.383	0.6	0.025	0.46	0.515			
800	0.009	0.281	0.71	0.015	0.35	0.635			
900	0.006	0.224	0.77	0.01	0.266	0.724			
1000	0.003	0.178	0.819	(0.006)	0.214	0.78			
1100	(0.0023)	0.146	0.852	(0.0045)	0.18	0.815			
1200	(0.002)	0.119	0.879	(0.003)	0.162	0.835			
1300	(0.0015)	0.099	0.9	(0.002)	0.15	0.848			
1400	(0.0012)	0.084	0.915	(0.0016)	0.135	0.863			
1500	(0.001)	0.073	0.926	(0.0014)	0.122	0.877			

The corresponding values of $F_{0\infty}$ and $F_{1\infty}$ are therefore shown in parentheses in the table.

The results of the measurements of the cross sections for electron loss σ_{12} and electron capture σ_{10} as a function of the He^+ ion energy are shown in Figs. 1 — 5. Also shown in these figures are the values of the cross sections for electron capture and loss σ_{21} and σ_{01} calculated from formula (3). Wherever possible, we give for comparison the data of Allison et al,[1] who measured the corresponding cross sections in the 100 — 450-kev interval in hydrogen, helium, and air. Our values are in satisfactory agreement with their data.

As seen from the figures, the cross sections for electron loss σ_{12} and σ_{01} for all the gases studied by us increase with energy, attain a broad maximum, and then slowly decrease with a further increase in the energy of the He^+ ions. The cross sections for electron capture σ_{10} and σ_{21} rapidly decrease monotonically with an increase in energy over the entire investigated interval. The values of the cross sections depend on the kind of target gas and increase with the atomic number of the target substance.

Also shown in Fig. 1 are the values of the cross sections for electron capture by doubly charged helium ions in hydrogen as calculated by Schiff.[7]

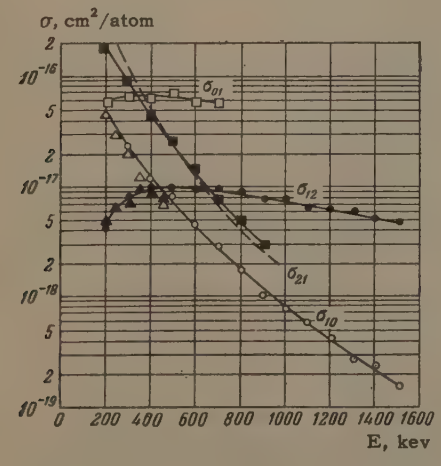

FIG. 1. Cross section for electron loss and capture by helium ions in hydrogen. △ – values of σ_{i0} from reference 1, ▲ – values of σ_{i2} from reference 1; dotted curve – according to data of reference 7.

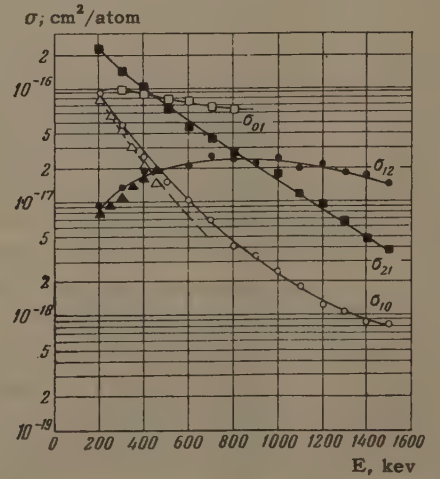

FIG. 2. Cross section for electron loss and capture by helium ions in helium △ – values of σ_{i0} from reference 1, ▲ – values of σ_{i2} from reference 1; dotted curve – according to data of reference 7.

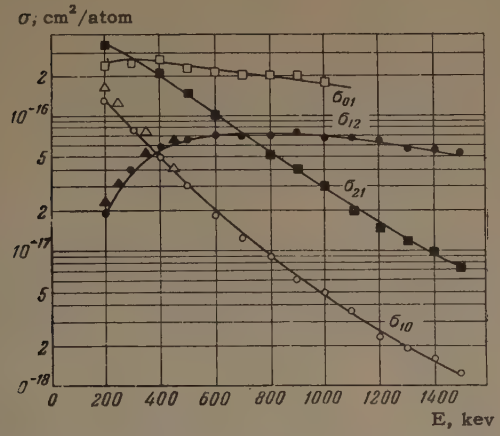

FIG. 3. Cross section for electron loss and capture by helium ions in nitrogen. △ – data from reference 1 for σ_{10} in air, ▲ – data from reference 1 for σ_{12} in air.

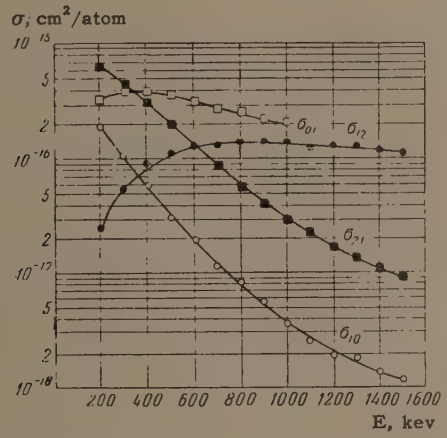

FIG. 4. Cross section for electron loss and capture by helium ions in argon.

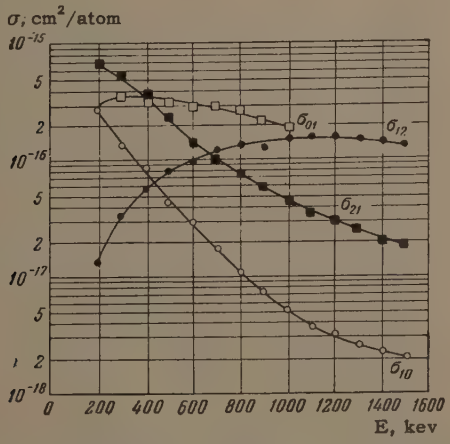

FIG. 5. Cross section for electron loss and capture by helium ions in krypton.

The theoretical and experimental curves in the 400 — 900 kev interval are in good agreement. It should be kept in mind, however, that such close agreement can be more or less accidental, if only because the experimental values of σ_{21} are given with a large error — this includes both the error of measurement of σ_{12} and the error of measurement of the equilibrium components $F_{1\infty}$ and $F_{2\infty}$.

Schiff[7] also calculated the cross sections for electron capture σ_{10} by He^+ ions in helium by means of the Born approximation. The corresponding values of σ_{10} are shown in Fig. 2 by the dotted curve. The theoretical curve systematically lies 20 — 40% below the experimental curve; the difference between them increases with energy. We note that this position of the theoretical curve with respect to the experimental curve of Fig. 2 was predicted by Schiff for ion velocities $v > v_0$ ($v_0 = q^2/\hbar$), which occurs in this case.

Since we measured the cross sections for ion velocities up to $v \approx 4v_0$, it is of interest to compare the data obtained in the velocity interval between $v \sim 3v_0$ and $v \sim 4v_0$ with the qualitative results obtained by Bohr for σ_{12} and σ_{21} in the case of light ions at velocities $v \gg v_0$.[8]

Assuming that the nucleus and the electron of the target atom act independently on the ion, Bohr obtained the following expression for light atoms:

$$\sigma_{12} \sim (v_0/v)^2. \qquad (4)$$

For substances of larger atomic number ($Z_1 \leq Z_2^{1/3}$), where the electrons and nucleus of the target atom do not act independently,

$$\sigma_{12} \sim v_0/v. \qquad (5)$$

For electron capture by an α particle in the case of atoms that are not very light, Bohr obtained the expression

$$\sigma_{21} \sim (v_0/v)^6. \qquad (6)$$

The experimental results do not strictly follow these functions of the ion velocity, but for H_2 and He the decrease in the cross sections for electron loss σ_{12} takes place more rapidly than for N_2, Ar, and Kr, which is in qualitative agreement with Bohr's conclusions.

The dependence of σ_{21} on the ion velocity obtained in this experiment for N_2, Ar, and Kr differs from expression (6) in the value of the exponent. The corresponding expressions can be written as follows: for nitrogen, $\sigma_{21} \sim (v_0/v)^{6.9}$; for argon, $\sigma_{21} \sim (v_0/v)^{6.7}$; and for krypton, $\sigma_{21} \sim (v_0/v)^{4.7}$. We note that Barnett and Reynolds[9] obtained similar results for hydrogen ion energies up to 1000 kev. For nitrogen, the exponent turned out to be ~ 6.5 and for argon 3.7.

In conclusion, the authors consider it their duty to express their gratitude to Academician A. K. Val'ter for his interest in and attention to this work.

[1] S. K. Allison, Revs. Modern Phys. **30**, 1137 (1958).

[2] Pivovar, Tubaev, and Novikov, JETP **40**, 34 (1961). Soviet Phys. JETP **13**, 23 (1961).

[3] Stier, Barnett, and Evans, Phys. Rev. **96**, 973 (1954).

[4] Dukel'skii, Afrosimov, and Fedorenko, JETP **30**, 792 (1956), Soviet Phys. JETP **3**, 764 (1956).

[5] E. Snitzer, Phys. Rev. **89**, 1237 (1953).

[6] C. F. Barnett and P. M. Stier, Phys. Rev. **109**, 385 (1958).

[7] H. Schiff, Can. J. Phys. **32**, 393 (1954).

[8] N. Bohr, The Passage of Atomic Particles through Matter, Kgl. Danske Videnskab. Selskab, Mat.-fys. Medd **18**, No. 8 (1948).

[9] C. F. Barnett and H. K. Reynolds, Phys. Rev. **109**, 355 (1958).

Translated by E. Marquit
6

ELASTIC SCATTERING OF 5.45 Mev *PROTONS BY ZIRCONIUM NUCLEI*

V. Ya. GOLOVNYA, A. P. KLYUCHAREV, and B. A. SHILYAEV

Physico-Technical Institute, Academy of Sciences, Ukrainian S.S.R.

Submitted to JETP editor January 24, 1961

J. Exptl. Theoret. Phys. (U.S.S.R.) **41**, 32-34 (July, 1961)

The angular distributions of 5.45-Mev protons elastically scattered by Zr^{90} and Zr^{91} nuclei were measured by the scintillation method. It is hardly possible that the great difference in the angular distribution curves can be explained only by the different threshold of the (p, n) reaction which competes with elastic pp scattering involving capture.

A change in the form of the angular distribution curves for elastically scattered protons, as a result of a change in mass number of the scattering nucleus by one or several units, shows up appreciably for energies of the bombarding protons below the Coulomb barrier. We have previously studied the angular distribution of elastically scattered protons by targets of separated isotopes of nuclei of medium atomic weight with an initial proton energy (5.45 Mev) lower than the Coulomb barrier by 1.0 — 1.5 Mev.[1,2] In the present work we present results of an investigation of the angular distribution of 5.45-Mev protons from Zr^{90} and Zr^{91} targets, which are considerably heavier than nuclei previously studied (the values of the Coulomb barriers in Zr^{90} and Zr^{91} are equal, respectively, to 8.66 and 8.63 Mev).

A scattering chamber described by Fedchanko and Vanetsian[3] was used in this work. The scattered protons were detected by a CsI scintillation crystal and a FÉU-S type photomultiplier with amplitude resolution not worse than 5%. The geometrical conditions of the experiment made it possible to obtain an angular resolution with a precision of ±2.5%. A current integrator[4] was used as monitor. Proton angular distribution curves can be measured reliably by this method. The inelastically scattered protons are easily differentiated from those elastically scattered, since the energies of the first levels of the Zr^{90} and Zr^{91} nuclei are 1.77 and 1.21 Mev respectively[5] and the targets were fairly thin: 3.5 and 2.2 μ. These targets were produced by thermal dissociation[6] from "raw material" with enrichment of 96.1 and 79.5% respectively for the Zr^{90} and Zr^{91} targets. A molybdenum substrate was used to obtain the targets. An x-ray structure analysis carried out showed a (10 ± 1) % molybdenum impurity for both targets. The contribution from scattering by molybdenum to the general scattering picture can, therefore, be considered the same.

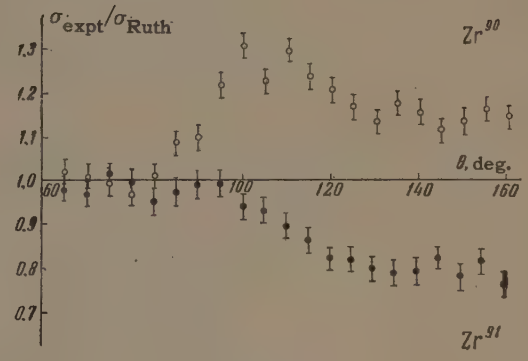

The angular dependence of the ratio of the experimentally measured cross-section to the Rutherford cross-section for the nuclei Zr^{90} and Zr^{91}.

The figure shows the results of the investigation. One notices first the effect of large nuclear elastic scattering at large angles, regardless of the considerable Coulomb barrier. The angular dependences of the scattering for nuclei differing by only one neutron differ appreciably. The form of the angular distribution curves of protons elastically scattered by Zr^{90} and Zr^{91} nuclei differ considerably from the form of the analogous curves for scattering by isotopes of nickel, cobalt and copper,[1] which have a clearly marked diffraction character. However, the qualitative dependence of the form of the curves on whether the mass number is even or odd remains.[2]

It was noted earlier[7,8] that the influence of reactions proceeding through elastic and inelastic channels, with capture of the primary proton, shows on the form of the angular distribution curves of elastically scattered protons. If the energy of the primary protons is higher than its threshold, the (p, n) reaction can have a consid-

erable effect. As a result of the strong competition of the (p,n) reaction, the emission of protons produced by pp scattering with capture, is greatly reduced. In our case the energy of the primary protons is above the threshold of the (p,n) reaction for both zirconium nuclei (the threshold is 5.22 Mev for Zr^{90} and 2.17 Mev for Zr^{91}). Consequently, the downward displacement of the curve of the ratio of the experimentally measured cross section to the Rutherford cross section for the Zr^{91} nucleus (compared with the curve for Zr^{90}), in the region of large angles, can be explained to some extent by the greater effectiveness of the (p,n) reaction for Zr^{91} at the given proton energy, because of its lower threshold. In order to elucidate this problem it is necessary to measure the neutron emission cross section for the (p,n) reaction as well as studying the angular distribution of elastically scattered protons.

The explanation of the different forms of the angular distribution curves for Zr^{90} and Zr^{91} only by the difference in the (p,n) reaction threshold, is not the unique possibility. The Zr^{90} nucleus has a completely filled neutron shell, while the Zr^{91} nucleus has one neutron in addition to the filled shell. From the point of view of the shell model, there are anomalously small level densities near the nuclear magic numbers and, as a result, a small proton capture cross section. The probability of processes which take place with the capture of protons is therefore reduced. Related to this, the contribution from (p,p) processes, with the formation of a compound nucleus, to the general elastic scattering balance may turn out not as great as for nuclei in the region Z = 24 – 30.

We have carried out preliminary studies of the angular distribution of elastically scattered protons for the Zr^{96} nucleus. As would be expected for a nucleus "overloaded" with neutrons, the form of the curve of the ratio of the experimentally measured cross section to the Rutherford cross section as a function of angle hardly differs from the form of the analogous curve for the Zr^{91} nucleus. However, the data obtained for Zr^{96} require further confirmation.

[1] Rutkevich, Golovnya, Val'ter, and Klyucharev, DAN SSSR **130**, 1008 (1960), Soviet Phys. Doklady **5**, 118 (1960).

[2] A. P. Klyucharev and N. Ya. Rutkevich, JETP **38**, 286 (1960), Soviet Phys. JETP **11**, 207 (1960).

[3] R. A. Vanetsian and E. D. Fedchenko, JETP **30**, 577 (1956), Soviet Phys. JETP **3**, 625 (1956).

[4] Golovnya, Zalyubovskii, and Shilyaev, PTÉ (Instrum. and Exptl. Techniques) No. 1, 99 (1961).

[5] B. S. Dzhelepov and L. K. Peker, Skhemy raspada radioaktivnykh yader (Decay Schemes of Radioactive Nuclei), AN SSSR 1958.

[6] Bondar', Emlyaninov, Klyucharev, Lishenko, Medyanik, Nikolaïchuk, and Shalaeva, Izv. Akad. Nauk SSSR, Ser. Fiz. **24**, 929 (1960), Columbia Tech. Transl. p. 926.

[7] A. P. Klyucharev, Proceedings of the All-Union Conference on Nuclear Reactions, Moscow, July 1960 (in press).

[8] A. P. Klyucharev, Proceedings of the International Conference on Nuclear Structure, Kingston, Canada 1960, p. 169.

Translated by R. Berman
7

CHARGE DISTRIBUTION OF FRAGMENTS IN NUCLEAR DISINTEGRATIONS

P. A. GORICHEV, O. V. LOZHKIN, and N. A. PERFILOV

Radium Institute, Academy of Sciences, U.S.S.R.

Submitted to JETP editor January 24, 1961

J. Exptl. Theoret. Phys. (U.S.S.R.) 41, 35-37 (July, 1961)

The charge distributions of fragments with $Z = 4 - 8$ produced in the disintegration of Ag and Br nuclei by 9-Bev protons, are investigated. The analysis is carried out for small and large energy transfers to the nucleus, for various directions of emission of the fragments, and for cases involving the emission of two or more fragments in a single disintegration. The fragment charge distributions are found to be practically the same in all indicated cases. A discussion of the obtained data is presented.

THE charge distribution of spallation products of Ag and Br has been investigated for different bombarding energies in a number of papers.[1-6] A comparison of the obtained results reveals the absence of any marked dependence of the charge distributions on the energy of the incoming particles. This result seems to be surprising since a number of quantities characterizing the spallation process (cross sections, multiplicities, angular distributions, and others) are known to depend on the energy of the incoming particle.

In this connection it is of interest to investigate directly the charge distribution of the fragments for a given energy of the incoming particles but for different conditions of the outgoing particles. Such conditions of interest are the magnitude of the energy transfer to the nucleus, or the direction of the outgoing particles with respect to the incoming particle, or the multiplicity of the reaction. This interest is due to the known dependence on the bombarding energy of these characteristics of the spallation process. Such an investigation was undertaken with 9-Bev protons. At this energy the spallation cross section is relatively large (100 mb), which allows one to accumulate a sufficiently large body of data to perform a statistically significant analysis.

The charge of the fragments was determined by measuring the total area of their tracks in P-9ch emulsion. This was done on a special semi-automatic optical photometric setup. The distribution of track areas was determined for each kind of disintegration (see Table I). The distributions of fragments with a charge of more than 3 were compared by means of two methods: (a) the method of statistical verification of hypotheses (calcula-

Table I. Results of the comparison of the distribution of the fragments in different disintegrations according to total track area.

Characteristics of the disintegrations		Number of analyzed fragments		Mean value of the total track area*		Value of the probability p from the comparison of two distributions***	
		Run I	Run II	Run I	Run II	Run I	Run II
Total number of light charged particles in the disintegration**	$\leqslant 12$	159	102	0.60	1.46	0.51	0.18
	>12	134	90	0.60	1.48		
Number of fragments N_f with $Z \geqslant 4$ in the disintegration	1	262	209	0.60	1.47	0.48	0.8
	$\geqslant 2$	112	187	0.60	1.45		
Emission direction of the fragments with respect to the incoming protons	$N_f = 1$ $\leqslant 90°$	150	130	0.59	1.49	—	0.6
	$N_f = 1$ $>90°$	58	56	0.60	1.49		
	$N_f \geqslant 2$ $\leqslant 90°$	112	95	0.63	1.49	—	0.4
	$N_f \geqslant 2$ $>90°$	63	51	0.61	1.46		

*The mean values of the total track area of the fragments is given in arbitrary units for track lengths $\geqslant 16\ \mu$ in Run I and $\geqslant 38\ \mu$ for Run II.

**Only for disintegrations with one fragment.

***p is the probability that the difference between two observations due to statistics is not smaller than the observed difference.

Table II. Charge distribution of the fragments in the different disintegrations.

Characteristics of the disintegrations*		Number of fragments				
		Be	B	C	N	$Z \geq 8$
$N_f = 1$	$n \leq 12$	76	24	4	2	0
	$n > 12$	68	22	9	4	0
	forward	102	34	11	4	0
	backward	42	12	2	2	0
	total	144	46	13	6	0
$N_f \geq 2$	forward	67	29	14	1	1
	backward	45	17	1	0	0
	total	112	46	15	1	1

*N_f is the number of fragments, and n is the number of the other charged particles in the disintegration.

tion of χ^2) and (b) comparison of the mean value of the track area in the distributions. Both methods showed that the distributions of track area, and thus the distributions of charge of the fragments, were practically indistinguishable for the following cases:

(1) for disintegrations which differ in the energy transfer to the recoiling nucleus from the incoming particle;

(2) for disintegrations which differ in the number of fragments;

(3) for disintegrations in which the fragments are emitted forward or backward relatively to the incoming particle.

In Table II are given the charge distributions of the fragment from the different disintegration types.

It must be mentioned that the above conclusions relate only to fragments within the range of the charge between 4 and around 8 and only to those which have an emission energy of ≥ 2 Mev per nucleon. At present one cannot say anything definite about the distribution of fragments with lower energy or with higher charge. However, it should be kept in mind that their relative contribution to the spallation process is not large, about 7%. Therefore the obtained results can be of more general importance and could be of significance for the understanding of certain aspects of the mechanism of production of higher charge fragments in the nuclear spallation process.

First, it becomes clear why the form of the charge distribution of the fragments does not change as a function of the energy of the incoming particles.

This situation could obtain if the relative probabilities of the production of fragments with different charge is independent of such factors as the temperature of the nucleus, and the angular and energy distribution of the cascade nucleons in the development of the cascade within the nucleus. The given results indicate that this apparently actually is true.

Secondly, in the given range it is unlikely that, as has been sometimes assumed, there exist several mechanisms (like, e.g., knock-on, evaporation, fission) each of which contributes a definite fraction to the total spallation cross section. To the contrary, the production of fragments evidently takes place by means of only one mechanism, independently of the energy of the incoming particle.

[1] Perfilov, Lozhkin, and Shamov, Usp. Fiz. Nauk **70**, 3 (1960), Soviet Phys. Uspekhi **3**, 1 (1960).

[2] Perfilov, Ivanov, Lozhkin, Makarov, Ostroumov, Solov'eva, and Shamov, JETP **38**, 345 (1960), Soviet Phys. JETP **11**, 250 (1960).

[3] Lozhkin, Perfilov, Rimskii-Korsakov, and Fremlin, JETP **38**, 1388 (1960), Soviet Phys. JETP **11**, 1001 (1960).

[4] Ivanova, Ostroumov, and Pavlov, JETP **37**, 1604 (1959), Soviet Phys. JETP **10**, 1137 (1960).

[5] Arifkhanov, Makarov, Perfilov, and Shamov, JETP **38**, 1115 (1960), Soviet Phys. JETP **11**, 806 (1960).

[6] O. Skjeggestad and S. O. Sörensen, Phys. Rev. **113**, 1115 (1959).

Translated by M. Danos
8

TOTAL CROSS SECTIONS FOR INTERACTIONS OF 4.75- *AND* 3.7-Bev/c K^+ *AND* π^+ *MESONS WITH PROTONS AND NUCLEI*

M. F. LIKHACHEV, V. S. STAVINSKII, HSÜ YÜN-CH'ANG and CHANG NAI-SEN

Joint Institute for Nuclear Research

Submitted to JETP editor January 24, 1961

J. Exptl. Theoret. Phys. (U.S.S.R.) **41**, 38-41 (July, 1961)

The total cross sections for interactions of K^+ and π^+ mesons with protons were measured. The following values were obtained: 21.3 ± 4.6 mb and 21 ± 4.3 mb for 4.75 ± 0.15 Bev/c and 3.7 ± 0.1 Bev/c K^+ mesons, respectively; the corresponding values for π^+ mesons of the same momenta were 33.3 ± 1.3 mb and 30 ± 1.2 mb. Data on the cross sections for inelastic collisions of K^+ and π^+ mesons with various nuclei have also been obtained.

ACCORDING to bevatron measurements,[1] the total cross section for interactions between K^+ mesons and protons attains a maximum of ~ 19 mb at a K^+-meson momentum of ~ 1.2 Bev/c and then drops to 13 mb at 2.4 Bev/c. In this connection, it is important to obtain data on the total cross sections for interactions between K^+ mesons and hydrogen at higher energies.

We carried out two series of measurements with the proton synchrotron of the High Energy Laboratory of the Joint Institute for Nuclear Research. The momentum of the particles bombarding a target-absorber was 4.75 ± 0.15 Bev/c in one case and 3.7 ± 0.1 Bev/c in the other. A diagram of the experimental layout is shown in Fig. 1.

As the source of K^+ mesons and other positive particles, we used a beryllium plate 20 × 2 × 4 cm bombarded by protons accelerated to ~ 10 Bev in the first series and to ~ 8 Bev in the second.

The K^+ and π^+ mesons of given momentum were deflected by the magnetic field of the proton synchrotron by an angle of ~ 18° relative to the primary proton direction. They passed through two quadrupole magnetic lenses focusing the particles in the vertical plane and defocusing them in the horizontal plane. After undergoing another deflection of ~ 8°, the particles passed through a system of scintillation and Cerenkov counters.[2]

The signals from the scintillator and Cerenkov radiator of each counter were picked up by a single photomultiplier tube (FÉU-33 or FÉU-24) and the pulses were applied to the electronic circuit. The basic block diagram of the electronic equipment used to measure the total cross section for interactions between K^+ mesons and hydrogen is shown in Fig. 2. This figure also shows the path of the signal from the photomultiplier, through the branching circuit, to the input of "fast" coincidence and anticoincidence circuits ($\tau \approx 5 \times 10^{-9}$ sec). The K^+ mesons were separated and recorded by two scintillation counters S_1 and S_2 and two gas Cerenkov counters Y_1 and Y_2 set to record K^+ mesons of a given momentum; these counters were connected in anticoincidence with a threshold gas Cerenkov counter P, which recorded π^+ and μ^+ mesons. In the separated K^+ meson beam (K^+ mesons constituted ~ 1% of all positive beam particles), π^+ and μ^+ mesons, positrons and random coincidences totaled no more than 0.5% of the K^+ mesons.

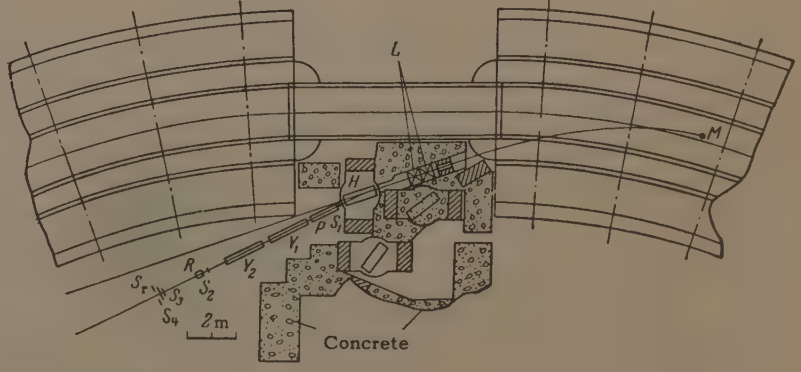

FIG. 1. Experimental layout: M – target; R – scatterer; H – magnet; L – magnetic lens; S – scintillation counters of diameter 9 cm (S_1), 6 cm (S_2), 14.5 cm (S_3), 16 and 30 cm (S_r); Y and P – Cerenkov counters.

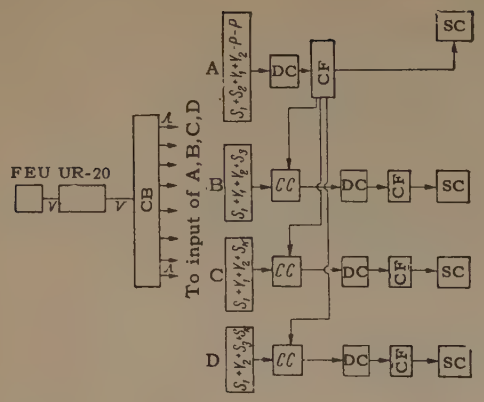

FIG. 2. Block diagram of the electronic equipment: A – four-channel coincidence circuit ($\tau \approx 5 \times 10^{-9}$ sec) with two anticoincidence channels; B, C, D – four-channel coincidence circuits ($\tau \approx 5 \times 10^{-9}$ sec); CC – two-channel coincidence circuits ($\tau \approx 5 \times 10^{-7}$ sec); DC – discriminators; CF – cathode followers; SC – scaler circuits. The path of the signal from the FÉU photomultiplier to the coincidence circuits is shown on the left: UR – amplifier with a mean amplification factor of 18 and bandwidth of 180 Mc; CB – clipper-branching circuit.

The π^+ mesons were separated by a threshold gas Cerenkov counter in coincidence with S_1 and S_2. The μ^+-meson and positron contamination in the π^+-meson beam was $(3 \pm 1)\%$ and $< 0.1\%$, respectively.

Liquid hydrogen (2.13 g/cm^2) in a foamed polysterene container was used as the target-absorber R in the experiments with hydrogen. In this case, the particles scattered out of the beam were measured at angles $\theta > 2.3°$ (in the laboratory system), where $\theta = \tan^{-1}(r/\rho)$; r is the radius of counter S_3 and ρ is the distance between S_3 and the center of the target.

In order to find the total interaction cross section, it is also necessary to take into account the particles scattered by angles $\leq 2.3°$. To do this at 3.7 Bev/c, we used a ring counter S_r located 1.9 m from the center of the target (see Fig. 1). The ring counter was connected in coincidence with counters S_1, S_2, Y_1, Y_2 and with S_1, S_2, Y_1, Y_2, S_3 in the measurements of K^+ mesons scattered out of the beam and with counters S_1, S_2, P and S_1, S_2, P, S_3 in the case of π^+ mesons (see Fig. 2).

Assuming an isotropic distribution (for small angles) for the secondary particles not recorded simultaneously by S_3 and S_r but recorded only by S_r, and knowing the probabilities that the secondary particles pass through only counter S_r and (owing to the multiplicity) simultaneously through both counters S_r and S_3, we found the cross-section correction $\Delta\sigma$ ($\leq 2.3°$) for processes in which at least one secondary particle traverses counter S_3. We call this cross section

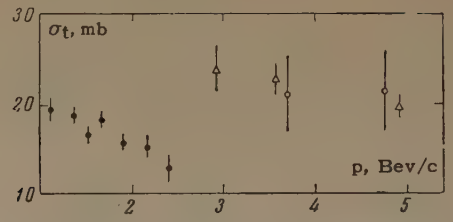

FIG. 3. Total cross sections for the interaction between K^+ mesons and hydrogen as a function of the K^+ momentum (in the laboratory system): ○ – present experiment, ● – data from,[1] Δ – data from[5]

correction the "forward-scattering" correction. This correction was 0.3 ± 0.3 mb for K^+ mesons and 3 ± 0.3 mb for π^+ mesons (of momentum 3.7 Bev/c).

The total cross sections for the interaction of K^+ mesons with hydrogen corrected for forward scattering were 21 ± 4.3 mb and 21.3 ± 4.6 mb at 3.7 and 4.75 Bev/c, respectively. For π^+ mesons, the corresponding values of the cross sections, corrected for forward scattering and the μ^+-meson contamination of the beam were 30 ± 1.2 and 33.3 ± 1.3 mb. Here we used the same forward scattering correction at 4.75 Bev/c as at 3.7 Bev/c.

The values of the total cross sections for the interaction between π^+ mesons and hydrogen are in agreement with the results obtained by Longo et al [3] for π^+ mesons of momentum up to 4 Bev/c.

The basic results of the present experiment were reported by I. V. Chuvilo at the 1960 Rochester Conference,[4] at which data obtained at CERN on the total cross sections for the interaction between K^+ mesons and hydrogen at approximately the same energy were also reported.[5] Figure 3 shows the data on the total cross sections for the interaction of K^+ mesons with hydrogen obtained at the bevatron,[1] at CERN,[5] and in the present experiment. As seen from the figure, the total cross section rises appreciably in the interval 2.4 – 3.5 Bev/c. Such a behavior of the cross section seems understandable if it is assumed that some resonance or threshold effects, for example, the production of K-meson pairs, occurs in this momentum region. Using the data obtained with the ring counters, we can draw some qualitative conclusions on the angular distribution of the secondary particles (to 5° in the laboratory system) in the interaction of K^+ and π^+ mesons with protons. For K^+ mesons, the probability density is less, and depends more weakly on the angle than for π^+ mesons of the same momentum (3.7 Bev/c).

Until now, data have been entirely lacking on the absorption cross sections (i.e., inelastic cross sections) of π^+ and K^+ mesons by nuclei

in the 3 — 5 Bev/c region. We measured the cross sections for the absorption of π^+ mesons by C, Al, Cu, Sn, and Pb nuclei and for K^+ mesons by C, Al, and Cu nuclei at 4.75 ± 0.15 Bev/c. The results are shown in the table.

Nucleus	Absorption cross section, mb	
	π^+ mesons	K^+ mesons
C	182 ± 8	136 ± 21
Al	344 ± 13	254 ± 33
Cu	689 ± 33	430 ± 120
Sn	1241 ± 190	—
Pb	1912 ± 161	—

In the experiment, we used absorbers of the following thicknesses: carbon — 21.15 g/cm^2, aluminum — 24.45 g/cm^2, copper — 13.30 g/cm^2, tin — 8.80 g/cm^2, and lead — 11.30 g/cm^2. Since the counter S_3 was seen from the center of the target-absorber at an angle of 3°, the absorption cross sections in the table have been corrected for Coulomb and diffraction scattering at angles $\leq 3°$ and for inelastic scattering at angles $\leq 3°$. In the case of π^+ mesons, we also introduced corrections for the μ^+ meson contamination of the beam.

The authors express their gratitude to V. I. Veksler and A. A. Lyubimov for discussion and aid in the work. We express our gratitude to I. V. Chuvilo, who reported the basic results of this work at the 1960 Annual International Conference on High Energy Physics in Rochester. We consider it our pleasant duty to express our gratitude to the proton synchrotron crew for the proper functioning of the accelerator. We thank Yu. D. Prokoshkin for providing the liquid hydrogen target.

[1] Burrowes, Caldwell, Frisch, Hill, Ritson, and Schulter, Phys. Rev. Lett. **2**, 117 (1959).

[2] Likhachev, Lyubimov, Stavinskii, and Chang, Report at the Conference on Experimental Techniques, Berkeley, 1960; PTÉ (Instruments and Meas. Techn.), in press.

[3] Longo, Helland, Hess, Moyer, and Perez-Mendez, Phys. Rev. Lett. **3**, 568 (1959).

[4] Proceedings 1960 Annual Intern. Conf. on High Energy Physics at Rochester, Univ. of Rochester, 1961.

[5] von Dardel, Frisch, Mermod, Milburn, Piroue, Vivargent, Weber, and Winter, Phys. Rev. Lett. **5**, 333 (1960). (see also Proceedings 1960 Annual Intern. Conf. on High Energy Physics at Rochester, Univ. of Rochester, 1961.

Translated by E. Marquit
9

SPECTROSCOPIC INVESTIGATION OF A TOROIDAL DISCHARGE

V. G. AVERIN, M. A. MAZING, and A. I. PISANKO

Submitted to JETP editor January 21, 1961

J. Exptl. Theoret. Phys. (U.S.S.R.) **41**, 42-48 (July, 1961)

A spectroscopic investigation is carried out of the plasma glow in the "Beta" installation (under various experimental conditions) and a study is made of the time dependence of the line intensities due to ions of different degrees of ionization. The results are interpreted on the basis of corresponding variations in the electron temperature of the plasma.

INTRODUCTION

THE installation "Beta" belongs to the class of toroidal chambers with a weak magnetic field, such as "Alpha" and "Zeta." In contrast to the other two installations a considerably higher current density is produced in "Beta."

It was of interest to carry out a spectroscopic investigation of the radiation from the discharge and, first of all, to study the variation with time of the intensity of the lines due to ions of different degrees of ionization (oxygen, fluorine, carbon and others) as the conditions of the discharge were varied.

As an interesting feature of the discharge we note that observation of the time dependence of the total radiation from the discharge by means of a photoelectric element with a "uviol" window (for the range 2200 — 6000 A) has shown that the intensity of the light passes through a minimum at the instant when the current reaches its maximum (Fig. 1).

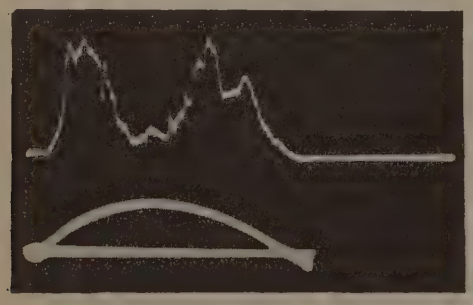

FIG. 1. Time dependence of the intensity of the spectroscopically unanalyzed light (in the range 2200-6000 A) (top) and of the magnitude of the discharge current (bottom).

DESCRIPTION OF THE EXPERIMENT

The installation "Beta" has the following parameters: principal diameter of the toroid 750 mm, diameter of the discharge chamber 210 mm, diameter of the external shell 250 mm, working pressure of hydrogen $(3-5)\times 10^{-3}$ mm Hg, maximum energy stored in capacitors 22 kilojoules, duration of the discharge 670 μsec, intensity of the longitudinal magnetic field 200 — 1100 oe, maximum discharge current with 1.5 kv initially applied 120 kamp, maximum current density evaluated for the total cross section of the discharge chamber 400 amp/cm^2, maximum conductivity of the discharge evaluated for the total cross section of the chamber (at a longitudinal magnetic field intensity of 640 oe) 4×10^{14} cgs esu.

The light was observed through a quartz window situated parallel to the plane of the large cross section of the discharge chamber. By means of a system of mirrors light from the same portion of the discharge was made to fall on the entrance slits of two monochromators ZMR-2 (Fig. 2), and this permitted simultaneous observation of the time dependence of the intensities of two different spectral lines.

At the exit of each monochromator there was placed an FÉU-18 photomultiplier, signals from which were applied to the input of two identical amplifiers of the OK-24MKB oscillograph.

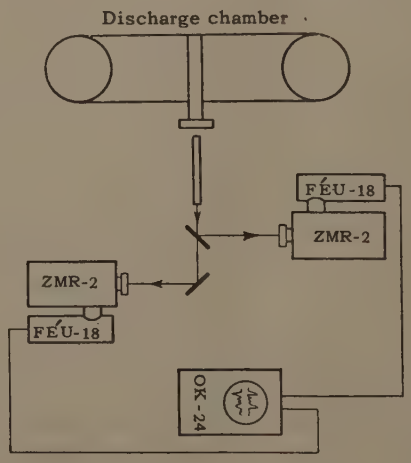

FIG. 2. Optical block diagram of the experimental arrangement.

Each photomultiplier had its own independent VS-9 rectifier. The photomultipliers and the connecting lines were carefully screened from all possible induction effects associated with the powerful gas discharge. The current in the discharge was measured by means of a Rogowski belt, the signal from which was integrated and applied to the input of an OK-17M oscillograph.

The voltage was measured by means of a turn of wire situated on the discharge chamber parallel to its axis. The voltage signal was applied to the second input of the OK-17M oscillograph.

EXPERIMENTAL RESULTS

1. Time dependence of the intensity of the spectral lines. Displays were obtained of the time dependence of the intensity of the spectral lines of oxygen, fluorine, nitrogen, carbon and helium. The wavelengths, the spectroscopic notations for all the lines, and the energies of the upper levels are shown in the table.

Line	λ, Å	Transition	Energy of the upper level, ev
OV	2781	$3s^3S_1—3p^3P_2$	81
OIV	3063	$3^2S_{1/2}—3^2P^0_{3/2}$	48
OIII	3047	$3s^3P^0_2—3p^3P_2$	37
FV	2707	$3s^4P^0_{7/2}—3p^4D_{9/2}$	81
FIV	2826	$3s^3P^0_2—3p^3D_3$	56
FIII	2994	$3s'''^6S^0_{5/2}—3p'''^6P_{7/2}$	53
NV	4945	$6^2G—7^2H^0$	91
NIV	3485	$3^3S_1—3^3P^0_1$	50
CIII	4650	$3^3S_1—3^3P^0_1$	32
He II	4685	$3^2D—4^2F$	51

The oscillograms exhibit the following phenomena:

1. The glow due to the ions of different degrees of ionization begins after different lapses of time from the beginning of the discharge: lines due to ions of higher degree of ionization (OV, FV) appear later than lines due to ions of lower degrees of ionization (OIII, FIII).

2. All the observed lines have a minimum intensity in the neighborhood of the maximum of the discharge current. The width and depth of this "dip" in the intensity depends on the degree of ionization of the emitting ion.

3. In contrast to the lines due to OIII and OIV, which have well defined intensity maxima at the beginning and at the end of the discharge, the line due to OV has a weakly pronounced second maximum at the end of the discharge, and sometimes the line due to OV does not get excited at all at the end of the discharge.

4. The time dependence of the intensities of the lines due to NV, NIV, CIII in its general behavior agrees with the time dependence of the lines due to OIII, OIV, FIII and FIV.

2. Effect of the initial conditions of the discharge. An investigation of the effect on the time dependence of the intensity of the spectral lines of the initial conditions of the discharge has shown that the appearance of the "dip" in the intensity of the lines is very sensitive to the variation of such parameters as the initial pressure, the discharge current and the initial longitudinal magnetic field.

It was established by means of preliminary experiments that the resistance of the plasma also depends on the variation of these three parameters, and it is possible to select such values of these parameters as to make the conductivity of the plasma a maximum. The corresponding values of the pressure p, of the maximum discharge current I_{max} and of the longitudinal magnetic field H_Z have been chosen by us for the operating values and in future shall be referred to as "optimum" values [$p = (3.5 — 4.5) \times 10^{-3}$ mm Hg, $I_{max} = 120$ kamp; $H_Z = 640$ oe].

It was found that a deviation of the longitudinal magnetic field from its optimum value by 150 — 200 oe in either direction leads to a change in the form of the time dependence of the intensity: to a diminution and even to a complete disappearance of the "dip" and to the appearance of strong fluctuations of intensity.

The same applies to the variation in initial pressure. The range of pressures for which a "dip" in the intensity of light is observed is $(3.5 — 4.5) \times 10^{-3}$ mm Hg. Outside this range a gradual smearing of the minimum is observed, accompanied by considerable fluctuations in the intensity of the glow.

The form of the time dependence of the lines due to OIII and OV for different values of the discharge current is shown in Fig. 3 (the longitudinal magnetic field and the pressure have been chosen equal to their optimum values).

It can be seen from the figure that a decrease in the discharge current leads to a decrease in the depth of the intensity minimum and to a complete disappearance of the minimum. We should particularly note the cases when a small dip in the intensity of the line due to OIII was observed while there was no such dip (Fig. 3d) in the line due to OV.

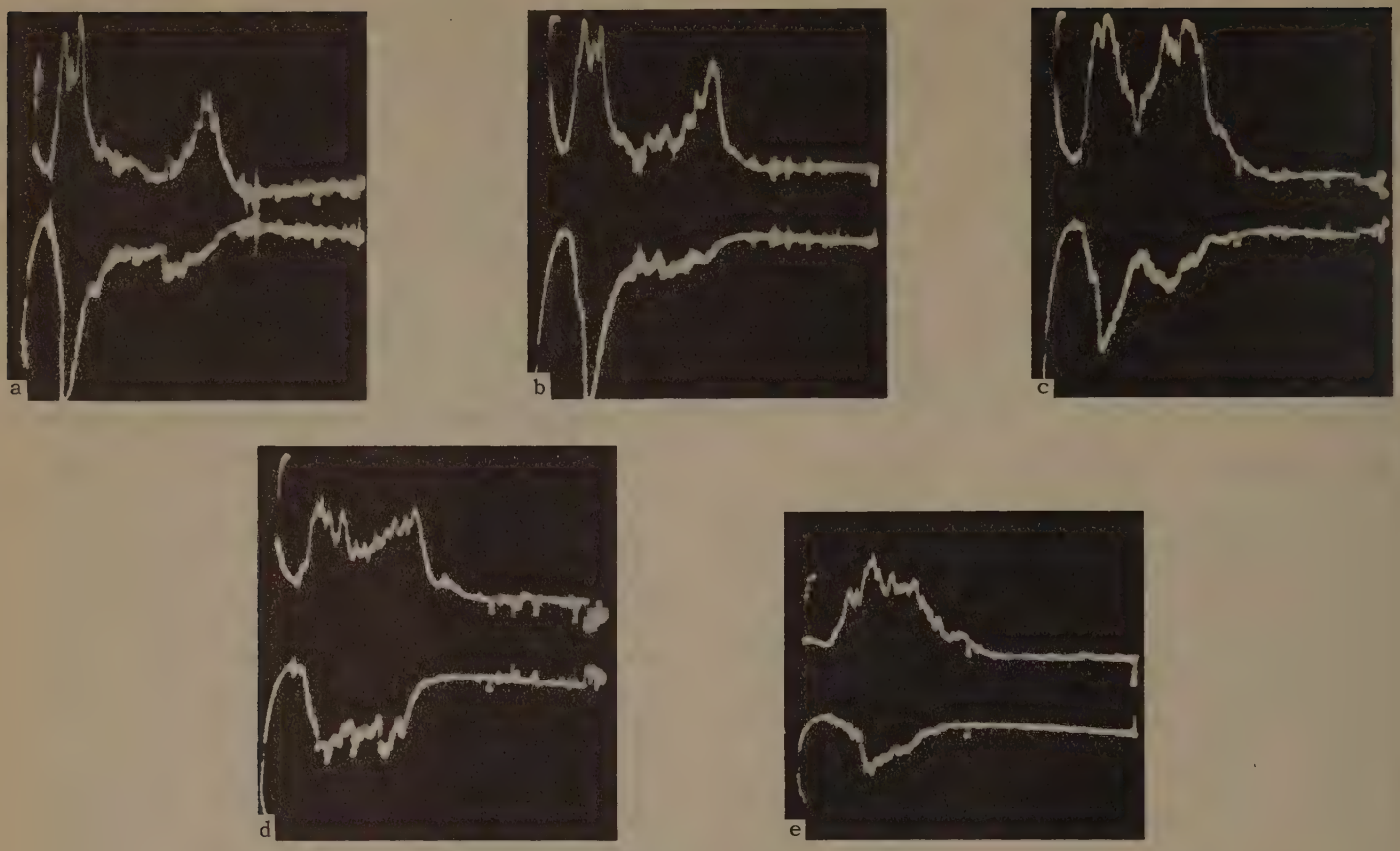

FIG. 3. Time dependence of the intensities of the OIII lines (upper trace) and OV lines (lower trace) for different values of the maximum discharge current: a – I_{max} = 120 kamp, b – 95 kamp, c – 75 kamp, d – 65 kamp, e – 50 kamp.

If we assume that the decrease in the intensity of the lines in the sequence from OII to OIV and OV is due to the transition of all the ions into a state of higher degree of excitation, then we can say that in the case of Fig. 3d we are observing by means of the line from OII the transition of the ion O^{++} into O^{+++}, while the ion O^{++++} (the line OV) does not have time to become ionized.

The oscillograms which give the dependence of the current on the voltage, and which were obtained under optimum conditions for the discharge, exhibit the well-known displacement (shift) of the current curve with respect to the voltage curve. This shift, as well as the dip in the light intensity, depends on the initial conditions of the discharge. But, the range of variation in the initial conditions within which the dip in the light intensity is preserved is considerably narrower than the range of variation in conditions within which the shift is preserved. For example, the values of the initial pressure, for which a dip in intensity is observed, lie within the range $(3.5 - 4.5) \times 10^{-3}$ mm Hg, while a shift is observed within the pressure range $(1 - 6) \times 10^{-3}$ mm Hg. Apparently, the dip in the intensity of the light is a very sensitive parameter characterizing the discharge.

3. Effect of impurities. The investigations which we have carried out on the effect of helium and argon impurities introduced into the discharge gave the following results:

1. The discharge in the presence of a 50% addition of He, and also in pure He, practically does not differ from the discharge in pure hydrogen. A dip in the light intensity is observed under optimum conditions of the discharge.

2. On the other hand, the discharge in the presence of an Ar impurity differs sharply from the "pure" discharge. Numerous sparkovers occur in the discharge chamber and as a result of this the pressure increases, and both the shift of the current with respect to the voltage mentioned earlier and the dip in the light intensity disappear.

The lines are excited only during the first half of the discharge, the time of emission of the OIII line does not exceed 200 μsec.

DISCUSSION OF RESULTS

At least two explanations are possible for the existence of the dip in the time dependence of the intensity of the lines.

As the electron temperature of the plasma increases the degree of ionization is increased and

transitions occur, for example, OIII → OIV → OV → OVI etc. Naturally, in this case the lines due to all ions of lower degree of ionization will exhibit a dip in intensity.

On the other hand, owing to instabilities arising in the discharge the plasma can touch the walls and in this way become cooled. This leads to a fall in the electron temperature and, correspondingly, also to a dip in the light intensity.

The weakness of the second explanation is immediately apparent. After the appearance of the instability and the cooling of the plasma at the moment of the maximum of the discharge current it is not very probable that the plasma will have time to be heated again towards the end of the discharge. And yet towards the end of the discharge all the observed lives due to OIII, OIV, FIII, FIV, NIV, and sometimes even OV exhibits a second light intensity maximum. Moreover, experiment shows that at sufficiently low currents the dip in the intensity disappears and this, in accordance with the second explanation, ought to indicate an increase in the stability of the discharge.

But experiment shows that at such low currents the radiation from the discharge becomes unstable, the reproducibility from discharge to discharge is strongly reduced, i.e., the discharge becomes less stable.

Both these circumstances support the first assumption. Indeed, the presence of the second intensity maximum at the end of the discharge denotes that as the plasma cools and its electron temperature falls a deionization process occurs in accordance with OVI → OV → OIV → OIII etc.

The dependence of the depth of the "dip" on the value of the discharge current shows that as the current decreases the electron temperature of the plasma falls, and in agreement with this the dip in the intensity decreases and disappears completely.

Apparently, we can assume that the reason for the appearance of the dip in the light intensity is an increase in the electron temperature of the plasma at the instant when the current is maximum. If we adopt this hypothesis, then from the time dependence of the intensity of the lines due to ions of different degrees of ionization we can attempt to evaluate the time dependence of the electron temperature and its maximum value.

Unfortunately, we could not investigate the intensity of the OVI line situated in the vacuum region of the spectrum. By utilizing data obtained only from the OIII, OIV, OV lines we can evaluate the time dependence of the electron temperature at the beginning and at the end of the discharge and its lower limit at the instant when the current is maximum.

As is well known, in the case of plasma of not excessively low density the main processes leading to the ionization of atoms are collisions with electrons. The inverse process of deionization also occurs in binary collisions with electrons (the probability of a triple collision is negligibly small at an electron density of $\sim 10^{14}$ cm^{-3}) and is accompanied by radiation (photorecombination).

In the steady state, the number of both kinds of effective collisions must be the same.

If we denote by S_i the ionization cross section, and by α_i the photorecombination cross section, then the ratio of the densities of ions of degrees of ionization $i+1$ and i will be given by:

$$n_{i+1}/n_i = \langle S_i v\rangle/\langle \alpha_{i+1} v'\rangle,$$

where v and v′ are respectively the velocities of the ionizing and the recombining electrons, while the brackets denote the averaging of the cross sections over the electron velocity distribution. If the velocities have a Maxwellian distribution, then the ratio n_{i+1}/n_i is a function of the electron temperature T_e.

Ions are also excited in collisions with electrons, and deexcitation occurs by radiation as a result of low particle density. In such a case the intensity of a spectral line is given by

$$I = I_0 n_i n_e \langle S^* v\rangle.$$

Here n_e is the electron density, n_i is the density of the emitting ions, $\langle S^* v\rangle$ is the excitation cross section averaged over the electron velocity distribution. The constant I_0 includes all the numerical coefficients.

We have utilized the values of the cross sections S_i and α_i averaged over the Maxwellian velocity distribution given in McWhirter's paper.[1] We have assumed the value of S^* to be equal to S_i at a potential equal to the excitation potential of the line under consideration. The last assumption will not lead to any appreciable error since we need only the relative values of the cross sections.

We have calculated the dependence of the relative intensities of the oxygen and fluorine lines on the electron temperature on the assumption that the total number of oxygen and fluorine atoms does not change in the course of the discharge. The results of the calculation using oxygen lines are shown in Fig. 4.

By utilizing the time dependence of the intensity of the OIII, OV, FIII, FIV, FV lines obtained by us we have measured the time intervals from

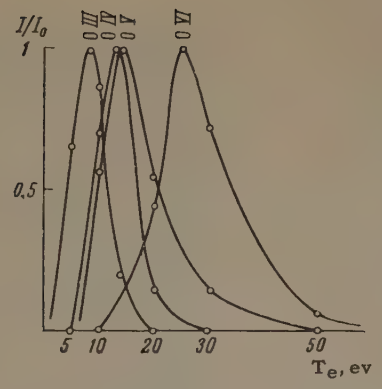

FIG. 4. Calculated dependence of the relative intensities of the OIII, OIV, OV, and OVI lines on the electron temperature of the plasma (wavelength of the OVI line is equal to 1036 A).

the instant of the beginning of the discharge to the instant when the first maximum of the lines is attained; to the instant when the intensity of these lines is equal to 20% of maximum intensity; to the instant when the same intensity is attained after the dip; and, finally, to the instant when the second maximum in the intensity is attained. The measured time intervals were averaged over three or four oscillograms. Each such point can be assigned a corresponding value of the electron temperature.

The time dependence of the electron temperature obtained in this manner for three different values of the discharge current is shown in Fig. 5. In making the transition from the variation of the line intensity with time to the variation of electron temperature we have not taken into account the change in the electron density after the lines have reached the first intensity maximm. Since by the time the current maximum is reached a simultaneous pinching of the discharge can occur, the electron density can increase by a factor of several fold during a time from 100 to 200 μsec after the beginning of the discharge. This must mean that the intensity attains not 20% of the maximum value, but an appreciably lower value, i.e., the electron temperature attains even greater values than shown in the figure.

The difference in the values of the electron temperature obtained from lines corresponding to different degrees of ionization is apparently associated with the fact that the discharge is observed over the whole cross section so that on the radiation coming from the hot central region consisting of light supplied by the "hot" OV and FV lines there is superimposed radiation coming from the colder external layers where the light is supplied by the OIII, FIV, FIII, etc lines. The existence of such stratification of the plasma has been

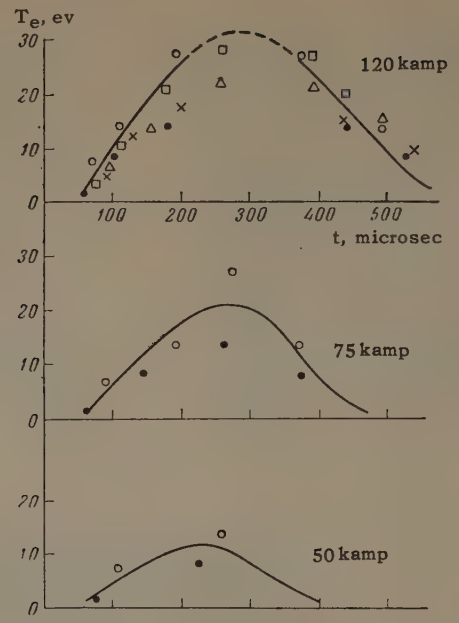

FIG. 5. Time dependence of the electron temperature for different values of the maximum discharge current determined from different lines: ○ – OV, ● – OIII, □ – FV, △ – FIV, × – FIII.

established by Kaufman [2] using the "Sceptre" apparatus.

As is shown in Fig. 5, corresponding to the greatest value of the discharge current (I_{max} = 120 kamp) the electron temperature attains a value not less than 25 — 30 ev after a lapse of time of 200 μsec after the beginning of the discharge. During the next 100 μsec the current continues to increase, and this can lead to a further increase in the electron temperature. After the current has passed through its maximum the electron temperature probably also begins to decrease and attains the value of 25 — 30 ev again after a time interval of 370 — 400 μsec after the beginning of the discharge, while after a lapse of 500 μsec it falls to a value ~ 10 ev.

At a discharge current of 75 kamp the electron temperature attains a value of 25 — 30 ev after a lapse of 300 μsec after the beginning of the discharge, and this high value of the electron temperature is apparently preserved only during 50 μsec. At a current of 50 kamp the maximum electron temperature does not exceed 14 ev.

It should be noted that in the first two cases when the OV line exhibits a dip in intensity the value of the electron temperature determined from the decrease in intensity gives a lower limit for the electron temperature. In the last case when there is no dip in the OV line the value of 14 ev is the upper limit on the electron temperature.

The electron temperature of the plasma can be estimated by utilizing the value of the plasma conductivity σ. For $\sigma = 4 \times 10^{14}$ cgs esu we obtain $T_e \sim 10 - 15$ ev. However, this value is without any doubt too low since the conductivity has been evaluated corresponding to the whole cross section of the discharge chamber. If we take pinching into account T_e can be increased by a factor of several fold.

Very recently communications have appeared in the literature on the observation of a "dip" in the time dependence of the intensities of spectral lines in installations where "slow" processes occur. In the "Alpha" installation two maxima in the intensity of the NIV line are observed corresponding to the greatest value of the capacitor bank voltage.[4] In the case of the "Tokamak" installation only the first intensity peak is observed[5] for the CIII line, $\lambda = 4651$ A.

In these two cases, apparently, we have the same mechanism as that described earlier.

In the same way Breton and Herman[6] attempt to explain the time dependence of line intensities in the TA-2000 installation. However, judging by the figure given in their paper, the intensity of the CIII line goes through a minimum twice during one half period of the current, and at the instant when the current reaches its maximum they observe not a minimum, but a second intensity maximum, and this is followed by a third one at the end of the half period of the current. It is doubtful that such a variation of intensity can be associated with a variation of the electron temperature of the plasma, it is more likely that it is due to some kind of instabilities of the discharge.

A similar dip in light intensity was observed[3] in the "Scylla" installation, where at the instant when the current reached its maximum a peak in the intensity of the OVII line was observed and a dip in the intensity of the OVI line. The authors working with "Scylla" explain such a time dependence of the line intensity by an increase in the electron temperature of the plasma and by a transition of all the O^{5+} ions into the O^{6+} state.

CONCLUSIONS

1. Spectroscopic measurements show that the intensity of radiation from a plasma in the range 2200 — 6000 A obtained in a toroidal discharge in a weak magnetic field passes through a minimum at the instant when the discharge current passes through a maximum.

2. The electron temperature of the plasma attains a value of not less than 30 ev for a maximum discharge current of 120 kamp. Such a value of the temperature persists for approximately 100 μsec.

3. The rate of growth of the temperature and its maximum value depend on the value of the discharge current. At a current of 50 kamp the electron temperature of the plasma does not exceed 14 ev at the time of maximum current.

4. For an exact determination of the maximum electron temperature under optimum conditions of the discharge it is necessary to investigate the time dependence of the intensities of the OVI, FVI, and, if possible, of the OVII lines.

The authors express their deep gratitude to Academician I. K. Kikoin and Prof. S. L. Mandel'shtam for valuable comments and for their continuing interest in this work, and also to V. V. Sokol'skii for his help with the work and for his discussion of the results.

[1] R. W. P. McWhirter, Proc. Phys. Soc. (London) **75**, 520 (1960).

[2] P. Williams and S. Kaufman, Proc. Phys. Soc. (London) **75**, 329 (1960).

[3] Jahoda, Little, Quinn, Sawyer, and Stratton, Phys. Rev. **119**, 843 (1960).

[4] Zaĭdel', Malyshev, Berezin, and Razdobarin, J. Tech. Phys. (U.S.S.R.) **30**, 1437 (1960), Soviet Phys. Tech. Phys. **5**, 1360 (1961).

[5] Dolgov-Savel'ev, Mukhovatov, Strelkov, Shepelev, and Yavlinskii, JETP **38**, 394 (1960), Soviet Phys. JETP **11**, 287 (1960).

[6] C. Breton and L. Herman, IV International Conf. on Ionization Phenomena in Gases, Uppsala, 1959, p. 17.

Translated by G. Volkoff
10

ELASTIC SCATTERING OF 10–15 Mev ALPHA PARTICLES BY GOLD AND ALUMINUM

M. P. KONSTANTINOV, E. V. MYAKININ, A. M. ROMANOV, and T. V. TSAREVA

Leningrad Physico-Technical Institute, Academy of Sciences, U.S.S.R.

Submitted to JETP editor February 4, 1961

J. Exptl. Theoret. Phys. (U.S.S.R.) **41**, 49-51 (July, 1961)

The angular distribution of 10 — 15 Mev α particles elastically scattered by gold and aluminum has been studied. The differential cross-sections for scattering of α particles by gold obey the Rutherford formula for angles between 10 and 140°. The angular distribution of α particles elastically scattered by aluminum is characterized by the presence of maxima and minima.

A study of the departures of the experimental cross sections for elastic scattering of α particles from the cross sections calculated by the Rutherford formula, makes it possible to obtain information on the radius and potential of the nuclear interaction of α particles. For this purpose the angular distributions of α particles with energies 20 — 43 Mev, scattered elastically by light and heavy nuclei, have been studied in detail.[1-6] The angular distribution of α particles with energies 8 — 20 Mev, elastically scattered by nuclei, has been insufficiently studied. In the present work measurements have been carried out on the angular distribution of 10 — 15 Mev α particles scattered by gold and aluminum nuclei.

The experiments were made with the cyclotron of the Physico-Technical Institute of the Academy of Sciences. The target — a thin gold or aluminum foil — was placed in the center of the 500 mm diameter brass chamber. Ya-2 photographic plates, with emulsion 100 μ thick, were placed around the target at equal distances and at equal angles of inclination to the axis of the collimated beams of scattered α particles. The windows of the casettes containing the plates were covered with 3.9 μ thick aluminum foil. Irradiation of the plates was carried out in several doses, and the ranges of angles 10 — 30, 30 — 50, 50 — 90 and 90 — 140° were covered consecutively. The overlap of angles in the ranges chosen made it possible to have "coupling plates," which provided a check on the readings of the monitor (Faraday cup with integrating circuit). The α-particle tracks with fixed (corresponding to calculation) values of range were counted with an MBI-2 microscope.

The energy of the primary α particle beam was determined from the range-energy curves in aluminum and in the photographic emulsion, for α particles scattered by gold, and for the protons from the reaction $Al^{27}(\alpha, p)Si^{30}$. In the latter case the Q values were used, determined by the magnetic analysis method[7] for transitions to the ground state and to the first, second and third excited states of Si^{30}.

The experimental scattering cross section in the center-of-mass system (for an angle $\Theta_{c.m.}$) was determined by using the formula

$$\sigma_{expt} = \frac{N_T(\theta_{lab})}{n_\alpha n_n G} \sin\theta_{lab} \frac{\sin^2\theta_{lab}}{\sin^2\theta_{c.m.}} \cos(\theta_{lab} - \theta_{c.m.}),$$

where $N_T(\Theta_{lab})$ is the number of α-particle tracks traversing a fixed area of plate examined at a given angle Θ_{lab} (laboratory system), n_α is the number of α particles falling on the target, determined from the charge in the Faraday cup, n_N is the number of nuclei referred to 1 cm^2 of target, and G is a coefficient determined by the geometrical conditions of the experiment.

The angular distribution of 10.4, 13.6, and 14.7 Mev α particles, elastically scattered by a 0.25 mg/cm^2 thick gold foil was studied by the method described. It was established that the differential cross section for scattering of α particles by gold satisfies the Rutherford formula in the range of angles 10 — 140°. The result holds generally for all α-particle energies studied here. The absolute values of the cross sections were determined with an error not exceeding 15%.

The elastic scattering of α particles by aluminum was studied for energies of 10.4 and 13.6 Mev in the primary beam (corresponding to α-particle energies in the c.m. system of 9.05 and 11.9 Mev). The target was 0.13 mg/cm^2 thick aluminum foil.

The points in the figure represent the ratio of the experimental cross sections for elastic scattering to the cross sections calculated by the

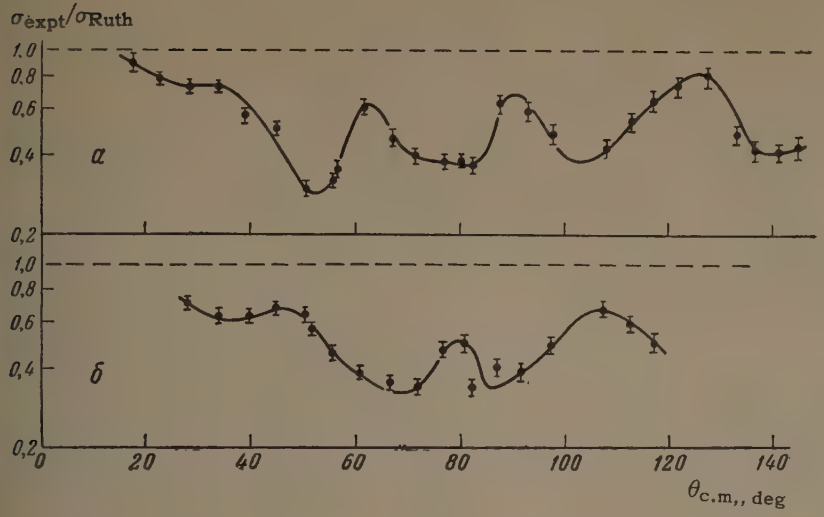

Angular distribution of α particles, elastically scattered by aluminum: a – for $E_{\alpha c.m.}$ = 11.9 Mev, b – for $E_{\alpha c.m.}$ = 9.05 Mev.

Rutherford formula. Apart from the statistical and geometrical errors of the experiment, errors related to incomplete separation of the groups of elastically and inelastically scattered α particles are also taken into account. For scattering at small angles the geometrical errors are dominant. while for scattering at large angles ($\Theta_{c.m.} > 90°$) the errors connected with separation of the inelastically scattered α particles are dominant.

It follows from the figure that the ratio $\sigma_{expt}/\sigma_{Ruth}$ is less than unity, and for $\Theta_{c.m.} > 30°$ a non-monotonic variation of angular distribution of the α particles is observed. Since the investigation was carried out with an angular interval of 5°, some details of the distribution could have passed unnoticed.

The results obtained are in qualitative agreement with the data on the distribution of elastically scattered α particles of energy 20 — 43 Mev [4–6] by aluminum. The difference consists in the maxima of this distribution being less pronounced for energies 10 — 14 Mev. If we proceed from the analogy between elastic scattering and the diffraction of light, [4] then we should expect the relative position of the maxima in the distribution of elastically scattered α particles to obey the relation

$$kR\Delta\left(\sin\frac{\theta}{2}\right)=\frac{\pi}{2},$$

where k is the α-particle wave-vector, R the interaction radius and Θ the scattering angle (c.m. system). For $E_{\alpha c.m.}$ = 11.9 Mev the mean distance between the maxima is 0.19 (on a sin Θ/2 scale). This corresponds to an interaction radius $R = 5.9 \times 10^{-13}$ cm.

[1] Kerlee, Blair, and Farwell, Phys. Rev. **107**, 1343 (1957).

[2] Wegner, Igo, and Eisberg, Phys. Rev. **99**, 825 (1955).

[3] H. E. Gove, Phys. Rev. **99**, 1353 (1955).

[4] P. C. Gugelot and M. Rickey, Phys. Rev. **101**, 1613 (1956).

[5] Igo, Wegner, and Eisberg, Phys. Rev. **101**, 1508 (1956).

[6] E. Bleuler and D. J. Tendam, Phys. Rev. **99**, 1605 (1955).

[7] Barros, Forsyth, Jaffe, and Taylor, Proc. Phys. Soc. **73**, 793 (1959).

Translated by R. Berman
11

ELASTIC BACK SCATTERING OF 2.8-Bev/c π^- *MESONS ON NEUTRONS*

Yu. D. BAYUKOV, G. A. LEKSIN, D. A. SUCHKOV, Ya. Ya. SHALAMOV, and V. A. SHEBANOV

Institute for Theoretical and Experimental Physics, Academy of Sciences, U.S.S.R.

Submitted to JETP editor February 2, 1961

J. Exptl. Theoret. Phys. (U.S.S.R.) **41**, 52-55 (July, 1961)

Cases of quasielastic π^-n-scattering into the back hemisphere in the laboratory system of coordinates were looked for in a 17-liter freon chamber. The cross section for this process evaluated per F nucleus has turned out to be < 0.1 mb. Recalculated for free nucleons the total cross section for the elastic π^-n-scattering process is less than 0.02 mb in the range of angles 140 — 180° in the center-of-mass system. Comparison of this result with theoretical estimates of the contribution to the scattering of the diagram with one virtual nucleon indicates that it is compensated by more complicated diagrams.

INTRODUCTION

ELASTIC scattering of π mesons by nucleons can be regarded as the result of simpler processes: of scattering by virtual π (or K) mesons in the "meson cloud" associated with the nucleon, of scattering by the nucleon "core" and, finally, as a result of penetration deep into the "core." For the process of elastic scattering of π^+-mesons by protons this may be written in the form of a symbolic equation for Feynman diagrams (Fig. 1).

Diagrams 1 and 2 lead to forward scattering for incident mesons of high energy. I. Ya. Pomeranchuk has noted a characteristic feature of the behavior of diagram 3 which, in contrast to diagrams of the form 1 or 2, should give at high energies a nonvanishing contribution to the back scattering of π^+ mesons. In the case of the scattering of π^- mesons by protons diagram 3 cannot occur in virtue of the law of conservation of charge. The analogous diagram of Fig. 2 with one virtual nucleon yields forward scattering at high energies. The angular distribution of π^+ mesons arising as a result of scattering described by diagram 3 has a maximum near 180° in the center-of-mass system (c.m.s.) with the width of the angular distribution being $\sim M/E$, where M is the nucleon mass and E is the energy of the incident meson in the c.m.s. An estimate of the cross section for the process with one virtual nucleon made by I. Ya. Pomeranchuk suggests the value $d\sigma/d\Omega(180°) \approx g^2k/4m^2 \approx 0.5$ mb. Here $\hbar = c = 1$, $g = 14$ is the meson-nucleon interaction constant, while $k \sim 1/40$ is an undetermined coefficient associated with the renormalization of the vertex parts and of the propagator in diagram 3. However, the

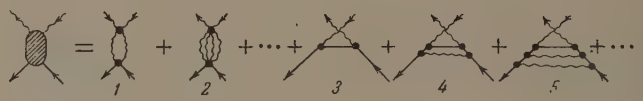

FIG. 1

contribution of diagram 3 can be compensated by the diagrams of the form 4, 5 etc. if they play a significant role in the scattering process.

EXPERIMENTAL ARRANGEMENT

At the present time there are no experimental data on the differential cross sections for the scattering of high-energy (several Bev) π^+ mesons by hydrogen. However, π^+p scattering is identical with π^-n scattering, data on which can be obtained if from the process of the interaction of mesons with nuclei we separate out the quasielastic π^-n scattering. On the other hand, a differential cross section for π^-n scattering in the backward direction ~ 0.5 mb/sr corresponding to an angular distribution of half-width 30 — 60° in the c.m.s. for incident mesons of energy of the order of several Bev leads to a total cross section ~ 1 mb.

A process with such a relatively large cross section can be studied well in a bubble chamber. Therefore, we have examined stereo-photographs obtained in the case of the interaction with matter of a beam of π^- mesons of momentum 2.8 Bev/c in a 17-liter freon bubble chamber [1] 50 cm long. The momentum spread of the beam is given by

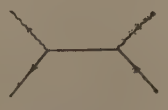

FIG. 2

$\Delta p/p = 10\%$. The working freon mixture (CF_3Cl and CF_2Cl_2) contains sufficiently light nuclei (the average atomic weight corresponds to a fluorine nucleus) and at the same time has a sufficiently high density (1.12 g/cm^3) and a sufficiently low value of the characteristic avalanche length (21.5 cm). This latter circumstance is particularly important, since the main background process has turned out to be the process involving the creation of π^0 mesons which were effectively recorded in the freon chamber by means of the decay γ quanta.

An incident meson momentum of 2.8 Bev/c in the laboratory system (l.s.) corresponds to a momentum of 1.05 Bev/c in the c.m.s. of the colliding meson and nucleon. Consequently, a sufficiently broad distribution of π^- mesons emerging in the backward direction ought to be observed. In the course of our work cases of scattering into the back hemisphere were recorded which corresponded in the c.m.s. to scattering in the angular interval 140 — 180°. The elastically back-scattered mesons must have momenta between 390 and 680 Mev/c and ranges greater than the length of the chamber.

The chamber was operated without a magnetic field. However, this is not particularly significant, since identification of elastic scattering by means of the correlation between the angle of scattering and the momentum of the π meson is in any case made difficult by the following circumstances: the relatively small change in the meson momentum as the scattering angle change from 90 to 180° in the l.s.; the 10% uncertainty in the momenta of the mesons in the beam; the uncertainty arising due to the Fermi motion of the nucleons in the target nucleus.

EXPERIMENTAL RESULTS

Three or four independent observers have examined ~ 2500 frames. These frames had recorded 36,000 meson traversals which gave rise to ~ 11,000 interactions with the working volume of the chamber, and this corresponds to a cross section of ~ 300 mb per average nucleus of the working mixture (F). Altogether there were recorded 14 single-prong events with one relativistic particle of momentum greater than 200 Mev/c emerging into the back hemisphere in the l.s. We have rejected the cases when the track ended in the chamber and when the ionization was twice the relativistic ionization. The efficiency of recording such events in the course of scanning the film is of the order of unity.

In ten of the recorded cases electron-positron pairs produced by the conversion of γ quanta appeared to radiate from the point of interaction (in one case there were four pairs, in two cases there were two pairs, and in seven cases there was one pair). It is natural to assume that the observed events are the result of an interaction involving the emission from a nucleus of one charged meson in the backward direction and of one or several π^0 mesons. The efficiency of recording a γ quantum within the chamber varies within the range from 0.6 to 0.23 depending on the spot at which the quantum was formed and on the scattering angle. There exists a certain probability of failing to record the π^0 mesons produced. This probability varies from ~ 10 to ~ 40%, depending on the angular distributions and on the multiplicity of production of π^0 mesons. Thus, events which are not accompanied by electron-positron pairs can also be included among the cases of multiple meson production. It is also possible that one of four cases is due to the reaction with the creation of a K^0 meson and its subsequent decay into two π^0 mesons, since in the chamber not far from the point of interaction there have been found three pairs radiating from a single point which is not associated with other interactions.

If, nevertheless, we assume that these four events are due to the elastic scattering of π^- mesons in the backward direction by the quasi-free neutrons in the nuclei, then the upper limit for the total cross section for scattering into the back hemisphere in the l.s. is $\sigma_n < 0.1$ mb per fluorine nucleus.

DISCUSSION OF RESULTS

On the basis of the experimental data obtained it is possible to make an estimate of the cross section for the process of elastic scattering of π^- mesons by a free neutron giving $\sigma < 0.1/n\eta$ mb ≈ 0.02 mb, where $n = 10$ is the number of neutrons in the fluorine nucleus, while $\eta \approx 0.5$ is a coefficient which takes into account the screening of nucleons in nuclei.

The choice of the value $\eta \approx 0.5$ may be justified in the following manner. Earlier Ballam et al[2] studied the elastic π^-n cross section at an energy of 460 Mev in a propane bubble chamber. A comparison was made of the angular distributions of π^- mesons scattered by neutrons contained in a carbon nucleus, and of π^+ mesons elastically scattered by hydrogen. It was shown that the data agreed well among themselves if we assume $\eta = 0.55$. The F nucleus is somewhat heavier than a C nucleus, so that one might expect that the coefficient η is smaller, but does not differ ap-

preciably from the value of η for C. An estimate made on the basis of data on small angle quasi-elastic scattering of 2.8 Bev/c π^- mesons by neutrons contained in the nuclei of which freon is composed shows that $\eta \approx 0.5$. Since the coefficient η is practically constant as the meson energy changes by almost an order of magnitude, it may be supposed that η will also not change in the case of back-scattering of mesons. Estimates of η made on the basis of the optical model also suggest a value ~ 0.5.

Thus, the cross section for back-scattering of π^--mesons by neutrons is smaller by more than an order of magnitude than the value estimated by means of diagram 3.

Moreover, as I. Ya. Pomeranchuk has noted, it is less than the value $\pi\lambda\!\!\!^{-2}/4\pi \approx 0.1$ mb ($\lambda\!\!\!^{-} = 1.9 \times 10^{-14}$ cm is the π-meson wavelength in the c.m.s.) which, generally speaking, should be expected for the contribution of just the S wave to the total cross section of elastic πN-scattering (in the present case independently of the sign of the meson charge) in the angular range studied (approximately 1 steradian in the c.m.s.). This means that the phases corresponding to low values of l are small, or else are such that the corresponding terms interfere and mutually cancel. The latter remark should be interpreted as an indication of the necessity for obtaining experimental data over a wider angular interval and with greater statistical accuracy rather than as a final result.

We express our deep gratitude to I. Ya. Pomeranchuk for suggesting the problem and for many discussions, and also to V. P. Rumyantseva and M. U. Khodakova for scanning photographs.

[1] Blinov, Lomanov, Meshkovskii, Shalamov, and Shebanov, PTÉ (Instruments and Experimental Technique) **1**, 35 (1958).

[2] Ballam, Hang, Scanreet, and Walker, Nuovo cimento **14**, 240 (1959).

Translated by G. Volkoff
12

SCATTERING OF 1–5 Bev/c MUONS IN LEAD

S. A. AZIMOV, G. G. ARUSHANOV, Kh. ZAĬNUTDINOV, R. KARIMOV, V. S. MASAGUTOV, and M. Kh. ÉSTERLIS

Physico-Technical Institute, Academy of Sciences, Uzbek S.S.R.

Submitted to JETP editor April 2, 1961

J. Exptl. Theoret. Phys. (U.S.S.R.) **41**, 56-59 (July, 1961)

The scattering of 1 — 5 Bev/c muons in 2-cm thick lead plates was studied in a cloud chamber. The experimental results are in good agreement with the multiple scattering theory of Cooper and Rainwater, in which the finite size of the nucleus is taken into account.

1. INTRODUCTION

DURING the last eight to ten years many studies of high-energy muon scattering have been published. Interest was aroused by the fact that the great majority of these investigations indicated the existence of so-called anomalous scattering. Large-angle muon scattering exceeded the predictions of electromagnetic theory. The results of many papers on interactions between muons and various substances have been collected in reference 1. All data for high-energy ($p \geq 1$ Bev/c) muon scattering, with the exception of the new data,[1] point to the existence of anomalies.

In the present work we studied the scattering of muons with momenta ranging from 1 to 5 Bev/c in five 2-cm lead plates inside of a cloud chamber. The experimental angular distribution was compared with theoretical integral curves of multiple scattering by a point-charge nucleus (Molière's theory)[2] as well as with the theory of Cooper and Rainwater[3] for an extended nucleus. The experimental results are found to be in good agreement with the latter theory after plural and single scattering are excluded and the so-called noise effect (errors in angle measurements and track distortions) is taken into account.

2. EXPERIMENTAL TECHNIQUE

The principal units of our apparatus (Fig. 1) were a large SP-29 electromagnet, a GK-7 hodoscope system, and a cloud chamber.

Three sets of coordinated counters (1, 2, and 3), each consisting of two trays, were placed parallel to the field in the $100 \times 30 \times 14$ cm pole gap of the electromagnet. The counter diameter was 0.46 cm; the working region was 12 cm long. The counter cathodes were aluminum tubes with $\sim 150\,\mu$ walls. Each set comprised 83 coordinated counters.

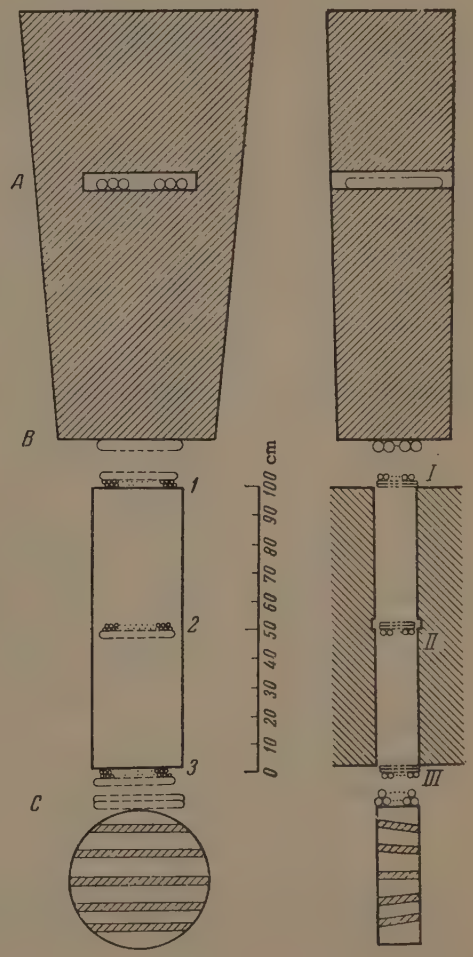

FIG. 1. Arrangement of apparatus (two views).

Aluminum counters with the dimensions 0.8×30 cm (trays I, II, and III containing 13 counters each) were placed directly above or below the coordinated counters and perpendicular to the latter. These counters, with $\sim 200\,\mu$ wall thickness, served to trace particle trajectories in a plane perpendicular to the field, as was required for the selection of the individual tracks whose momenta were to be determined.

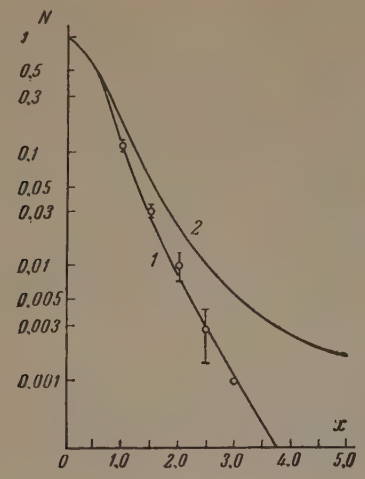

FIG. 2. Integral distribution in the dimensionless variable x. Ordinates represent the number of instances in which x is greater than the indicated value. Theoretical curves: 1 – representing theory of Cooper and Rainwater; 2 – representing theory of Molière.

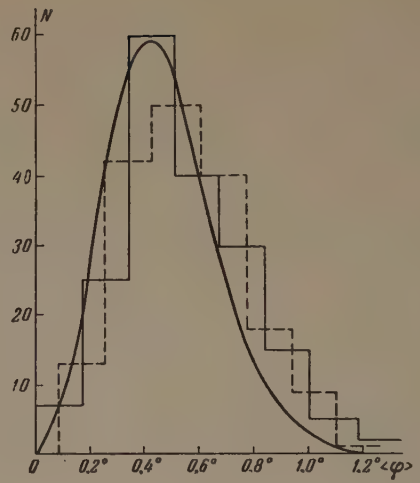

FIG. 3. Distribution of rms scattering angles on 200 tracks. The dashed and solid histograms were plotted for two groups of tracks selected at random. The theoretical curve was plotted for $n = 3$ and $\sigma_i = 0.5°$.

Pulses produced by triple coincidences in counters A, B, and C were fed simultaneously to the hodoscope and to the cloud chamber control. The cloud chamber containing the five plates each 2 cm thick, was placed under the electromagnet gap. The chamber was side-illuminated by two pulsed lamps, and a mirror forming an angle of 45° with the bottom of the chamber was used in photographing. A 1700 g/cm^2 lead layer above the magnet gap excluded electrons, protons, and pions, thus permitting the registration of muons alone.

Momenta were determined from the conventional formula $pc = 300\,H\rho$, where H is the magnetic field strength (10 000 oe in our experiment), and ρ is the track radius of curvature. Errors in measuring momenta of 1, 3, and 5 Bev/c were 2.5, 5, and 11%, respectively.

The photographed angles of scattering in the lead plates were measured with a UIM-21 microscope; the errors did not exceed 40′.

3. EXPERIMENTAL RESULTS AND DISCUSSION

We investigated 1134 muon scattering events in lead, with momenta in the range 1 – 5 Bev/c. Our results were compared with the integral curves for multiple Coulomb scattering by both point [2] and extended [3] nuclei. The data were compared with the theory of Cooper and Rainwater, [3] but not with Olbert's theory, [4] because the latter overestimates greatly the effect of an extended nucleus, whereas Cooper and Rainwater use a nuclear form factor based upon Hofstadter's well-known experiments [5] on fast electron scattering by nuclei.

The theory employs the variable

$$x = \varphi / \sqrt{B}\chi_c,$$

which is proportional to the product of the scattering angle by pv; $\sqrt{B}\,\chi_c$ is the characteristic angle in the theory of multiple Coulomb scattering. For a complete comparison of theory with experiment it is therefore desirable to determine experimentally the momentum of each scattered particle. In the great majority of experiments on muon scattering the momentum of each particle was not measured and multiple scattering curves were plotted for the momentum spectrum. Our data afford an advantage in this respect.

Our results are shown in Fig. 2. The experimental points represent 1134 muon traversals of a 2-cm lead plate. The theoretical curves represent integrals of the form $2\int_x^\infty f(\alpha)\,d\alpha$. The advantage of plotting scattering curves in the variable x lies in the fact that scattering data can be combined for different energies, different plate thicknesses, and even for different substances. Integral curves for particles with a momentum spectrum S(p) are customarily plotted according to the formula

$$\int_\varphi^\infty f(\varphi, p)\,d\varphi \int_{p_1}^{p_2} S(p)\,dp = (p_2 - p_1)\sqrt{B}\chi_c(p_0)\,S(p_0) \int_{x(p_0)}^\infty f(x)\,dx,$$

where p_2 and p_1 are the boundary values of the momenta, with $p_1 \le p_0 \le p_2$, where p_0 is the "average" momentum. Arushanov [6] has obtained different expressions in the form of series for the integral when f(x) is given by Molière's theory.

In treating the experimental results it is necessary to keep in mind the so-called noise effect, which has various causes. One particular cause can be distortion (such as that resulting from track diffusion or turbulent eddies associated with the operation of the cloud chamber), which leads to uncertainty of the scattering angle measurements. It is especially difficult to measure the projections of scattering angles in the first and last plates of the chamber, and we have not included the data obtained from these plates.

We have followed the procedure of McDiarmid [7] for the purpose of excluding plural and single scattering, which cause large scattering angles. We also followed McDiarmid in taking account of the noise effect. Figure 3 shows histograms of the rms scattering angle distribution for 200 tracks selected at random. Increased dispersion of the distribution as a result of the noise effect is associated with a diminishing true value of x:

$$x \to x\sqrt{1 + 2\sigma_1^2/B\chi_c^2},$$

where σ_1^2 is the variance of spurious scattering (noise), and n is the number of plates.

Figure 2 shows that our results are in good agreement, within the limits of experimental accuracy, with Cooper and Rainwater's theory, but that the experimental values lie below the Molière curve.

It should be noted that experiments with δ rays ejected by muons, [8] underground detection of muon pairs, [9] experiments with μ-mesic atoms, [10] and muon pair production by γ rays [11] all confirm the purely electromagnetic character of the muon-nucleon interaction.

The authors wish to thank R. Kamaletdinov and A. A. Yuldashev for the uninterrupted operation of the electronic equipment. We are also indebted to A. I. Alikhanov and G. B. Zhdanov for reading of the manuscript.

[1] Fukui, Kitamura, and Watase, Phys. Rev. **113**, 315 (1959).

[2] G. Molière, Z. Naturforsch. **3a**, 78 (1948); H. A. Bethe, Phys. Rev. **89**, 1256 (1953).

[3] L. N. Cooper and J. Rainwater, Phys. Rev. **97** 492 (1955).

[4] S. Olbert, Phys. Rev. **87**, 319 (1952).

[5] R. Hofstadter, Revs. Modern Phys. **28**, 214 (1956).

[6] G. G. Arushanov, Izv. AN UzbSSR **1**, 81 (1961).

[7] B. McDiarmid, Phil. Mag. **45**, 933 (1954); **46**, 177 (1955).

[8] W. D. Walker, Phys. Rev. **90**, 234 (1953); J. L. Lloyd and A. W. Wolfendale, Proc. Phys. Soc. (London) **73**, 178 (1959).

[9] Barrett, Bollinger, Cocconi, Eisenberg, and Greisen, Revs. Modern Phys. **24**, 133 (1952).

[10] V. L. Fitch and J. Rainwater, Phys. Rev. **92**, 789 (1953).

[11] G. E. Masek and W. K. H. Panofsky, Phys. Rev. **101**, 1094 (1956); Masek, Lazarus, and Panofsky, Phys. Rev. **103**, 374 (1956).

Translated by I. Emin
13

YIELD OF FAST PHOTONEUTRONS FROM C^{12} *AND* Al^{27}

V. PRESPERIN and L. A. KUL'CHITSKII

Leningrad Physico-Technical Institute, Academy of Sciences, U.S.S.R.

Submitted to JETP editor February 6, 1961

J. Exptl. Theoret. Phys. (U.S.S.R.) **41**, 60-63 (July, 1961)

A threshold detector was employed to measure the yield of fast photoneutrons ($E_n \geq 11$ Mev) produced by γ quanta with energies up to 85 Mev on C^{12} and Al^{27} nuclei. The experimental results indicate the predominance of a single-particle mechanism of fast photoneutron production (in which only one fast neutron is emitted from the nucleus).

MEASUREMENTS of the yield of fast photoneutrons (> 11 Mev) from C^{12} and Al^{27} were carried out to obtain additional information on the production mechanism for these particles. The fast neutrons were recorded by the method of threshold detectors. A natural mixture of the isotopes of copper served as the detector. In the interaction of neutrons of energies > 11 Mev with Cu^{63} nuclei, an active isotope appears with a half-life of 10 min and a maximum positron energy of 2.9 Mev.[1]

The positrons were recorded by a self-quenching Geiger counter of the type STS-6. To decrease the noise, this counter was surrounded by a guard ring of nine other counters of the same type, connected in parallel and in anticoincidence with the working counter. The system of counters was surrounded by a protective layer of iron of 150 mm thickness, and by a lead layer of 100 mm thickness. It was possible to decrease the background of the working counter by such means to ~ 3 counts/min. The background remained constant during the entire period of measurement. A hollow iron cylinder was placed between the ring and the working counter for the purpose of preventing the simultaneous incidence of positrons in the working counter and in one of the counters of the protective ring.

To lessen the effect of oscillations in the radiation intensity, the relative radiation dose was measured by the method of activation of a thin copper foil placed directly in the beam of the γ rays. The resultant β^+ activity was measured by an end-window counter. The equivalent dose of γ radiation (in absolute units) was determined from calibration measurements at constant radiation intensity with the help of a so-called quantometer.[2]

The target had the shape of a cylinder 100 mm long and 58 mm in diameter. Copper activated by photoneutrons was prepared in the shape of hollow cylinders with walls 0.6 mm thick.

Other possible reactions cannot give an appreciable contribution to the measured activity of the reactions $Cu^{63}(n, 2n)Cu^{62*}$ and $Cu^{63}(\gamma, n)Cu^{62*}$, as verified by the results of control measurements of the decay period. Measurement of the effect was alternated with measurement of the background (in the absence of a target). The background did not exceed 30 percent on average. A systematic control was maintained on the stability of the apparatus.

The method used makes it possible to determine the relative number of fast neutrons by the number of radioactive decays in the copper specimen per unit of monitor reading. For this purpose, it is necessary to know the neutron energy dependence of the cross section σ of the reaction $Cu^{63}(n, 2n)Cu^{62*}$, and the form of the energy spectrum of the photoneutrons from a target irradiated by bremsstrahlung with different maximum γ-quantum energies, $E_{\gamma max}$.

The dependence of σ on the neutron energy is sufficiently well known.[3] Information on the energy spectra of photoneutrons is limited. Only the energy spectrum of photoneutrons emitted from the C^{12} nucleus in the photodecay of bremsstrahlung with $E_{\gamma max} = 88$ Mev has been studied.[4] However, the dependence of the cross section of the reaction $C^{12}(\gamma, n)C^{11}$ on the energy of the γ rays is known.[5] On the basis of available data,[3,5] we can compute the energy spectra of the photoneutrons, assuming that the product nucleus in the reaction $C^{12}(\gamma, n)C^{11}$ remains in the ground state or in a weakly excited state. The results of the study of the reaction $C^{12}(\gamma, p)B^{11}$ can serve as the basis of such an assumption.[6] Calculations have shown that the shapes of the energy spectra of fast neutrons emitted by a C^{12} nucleus

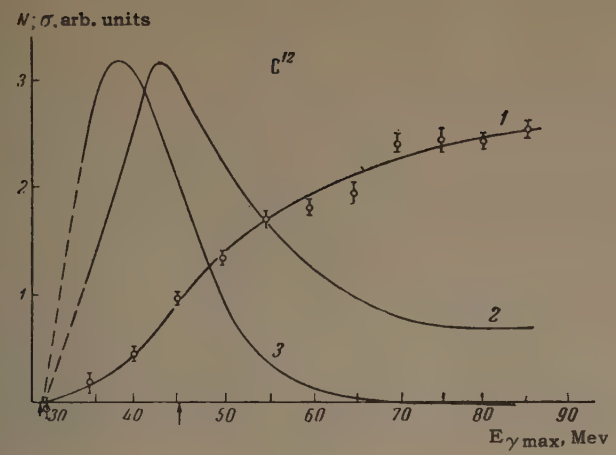

FIG. 1

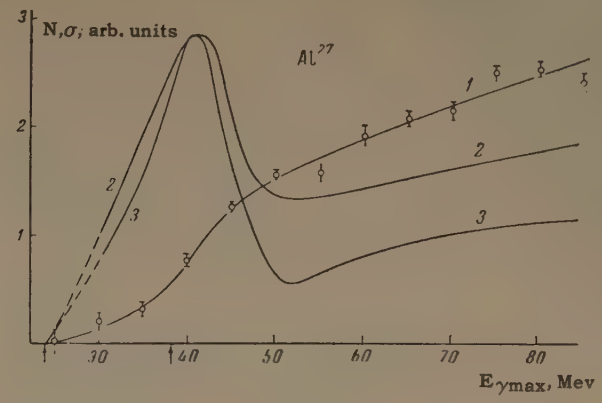

FIG. 2

are virtually identical for different $E_{\gamma max}$ over a rather wide range of values of the latter. Therefore, it was taken into account in the treatment of the experimental data for C^{12} that the neutron spectrum in the case $E_{\gamma max} = 85$ Mev decays as E^{-n} with $n = 1.5$, as was found by us earlier.[4] The same form of the neutron spectrum was assumed for all values of $E_{\gamma max} < 85$ Mev. Measurements of the energy spectrum of fast photoneutrons from Al^{27} were not carried out in the energy range studied. Experimental points of the yield for Al^{27} were computed by us, initially under the assumption that the neutron spectrum decays in the same way as in the case of C^{12} ($\sim E^{-1.5}$), and then under the assumption of a spectrum of the form $E^{-2.5}$, which corresponds approximately to the decay of the spectrum of protons from the Al^{27} nucleus.[7]

The cross sections were determined by the method of Penfold and Leiss.[8] They were computed from the yield curves, which were drawn through the experimental points and smoothed according to their first differences.

The results obtained for C^{12} are plotted in Fig. 1. The experimental points represent the number of fast neutrons N with energy > 11 Mev per unit reading of the monitor for a given $E_{\gamma max}$. The curve 1 is a smoothed one, drawn through the experimental points. The curve of the cross section of all the fast neutrons (> 11 Mev), calculated on the basis of curve 1, is given by curve 2, and the cross section for photoneutrons in the energy range 11 — 21 Mev is shown by curve 3.

The results of an experimental investigation of photoneutrons with energies > 11 Mev are given in Fig. 2 for the case of Al^{27}. The computed curves 2 and 3 are constructed under the assumption that the spectrum of photoneutrons decays according to the laws $E^{-1.5}$ and $E^{-2.5}$, respectively.

In both drawings, the arrows at the left on the abscissa indicate the energy threshold of the reaction (γ, n) with emergence of a neutron having the energy 11 Mev (minimum recording energy, E_n^{min}). The arrows to the right show the energy of a γ quantum, E_γ, necessary for the formation of a neutron with energy E_n^{min} under the condition that there exists a quasideuteron mechanism of γ quantum absorption. In this case, E_γ was computed according to a formula obtained from the conservation laws for the photodecay of a deuteron

$$E_\gamma = 2E_n/[1 - E_n/Mc^2 + (P/Mc)\cos\vartheta],$$

where $E_n = E_n^{min} + E_0/2$ [E_0 is the threshold of the reaction (γ, pn)], M is the mass of the neutron, P is the momentum of the neutron, c is the speed of light, and ϑ the angle of flight of the neutron relative to the direction of the γ quanta (in the laboratory system of coordinates).

As follows from Fig. 1, the cross section for all neutrons with energy 11 Mev in the case of the C^{12} nucleus is a curve with a broad maximum, which falls off slowly in the high-energy region. For a narrower range of energies of recorded neutrons, one can expect a contraction of the cross section curve and its displacement in the direction of lower energies, which is also confirmed by curve 3 in the same drawing. The experimentally measured threshold for formation of neutrons with energies > 11 Mev is in excellent agreement with the value computed under the assumption that a neutron with energy 11 Mev is produced in the single-particle reaction $C^{12}(\gamma, n)C^{11}$.

An important part of the curves, especially for curve 3, lies below the region corresponding to the quasideuteron mechanism. It obviously can be shown that an important part of the curves lies in an energy range where emission of only a single neutron is possible from the nucleus without the simultaneous emission of a proton. It is known that the difference in the thresholds of the reac-

tions (γ, n) and (γ, np) is equal to ~ 9 Mev. If we take it into account that in the emission of the neutron the C^{11} nucleus remains in an excited state in half the cases (by analogy with the results of the study of the reaction $C^{12}(\gamma, p)B^{11}$,[6] and also consider the great width of the energy recording range, then we see that in the region close to the right-hand arrow there should be very few neutrons accompanied by an emission of protons.

Similar conclusions can be drawn relative to the results for Al^{27} shown in Fig. 2, although here some difference is observed from the results for C^{12} (the width of the maximum is significantly less and, in the region of high energies, an increase in cross section is observed).

In conclusion, it can be shown that the value of the threshold for production of fast photoneutrons and the existence of a broad maximum in the region of comparatively low energies of the γ quanta indicate the predominance of a mechanism for which only a single fast neutron is emitted from the nucleus in the reaction (γ, n). However, it is impossible to deny that the quasideuteron absorption mechanism plays a substantial role in the region of energies of γ quanta behind the broad maximum.

It should be observed that the cross sections of the reaction (γ, n) are of the same form as those of the (γ, p) reaction for the C^{12} nucleus.[9] In this case the experimental points on the yield curves of the reaction (γ, n) reveal a break for high energies of the γ quanta, corresponding to the inflexion in the yield curve for the (γ, p) reaction. This can serve as proof of the possibility of the existence of a second maximum in the cross section curves. However, this maximum is not shown in Fig. 1, since the cross section curve was computed on the basis of a smoothed yield curve.

The angular distribution and the values of the cross section for fast photoneutron production[4,10] do not agree with the calculations,[11] which are based on the single nucleon mechanism of absorption of γ quanta.

In previous researches,[4,10] qualitative agreement has been observed in the angular distributions of fast photoneutrons with calculations according to the quasideuteron model. However, the results of the present work show that the quasideuteron mechanism does not appear to be dominant for fast photoneutron production in the nuclei investigated. Recently, calculations of the cross sections of fast photonucleon production were carried out by Shklyarevskii on the basis of the shell model, with account of pair correlations of nucleons in the nucleus. Account of pair correlations leads to the correct value of the cross section of fast photonucleon production; as calculations on a simplified model have shown, this makes it possible to explain qualitatively the shift forward in the angular distribution of fast photoneutrons.

[1] Seaborg, Perlman, and Hollander, Tables of Isotopes, Revs. Modern Phys. **25**, 469 (1953).

[2] A. P. Komar and S. P. Kruglov, J. Tech. Phys. (U.S.S.R.) **30**, 1369 (1960), Soviet Phys. Tech. Phys. **5**, 1299 (1961).

[3] Encyclopedia of Physics, **45**, Springer-Verlag, 1958, p. 507.

[4] L. A. Kul'chitskii and V. Presperin, JETP **37**, 1524 (1959), Soviet Phys. JETP **10**, 1082 (1960).

[5] Barber, George, and Reagan, Phys. Rev. **98**, 73 (1955).

[6] S. Penner and J. E. Leiss, Phys. Rev. **114**, 1101 (1959).

[7] Bazhanov, Volkov, and Kul'chitskii, JETP **35**, 322 (1958), Soviet Phys. JETP **8**, 224 (1959).

[8] A. S. Penfold and J. E. Leiss, Analysis of Photo Cross-Sections (University of Illinois, 1958).

[9] E. B. Bazhanov, JETP **38**, 267 (1960), Soviet Phys. JETP **11**, 193 (1960).

[10] L. A. Kul'chitskii and V. Presperin, JETP **39**, 1001 (1960), Soviet Phys. JETP **12**, 696 (1961).

[11] G. M. Shklyarevskii, JETP **36**, 1492 (1959), Soviet Phys. JETP **9**, 1057 (1959).

[12] G. M. Shklyarevskii, JETP **41**, 451 (1961), Soviet Phys. **14**, in press.

Translated by R. T. Beyer
14

EXCITED LEVELS OF Ne^{22}

A. M. ROMANOV, E. V. MYAKININ, and M. P. KONSTANTINOVA

Leningrad Physico-Technical Institute, Academy of Sciences, U.S.S.R.

Submitted to JETP editor February 13, 1961

J. Exptl. Theoret. Phys. (U.S.S.R.) **41**, 64-65 (July, 1961)

The levels of the Ne^{22} nucleus in the interval from 1 to 9 Mev are determined from the proton spectrum of the $F^{12}(\alpha, p)Ne^{22}$ reaction.

WE obtained information concerning the levels of Ne^{22}, especially above 3.3 Mev, by studying the energy spectra of protons emitted at the laboratory angles 60° and 90° from the reaction $F^{19}(\alpha, p)Ne^{22}$. The α-particle energies were 10.3, 13.6, and 14.7 Mev. The experimental arrangement and the treatment of the experimental results were the same as in [1]. The target was a 1.3-mg/cm^2 tetrafluoroethylene film positioned at a 45° angle to the α-particle beam. Protons were registered on Ya-2 photographic plates. The mean energies of proton groups were determined from the range-energy curves for aluminum and nuclear emulsion. We used as reference points the energy of protons from $C^{12}(\alpha, p)N^{15}$ ($Q_0 = -4.965$ Mev) and of the p_2 proton group from $F^{19}(\alpha, p)Ne^{22}$, emitted when Ne^{22} is formed in its second excited state.

Our results for the Ne^{22} energy levels are compared in the table with values given in [2] and [3]. Levels at 6.37, 7.52, and 8.54 Mev are here reported for the first time. Our value for the third excited level agrees with [3] but differs considerably from [2].

Our data	Reference 2	Reference 3
1.30±0.05	1.28	1.3
3.36±0.05	3.3	3.3
4.46±0.10	4.9	4.4
5.30±0.10	—	5.4
5.76±0.15	—	5.7
6.37±0.12	—	—
7.52±0.15	—	—
8.54±0.15	—	—

In all instances the intensity of p_0 protons (associated with the formation of Ne^{22} in its ground state) was considerably lower than that of protons accompanying Ne^{22} formation in the first and second excited states. The p_1 intensity was 6 — 12 times greater than the p_0 intensity. This effect is apparently associated with the character of the shell structure in the initial F^{19} and final Ne^{22} nuclei. It should also be noted that in the case of the reaction $Al^{27}(\alpha, p)Si^{30}$ investigated by us previously [1] the energy spectra were similar, but the angular distributions of p_0 and p_1 protons indicated that direct interactions played a considerable role.

Note added in proof (June 15, 1961). A recent paper by Martin et al. [Phys. Rev. **121**, 866 (1961)] reports Ne^{22} levels up to 7.5 Mev, which agree with our results.

[1] A. M. Romanov, JETP **39**, 1540 (1960), Soviet Phys. JETP **12**, 1072 (1961).

[2] Foster, Stanford, and Lee, Phys. Rev. **93**, 1069 (1954).

[3] T. R. Ophel and I. F. Wright, Proc. Phys. Soc. (London) **71**, 389 (1958).

Translated by I. Emin
15

EXCITATION OF NUCLEAR ROTATIONAL LEVELS IN μ-MESIC ATOMIC TRANSITIONS

G. E. BELOVITSKII

P. N. Lebedev Physics Institute, Academy of Sciences, U.S.S.R.

Submitted to JETP editor February 14, 1961

J. Exptl. Theoret. Phys. (U.S.S.R.) 41, 66-70 (July, 1961)

The occurrence of Coulomb excitation of nuclear rotational levels in the U^{238} nucleus accompanying μ^--mesic atomic transitions is established by means of the thick nuclear emulsion technique. The probability of this process has turned out to be ~ 0.5 in satisfactory agreement with the theoretically expected value.

SLOW μ^- mesons brought to rest in a medium are captured by atoms forming a bound system consisting of a μ-mesic atom in a highly excited state. Transition to the 1s ground state takes place by means of a cascade process. The energy of the μ-mesic atomic transitions is expended in the emission of Auger electrons and of x rays.

In the case of μ-mesis atomic transitions to the 2p state in mesic atoms with highly deformed nuclei ($155 < A < 185$ and $A > 225$) there exists an additional interaction of the μ^- meson with the quadrupole moment of the nucleus. As a result of this, in the case of such transitions the probability for the excitation of low lying nuclear rotational levels[1,2] is high (~ 0.5). There exists a low probability (~ 0.05) for the excitation of rotational levels also in the case of transitions to the 3d state, but such excitation does not take place at all in the case of transitions to the 1s state.[1]

The lifetime of the first excited level of a heavy nucleus ($\leq 10^{-9}$ sec) is considerably shorter than the lifetime of a μ^- meson in its K shell prior to its capture (~ 10^{-7} sec). Therefore, the nucleus has time to make the transition to its ground state before the μ^- meson is captured by the nucleus. A measurement of the number of corresponding γ quanta and conversion electrons normalized per μ^--meson capture yields directly the probability of Coulomb excitation of the nucleus W_μ.

The probability W_μ depends both on the magnitude and on the sign of the intrinsic quadrupole moment of the nucleus Q_0. Therefore, a measurement of W_μ enables us, in principle, to determine one of these two quantities, for example, the sign of the quadrupole moment Q_0, if its absolute value is known. In nuclei for which the first excited state is not a purely rotational state, W_μ also depends on the quadrupole moment of the excited state.

Another possible method of determining all the characteristics of the quadrupole moment consists of measuring the hyperfine structure of the $2p \rightarrow 1s$ γ transitions due to the splitting of the fine structure of the 2p level caused by the interaction of the μ^- meson with the quadrupole moment of the nucleus. As a result of the stringent requirements on the degree of accuracy in the measurement of the energy of the γ quanta (1%) such experiments also have not been performed to date. Both types of experiments are of considerable interest, since no other methods of determining the sign of Q_0 are known at the present in the case of even-even nuclei.

1. EXPERIMENTAL PROCEDURE AND RESULTS

In the present work an experimental attempt is made for the first time to observe the Coulomb excitation of rotational levels of U^{238} nuclei accompanying μ^--mesic atomic transitions. The energy of the first rotational level (2^+) in U^{238} is 45 kev. Transitions to the ground state occur entirely by means of conversion. Conversion is possible only from L and higher shells. The energy of conversion electrons from the L shell amounted to 25 — 28 kev, and from the M shell amounted to 40 kev.

The effect under investigation was studied by observing conversion electrons. Photoplates NIKFI-R of 200 μ thickness were used to record the electrons. To achieve more reliable recording and greater accuracy in the measurement of the ranges of slow electrons the plates were first treated with a solution of triethanolamine which produced a grain density in relativistic electron tracks up to 50 per 100 μ. Then photoplates doped with uranyl acetate[3] were irradiated by the beam of slow μ^- mesons produced by the synchrocyclotron of the Joint Institute for Nuclear Research.[4]

The capture of a μ^- meson in uranium was identified by means of the fission of the uranium nucleus to which it gives rise. Emission of one or more electrons from the point at which fission occurred was frequently observed.

The energy of the electrons was determined from their range. The range-energy curve was calibrated at one point (~ 30 kev) by means of conversion electrons accompanying the α decay of uranium isotopes as observed in the same photoplates. The accuracy of energy determination is 15%. The efficiency for recording electrons of the given energy has turned out to be close to 100%.

We have analyzed 220 cases of fission of uranium nuclei by μ^- mesons and we have determined the energy of all the electrons emitted from the point at which fission occurs. We have selected only electrons of energy > 20 kev. This has enabled us to exclude the Auger electrons emitted as a result of filling a vacancy in the L and higher shells.

Electrons of energy > 20 kev can be produced in three ways: excitation of rotational levels, mesic atomic transitions and nuclear fission. The existing theories of the Auger effect in mesic atoms do not allow us to calculate exactly the number of electrons emitted in a mesic atomic transition in an atom of given Z. Therefore, electrons arising in μ^--mesic atomic transitions in uranium were eliminated by means of comparison with the number of electrons per π^- meson stopped in uranium ($\bar{N}_\pi$). Even if π^- mesons do give rise to excitation of rotational levels in a uranium nucleus this process cannot be observed since nuclear capture of a π^- meson occurs in a time which is much shorter than the lifetime of the 2^+ excited level. But the nature of mesic atomic transitions does not depend on the nuclear properties of the mesons and must be the same both for μ^- and π^- mesons.

The number of electrons per π^- meson stopped in uranium was determined in the same manner as in the case of μ^- mesons. On plates irradiated by a beam of slow π^- mesons we have analyzed 132 cases of fission of a uranium nucleus by π^- mesons, and we have determined the energy of all the electrons emitted from points at which fission has occurred.

The fission of uranium nuclei is accompanied by a rearrangement of the electronic shell structure and by other processes as a result of which electrons can be emitted from the point at which fission occurs. In order to determine the number of such "parasitic" electrons control experiments were carried out involving the fission of U^{238} nuclei by 14-Mev neutrons and of U^{235} nuclei by thermal neutrons.

In the case of neutron-induced fission of uranium nuclei it is impossible to determine the point at which fission occurs. However, it is known [5] that the ratio of the ranges l_l of the light and l_h of the heavy fragments satisfies $l_l / l_h \leq 2$. Therefore, it was assumed that fission is accompanied by the emission of an electron if the ratio of the ranges measured for a point from which the emission of an electron is observed satisfies the condition $l_l / l_h \leq 2$. It turned out that fission brought about both by thermal neutrons (600 cases) and by 14-Mev neutrons (500 cases) is accompanied in $\sim 3\%$ of the cases by the emission of $20 - 50$ kev electrons (50 kev electrons were observed in 1% of the cases). This is approximately 10 times less than the number of electrons observed when the fission of uranium nuclei is induced by μ^- and π^- mesons. This result was used in evaluating the true number of electrons per μ^- meson and per π^- meson stopped in uranium.

Control experiments were also carried out with Ag and Br nuclei.

In the slightly deformed Ag and Br nuclei the value of Q_0 is approximately 10 times smaller than in uranium, and this, taken together with a number of other factors, leads to a low probability for Coulomb excitation to accompany μ^--mesic atomic transitions. It follows from general considerations that in such nuclei the number of observed electrons emitted in mesic atomic transitions increases with increasing meson mass. This had been previously demonstrated in experiments involving π^- and K^- mesons. [6]

Below we exhibit results obtained by us for μ^- and π^- mesons. In the same photoplates in which we have observed the fission of uranium nuclei by μ^- and π^- mesons, we have also found and analyzed 1,000 μ^- mesons brought to rest and 850 stars with one or more prongs due to π^- mesons.

Capture of μ^- mesons by AgBr nuclei was inferred from the absence of the electron arising from $\mu \rightarrow e$ decay as was done, for example, in Fry's paper. [7] It turned out that 60% of the mesons are captured by AgBr nuclei. According to the data of Brown and Hughes, [8] 56% of the stars with one or more prongs, induced by π^- mesons, come from AgBr nuclei. An analysis of stars accompanied by the emission of Auger electrons of mesic atomic origin has shown that with rare exceptions they all come from AgBr nuclei. This last result is in good agreement with the results of other papers, for example [9].

Nucleus	Kind of meson	20–50 kev	> 50 kev	$\bar{N}_\mu/\bar{N}_\pi$ (for 20–50 kev electrons)	
				experimental value	calculated value
U	μ^-	0.65±0.08	0.22±0.04	2.3 ±0.7	~0.8
	π^-	0.28±0.06	0.15±0.04		
AgBr	μ^-	0.15±0.02	0.14±0.02	0.58±0.14	~0.75
	π^-	0.26±0.03	0.19±0.02		

The table shows experimental data on the average number $\bar{N}$ of electrons of 20 — 50 kev and > 50 kev energy evaluated per μ^- meson and per π^- meson stopped by AgBr and by uranium nuclei (after the background due to the "parasitic" electrons has been subtracted). The table also gives experimental and theoretical values of $\bar{N}_\mu/\bar{N}_\pi$ for uranium and for AgBr (for 20 — 50 kev electrons).

The calculation of $\bar{N}_\mu/\bar{N}_\pi$ was carried out in the following manner. The energy levels for μ^- and π^- mesons in mesic atoms of Ag, Br, and uranium, and also the energies of the mesic atomic transitions were calculated on the assumption that $\Delta n = \Delta l = 1$, where n and l are the principal and the orbital quantum numbers. In evaluating the internal-conversion coefficients for each transition theoretical results on mesic atomic transitions were utilized.[10,11]

2. DISCUSSION OF RESULTS

From the table it can be seen that for uranium $\bar{N}_\mu > \bar{N}_\pi$, while for AgBr, as should have been expected, $\bar{N}_\mu < \bar{N}_\pi$. The values of $\bar{N}_\pi$ for uranium and for AgBr have turned out to be close to each other, and this is due to the weak dependence of the Auger effect on Z.

The value of $\bar{N}_\mu$ for uranium for 20 — 50 kev electrons is approximately four times larger than for AgBr. This difference can be due to: a) Coulomb excitation of nuclear rotational levels in uranium, b) excitation of the nucleus as a result of direct transfer to the nucleus of the energy of the 2p → 1s mesic atomic transition.

The latter process was discussed in the theoretical paper of Zaretskii.[12] Its probability in U^{238} was measured in the paper by Balats, Kondrat'ev, et al.[13] and has turned out to be equal to (0.23 ± 0.04). In the case of such excitation the energy transferred to the nucleus is 6.3 Mev and this can be expended in the emission of a neutron, γ rays and conversion electrons. The latter are, perhaps, responsible for the slight excess in uranium of the number $\bar{N}_\pi$ over $\bar{N}_\mu$ for electrons of energy > 50 kev (in AgBr in the case of electrons of energy > 50 kev the opposite inequality $\bar{N}_\mu < \bar{N}_\pi$ holds).

For the experimentally observed probability of excitation of rotational levels we obtain the value

$$(W_\mu)_{obs} = (\bar{N}_\mu)_U - \left(\frac{\bar{N}_\mu}{\bar{N}_\pi}\right)_{AgBr} (\bar{N}_\pi)_U = 0.5 \pm 0.1. \quad (1)$$

The true value of the probability W_μ can be obtained from $(W_\mu)_{obs}$ in the following manner:

$$(W_\mu)_{obs} = W_\mu (1 - 0.23) + 0.23\ \alpha, \quad (2)$$

where α is the probability that the transition from the excited (6.3 Mev) to the ground level will take place via the first excited level of the U^{238} or U^{237} nucleus. On substituting into (2) the value $(W_\mu)_{obs}$ we obtain

$$W_\mu = 0.65 - 0.3\ \alpha,$$

and since $0 < \alpha < 1$, then $0.35 < W_\mu < 0.65$. The spin and parity of the excited (as a result of the 2p → 1s transition) U^{238} nucleus are given by 1^-. If a neutron is not emitted by the nucleus then transitions to the ground state (0^+) or to the first excited state (2^+) will apparently be equally probable. From this it follows that $\alpha = 0.5$. However, if a neutron is emitted then U^{237} is formed for which the value of the spin in the excited state is unknown.

Apparently, we can assume without gross error that $\alpha = 0.5$ in all cases, so that $W_\mu = 0.5 \pm 0.1$. Thus, it is quite probable that the excitation of the nucleus as a result of the 2p → 1s transition does not appreciably alter the value of W_μ.

The theoretical values[1] of W_μ for $Q_0 > 0$ and $Q_0 < 0$ are respectively equal to 0.5 and 0.4. Therefore, in order to obtain a definitive solution of the problem of the sign of Q_0 it is necessary to increase the experimental accuracy of the determination of W_μ and to eliminate reliably the influence of side effects. Moreover, it is desirable to know more accurately the theoretical value of the probability of excitation of rotational levels from the 3d state.

The high value of W_μ (~ 0.5) makes experiments of such type for the determination of the sign of Q_0 appropriate in the case of even-even nuclei. These experiments can also be carried out using pure samples of the elements in a Wilson

cloud chamber or in a diffusion chamber, utilizing thin solid or gaseous targets.

The excitation of rotational levels in μ^--mesic atomic transitions leads to another effect discussed in the theoretical paper of Zaretskii and Novikov.[14] This effect consists of the fact that in deformed even-even nuclei as a result of the excitation of rotational levels the spin of the excited level turns out to be different from zero with a probability of ~ 0.5. This results in additional depolarization of μ^- mesons in transitions to the 1s state due to the hyperfine splitting of the 1s level.

I express my gratitude to I. M. Frank, I. Ya. Barit and F. L. Shapiro for valuable comments in the discussion of this work, and to V. P. Zavarzina and I. V. Surkova for aid in scanning the photoplates.

[1] L. Wilets, Kgl. Danske Videnskab. Selskab, Mat.-fys. Medd. **29**, 3 (1954).

[2] B. A. Jacobsohn, Phys. Rev. **96**, 1637 (1954).

[3] T. A. Romanova and L. D. Chikil'dina, Proc. Third International Conference on Nuclear Photography, Moscow, 1960 (in press).

[4] Belovitskii, Kashukeev, Mikhul, Petrashku, Romanova, and Tikhomirov, JETP **38**, 404 (1960), Soviet Phys. JETP **11**, 296 (1960).

[5] V. P. Shamov and O. V. Lozhkin, JETP **29**, 286 (1955), Soviet Phys. JETP **2**, 111 (1956).

[6] E. B. Chesick and J. Schneps, Phys. Rev. **111**, 1810 (1958).

[7] W. F. Fry, Nuovo cimento **10**, 490 (1953).

[8] G. Brown and J. S. Hughes, Phil. Mag. **2**, 777 (1957).

[9] A. O. Vaĭsenberg, JETP (in press).

[10] C. R. Burbidge and A. H. de Borde, Phys. Rev. **89**, 189 (1953).

[11] R. A. Ferrell, Phys. Rev. Letters **4**, 420 (1960).

[12] D. F. Zaretskii, Proc. Second International Conference on Peaceful Uses of Atomic Energy, Geneva, 1958. Reports by Soviet Scientists, v. 1, Moscow, Glavatom, 1959.

[13] Balats, Kondrat'ev, Lansberg, Lebedev, Obukhov, and Pontecorvo, JETP **39**, 1168 (1960), Soviet Phys. JETP **12**, 813 (1961).

[14] D. F. Zaretskii and V. M. Novikov, JETP **37**, 1824 (1959), Soviet Phys. JETP **10**, 1287 (1960).

Translated by G. Volkoff
16

ANGULAR DISTRIBUTION OF 6.8-Mev *PROTONS ELASTICALLY SCATTERED ON NICKEL AND ZIRCONIUM ISOTOPES*

A. K. VAL'TER, I. I. ZALYUBOVSKII, A. P. KLYUCHAREV, V. A. LUTSIK, B. F. ORLENKO, M. V. PASECHNIK, V. S. PROKOPENKO, and N. N. PUCHEROV

Institute of Physics, Academy of Sciences, Ukrainian S.S.R.; Physico-Technical Institute, Academy of Sciences, Ukrainian S.S.R.

Submitted to JETP editor February 17, 1961

J. Exptl. Theoret. Phys. (U.S.S.R.) **41**, 71-74 (July, 1961)

The angular distribution of 6.8-Mev protons elastically scattered by Ni^{64}, Zr^{90-92} and Zr^{96} nuclei is investigated. A large difference is found between the angular distributions of the various isotopes.

THE study of the scattering of medium-energy nucleons by atomic nuclei is a source of considerable information on the properties of atomic nuclei. Interest in experiments of this kind is greatly due to the development of the optical model of the nucleus. Very interesting results are those obtained from experiments on elastic scattering of protons by separated isotopes at energies below 10 Mev. A considerable difference was observed in the angular distributions even in scattering by neighboring isotopes.[1-5]

The fact that these effects cannot be fully described theoretically necessitates gathering additional experimental facts to permit subsequent generalization. It is natural to attempt to relate the difference in the scattering to the shell structure of nuclei.

The isotopes of nickel have filled proton shells ($Z = 28$). The filling of the neutron shells has the following singularity: the filling of the sublevel $2p_{3/2}$ ends with the isotopes N^{58} and Ni^{60}, and the filling of the sublevel $1f_{5/2}$ begins with Ni^{62}. The isotope Zr^{90} has filled neutron shells ($N = 50$), and completes the filling of the level $1g_{9/2}$. The sublevel $2d_{5/2}$ is filled for the following isotopes of zirconium.

It is therefore quite probable that the nuclei Ni^{62} and $Zr^{91,92,96}$ have a more "diffuse" surface, bringing about an increase in the absorption of neutrons by these nuclei.[6] An experimental manifestation of this is the fact that the differential cross section of elastic scattering at large angles is much less for Ni^{62} than for Ni^{58} and Ni^{60}, and is much greater for Zr^{90} than for the heavier zirconium isotopes.

From this point of view, great interest is attached to a study of the scattering on Ni^{64} and various isotopes of zirconium. The addition of the succeeding neutrons can be expected to "loosen" the surface of the nucleus even more and increase the probability of absorption of the incident protons. This should be accompanied by a reduction in the differential cross section in the region of large scattering angles.

The experimental procedure did not differ in principle from that described earlier.[5] However, several improvements were made to increase the measurement accuracy. Thus, the current of the protons incident on the target was measured with the aid of a current integrator. Simultaneously, the intensities of the scattered protons were measured with a scintillation spectrometer, mounted at an angle of 90° to the direction of the primary protons. Thus, a double check on the measurement of the intensity of the incident protons was accomplished.

The targets were thin free metallic foils, enriched with the investigated isotopes in the following fashion: Ni^{64}—79.8 per cent, Zr^{90}—96.1 per cent, Zr^{91}—73.5 per cent, Zr^{92}—88.6 per cent, and Zr^{96}—31.3 per cent.

MEASUREMENT RESULTS AND DISCUSSION

Nickel. The results of the measurements for Ni^{64} are shown in Fig. 1, in the form of the ratio of the measured scattering cross section to the Coulomb scattering cross section ($\sigma_{exp}/\sigma_{res}$) as a function of the scattering angle. The measurement error did not exceed 3 per cent. As can be seen from Fig. 2, where a comparison is made with the already known data for the other three nickel isotopes,[5] this ratio has the lowest values for Ni^{64} at the largest angles, apparently owing to the stronger absorption of the protons by the Ni^{64}

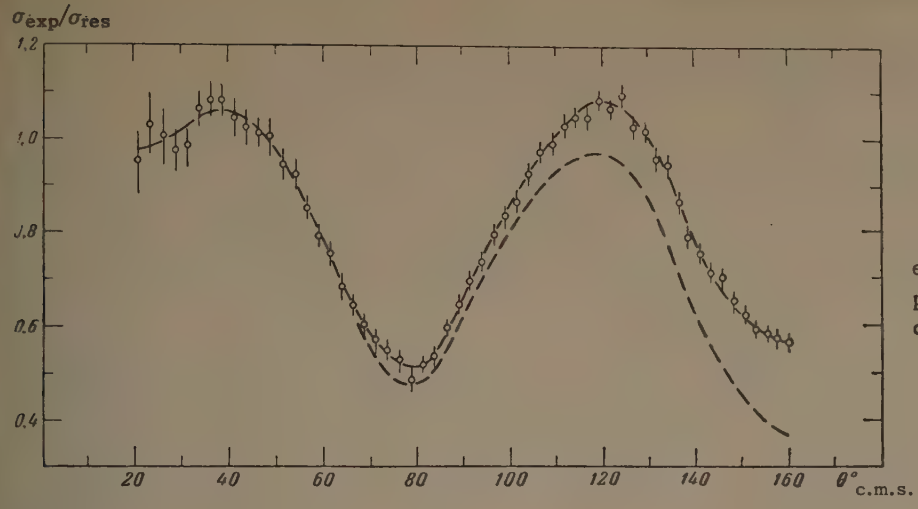

FIG. 1. Angular distribution of protons in elastic scattering on nickel enriched with 79.8 per cent Ni^{64}. The dotted curve has been recalculated for pure Ni^{64} ($E_p \approx 6.8$ Mev).

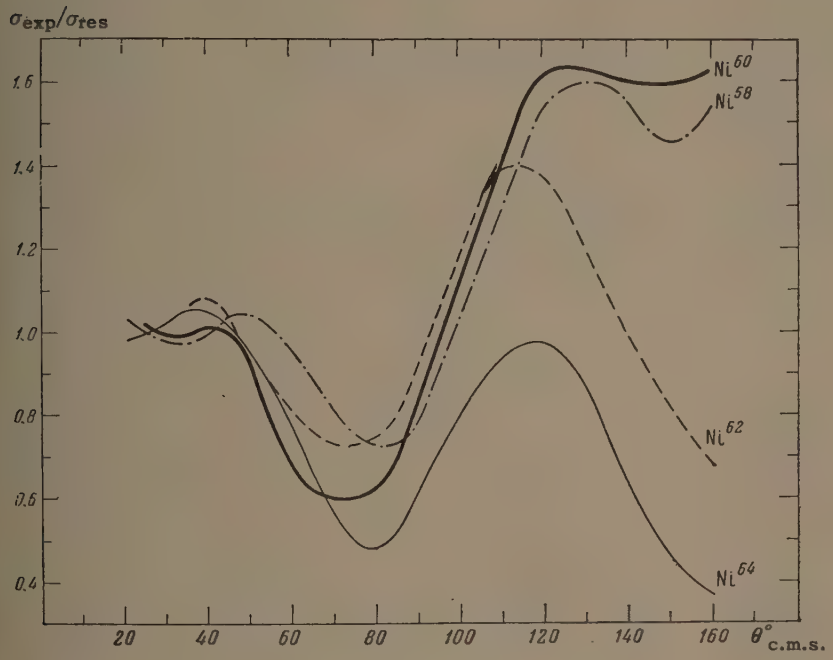

FIG. 2. Comparison of angular distributions of protons elastically scattered by different nickel isotopes, at $E_p = 6.8$ Mev.

nucleus, compared with other isotopes. An analogous result was observed earlier in the scattering of 5.4-Mev protons by the same isotopes.[4] We can therefore expect for Ni^{64} a much larger cross section for the reactions that compete with elastic scattering with capture. In particular, this takes place for the (p, n) reaction, the thresholds of which are 4.77 and 2.49 Mev for Ni^{62} and Ni^{64}, respectively.

Zirconium. In connection with the noticeable solubility of molybdenum in zirconium at high temperatures, molybdenum impurities were found in the zirconium targets. It was established by x-ray spectroscopy that this impurity is the same for all targets, 10 per cent by weight.

The results of the investigation of elastic scattering of 6.8-Mev protons by enriched zirconium targets are shown in Fig. 3. The ratio $\sigma_{exp}/\sigma_{res}$ is much higher for Zr^{90} than for the heavier isotopes in the large-angle region. Addition of merely one odd neutron to the Zr^{90} nucleus greatly reduces this ratio, which is much less in the maximum region than for Zr^{90}.

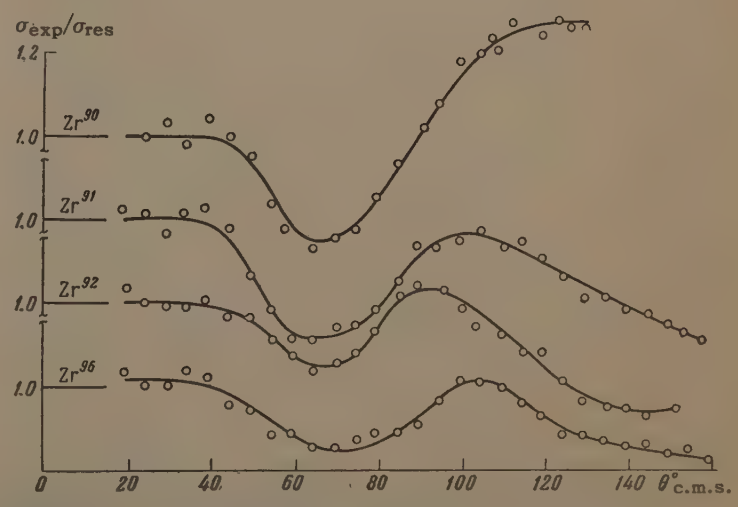

FIG. 3. Angular distribution of protons in elastic scattering by zirconium isotopes ($E_p = 6.8$ Mev).

Inasmuch as the enrichment of the target with

Zr^{96} was merely 31 percent, we can only note that in the large-angle region the cross section for the elastic scattering by this isotope is apparently much smaller than for scattering by light isotopes.

Our results on Zr^{90} and Zr^{91} agree with the results of an investigation of elastic scattering of 5.45-Mev protons by the same isotopes.[7]

Thus, in the scattering of protons by zirconium isotopes, a noticeable difference is observed in the course of the angular dependence of $\sigma_{exp}/\sigma_{res}$. A comparison of this course of the angular dependence with the magnitude of the (p, n) reaction threshold for the same isotopes again confirms the important role played by the reactions that compete with the (p, p) reaction with capture.

In conclusion, the authors are grateful to the cyclotron crew of the Institute of Physics of the Ukrainian Academy of Sciences for producing the proton beam.

The authors are grateful to Zh. I. Pisanko and A. G. Beletskii for help with the measurements, and also to A. D. Nikolaĭchuk and V. N. Medyanik for preparation of the targets.

[1] A. P. Klyucharev and N. Ya. Rutkevich, JETP **38**, 285 (1960), Soviet Phys. JETP **11**, 207 (1960).

[2] Rutkevich, Golovin, Val'ter, and Klyucharev, DAN SSSR **130**, 1008 (1960), Soviet Phys. Doklady **5**, 118 (1960).

[3] Vanetsian, Klyucharev, and Fedchenko, Atomnaya énergiya (Atomic Energy) **6**, 661 (1959).

[4] A. P. Kliutcharev, Proc. Intern. Conf. on Nuclear Structure, Univ. of Toronto Press, 1960, p. 169.

[5] Val'ter, Zalyubovskii, Klyucharev, Pasechnik, Pucherov, and Chirko, JETP **38**, 1419 (1960), Soviet Phys. JETP **11**, 1025 (1960).

[6] A. P. Klyucharev, Izv. AN SSSR, ser. fiz. **24**, 887 (1960), Columbia Tech. Transl. p. 888.

[7] Golovnya, Klyucharev, and Shilyaev, JETP **41**, 32 (1961), this issue, p. 25

Translated by J. G. Adashko
17

THE CROSS SECTION FOR PRODUCTION OF HYPERNUCLEI IN EMULSION BY 9-Bev PROTONS

I. B. BERKOVICH, A. P. ZHDANOV, F. G. LEPEKHIN, and Z. S. KHOKHLOVA

Radium Institute, Academy of Sciences, U.S.S.R.

Submitted to JETP editor February 17, 1961

J. Exptl. Theoret. Phys. (U.S.S.R.) **41**, 75-77 (July, 1961)

The cross section for the production of hypernuclei in NIKFI-R photographic emulsion exposed to 9-Bev protons is found to be $\sigma_{Hf} = (0.2 \pm 0.1)$ mb.

1. INTRODUCTION

A number of articles on hypernuclei have already been published. These articles deal mainly with the study of the decay of hypernuclei stopping in photographic emulsion. As a result, many valuable data have been obtained on the properties of Λ^0 particles in the bound state and on the character of the Λ^0N interaction. Only some of the articles (see for example, [1]) deal with questions connected with the mechanism of hypernucleus production. The study of the act of production of hypernuclei can give valuable information on strong interactions of nucleons in which strange particles are produced and on the character of the interaction of strange particles with each other, with nucleons, and with π mesons. Qualitative ideas on the mechanism of hypernucleus production are based on the assumption that the formation of hypernuclei is preceded by the production of Λ^0 particles along with other strange particles, and, possibly, π mesons in the elementary act of NN interactions. It is natural to begin a study of the mechanism of hypernucleus production with the determination of their production cross section and the dependence of this cross section on the energy of the bombarding protons. Blau[2] and Fry et al[3] have determined the frequency of production of hypernuclei by 3- and 6-Bev protons. In this article, we shall present an estimate of the cross section for this process in the case of 9-Bev protons.

2. EXPERIMENTAL METHOD

A stack of 400-μ NIKFI-R emulsion pellicles was exposed to 9-Bev protons from the proton synchrotron of the Joint Institute for Nuclear Research. The primary proton flux, estimated from a direct count of tracks over successive 34-μ intervals, 500 μ apart, with allowance for the change in thickness of the pellicle, was $(1.36 \pm 0.06) \times 10^5$ cm^{-2}. The emulsion was scanned under a magnification of $20 \times 1.5 \times 10$. All double stars were recorded. After scanning part of the material a second time and taking into account the geometrical conditions of observation of the stars and the connecting tracks, we were able to estimate the scanning efficiency on the basis of double stars missed in the scanning. In the entire scanned volume, 443 double stars were observed (without taking into account L-shaped tracks). They were all analyzed with a view to selecting hypernuclei.

The analysis was based on the laws of conservation of energy, momentum, and charge of the particles with the best possible determination of the charge, and measurement of the track lengths and angles between tracks. The charge was determined by the track-width method.*

In selecting the cases with hypernuclei from among the double stars, we excluded all cases of interaction of π^- and K^- mesons with nuclei on the basis of the law of conservation of charge; elastic pp interactions were eliminated by means of the law of conservation of momentum. Interactions between nuclei and emulsion nuclei were distinguished from hypernucleus decays by the track-width measurements. The thinning down of the connecting track was evidence of the stopping of the particle. Cases in which there was no thinning down of the connecting track were attributed to nuclear-nuclear interactions. In about 2% of the cases, the measurements could not give information on the thinning down (tracks $\leq 20\,\mu$ in length).

3. RESULTS

As a result of the analysis of all double stars, 20 cases were attributed to hypernuclei: 18 with nonmesic decay and 2 with mesic decay. It should be noted that we did not take into account cases

*Details on the track-width measurements in NIKFI-R emulsion will be presented in a separate report.

with L-shaped tracks, which are (except for scatters) either nonmesic decays of hypernuclei with Z = 1, 2 or π^0-mesic decays. These cases were very rare, and, in our opinion, do not make any essential contribution to the value of the cross section.

Most hypernuclei have a charge ≥ 3. The charge distribution was as follows:

Z:	1	2	3	>3
Number of hypernuclei:	2	3	6	9

The mean number of gray and black tracks in the parent stars with hypernuclei was 14 ± 1.4. This gives a basis to assume that all observed hypernuclei are produced as a result of the interaction of primary protons with heavy nuclei of the emulsion (Ag and Br).

The angular distribution of the hypernuclei (see figure) indicates that the direction of emission is preferentially in the forward hemisphere (i.e., in the direction of the primary proton. The ratio of the number of cases of forward emission to the number of cases of backward emission was 2.3, which is in good agreement with the data given in Silverstein's survey.[1]

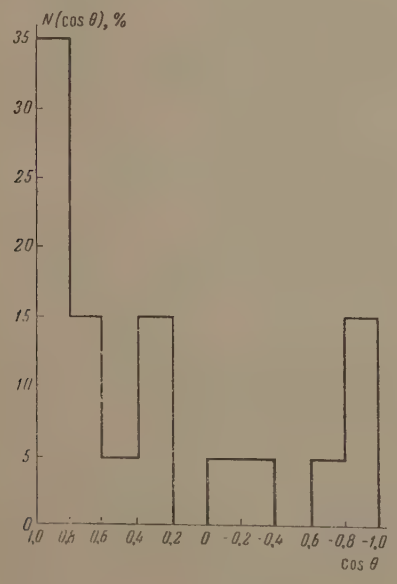

4. DISCUSSION OF RESULTS

The cross section determined by us, after all corrections, was $\sigma_{Hf} = 0.2 \pm 0.1$ mb.

If we compare this value with the cross section for the production of free Λ^0 particles,[4] then it turns out that $\sigma_{\Lambda^0}/\sigma_{Hf} \approx 15$. This apparently indicates that only a small part of the produced Λ^0 particles give rise to hypernuclei. Blau[2] and Fry et al[3] at 3 Bev and 6 Bev, respectively, observed 14 and 7 hypernuclei out of 14 480 and 10 000 stars; the corresponding frequencies of hypernuclei per star were 1×10^{-3} and 0.7×10^{-3}. Comparison with our data indicates that the hypernucleus production cross section in the 3 — 9 Bev region decreases with an increase in the primary proton energy. In all probability, this decrease in cross section is connected with the decrease in the cross section for NN interactions[5] and the decrease in cross section for the production of Λ^0 particles with an increase in energy of the primary nucleon.

[1] E. M. Silverstein, Nuovo cimento Suppl. **10**, 41 (1958).

[2] M. Blau, Phys. Rev. **102**, 495 (1956).

[3] Fry, Schneps, and Swami, Phys. Rev. **101**, 1526 (1956).

[4] Belyakov, Glagolev, Kirillova, Mel'nikova, Suk, and Tolstov, Preprint R-434, Joint Institute for Nuclear Research, 1959.

[5] V. I. Veksler, Report at the Ninth Annual Conference on High Energy Physics at Kiev, 1959.

[6] Barashenkov, Barbashov, and Bubelev, Statisticheskaya teoriya mnozhestvennogo rozhdeniya pri stolknovenii bystrykh nuklonov (Statistical Theory of Multiple Production in the Collision of Fast Nucleons), Preprint, Joint Institute for Nuclear Research, 1958.

Translated by E. Marquit
18

INTERACTION OF 78-Mev π^+ MESONS IN PROPANE

R. G. SALUKVADZE and D. NEAGU

Joint Institute for Nuclear Research

Submitted to JETP editor February 16, 1961

J. Exptl. Theoret. Phys. (U.S.S.R.) **41**, 78-80 (July, 1961)

The interaction of π^+ mesons of 78 ± 3 Mev with hydrogen and carbon was studied in a bubble chamber. The scattering cross sections on hydrogen and carbon and the absorption cross section in carbon were determined. The prongs of the stars formed in the absorption of a meson go predominantly forward. This points to the existence of quasi-elastic collisions of the mesons in the nucleus prior to their absorption.

WE have investigated the interaction of π^+ mesons with hydrogen and carbon at the synchrocyclotron of the Joint Institute of Nuclear Research by means of a small propane bubble chamber.[1] The energy of the π^+ mesons and the admixture of positrons and μ mesons to the beam, η, were determined by range measurements in polyethylene. These values were obtained: $E_{\pi^+} = (78 \pm 3)$ Mev; $\eta = (25 \pm 2)\%$. In 2852 stereoscopic pictures we found 400 interactions. The scanning efficiency was 0.90 ± 0.03. The results are given in Table I. The scattering from hydrogen and carbon was investigated for scattering angles $\theta \geq 41°$. The cross sections agree with the known values contained in the literature (see, e.g., the review article by Barkov and Nikol'skii[2]).

The experimental value of the cross section for reaction (4) (Table I) includes the process of exchange scattering and absorption of the mesons. Taking into account that the exchange scattering cross section of π^- mesons on hydrogen at 79 Mev equals 15 mb,[2] one has $\sigma_{abs} = 180 \pm 20$ mb and a mean free path $\lambda_{abs} = (7.6 \pm 0.9) \times 10^{-13}$ cm.

The mean number of prongs of the stars is $\bar{f} = 2.50 \pm 0.18$. Comparison with the data of different investigations[4,5] shows that this distribution depends very little on the energy of the π^+ mesons (Table II).

Among the two-prong stars 36 of the 92 events have an angle between the emitted protons of > 140° which allows to classify them as due to absorbtion of the meson by an n-p pair. If one takes into account the collisions of the protons in the nucleus and one considers that capture of mesons by an n-n pair is 2 — 3 times less probable than by an n-p pair,[6] it follows from the experimental data that approximately in 70% of the cases mesons are absorbed by nucleon pairs. This agrees well with the estimates obtained by different authors.[7,8]

The angular distribution of the prongs (see Table II) has a forward-backward asymmetry with respect to the incoming π^+ beam: about 30% more prongs go forward than backward. The asymmetry coefficient $\xi = 2(N_\rightarrow - N_\leftarrow)/(N_\rightarrow + N_\leftarrow)$ decreases with increasing number of prongs in the star. (Here $N_\rightarrow$ and $N_\leftarrow$ is the number of prongs going forward and backward respectively).

The similarity of the experimental conditions and of the analysis between the present work and Ref. 4 allows also to determine the weighted mean value of the asymmetry coefficient. It is also given in Table II.

A large contribution to the anisotropy of single prong stars certainly is due to protons leaving the nucleus as a result of the exchange scattering process ($\pi^+ + n \rightarrow \pi^0 + p$). The anisotropy of the other stars and the character of its dependence on the prong number must be connected with the meson absorption mechanism. The appearance of a large isotropic "background" (more than 30% of the total number of prongs) of low energy prongs (E < 15 Mev) indicates that the mesons sometimes are absorbed by a large cluster of nucleons or by the nucleus as a whole. The overall anisotropy of the prongs can be explained by quasi-elastic collisions of the meson in the nucleus before its absorption. This has been already suggested in Ref. 4. It should be mentioned that any reasonable assumptions concerning the meson absorption mechanism must also lead to an anisotropy of the emitted particles and fragments (the meson-nucleus system contains forward momentum). However, no other assumption (e.g., absorption of the meson by the nucleus as a whole) can yield an anisotropy in the distribution of the emitted protons. Evidently, the angular distribution of the residual nuclei could

Table I. Cross section of π^+ mesons of 78 Mev with hydrogen and carbon

Reaction	Number of events	σ_{exp}, mb	Remarks	σ, mb
(1) $\pi^+ + p \to \pi^+ + p$	72	36± 5	$\theta_{\pi^+} \geqslant 41°$ (lab syst.)	$\sigma_{el}(0° - 180°) = 39 \pm 6$ [3]
(2) $\pi^+ + C \to \pi^+ + C$ (3) $\pi^+ + C \to \pi^+ + A + f$ prongs $f = 0,1,2,\ldots$	177	166±14	$\theta_{\pi^+} \geqslant 41°$ (lab syst.)	
Absorption and exchange scattering: (4) $\pi^+ + C \to A + f$ prongs $f = 1,2,\ldots$	201	195±20	$\delta(\pi^+ \to \pi^0) = 15$ mb [2]	$\sigma_{abs} = 180 \pm 20$

Table II. Distribution of the prong number and asymmetry coefficient

	Number of prongs in star							E_{π^+}, Mev	Reference
	1	2	3	4	5	6	7		
Number of stars	17	45 (+8) *	35	14	2	1	1	250—270	[5]
	9 (+14) *	66 (+18) *	58 (+5) *	32	8	—	—	~50	[4]
	24	92	56	21	6	2	—	78	[**]
Asymmetry coefficient ξ	0.50 ± 0.30	0.26 ± 0.12	0.18 ± 0.13	0.14 ± 0.18	0.14 ± 0.31	—	—	78	[**]
	0.90 ± 0.23	0.44 ± 0.10	0.46 ± 0.09	0.28 ± 0.10	0.28 ± 0.20	—	—	50—80	[4] and [**]

*The error is due to the uncertainty in the prong number.
**This paper.

give additional evidence concerning the meson absorption mechanism.

The authors express their sincere gratitude to A. M. Pontecorvo for his interest in this work. They also are indebted to N. I. Petrov for useful criticisms.

[1] D. Neagu and R. G. Salukvadze, Proc. Physics Inst. Acad. Sci. Georgian S.S.R. (in press).

[2] L. M. Barkov and B. A. Nikol'skii, Usp. Fiz. Nauk **61**, 341 (1957).

[3] Anderson, Fermi, Nagle, and Yodh, Phys. Rev. **86**, 413 (1952); **91**, 155 (1953).

[4] Laberigue-Frolova, Balandin, and Otvinovskii, JETP **37**, 634 (1959), Soviet Phys. JETP **10**, 452 (1960).

[5] Wang Kang-Ch'ang, Wang Tso-Tsiang, Ding Ta-Tsao, Dubrovskii, Kladnitskaya, and Solov'ev, JETP **35**, 899 (1958), Soviet Phys. JETP **8**, 625 (1959).

[6] Petrov, Ivanov, and Rusakov, JETP **37**, 957 (1959), Soviet Phys. **10**, 682 (1960).

[7] Byfield, Kessler, and Lederman, Phys. Rev. **86**, 17 (1952).

[8] F. N. Tenney and J. Tinlot, Phys. Rev. **92**, 974 (1953).

Translated by M. Danos
19

THE EFFECT OF UNILATERAL COMPRESSION ON THE ELECTRICAL PROPERTIES OF p-TYPE GERMANIUM AT LOW TEMPERATURES

M. A. IL'INA and I. A. KUROVA

Moscow State University

Submitted to JETP editor February 22, 1961

J. Exptl. Theoret. Phys. (U.S.S.R.) 41, 81-82 (July, 1961)

The resistance, Hall constant, and the variation of resistance in a magnetic field were measured at temperatures between 4.2 and 3.7° K for p-type Ge subjected to unilateral compression. The change in conductivity of hole type Ge caused by the pressure is due both to a variation in the number of carriers in the band and to a change in their mobility. The sign of the deformation potential is determined from the ratio of the mobilities for different crystallographic directions.

UNDER a unilateral deformation the valence band in germanium, which is fourfold degenerate in the normal state, is split into two doubly degenerate bands and is deformed. This produces a change in the electrical properties of p-type germanium. Several works[1-6] have been devoted to a study of the effect of unilateral deformation on the electrical properties of p-type germanium. The problem has been most fully considered theoretically by Pikus and Bir.[5] Smith[1] and Morin et al[2] studied the change of resistivity on deformation and its temperature dependence down to 20° K.

The purpose of the present work was to study the electrical properties at lower temperatures, where the effects should be greater and should have some features pointed out by Pikus and Bir. After this investigation had started, we heard of the work of Koenig and Hall[6] in which the electrical properties of p-type germanium under unilateral compression in the [111] and [100] directions were studied down to 4.2° K. Our results are in general agreement with their data and the sign of the deformation potential d agrees with the sign determined by Koenig.

We measured the resistance, Hall constant, and the variation of resistance in a magnetic field for unilateral compression, on p-type germanium having $\rho = 20$ ohm-cm at room temperature. The measurements were carried out at temperatures from 4.2 to 3.7° K. In this temperature range the conductivity of such specimens is due to holes in the valence band, and the impurity band conductivity does not show up, as is indicated by the exponential variation of the resistivity and Hall constant with decreasing temperature. The temperature range is limited by the value of the resistivity of the specimen: for $T < 3.7°$ K we have $R > 10^{12}$ ohm, and measurement becomes difficult. Measurements were made in the direction of the deformation, [110], and perpendicular to it, along [$\bar{1}$10]. The load varied from zero to 600 kg/cm^2 and was produced by beryllium bronze springs.*

The measurements were carried out in an apparatus thoroughly shielded from radiation, since the magnitude of the measured effects decreases in the presence of radiation and becomes zero for a large amount of radiation. All measurements were made with such electric field strengths in the specimen that Ohm's law was obeyed. The magnetic field was ~ 1,500 oe.

Figure 1 shows the variation of conductivity with pressure for the conductivity parallel to the pressure direction and perpendicular to it. It can be seen that the conductivity changes by more for the [$\bar{1}$10] direction than for the [110] direction. If we assume that the scattering is little anisotropic, then according to Pikus and Bir[5] the sign of the product dD can be deduced as negative, from the value of the ratio of mobilities $\mu_\perp/\mu_\parallel = \sigma_\perp/\sigma_\parallel > 1$; d is the deformation potential and D is the matrix element of the spin-orbit coupling.

Figure 2 shows the ratios of the mobilities μ/μ_0 and of the concentration of carriers $n/n_0 = R_0/R$ (where R is the Hall constant) with and without deformation, as a function of pressure, when these are measured in the direction of deformation, [110], at 4.2° K. It can be seen from these curves that the conductivity of germanium changes on deformation not only because of an increase in hole mobility,

*The apparatus for producing the unilateral compression was developed by N. B. Brandt.

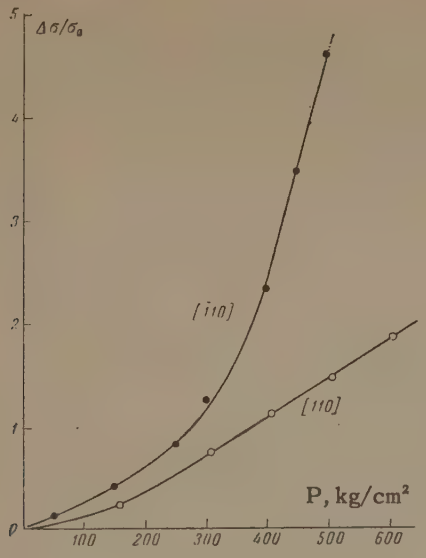

FIG. 1

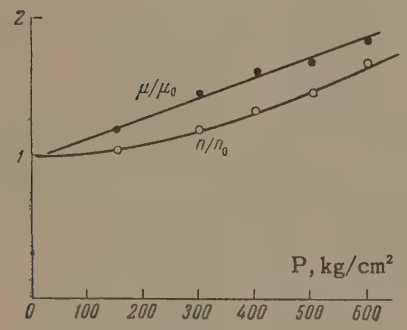

FIG. 2

but also because their number increases. Measurement of the temperature dependence of the Hall constant at zero and at the maximum deformation for these experiments, showed that the ionization energy of the holes changed by 5×10^{-4} ev, which represents 5% of the ionization energy, and is close to the accuracy of measurement in our experiments (~3%). However, the increase in the number of carriers with pressure, found in these experiments, gives the same change of ionization energy.

We thank N. B. Brandt, A. I. Shal'nikov, and G. E. Pikus for their interest and help with this work.

[1] C. S. Smith, Phys. Rev. **94**, 42 (1954).

[2] Morin, Geballe, and Herring, Phys. Rev. **105**, 525 (1957).

[3] E. N. Adams, Phys. Rev. **96**, 803 (1954).

[4] W. H. Kleiner and L. M. Roth, Phys. Rev. Lett. **2**, 334 (1959).

[5] G. E. Pikus and G. L. Bir, Fiz. tverdogo tela **1**, 154, 1828 (1958), Soviet Phys. Solid State **1**, 136 (1959), **1**, 1675 (1960).

[6] S. H. Koenig and J. J. Hall, Phys. Rev. Lett. **5**, 550 (1960).

Translated by R. Berman
20

CORRELATION BETWEEN THE NORMAL POLARIZATION COMPONENTS IN pp SCATTERING AT 650 Mev. I

B. M. GOLOVIN, V. P. DZHELEPOV, and R. Ya. ZUL'KARNEEV

Joint Institute for Nuclear Research

Submitted to JETP editor February 27, 1961

J. Exptl. Theoret. Phys. (U.S.S.R.) **41**, 83-88 (July, 1961)

In a program including a complete set of experiments for the determination of nucleon-nucleon scattering amplitudes, we measured the coefficient of correlation between the normal polarization components (the parameter C_{nn}) in elastic pp scattering at 650 Mev and 90° (c.m.s.). We obtained $C_{nn}(90°) = 0.93 \pm 0.20$. The moduli of the respective amplitudes contained in the elastic pp-scattering matrix were calculated on the basis of the obtained experimental values.

1. INTRODUCTION

In one of our earlier papers[1] we formulated several possible sets of experiments, by which the amplitudes of nucleon-nucleon scattering can be determined by a simultaneous analysis of data on np and pp scattering. All these sets involve a determination of the correlation coefficient $C_{nn}(\vartheta)$ of the normal components of the polarization of nucleons in pp scattering. This coefficient is determined in terms of the average value of the operator $(\sigma_1 \cdot \mathbf{n})(\sigma_2 \cdot \mathbf{n})$, the value of which is

$$\langle (\sigma_1 \mathbf{n})\,(\sigma_2 \mathbf{n})\rangle = \mathrm{Sp}\, MM^+ (\sigma_1 \mathbf{n})\,(\sigma_2 \mathbf{n})/\mathrm{Sp}\, MM^+, \quad (1)$$

and the quantity

$$I_0(\vartheta) = \tfrac{1}{4}\,\mathrm{Sp}\, MM^+, \quad (1a)$$

where M is the amplitude of elastic pp scattering; σ_i is the spin matrix of the i-th nucleon; $\mathbf{n} = [\mathbf{k}_i \times \mathbf{k}_f]/|[\mathbf{k}_i \times \mathbf{k}_f]|$ is a unit vector normal to the nucleon scattering plane; $I_0(\vartheta)$ is the scattering cross section of unpolarized nucleons by unpolarized nucleons through an angle ϑ in the c.m.s. of both nucleons.

Using for M the expression proposed by Wolfenstein[2]

$$M = BS + C(\sigma_1 + \sigma_2)\,\mathbf{n} + N(\sigma_1 \mathbf{n})(\sigma_2 \mathbf{n})\,T + \tfrac{1}{2} G\,[(\sigma_1 \mathbf{m})(\sigma_2 \mathbf{m}) + (\sigma_1 \mathbf{l})(\sigma_2 \mathbf{l})]T + \tfrac{1}{2} H\,[(\sigma_1 \mathbf{m})(\sigma_2 \mathbf{m}) - (\sigma_1 \mathbf{l})(\sigma_2 \mathbf{l})]T, \quad (2)$$

we write the pp-scattering cross section in the form

$$I(\vartheta) = \tfrac{1}{4}|B|^2 + 2|C|^2 + \tfrac{1}{4}|G - N|^2 + \tfrac{1}{2}|N|^2 + \tfrac{1}{2}|H|^2. \quad (3)$$

The coefficient of spin correlation $C_{nn}(\vartheta)$ is defined here as

$$I_0(\vartheta)\, C_{nn}(\vartheta) = -\tfrac{1}{4}|B|^2 + 2|C|^2 - \tfrac{1}{4}|G - N|^2 + \tfrac{1}{2}|N|^2 + \tfrac{1}{2}|H|^2. \quad (3a)$$

If we use for the scattering amplitude another frequently employed expression[1,3,4]

$$M = \alpha + \beta(\sigma_1 + \sigma_2)\,\mathbf{n} + \gamma(\sigma_1 \mathbf{n})(\sigma_2 \mathbf{n}) + \delta(\sigma_1 \mathbf{l})(\sigma_2 \mathbf{l}) + \varepsilon(\sigma_1 \mathbf{m})(\sigma_2 \mathbf{m}), \quad (4)$$

then the scattering cross section $I_0(\vartheta)$ and the coefficient of spin correlation $C_{nn}(\vartheta)$ assume the form

$$I_0(\vartheta) = \tfrac{1}{2}(|a|^2 + |b|^2 + |c|^2 + |d|^2 + |e|^2), \quad (5)$$

$$I_0(\vartheta)\, C_{nn}(\vartheta) = \tfrac{1}{2}(|a|^2 - |b|^2 - |c|^2 + |d|^2 + |e|^2); \quad (5a)$$

$$a = \alpha + \gamma, \quad b = \alpha - \gamma, \quad c = \delta + \varepsilon, \quad d = \delta - \varepsilon, \quad e = 2\beta. \quad (6)$$

The main principles of the determination of the coefficient $C_{nn}(\vartheta)$ were considered by Smorodinskii et al.[4,5] In the present communication, which is the first part of a paper on the determination of the coefficients $C_{nn}(\vartheta)$ for pp scattering at 650 Mev, we describe the research procedure and report the results of the measurement of C_{nn} at 90° (c.m.s.).[6]

For this angle, expressions (3), (5) and (3a), (5a) are made simpler by the symmetry of the coefficients of the scattering amplitude:

$$I_0(90°) = \tfrac{1}{4}|B|^2 + 2|C|^2 + \tfrac{1}{2}|H|^2 = \tfrac{1}{2}(2|b|^2 + |d|^2 + |e|^2), \quad (7)$$

$$I_0(90°)\,C_{nn}(90°) = -\tfrac{1}{4}|B|^2 + 2|C|^2 + \tfrac{1}{2}|H|^2$$
$$= \tfrac{1}{2}(-2|b|^2 + |d|^2 + |e|^2). \quad (8)$$

In addition, the value of $C_{nn}(90°)$ is simply related to the contributions of the triplet I_{tr} and singlet I_S interactions to the scattering cross section $I_0(90°)$:

$$I_{tr}(90°)/I_0(90°) = \tfrac{1}{2}[1 + C_{nn}(90°)], \quad (9)$$

$$I_s(90°)/I_0(90°) = \tfrac{1}{2}[1 - C_{nn}(90°)]. \quad (10)$$

2. EXPERIMENTAL LAYOUT

The experimental determination of the spin-correlation coefficients is based on the measurement of the asymmetry produced when the two protons from elastic pp scattering are simultaneously scattered on the polarization-analyzer targets. Our experimental layout is shown in the figure. An unpolarized proton beam, extracted from the synchrocyclotron chamber of the Joint Institute for Nuclear Research and cleared by the stray field of the accelerator magnet, was shaped by quadrupole lenses and then, after passing through steel collimators 20 mm in diameter in the main shielding wall and in the local shielding of the layout, struck a liquid-hydrogen target. The proton energy at the center of the liquid-hydrogen target was 650 ± 12 Mev.

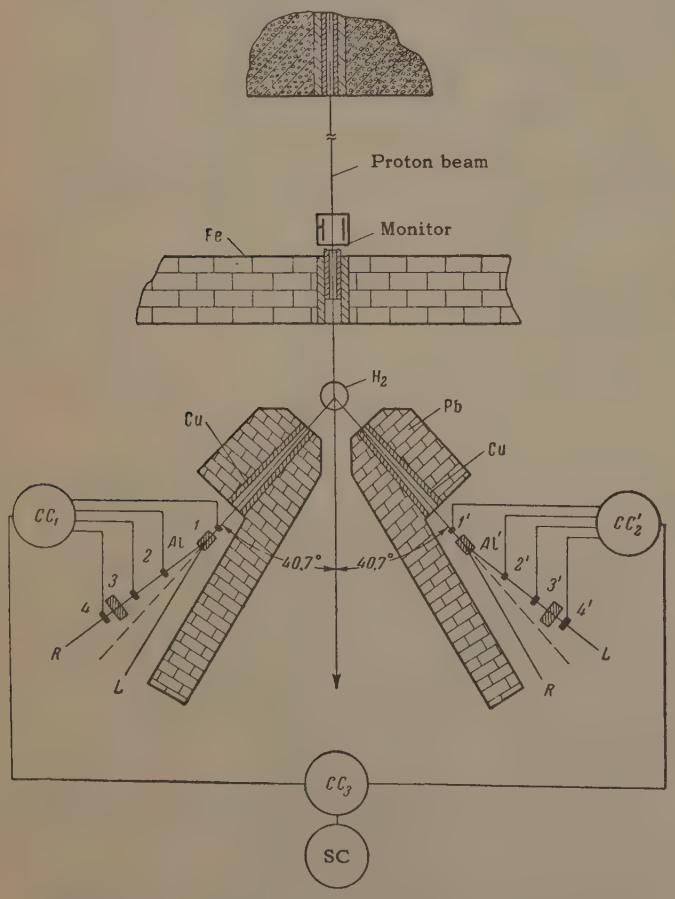

Layout of apparatus in experiments for the measurements of the parameter $C_{nn}(90°)$.

The density of the proton current incident on the liquid-hydrogen target was monitored with an ionization chamber filled with helium at a pressure of 0.4 atm, and did not exceed $(3.3 \pm 0.3) \times 10^8$ cm^{-2} in this experiment. A check was made also in the experiments on the homogeneity of the density distribution of the proton current incident on the target.

The two protons involved in each event of elastic scattering by 90° in the c.m.s. were detected by conjugated scintillation counters 1 and 1′ with 20×60×10 mm plastic scintillators. The angular resolutions of the first scattering in the horizontal projection were ±1.5°, and the resolution in the azimuthal angle was ±3.6°.

The scattered protons and the recoil protons passed through collimating slots in the supplementary shielding of the layout and struck aluminum polarization-analyzer targets (20 g/cm^2). The counter system 2, 3, 4 and 2′, 3′, 4′, with scintillator dimensions 23×50×10, 40×90×10, and 50×110×10 mm respectively, detected the protons scattered in the analyzers by an angle 11 ± 2.5° (l.s.).

Pulses from the photomultiplier anodes were fed first to shaping networks, where they were limited in amplitude and shaped in duration, and then to the inputs of two four-channel coincidence circuits, CC_1 and CC'_2, with resolution time $\tau = 7.5 \times 10^{-9}$ sec. The pulses produced at the outputs of these circuits were additionally shaped in amplitude and duration, and then analyzed for coincidence with each other within the limits of a resolving time of 7.5×10^{-8} sec.

Thus, the two-channel coincidence circuit CC_3, connected with scaler circuit SC, picked out the "triple" scattering cases, i.e., cases when the scattered particle and the recoil particle were simultaneously scattered in the analyzing targets through angles specified by the geometry of the experiment.

In 90° (c.m.s.) elastic pp scattering the polarization of the two proton beams (scattered and recoil protons) incident on the analyzer targets should, as is well known, be equal to zero. The polarization of this beam was monitored simultaneously with the main measurements and it was found that the polarization of the proton beams (due, for example, to imperfect alignment of the beams and counters), if it exists at all, does not exceed 0.003 ± 0.002 in absolute magnitude.

3. CALIBRATION EXPERIMENT

A calibration experiment was carried out to determine the analyzing ability of the second-scattering targets. In this experiment the protons were slowed down to 385 Mev by polyethylene absorbers placed near the accelerator chamber, while counters 1 and 1′, used to determine the first-scattering angle, where so placed as to separate the protons scattered in the c.m.s. through an angle $\vartheta = 41°$ ($\theta_{l.s.} = 19°$). The protons incident on the second scatterers had then the same energy, 325 Mev, as in the correlation experiments, and their polarization under these conditions was $P = 0.39 \pm 0.03$.*

It was found that when a copper absorber is placed between the counters (together with an aluminum scatterer), so that the proton registration threshold is set at 260 Mev, the asymmetries E_1 and E_2 in the scattering of the protons by the analyzer targets are given by $E_1 = 0.200 \pm 0.015$ and $E_2 = 0.210 \pm 0.016$. This corresponds to second-scattering analyzing abilities

$$P_1 = 0.51 \pm 0.056, \qquad P_2 = 0.54 \pm 0.06. \tag{11}$$

4. CORRELATION ASYMMETRY AND THE COEFFICIENT $C_{nn}(90°)$

The coefficient $C_{nn}(90°)$ is given by the expression $C_{nn}(90°) = e/P_1P_2$, where e is the correlation asymmetry. The experimental value of the correlation asymmetry e′ was determined from the relation

$$e' = \frac{(N_{LL} + N_{RR}) - (N_{RL} + N_{LR})}{N_{LL} + N_{RR} + N_{RL} + N_{LR}}, \tag{12}$$

where N_{LL}, N_{RR}, N_{LR}, and N_{RL} are the counting rates of the double coincidence circuit CC_3 in the positions LL, RR, LR, and RL, respectively (see the figure). The values of N_{LL}, N_{RR}, N_{LR}, and N_{RL} were determined by subtracting the background of the layout from the total counting rates of the CC_3 circuit with both analyzing targets in place.

The background of the layout is:

$$N_b = N^{+-} + N^{-+} - N^{--} + 0.05\,N^{++}. \tag{13}$$

Here N is the counting rate of the coincidence circuit CC_3, and the index + or − denotes the respective presence or absence of the first and second analyzing targets. The measurements have shown that $N^{--} \ll N^{++}$ and $N^{+-} = N^{-+}$. The correction term $0.05\,N^{++}$ is due to the 5-percent background of random coincidences in coincidence circuit CC_3. The total background N_b amounts to approximately 25 percent of N^{++}.

As a result of several measurement runs and subsequent averaging, the correlation asymmetry was found to be $e' = 0.267 \pm 0.037$. To determine the true correlation asymmetry e it is necessary to introduce into the obtained value e′ a correction for false correlation e_f, due to the geometry of the layout. Calculations have shown that $e_f = 0.01 \pm 0.04$.

From the resultant values

$$P_1 = 0.51 \pm 0.056, \quad P_2 = 0.54 \pm 0.060, \quad e = e' - e_f = 0.257 \pm 0.37, \tag{14}$$

it follows that

$$C_{nn}(90°) = 0.93 \pm 0.20. \tag{15}$$

5. DISCUSSION OF RESULTS

1. By using relations (9) and (10), as well as the average value of the spin-correlation coefficient (15), we find that at 650 Mev the triplet interaction produces a contribution of 96 percent to the cross section for elastic scattering $I_0(90°)$. The contribution of the singlet interaction is merely 4 percent.

A comparison of the value of the parameter $C_{nn}(90°) = 0.93 \pm 0.20$, obtained at 650 Mev proton energy, with the known values of this parameter for 310 Mev[8] [$C_{nn}(90°) = 0.84^{+0.10}_{-0.22}$] and 382 Mev[9] [$C_{nn}(90°) = 0.416 \pm 0.084$] points to a possible non-monotonicity in the variation of the ratio of the contributions of the triplet and singlet interactions to elastic pp scattering in the energy interval 300 — 650 Mev.

2. If we take into consideration the connection existing between the experimentally measured values of the parameters $C_{nn}(\vartheta)$ and $D_{nn}(\vartheta)$ (the depolarization coefficient) and the absolute values of the quantities B, C, H, G, N or a, b, c, d, and e, then the experimental data presently available on pp scattering at 650 Mev are sufficient to determine the moduli of the amplitudes contained in the matrix of elastic pp scattering by an angle $\vartheta = 90°$. The calculated moduli of the coefficients of the scattering matrix (2) and moduli of the quantities (6) are

$$\frac{1}{4}\frac{|B(90°)|^2}{I_0(90°)} = \frac{1}{2}\frac{|b(90°)|^2}{I_0(90°)} = \frac{1 - C_{nn}(90°)}{2} = 0.035 \pm 0.1, \quad |b(90°)|^2 = |c(90°)|^2, \tag{16}$$

*This value of the polarization was obtained by averaging the data contained in the review by Hess[7] for polarization at 314 Mev (P = 0.38 ± 0.02), 315 Mev (P = 0.38 ± 0.02), and 415 Mev (P = 0.41 ± 0.03).

$$\frac{2|C(90°)|^2}{I_0(90°)} = \frac{1}{2}\frac{|e(90°)|^2}{I_0(90°)} = \frac{1}{4}(1 + C_{nn}(90°) + 2D_{nn}(90°)) = 0.95 \pm 0.1, \quad (17)$$

$$\frac{1}{2}\frac{|H(90°)|^2}{I_0(90°)} = \frac{1}{2}\frac{|d(90°)|^2}{I_0(90°)} = \frac{1}{4}(1 + C_{nn}(90°) - 2D_{nn}(90°)) = 0.02 \pm 0.1 \quad (18)$$

$$N(90°) = G(90°) = a(90°) = 0. \quad (19)$$

We used here the value of the parameter $D_{nn}(90°) = 0.93 \pm 0.17$, obtained in [10] at practically the same proton energy.

3. Knowledge of the values of the moduli of the amplitudes B, C, and H permits, in principle, an estimate of the Wolfenstein parameters R(90°) and A(90°) at 650 Mev. It is necessary to use for this purpose, for example, the analytic expressions for the relative phase shifts of these amplitudes. The estimates carried out have shown that when $C_{nn}(90°) = 0.93$ the parameters R(90°) and A(90°) differ little in magnitude and do not exceed 0.25.

[1] Golovin, Dzhelepov, Nadezhdin, and Satarov, JETP **36**, 433 (1959), Soviet Phys. JETP **9**, 302 (1959).

[2] L. Wolfenstein, Phys. Rev. **96**, 1654 (1954).

[3] R. Oehme, Phys. Rev. **98**, 147 (955).

[4] Puzikov, Ryndin, and Smorodinskii, JETP **32**, 592 (1957), Soviet Phys. JETP **5**, 489 (1957).

[5] V. Vladimirskii and Ya. Smorodinskii, DAN SSSR **104**, 713 (1955).

[6] V. P. Dzhelepov, Proc. 1960 Ann. Intern. Conf. on High-Energy Physics at Rochester, Publ. Univ. Rochester, 1961, p. 115.

[7] H. Hess, Revs. Modern Phys. **30**, 368 (1958).

[8] Vasilevsky, Visnyakov, Iliesku, and Tyapkin, op. cit. [6] p. 200.

[9] Ashmore, Diddens, Huxtable, and Skarvag, Proc. Phys. Soc. **72**, 289 (1958).

[10] Kumekin, Meshcheryakov, Nurushev, and Stoletov, JETP **35**, 1398 (1958), Soviet Phys. JETP **8**, 977 (1959).

Translated by J. G. Adashko
21

CAPTURE OF SEVERAL ELECTRONS BY FAST MULTICHARGED IONS

V. S. NIKOLAEV, L. N. FATEEVA, I. S. DMITRIEV, and Ya. A. TEPLOVA

Institute of Nuclear Physics, Moscow State University

Submitted to JETP editor February 27, 1961

J. Exptl. Theoret. Phys. (U.S.S.R.) **41**, 89-99 (July, 1961)

The capture cross sections of two or more electrons by multicharged ions of light elements in helium, nitrogen, argon and krypton have been measured for velocities from 2.6×10^8 to 12×10^8 cm/sec. In most cases, the electron capture probability is determined by the magnitude of the ionization potential of the resulting ions and depends weakly on the number of captured electrons. It is shown that the simultaneous capture of several electrons in a beam of particles with an equilibrium charge distribution is the chief mode of formation of low charge ions.

1. INTRODUCTION

IN the collision of multicharged ions with atomic matter, the simultaneous capture of several electrons can take place in addition to the capture of a single electron by the ion. As a consequence of the great change in the charge of the ion in such collisions, the latter can have a significant effect on the charge composition of a beam of ions passing through the material.

However, the actual role of these phenomena, especially for ionic velocities close to those of the orbital electrons, has been insufficiently discussed. The cross sections for capture of several electrons by multicharged ions of Ne, Ar, and Kr are known for ionic velocities $v < 10^8$ cm/sec.[1-3] For higher velocities, there are data on capture cross sections of two electrons by He ions[4] and estimates of the cross sections for N ions.[5] Theoretical calculations of the cross sections for capture of two electrons by He ions in helium have been carried out.[6]

In the present research, results are given of an experimental study of the capture cross sections of several electrons by multicharged ions of He, Li, B and N for velocities from $(2.6-4) \times 10^8$ to 12×10^8 cm/sec, by Ne ions for $v = (2.6-6) \times 10^8$ cm/sec, by P and Ar ions for $v = 2.6 \times 10^8$ and 4.1×10^8 cm/sec, and by Na, Mg, Al and Kr ions for $v = 2.6 \times 10^8$ cm/sec. The measurements were carried out in helium, nitrogen, argon and krypton. The two-electron capture cross sections $\sigma_{i,i-2}$ were determined for all the ions. Values of the three-electron capture cross sections of $\sigma_{i,i-3}$ were obtained for B, N, P, and Ar ions. An estimate of the simultaneous capture of four electrons, not previously observed, was obtained for N ions. The capture of more than two electrons was not observed in the passage of the ions through helium, as was to be expected.

The method for determining the cross sections and the experimental setup were described in a previous paper.[7] In the determination of the capture cross sections of several electrons, statistical errors were the most important, and also those errors produced by the small background of random pulses. In most cases, the total error did not exceed 15 — 20 percent for $\sigma_{i,i-2}$ and 20 — 30 percent for $\sigma_{i,i-3}$. The values of $\sigma_{i,i-4}$ were determined with an accuracy ~ 50 percent.

The resultant cross sections refer to cases of capture of electrons accompanied by scattering of the ions through an angle θ which did not exceed 0.005 radian on the average. For scattering at larger angles, a much smaller part of the scattered ions were incident on the recording system than in the case $\theta < 0.005$. In this case, the ratio of the number of recorded ions to the total number of ions scattered through an angle θ was proportional to the geometrical factor $S(\theta) = 1 - 50\,\theta$ for $0 \leq \theta \leq 0.0036$, and $S(\theta) \approx \exp(0.9 - 300\,\theta)$ for $\theta > 0.0036$. In particular, for $\theta = 0.003$, 0.005, and 0.010, the relative fraction of recorded particles $S(\theta)$ was equal to 85, 53 and 13 percent, respectively. The number of recorded ions with scattering angle $\theta \gtrsim 0.008$, which are produced principally by entrance into the counter close to the edges of the input window, was small and did not exceed the background of random pulses. This means that, in comparison with the cross sections obtained, the part of the capture cross section of the electrons associated with the scattering of the

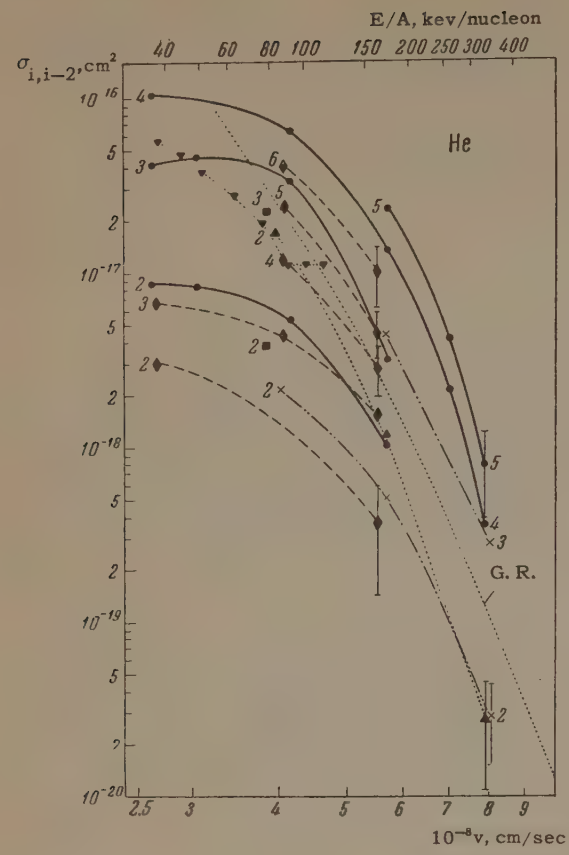

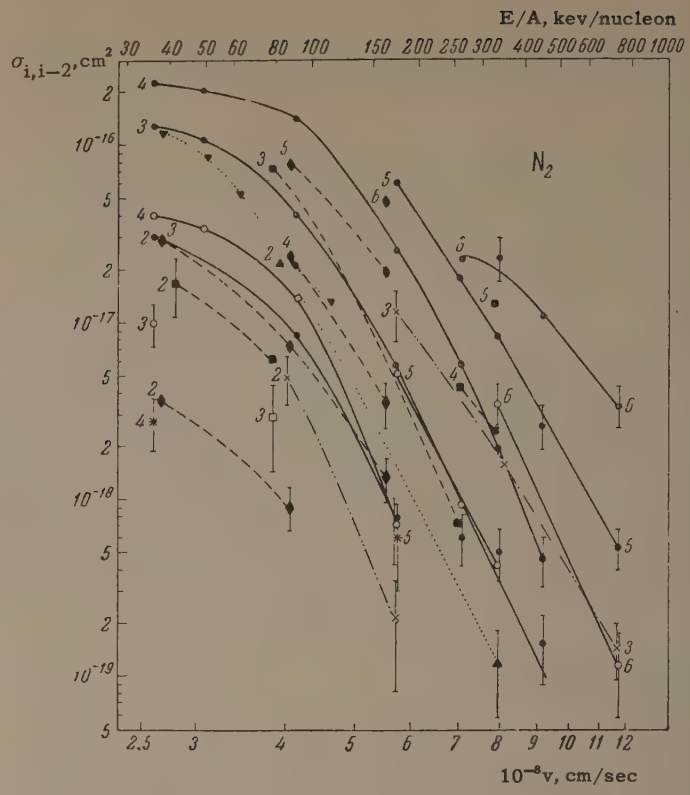

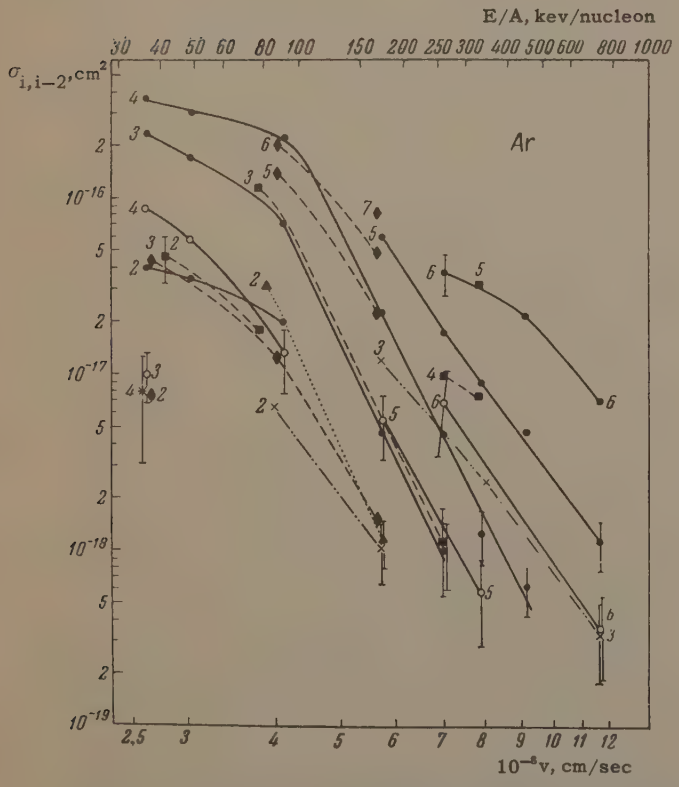

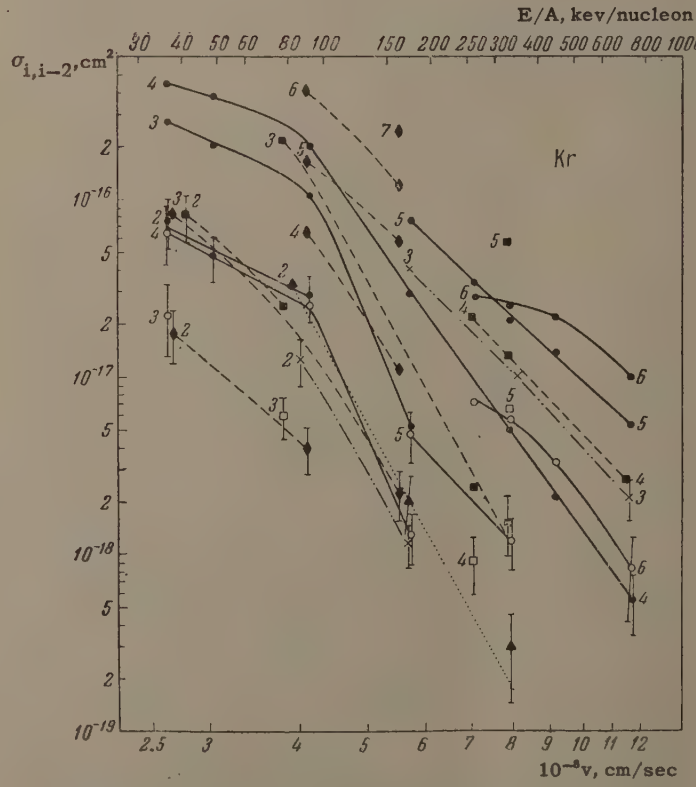

FIG. 1. Cross sections for capture of several electrons in different gases as a function of the velocity v and the energy per nucleon of the ion, E/A, for the ions He (▲), Li (×), B (■, □), N (●, ○) and Ne (◆). The blackened points correspond to the cross section $\sigma_{i,i-2}$, the clear ones to $\sigma_{i,i-3}$, × to $\sigma_{i,i-4}$ for the N ion. The numbers on the points and curves denote the initial charge of the ions, i; ▼ is the value of σ_{20} for helium ions from,[4] G. R. is the theoretical curve of Gerasimenko and Rozentsveig.[6] The measurement errors are shown only if they exceed 20 per cent.

ions by an angle of $\theta \gtrsim 0.008$ is usually small and does not exceed the range of random error.

2. EXPERIMENTAL RESULTS

The results of measurements of capture cross sections of several electrons (referred to a single atom) have been plotted in Figs. 1, 2, and 3.

As is seen from Fig. 1, the two-electron capture cross sections $\sigma_{i,i-2}$ decrease with increase in speed of the ions, while for a given gas the dependence of $\sigma_{i,i-2}$ on v is approximately the same for all ions. For increase in velocity, the capture cross sections of two electrons decrease more rapidly than the single-electron capture cross section $\sigma_{i,i-1}$.[7] An especially large difference is observed in the dependence of $\sigma_{i,i-2}$ and $\sigma_{i,i-1}$ on v for $v \sim (6-8) \times 10^8$ cm/sec in helium:

$$-d\log \sigma_{i,i-1}/d\log v = 5\text{—}6, \quad -d\log \sigma_{i,i-2}/d\log v = 8\text{—}14.$$

With increase in the ionic charge i, the two-electron capture cross sections increase monotonically, approximately as i^m, while the index m is approximately 1.5 times larger than the corresponding exponent for the single-electron capture cross section. With change in charge of the nucleus of the ions Z, the two-electron capture cross section $\sigma_{i,i-2}$, as well as the single-electron capture cross section $\sigma_{i,i-1}$, do not change monotonically (Fig. 2). The dependence of the cross section $\sigma_{i,i-2}$ on the medium (Fig. 3) is qualitatively similar to the corresponding dependence of $\sigma_{i,i-1}$.

From the experimental data which are given in the present work and elsewhere,[7] one can determine the ratio of the two-electron capture cross sections to the single-electron capture cross section, $\eta_{i,i-2} = \sigma_{i,i-2}/\sigma_{i,i-1}$. Typical values of $\eta_{i,i-2}$ are shown in Figs. 4 and 5. In all cases, $\eta_{i,i-2} < 1$. The largest values of $\eta_{i,i-2} \sim 0.2$ were obtained for N, P, Ar, and Kr ions with $i = 4-6$, and the smallest values, $\eta_{i,i-2} \sim 0.01$, for doubly charged ions of He, Li, B, Ne, Na, and Mg. For ions of a given element the values of $\eta_{i,i-2}$ increase along with increase of i; however, for large values of $\eta_{i,i-2} \sim 0.2$, the dependence of $\eta_{i,i-2}$ on i weakens and the $\eta_{i,i-2}$ become practically constant. With increase in the velocity, the values of $\eta_{i,i-2}$ decrease (Fig. 5).

The values of $\eta_{i,i-2}$ depend weakly on the medium (Fig. 4) and only in helium at $v \geq 8 \times 10^8$ cm/sec are they much less than in the other gases: for all ions, $\eta_{i,i-2} < 0.01$.

Like the one- and two-electron capture cross sections, the values of $\eta_{i,i-2}$ depend strongly on Z. The dependence of $\eta_{i,i-2}$ on i and Z can usually be reduced to a dependence of this quantity on I — the binding energy of the electron in the ground state of an ion with charge $i-2$ (Fig. 4). Exceptions are the ratios $\eta_{i,i-2}$ for neon ions with various charges i and for the ions Na^{+3} and Ar^{+2}, which are shown to be much smaller than for the other ions. As is seen from Fig. 4, at $v = 2.6 \times 10^8$ cm/sec, the values of $\eta_{i,i-2}$ are identical in the case of capture of electrons by the L and M shells, while for $v = 4.1 \times 10^8$ cm/sec, they differ by not more than a factor of two. For ions with $i = Z$ at $v \geq 4 \times 10^8$ cm/sec, the values of $\eta_{i,i-2}$ are approximately one-half those for the capture of L electrons.

The three-electron capture cross sections $\sigma_{i,i-3}$, as the experimental results for ions of B, N, and Ar show, are changed more strongly with a

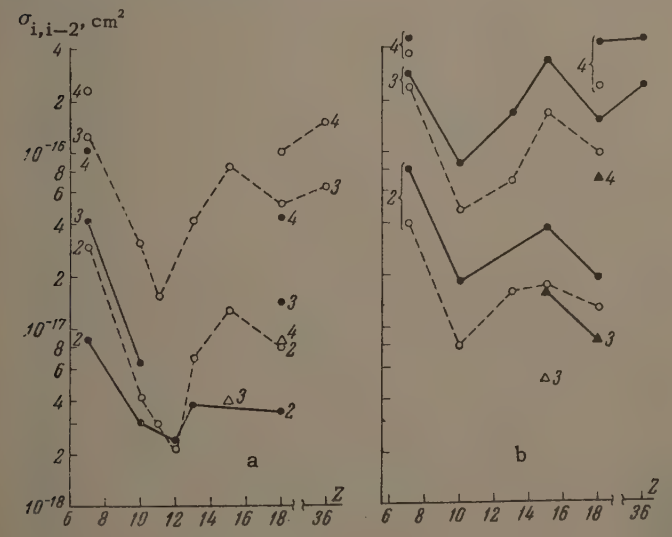

FIG. 2. Dependence of $\sigma_{i,i-2}$ on the charge of the ion nucleus Z for $v = 2.6 \times 10^8$ cm/sec; a — in helium (●) and nitrogen (○); b — in krypton (●) and argon (○). For P and Ar ions (Z = 15 and 18), the values of $\sigma_{i,i-3}$ are also shown (△ and ▲). The values of i are given at the points and curves.

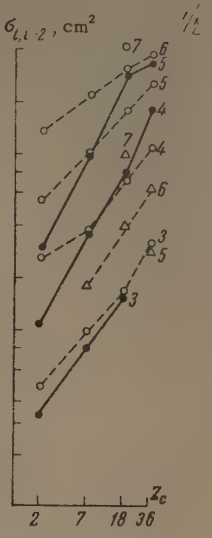

FIG. 3. Capture cross sections of two electrons by ions of phosphorus (●) and nitrogen (○) in gases with atomic number Z_c for $v = 4.1 \times 10^8$ cm/sec. The values of $\sigma_{i,i-3}$ (△) are also given for argon ions. The initial charge of the ions is shown on the curves.

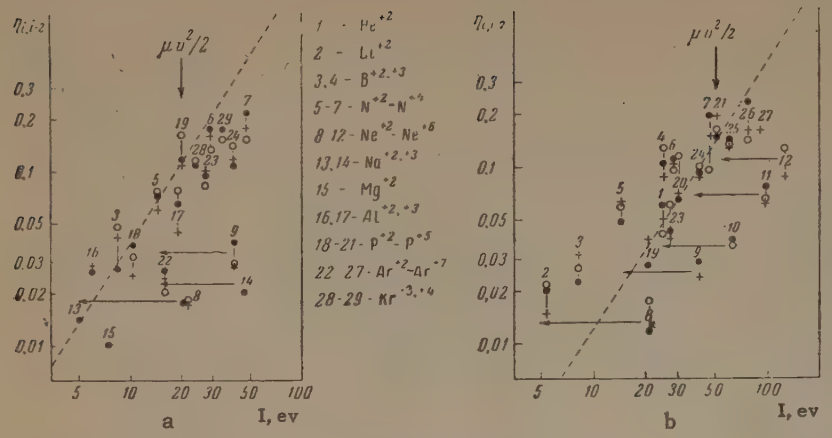

FIG. 4. Values of $\eta_{i,i-2} = \sigma_{i,i-2}/\sigma_{i,i-1}$ for different ions in nitrogen (●), argon (+) and krypton (○) as a function of the binding energy I of the electron in the ground state of the ion that is formed; a – for $v = 2.6 \times 10^8$ cm/sec, b – for $v = 4.1 \times 10^8$ cm/sec. The arrows indicate the maximum value of the binding energy of the electron (for Ne and Na ions) for its capture by the M shell. The dashed lines correspond to a dependence of the form $I^{3/2}$ (μ = mass of the electron).

change of i than the two-electron capture cross sections. Therefore, for increase of i, the ratio of the three-electron capture cross section to the two-electron capture cross sections ($\eta_{i,i-3} = \sigma_{i,i-3}/\sigma_{i,i-2}$) increases, as does $\eta_{i,i-2}$. Moreover, for all ions for which the three-electron capture cross sections have been determined, the values of $\eta_{i,i-3} = \sigma_{i,i-3}/\sigma_{i,i-2}$ coincide, within the limits of experimental error, with the values of $\eta_{i-1,i-3} = \sigma_{i-1,i-3}/\sigma_{i-1,i-2}$ for ions of the same element with initial charge smaller by one. For N ions in nitrogen, this coincidence is shown in Fig. 5.

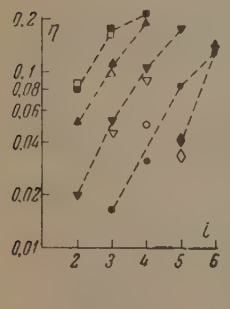

FIG. 5. Values of $\eta_{i,i-2} = \sigma_{i,i-2}/\sigma_{i,i-1}$ (blackened points) and $\eta_{i+1,i-1} = \sigma_{i+1,i-2}/\sigma_{i+1,i-1}$ (clear points) as a function of i for N ions in nitrogen at the velocities: □, ■ – 2.6×10^8; ▲, △ – 4.1×10^8; ▼, ▽ – 5.7×10^8; ●, ○ – 8.0×10^8; ◆, ◇ – 10.7×10^8 cm/sec.

In a similar way, the four-electron capture cross sections $\sigma_{i,i-4}$ give values of $\eta_{i,i-4} = \sigma_{i,i-4}/\sigma_{i,i-3}$ close to $\eta_{i-1,i-4} = \sigma_{i-1,i-4}/\sigma_{i-1,i-3}$. Thus for ions of a given element, $\eta_{i,i-2} \approx \eta_{i+1,i-2} \approx \eta_{i+2,i-2}$ or $\sigma_{i,i-2}/\sigma_{i,i-1} \approx \sigma_{i+1,i-2}/\sigma_{i+1,i-1} \approx \sigma_{i+2,i-2}/\sigma_{i+2,i-1}$; that is, the ratio of the cross sections for the capture of s and s – 1 electrons, $\eta_{i,i-s}$, is determined by the value of the charge of the ions formed, i – s and i + 1 – s, and for fixed value of the latter does not depend on s.

If we compare the cross section for the capture of different numbers of electrons, leading to the formation of ions with the same final charge k, then it is shown that the cross sections $\sigma_{k+s,k}$ decrease with increase in the number of captured electrons, while the ratio of the cross sections $\sigma_{k+s+1,k}/\sigma_{k+s,k}$ does not exceed 0.5. For approximate estimates, one can assume that $\sigma_{k+s,k} \sim \exp(-as)$ with an exponent $a \sim 1-3$.

3. DISCUSSION OF RESULTS

Experimental data which can be directly compared with the results of the present research exist only for ions of He in helium and air at $v < 5 \times 10^8$ cm/sec in the work of Allison.[4] For $v = 4 \times 10^8$ cm/sec, the value of σ_{20} in helium which we obtained is the same as the result of Allison, while the value of σ_{20} in nitrogen is 25 percent smaller than σ_{20} in air, i.e., the difference lies within the limits of experimental error. For $v = 4.7 \times 10^8$ cm/sec, the values of σ_{20} of Allison[4] are evidently too high, since the experimental data of the present work and theoretical calculations[6] demonstrate the rather rapid drop in the cross section σ_{20} with increase in the speed of the ions. Experimental data on two-electron capture cross sections of nitrogen ions, which we obtained earlier,[5] are in agreement with the results of the present research. The values of σ_{20} for He ions in helium, computed in the Born approximation by Gerasimenko and Rozentsveĭg,[6] are approximately twice as large as the experimental; the dependence of the computed cross sections on v is close to the experimental dependence. The speed of the ions in our cases is still not so large that one can expect better agreement with experiment from calculations in the Born approximation.

According to representations of the capture of electrons formulated in a general form by Bohr[8] and developed in application to multicharged ions in the researches of our group,[7,9] the single-electron capture cross section $\sigma_{i,i-1}$ can be represented in the form of a product $\sigma_i' n f_{i,i-1}$, where σ_i' is the collision cross section of an ion possessing a charge i with an electron of an atom of the medium, with a transfer to the latter of an energy of the order of $\mu v^2/2$ (μ is the mass of the electron); n is the number of electrons in an atom of the medium which effectively take part in the capture; $f_{i,i-1}$ is the capture probability of the electron after the collision mentioned, as a result of which an ion is formed with charge i – 1.

Applying a similar consideration to the phenomena of capture of several electrons, we can write

$$\sigma_{i,i-2} = \sigma_i' n f_{i,i-1} w_2 f_{i,i-2},$$
$$\sigma_{i,i-3} = \sigma_i' n f_{i,i-1} w_2 f_{i,i-2} w_3 f_{i,i-3} \text{ etc.}$$

where w_2 and w_3 are the collision probabilities of an ion with the second and third electrons of the atom of the medium, in the presence of a collision with one and two electrons, respectively; $f_{i,i-2}$ and $f_{i,i-3}$ are the capture probabilities of the second and third electrons with the formation of ions possessing charges of $i-2$ and $i-3$, respectively. It is then seen that in comparison with the s-electron capture cross section, $\sigma_{i,i-s}$, the ratio of the s- and $(s-1)$-electron capture cross sections, $\eta_{i,i-s} = \sigma_{i,i-s}/\sigma_{i,i+1-s}$, is a much simpler quantity, equal to $w_s f_{i,i-s}$, while the quantities w_s must by their physical meaning be determined by the properties of the atoms of the medium, and the quantities $f_{i,i-s}$ should be functions of the ionic parameters.

In correspondence with what has been pointed out above, the experimentally observed dependence of the ratio $\sigma_{i,i-2}$ on I should be due to the dependence of the quantity $f_{i,i-2}$ on I. The decisive influence of the electron binding energy I on the capture probability f, established in the present research, is seen to be in full correspondence with the electron-capture probability estimated by a statistical method suggested by Bohr.[8] The general experimental dependence of $\eta_{i,i-2}$ on I for most ions is close to the dependence of f on I, which was suggested by one of us,[9] according to which $f \approx (2I/\mu v^2)^{3/2}$ for $I < \mu v^2/2$ and $f \sim 1$ for $I > \mu v^2/2$. The difference is that the actual transition to constant values $\eta_{i,i-2}$, at least for $v \sim 3 \times 10^8$ cm/sec, takes place at values of I somewhat larger than $\mu v^2/2$ (Fig. 4). As experimental results show, there also exists a certain dependence of the quantity $f_{i,i-2}$ on the number of the shell being filled (Fig. 4b).

The presence of a decisive influence of the binding energy of the electron in the ground state of the ion that is formed on the probability of capture $f_{i,i-2}$ indicates that for $I < \mu v^2/2$ the capture of electrons takes place predominantly into the ground state or in a state close to it with the smallest possible values of the principal quantum number and with a binding energy close to I, since the binding energy of the electron captured from the next shell depends essentially on the charge of the ion i, and is weakly associated with the value of I. The weakening of the dependence of the ratio $\eta_{i,i-2}$ on I for $I \gtrsim \mu v^2/2$ can be considered as proof of the growth of the role of electron capture in highly excited states. Inasmuch as the velocity of the captured electrons relative to the ion is on the order of v, then for $I \gtrsim \mu v^2/2$ the electrons should be captured principally in states with binding energy $\sim \mu v^2$.

As can be seen from Fig. 4, in the case of capture of different (in order of enumeration) L or M electrons, the values of $\eta_{i,i-2}$ for the same I are practically identical. This means that the probability of capture of the second electron $f_{i,i-2}$ does not depend on the number of electrons in the outer shell of the ion. Only in the capture of the last (eighth) M electron (η_{20} for Ar^{+2} ions) and in the capture of the seventh and eighth L electrons ($\eta_{i,i-2}$ for the ions $Ne^{+2,+3}$ and Na^{+3}) does a decrease in the probability of capture $f_{i,i-2}$ take place, which can explain the filling of the shell. A similar decrease of $f_{i,i-2}$ obviously takes place also in the capture of K electrons, as a result of which the values of $\eta_{i,i-2}$ for the ions He^{+2}, Li^{+3} and B^{+5} are shown to be one half the size of $\eta_{i,i-2}$ corresponding to capture of L electrons.

Similarly, small values of $\eta_{i,i-2}$ for the ions $Ne^{+5,+6,+7}$ cannot be explained by a decrease in the probability of electron capture as a consequence of the filling of the L shell, since a decrease in the values of $\eta_{i,i-2}$ is not observed for nitrogen ions with the same number of electrons. Decrease in the probability of capture in these cases can be brought about by the small dimensions of the region occupied by the L electrons in the neon ions. In the case of a sharp decrease in the capture probability of electrons in the L shell, the electrons should be captured principally in the following M shell. If the experimental values of $\eta_{i,i-2}$ for neon ions refer to the maximum binding energy of the electron in the M shell, then they are shown to be on the general curve of the dependence of $\eta_{i,i-2}$ on I for other ions which capture electrons in the M shell (Fig. 4). This gives us a basis for assuming that the neon ions capture the second electron in the M shell.

In consideration of the values of $\eta_{i,i-2}$, attention is called to the sharp decrease in the values of $\eta_{i,i-2}$ in helium for $v > 6 \times 10^8$ cm/sec, as a result of which (for $v \gtrsim 8 \times 10^8$ cm/sec) the values of $\eta_{i,i-2}$ for arbitrary ions in helium become much less than in other gases. The atoms of helium differ from the atoms of other gases used in that electrons with orbital velocities of the order of 10^9 cm/sec are lacking. In this connection, the observed decrease in the probability of capture of electrons in helium at $v > 6 \times 10^8$ cm/sec can be regarded as a direct verification of the general results of theoretical calculations carried out in

the Born approximation[10,11] and the corresponding qualitative considerations of Bohr,[8] according to which the probability of electron capture reaches a large value only in those cases when the orbital velocity of the captured atomic electron is close to the velocity of the ion. It then follows that in all cases (except for capture of electrons in helium at $v \gtrsim 8 \times 10^8$ cm/sec) we are dealing with the capture of electrons with orbital velocity close to the velocity of the ion. Inasmuch as the velocities of the electrons found in the different shells differ widely, then one can establish the result that the electrons are almost always captured from one definite shell of the atoms of the medium for a given velocity of the ions. This conclusion is also supported by the coincidence of the ratios of one-electron capture cross sections in different gases with the ratios of the number of electrons in the corresponding shells of the atoms of these gases.[7]

As the resultant experimental data show, in the presence in the atoms of the medium of electrons with orbital velocities close to the velocity of the ions v, the values of $\eta_{i,i-2} = w_2 f_{i,i-2}$ depend weakly on the atomic number of the medium Z_m. It then follows that the probability w_2 of collision of the ion with the second electron is approximately the same in all the gases used.

One can determine the value of w_2 from the values of $\eta_{i,i-2}$ for those ions for which $\eta_{i,i-2}$ does not depend on I, when one can assume that $f_{i,i-2} \approx 1$. In such estimates, $w_2 \sim 0.1 - 0.2$. One can then draw the conclusion that in such a collision of the ion with one of the atomic electrons, which is necessary for capturing the latter, a similar collision with another electron takes place only in the case in which the distance R between the two electrons is not very large. The size of the distance R can be estimated from the relation $w_2 \sim (4/3)\pi R^3 \rho$, where ρ is the mean density of the electrons remaining after removal of the first electron in the shell of the atom of the medium from which capture takes place. If one assumes that the electrons are captured from the outer shell of the atoms at low ion velocities, and from the next shell when $v \sim 10^9$ cm/sec, then it is shown that in the first case $R \sim (0.5 - 0.7)\, a_0$, and in the second, $R \sim 0.15\, a_0$, where $a_0 = 0.53 \times 10^{-8}$ cm. These values of R amount to between 0.5 and 1.0 of the mean radius of the electron shell from which the electrons are captured.

Inasmuch as the experimental data obtained for different ions of the same element yield $\eta_{i,i-2} \approx \eta_{i+1,i-2} \approx \eta_{i+2,i-2}$, one can assume that $w_2 \approx w_3 \approx w_4$ and $f_{i,i-2} \approx f_{i+1,i-2} \approx f_{i+2,i-2}$. The equality of values of f means that the probability of electron capture depends only on the charge of the ion formed, and does not depend on the number of captured electrons or the initial charge. The latter is quite natural, since the interaction between the electrons is weaker than their interaction with the field of the atom and the ion, and therefore the electrons can be regarded as noninteracting with one another in the capture process.

In this connection, it should be expected that the probability of capture of the first electron $f_{i-1,i-2}$ must also enter into the equation for f. If we assume that $f_{i,i-1} = f_{i+1,i-1} = \eta_{i+1,i-1}/w_2$, then the total collision cross section of the ion with electrons of the atom of the medium $n\sigma'_i = \sigma_{i,i-1}/f_{i,i-1}$ can be determined from the experimental values of $\sigma_{i,i-1}$ (Fig. 6). If the ion in the collision of ion with electron were to act as a point charge of value i, then $n\sigma'_i$ would be proportional to i^2. Actually, for all ions except the ions of Ne, the values of $n\sigma'_i$ increase very slowly with increase of i. This means that the principal change in the momentum of the electron takes place at such small distances from the nucleus of the ion that the effective charge of the ion i* acting on the electron is larger than the charge of the ion i, and therefore depends weakly on i.

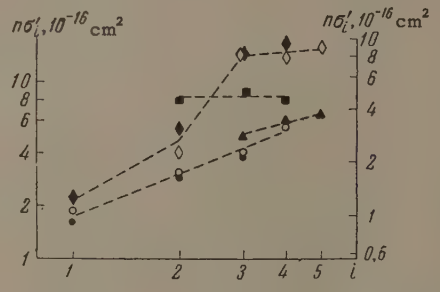

FIG. 6. Values of $n\sigma'_i = \sigma_{i,i-1}/f_{i,i-1} = \dfrac{w\sigma_{i,i-1}\sigma_{i+1,i}}{\sigma_{i+1,i-1}}$ as a function of i for N ions (●, ○), Ne ions (◆, ◇), P ions (□, ■) and Ar ions (▲, △) in nitrogen. The scale at the left and the blackened points correspond to $v = 4.1 \times 10^8$ cm/sec, the scale at the right and the clear points correspond to $v = 5.6 \times 10^8$ cm/sec; $w = 0.2$.

This conclusion is also substantiated by the fact that $n\sigma'_i \lesssim \pi R_i^2$, where R_i is the radius of the outer electron shell of the ion. The difference in values of $n\sigma'_i$ for ions of different elements, excluding the ions of Ne, and also the values of R_i of these ions, can be found qualitatively from the differences in the values of i*. Thus the assumption that $f_{i,i-1} = f_{i+1,i-1}$ for most ions does not contradict experimental data and is acceptable.

For the ions of Ne, for which the probability of capture of a second electron is anomalously small, and corresponds to its capture by the M shell

(Fig. 4), the values of $n\sigma_i'$ calculated under the assumption that $f_{i,i-1} = f_{i+1,i-1}$ are several times larger than those for the other ions (Fig. 6). Therefore, if this assumption is made, then it is necessary to assume that the effective charge for Ne ions is at least 1.5 times larger than for N ions. The latter can take place at distances from the nucleus less than $\sim 0.6\,a_0$,[12] while $n\sigma_i' \approx 10\,a_0^2$.

Thus the assumption that the capture probability of the first electron for neon ions, $f_{i,i-1}$, is close to the capture probability of the second electron, $f_{i+1,i-1}$, leads to contradictions. If we now assume that $f_{i,i-1}$ is larger than $f_{i+1,i-1}$, and is identical with the capture probability of the L electron for other ions with the same values of I, then the values of $n\sigma_i'$ are shown to be approximately as for N ions, and no difficulties arise in their interpretation. It then follows that the significant decrease in the electron capture probability because of the small dimensions of Ne ions takes place only in the capture of two (or more) electrons.

This phenomenon becomes understandable if we take it into account that for $v \sim (3-5) \times 10^8$ cm/sec, the capture of several electrons usually takes place from a region with dimensions $(0.5 - 0.7)\,a_0$ in a state with mean radius of the electron orbit greater than this quantity. However, with Ne ions, the radius of the L shell is known to be less than this value. Therefore, the electrons of the atom of the medium located at a distance of $(0.5 - 0.7)\,a_0$ from the first captured electron cannot be trapped in this shell; capture of several electrons in the L shell of Ne ions will take place from a smaller region than usual and the probability of capture of several electrons will be diminished. The probability of capture of the first electron is not associated with the dimensions of this region and therefore should not be diminished.

In contrast with the capture of electrons for $v < 10^8$ cm/sec,[1-3] a definite connection between the cross sections and the resonance defect ΔE was not observed in the region studied by us (ΔE is the change in binding energy of the electron in its transition from the atom of the medium to the ion). The resonance charge-exchange cross sections corresponding to $\Delta E = 0$ (σ_{20} for He ions in helium and Ar ions in argon) are not at all distinguished from the remaining cases of electron capture. At the same time, it is interesting to note that a change in velocity by one order of magnitude (from $2-5$ to 26×10^7 cm/sec) cause the ratios of the cross sections for nonresonance capture of electrons by ions of Ne, Ar and Kr (σ_{20} and σ_{31} in krypton) to be changed by no more than a factor of two. The dependence of the cross section on the medium is also little changed (σ_{20} for Ne ions in helium, argon and krypton, σ_{31} for Kr ions in nitrogen and argon). The latter means that the behavior of the number of electrons effectively participating in the capture in atoms of the media under consideration and in the velocity range from $\sim 0.3 \times 10^8$ to $\sim 4 \times 10^8$ cm/sec changes very slowly. Since the cross sections for electron capture decrease with increase in velocity for $v > 2.6 \times 10^8$ cm/sec, while they increase for $v \lesssim 5 \times 10^7$ cm/sec in a majority of cases of nonresonance capture, a maximum cross section should be observed in the unstudied range of velocities between the values mentioned.

The given results make it possible to clarify the relative role of capture of a different number of electrons in the formation of charged groups of an equilibrium charge distribution which is established in the ion beam as a result of multiple collisions of ions and atoms of the material. Inasmuch as the capture cross sections of several electrons are much less than the cross sections of capture of a single electron, they do not show any significant effect on the distribution of ions among the most intense charge groups. However, the relative number of ions comprising low intensity groups, with charge i several units less than the mean charge $\bar{i}$, should be determined by the cross sections of capture of several electrons.

Actually, the number of ions of charge i formed from ions with charge j is proportional to the quantity $\Phi_j\sigma_{ji}$, where Φ_j is the relative number of ions with charge j in the equilibrium distribution. If i differs from $\bar{i}$ by not more than $2-3$, then the values of Φ_j, as established in our earlier work,[13] are proportional to $\exp[-(j-\bar{i})^2/2\sigma^2]$. The cross sections σ_{ji}, as shown in Sec. 2, are approximately proportional to $\exp[-(j-i)/a]$. It then follows that

$$\Phi_j\sigma_{ji} \sim \exp[-(j - i_0)^2/2\sigma^2],$$

where $i_0 = \bar{i} - \sigma^2 a$. Since $j \geq i + 1$, then the value of $\Phi_j\sigma_{ji}$ for $i \geq i_0 + 1$ takes on a maximum value for $j = i + 1$, while for $i \lesssim i_0 - 2$, it does so for $j \sim i_0$. The latter means that ions with charges $i \lesssim i_0 - 2$ are formed principally from ions with charge $j \sim i_0$ as the result of simultaneous capture of several electrons; in this case $\Phi_i \approx \Phi_{i_0}\sigma_{i_0,i}/\sigma_{i,i+1}$.

For $i < i_0 - 2$ significant deviations from the Gaussian distribution should exist in the equilibrium distribution of ions. This Gaussian distribution holds in the region of values of i where the capture and loss of several electrons have little

effect on the equilibrium distribution of the charges and $\Phi_i \approx \Phi_{i+1}\sigma_{i+1,i}/\sigma_{i,i+1}$. For $i < i_0 - 2$ we have $\Phi_{i_0}\sigma_{i_0,i} > \Phi_{i+1}\sigma_{i+1,i}$; therefore, the values of Φ_i should be larger than the values given by the Gaussian formula. In most cases $a \sim 1-3$ and $\sigma^2 \sim 0.5-1$. Therefore, $\sigma^2 a$ is of the order of several units. For example, for N ions and v $\sim 8 \times 10^8$ cm/sec, the value of $a \approx 2-2.5$, $\sigma^2 \approx 0.6$, $i \approx 4$, so that $i_0 \sim 2.5$; it then follows that the particles with $i = 0$ should be formed principally from doubly and triply charged ions as the result of simultaneous capture of two or three electrons.

[1] N. V. Fedorenko, J. Tech. Phys. (U.S.S.R.) **24**, 769 (1954).

[2] I. P. Flaks and E. S. Solov'ev, J. Tech. Phys. (U.S.S.R.) **28**, 599, 612 (1958), Soviet Phys. Tech. Phys. **3**, 564, 577 (1958).

[3] I. P. Flaks and L. G. Filippenko, J. Tech. Phys. (U.S.S.R.) **29**, 1100 (1959), Soviet Phys. Tech. Phys. **4**, 1005 (1959).

[4] S. K. Allison, Phys. Rev. **109**, 76 (1958).

[5] Nikolaev, Fateeva, Dmitriev, and Teplova, JETP **33**, 306 (1957), Soviet Phys. JETP **6**, 239 (1958).

[6] V. K. Gerasimenko and L. N. Rozentsveĭg, JETP **31**, 684 (1956), Soviet Phys. JETP **4**, 509 (1957).

[7] Nikolaev, Dmitriev, Fateeva, and Teplova, JETP **40**, 989 (1961), Soviet Phys. JETP **13**, 695 (1961).

[8] N. Bohr, The Passage of Atomic Particles through Matter, Kgl. Danske Vidensk. Selsk. Mat.-Fys. Medd. **18**, 8 (1948).

[9] V. S. Nikolaev, JETP **33**, 534 (1957), Soviet Phys. JETP **6**, 417 (1958).

[10] D. R. Bates and A. Dalgarno, Proc. Phys. Soc. (London) **A66**, 962 (1953).

[11] H. Schiff, Canad. J. Phys. **32**, 393 (1954).

[12] Landolt-Börnstein, Zahlenwerte und Funktionen aus Physik, Chemie, Astronomie, Geophysik, Technik, Band I, Teil I, Springer-Verlag, Berlin (1950).

[13] Nikolaev, Dmitriev, Fateeva, and Tepolova, JETP **39**, 905 (1960), Soviet Phys. JETP **12**, 627 (1961).

Translated by R. T. Beyer
22

RELAXATION PHENOMENA IN THE PARAMAGNETIC RESONANCE OF Mn^{2+} *IONS IN THE CUBIC CRYSTAL FIELD OF* SrS

A. A. MANENKOV and V. A. MILYAEV

P. N. Lebedev Physics Institute, Academy of Sciences, U.S.S.R.

Submitted to JETP editor February 25, 1961

J. Exptl. Theoret. Phys. (U.S.S.R.) **41**, 100-105 (July, 1961)

Relaxation phenomena in the electron paramagnetic resonance spectrum of Mn^{2+} ions in the SrS lattice were studied at a frequency of 9,300 Mc/sec in polycrystalline specimens containing ~ 0.05% Mn. The spin-lattice relaxation time T_1 is 5×10^{-8} sec at 300° K, 1.5×10^{-6} sec at 77° K, 9×10^{-2} sec at 4.2° K and 2.1×10^{-1} sec at 1.6° K. The spin-spin relaxation time T_2, determined from the line width at 77° K, is 6×10^{-8} sec.

Pronounced spin-spin cross relaxation effects were observed at liquid helium temperatures. The spin-spin cross relaxation times in the Mn^{2+} spectrum lie between 2×10^{-3} and 1×10^{-2} sec. The features of spin-lattice relaxation of ions in the S state are discussed. It is indicated that spin-lattice interaction may play an effective role via the covalent bond between the Mn^{2+} ions and the surrounding crystal ions.

1. INTRODUCTION

In the existing theory of spin-lattice relaxation in paramagnetic crystals it is assumed that the Kronig mechanism is the most effective in the exchange of the electron spin energy of the paramagnetic ions with the thermal vibrations of the lattice. This consists in the modulation of the crystal electric field by the thermal vibrations of the lattice, which is transmitted to the electron spins by means of the spin-orbit coupling.

The case of ions in an S state (Mn^{2+}, Fe^{3+}, Gd^{3+}, Eu^{2+}) in a cubic crystal field is of special interest in connection with the efficiency of this mechanism. In so far as the orbital momentum of such ions is zero in the ground state, there is no spin-orbit coupling, so that the Kronig mechanism should be little effective. This mechanism can only occur for ions in an S state if there is admixture of higher orbital states, with non-zero orbital momentum, to the ground state.

In the present work we have undertaken a study of the spin-lattice relaxation of Mn^{2+} ions in SrS crystals. As was shown by a study of the paramagnetic resonance spectrum of Mn^{2+} in SrS,[1] the crystal field has cubic symmetry and the ^6S ground state is very weakly split (splitting ~ 10^{-4} cm^{-1}). This indicates that the ground state of Mn^{2+} in the SrS cubic lattice is almost a pure S state, and it would, therefore, be expected that the spin-lattice relaxation time should be large even at room temperature. However, it turned out that the spin-lattice relaxation time of Mn^{2+} in SrS is fairly short (~ 10^{-8} sec at room temperature and ~ 10^{-6} sec at liquid-nitrogen temperature). We discuss below these results on the basis of possible relaxation mechanisms.

Apart from features connected with spin-lattice relaxation, the case of Mn^{2+} ions is also of interest from the point of view of the elucidation of the role of spin-spin cross relaxation, since Mn^{2+} ions have a large number of hyperfine structure energy levels, brought about by the interaction of the electron spin of Mn^{2+} ($S = 5/2$) with the nuclear spin of Mn^{55} ($I = 5/2$). The phenomenon of cross relaxation was analyzed in detail theoretically by Bloembergen et al[2] and was found experimentally and studied in various substances by several authors (see, for example,[3,4]).* We have observed very pronounced cross relaxation effects in the spectrum of Mn^{2+} in SrS at liquid-helium temperatures.

2. EXPERIMENTAL METHODS OF STUDYING RELAXATION PROCESSES

The investigation of relaxation was carried out on SrS · Mn single crystal specimens with a Mn^{2+} ion concentration of about 0.05%.

The measurements of relaxation time were made with a superheterodyne radiospectrometer at a frequency of 9,300 Mc/sec at room temperature

*The cross relaxation effects observed by Giordmaine et al[3] were explained by Bloembergen et al[2] as spin-spin cross relaxation phenomena.

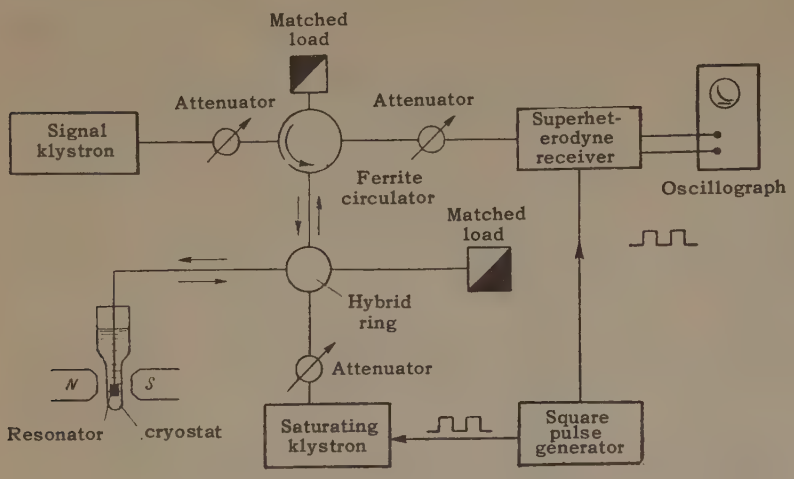

FIG. 1. Block diagram of apparatus used in the relaxation studies.

(300° K), liquid-nitrogen (77° K) and liquid-helium temperatures (4.2° and 1.6° K).

All the measurements were carried out for different hyperfine structure components, $m = \pm 1/2$; $\pm 3/2$; $\pm 5/2$ on the lines corresponding to the electronic transition $M = 1/2 \rightarrow -1/2$. At 300° K the spin-lattice relaxation time T_1 was calculated from the line broadening produced by spin-lattice interaction. This broadening was determined by a comparison of the line widths at 300 and at 77° K.

The value of T_1 at 77° K was determined by the method of continuous saturation of the lines. The method of measurement is analogous to that described earlier.[8]

The relaxation phenomena at liquid helium temperatures were mainly studied by the method of pulsed saturation of the lines of the spectrum. The block diagram of the apparatus used in these experiments is shown in Fig. 1. Saturation was produced by square pulses from an auxiliary klystron generator, the frequency of which was made equal to the frequency of the signal klystron.

The heterodyne only works in the intervals between the saturating pulses, in order to avoid saturation of the heterodyne receiver by the strong signal from the auxiliary klystron. The pulse mode of operation of the saturating klystron and of the heterodyne klystron is produced by feeding the voltages from the square pulse generator onto the reflector.

The observation of the relaxation curves of the recovery of the intensity of the absorption lines in the periods between the saturating pulses is carried out for low power levels of the signal klystron, working under continuous wave conditions.

The duration of the saturating pulses τ was varied in two series of experiments. Saturation by narrow ($\tau = 0.1 - 1$ μsec) and by wide ($\tau = 70$ μsec) pulses was carried out in order to separate the effects of spin-spin cross relaxation and of spin-lattice relaxation (for further details, see Sec. 3).

At 4.2° K the relaxation times were also determined by continuous saturation, in order to compare the values obtained by this method with the values of relaxation time determined by the pulsed saturation method.

3. EXPERIMENTAL RESULTS

The spin-lattice relaxation time T_1 for Mn^{2+} ions in SrS at room temperature was determined from the line broadening, produced by spin-lattice interaction, of the electronic transition $M = 1/2 \rightarrow -1/2$ for the two hyperfine structure components corresponding to values of the nuclear magnetic quantum number $m = \pm 5/2$.* The $M = 1/2 \rightarrow -1/2$ lines are best resolved for these components. For both lines the value of T_1 is the same, equal to $T_1 = 5 \times 10^{-8}$ sec. At 77° K, T_1 was determined by the continuous line saturation method. As is well known, the product $T_1 \cdot T_2$ is determined directly by this method. We obtained the value 9.2×10^{-14} sec^2 for this product at 77° K, and this was the same for the two lines studied, $M = 1/2 \rightarrow -1/2$, $m = \pm 5/2$. The spin-spin relaxation time T_2 calculated from the observed width $\Delta\nu$ of these lines at T = 77° K, using the relation $T_2 = 1/\pi\Delta\nu$, is 6×10^{-8} sec and the spin-lattice relaxation time is consequently $T_1 = 1.5 \times 10^{-6}$ sec.

At liquid helium temperature, T = 4.2° K, the continuous saturation method for the transition $M = 1/2 \rightarrow -1/2$, $m = \pm 5/2$ gave the value $T_1 = 2.9 \times 10^{-2}$ sec, if the same value of T_2 is used as at T = 77° K. However, in the presence of spin-spin

*Detailed data on the spectrum of Mn^{2+} in SrS at 300 and at 77°K were obtained earlier.[1] The spectrum observed at liquid helium temperatures was little different from the spectrum at 77°K.

cross relaxation, which is strongly marked in the spectrum of Mn^{2+} in SrS at helium temperatures, the effective value of T_2 must be reduced threefold in order that the value of T_1 should agree with the true value of the spin-lattice relaxation time $T_1 = 9 \times 10^{-2}$ sec, determined by the direct method of pulsed saturation (see below). For a more detailed investigation of relaxation processes in the paramagnetic resonance spectrum of Mn^{2+} in SrS at helium temperatures, we applied the method of pulsed saturation of the lines.

On saturating by narrow pulses of duration $\tau = 0.1 - 1$ μsec, it was immediately noticed that the relaxation curve of the recovery of the absorption line intensity J, after the action of the saturating pulses, consists of several exponentials and can be expressed by the formula

$$J = \sum_i [A_i \exp(-\alpha_i t) + B_i],$$

where A_i, α_i, and B_i are constants independent of the time t.

Figure 2 shows an oscillogram of a typical relaxation curve, obtained for a saturating pulse duration $\tau = 1$ μsec, for the line of the transition $M = 1/2 \rightarrow -1/2$, $m = -1/2$ at $T = 4.2°$ K. The base line below the relaxation curve corresponds to the equilibrium intensity of the line in the absence of saturation $J_0 = \sum_i B_i$. It was established that the coefficients α_i of the rapidly falling exponential are independent of temperature in the range $4.2 - 1.6°$ K for all the transitions studied $M = 1/2 \rightarrow -1/2$, $m = \pm 1/2; \pm 3/2; \pm 5/2$, while $T_i = 1/\alpha_i$ has values within the limits $2 - 10$ μsec. For all the transitions $M = 1/2 \rightarrow -1/2$, $m = \pm 1/2; \pm 3/2; \pm 5/2$ there is a slowly falling exponential in the overall relaxation curve, the exponent of which decreases with decreasing temperature. The weighting factor of this exponential for all the transitions studied is on the average ~ 50% of the equilibrium line intensity ($A/J_0 \sim 0.5$). The values of $1/\alpha_i$ for the slowly falling exponentials varied between $23 - 46$ μsec at 4.2° K and $150 - 200$ μsec at 1.6° K for the transitions $M = 1/2 \rightarrow -1/2$, corresponding to different components of the hyperfine structure (to different values of m).

The fact that the relaxation times $T_i = 1/\alpha_i$ for the rapidly falling exponentials are independent of temperature, shows that these exponentials characterize the spin-spin interaction. The slowly falling exponentials evidently characterize the spin-lattice interaction, since the relaxation times corresponding to them depend on temperature.

We carried out an experiment with saturation of the lines by broad pulses of duration $\tau = 70$ μsec

FIG. 2. Oscillogram of relaxation curve for the transition $M = 1/2 \rightarrow -1/2$, $m = -1/2$ at $T = 4.2°$K. Saturating pulse duration $\tau = 1$ μsec, pulse repeat time $\tau_1 = 50$ μsec.

in order to elucidate the nature of these two processes. During the time of action of the saturating pulse, the duration of which is greater than the spin-spin cross relaxation time, the saturation processes within the spin system have time to get established, and after the removal of the saturating pulse only spin-lattice relaxation should be observed.

It turned out in fact that on saturating by a broad pulse, the relaxation curve was in the form of only one slowly falling exponential. Thus the relaxation time corresponding to this exponential is the spin-lattice relaxation time T_1. The time T_1 is the same for all transitions

$$M = 1/2 \rightarrow -1/2, \quad m = \pm 1/2; \quad \pm 3/2; \quad \pm 5/2$$

and has the value $T_1 = 90$ μsec at 4.2° K and $T_1 = 210$ μsec at 1.6° K. The values $1/\alpha_i$ for the slowly falling exponentials, obtained on saturating by narrow pulses, are less than the values of T_1. This fact shows that the long exponentials on saturating with narrow pulses characterize a mixture of spin-lattice and spin-spin cross relaxation processes. After carrying out the experiments on saturation by broad pulses it becomes more certain that the times $T_i = 2 - 10$ μsec for the rapidly falling exponentials, observed in the experiments on saturation by narrow pulses, refer to spin-spin cross relaxation.*

4. DISCUSSION OF RESULTS

The following conclusions about the character of the relaxation processes in the spectrum of Mn^{2+} in SrS can be drawn from the experimental results.

1. The temperature dependence of the spin-lattice relaxation time follows the law $T_1 \sim T^{-1}$ in the range $4.2 - 1.6°$ K. This shows that single phonon processes are dominant in spin-lattice relaxation at helium temperatures. At higher temperatures the $T_1 = f(T)$ dependence becomes steeper. It is interesting to note that the reduction of T_1 on increasing the temperature from 4.2 to

*Analogous phenomena of cross relaxation were observed in the spectrum of Co^{2+} in Al_2O_3.[6]

300° K appears not to proceed monotonically. This deduction follows from the fact that the temperature dependence follows a law $T_1 \sim T^{-n}$, where the power n, using the values of T_1 determined at 300, 77 and 4.2° K, comes out larger in the range 4.2 — 77° K than in the range 77 — 300° K. We may also note that at 300° K, $T_1 \approx T_2$ within the limits of experimental errors. Investigations of spin-lattice relaxation at other points in the range are essential for drawing more reliable conclusions about the temperature dependence of T_1 in the range 300 — 4.2° K.

2. The Mn^{2+} ions are in an S-state and the crystal field splits the energy levels of Mn^{2+} in SrS little. We could therefore have assumed that the Kronig mechanism would be little effective for spin-lattice relaxation of Mn^{2+} in SrS, and expect a reasonably large relaxation time T_1 even at room temperature. However, the values of T_1 turned out to be unexpectedly small at 300 and at 77° K. Although the Kronig mechanism can make a contribution to spin-lattice relaxation through the admixture of higher orbital states, it is possible that other relaxation mechanisms play a part in the case of Mn^{2+} in SrS.

Al'tshuler[9] discusses theoretically two mechanisms which may be important for the relaxation of ions in an S-state: modulation, by the thermal vibrations of the lattice, of the magnetic (the Waller mechanism) and exchange interactions between paramagnetic ions. Detailed calculations are necessary to estimate the contribution of these mechanisms to the spin-lattice relaxation of Mn^{2+} in SrS, although it appears unlikely that it can be large, in so far as the concentration of Mn^{2+} ions in the specimens studied is small ($\sim 0.05\%$).

Apart from the relaxation mechanisms noted above, we assume that for Mn^{2+} in SrS, spin-lattice relaxation can be brought about by the modulation of the covalent bonding of Mn^{2+} with the surrounding diamagnetic ions. This mechanism has not so far been discussed theoretically, but it may be effective in substances with covalent bonding. The reduction in the hyperfine structure constant for Mn^{2+} in this compound[1] indicates the existence of covalent bonding of Mn^{2+} in SrS with the surroundings.

3. Spin-spin cross relaxation is strongly marked in the relaxation processes of Mn^{2+} in SrS at liquid helium temperatures.

This cross relaxation may be brought about in the spin system by transitions between energy levels of the electron spin of Mn^{2+}, corresponding to different electron and nuclear states (different values of the electronic, M, and nuclear, m, magnetic quantum numbers). In other words, cross relaxation in the paramagnetic resonance spectrum of Mn^{2+} may proceed between different components of the hyperfine structure, corresponding to one and the same electronic transition, and also between lines belonging to different electronic transitions within each component of the hyperfine structure. Mn^{2+} ions have a large number of energy levels, equal to $(2S + 1)(2I + 1) = 36$, and a complicated paramagnetic resonance spectrum consisting of six groups of hyperfine structure lines, with splittings in these groups into several lines belonging to different electronic transitions. It is therefore difficult to give a definite interpretation of the cross relaxation times observed by us in experiments with pulsed saturation of absorption lines, since there are a large number of routes by which cross relaxation processes may proceed.

The authors express their thanks to Professors A. M. Prokhorov and S. A. Al'tshuler for a discussion of the results. We also want to thank R. M. Medvedev for preparing the specimens of SrS · Mn.

[1] A. A. Manenkov and A. M. Prokhorov, JETP **40**, 1606 (1961), Soviet Phys. JETP **13**, 1129 (1961).

[2] Bloembergen, Shapiro, Pershan, and Artman, Phys. Rev. **114**, 445 (1959).

[3] Giordmaine, Alsop, Nash, and Townes, Phys. Rev. **109**, 302 (1958).

[4] K. D. Bowers and W. B. Mims, Phys. Rev. **115**, 285 (1959).

[5] S. Shapiro and N. Bloembergen, Phys. Rev. **116**, 1453 (1959).

[6] G. M. Zverev and A. M. Prokhorov, JETP **39**, 545 (1960), Soviet Phys. JETP **12**, 382 (1961).

[7] Castle, Chester, and Wagner, Phys. Rev. **119**, 953 (1960).

[8] A. A. Manenkov and A. M. Prokhorov, JETP **38**, 729 (1960), Soviet Phys. JETP **11**, 527 (1960).

[9] S. A. Al'tshuler, Doctoral Thesis, Phys. Inst., Acad. Sci., 1955.

Translated by R. Berman
23

ANGULAR DISTRIBUTION OF μ MESONS FROM π-μ DECAY

A. O. VAĬSENBERG, É. D. KOLGANOVA, and Z. V. MINERVINA

Institute of Theoretical and Experimental Physics, Academy of Sciences, U.S.S.R.

Submitted to JETP editor February 28, 1961

J. Exptl. Theoret. Phys. (U.S.S.R.) **41**, 106-108 (July, 1961)

It is shown that the angular distribution of μ mesons from the decay of π mesons produced in strong interactions is isotropic. The deviation from isotropy observed in some cases may be due to the omission of some of the π-μ decays when their density is very high. Emulsion and microscope distortions are shown to have no effect on the angular distribution.

FOLLOWING the detection of asymmetry in the spatial distribution of electrons from the π-μ-e decay a number of experiments were performed in order to verify that the distribution of μ mesons from the π-μ decay is isotropic. Nearly all the authors who studied the π-μ decay[1-6] arrived at the conclusion that the distribution of interest was isotropic. The work of Hulubei et al[1] provides an exception: with a statistics of approximately 8000 π-μ decays the number of μ mesons emitted "forward" (relative to the direction of the π-meson beam) and "backwards" was found to be smaller by 20-25% than the number emitted "right" and "left." Another exception is the work of Garwin et al,[6] who studied the distribution of μ mesons from the decay of π mesons produced in the decay of τ mesons in emulsions. In this work the following data were obtained on the distribution of μ mesons relative to the direction of motion of the π meson at the instant of decay:

	$E_\pi < 12$ Mev	$E_\pi < 15$ Mev	All π mesons
Back/front ratio:	71/39 = 1.8	85/54 = 1.6	186/160 = 1.16

These data indicate the existence not only of a considerable "forward-backward" asymmetry but also the dependence of it on the energy of the π meson from the τ-meson decay.

The photoemulsion method makes it possible to identify errorlessly π-μ decays and to measure with exceptional accuracy the projection onto the plane of the emulsion of the angles between a given direction and the direction of emission of the μ meson. It therefore seemed to us important to understand how a method so well adapted to the observation of π-μ decays undistorted by systematic errors, could give rise to the results observed by Hulubei et al[1] and Garwin et al.[6]

We carried out measurements in one of the available to us emulsion chambers (NIKFI-R type emulsion), with layers $10\times10\times0.04$ cm, irradiated by a π^+-meson beam whose energy at the output of the collimator was equal to 150 Mev. These π^+ mesons were slowed down by additional filters and the density of the π-μ decays in the emulsion itself was close to 500 events per cm^2 at a distance of 2 cm from the incoming end of the emulsion layer, and close to 60 cm^{-2} at a distance of 2 — 3 cm from the opposite end.

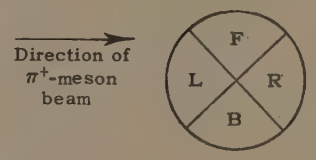

Prior to the measurement of the distribution of μ mesons from the π-μ decay we performed for control purposes measurements of the angular distribution of α particles from thorium stars with 3 to 5 prongs. The measurements were performed with a 20×15 magnification in the following manner. Into the field of view of the microscope ocular was inserted a scale, marked as shown on the figure, and the observers recorded with the letters B, F, L and R the occurrence of an α particle from a thorium star in the corresponding quadrant of the scale. The results obtained by seven observers were in excellent agreement with each other and are given below:

Scale quadrant	B	F	L	R
Number of particles	1292	1344	1266	1253

This distribution is for practical purposes isotropic: thus for example an analysis according to the χ^2 test gives the magnitude $\chi^2 = 3.7$ for three degrees of freedom.

The second control experiment consisted of measurements of the angular distribution of electrons from the μ-e decay relative to the same direction of the collimator axis. It is obvious that

this distribution too should be isotropic. We have selected, under 20×15 magnification, some 4100 π-μ-e decays wholly contained in the emulsion layer. The following angular distribution was found for the electrons:

Scale quadrant	B	F	L	R
Number of electrons	1027	1048	1002	1013

Just like the previous distribution these results indicate isotropy. On the basis of these observations we conclude that distortions of first order in the emulsion, as well as distortions that could be due to the microscope, have no noticeable effect on our measurements of angular distributions.

Let us pass now to the consideration of the data on the angular distribution of μ mesons from π-μ decay.

The microscope operator would find (at 20×10 magnification) a π-μ-decay event by its vertex. From all π-μ decays only those were selected for which the subsequent μ-e decay took place in the same emulsion layer. The decay was drawn in and its coordinates recorded. After the scanning was completed the same observers would repeat it using unchanged selection criteria and recording rules. This double scanning permits one to find events that were missed the first time and also determines the scanning efficiency for each observer. The first measurements were carried out in that region of the emulsion where the density of π-μ decays was small and amounted to approximately 60 cm^{-2}. The resultant angular distribution (from the data of seven observers) and average scanning efficiency of seven observers were as follows:

Scale quadrant:	F	B	L	R
Number of mesons:	504	540	508	487
Scanning efficiency:	0.86±0.03	0.85±0.03	0.87±0.03	0.82±0.03

An analysis according to the χ^2 test gives $\chi^2 \approx 3$ for three degrees of freedom which indicates the absence of statistically significant deviations from isotropy. Furthermore, it turned out that the scanning efficiency was practically the same in all four quadrants.

We shall now give the results obtained in the part of the chamber where the density of π-μ decays was high and approximately equal to $400 - 500$ cm^{-2}. Here the data obtained by different observers were in strong disagreement. The measurements of one group of observers (whom we might denote as A, B, C, D) were, as before, in agreement with an isotropic distribution and with a scanning efficiency independent of the quadrant:

Scale quadrant:	F	B	L	R
Number of mesons:	389	405	375	360
Scanning efficiency:	0.80±0.05	0.73±0.05	0.73±0.05	0.76±0.05

A second group (E, F, G) showed an effect analogous to the one found by Hulubei et al.[1]

Scale quadrant:	F	B	L	R
Number of mesons:	593	647	560	479
Scanning efficiency:	0.77±0.03	0.72±0.03	0.66±0.03	0.63±0.03

This result points to a large anisotropy (the deviation from isotropy is characterized by a χ^2 of approximately 37 for three degrees of freedom), but the analysis indicates that it is due to weakening of scanning efficiency of operators E, F, and G in the quadrants L and R.

We conclude that the present data indicate that the angular distribution of μ mesons from the decay of π mesons produced in strong interactions is isotropic. The asymmmetry found by some of the observers is explained by scanning omissions. These omissions are apparently caused by psychological factors: they arise under conditions of high π-μ-decay density. If on the average several π-μ decays appear in the field of view of the microscope operator he will leave out those decays which require greater attention for their identification, i.e., the "backward" and "forward" decays (quadrants L and R). These considerations do not apply to π mesons produced in the τ decay, where the π meson can be traced from the point of its production, however the statistical accuracy of the data of Garwin et al.[6] is insufficient. The accumulation of large numbers of τ decays in emulsion and in bubble chambers will show whether one is dealing here with an exceptionally large fluctuation or an extraordinarily important physical phenomenon.

[1] Hulubei, Auslander, Balea, Friedlander, and Titeica, International Conference on Peaceful Uses of Atomic Energy, NP 1283, Geneva (1958).

[2] Bogachev, Mikhul, Petrashku, and Sidorov, JETP **34**, 531 (1958), Soviet Phys. JETP **7**, 367 (1958).

[3] Castagnoli, Ferro-Luzzi, and Manfredini, La Ricerca Scientifica **28**, 1644 (1958).

[4] R. L. Connoly and G. R. Lynch, Nuovo cimento **9**, 1077 (1958).

[5] Crewe, Kruse, Miller, and Pondrom, Phys. Rev. **108**, 1531 (1957).

[6] Garwin, Gidal, Lederman, and Weinrich, Phys. Rev. **108**, 1589 (1957).

Translated by A. M. Bincer
24

μ^- MESON CAPTURE IN CARBON WITH FORMATION OF B^{12*}

A. O. VAĬSENBERG

Institute of Theoretical and Experimental Physics, Academy of Sciences, U.S.S.R.

Submitted to JETP editor February 28, 1961

J. Exptl. Theoret. Phys. (U.S.S.R.) **41**, 109-112 (July, 1961)

Approximately 500 two-prong stars produced in the capture of μ^- mesons by light emulsion nuclei are examined. The probability for emission of an Auger electron in a capture of this type is of the order of a tenth of a percent. Nine stars of the type $\mu^- + C^{12} \rightarrow B^{12*} + \nu$; $B^{12*} \rightarrow Li^8 + He^4$ have been detected. The probability of such a reaction is 2×10^{-3} per capture in a carbon nucleus. It is shown that there should exist excited levels in the B^{12} nucleus with an energy $\sim 19 - 26$ Mev, from which breakup into Li^8 and He^4 is possible.

In the study of stars from μ^- meson capture in nuclear emulsion one's attention is attracted to characteristic two-prong stars, consisting of approximately collinear tracks. The short prong of the star represents the track of the recoil nucleus, whose range is, as a rule, under 10 μ. The presence of visible tracks of the recoil nuclei shows that these stars are produced as a result of μ^- meson capture by light, and not heavy, emulsion nuclei. Occasionally the recoil nucleus turn out to be β-active (Fig. 1), and in a few cases, discussed in detail below, we have observed its decay into two α particles. Additional evidence in favor of the hypothesis that the stars in question arise from capture in light nuclei is provided by the absence of Auger electrons from the center of the star. Among the ~ 500 stars of the type under consideration only 2 electron tracks with energy $\gtrsim 25$ kev were found, whereas approximately 20% of captures in heavy nuclei are accompanied by the emission of such electrons.

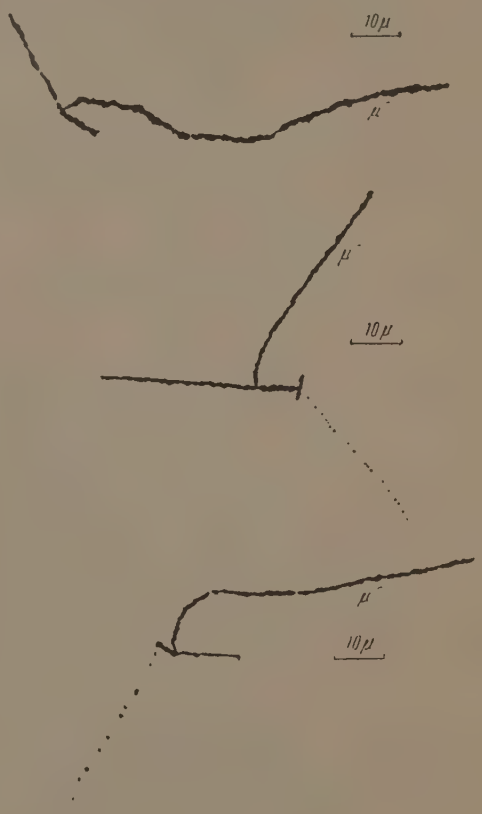

FIG. 1

We remark that the practical absence of Auger electrons among the 500 stars considered by us has additional meaning in connection with the well known experiments of Stearns et al,[2] who noted a considerable deficiency of radiative transitions in μ^- meson captures by light nuclei. According to their data this deficiency amounts to respectively ~ 40 and 20% on C and N nuclei.

It is reasonable to assume that this decrease in the probability of radiative transitions is accompanied by a corresponding increase in the probability of emission of Auger electrons. If this assumption is correct we should have observed ~ 100 Auger electrons with energy > 25 kev, instead of the two that were seen. The number of Auger electrons seen by us is in agreement with that expected from the theory of radiationless transitions,[3,4] and we conclude that there are no additional radiationless transitions to compensate for the deficiency of radiative transitions observed by Stearns et al.[2]

As a rule the two particles observed by us are emitted in approximately opposite directions. This can be seen from the distribution of the projection of the angles ϑ between the directions of the tracks of the recoil nucleus and the other, lighter, particle (Fig. 2). The small deviation from colline-

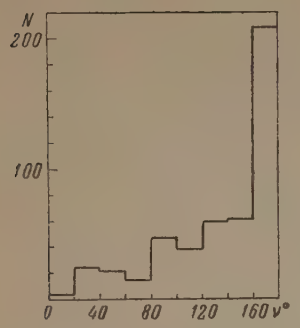

FIG. 2. Distribution of the angles between the tracks of the α particle and the recoil nucleus.

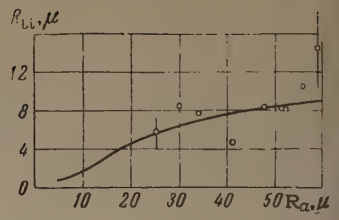

FIG. 3. Correlation between the ranges of the α particle, R_α, and the recoil nucleus, R_{Li}.

arity may be explained by the recoil of the nucleus, which captured the μ^- meson, as a result of emission of a neutrino:

$$\mu^- + N \rightarrow N^* + \nu.$$

From among all observed stars of this type we shall discuss those which could be reliably identified. Such stars (see Fig. 1) arise from capture of a μ^- meson by a C^{12} nucleus:

$$\mu^- + C^{12} \rightarrow B^{12*} + \nu$$

followed by the breakup of the excited B^{12*} nucleus into a Li^8 nucleus and an α particle:

$$B^{12*} \rightarrow Li^8 + \alpha.$$

After stopping the Li^8 nucleus decays:

$$Li^8 \rightarrow Be^8 + \nu + \beta,$$

and the resultant Be nucleus breaks up into two α particles. We have discovered nine disintegrations of this type. Their characteristics are given in the table, where we show the projection ϑ on the emulsion plane of the angle of emission of the two particles, the noncoplanarity angle $\Delta\varphi$ in the perpendicular plane, the ranges of the two particles R_α and R_{Li}, and the total range $R_{2\alpha}$ of the collinear α particles produced in the decay of Be.

If our treatment of these stars is correct then there should exist a correlation between the ranges of the α particles and the recoil nucleus. The solid curve in Fig. 3 shows the dependence between the α-particle range R_α and the recoil nucleus range R_{Li}, calculated on the assumption that in the breakup of the B^{12*} nucleus the momenta of the two particles are equal and opposite. In the construction of this curve we have made use of the range-energy relations for α particles and Li nuclei as given by Bujdoso[5] and Powell.[6] The experimental points on the graph correspond to values of R_α and R_{Li} from the table. If one keeps in mind that the errors in the measurement of the range of the recoil nucleus in the $4 - 10\,\mu$ region can amount to 25 — 30%, one concludes that the agreement found should be considered satisfactory.

Another test of the correctness of our treatment is to be found in the degree of deviation of the tracks from collinearity. If it is assumed that the momentum carried away by the neutrino is close to a 100 Mev, then it is easy to show that for the observed ranges of α particles and lithium nuclei the maximum deviation from collinearity should lie between 15 and 20°. This is in good agreement with the data in the table.

It is of interest to estimate the probability for μ^- meson capture in C^{12}, followed by a reaction of the type considered. According to an approximate estimate the nine stars were found among 160,000 μ^- decays, which can be assumed without too much of an error to be the number of μ^- mesons stopped in the gelatin (C, N, and O nuclei). Let us assume further that the stoppings are equally divided among the nuclei of C, N, and O. It is known that approximately 10% of μ^- mesons in carbon mesic atoms are captured by the nucleus.[7] In this manner we find for the desired probability

$$W \approx 9/\frac{160\,000}{3} \times 0.1 \approx 2 \times 10^{-3},$$

i.e., approximately 2×10^{-3} captures of μ^- mesons

R_α, μ	R_{Li}, μ	$E_\alpha + E_{Li}$, Mev	$R_{2\alpha}$, μ	ϑ, degrees	Δφ, degrees
29.9	8.4	11.5	13	180	2
47.9	8.2	13.8	12.9	156	7
25.2	5.6	8.9	13.6	145	1
51.8	8.1	14.2	10.6	175	4
34.3	7.7	11.9	10.8	166	4
56.3	10.5	16.2	9.6	180	10
59.6	14.4	19.5	9.9	177	4
52	8.1	14.1	15.4	180	8
41.4	4.6	10.7	22.4	175	8

by carbon nuclei lead to the reaction under consideration.

If we turn to the energy level diagram of C^{12},[8] we see that the investigated levels extend all the way to the excitation energy of 5.73 Mev, whereas the rest energy of the $Li^8 + \alpha$ system exceeds this excitation energy by 4.23 Mev. The particles in our stars, resulting from the breakup of the B^{12*} nucleus, have an energy of 9 — 16 Mev. This means that in the region of excitation energies of 5.73 + 4.23 + (9 — 16) Mev, i.e., in the region of 19 — 26 Mev, there should exist levels in the B^{12} nucleus capable of decay into Li^8 and an α particle.

In principle, in addition to the reaction here considered, many of the reactions on light emulsion nuclei can be identified. To that end it is necessary to measure more precisely the range and charge of the recoil nucleus, which, apparently, can be done with the help of fine-grained and diluted emulsions. The capture of μ^- mesons by nuclei may turn out to be a tool for obtaining information on the properties of light nuclei for excitation energies of 10 — 20 Mev.

The author is grateful to E. A. Pesotskaya, Z. V. Minervin, E. D. Kolganov, and V. A. Smirnit-skii for help in measurements.

[1] W. F. Fry, Phys. Rev. **85**, 676 (1952).

[2] Stearns, Stearns, and Leipuner, Phys. Rev. **108**, 445 (1957).

[3] G. R. Burbridge and A. H. de Borde, Phys. Rev. **89**, 189 (1953).

[4] M. A. Ruderman, Phys. Rev. **118**, 1632 (1960).

[5] E. Bujdoso, Nucl. Phys. **6**, 107 (1958).

[6] C. F. Powell et al., The Study of Elementary Particles by the Photographic Method, Pergamon Press, 1959.

[7] Argo, Harrison, Kruse, and McGuire, Phys. Rev. **114**, 626 (1959).

[8] F. Aisenberg-Selove and T. Lauritsen, Nucl. Phys. **11**, 1 (1959).

Translated by A. M. Bincer
25

WAVE RESONANCE OF LIGHT AND GRAVITIONAL WAVES

M. E. GERTSENSHTEĬN

Submitted to JETP editor July 29, 1960

J. Exptl. Theoret. Phys. (U.S.S.R.) **41**, 113-114 (July, 1961)

The energy of gravitational waves excited during the propagation of light in a constant magnetic or electric field is estimated.

ACCORDING to general relativity, light and gravitational waves propagate at the same speed, and their rays coincides with no geodetics. Therefore, if the waves of gravitational and light waves are linearly related, wave resonance, a well known phenomenon in radio physics, sets in and makes possible an appreciable transfer of energy even at low coupling. In the present note we estimate the extent of excitation of gravitational waves by light.

The equations of a weak gravitational field in the presence of an electromagnetic field (see [1]) are

$$\Box\psi^{ik} = -16\pi\gamma c^{-4}\tau^{ik}, \qquad \tau^{k}_{k} = 0, \qquad \tau^{ik}_{,k} = 0,$$

$$\tau^{i}_{k} = \frac{1}{4\pi}\left[F^{il}F_{kl} - \frac{1}{4}\,\delta^{i}_{k}\,(F^{lm}F_{ml})\right], \qquad \psi^{k}_{i} = h^{k}_{i} - \frac{1}{2}\,h\delta^{k}_{i}, \tag{1}$$

where τ^{ik} is the energy-momentum tensor of the electromagnetic field, F^{ik} is the electromagnetic field tensor, γ is the gravitational constant, and h_{ik} is the perturbation of the metric tensor.

Let us apply Eq. (1) to the propagation of light (field F^{ik}) in the presence of a strong "magnetizing" field $F^{(0)ik}$, constant in space and in time. The energy-momentum tensor will be the sum of three terms: the square of the constant term, the square of the field of the light wave, and an interference term describing the wave resonance. Leaving out the nonresonant terms we obtain

$$\Box\psi^{i}_{k} = -\frac{8\gamma}{c^4}\left[F^{(0)il}\,F_{kl} - \frac{1}{4}\,\delta^{i}_{k}\,(F^{(0)lm}F_{lm})\right]. \tag{2}$$

We align the x axis with the wave vector and normalize the wave amplitudes to unit energy density:

$$F_{kl} = b(x)\,f_{kl}\,e^{ikx}, \qquad f^{0l}f_{0l} = 1, \qquad k = \omega/c,$$

$$\psi^{ik} = a(x)\sqrt{16\pi\gamma/c^4k^2}\,\zeta^{ik}\,e^{ikx}, \qquad \zeta_{ik}\zeta^{ik} = 1, \qquad \zeta^{i}_{i} = 0; \tag{3}$$

The amplitudes f_{kl} and ζ^{ik} are dimensionless. We then have in the approximation of slowly varying amplitudes [2]:

$$ida(x)/dx = \sqrt{\gamma/\pi c^4}\,F^{(0)il}\,f_{kl}\,\zeta^{k}_{i}\,b(x). \tag{4}$$

The solution of (4) has the form

$$a(x) = i\sqrt{\gamma/\pi c^4}\,f_{kl}\,\zeta^{k}_{i}\int_{0}^{x}F^{(0)il}(s)\,b(s)\,ds + a(0), \tag{5}$$

where the integration is along the ray. If a(0) = 0, the external field is constant and the absorption or scattering of light along the ray is small in the region under consideration, i.e., b(s) = const, and then

$$|a(x)/b(0)|^2 = (\gamma/\pi c^2)\,F^{(0)2}T^2, \tag{6}$$

where T is the time of travel of the ray in a constant field. In the derivation of (6) we assumed the convolutions of the dimensionless amplitudes to be equal to unity. If the field $F^{(0)}$ is turbulent and random, we can estimate the energy of the gravitational wave by assuming that $F^{(0)}$ is constant over a section of length R_0 (where R_0 is the correlation radius of the field $F^{(0)}$), after which it changes abruptly and at random. The amplitude of the light b(x) is practically constant along the ray. We then have for the amplitude of the gravitational wave

$$a(x) = \sum a_n; \qquad a_n = i\sqrt{\gamma/\pi c^4}\,f_{kl}\,\zeta^{k}_{l}\int_{x_{n-1}}^{x_n}F^{(0)il}(s)b(s)ds.$$

The gravitational waves excited on each section will be incoherent, and we must add their energies and not their amplitudes. As a result we obtain

$$|a(x)/b|^2 = (\gamma/\pi c^3)\,F^{(0)2}R_0\,T. \tag{7}$$

For interstellar fields, putting $F^{(0)} = 10^{-5}$ gauss, $R_0 = 10$ light years, and $T = 10^7$ years, we obtain $|a/b|^2 \sim 10^{-17}$. The frequency of the excited gravitational wave is determined by the frequency of the light.

There are strong magnetic fields also inside the stars, and consequently generation of gravitational waves is also possible. Formula (5) is applicable in this case, too, and the "constant" field $F^{(0)}$ changes relatively slowly, whereas the amplitude

b(s) varies rapidly as a result of light scattering. Thus, the correlation radius a(x) is determined for this case essentially by the free path of the radiation, which is the reciprocal of the opacity.[3] Since the star is transparent to the exciting gravitational radiation, we can show that formula (7) yields the ratio of the gravitational radiation of the star to the optical one. The intensity of the gravitational radiation is small and of no importance to the energy balance. The frequency of the gravitational radiation is determined essentially by the electromagnetic radiation inside the star, where γ quanta predominate.

Thus, the spectrum of the gravitational radiation of stars has maxima both at very low frequencies (the frequencies of planetary orbits), as well as in the range of γ-quantum frequencies; both portions of the spectrum have comparable energy.

From general relativity follows also the possibility of the inverse conversion of gravitational waves into light waves, but this problem is hardly of interest.

[1] L. D. Landau and E. M. Lifshitz, Teoriya polya (Field Theory), 3d Ed., Fizmatgiz, 1960.

[2] M. E. Gertsenshteĭn and N. F. Funtova, Radiotekhnika i elektronika (Radio Engineering and Electron Physics) 4, 805 (1959).

[3] D. A. Frank-Kamenetskii, Fizicheskie yavleniya vnutry zvezd (Physical Phenomena Inside the Stars), Fizmatgiz, 1959.

Translated by J. G. Adashko
26

ANISOTROPY OF GAMMA RADIATION IN THE MÖSSBAUER EFFECT

A. GEL'BERG

Institute of Atomic Physics, Roumanian Academy of Sciences, Bucharest

Submitted to JETP editor August 3, 1960

J. Exptl. Theoret. Phys. (U.S.S.R.) 41, 115-117 (July, 1961)

Anisotropy of γ radiation in the Mössbauer effect is calculated for the case when the source is in a magnetic field (external magnetic field or field of ferromagnetic domains).

MÖSSBAUER[1,2] pointed out the possibility of direct observation of resonance scattering of γ rays in the case when the nucleus is sufficiently rigidly bound to the crystal lattice. Under this condition, the recoil momentum can be transferred not to the individual nucleus, but to the lattice as a whole; consequently, both the emission and the absorption of the γ quantum proceed without energy loss. Thus, realization of resonance scattering requires no additional Doppler shift of the photon energy, and the effective scattering cross section reaches thereupon a large value.

The sensitivity of the Mössbauer effect to minute energy changes has made it possible to observe heretofore undetected phenomena, such as the transverse Doppler effect or the Zeeman splitting of nuclear levels.[3,4] The Zeeman effect was investigated in the decay of Co^{57}, as was the polarization of γ radiation. The latter phenomenon was observed with a source and absorber placed in a magnetic field sufficiently strong to orient the ferromagnetic domains.

The positive results of these experiments indicate that the anisotropy of the emission of γ radiation in the Mössbauer effect can be observed when the source is in a magnetic field. Unlike ordinary experiments with oriented nuclei, such a phenomenon can be observed at high temperatures.

We assume that the source is situated in a magnetic field strong enough to cause a noticeable Zeeman splitting. This can be either an external field or the field of ferromagnetic domains oriented by means of a weak external field.[5]

Let us examine a nucleus situated in a magnetic field H, directed along the z axis, and let the nucleus emit a quantum on going from a state with spin J_1 into a ground state with spin J_0. When the magnetic field is applied, these two levels are split into $2J_1+1$ and $2J_0+1$ levels, respectively. Let 2^L be the multipolarity of the γ quantum. If we do not measure the polarization, we need not distinguish between magnetic and electric radiation.

The angular distribution of radiation of multipolarity 2^L with magnetic quantum number M is given by the expression

$$I_M^L(\theta) = \sum_k a_k(L, M) P_k(\cos\theta),$$

$$a_k = (2k+1)\left[1 - \frac{k(k+1)}{2L(L+1)}\right] C(kLL; 00) C(kLL; 0M),$$

where θ is the angle between the direction of radiation and the z axis, P_k a Legendre polynomial, k an even number, and C a Clebsch-Gordan coefficient.

The relative probability of radiation of an (LM) transition going to a level with magnetic quantum number m_0, is

$$g(m_0 M) = |C(J_0 L J_1; m_0 M)|^2 \Big/ \sum_{m_0 M} |C(J_0 L J_1; m_0 M)|^2,$$

where the summation is over all the Zeeman components; we note that

$$\sum_{m_0 M} g(m_0 M) = 1.$$

The intensity of the (LM) component in the θ direction is $I_M^L(\theta)\, g(m_0 M)$, with

$$\sum I_M^L(\theta) g(m_0 M) = 1.$$

We assume that an absorber, in which resonance scattering can take place, is located in this direction. We shall assume that the absorber is not in an external magnetic field. Two cases are then possible:

a) The intensity of the magnetic field inside the absorber is zero, as for example in the case of $Na_4Fe(CN)_6 \cdot 10H_2O$.[6] In this case there is no Zeeman splitting and the resonant absorption takes place only for the transition $m_1 = 0 \rightarrow m_0 = 0$, if this is possible. In the opposite case, and in general for the observation of other components, it is necessary to compensate for the energy difference in the radiation and absorption with a Doppler

shift.[2] In this case the intensity of the transmitted radiation will depend only on the function $I_M^L(\theta)$ for the given multipole.

b) Inside the absorber there is an unordered magnetic field, for example a ferromagnetic-domain field strong enough to produce a noticeable Zeeman effect. If the Zeeman splitting is sufficiently large, then the radiation (m_0M) can produce only a transition $J_0m_0 \to J_1m_1$, which is the inverse of the transition that takes place in the source nucleus. The quantization axis will coincide for each nucleus with the direction of the local magnetic field. The probability of absorption of the component (m_0M) by the unoriented nuclei of the absorber is proportional to the probability of radiation by the unoriented nuclei, i.e., it can be written in the form $p_{Rg}(m_0M)$.

In experiments on the nuclear Zeeman effect it is also customary to use sources with unordered magnetic field. The share of the component (m_0M) in the radiation from such a source is $g(m_0M)$, and the observed summary probability of absorption is

$$\bar{p}_R = p_R \sum_{m_0M} g^2(m_0M) = p_R/\alpha, \qquad 1/\alpha = \sum g^2(m_0M).$$

We assume for the time being that all the absorption is resonant. The probability of passage of the radiation through the absorber is equal, for each individual component,

$$1-\alpha\,\bar{p}_R\,g(m_0M),$$

and the angular distribution of the transmitted radiation is given by

$$F(\theta) = 1 - p - \alpha\bar{p}_R \sum_{m_0M} I_M^L(\theta) g^2(m_0M),$$

where p is the probability of electron absorption. If the fraction of the resonant radiation is f, the sum in this formula should be multiplied by f.

In order to perform such an experiment it is necessary that the Zeeman splittings in the source and in the absorber be the same. If a source is used with domains oriented by an external field, it should be sufficiently weak so that its influence on the Zeeman splitting can be neglected. The work described in [5] was performed precisely under these conditions.

We shall consider briefly the case of a 14.4-kev transition in the decay of Co^{57}, between the levels $J_1 = 3/2$ and $J_0 = 1/2$ of the Fe^{57} nucleus. Because of the high intensity of the magnetic field of the domains ($\sim 10^5$ oe), the Zeeman splitting exceeds the width of the level. The angular distribution of M1 radiation has the form

$$F(\theta) = 1 - p - \frac{3}{28} f \bar{p}_R [9 + \cos^2\theta].$$

Thus, for an absorber 3 mg/cm^2 thick, containing 76% Fe^{57}, we have[5]

$$\bar{p}_R = 0.543, \qquad f \approx 0.9.$$

Under these conditions the anisotropy obtained is

$$[F(\pi/2) - F(\pi)]/F(\pi) \approx 0.018.$$

In conclusion, the author takes pleasure in thanking Prof. S. Titeica for a discussion of the results of this work.

[1] R. L. Mössbauer, Z. Physik **151**, 124 (1958).
[2] R. L. Mössbauer, Z. Naturforsch. **14a**, 211 (1959).
[3] Pasquali, Frauenfelder, Margulis, and Peacock, Phys. Rev. Lett. **4**, 71 (1960).
[4] Hanna, Heberle, Littlejohn, Perlow, Preston, and Vincent, Phys. Rev. Lett. **4**, 177 (1960).
[5] Hanna, Heberle, Littlejohn, Perlow, Preston, and Vincent, Phys. Rev. Lett. **3**, 28 (1960).
[6] Ruby, Epstein, and Sun, Rev. Sci. Instr. **31**, 580 (1960).

Translated by J. G. Adashko
27

PRODUCTION OF TRITIUM IN COLLISIONS OF FAST PROTONS WITH HEAVY NUCLEI

S. V. IZMAĬLOV and I. I. P'YANOV

Radium Institute, Academy of Sciences, U.S.S.R.

Submitted to JETP editor September 16, 1960

J. Exptl. Theoret. Phys. (U.S.S.R.) **41**, 118-126 (July, 1961)

The probability of the production of tritons as a result of the indirect evaporation process when heavy nuclei are bombarded by protons of energy ~ 100 Mev is calculated.

1. INTRODUCTION

IT is known that nucleons, deuterons d, tritons t, helium nuclei α, and other heavier particles are produced in collisions between high-energy nucleons and nuclei. As a rule, these particles are produced as a result of a direct interaction between the bombarding nucleon and the nucleus and the subsequent evaporation of the residual excited nucleus. However, at incident nucleon energies up to 100 Mev, the production reaction can take place through a compound state. For example, at an incident nucleon energy of 100 Mev (mean free path of a nucleon in the nucleus $\sim 4 \times 10^{-13}$ cm), the nucleon, in the case of a central collision with a heavy nucleus, can experience several collisions in the nucleus and lose a large part of its energy, as a result of which it is trapped in the nucleus and produces an excited compound nucleus. We shall consider such a mechanism of emission of particles.

It is usually assumed that entire compound particles (d, t, α) are evaporated from the compound nucleus, but the excitation can be removed by other channels, in particular, by the evaporation of individual nucleons (or various combinations of them) and their subsequent uniting into d, t, or α close to the boundary of the nucleus (indirect process).

Kikuchi[1] calculated the deuteron yield by means of the indirect process. The basic difference in comparison with ordinary evaporation is in an increase in the mean kinetic energy of the emitted deuterons and a change in the shape of the energy distribution. The probability of deuteron emission in the indirect process, at large excitation, exceeds the corresponding probability for ordinary evaporation.

In contrast to the case of deuterons, the indirect process for triton production can proceed via two channels: by the evaporation of two neutrons and one proton and their subsequent union and by the evaporation of a deuteron and neutron and their subsequent union. We calculated the triton yield via the first channel only and determined its energy spectrum. The calculations were based on the method of Kapur and Peierls[2] (see also [1] and [3]).

2. DETERMINATION OF THE REACTION MATRIX

We shall consider the reaction in which a triton is produced in a heavy nucleus by a high-energy proton p

$$p + A_Z \rightarrow C \rightarrow (A-2)_Z + t, \qquad (1)$$

where C denotes a compound nucleus, A_Z is the target nucleus of mass number A and charge Z. The production of a triton can take place through the union of combinations of two neutrons and one proton undergoing evaporation. In order to take into account all possibilities, we divide the configuration space of two neutrons (n_1 and n_2) and a proton p, which form the triton, into eight regions corresponding to different combinations of these particles with respect to a surface S of given radius r_0 (r_0 is the distance at which the potential energy between nucleons n_1, n_2, p and the residual nucleus $(A-2)_Z$ is sufficiently small; r_0 is a little bigger than the radius of the nucleus). The configuration space is divided in the following way:

N regions	1	2	3	4	5	6	7	8
Particles outside S	n_1, n_2, p	n_1, p	n_2, p	n_1, n_2	p	n_1	n_2	—
Particles inside S	—	n_2	n_1	p	n_1, n_2	n_2, p	n_1, p	n_1, n_2, p

In region 1, the particles n_1, n_2, and p unite into a triton. The transition from 8 to 1 can take place through one of the regions 5, 6, 7, and then, depending on the case, through one of the regions 2, 3, 4. In all, there are six ways of transition from 8 to 1. We shall consider below one of these transitions: 8-5-2-1.

The Hamiltonian of the entire system H is written in the form

$$H = H_0 + K_p + K_1 + K_2 + V_p + V_1 + V_2 + V_{p1} + V_{p2} + V_{12}, \quad (2)$$

where H_0 is the Hamiltonian of the residual nucleus $(A-2)_Z$; K_p, K_1, K_2 are the kinetic energy operators of the nucleons p, n_1, n_2; V_p, V_1, V_2 are the potential energies of interaction of nucleons p, n_1, n_2 with the residual nucleus $(A-2)_Z$; V_{p1}, V_{p2}, V_{12} are the potential energies of interaction of nucleons p and n_1, p and n_2, n_1 and n_2. It is convenient to express the matrix of the transition T by means of wave functions of the final state $\Psi_f^{(-)}$, which are solutions of Schrödinger's equation

$$H\Psi_f^{(-)} = E\Psi_f^{(-)}. \quad (3)$$

To do this, we consider the initial $(p + A_Z)$ and final $[(A-2)_Z + t]$ states of the system.

The splitting up of the Hamiltonian into an unperturbed part and a perturbation is different for the initial (i) and final (f) states. In the initial state

$$H = H_i + V_i, \qquad V_i = V_p + V_{p1} + V_{p2}. \quad (4)$$

In the final state

$$H = H_f + V_f, \qquad V_f = V_p + V_1 + V_2. \quad (5)$$

Here H_i is the unperturbed Hamiltonian of the initial state, V_i is its perturbation; H_f and V_f are the corresponding quantities in the final state.

We also introduce the wave functions Φ_i and Φ_f of the unperturbed Hamiltonians H_i and H_f, respectively:

$$H_i\Phi_i = E\Phi_i, \qquad H_f\Phi_f = E\Phi_f. \quad (6)$$

Then the matrix T is written in the form:[4,5]

$$T = \langle \Psi_f^{(-)} | V_i | \Phi_i \rangle, \quad (7)$$

$$\Psi_f^{(-)} = [1 + (E - i\varepsilon - H)^{-1} V_f]\, \Phi_f. \quad (8)$$

We are interested in those transitions which go through the compound state. It is therefore necessary to exclude from matrix (7) those processes of triton production in which the incident proton p is not inside the region bounded by the surface S and interacts with the tails of the wave functions of neutrons n_1 and n_2 (direct capture). For this purpose, we split the perturbation V_i occurring in (7) into two parts corresponding to the positions of the proton p in the initial state outside and inside the nucleus:

$$V_i = V_i^{(5)} + V_i^{(8)}. \quad (9)$$

We now introduce the Hamiltonian $H^{(2)}$ describing the decaying intermediate nucleus after p and n_1 have left it:

$$H^{(2)} = H_0 + K_2 + V_2,$$

the Hamiltonian $H^{(5)}$ describing the decaying intermediate nucleus after the proton has left it:

$$H^{(5)} = H_0 + K_1 + K_2 + V_1 + V_2 + V_{12}$$

and the Hamiltonian of the compound nucleus $H^{(8)}$:

$$H^{(8)} = H_i + V_i^{(8)}.$$

We also introduce the quantities $E^{(2)} = E - \hbar^2(k_p^2 + k_1^2)/2M$, $E^{(5)} = E - \hbar^2 k_p^2/2M$, where $\hbar k_p$ and $\hbar k_1$ are the momenta of p and n_1, and M is the mass of the nucleon.

We shall consider the eigenfunctions $\varphi_\nu^{(2)}$, $\varphi_\mu^{(5)}$, $\varphi_\lambda^{(8)}$ of the Hamiltonians $H^{(2)}$, $H^{(5)}$, $H^{(8)}$, respectively, which have complex eigenvalues $W_\nu^{(2)}$, $W_\mu^{(5)}$, $W_\lambda^{(8)}$ (the subscripts ν, μ, λ indicate the level number). The function φ satisfies on the surface S the boundary conditions

$$(\partial/\partial r_2 - f(k_2 r_2))\, \varphi_\nu^{(2)}|_{r_2 = r_0} = 0, \quad (\partial/\partial r_1 - f(k_1 r_1))\, \varphi_\mu^{(5)}|_{r_1 = r_0} = 0,$$

$$(\partial/\partial r_p - f(k_p r_p))\, \varphi_\lambda^{(8)}|_{r_p = r_0} = 0, \quad (10)$$

where the function f is given by Kapur and Peierls.[2] The functions $\varphi_\nu^{(2)\prime}$, $\varphi_\mu^{(5)\prime}$, $\varphi_\lambda^{(8)\prime}$ corresponding to the complex conjugate eigenvalues $W_\nu^{(2)*}$, $W_\mu^{(5)*}$, $W_\lambda^{(8)*}$ satisfy the complex conjugate boundary conditions.

The functions φ are normalized in the following way:

$$\sum_\nu |\varphi_\nu^{(2)}\rangle \frac{1}{N_\nu^{(2)}} \langle \varphi_\nu^{(2)\prime}| = 1, \qquad \langle \varphi_\nu^{(2)\prime} | \varphi_\mu^{(2)} \rangle = N_\nu^{(2)} \delta_{\nu\mu}, \quad (11)$$

$|N_\nu^{(2)}| = 1$, and similarly for $\varphi^{(5)}$ and $\varphi^{(8)}$. The complex factor N occurs when $\varphi^{(2)}$ is replaced by $\varphi^{(2)\prime}$ in the usual normalization conditions

$$\sum_\nu |\varphi_\nu^{(2)}\rangle \langle \varphi_\nu^{(2)}| = 1, \qquad \langle \varphi_\nu^{(2)} | \varphi_\mu^{(2)} \rangle = \delta_{\nu\mu}.$$

We now separate out of the matrix T given by formula (7) the part $T^{(c)}$ associated with the transition through the compound nucleus:

$$T^{(c)} = \langle F_f^{(-)} | V_i^{(8)} | \Phi_i \rangle. \quad (12)$$

Here[5]

$$F_f^{(-)} = \Omega_3\Omega_2\Omega_1\Phi_f,$$

$$\Omega_1 = 1 + [E - i\varepsilon - H^{(5)} - K_p - (V_{p1} + V_{p2})^{(8)} - L_{12} + V_1 + V_2]^{-1}L_{12},$$

$$\Omega_2 = 1 + (E - i\varepsilon - H^{(5)} - K_p)^{-1}[V_1 + V_2 - (V_{p1} + V_{p2})^{(8)} - L_{12}],$$

$$\Omega_3 = 1 + (E - i\varepsilon - H^{(5)} - K_p - V_i^{(8)})^{-1}V_i^{(8)}, \qquad (13)$$

where L_{12} is an arbitrary interaction potential, which it is convenient to choose in the form of a potential of a rigid sphere.

We now expand the matrix $T^{(c)}$ in the wave functions $\varphi^{(2)}$, $\varphi^{(5)}$, $\varphi^{(8)}$. However, the function $F_f^{(-)}$ in (12) does not satisfy on the surface S the boundary conditions of the type (12) corresponding to the decay. Kapur and Peierls[2] showed that the function $F_f^{(-)} - \chi$ can be expanded in terms of φ if χ is chosen so that the difference satisfies the boundary conditions. The quantity χ is taken in such a way that all final expressions containing it vanish.

It is also convenient to introduce the potential energy[3] L_p [in analogy to the quantity L_{12} introduced in (13)] in order to separate out of $T^{(c)}$ terms responsible for potential scattering. The matrix $T^{(c)}$ then takes the form

$$T^{(c)} = \langle\chi_f^{(-)}|L_p|\Phi_i\rangle + \langle F_f^{(-)}|V_i^{(8)} - L_p|\chi_i^{(+)}\rangle; \qquad (14)$$

$$\chi_i^{(+)} = [1 + (E + i\varepsilon - H^{(5)} - K_p - L_p)^{-1}L_p]\,\Phi_i,$$

$$\chi_f^{(-)} = [1 + (E - i\varepsilon - H^{(5)} - K_p - L_p)^{-1}L_p] \times [1 + (E - i\varepsilon - H^{(5)} - K_p)^{-1} \times (V_1 + V_2 - V_{p1} - V_{p2})]\,\Phi_f. \qquad (15)$$

The first term in (14) vanishes, since it describes the elastic scattering of the proton, and its interaction with nucleons n_1 and n_2 does not lead to the production of a triton because of the endothermic character of this transition.

For the expansion of $T^{(c)}$ in terms of $\varphi^{(2)}$, we note that the function $\Omega_1\Phi_f$ in (12) satisfies the equation

$$(E - H^{(2)} - K_p - K_1)\,\Omega_1\Phi_f = [(V_{p1} + V_{p2})^{(8)} + V_{12} + L_{12} - V_2]\,\Omega_1\Phi_f. \qquad (16)$$

We multiply (16) on the left by the wave function $\langle \mathbf{k}_1\mathbf{k}_p|$ of the free neutron n_1 (momentum $\hbar\mathbf{k}_1$) and the proton p ($\hbar\mathbf{k}_p$); we take the transposed matrix (we shall denote it with the tilde) and act with it on the function $\varphi_\nu^{(2)}$. Then, using the identity

$$\frac{1}{(E^{(2)} - W_\nu^{(2)})\,N_\nu^{(2)}}\langle\varphi_\nu^{(2)'}\mathbf{k}_1\mathbf{k}_p| = \frac{1}{N_\nu^{(2)}}\langle\varphi_\nu^{(2)'}\mathbf{k}_1\mathbf{k}_p|\,\frac{1}{E + i\varepsilon - \tilde{H}^{(2)} - \tilde{K}_p - \tilde{K}_1}$$

and carrying out the summation over ν, $\mathbf{k}_1$, and $\mathbf{k}_p$, we obtain

$$\sum_{\nu\mathbf{k}_1\mathbf{k}_p}\Delta^{(2)}(\nu;\,\mathbf{k}_2)\,[N_\nu^{(2)}(E^{(2)} - W_\nu^{(2)})]^{-1}\langle\varphi_\nu^{(2)'}\mathbf{k}_1\mathbf{k}_p| = \langle\{1 + (E - i\varepsilon - H^{(2)} - K_p - K_1)^{-1}[V_2 - L_{12} - V_{12} - (V_{p1} + V_{p2})^{(8)}]\}\,\Omega_1\Phi_f|, \qquad (17)$$

$$\Delta^{(2)}(\nu;\,\mathbf{k}_2) = \langle\Omega_1\Phi_f|\,\tilde{H}^{(2)} - H^{(2)}\,|\mathbf{k}_1\mathbf{k}_p\varphi_\nu^{(2)}\rangle. \qquad (18)$$

Multiplying (17) by

$$1 + (E - i\varepsilon - H^{(5)} - K_p)^{-1}(V_1 + V_2),$$

we obtain $\langle\Omega_2\Omega_1\Phi_f|$ in the right-hand part. After inserting this expression into (14), $T^{(c)}$ takes the form

$$T^{(c)} = \sum_{\nu\mathbf{k}_1\mathbf{k}_p}\Delta^{(2)}(\nu;\,\mathbf{k}_2)\,[N_\nu^{(2)}(E^{(2)} - W_\nu^{(2)})]^{-1} \times \langle\mathbf{k}_1\mathbf{k}_p\varphi_\nu^{(2)'}[1 + (\tilde{V}_1 + \tilde{V}_2) \times (E + i\varepsilon - \tilde{H}^{(5)} - \tilde{K}_p)^{-1}]\,\tilde{\Omega}_3|V_i^{(8)} - L_p|\chi_i^{+}\rangle. \qquad (19)$$

The quantity $\Delta^{(2)}$ occurring here characterizes the probability of the evaporation of the neutron n_2 from the intermediate state of the nucleus $(A-1)_Z$ and the subsequent formation of a triton.

Carrying out the expansion of matrix (19) in terms of $\varphi^{(5)}$ and $\varphi^{(8)}$, we obtain, by similar arguments,

$$T_1^c = \sum_{\substack{\nu\mu\lambda\\ \mathbf{k}_1\mathbf{k}_p}}\Delta^{(2)}(\nu;\,\mathbf{k}_2)\,[N_\nu^{(2)}(E^{(2)} - W_\nu^{(2)})]^{-1}\Delta_{(2)}^{(5)}(\mu;\,\nu\mathbf{k}_1) \times [N_\mu^{(5)}(E^{(5)} - W_\mu^{(5)})]^{-1}\Delta_{(5)}^{(8)}(\lambda;\,\mu\mathbf{k}_p)\,[N_\lambda^{(8)}(E - W_\lambda^{(8)})]^{-1}\,y_{\lambda p}. \qquad (20)$$

Here

$$\Delta_{(2)}^{(5)}(\mu;\,\nu\mathbf{k}_1) = \langle\mathbf{k}_1\varphi_\nu^{(2)'}|\,\tilde{H}^{(5)} - H^{(5)}\,|\varphi_\mu^{(5)}\rangle,$$

$$\Delta_{(5)}^{(8)}(\lambda;\,\mu\mathbf{k}_p) = \langle\mathbf{k}_p\varphi_\mu^{(5)'}|\,\tilde{H} - H\,|\varphi_\lambda^{(8)}\rangle \qquad (21)$$

characterize the probabilities of transition of the system from region 5 to region 2 (with the emission of the neutron n_1) and from region 8 to region 5 (with the emission of the proton). The quantity

$$y_{\lambda p} = \langle\varphi_\lambda^{(8)'}|H - \tilde{H}\,|\chi_i^{(+)}\rangle \qquad (22)$$

characterizes the probability of the formation of a

compound nucleus in the state λ when the target nucleus is bombarded by protons.

The subscript 1 of the matrix $T_1^{(c)}$ denotes a given channel for the reaction; we did not indicate this earlier for the sake of brevity. The matrices for processes taking place by other channels are written in a similar way. The complete matrix element is, of course, equal to their sum

$$T^{(c)} = \sum_{j=1}^{n} T_j^{(c)}. \qquad (23)$$

3. CALCULATION OF THE CROSS SECTION FOR THE PRODUCTION OF TRITONS

We shall calculate the cross section $\sigma(p, t)$ for the process corresponding to the matrix $T^{(c)}$ (23). It is convenient to write it in the form of a dispersion formula in which terms characterizing the formation of a compound nucleus are separated:

$$\sigma(p, t) = \frac{\pi}{k_p^2}\left|\sum_{\lambda}\frac{(\Gamma_t\Gamma_{\lambda p})^{1/2}}{N_\lambda^{(8)}(E - W_\lambda^{(8)})}\right|^2. \qquad (24)$$

Here $\Gamma_{\lambda p} = |y_{\lambda p}|^2$ is the width for the formation of a compound nucleus by the incident proton and the nucleus A_Z; Γ_t is the width corresponding to the formation of a triton; $W_\lambda^{(8)} = E_\lambda - \frac{1}{2}i\Gamma_\lambda$, where E_λ is the energy level of the compound nucleus in the state λ, and Γ_λ is the width of this level.

The expression for the cross section (24) must be averaged over the initial state and summed over all final states. To do this, we consider the average of $\sigma(p, t)$ with respect to the energy of the bombarding beam, where we neglect the contribution from cross terms:

$$\sigma(p, t) = \frac{\pi}{k_p^2}\frac{1}{D(E_c)}\int\frac{\Gamma_t\Gamma_{\lambda p}}{(E - E_\lambda)^2 + \Gamma_\lambda^2/4}dE = \frac{2\pi}{k_p^2}\frac{\Gamma_t\Gamma_{\lambda p}}{\Gamma_\lambda D(E_c)}; \qquad (25)$$

here $D(E_c)$ is the average distance between the compound nucleus levels for an excitation energy $E_c \equiv E_\lambda$.

Taking into account the fact that the density of the final states of the triton is

$$2\cdot 4\pi K_t^2 dK_t/(2\pi)^3\, dE_t = 3MK_t/\pi^2\hbar^2$$

where K_t is the wave number of the emitted triton, $E = \hbar^2K_t^2/6M$ is the kinetic energy of the triton, we obtain the expression for the width Γ_t:

$$\Gamma_t = \Sigma_f\frac{3}{\pi}\frac{MK_t}{\hbar}|B|^2, \qquad (26)$$

$$B = \sum_{\mu\nu\mathbf{k}_1\mathbf{k}_p}\Delta^{(2)}(\nu; \mathbf{k}_2)\,[N_\nu^{(2)}(E^{(2)} - W_\nu^{(2)})]^{-1}\,\Delta_{(2)}^{(5)}(\mu; \nu\mathbf{k}_1)$$
$$\times\,[N_\mu^{(5)}(E^{(5)} - W_\mu^{(5)})]^{-1}\,\Delta_{(5)}^{(8)}(\lambda, \mu\mathbf{k}_p)$$
$$+ 5 \text{ similar terms from (23)} \qquad (27)$$

Here the symbol Σ_f denotes summation over all final states.

We estimate the first term B_1 in the sum (27). Introducing the notation

$$g(\mathbf{r}_2, \mathbf{R}; \mathbf{k}_1, \mathbf{k}_p) = \langle\mathbf{k}_1\mathbf{k}_p|\,\Phi_f\rangle \approx \langle\mathbf{k}_1\mathbf{k}_p|\,\Omega_1\Phi_f\rangle, \qquad (28)$$

we rewrite (18) in the form

$$\Delta^{(2)}(\nu; \mathbf{k}_2) \approx \langle g|\,\widetilde{H}^{(2)} - H^{(2)}\,|\varphi_\nu^{(2)}\rangle. \qquad (29)$$

In (29), we neglected the effect of L_{12} on the wave function Φ_f. The error in doing this is small, since, by choosing L_{12} in the form of a potential of a rigid sphere, we extrapolate the given form of g (28) to the small volume bounded by the surface S.

In (28), R denotes the coordinates of all the particles except n_1, n_2, p. Then

$$g = \frac{1}{(2\pi)^3}$$
$$\times\int d\mathbf{r}_1 d\mathbf{r}_p e^{-i\mathbf{k}_1\mathbf{r}_1}e^{-i\mathbf{k}_p\mathbf{r}_p}\,\Phi_t(\mathbf{r}_1, \mathbf{r}_2, \mathbf{r}_p)\,e^{i\mathbf{K}_t(\mathbf{r}_1+\mathbf{r}_2+\mathbf{r}_p)/3}\Psi_f(\mathbf{R}). \qquad (30)$$

Here $\Psi_f(\mathbf{R})$ is the wave function of the residual nucleus $(A-2)_Z$; $\Phi_t(\mathbf{r}_1, \mathbf{r}_2, \mathbf{r}_p)$ is the wave function of the internal motion of the triton; for our problem it is convenient to choose it in the form

$$\Phi_t = \frac{\alpha}{2\sqrt{7}\pi}\left[\frac{\exp\{-\alpha(\rho_1+\rho_2)\}}{\rho_1\rho_2} + \frac{\exp\{-\alpha(\rho_2+\rho_3)\}}{\rho_2\rho_3}\right.$$
$$\left. + \frac{\exp\{-\alpha(\rho_3+\rho_1)\}}{\rho_3\rho_1}\right]. \qquad (31)$$

We note that here Φ_t is normalized, the parameter α characterizes the dimensions of the nucleus and the binding energy of the triton, and

$$\boldsymbol{\rho}_1 = \mathbf{r}_1 - \mathbf{r}_2, \qquad \boldsymbol{\rho}_2 = \mathbf{r}_2 - \mathbf{r}_p, \qquad \boldsymbol{\rho}_3 = \mathbf{r}_p - \mathbf{r}_1.$$

The calculation of g (28) gives

$$g \approx \xi(\mathbf{k}_1, \mathbf{k}_p, \mathbf{K}_t)\,\Psi_f(\mathbf{R})\exp(i\mathbf{q}\mathbf{r}_2), \qquad (32)$$

$$\xi = \frac{\alpha}{\pi^2\sqrt{7}}\left[\frac{1}{(\alpha^2+q_1^2)(\alpha^2+q_2^2)} + \frac{1}{(\alpha^2+q_2^2)(\alpha^2+q_3^2)}\right.$$
$$\left. + \frac{1}{(\alpha^2+q_3^2)(\alpha^2+q_1^2)}\right],$$

$$\mathbf{q} = \mathbf{K}_t - \mathbf{k}_1 - \mathbf{k}_p, \quad \mathbf{q}_1 = \tfrac{2}{3}\mathbf{K}_t - \mathbf{k}_1 - \mathbf{k}_p,$$

$$\mathbf{q}_2 = \tfrac{1}{3}\mathbf{K}_t - \mathbf{k}_1, \quad \mathbf{q}_3 = \tfrac{1}{3}\mathbf{K}_t - \mathbf{k}_p. \qquad (33)$$

For greater accuracy in the estimate (28), we take into account the spin components of all particles, except n_1 and p. After lengthy calculations, in which we neglect the recoil of the nucleus (so that $\mathbf{q} = \mathbf{K}_t - \mathbf{k}_1 - \mathbf{k}_p \approx \mathbf{k}_2$), and going over to the integral over the surface,[6] we obtain for the average value of (29)

$$|\Delta^{(2)}(\nu;\mathbf{k}_2)|^2_{\mathrm{av}} \approx (\pi\hbar^2/8Mk_2)\,\xi^2\Gamma_{2\nu}(k_2), \quad \Gamma_{2\nu}(k_2) = |\gamma_2(\nu)|^2, \tag{34}$$

where, according to reference 1,

$$\gamma_2(\nu) = -\left(\frac{\hbar^2 k_2}{M}\right)^{1/2} \times \int_S \left\langle \Psi_f(\mathbf{R})\, Y_{JMl_2\sigma} \middle| \varphi^{(2)}_\nu \left(\frac{\partial}{\partial r_2} - f(k_2 r_2)\right) j_{l_2}(k_2 r_2) \right\rangle dS \tag{35}$$

is the amplitude of the width of the emission of nucleon n_2 with a momentum $\hbar k_2$ from the intermediate nucleus $(A-1)_Z$ in the state ν. In (35), $j_{l_2}(k_2 r_2)$ is the spherical Bessel function of the first kind and of order l_2, and

$$Y_{JMl_2\sigma} = \sum_{m_2\mu\mu_2\mu_0} (l_2\sigma m_2\mu \,|\, JM)\,(\sigma_2\sigma_0\mu_2\mu_0 \,|\, \sigma\mu) \times \chi_{\mu_2}(\sigma_2)\,\chi_{\mu_0}(\sigma_0)\,Y_{l_2 m_2}(\Omega_2),$$

where $\chi_{\mu_2}(\sigma_2)$ and $\chi_{\mu_0}(\sigma_0)$ are the spin functions of the neutron n_2 and the residual nucleus $(A-2)_Z$, respectively; $(\ldots|\ldots)$ are the Clebsch-Gordan coefficients; $Y_{l_2 m_2}$ are spherical functions.

The calculation of (21) gives

$$|\Delta^{(5)}_{(2)}(\mu;\nu\mathbf{k}_1)|^2_{\mathrm{av}} \approx (\pi\hbar^2/Mk_1)\,\Gamma_{1\mu}(k_1);$$
$$|\Delta^{(8)}_{(5)}(\lambda;\mu\mathbf{k}_p)|^2_{\mathrm{av}} \approx (\pi\hbar^2/Mk_p)\,\Gamma_{p\lambda}(k_p), \tag{36}$$

where $\Gamma_{1\mu}(k_1)$ is the width for the emission of neutron n_1 with momentum $\hbar k_1$ from the intermediate nucleus A_Z in the state μ; $\Gamma_{p\lambda}(k_p)$ is the width for the emission of the proton with momentum $\hbar k_p$ from the compound nucleus in the state λ.

We insert (34) and (36) into (27) and make the substitution for the widths in accordance with Weisskopf's formulas:[7]

$$\Gamma_{1\mu} = \frac{1}{w(E^{(5)})}\frac{2ME_1}{\pi^2\hbar^2}\sigma^{(1)}(E_1),$$
$$\Gamma_{2\nu} = \frac{1}{w(E^{(2)})}\frac{2ME_2}{\pi^2\hbar^2}\sigma^{(2)}(E_2), \qquad \Gamma_{p\lambda} = \frac{1}{w(E_c)}\frac{2ME_p}{\pi^2\hbar^2}\sigma^{(p)}(E_p), \tag{37}$$

here $w(E^{(5)})$, $w(E^{(2)})$, and $w(E_C)$ are the level densities of the intermediate nuclei A_Z, $(A-1)_Z$, and the compound nucleus C, respectively, with excitation energies $E^{(5)}$, $E^{(2)}$, and E_C; $\sigma^{(1)}(E_1)$, $\sigma^{(2)}(E_2)$, and $\sigma^{(p)}(E_p)$ are the cross sections for the formation of intermediate nuclei A_Z, $(A-1)_Z$, and the compound nucleus C by the incident nucleons n_1, n_2, and p of energy E_1, E_2, and E_p, where these cross sections are slowly varying functions of the energy, and E_1, E_2, and E_p are eigenvalues of the operators K_1, K_2, K_p, respectively. After integration, we obtain the quantity B_j (j = 1, 2, 3, 4, 5, 6):

$$B_j \approx 10^{-2}\left(\frac{M}{\hbar^2}\right)^{1/4}\alpha\,[w(E_c)\,\sigma^{(1)}\,\sigma^{(2)}\,\sigma^{(p)}]^{1/2} \times \exp\left[-\frac{3S_1+E_t}{2\Theta_c}\right] f(E_t)\,E_t^{7/4},$$

$$f(E_t) = \left\{\left[\ln\frac{\hbar^2\alpha^2/M + 8E_t/3}{\hbar^2\alpha^2/M}\right]^2 + \frac{1}{2}\ln\frac{\hbar^2\alpha^2/M+8E_t/3}{\hbar^2\alpha^2/M}\ln\frac{\hbar^2\alpha^2/M+32\,E_t/3}{\hbar^2\alpha^2/M}\right\}. \tag{38}$$

In the calculation of (38), we took into account the fact that[8]

$$w(E^{(2)}) \approx w(E_c)\exp\left(-\frac{E_1+E_p+S_1+S_p}{\Theta_c}\right),$$
$$w(E^{(5)}) = w(E_c)\exp\left(-\frac{E_p+S_p}{\Theta_c}\right),$$

where S_p and S_1 are the binding energies of the nucleons p and n_1 in nuclei A_Z and $(A-1)_Z$, respectively, Θ_C is the temperature of the compound nucleus C; we also took into account the fact that, according to reference 9, $S_1 \approx S_2 \approx S_p$ in the case of heavy nuclei.

Inserting the value of B_j (38) into (26) and carrying out the summation over all final states (after going over from summation to integration):

$$\Sigma_f \to \int \frac{dE_f}{D(E_f)} = \int_0^{E_c-S_t} w(E_c)\exp\left(-\frac{E_t+S_t}{\Theta_c}\right)dE_t$$

(S_t is the binding energy of a triton in the residual nucleus $(A-2)_Z$, $E_f = E_c - E_t - S_t$), we obtain the width for the triton production:

$$\Gamma_t \approx 1.4\cdot 10^{-3}\,(M\alpha/\hbar^2)^2\,\sigma^{(1)}\sigma^{(2)}\sigma^{(p)}\exp\left[-(3S_1+S_t)/\Theta_c\right] \times \int f^2(E_t)\,E_t^4\exp(-2E_t/\Theta_c)\,dE_t. \tag{39}$$

If we neglect the slowly varying logarithmic term, the integrand gives the energy spectrum $dw(E_t)$ of the emitted tritons:

$$dw(E_t) \sim E_t^4\exp(-2E_t/\Theta_c)\,dE_t. \tag{40}$$

Calculation of the integral in (39) by the method of steepest descent leads to

$$\Gamma_t \approx 1.1\cdot 10^{-3}\left(\frac{M\alpha}{\hbar^2}\right)^2\sigma^{(1)}\sigma^{(2)}\sigma^{(p)}\,w^2(E_c) \times \exp\left[-\left(\frac{3S_1+S_t}{\Theta_c}\right)\right] f^2(2\Theta_c)\,\Theta_c^5. \tag{41}$$

Finally, we compare the width (41) with the width for the evaporation of a triton Γ_{tc} obtained from the ordinary theory of evaporation. For this, we introduce[1] the integral width for the evaporation of nucleons n_1 and p and a triton by the compound nucleus:

$$\Gamma_{ic} = \int \Gamma_{ic}(E_i)\, dE_i \qquad (i = 1, p, t)$$

$$\Gamma_{1c} = (2M/\pi^2\hbar^2)\, \sigma^{(1)}\, \Theta_c^2 \exp(-S_1/\Theta_c),$$

$$\Gamma_{pc} = (2M/\pi^2\hbar^2)\, \sigma^{(p)}\, \Theta_c^2 \exp(-S_p/\Theta_c),$$

$$\Gamma_{tc} = (6M/\pi^2\hbar^2)\, \sigma^{(t)}\, \Theta_c^2 \exp(-S_t/\Theta_c), \qquad (42)$$

where $\sigma^{(1)}$, $\sigma^{(p)}$, and $\sigma^{(t)}$ are the cross sections for the formation of a compound nucleus by the incident nucleons n_1 and p and the triton. We note that formulas (42) are readily derived from (37). As a result, we obtain

$$\Gamma_t/\Gamma_{tc} \approx 4.5 \cdot 10^{-2} \frac{\Gamma_{1c}\Gamma_{pc}}{D^2(E_c)} \frac{\sigma^{(2)}}{\sigma^{(t)}} f^2(2\Theta_c) \frac{\hbar^2\alpha^2}{M\Theta_c} \exp(-S_1/\Theta_c). \quad (43)$$

The quantity $\Gamma_{1c}\Gamma_{pc}/D^2(E_c)$ is of the order of unity, since the excitation energy is large.[8] The ratio $\sigma^{(2)}/\sigma^{(t)}$ is also of the order of magnitude of unity; the term $\hbar^2\alpha^2/M$ is equal to 0.3 Mev.* The binding energy S_1 can be taken equal to 6 Mev (heavy nuclei). Then

$$\Gamma_t/\Gamma_{tc} \approx 1.4 \cdot 10^{-2}\, \Theta_c^{-1} f^2(2\Theta_c) \exp(-6/\Theta_c) \qquad (\Theta_c \text{ in Mev}). \quad (44)$$

For $\Theta_c \approx 2.5$ Mev, which corresponds to an excitation energy of 100 Mev for heavy nuclei with A > 200, we have

$$\Gamma_t/\Gamma_{tc} \sim 0.3. \qquad (45)$$

Hence the indirect evaporation process associated with the evaporation of the three nucleons n_1, n_2, and p and their subsequent uniting makes an appreciable contribution to the cross section for the production of tritons.

We note that this result does not take into account the probability that the particles cross the Coulomb barrier. If this is taken into account, the ratio (45) will be somewhat larger.

*The quantity α is estimated from the value of the triton radius $R_t = 2.24 \times 10^{-13}$ cm determined from a comparison of the binding energies of the mirror nuclei t and He_2^3:

$$R_t = r_1 - \frac{r_1 + r_2 + r_3}{3} = \frac{1}{3}(\rho_1 - \rho_3),$$

$$R_t = \frac{1}{3}\int |\rho_1 - \rho_3|\, |\Phi_t|^2\, \delta(\rho_1 + \rho_2 + \rho_3)\, d\rho_1\, d\rho_2\, d\rho_3.$$

Hence $\alpha = 0.85 \times 10^{12}$ cm^{-1} and $\hbar^2\alpha^2/M = 0.3$ Mev.

[1] K. Kikuchi, Progr. Theoret. Phys. (Kyoto) **18**, 503 (1957).

[2] P. Kapur and R. Peierls, Proc. Roy. Soc. (London) **A166**, 277 (1938).

[3] H. Ui, Progr. Theoret. Phys. (Kyoto) **16**, 299 (1956).

[4] B. Lippman and J. Schwinger, Phys. Rev. **79**, 469 (1950).

[5] M. Gell-Mann and M. Goldberger, Phys. Rev. **91**, 398 (1953).

[6] V. I. Smirnov, Kurs vysshei matematiki (Course in Higher Mathematics), Gostekhizdat, 1951, vol. 2, Sec. 193.

[7] V. F. Weisskopf, Phys. Rev. **52**, 295 (1937).

[8] A. Akhiezer and I. Pomeranchuk, Nekotorye voprosy teorii yadra (Some Problems on the Theory of the Nucleus), Gostekhizdat, 1950.

[9] J. M. Blatt and V. F. Weisskopf, Theoretical Nuclear Physics, John Wiley and Sons, New York, 1952, Chap. 1.

Translated by E. Marquit
28

CALCULATION OF THE SPIN-LATTICE RELAXATION TIME FOR RADICALS IN MOLECULAR CRYSTALS

I. V. ALEKSANDROV and G. M. ZHIDOMIROV

Institute of Chemical Physics, Academy of Sciences, U.S.S.R.

Submitted to JETP editor December 19, 1960

J. Exptl. Theoret. Phys. (U.S.S.R.) 41, 127-132 (July, 1961)

It is shown that anisotropy of the g factor (i.e., anisotropy of the hyperfine structure) can lead to a spin-lattice relaxation time for radicals in molecular crystals that is of the order of 10^{-3} sec or less in the presence of orientational oscillations.

THE spin-lattice relaxation mechanism of radicals in liquids is well understood at the present time.[1] We have already shown[2] that in most cases relaxation in liquids results from Brownian rotation of the radicals, as was suggested by McConnell.[1] It is obvious, however, that McConnell's mechanism is ineffective in solids, where all internal rotations are usually frozen. It can therefore be assumed that the spin-lattice relaxation time T_1 in a solid will be considerably longer than in a liquid, and the literature contains indications[3] that we can expect T_1 to be of the order of one second.

We shall consider spin-lattice relaxation of a radical in a magnetically dilute molecular crystal, which is the most characteristic case. It is evident at once that the method of calculating the relaxation transition probability in [2] cannot be applied to a solid, where the spectrum of thermal motions differs essentially from that given in Eqs. (5) and (8) of [2]. In complete analogy with liquids, the interaction between electron spin and the oscillations of individual atoms of a radical in molecular crystals appears to be considerably weaker than that between spin and orientational motions of the radical as a whole.[4]

Let the spin Hamiltonian be

$$\mathcal{H} = \beta g_{\alpha\gamma} S_\alpha H_\gamma + A_{\alpha\gamma} S_\alpha I_\gamma, \qquad (1)$$

where $g_{\alpha\gamma}$ and $A_{\alpha\gamma}$ are the tensors of the spin-orbit and hyperfine interaction, respectively, with summation over Greek subscripts. H_α is the external magnetic field component in the α direction; S_α and I_α are the projections of the electron and nuclear spin operators on the α axis (assuming that the electron spin interacts with the spin of only one nucleus); β is the Bohr magneton. We shall assume for the sake of simplicity that the spin-orbit and hyperfine interactions are axially symmetric, i.e., in some system of coordinates x″y″z″ fixed rigidly in the radical the tensors $g_{\alpha\gamma}$ and $A_{\alpha\gamma}$ are diagonal, with

$$g_{x''x''} = g_{y''y''} = g_\perp, \quad g_{z''z''} = g_\parallel, \qquad A_{x''x''} = A_{y''y''} = A_\perp, \quad A_{z''z''} = A_\parallel. \qquad (2)$$

We shall use the linear model of orientational waves in a molecular crystal that was investigated in [4], assuming that in the equilibrium position the principal (z″) axis of g and A is parallel to the direction of propagation κ of orientational waves. Assuming that the angular deviation χ from equilibrium is small and denoting the angle between κ and the magnetic field H by φ, we find that when χ lies in a plane passing through κ and H (the z′y′ plane in Fig. 1), the spin Hamiltonian (1) becomes

$$\mathcal{H} = \beta H g_{zz}(\varphi) S_z + A(\varphi) S_z I_z + \beta H g_{xz}(\varphi, \chi) S_x + A_{xx}(\varphi, \chi) S_x I_x + A_{xz}(\varphi\chi) S_x I_z, \qquad (3)$$

$$g_{zz}(\varphi) = g_\perp \sin^2\varphi + g_\parallel \cos^2\varphi,$$
$$A_{zz}(\varphi) = A_\perp \sin^2\varphi + A_\parallel \cos^2\varphi,$$
$$g_{xz}(\varphi, \chi) = \Delta g\, [\chi \cos 2\varphi + \chi^2 \sin 2\varphi],$$
$$A_{xx}(\varphi, \chi) = \Delta A\, [-\chi \sin 2\varphi + \chi^2 \cos 2\varphi],$$
$$A_{xz}(\varphi, \chi) = \Delta A\, [\chi \cos 2\varphi + \chi^2 \sin 2\varphi],$$
$$\Delta g = g_\parallel - g_\perp, \quad \Delta A = A_\parallel - A_\perp. \qquad (4)$$

In (3) we have neglected terms of the form $(A_\perp \cos^2\varphi + A_\parallel \sin^2\varphi) S_X I_X$, which cause small level shifts in higher approximations, as well as $\chi \Delta A \cos^2 2\varphi\, S_Z I_X$ terms, which do not induce electron spin flip.

When waves are polarized in the perpendicular direction (i.e., the deviation from equilibrium occurs in the z′x′ plane, as shown in Fig. 2), Eq. (1) becomes

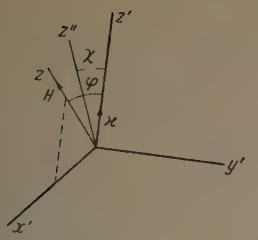

FIG. 1

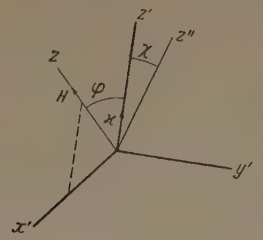

FIG. 2

$$\mathcal{H} = \beta H g_{zz}(\varphi)\, S_z + A_{zz}(\varphi)\, S_z I_z + \beta H g_{xz} S_x + \beta H g_{yz} S_y + A_{xx} S_x I_x + A_{xy} S_x I_y + A_{xz} S_x I_z + A_{yx} S_y I_x + A_{yy} S_y I_y + A_{yz} S_y I_z, \quad (5)$$

where

$$g_{xz} = \tfrac{1}{2}\Delta g \chi^2 \sin 2\varphi,\ g_{yz} = \Delta g \chi \cos\varphi,\ A_{xx} = -\Delta A \chi^2 \sin^2\varphi,$$
$$A_{xy} = A_{yx} = -\Delta A\, \chi \sin\varphi,\quad A_{xz} = \tfrac{1}{2}\Delta A \chi^2 \sin 2\varphi,$$
$$A_{yy} = \Delta A \chi^2,\quad A_{yz} = \Delta A \chi \cos\varphi. \quad (6)$$

In (5), as in (3), we have omitted all terms that are unimportant for our purposes.

We thus find that in the cases of both (3) and (5), when calculating the probability of a relaxation transition between any two levels of the spin system, the spin Hamiltonian can be put into the form

$$\mathcal{H} = \beta H g(\varphi)\, S_z + A(\varphi)\, S_z I_z + \chi R_1(\varphi) + \chi^2 R_2(\varphi), \quad (7)$$

where $R_1(\varphi)$ and $R_2(\varphi)$ are linear combinations of the spin operators with nonvanishing matrix elements for the transition of interest. The coefficients in these linear combinations are functions of the angle φ.

In (7) we shall first consider the term linear in χ that is responsible for transitions involving absorption of a single orientational phonon. The probability per unit time of a relaxation transition between spin levels (with spin flip) is given by[5]

$$w_{12} = \frac{2\pi}{\hbar^2} |(1|R_1|2)|^2 \langle |\chi_{n,n+1}(\omega_L)|^2 \rangle g(\omega_L), \quad (8)$$

where $(1|R_1|2)$ is the matrix element between spin states 1 and 2, $\chi_{n,n+1}(\omega) = (n\hbar/2J\omega)^{1/2}$ is the matrix element between states n and n+1 of the rotational oscillator, where J is the moment of inertia of the rotational oscillator, i.e., of the radical with respect to the appropriate axis; $g(\omega)\,d\omega$ is the number of normal orientational oscillations with frequencies from ω to $\omega+d\omega$; the sign $\langle\ \rangle$ denotes averaging over the quantum numbers n; and $\hbar\omega_L$ is the separation between the magnetic levels 1 and 2.

It follows from [4] that for the linear model of orientational waves, when the centers of rotational oscillations of individual molecules are fixed (i.e., there are no interactions between orientational and translational oscillations) the frequencies ω are determined from

$$\omega = \Omega_2 \sqrt{1 + q\cos\eta}\ , \quad (9)$$

where Ω_2 is the frequency of rotational oscillations of an individual molecule if all other molecules are at their equilibrium positions, q is determined by the interaction constants of the individual molecules and can assume values from -1 to $+1$, and η varies from 0 to π. It is easily seen that $g(\omega)$, normalized to 1, is then represented by

$$g(\omega) = \begin{cases} 2\omega\,(\pi q \Omega_2^2)^{-1}\left[1 - \frac{1}{q^2}\left(\frac{\omega^2}{\Omega_2^2} - 1\right)^2\right]^{-1/2} & \text{for } \Omega_2\sqrt{1-|q|} < \omega < \Omega_2\sqrt{1+|q|} \\ 0 & \text{for } \omega < \Omega_2\sqrt{1-|q|} \text{ and for } \omega > \Omega_2\sqrt{1+|q|}\,. \end{cases} \quad (10)$$

In other words, unlike the spectrum of translational vibrations, the frequency spectrum of orientational waves generally starts at some lower limit $\Omega_{min} = \Omega_2\sqrt{1-|q|}$ instead of zero frequency.

From the Raman scattering spectra in molecular crystals it follows that the frequency threshold Ω_{min} lies in the optical infrared region ($\Omega_{min} \gg \omega_L$). We then obviously have $g(\omega_L) = 0$ in (8). This corresponds to the fact that the minimum energy of an orientational phonon is considerably greater than the Zeeman quantum. Consequently, one form of energy cannot be converted directly into the other, and spin energy transfer to the lattice requires at least two orientational phonons (a Raman transition).

Relaxational transitions of this kind involving two phonons are induced by the last term in (7).

The transition probability per unit time is then

$$w_{12} = (2\pi/\hbar^2)\,|(1|R_2|2)|^2 \int_{\Omega_{min}}^{\Omega_{max}} \langle |\chi_{n,n+1}(\omega) \times |^2 \rangle \langle |\chi_{n,n+1}(\omega+\omega_L)|^2 \rangle\, g(\omega)\, g(\omega+\omega_L)\, d\omega,$$
$$\Omega_{max} = \Omega_2\sqrt{1+|q|}. \quad (11)$$

Averaging over n and using (10), we obtain

$$w_{12} = (2/\pi)\,(|(1|R_2|2)|/qJ\Omega_2^2)^2 \times \int_{\Omega_{min}}^{\Omega_{max}-\omega_L} F(\omega)\left[\left(1 - \frac{1}{q^2}\left(\frac{\omega^2}{\Omega^2} - 1\right)^2\right) \times \left(1 - \frac{1}{q^2}\left(\frac{(\omega+\omega_L)^2}{\Omega^2} - 1\right)\right)\right]^{-1/2} d\omega,$$
$$F(\omega) = \exp\{\hbar(\omega+\omega_L)/kT\}\,/\,\{(\exp\{\hbar\omega/kT\} - 1) \times (\exp\{\hbar(\omega+\omega_L)/kT\} - 1)\}. \quad (12)$$

It is easily shown that although the integrand in (12) has singularities at the ends of the integration range, the integral always converges when $|q| \neq 1$. The divergence when $|q| = 1$ is associated with the use of a linear model for the orientational waves, and can be eliminated by employing a two-dimensional model.

The evaluation of (12) given below leads to the result

$$w_{12} \geqslant \frac{2}{\pi}\left(\frac{|(1|R_2|2)|}{qJ\Omega_2^2}\right)^2 \frac{\exp\{\hbar\Omega_{max}/kT\}}{(1-\exp\{\hbar\Omega_{max}/kT\})^2}(\Omega_{max}-\Omega_{min}). \tag{13}$$

It can be shown that in the most interesting case, $\hbar\Omega_2/kT \ll 1$, we have

$$w_{12} = \frac{2}{\pi}\xi(q)\left(\frac{|(1|R_2|2)|}{q\Omega_2^2 J}\right)^2 \frac{1}{\Omega_2}\left(\frac{kT}{\hbar}\right)^2, \tag{14}$$

where

$$\xi(q) = \frac{27q^2(\sqrt{1-|q|}+\sqrt{1-|q|})}{4[1+1/2\sqrt{1+3q^2}][3q^2-1+\sqrt{1+3q^2}]}.$$

By calculating the matrix elements $(1|R_2|2)$ we can obtain from Eqs. (12) — (14) the probability of a relaxational transition between any spin levels.

We shall now consider as a specific example the transition $\frac{1}{2}, \frac{1}{2} \rightarrow -\frac{1}{2}, -\frac{1}{2}$ in which the electron spin and nuclear spin are flipped simultaneously. For an orientational wave polarized in the z'x' plane Eqs. (3) and (4) give

$$|(1|R_2|2)|^2 = \frac{1}{16}\Delta A^2 \cos^2 2\varphi.$$

With polarization in the z'y' plane, Eqs. (5) and (6) give

$$(1|R_2|2)|^2 = \frac{1}{16}\Delta A^2 (1+\sin^2\varphi)^2.$$

Finally, adding the probabilities of transitions induced by each of the waves, we obtain

$$w_{12} = \frac{1}{8\pi}\xi(q)\left(\frac{\Delta A}{qJ\Omega_2^2}\right)^2 [\cos^2 2\varphi + (1+\sin^2\varphi)^2]\left(\frac{kT}{\hbar\Omega_{max}}\right)^2 \Omega_2. \tag{15}$$

Averaging this expression over all angles, we obtain a mean value of T_1 that is characteristic of a polycrystalline sample. The final evaluation of w_{12}, with $\Delta A = 10$ gauss and $q = \frac{1}{2}$,[6] gives

$$1/T_1 = w_{12} \approx 5\cdot 10^7\, T^2/\nu^5 J^2. \tag{16}$$

Here T is the absolute temperature, $\nu = \Omega_2/2\pi$ in cm^{-1}, and J is the corresponding moment of inertia of the radical in the unit 10^{-40} g-cm^2. Since the Raman scattering spectra in molecular crystals[7] show that the minimum frequencies of orientational oscillations lie in a region below 10 — 100 cm^{-1} for J = 100 and T = 200°, we obtain $1/T_1 = w_{12} \gtrsim 2 \times 10^3$ sec^{-1}.

When orientational oscillations exist in a molecular crystal the spin-lattice relaxation time can thus be smaller than 1 sec by a few orders of magnitude. This result agrees well with data obtained in the laboratory of V. V. Voevodskii at the Institute of Chemical Physics of the U.S.S.R. Academy of Sciences. According to these data the absence of saturation in the electron paramagnetic resonance spectrum of some molecular crystal radicals shows that $T_1 < 10^{-4}$ sec. (We have confined ourselves to estimating the order of magnitude of T_1 from the simplest model of orientational waves, making no comparison with specific experimental results, since the literature contains no direct measurement of T_1 in molecular crystals, and whenever indirect data for T_1 are obtained in the absence of saturation we lack optical data for the frequency thresholds of orientational oscillations.)

We have pointed out above that a direct transformation of a Zeeman quantum into an orientational phonon is impossible, since the spectrum of orientational waves begins at a minimum frequency $\Omega_{min} \gg \omega_L$; this result does not depend on whether a linear or a spatial model is being considered. However, the situation changes if orientational and translational oscillations interact. In this case (in the linear model) the frequency spectrum consists of two branches, one of which, as previously, begins at Ω_{min}, while the other branch begins at zero frequency. In the absence of coupling between orientational and translational oscillations the second branch represents pure translational waves. However, the presence of coupling results in the mixing of orientational and translational motions.[4] The amplitude of orientational oscillations will, of course, approach zero as $\omega \rightarrow 0$, but remain finite for any $\omega \neq 0$. Direct (single-phonon) relaxational transitions thus become possible.

If the indicated interaction is represented in the potential energy of the system by terms of the form

$$U_l = g(\chi_{l-1}x_l + \chi_l x_{l-1} + 2\chi_l x_l), \tag{17}$$

where χ_l is the angle of deviation from the equilibrium position and x_l is the shift of the center of gravity of a molecule with index l, then at low frequencies the amplitudes of rotational and translational oscillations are related by

$$\frac{\chi}{x} = -\frac{2g_0\omega}{(1+q)\Omega_2^2}\left[\frac{1}{2}\Omega_1^2 - \frac{4g_0^2}{(1+q)\Omega_2^2}\right]^{-1/2}\sqrt{\frac{M}{J}}, \tag{18}$$

where M is the molecular mass, $g = g_0(MJ)^{-1/2}$, and Ω_1 is the frequency of translational oscilla-

tions of an individual molecule if all other molecules are at their equilibrium positions.

From (18), assuming in first approximation that at low frequencies translational oscillations are independent of orientational oscillations, the probability of a single-phonon relaxational transition is easily calculated:

$$w_{12} = \frac{4\sqrt{2}}{\pi(1+q)^2} \frac{|(1|R_1|2)|^2}{\hbar} \frac{\omega_L}{e^{\hbar\omega/kT}-1} \frac{g_0^2}{J\Omega_1^3\,\Omega_2^4}. \qquad (19)$$

This result obviously is subject to the condition of weak interactions between orientational and translational oscillations. Using (17) of [4], we can show that this condition has the form

$$\Omega_1^2\Omega_2^2 \gg 8g_0^2/(1+q).$$

When $\hbar\Omega_L/kT \ll 1$, Eq. (19) becomes

$$w_{12} = \frac{4\sqrt{2}}{\pi(1+q)^2} \frac{|(1|R_1|2)|^2}{\hbar^2} \frac{g_0^2}{J\Omega_1^3\,\Omega_2^4} kT. \qquad (20)$$

In order to determine the order of magnitude represented by (19) and (20) it is necessary to know the value of g_0, which can be determined experimentally only with great difficulty.

It is easily seen that in determining the temperature dependence of relaxational transition probabilities when $\hbar\Omega_2/kT \ll 1$ it is not important to distinguish between a linear and a spatial model. In this case we always have $W_{12} \sim T^2$ for Raman transitions, and $W_{12} \sim T$ for direct transitions; this follows directly from (8) and (12). Thus the experimental temperature dependence of the spin-lattice relaxation time in conjuction with a specific model as described above would yield the characteristic parameters of a molecular crystal.

We note, finally, that since the matrix elements $(1|R_{1,2}|2)$ differ for transitions between different spin levels, the values of T_1 must differ for different hyperfine lines. Moreover, (14) and (20) show that for a single crystal T_1 depends, as a general rule, on crystal orientation in an external magnetic field. Experimental confirmation of the indicated regularities would constitute direct evidence for the proposed relaxation mechanism.

The authors wish to thank Professors A. S. Kompaneets and N. D. Sokolov for discussions.

[1] H. M. McConnell, J. Chem. Phys. **25**, 709 (1956).

[2] I. V. Aleksandrov and G. M. Zhidomirov, JETP (in press).

[3] D. I. E. Ingram, Free Radicals as Studied by Electron Spin Resonance, Academic Press, London, 1958.

[4] A. I. Ansel'm and N. N. Porfir'eva, JETP **19**, 438 (1949).

[5] J. H. Van Vleck, Phys. Rev. **57**, 426 (1940).

[6] Ya. I. Frenkel', Kinetic Theory of Liquids, Oxford University Press, 1946, and Dover Publications, New York.

[7] E. Gross and A. Korshunov, JETP **16**, 53 (1946); M. Vuks, JETP **16**, 410 (1946).

Translated by I. Emin
29

DISPERSION IN FERROELECTRICS

D. G. SANNIKOV

P. N. Lebedev Physics Institute, Academy of Sciences, U.S.S.R.

Submitted to JETP editor December 23, 1960

J. Exptl. Theoret. Phys. (U.S.S.R.) **41**, 133-138 (July, 1961)

The frequency dependence of the permittivity of a ferroelectric associated with domain wall displacements is considered. Numerical calculations have been made, and are compared with experiment for $BaTiO_3$.

THE motion of domain walls in ferromagnetics under the influence of an external magnetic field has been discussed theoretically in a number of papers.[1-3] Dispersion of the magnetic permeability associated with domain wall motion has been observed experimentally in ferrites (e.g., see [4-5]). The ideas developed for ferromagnetic materials are applied in the present paper to ferroelectrics.

We consider a free boundary separating two ferroelectric regions polarized parallel to the boundary in opposite directions, i.e., to be definite, we consider a single 180-degree boundary. It follows from energy considerations that the wall will be displaced by a uniform external electric field if it has a component parallel to the spontaneous polarization inside the domains. We take this direction as the z axis, and the direction perpendicular to the wall as the x axis. We take as the steady-state solution, i.e., the structure of the stationary wall in the absence of external field, the solution obtained by Zhirnov.[6] A feature of this solution is that the change with x coordinate of the polarization vector P is confined to the P_z component, and $P_y = 0$. If we take the external electric field E along the z axis, the only component of the polarization vector P different from zero will be, as before, P_z, which for brevity we will simply call P.

It is convenient to write the thermodynamic potential of unit volume of a ferroelectric with cubic symmetry in terms of the variables P and u_{ij} (the deformation tensor):

$$\begin{aligned} F = F_0 &+ \tfrac{1}{2}\varkappa\,(\partial P/\partial x)^2 + \alpha P^2 + \tfrac{1}{2}\beta P^4 \\ &+ \tfrac{1}{2}c_1\,(u_{xx}^2 + u_{yy}^2 + u_{zz}^2) \\ &+ c_2\,(u_{xx}u_{yy} + u_{xx}u_{zz} + u_{yy}u_{zz}) \\ &+ \tfrac{1}{2}c_3\,(u_{xy}^2 + u_{xz}^2 + u_{yz}^2) + q_1 u_{zz}P^2 \\ &+ q_2\,(u_{xx} + u_{yy})\,P^2 - PE, \end{aligned} \tag{1}$$

where the energy of anisotropy, the elastic and electrostrictive energies, and the correlation energy associated with the nonuniformity of P are included explicitly.

We write the density of kinetic energy in the form

$$T = \frac{1}{2}\rho\left(\frac{\partial u_i}{\partial t}\right)^2 + \frac{1}{2}\frac{m}{ne^2}\left(\frac{\partial P}{\partial t}\right)^2, \tag{2}$$

where the first term is the energy of elastic oscillations (ρ is the density, and u_i is the displacement vector), and the second term is the energy of the oscillations of the ions (it is assumed[7,8] that the polarization in a ferroelectric is due to the displacement of a definite ion, P = nez, where z is the displacement of the ion, e is the effective charge, m is the effective mass, and n is the number of ions in unit volume).

The equations connecting P, u_i, and σ_{ij}, the deformation tensor, are now obtained, following the usual rule, from the Lagrange density L = T − F by allowing variations with respect to P and u_i:

$$\begin{aligned} \frac{m}{ne^2}\frac{\partial^2 P}{\partial t^2} + \frac{m}{ne^2}\omega_r\frac{\partial P}{\partial t} = \varkappa\frac{\partial^2 P}{\partial x^2} - 2\alpha P - 2\beta P^3 - 2q_1 u_{zz}P \\ - 2q_2\,(u_{xx} + u_{yy})\,P + E, \end{aligned} \tag{3}$$

$$\rho\partial^2 u_i/\partial t^2 = \partial\sigma_{ij}/\partial x_j, \qquad \sigma_{ij} = \partial F/\partial u_{ij}, \tag{4}$$

where a decay term has been added to the left-hand side of equation (3); ω_r is the frequency of the ion causing the decay. In what follows we will take the field to depend harmonically on the time $E = E_0 \times e^{i\omega t}$.

The longitudinal acoustic wave along the z axis, arising when the field is switched on, decays with time. A solution can, therefore, be sought in the variables x and t. We introduce the dimensionless variable $\xi = (x - X)/\delta$, which is a measure of the distance from the instantaneous center of the wall X(t); V = dX/dt is the velocity of the wall, δ

$= \sqrt{\kappa/(\beta - q_2^2/c_1)\,P_0^2}$ is a parameter of the wall thickness, and P_0 is the static polarization in the uniform ferroelectric. We also introduce the notation

$$\omega_p^2 = E_0 ne^2/P_0 m, \qquad \omega_q^2 = 4\beta P_0^2 ne^2/m. \tag{5}$$

We seek a solution of the system (3) and (4) in the special form

$$P(x, t) = P^c(\xi) + p(\xi)\, e^{i\omega t}, \qquad V = ve^{i\omega t},$$
$$u_i(x, t) = u_i^c(\xi) + u_i(\xi)\, e^{i\omega t}, \tag{6}$$

where the field P_0 is considered to be sufficiently small [see inequality (10) below] so that it is possible to use perturbation theory with respect to p and u_i. A solution in the form of (6) means that the wall, without changing its form ($P^c(x)$, $u_i^c(x)$ is the static solution[6] in the absence of the field E), oscillates with frequency ω and velocity V. A small distortion of the form of the wall occurs due to the superposition of the small oscillations of ions with the same frequency ω about the equilibrium position in the moving boundary. Such a type of solution is dictated by the physics of the situation, and is justified by the fact that a solution of (3) and (4) in the form given by (6) exists, and is determined uniquely.

By substituting (6) in (3) and (4) we obtain, in the linear approximation with respect to p and u_i, a system of linear equations in total differentials for p and u_x ($u_y = u_z = 0$).*

In the particular case $q_2 = 0$ (according to the data of Devonshire[8] $q_2 = 0$ for $BaTiO_3$), and on satisfying the inequalities

$$\omega^2 \ll \omega_q^2, \qquad \omega\omega_r \ll \omega_q^2 \tag{7}$$

this system of equations becomes simpler, and leads to a single equation for p:

$$\frac{d}{d\eta}\left[(1-\eta^2)\frac{d}{d\eta}\right]p + \left[6 - \frac{4}{1-\eta^2}\right]p - \frac{4}{1-\eta^2}\frac{\omega_p^2}{\omega_q^2}P_0 = 4i\frac{\omega}{\omega_q^2}\frac{v}{\delta}\left(1 - i\frac{\omega_r}{\omega}\right)P_0. \tag{8}$$

Here we have written $\eta = \tanh \xi$. For the inhomogeneous equation (8) to have a finite solution, the following condition must be satisfied†

$$\int_{-1}^{+1} d\eta P_2^2(\eta)\, F(\eta) = 0,$$

where $F(\eta)$ is the right-hand side of (8), and $P_2^2(\eta)$, the associated Legendre polynomial, is the finite solution of the corresponding homogeneous equation. From this condition is obtained the solution for the wall velocity of interest to us:

$$V = \frac{dX}{dt} = -\frac{3}{2}\delta\frac{\omega_p^2}{\omega^2}\frac{1}{1 - i\omega_r/\omega}\, i\omega e^{i\omega t}. \tag{9}$$

We now make more precise the conditions under which expression (9) was obtained. The condition for a linear approximation in p and u_i is the satisfying of the weaker of the inequalities

$$\omega_p^2 \ll \omega^2 \quad \text{or} \quad \omega_p^2 \ll \omega_r^2. \tag{10}$$

For a fixed frequency of the external field ω, the first of these inequalities imposes a limitation on the value of the field strength E_0. The presence of significant ionic damping ($\omega < \omega_r$) allows the requirement that E_0 be small to be weakened. The satisfying of conditions (10) ensures that the distortion of the form of the moving boundary, as compared with that of the stationary boundary, is small. The velocity of wall displacement, as is seen from Eq. (9), is also small, and is proportional to the strength of the external field E_0.

Condition (7), if decay is neglected, assumes that the frequency of the external field is small in comparison with the resonance frequency of the ions in the internal field [see formula (19) below]. The wall oscillates with the frequency of the external field, and thus condition (7) means neglecting the interaction of the wall oscillations with the intrinsic oscillations of the ions in the internal field. This simplifies the problem and allows us to find without difficulty solution (9) for the wall velocity. If P_0^2 depends on the temperature T linearly, $P_0^2 \sim \Theta - T$ (second order phase transition), then, for a fixed frequency of the external field ω, condition (7) imposes a limitation on the temperature, which must not be too close to the Curie temperature Θ. The greater the ionic damping, i.e., the greater ω_r, the stronger becomes this limitation [see the second inequality of condition (7)].

We now calculate the energy W of the boundary layer per square centimeter of surface:

$$W = \int_{-\infty}^{\infty} dx\,(T + F) - \int_{-\infty}^{\infty} dx\,(T + F)_{\text{uniform}}, \tag{11}$$

where the integral of the energy density of the uniformly polarized ferroelectric has been subtracted. To do this it is necessary to use solutions (6). We substitute them into (11) and expand

*The latter is derived from the boundary conditions $u_{ij}(x) = 0$ deep in the domains ($x = \pm\infty$). Such boundary conditions are valid at sufficiently high frequencies: $c/l \ll \omega$, where c is the velocity of sound, l is the dimension of the crystal. If the reverse inequality is true, in particular when $\omega = 0$, the boundary conditions will be different: $\sigma_{ij}(x) = 0$ at $x = \pm\infty$.

†This condition becomes obvious if the solution of the inhomogeneous second-order linear equation is written in the general form, and it is remembered that the second linearly independent solution of the homogeneous equation (8) is infinite.

the integrands in series, whilst observing conditions (7), (10) and $q_2 = 0$. After integrating we obtain

$$W = W_0 + \frac{1}{2} MV^2 - FX + \ldots. \qquad (12)$$

The first term of this expression

$$W_0 = \frac{1}{3} P_0^2 \varkappa / \delta \qquad (13)$$

is the energy per unit surface area of the stationary wall.* The second term, proportional to the square of the velocity, is the kinetic energy of the wall. It is natural to call the coefficient M the effective mass of the wall, where

$$M = 4W_0/\delta^2 \omega_q^2 = mW_0/ne^2\varkappa. \qquad (14)$$

The third term, proportional to the displacement, is the potential energy of the wall in the external field.† The coefficient F is the pressure exerted by the field on the wall, $F = -2P_0E$.

According to (12) the equation of motion of the boundary will be

$$MdV/dt + M\omega_r V = F, \qquad (15)$$

where a decay term proportional to the wall velocity has been added. Its solution, as would be expected, is expression (9). It would, of course, have been possible to write down (15) (accurate to within an arbitrary constant multiplier) starting from the solution (9) obtained previously, without resorting to a calculation of the wall energy (12). However, the calculations presented confirm once more the correctness of the result obtained (9), and enable the physical meaning to be made more precise, and the coefficients M and F to be written down explicitly.

So far the domain wall has been considered to be free (if we neglect the ionic damping). This will apparently be the case in an ideal crystal. However, when inclusions and deformations are present in the crystal, the boundary can have equilibrium positions which are energetically more favorable, and can also encounter in its motion additional resistance. If it is supposed that the wall is elastically coupled in an equilibrium position, then (15) must be generalized as follows:‡

$$Md^2X/dt^2 + M(\omega_r + \omega_r')\, dX/dt + M\omega_0^2 X = F, \qquad (16)$$

where $M\omega_r'$ is the additional frictional coefficient, and $M\omega_0^2$ is the elastic coupling constant. Both these coefficients must depend greatly on the structure of the material.

The polarization of the crystal changes, when the boundary is displaced a distance X, by the amount $\Delta P = -2P_0X/l$ (under conditions such that the small distortion in the form of the wall can be neglected), where l is the dimension of the crystal. If the specimen is subdivided into many domains, then l should be understood to be the mean domain width. Solving (16), we obtain an expression for the electric susceptibility χ of the ferroelectric due to the domain wall displacement:

$$\chi(\omega) = \frac{\Delta P}{E} = \frac{\chi_0 \omega_0^2}{\omega_0^2 - \omega^2 + i(\omega_r + \omega_r')\,\omega}, \qquad (17)$$

where χ_0 is the susceptibility at the frequency $\omega = 0$:

$$\chi_0 = 4P_0^2/lM\omega_0^2. \qquad (18)$$

The resonance frequency ω_0 is related to χ_0 by (18).

We now make some numerical estimates for $BaTiO_3$ and compare the formula obtained, (17), with the experimentally observed[9] variation of the dielectric constant ϵ of polycrystalline $BaTiO_3$ on the frequency of the external field $\omega/2\pi$. In order of magnitude, the effective mass of the ion is $m = 10^{-22}$g (the reduced mass of Ba and the TiO_3 group is 9.4×10^{-23}g,[10] or the mass of Ti is 8×10^{-23}g). The effective charge is $e = 4 \times 4.8 \times 10^{-10}$ (twice the charge of Ba and TiO_3, or four times the charge of Ti). The number of ions per cc is $n = (4 \times 10^{-8})^{-3}$ cm^{-3}. Thus, we have $ne^2/m = 6 \times 10^{26}$ sec^{-2}. The experimental value of P_0 is 4.8×10^4; according to Devonshire's data,[8] we have $\beta = 7 \times 10^{-12}$. Thus, $\omega_q/2\pi = 1.2 \times 10^{12}$ sec^{-1} [see Eq. (5)]. Taking for κ the value 3×10^{-16} cm^2 (see [10]), we obtain $\delta = 1.3 \times 10^{-7}$ cm. The energy of unit area of the wall is, according to (13), $W_0 = 8$ erg/cm^2. The effective mass of the wall is, according to (14), $M = 0.4 \times 10^{-10}$ g/cm^2. Taking the experimental value[9] of the susceptibility at the frequency $\omega = 0$ as $\chi_0 = 1300/4\pi$ ($\epsilon = \epsilon_\infty + 4\pi\chi$), and taking the domain thickness as $l = 10^{-3}$ cm, we obtain for the resonance frequency ω_0 from formula (18) the value $\omega_0/2\pi = 0.8 \times 10^{10}$ sec^{-1}, which agrees in order of magnitude with the experimental value[9] of 3×10^{10} sec^{-1}.

Since there are two damping mechanisms, it can be expected that the sum of the damping frequencies $\omega_r + \omega_r'$ will be much greater than the

*There are misprints in the analogous expressions in Zhirnov's paper:[6] in all formulae for σ a multiplier ½ must be added.

†When calculating the energy of a wall in a ferromagnetic a similar term was erroneously omitted in [5] as well as in[3] (this did not, however, affect the result). The integral of the type $\int_{-\infty}^{+\infty} dx P^c(x)$ is, in fact, different from zero, and is proportional to the displacement of the boundary X.

‡It would be more logical to include the imperfection of the crystal in the original expression (1) for the thermodynamic potential and hence obtain Eq. (16).

resonance frequency ω_0 (ω_r has been experimentally determined for Rochelle salt,[11] and gives $\omega_r/\omega_q^2 = 2.6 \times 10^{-8}/(\Theta - T)$ sec^{-1}). In this case the dispersion (17) will show, not a resonant, but a relaxation behavior, which is observed in experiment.[9]

It is still necessary to verify that conditions (7) and (10) for the applicability of formula (17) are satisfied. If we take $E_0 \leq 1$ v/cm, then $\omega_p/2\pi = 10^9$ sec^{-1}. The value of ω_q has been obtained above. By comparing these values with the resonance frequency ω_0, we see that in the dispersion region the frequency ω in fact satisfies inequalities (7) and (10).

The treatment given and the numerical calculations show that the experimentally observed dispersion in $BaTiO_3$ can be considered as due to processes of domain wall displacement (this idea was first advanced by Kittel[12]).

Apart from the dispersion considered, there exists in ferroelectrics another dispersion region at a higher frequency, associated with the intrinsic oscillations of the ions [the resonance frequency ω_q, (5)].[7,10] In distinction from the first, the second dispersion region should also be observed in a homogeneous (single-domain) ferroeletric. Solving the system of linearized equations in the case of the homogeneous ferroelectric, we obtain for the susceptibility

$$\chi = \chi_\infty \omega_q^2/(\omega_q^2 - \omega^2 + i\omega_r\omega), \qquad (19)$$

where $\chi_\infty = \frac{1}{4}\beta P_0^2$. In distinction from formula (10) of [10], Eq. (19) was derived taking into account the elastic energy and the electrostrictive energy. The applicability of formula (19) for all frequencies is limited by the single inequality $\omega_p^2 \ll \omega_0^2$, i.e., $E_0 \ll 4\beta P_0^3$. Taking into account that in a phase transition of the second kind we have $P_0^2 \sim \Theta - T$, this inequality imposes at a fixed field strength E_0 a limitation on the temperature T, which must not be too close to the Curie temperature Θ (for more detail on this question see [10]).

In conclusion, it should be noted that the entire treatment is valid if there is a second order (but not a first order) phase transition in the ferroelectric.

The author thanks V. L. Ginzburg and A. P. Levanyuk for discussing the work and for valuable counsels.

[1] L. D. Landau and E. M. Lifshitz, Physik Z. Sowjetunion **8**, 153 (1935).

[2] W. Döring, Z. Naturforsch. **3a**, 373 (1948).

[3] G. T. Rado, Phys. Rev. **83**, 821 (1951).

[4] Rado, Wright, and Emerson, Phys. Rev. **80**, 273 (1950).

[5] Perekalina, Askochenskii, and Sannikov, JETP **40**, 441 (1961), Soviet Phys. JETP **13**, 303 (1961).

[6] V. A. Zhirnov, JETP **35**, 1175 (1958), Soviet Phys. JETP **8**, 822 (1959).

[7] V. L. Ginzburg, Usp. Fiz. Nauk **38**, 490 (1949).

[8] A. F. Devonshire, Phil. Mag. **40**, 1040 (1949).

[9] A. Hippel, Revs. Modern Phys. **22**, 221 (1950).

[10] V. L. Ginzburg, Fiz. Tverd. Tela **2**, 2031 (1960), Soviet Phys.-Solid State **2**, 1824 (1961).

[11] I. A. Yakovlev and T. S. Velichkina, Usp. Fiz. Nauk **63**, 411 (1957).

[12] C. Kittel, Phys. Rev. **83**, 458 (1951).

Translated by K. F. Hulme
30

ANALYSIS OF COSMIC-RAY SHOWERS PRODUCED BY HIGH ENERGY PRIMARY PARTICLES: BASED ON THE EXCITED NUCLEON MODEL

L. A. SAN'KO, Zh. S. TAKIBAEV, and P. A. USIK

Institute of Nuclear Physics, Academy of Sciences, Kazakh S.S.R.

Submitted to JETP editor December 26, 1960

J. Exptl. Theoret. Phys. (U.S.S.R.) 41, 139-145 (July, 1961)

High-energy ($E > 10^{11}$ ev) interactions of cosmic-ray nucleons in emulsion are analyzed on the basis of the excited nucleon model. The c.m.s. angular distribution of the excited nucleons is given. The anisotropy of the angular distribution of the shower particles and the multiplicity of the shower particles are examined in relation to the velocity and the emission angle of the excited nucleons in the c.m.s. The experimental results are compared with the prediction of the single-meson pole approximation.

THE two-center model,[1] without stipulating a specific mechanism for the interaction between the nucleons or a mechanism for their decay, presupposes that the two colliding nucleons are excited to certain isobaric states. The excited nucleons, which have large masses, rapidly decay independently of each other with formation of pions, and go to the ground state. In a frame fixed to the excited nucleon (radiating center), the pions are isotropically distributed, as confirmed by numerous experimental data obtained at high energies (see for example,[2]), and their angular distribution in the center of mass system (c.m.s.) depends on the velocity of motion of the radiating centers in this system, $\bar{v}$, or on the quantity $\bar{\gamma} = (1-\bar{v}^2)^{-1/2}$.*

If $\bar{\gamma}$ is close to unity, the angular distribution of the shower particles is almost isotropic in the c.m.s., and if $\bar{\gamma} > 1$, the distribution of the shower particles is anisotropic in the c.m.s. Thus, the model of excited nucleons describes various angular distributions, the form of which in the c.m.s. depends on the value of $\bar{\gamma}$. The value of $\bar{\gamma}$ can be determined from the angular distribution of the shower particles in the laboratory system (l.s.) and from the number of mesons n_1 and n_2 produced by the decay of each of the excited nucleons[2]:

$$\bar{\gamma} = (\gamma_1 + \gamma_2)/2\gamma_c.$$

In the experiments, γ_1 and γ_2 are determined from the angular distribution of the particles in the narrow and diffuse cones of the shower. In the determination of γ_1 and γ_2 we do not assume that the pions have a monoenergetic distribution in the system of the excited nucleon.

Making use of the experimental data of Boos et al,[3] who investigated showers with low anisotropy (corresponding to $\bar{\gamma} \approx 1$), we assume that the energy spectrum of the shower particles obeys in the system of the excited nucleon a power law:

$$N(E') \sim \frac{1}{E'^2} dE'$$

and therefore[4] *

$$\gamma_1 = 0.77\,\gamma_1', \qquad \lg \gamma_1' = -\frac{1}{n_1}\sum_{i=1}^{n_1} \lg \operatorname{tg} \theta_i;$$

$$\gamma_2 = 0.77\,\gamma_2', \qquad \lg \gamma_2' = -\frac{1}{n_2}\sum_{i=1}^{n_2} \lg \operatorname{tg} \theta_i;$$

$$n_s = n_1 + n_2.$$

Taking account of the fact that the excited nucleons can be emitted at arbitrary c.m.s. angles ϑ' to the primary direction, we must determine the parameter γ_c not from the formula $\gamma_c = \sqrt{\gamma_1\gamma_2}$, but from the expression[5]

$$\gamma_c = 2^{-1/2}\left[\gamma_1 + \gamma_2 + \tfrac{3}{2}E'(n_1\gamma_1 + n_2\gamma_2)\right]^{1/2},$$

where $E' = 0.4$ Bev is the average meson energy in the radiating-center system.

The emission angle ϑ is calculated, using the energy and momentum conservation law, from the values of γ_1, γ_2, and γ_c[6]:

$$\cos \vartheta' = (\gamma_1 - \gamma_2)/\sqrt{(\gamma_1 + \gamma_2)^2 - 4\gamma_c^2}.$$

The purpose of the present investigation was a study of the angular distribution of the excited nucleons in the c.m.s., its connection with the form of the angular distribution of the generated shower

*We use a system of units in which the velocity of light and the mass of the nucleon are equal to unity.

*lg = log, tg = tan.

particles in the l.s. and with their multiplicity, and also a check on the theory of peripheral interactions in the region of superhigh energies.

EXPERIMENTAL RESULTS

We chose for the analysis showers with $N_n \leq 2$ and $n_s \geq 6$, formed by singly-charged or neutral cosmic-ray particles (nucleons) with energy $E > 10^{11}$ ev interacting in emulsion. The total number of showers was forty-two.* We plotted the integral and differential angular distributions of the shower particles in coordinates log tan θ – log tan θ, and determined the approximate number of particles radiated by each nucleon. If the integral-distribution curve split into two branches, we determined n_1 and n_2 as the number of particles in each branch, and if there was no split we assumed that the nucleons are similarly excited, i.e., their masses after collision are $m_1 = m_2 = m$, and consequently the same number of mesons $n_1 = n_2 = n_s/2$ is produced by their decay. We then calculated γ_1, γ_2, γ_c, $\bar{\gamma}$, and cos ϑ', for all the analyzed showers.

The angular distribution of the excited nucleons in the c.m.s. is highly anisotropic (Fig. 1), with small emission angles predominating (25 – 30°),

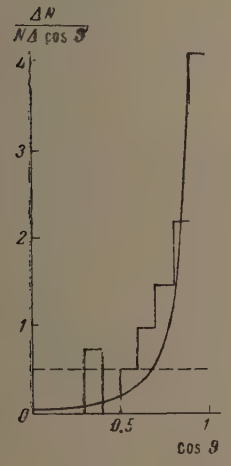

FIG. 1. Angular distribution of excited nucleons in the c.m.s. The curve was calculated with formula (5) (see below) and normalized in area with the histogram; the dashed line corresponds to isotropic distribution in the c.m.s.

but the angle reaches 70° in some showers with low multiplicity. Considering that the influence of fluctuations is particularly great at small n, we disregarded showers with $n_s < 10$, and the form of the distribution of the excited nucleons was not changed thereby. For comparison we calculated the angular distribution by the theory of peripheral interactions in the single-meson pole approximation. In view of the fact that the multiplicities of the shower particles of the analyzed showers are small on the average, it becomes necessary to take account of the influence of fluctuations in the number of particles.

Podgoretskii et al[7] define the fluctuations in the number of particles as quantities proportional to the square root of the number of particles: $n_s \pm \alpha\sqrt{n_s}$. The proportionality coefficient α depends on the type of generated particles and is close to unity for the case of pions. We have calculated the fluctuations in the number of particles generated by each excited nucleon: $n_1 \pm \sqrt{n_1}$ and $n_2 \pm \sqrt{n_2}$, and then determined the corresponding γ_1 and γ_2 and evaluated the angles ϑ' for several showers with different multiplicities. As a result it became clear that an account of the fluctuations in the number of particles n_1 and n_2 produced by each excited nucleon changes the value of the angle ϑ' very little, and the change $\Delta \cos \vartheta' = 0.03 - 0.04$ is insignificant. Thus, fluctuations in the number of particles do not change the form of the c.m.s. angular distribution of the excited nucleons. The fluctuations in the angular distributions were not taken into account rigorously, but we assume that such an account would not change appreciably the angular distribution, for otherwise there would be no regular connection between the multiplicity n_s and cos ϑ', and a much greater straggle in the points would be observed in Fig. 2.

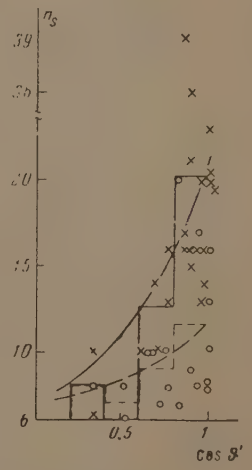

FIG. 2. Dependence of the multiplicity on the cosine of the angle of emission of excited nucleons in the c.m.s. The solid and dashed curves were calculated by the least-squares method. The points × and o pertain to showers with $\gamma_c \geq 12$ and with $5 \leq \gamma_c < 12$, respectively.

In the two-center model the multiplicity of shower particles is determined by the momentum transfer, and depends on the degree of excitation of the colliding nucleons, i.e., on their mass m after collision. We find from the experimental data that the masses of the excited nucleons (or the multiplicity of the shower mesons) depend on the angle at which they are emitted in the c.m.s., and the smaller the angle ϑ', the larger the multiplicity for a given primary-particle energy (for specified γ_c). As can be seen from Fig. 2, where the experimental values of the multiplicity n_s and of cos ϑ' were plotted for two energy intervals

*In many cases data on the showers were taken from published papers or obtained from other laboratories (Moscow, Leningrad, Prague, Berlin, Budapest, Krakow).

and the corresponding curves then calculated by the method of least squares, the multiplicity increases with decreasing angle ϑ'. We excluded from consideration showers with $n_s < 10$, but these do not change the general character of this dependence.

We next investigated the dependence of the form of the angular distribution of the shower particles on the velocity of motion and angle of emission of the excited nucleons in the c.m.s. We chose as a characteristic of the form of the angular distribution of the shower particles the mean-square deviation[4]

$$\sigma = \left[\frac{1}{n_s} \sum_{i=1}^{n_s} (\lg \operatorname{tg} \theta_i - \overline{\lg \operatorname{tg} \theta})^2 \right]^{1/2},$$

and the measure of departure from isotropy was the ratio σ/σ_{is}, where $\sigma_{is} = 0.31$ corresponds to isotropic angular distribution of the particles and to a power-law energy spectrum.

Figure 3 shows the values of σ/σ_{is} as a function of $\bar{\gamma}$. The parameter σ/σ_{is} characterizes the degree of anisotropy and increases (on the average) with increasing $\bar{\gamma}$, i.e., the velocity of motion of the excited nucleons in the c.m.s. The angle at which the excited nucleons are emitted in the c.m.s. is also connected with the form of the angular distribution of the shower particles, i.e., with the anisotropic parameter σ/σ_{is}. It is seen in Fig. 4 that the greater ϑ', the closer the angular distribution is to isotropic; at small angles the distribution is in most cases anisotropic.

For many cases (see Figs. 3 and 4) the values of the parameter σ/σ_{is} were found to be less than unity. Were the model to be confined to an examination of the angles $\vartheta' = 0$, this fact would remain unexplained. The admission of large ϑ' into the model provides us with the following explanation:

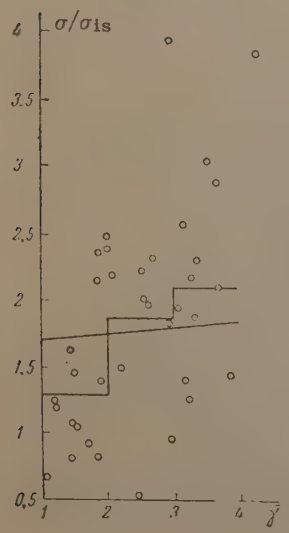

FIG. 3. Dependence of the anisotropy parameter σ/σ_{is} on $\bar{\gamma}$ for the analyzed nucleon-nucleon showers. The histogram was constructed from the average values of σ/σ_{is} in each chosen interval of $\bar{\gamma}$, while the straight line was calculated by the method of least squares.

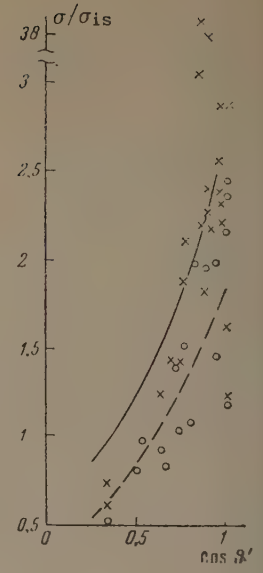

FIG. 4. Dependence of σ/σ_{is} on the cosine of the angle of emission of the excited nucleons in the c.m.s. The curves (solid and dashed) were calculated by the method of least squares. The points × and ○ pertain to showers with $\gamma_c \geq 12$ and with $5 \leq \gamma_c < 12$, respectively.

the measure of the anisotropy σ/σ_{is} depends on two parameters $\bar{\gamma}$ and ϑ'; if $\bar{\gamma} \approx 1$, then the distribution is isotropic for all emission angles and $\sigma/\sigma_{is} \approx 1$; on the other hand, if $\gamma > 1$, then the distribution should be anisotropic but the anisotropy parameter σ/σ_{is}, calculated from angles obtained in the l.s., is less than unity at large emission angles ϑ'.

The experimental data cited are comparable with the deductions of the theory of peripheral interactions. This comparison is essentially qualitative, since the results shown in Figs. 1 and 2 are, first, summary material for a rather extensive interval of values of γ_c ($5 \leq \gamma_c \leq 70$), and second, they are subject to unaccountable errors. Furthermore, it must be noted that apparently not all forty-two interactions correspond to the case of nucleon excitation, and a certain fraction of the showers may correspond to a virtual $\pi\pi$ interaction.[8] However, in the comparison of experiment with theory we shall assume that all the analyzed showers correspond to excitation of nucleons.

COMPARISON OF THE RESULTS OF THE THEORY OF PERIPHERAL INTERACTIONS WITH EXPERIMENT

A method based on perturbation theory has been developed in a series of papers[9-11] for the description of peripheral interaction of high-energy nucleons. In the single-meson pole approximation, the results of this method are in satisfactory agreement with experiments on nucleon-nucleon interactions at energies of 9 Bev[9,10] and 200 — 300 Bev,[11,12] indicating that the peripheral interactions make the principal contribution at these energies. It is interesting to compare the theory in this approximation with the experimental data at higher energies. In view of the fact that the experimental

material at our disposal pertains to a broad energy interval, a detailed comparison between theory and experiment is impossible. We can, however, present an analysis that pertains to an important characteristic of the interaction, namely the 4-momentum of the intermediate pion, exchanged by the interacting nucleons.

The single-meson interaction of these nucleons, which leads to their excitation and subsequent decay, is described by the Feynman diagram shown in Fig. 5. For the left node of this diagram, the 4-momentum conservation law has the form

$$k = p_0 - p_1.$$

Squaring both halves of this expression we have

$$k^2 = p_0^2 + p_1^2 + 2\varepsilon_0\varepsilon_1 - 2\,|\mathbf{p}_0|\,|\mathbf{p}_1|\cos\vartheta, \qquad (1)$$

where $k^2 = \mathbf{k}^2 - k_0^2$ is the square of the 4-momentum of the intermediate pion, ϵ_0 is the nucleon energy prior to interaction, ϵ_1 the energy of the excited nucleon, and ϑ the angle between the directions of motion of the nucleon before and after the interaction.

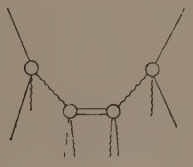

FIG. 5

Denoting by m_1 and m_2 the masses of the excited nucleons, we can rewrite (1) as

$$k^2 = -1 - m_1^2 + 2\varepsilon_0\varepsilon_1 - 2\sqrt{(\varepsilon_0^2 - 1)(\varepsilon_1^2 - m_1^2)}\cos\vartheta. \qquad (2)$$

For the c.m.s. of the colliding nucleons, the energy-momentum conservation law is given by the equations

$$\varepsilon_1 + \varepsilon_2 = 2\gamma_c, \qquad \varepsilon_1^2 - m_1^2 = \varepsilon_2^2 - m_2^2. \qquad (3)$$

Hence

$$\varepsilon_1 = (4\gamma_c^2 + m_1^2 - m_2^2)/4\gamma_c \qquad (4)$$

and we obtain finally for the momentum of the intermediate pion

$$k^2 = -1 - m_1^2 + \frac{4\gamma_c^2 + m_1^2 - m_2^2}{2} - 2\cos\vartheta'\sqrt{\gamma_c^2 - 1} \times \left[\left(\frac{4\gamma_c^2 + m_1^2 - m_2^2}{4\gamma_c}\right)^2 - m_1^2\right]^{1/2}. \qquad (5)$$

In the case of symmetrical excitation of the nucleons we have $m_1 = m_2 = m$; for k^2 we obtain from (5)

$$k^2 = -1 - m^2 + 2\gamma_c^2 - 2\sqrt{(\gamma_c^2 - 1)(\gamma_c^2 - m^2)}\cos\vartheta'. \qquad (6)$$

Using (6), we have calculated for the analyzed interaction cases the distribution over k^2, shown in Fig. 6.

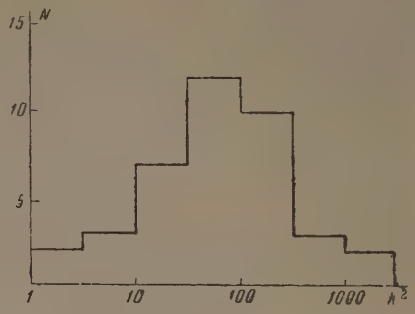

FIG. 6. Distribution of showers with respect to the value of k^2 calculated from formula (6).

The result obtained can be compared with the data of Dremin and Chernavskii,[11] who found that the total cross section $\sigma_{NN}(E)$ of the single-meson interaction of two nucleons agrees at energies $E \sim 200$ Bev with the corresponding experimental value only if it is assumed that the total cross section of the interaction of a virtual pion with the nucleon, $\sigma_{\pi N}(k^2)$, is a smooth function of k^2 when $k^2 \leq (7\mu)^2$, and decreases sharply with further increase in k^2. In our case, however, $k^2 \ll (7\mu)^2$ for all showers (Fig. 6). This indicates that the showers which we are considering cannot be described by perturbation theory in the single-meson approximation.

It was noted in several papers[9-11] that in the single-meson approximation the c.m.s. angular distribution of the excited nucleons should be strongly anisotropic; the degree of anisotropy should increase with increasing γ_c. In addition, the width of the angular distribution of the excited nucleons is determined by the cross section $|\sigma_{\pi N}(k^2)$. If this cross section decreases sharply, starting with $k^2 \sim (7\mu)^2$, then this is equivalent to the existence of a maximum angle ϑ'_{max}, which should be considerably smaller than $\pi/2$. Actually, if we determine ϑ'_{max} from the formula

$$\cos\vartheta' = (2\gamma_c^2 - 1 - m^2 - k^2)/2\sqrt{(\gamma_c^2 - 1)(\gamma_c^2 - m^2)},$$

which follows from (6), we have $\vartheta'_{max} = 6°\,6'$ when $\gamma_c = 10$, $m = 1.32$ [mass of the isobar $(3/2, 3/2)$] and $k^2 = (7\mu)^2$, whereas $\vartheta_{max} = 2°\,54'$ when $\gamma_c = 20$ and $m = 1.32$.

Greater values of m correspond to even smaller limiting angles. Thus, the observed angular distribution of the excited nucleons (Fig. 1) goes far beyond the limits permissible in our theory. However, if no limitations are imposed on the virtuality, we can readily obtain the theoretical angular distribution for fixed γ_c and m by using the results of Dremin and Chernavskii.[9] The curve shown in Fig. 1 is calculated for average experimental values of γ_c and m ($\gamma_c = 20$, $m = 4.5$).

In spite of the fact that the assumption of the large virtualities is unfounded, the curve fits the observed angular distribution quite satisfactorily.

In addition to the features of the angular distribution, the theory predicts a reduction (for γ_c = const) in the mass of the excited nucleons (or in the multiplicity of the shower particles) with increasing angle ϑ'. The prediction of such a tendency does not contradict experiment (Fig. 2). However, inasmuch as the experimental angular distribution is much broader than that admitted by the theory, it is impossible to carry out a complete graphic comparison.

CONCLUSIONS

1. The mass of the excited nucleons, and consequently the multiplicity of the generated mesons, depends on the direction of motion of the excited nucleons in the c.m.s.

2. The form of the angular distribution of the shower particles in the laboratory system depends on the velocity and direction of motion of the excited nucleons in the c.m.s.

3. The transfer of 4-momentum, occurring upon interaction of the nucleons, is in all cases large compared with $(7\mu)^2$. Therefore, if the centers of emission of the shower mesons are actually the excited nucleons and if the directions of their motion coincide with the axes of the cones, then the mechanism of excitation of the nucleons should be appreciably different from the single-meson interaction.

[1] S. Takagi, Progr. Theoret. Phys. **7**, 123 (1952); W. L. Kraushaar and L. J. Marks, Phys. Rev. **93**, 326 (1954).

[2] Ciok, Coghen, Gierula, Holynski, Jurak, Miesowicz, Saniewska, and Pernegr, Nuovo cimento **10**, 741 (1958).

[3] Boos, Vinitskii, Takibaev, and Chasnikov, JETP **34**, 622 (1958), Soviet Phys. JETP **7**, 430 (1959).

[4] L. V. Lindern, Nuovo cimento **5**, 491 (1957).

[5] Burmeister, Lanius, and Meier, ibid. **11**, 12 (1959).

[6] H. W. Meier, ibid. **11**, 307 (1959).

[7] Podgoretskii, Rozental', and Chernavskii, JETP **29**, 296 (1955), Soviet Phys. JETP **2**, 211 (1956).

[8] P. A. Usik and V. I. Rus'kin, JETP **39**, 1718 (1960), Soviet Phys. JETP **12**, 1200 (1961).

[9] I. M. Dremin and D. S. Chernavskii, JETP **38**, 229 (1960), Soviet Phys. JETP **11**, 167 (1960).

[10] Gramenitskii, Dremin, Maksimenko, and Chernavskii, Nucleon-nucleon Interaction at 9 Bev, preprint, 1960.

[11] D. S. Chernavski and J. Dremin, On Nucleon-Nucleon Interactions at Energies of 10^{11} ev, preprint, 1960.

[12] S. A. Slavatinskii and D. S. Chernavskii, Trans. Intl. Conf. on Cosmic Rays, **1**, AN SSSR, 1960, p. 161.

Translated by J. G. Adashko
31

LIMITING VALUES OF THE $\pi^{\pm}$p SCATTERING AMPLITUDE

V. P. KANAVETS, I. I. LEVINTOV, and B. V. MOROZOV

Institute of Theoretical and Experimental Physics, Academy of Sciences, U.S.S.R.

Submitted to JETP editor December 28, 1960

J. Exptl. Theoret. Phys. (U.S.S.R.) **41**, 146-153 (July, 1961)

Dispersion relations in which subtraction is transferred to points located at infinity are derived on the basis of Pomeranchuk's assumptions regarding the asymptotic behavior of the scattering amplitude. In this form, the dispersion relations are most convenient for estimating the asymptotic behavior of the amplitude on the basis of the experimental data on $\pi^{\pm}$p scattering. A preliminary numerical estimate of the asymptotic behavior of the $\pi^{\pm}$p scattering amplitude is presented. The question whether the validity of the dispersion equations at high energies is consistent with the statistical theory is considered.

POMERANCHUK[1] has shown that if the existence of an energy-independent limited radius of interaction is assumed, the behavior of the complex scattering amplitude of particles and antiparticles for an arbitrary scatterer at an angle 0° should be described by a function which increases to infinity no faster than the first power of the energy. A consequence of this is the equality of the limiting values of the total interaction cross sections for particles and antiparticles:

$$\sigma_t^+(\infty) = \sigma_t^-(\infty). \tag{1}$$

Experimental studies of the total cross sections of $\pi^{\pm}$p interactions apparently confirm Pomeranchuk's conclusions that at high energies the cross sections for π^+ and π^- approach the same, almost constant value.

In this connection, it is of interest to estimate, within the framework of these theoretical assumptions, the asymptotic value of the real part of the $\pi^{\pm}$p scattering amplitude on the basis of the latest data on the behavior of the total cross sections at high energies. For this, it will be convenient to start from symmetric and antisymmetric combinations of the amplitudes $D_+(E) \pm D_-(E)$, where $D_{\pm}(E)$ are the real parts of the $\pi^{\pm}$p scattering amplitudes at 0°. For such combinations at sufficiently high energy E, according to Pomeranchuk's assumptions, the following relations should hold:

$$C(E) \equiv [D_+(E) - D_-(E)]/2E = C_\infty, \tag{2}$$

$$\tfrac{1}{2}[D_+(E) + D_-(E)] = Q(E), \tag{3}$$

where $Q(E)$ is a function that increases more slowly than the first power of the energy, an C_∞ is a constant.

For an estimate of quantities (2) and (3), we should let the energy go to infinity in the dispersion relations. For this, it is convenient not to fix the energy at which the second subtraction is made. Since many values of $D_{\pm}(E)$ are now known with good accuracy over a rather large energy interval, the method permits an essential increase in the accuracy of the determination of $D_{\pm}(\infty)$ in comparison with calculations by means of the dispersion relations in Goldberger's form, in which the second subtraction is fixed at $E = m$ (m is the meson mass). We note that the transfer of the subtraction to infinity leads [together with condition (2)] to definite restrictions on the way the cross sections approach their limiting values.

We shall start from the dispersion relations for the case of forward scattering of charged mesons in the form in which they were written by Bogolyubov, Medvedev, and Polivanov:[2]

$$C(E) - C(E_0) = \frac{1}{4\pi^2}(E^2 - E_0^2)\,\mathrm{P}\int_m^\infty \frac{k'[\sigma_t^+(E') - \sigma_t^-(E')]\,dE'}{(E'^2 - E_0^2)(E'^2 - E^2)} + 2f^2\frac{E^2 - E_0^2}{(E^2 - r^2)(E_0^2 - r^2)}, \tag{4}$$

$$Q(E) - Q(E_0) = \frac{1}{4\pi^2}(E^2 - E_0^2)\,\mathrm{P}\times\int_m^\infty \frac{k'E'[\sigma_t^+(E') + \sigma_t^-(E')]}{(E'^2 - E_0^2)(E'^2 - E^2)}\,dE' + 2f^2\frac{r(E^2 - E_0^2)}{(E^2 - r^2)(E_0^2 - r^2)}. \tag{5}$$

Here $E^2 = m^2 + k^2$, $r = m^2/2M$, $f^2 = 0.08$, M is the mass of the nucleon.

Setting $E^2 \ll \epsilon^2 \ll E_0^2$, we can rewrite (4) in the form

$$p(\varepsilon) = C(E) - \frac{1}{4\pi^2} P \int_m^{\varepsilon} \frac{k'(\sigma_t^+ - \sigma_t^-)}{E'^2 - E^2} dE' + 2f^2 \frac{1}{E^2 - r^2}$$

$$= C(E_0) - \frac{1}{4\pi^2} P \int_{\varepsilon}^{\infty} \frac{E_0^2(\sigma_t^+ - \sigma_t^-)}{E'(E'^2 - E_0^2)} dE', \quad (6)$$

where $p(\epsilon)$ is obviously a function of ϵ only.

We now let E_0 go to infinity for any fixed value of ϵ. According to (2), the function $C(E_0)$ should then go over into C_∞. Since $p(\epsilon)$ is constant, the integral with E_0 in (6) also should go over to a constant as $E_0 \to \infty$. The necessary condition for this is the existence of the integral*

$$\int_{\varepsilon}^{\infty} dE' (\sigma_t^+ - \sigma_t^-)/E' = A(\varepsilon).$$

We then have the condition

$$\lim_{E_0 \to \infty} \left(-\frac{1}{4\pi^2} P \int_{\varepsilon}^{\infty} \frac{E_0^2(\sigma_t^+ - \sigma_t^-)}{E'(E'^2 - E_0^2)} dE' \right) = \frac{1}{4\pi^2} \int_{\varepsilon}^{\infty} \frac{\sigma_t^+ - \sigma_t^-}{E'} dE'. \quad (7)$$

From (6) and (7) it follows that

$$C(E) - \frac{1}{4\pi^2} P \int_m^{\varepsilon} \frac{k'(\sigma_t^+ - \sigma_t^-)}{E'^2 - E^2} dE' - \frac{1}{4\pi^2} \int_{\varepsilon}^{\infty} \frac{\sigma_t^+ - \sigma_t^-}{E'} dE'$$

$$+ 2f^2 \frac{1}{E^2 - r^2} = C(E) - \frac{1}{4\pi^2} P \int_m^{\infty} \frac{k'(\sigma_t^+ - \sigma_t^-)}{E'^2 - E^2} dE'$$

$$+ 2f^2 \frac{1}{E^2 - r^2} = C_\infty. \quad (8)$$

Formula (8) represents the dispersion relation for the difference in amplitudes in which the subtraction is transferred to points located at infinity. Setting $C_\infty = 0$ and $E = m$ in (8), we arrive at the summation rule of Goldberger et al.[4]

We do not know whether the function $Q(E)$ remains bounded as $E \to \infty$. The asymptotic behavior of $Q(E)$ is determined by how fast $\sigma_t^+(E) + \sigma_t^-(E)$ approaches the limiting value $2\sigma_\infty$. If $\sigma_t^\pm$ decreases monotonically beginning at some energy, then it can be shown (see Appendix) that, for sufficiently large E, a necessary condition for the relation

$$Q(E) = Q_\infty, \quad (9)$$

where Q_∞ is a bounded quantity, is the existence of the integral

$$\int_{\varepsilon}^{\infty} [\sigma_t^+(E') + \sigma_t^-(E') - 2\sigma_\infty] dE' = B(\varepsilon) < \infty. \quad (10)$$

This means that the difference $\sigma_t^+ + \sigma_t^- - 2\sigma_\infty$ should, under condition (9), tend to zero as $E \to \infty$ faster, on the average, than $(E \ln E)^{-1}$. At present, however, we cannot give definite theoretical arguments in favor of assumptions (9) or (10),* and the transferring of the substraction points $\pm E_0$ to infinity in relation (5) does not lead to definite results.

Nevertheless, to investigate the behavior of $Q(E)$ at high energies, it is useful to introduce the function $q(\epsilon)$, which is determined by experimentally measured quantities:

$$q(\varepsilon) = Q(E) - \frac{1}{4\pi^2} P \int_m^{\varepsilon} \frac{E'k'(\sigma_t^+ + \sigma_t^-)}{E'^2 - E^2} dE'$$

$$+ \frac{\varepsilon}{4\pi^2} [\sigma_t^+(\varepsilon) + \sigma_t^-(\varepsilon)] + 2f^2 \frac{r}{E^2 - r^2}, \quad (11)$$

$$\varepsilon^2 \gg E^2.$$

In the Appendix, it is shown that $q(\epsilon)$ has the following properties: 1) it does not depend on E under the condition that $\epsilon^2 \gg E^2$; 2) if (9) and (10) are fulfilled, then $\lim q(\epsilon) = \bar{Q}_\infty$ as $\epsilon \to \infty$; 3) if (9) and (10) are not fulfilled, then the absolute value of $q(\epsilon)$ increases without limit as ϵ increases.

COMPARISON WITH EXPERIMENT

Experimental information concerning $\sigma_t^\pm$ and $D_\pm(E)$ is available only up to a certain energy. For a number of reasons, the energy ϵ to which information on $\sigma_t^\pm$ is available is considerably higher than the energy E to which $D_\pm(E)$ is known. This is in accord with the conditions of separation $\epsilon^2 \gg E^2$. Hence, for comparison with experiment it is convenient to separate out of (8), along with C_∞, that part of the integral in the limits between ϵ and ∞ for which $\sigma_t^\pm$ is not known at present.

Adding and subtracting (6) and (11), we arrive at a system of two equations valid for $E^2 \ll \epsilon^2$:

$$q(\varepsilon) \pm Ep(\varepsilon) = D_\pm(E)$$

$$- \frac{1}{4\pi^2} P \int_m^{\varepsilon} \frac{E'k'(\sigma_t^+ + \sigma_t^-) \pm Ek'(\sigma_t^+ - \sigma_t^-)}{E'^2 - E^2} dE'$$

$$+ \frac{\varepsilon}{4\pi^2} [\sigma_t^+(\varepsilon) + \sigma_t^-(\varepsilon)] \pm \frac{2f^2}{r \mp E}, \quad (12)$$

where

$$p(\varepsilon) = C_\infty + \frac{1}{4\pi^2} \int_{\varepsilon}^{\infty} \frac{\sigma_t^+ - \sigma_t^-}{E'} dE'. \quad (13)$$

If, in fixing ϵ, we subtract from the experimental data on $D_\pm(E)$ and $\sigma_t^\pm$ the right-hand part of (12) and plot the result as a function of E, we consequently obtain a straight line whose parameters determine $q(\epsilon)$ and $p(\epsilon)$. From (12) it follows that any error in the information on the total cross

*The condition under which (2) is fulfilled was obtained earlier by Amati, Fierz, and Glaser.[3]

*For this reason, the conclusions on the behavior of the cross sections made by Lomsadze, Lend'el and Érnst[5] on the basis of assumption (9) cannot be considered well-founded.

sections at energies much higher than E does not disturb the linear dependence of the right-hand part of (12) on E, but changes the values of $q(\epsilon)$ and $p(\epsilon)$ by the quantities $\delta q(\epsilon)$ and $\delta p(\epsilon)$:

$$\delta q(\varepsilon) = \int \frac{[\delta\sigma_t^+(E') + \delta\sigma_t^-(E')]\,dE'}{4\pi^2},$$

$$\delta p(\varepsilon) = \int \frac{\delta\sigma_t^+ - \delta\sigma_t^-}{4\pi^2 E'}\,dE'. \qquad (14)$$

Therefore the errors in the cross sections at high energies have a far greater effect on the determination of $q(\epsilon)$ than on $p(\epsilon)$.

To determine the parameters $p(\epsilon)$ and $q(\epsilon)$, we used the experimental data[6-9] on the values of $D_{\pm}(E)$. In the calculations, we used the values of $D_{\pm}(E)$ in the laboratory system. For the calculation of the integrals in the right-hand part of (12), we took all the values for $\sigma_t^{\pm}$ up to 5.2 Bev published by the middle of 1960, except for the data of Devlin et al,[10] since they are in poor agreement with the results of the measurements of other authors in this energy interval.[11-13]

The energy interval in which the total cross sections are known were divided into 14 subintervals for σ_t^- and 13 subintervals for σ_t^+. In each subinterval, the cross section was approximated by a quadratic parabola by the method of least squares. The values of the right-hand part of (12) as a function of E are shown in the figure in units of 10^{-13} cm.

The parameters of the line for $\epsilon = 5.2$ Bev determined by the method of least squares are:

$$p(\varepsilon) = (-0.069 \pm 0.03)\cdot 10^{-13}\ \text{cm/Bev},$$

$$q(\varepsilon) = (-0.395 \pm 0.01)\cdot 10^{-13}\ \text{cm}.$$

In the calculation, we took $f^2 = 0.08$.

Data on $D_{\pm}(m)$, shown in the dotted circles in the figure, were not included in the calculation of $p(\epsilon)$ and $q(\epsilon)$, since they were calculated from the experimental results used for the determination of $D_{\pm}(\epsilon)$ at low energies, and have already been included in the calculations. The errors given for $p(\epsilon)$ and $q(\epsilon)$ were determined by the statistical errors in $D_{\pm}(E)$ and do not take into account uncertainties connected with the experimental data on the total cross sections and the approximation of the cross sections, or the uncertainty in f^2.

The parameter $q(\epsilon)$, because of (14), is very sensitive to the behavior of the cross section in the high-energy region, and since the behavior of σ_t^- in the energy interval 1.9 – 4.15 Bev is not known, the actual error in the value of $q(\epsilon)$ can be several times the value cited. Therefore we refrain from analyzing the variation of $q(\epsilon)$ with energy.

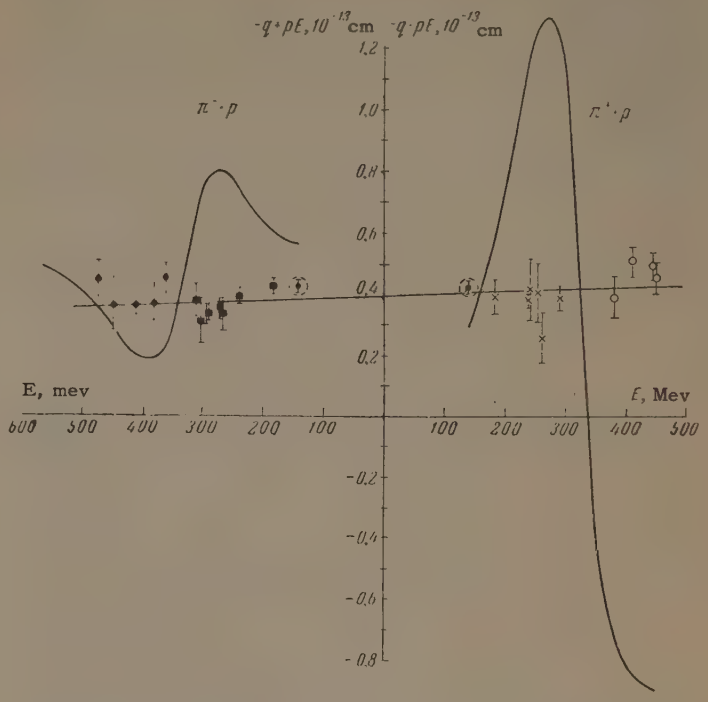

Values of the right-hand part of (12) for $\varepsilon = 5.2$ Bev based on the following data for $D_{\pm}(E)$: ● – reference 6; ■ – reference 7; × – reference 8; ○ – reference 9. The parameters of the line $q(\varepsilon) \pm Ep(\varepsilon)$ are: $q = (-0.395 \pm 0.010) \times 10^{-13}$ cm, $p = (-0.069 \pm 0.030) \times 10^{-13}$ cm/Bev. The curves represent the right-hand part of expression (12) after subtraction of the term $D_{\pm}(E)$.

It should be stressed that, although the quantity $p(\epsilon)$ is not very sensitive [as follows from (14)] to the measurement errors and the approximation of the total cross sections in the high-energy region, an error in the approximation in the low-energy region can lead to a shift in the calculated points, and consequently, to important errors in $p(\epsilon)$. This is connected with the fact that the magnitudes of the principal values of the integrals in (12) are very sensitive to the behavior of the cross section in the region of resonances, and the contribution of the integral terms is very large. (The right-hand part of expression (12), after subtraction of the term $D_{\pm}(E)$, is shown in the figure as a solid line.)

The only objective criterion for errors of this kind in the estimate of $p(\epsilon)$ is the degree to which the data shown in the figure are consistent with a linear dependence. In our case, the degree of agreement is characterized by the value $\chi^2 = 26.3$ for 21 degrees of freedom, which corresponds to $P(\chi^2) = 15.5\%$. In this connection, we note the following. It can be shown that a linear dependence of the right-hand part of (12) on E is equivalent to a linear dependence of the right-hand part

of Schnitzer and Salzman's[14] formula (1±) on the energy.*

Hence, experimental confirmation of a linear dependence of (12) reflects the validity of the dispersion relations in the form given by Goldberger et al.[4] Moreover, a check of these dispersion relations, particularly that by Zinov et al.[15] leads to excellent agreement with experiment. We therefore believe that more accurate values of $p(\epsilon)$ can be obtained on the basis of recent experimental data after a more correct approximation of the total cross sections by means of resonance curves, as was done, for example in [15] and [16]

In conclusion, we note that the method by which we determined the parameters $p(\epsilon)$ and $q(\epsilon)$ is of full statistical value since it permits the utilization of all the experimental data concerning $D_{\pm}(E)$. The statistical error in the value of $p(\epsilon)$ in the determination of the latter by $D_{\pm}(m)$ only, i.e., by means of the formulas of Goldberger et al[4] [in this case, the straight line in the figure passes only through the points $D_{\pm}(m)$] is five times the statistical error obtained in this work. Another important advantage of the method is the fact that uncertainty in f^2 has comparatively little effect, since the contribution of the term with f^2 to (12) decreases with the energy as $(m/E)^2$.

DISCUSSION

From the principle of isotopic invariance, it follows that the charge-exchange cross section at 0° is[17]

$$k^{-2}\sigma_{ex}(0) = 2\,[C(E)]^2 + 2\,(4\pi)^{-2}\,(\sigma_t^+ - \sigma_t^-)^2. \qquad (15)$$

If the statistical view is correct, then, as $E \to \infty$, the total cross section for charge-exchange $(\sigma_{ex})_t$ should drop very rapidly to zero (as $e^{-\sqrt{E}}$). This means that the right-hand part of (15) tends to zero as $E \to \infty$, and, consequently,†

$$C_\infty = 0. \qquad (16)$$

We have estimated $p(\epsilon)$ for ϵ = 590 and 930 Mev, corresponding to the intergration up to the second and third maxima in σ_t^- and obtained the following values (in units of cm/Bev):

$$p\,(590\,\text{Mev}) = -0.29\cdot10^{-13}, \quad p\,(930\,\text{Mev}) = -0.17\cdot10^{-13},$$
$$p\,(5.2\,\text{Bev}) = -0.069\cdot10^{-13}.$$

Hence, the absolute value of $p(\epsilon)$ decreases rapidly. The value of $(\sigma_{ex})_t$ corresponding to p (5.2 Bev) estimated by means of (15) is $\sim 2\times10^{-29}$ cm^2. Shalamov and Shebanov[19] obtained the value $(0.2 \pm 0.25)\times10^{-27}$ cm^2 at 2.8 Bev. All this is in good agreement with the statistical view.

In view of this and also in view of the already-mentioned uncertainties in $p(\epsilon)$ connected with the approximation of the cross sections, we do not believe that the statistically significant deviation of our value of p (5.2 Bev) from zero definitely contradicts condition (16), even though in the estimate of p (5.2 Bev) it was assumed that $\sigma_t^+ = \sigma_t^-$ at E = 5.2 Bev.

It is of interest to estimate, starting from the relation

$$p\,(5.2\,\text{Bev}) = C_\infty + \frac{1}{4\pi^2}\int_{5.2\,\text{Bev}}^{\infty}\frac{\sigma_t^+ - \sigma_t^-}{E'}\,dE'$$

$$= 0.069\cdot10^{-13}\ \text{cm/Bev}, \qquad (17)$$

how the cross sections should behave at E > 5.2 Bev under the assumption that $C_\infty = 0$. It follows from (17) that the difference $\sigma_t^- - \sigma_t^+$ should be $\sim 2\times10^{-27}$ cm^2 for E > 5.2 Bev in the energy region of ~ 50 Bev.

The absence of information on the behavior of the cross section σ_t^- in the 1.9 — 4.15 Bev region can also lead to a deviation of p (5.2 Bev) from zero. We obtain the value p (5.2 Bev) = 0 if it is assumed that σ_t^- has a maximum of area ~ 8 Bev-mb in the region 1.9 — 4.15 Bev, while we obtain $\sigma_t^+ = \sigma_t^-$ for $E \geq 5.2$ Bev.

From the above, it is clear that a more accurate estimate of the value of $p(\epsilon)$ is important.

We express our deep gratitude to E. M. Landis for investigating the passing to the limit in expressions (5) and (6) and I. Ya. Pomeranchuk for constant interest in this work and for helpful discussions, and also I. M. Shmushkevich for his critical remarks.

APPENDIX

E. M. Landis has shown that if, as $x \to \infty$, the function f(x) tends to zero, so that, beginning with some value of x, it is positive and monotonic, then the following equality holds:

$$\lim_{N\to\infty}\frac{N^2}{I_N}\int_{\varepsilon}^{\infty}\frac{f(x)\,dx}{x^2 - N^2} = 1, \qquad I_N = \int_{\varepsilon}^{N} f(x)\,dx. \qquad (A.1)$$

Here, by lim we understand the low side of the limits over all possible sequences of N which go

*This statement means that, although the parameters of a straight line in formula (1 ±) of reference 14 and formulas (12) of the present work are quite different quantities [C(m) and Q(m) in reference 14 and p(ε) and q(ε) in the present work], the same errors in the total cross sections and the values of $D_{\pm}(E)$ lead in both cases to the same deviation of the calculated points from a straight line.

†Amati, Fierz, and Glasser[3] maintain that it follows from assumption (2) that $C_\infty = 0$. However, they did not actually prove this statement (in this connection, see Chew's article).[18]

to infinity. If, in particular, the limit of the numerator in (A.1) exists and is equal to A, then the integral I_∞ exists and is equal to $-A$.

To elucidate the properties of the function $q(\epsilon)$ given in (11) and $Q(E_0)$ of the form (9) and (10), we set in (5)

$$E^2 \ll \varepsilon^2 \ll E_0^2. \tag{A.2}$$

Then (5) can be represented in the form

$$Q(E) = \frac{1}{4\pi^2} P \int_m^{\varepsilon} \frac{E'k'(\sigma_t^+ + \sigma_t^-)}{E'^2 - E^2} dE' + \frac{\varepsilon}{4\pi^2}[\sigma_t^+(\varepsilon) + \sigma_t^-(\varepsilon)]$$
$$+ 2f^2 \frac{r}{E^2 - r^2} \cdot Q(E_0) - \frac{1}{4\pi^2} P \int_{\varepsilon}^{\infty} \frac{E_0^2(\sigma_t^+ - \sigma_t^-)}{E'^2 - E_0^2} dE'$$
$$\frac{\varepsilon}{4\pi^2}[\sigma_t^+(\varepsilon) + \sigma_t^-(\varepsilon)] = q(\varepsilon). \tag{A.3}$$

If (A.2) is fulfilled, then (A.3) is fulfilled for any arbitrary values of E and E_0, from which it follows that $q(\epsilon)$ is independent of E in (11).

We shall now show the validity of (9) and (10). Using the auxiliary identity valid for $\epsilon^2 \ll E_0^2$,

$$\varepsilon = P \int_{\varepsilon}^{\infty} \frac{E_0^2 dE'}{E'^2 - E_0^2}, \tag{A.4}$$

we can represent $Q(E_0)$ in (A.3) in the form

$$Q(E_0) = \frac{1}{4\pi^2} P \int_{\varepsilon}^{\infty} \frac{f(E')E_0^2 dE'}{E'^2 - E_0^2} - \frac{\varepsilon}{4\pi^2} f(\varepsilon) + q(\varepsilon), \tag{A.5}$$

where $f(x) = \sigma_t^+(x) + \sigma_t^-(x) - 2\sigma_\infty$. If we allow E_0 to go to infinity in (A.5), we then have, owing to (A.1),

$$Q(E_0) \text{ bound from above } I_\infty < \infty,$$
$$Q(E_0) = \infty \text{ for } I_\infty = \infty,$$

i.e., we obtain (9) and (10).

Using (A.5) and (A.4), we can also investigate the behavior of $q(\epsilon)$ as $\epsilon \to \infty$. If $\bar{Q}_\infty$ is the upper limit of Q_∞, then from (A.5) and (A.1) we find

$$\lim_{\varepsilon\to\infty} q(\varepsilon) = \lim_{\varepsilon\to\infty}\left[\bar{Q}_\infty + \lim_{E_0\to\infty}\left(-\frac{1}{4\pi^2} P \int_{\varepsilon}^{\infty} \frac{f(E')E_0^2}{E'^2 - E_0^2} dE'\right)\right.$$
$$\left. + \frac{\varepsilon}{4\pi^2} f(\varepsilon)\right] = \lim_{\varepsilon\to\infty}\left(\bar{Q}_\infty + \frac{1}{4\pi^2}\int_{\varepsilon}^{\infty} f(E')\,dE'\right.$$
$$\left. - \frac{\varepsilon}{4\pi^2} f(\varepsilon)\right) = \bar{Q}_\infty,$$

since $\lim \epsilon f(\epsilon) = 0$ as $\epsilon \to \infty$. If conditions (9) and (10) are not fulfilled, then $q(\epsilon) \to \infty$, when $\epsilon \to \infty$, since the integral in the left-hand part of (A.3) diverges.

In conclusion, we give the dispersion relation for $Q(E)$ with the subtracted points transferred to infinity. This relation holds when (9) and (10) are fulfilled:

$$Q_\infty = Q(E) - \frac{1}{4\pi^2}\int_m^{\varepsilon_1} \frac{E'k'(\sigma_t^+ + \sigma_t^-)}{E'^2 - E^2} dE'$$
$$+ \frac{\varepsilon_1}{2\pi^2}\sigma_\infty + 2f^2 \frac{r}{E^2 - r^2};$$

for $E \geq \epsilon_1$ we have $\sigma_t^+ = \sigma_\infty$.

Note added in proof (June 9, 1961): We recently calculated $p(\varepsilon)$ with the aid of the data of Klepikov et al[16] in which the total cross sections were approximated by resonance curves. The new result is $p(5.2\ \text{Bev}) = -0.085 \pm 0.03$ cm/Bev. On the other hand, according to data obtained at the Joint Institute for Nuclear Research and kindly communicated to us by A. L. Lyubimov, σ_t for π^-p has no maximum in the 2–7 Bev energy region. Hence our result can signify the existence of the difference $\sigma_t^- - \sigma_t^+$ in a broad energy interval of over 5 Bev if C_∞ is not different from zero.

[1] I. Ya. Pomeranchuk, JETP **34**, 725 (1958), Soviet Phys. JETP **7**, 499 (1958).

[2] Bogolyubov, Medvedev, and Polivanov, Voprosy teorii dispersionnykh sootnoshenii (Problems in the Theory of Dispersion Relations), Gostekhizdat, 1958.

[3] Amati, Fierz, and Glaser, Phys. Rev. Lett. **4**, 89 (1960).

[4] Goldberger, Miyazawa, and Oehme, Phys. Rev. **99**, 986 (1955).

[5] Lomsadze, Lend'el, and Érnst, JETP **39**, 1154 (1960), Soviet Phys. JETP **12**, 803 (1961).

[6] Zinov, Korenchenko, and Tentyukova, JETP **38**, 1407 (1960), Soviet Phys. JETP **11**, 1016 (1960).

[7] Zinov, Konin, Korenchenko, and Pontecorvo, JETP **38**, 1708 (1960), Soviet Phys. JETP **11**, 1233 (1960).

[8] H. P. Noyes and D. N. Edwards, Phys. Rev. **118**, 1409 (1960).

[9] G. Puppi and A. Stanghellini, Nuovo cimento **5**, 1305 (1957).

[10] Devlin, Barish, Hess, Perez-Mendez, and Solomon, Phys. Rev. Lett. **4**, 242 (1960).

[11] Burrowes, Caldwell, Frisch, Hill, Ritson, Schluter, and Wahlig, Phys. Rev. Lett. **2**, 119 (1959).

[12] Brisson, Detoeuf, Falk-Vairant, van Rossum, Valladas, and Yuan, Phys. Rev. Lett. **3**, 561 (1959).

[13] Longo, Helland, Hess, Moyer, and Perez-Mendez, Phys. Rev. **3**, 568 (1959).

[14] H. J. Schnitzer and G. Salzman, Phys. Rev. **113**, 1153 (1958).

[15] Zinov, Konin, Korenchenko, and Pontecorvo, JETP **38**, 1708 (1960), Soviet Phys. JETP **11**, 1233 (1960).

[16] Klepikov, Sokolov, and Meshcheryakov, Preprint, Joint Institute for Nuclear Research.

[17] L. B. Okun' and I. Ya. Pomeranchuk, JETP **30**, 424 (1956), Soviet Phys. JETP **3**, 307 (1956).

[18] H. Chew, Nuovo cimento **17**, 619 (1960).

[19] Ya. Ya. Shalamov and V. A. Shebanov, JETP **39**, 1232 (1960), Soviet Phys. JETP **12**, 859 (1961).

Translated by E. Marquit
32

INTERACTION OF TRANSVERSE OSCILLATIONS IN A PLASMA

A. P. KAZANTSEV and I. A. GILINSKII

Institute of Radiophysics and Electronics, Siberian Branch, Academy of Sciences, U.S.S.R.

Submitted to JETP editor December 30, 1960

J. Exptl. Theoret. Phys. (U.S.S.R.) 41, 154-158 (July, 1961)

The role of a nonlinear effect associated with the influence of the magnetic field of transverse waves in a plasma is discussed. It is shown that the waves are modulated if the frequency difference of two transverse waves is equal to the plasma frequency (resonance interaction). In a nonresonance interaction only a weak frequency shift occurs. The adiabatic invariants for the problem are found.

In the usual analysis of small oscillations of a plasma the effect of the self magnetic field on the plasma is neglected because this effect is of order nv/c (n is the refractive index and v is some characteristic velocity) as compared with the effect of the electric field. It is of interest, however, to examine this effect because it can lead to an additional interaction between the waves.* It is clear that this effect will be of greatest importance in a magnetoactive plasma when the refractive index n becomes large.

We shall limit ourselves to the case of wave propagation along a uniform magnetic field H (0, 0, H). In this case the transverse waves interact via the excitation and absorption of longitudinal oscillations.

1. BASIC EQUATIONS

The equations that describe the plasma (hydrodynamic approximation) and the electromagnetic field are

$$du/dt + eE/m = -(e/2mc)(v\partial A^*/\partial z + v^*\partial A/\partial z), \quad (1)$$

$$\partial E/\partial z + 4\pi e n_0 \rho = 0, \qquad d\rho/dt + (1+\rho)\,\partial u/\partial z = 0, \quad (2)$$

$$\frac{d}{dt}\left(v - \frac{e}{c}A\right) = i\frac{eH}{mc}v, \quad (3)$$

$$\frac{1}{c^2}\frac{\partial^2 A}{\partial t^2} - \frac{\partial^2 A}{\partial z^2} = -\frac{4\pi}{c}en_0(1+\rho)v. \quad (4)$$

Here $d/dt = \partial/\partial t + u\partial/\partial t$; u and E are the electron velocity and the electric field along the z axis, and $\rho = (n - n_0)/n_0$ is the relative variation in electron density. The ions are fixed and characterized by a density n_0.

The transverse electromagnetic field is described by the vector potential $\mathbf{A}(A_x, A_y, 0)$ and $A = A_x + iA_y$, $v = v_x + iv_y$, where v_x and v_y are the transverse electron velocities. The electrons are assumed to be at zero temperature and dissipative processes are neglected.

Hereinafter we assume that no longitudinal self oscillations are excited. Taking the right-hand side of (1) to be small, we neglect quadratic terms in u and ρ.* Then, Eqs. (1) — (4) can be written in dimensionless form

$$\frac{\partial^2\rho}{\partial t^2} + \rho = \varepsilon^2\frac{\partial}{\partial z}\left(v\frac{\partial A^*}{\partial z} + v^*\frac{\partial A}{\partial z}\right), \quad (5)$$

$$\frac{\partial\rho}{\partial t} + \frac{\partial u}{\partial z} = 0, \qquad \frac{d}{dt}(v - A) = i\omega_H v, \quad (6)$$

$$\partial^2 A/\partial t^2 - \partial^2 A/\partial z^2 + (1+\rho)v = 0. \quad (7)$$

Here, time, length, and longitudinal velocity are expressed in units of $1/\omega_0 = (m/4\pi e^2 n_0)^{1/2}$, c/ω_0, and c respectively. The unit of vector potential is some characteristic initial amplitude A_0 so that the dimensionless quantity A is of order unity. The transverse velocity is measured in units of $v_0 = eA_0/mc$; $\epsilon = |v_0|c\sqrt{2}$ is a small parameter and $\omega_H = eH/mc\omega_0$ is the dimensionless Larmor frequency.

2. APPROXIMATE SOLUTION

We seek an approximate solution of Eqs. (5) — (7) in the form of a superposition of plane waves with amplitudes that vary slowly in time:

$$A(z,t) = \sum_\omega A_\omega(t)\,e^{i\varphi_\omega},$$

$$v(z,t) = \sum_\omega \frac{\omega}{\omega - \omega_H}(A_\omega + B_\omega)\,e^{i\varphi_\omega},$$

$$\rho(z,t) = \sum_{\omega>\omega'}{}' a_{\omega\omega'}(t)\,e^{i(\varphi_\omega - \varphi_{\omega'})} + \text{c.c.} \quad (8)$$

*Wave interactions due to dissipation processes have been investigated in detail in a number of papers (cf. the review by Ginzburg and Gurevich[1]).

*The interaction of longitudinal oscillations in a plasma has been investigated by Sturrock.[2]

where

$\varphi_\omega = \omega t + k_\omega z$, $k_\omega = \omega n_\omega$ and $n_\omega^2 = 1 - 1/\omega\,(\omega - \omega_H)$

is the refractive index, which is determined from the solution of the linearized problem.

In (8) we have neglected combination waves since the amplitudes of these waves are proportional to a power of the small parameter. By slowly varying amplitudes here we mean that $\dot{A}_\omega \ll \omega A_\omega$, etc ($\dot{A}_\omega$ is also proportional to a power of ϵ). The quantity B_ω is a correction ($B_\omega \ll A_\omega$) that takes account of the deviation of v from the solution of the corresponding linearized problem. It is also assumed that any frequency of interest is not too close to ω_H.

Substituting Eq. (8) in Eqs. (5) — (7) and equating coefficients for the same phase we obtain a system of equations for the amplitudes:

$$2i\,(\omega - \omega')\,\dot{\alpha}_{\omega\omega'} + [1 - (\omega - \omega')^2]\,\alpha_{\omega\omega'} = -\varepsilon^2 \lambda_{\omega\omega'} A_\omega A^*_{\omega'}, \tag{9}$$

$$\mu(\omega)\,\dot{A}_\omega = i \sum_{\omega'} \alpha_{\omega\omega'} \frac{\lambda_{\omega\omega'}}{(k_\omega - k_{\omega'})^2} A_{\omega'}, \tag{10}$$

$$B_\omega = i \frac{\omega_H}{\omega} \left(\frac{\dot{A}_\omega}{\omega - \omega_H} + \sum_{\omega'} \frac{k_{\omega'}(\omega - \omega')\,\alpha_{\omega\omega'} A_{\omega'}}{(k_\omega - k_{\omega'})(\omega' - \omega_H)} \right), \tag{11}$$

where

$$\lambda_{\omega\omega'} = (k_\omega - k_{\omega'}) \left(\frac{k_\omega \omega'}{\omega' - \omega_H} - \frac{k_{\omega'} \omega}{\omega - \omega_H} \right),$$

$$\mu(\omega) = 2\omega + \frac{\omega_H}{(\omega - \omega_H)^2}.$$

Equations (9) — (10) have the following integrals:

$$\mu(\omega)\,|A_\omega|^2 + \frac{2}{\varepsilon^2} \sum_{\omega'} \frac{\omega - \omega'}{(k_\omega - k_{\omega'})^2} |\alpha_{\omega\omega'}|^2 = \text{const}. \tag{12}$$

In the summation in the last expression only the resonance and (near-resonance) terms $\alpha_{\omega\omega'}$ are important; these terms satisfy the condition

$$(\omega - \omega')^2 = 1. \tag{13}$$

The resonance terms can be of order ϵ; far from resonance $\alpha_{\omega\omega'}$ is smaller than ϵ^2. It follows from (12) that in general when different waves interact the energy of the high-frequency waves is reduced while the energy of the low-frequency waves is increased.

Summing over ω in (12) we find that the following quantity is conserved:

$$\sum_\omega \mu(\omega)\,|A_\omega|^2 = \text{const}. \tag{14}$$

The integrals in (12) and (14) represent adiabatic invariants of the problem being considered. The quantity $\mu(\omega)|A_\omega|^2/8\pi$ is the energy density of the plane waves divided by the frequency. In a dispersive medium this energy density is [3]

$$\frac{\omega}{8\pi} |A_\omega|^2 \left[n_\omega^2 + \frac{d}{d\omega} (\omega n_\omega^2) \right]. \tag{15}$$

The quantity in the summation sign in (12) is proportional to the energy density of the longitudinal oscillations interacting with a given wave, divided by the frequency.

We note that (14) may be given the following quantum-mechanical interpretation. If we introduce the notion of transverse quasiparticles (A) and longitudinal quasi-particles (α), then the Hamiltonian of the interaction between them is cubic in the amplitude (quadratic with respect to A). Thus the meaning of (14) is that the number of transverse quasi-particles is conserved.*

Further investigation of Eqs. (9) — (10) is difficult for the general case. For this reason we make separate analyses of the resonance interaction of two waves and the nonresonance interaction (in which case the quantity $|\omega - \omega'|$ does not approach unity at any frequency).

In the nonresonance case we can omit $\dot{\alpha}$ in (9) and the solution of (9) — (10) can be easily found in the form

$$A_\omega(t) = A_\omega(0)\, e^{i\Delta\omega t}, \tag{16}$$

where

$$\Delta\omega = -\frac{\varepsilon^2}{\mu(\omega)} \sum_{\omega'}' \frac{\lambda^2_{\omega\omega'} |A_{\omega'}(0)|^2}{(k_\omega - k_{\omega'})^2 [1 - (\omega - \omega')^2]}.$$

The applicability condition for the last relation ($\Delta\omega \ll \omega$) is the inequality $\epsilon(\omega_H - \omega)^{-1} \ll 1$.

3. INTERACTION OF TWO WAVES

We now consider the case of a resonance interaction between two extraordinary waves ($\omega_1 - \omega_2 = 1$) assuming that $\omega_1, \omega_2 < \omega_H$ and $\omega_H > 1$. For definiteness we denote quantities pertaining to the high-frequency wave by the subscript "1." We also introduce the notation

$$I_{1,2} = \mu_{1,2}(\omega)\,|A_{1,2}|^2, \qquad |\alpha|^2 = \tfrac{1}{2} \varepsilon^2 I_{10} (k_1 - k_2)^2 \zeta.$$

If it is assumed that there are no longitudinal oscillations at the initial time [$\dot{\xi}(0) = \xi(0) = 0$], then (12) can be written in the form

$$I_1 + I_{10}\zeta = I_{10}, \qquad I_2 - I_{10}\zeta = I_{20}, \tag{17}$$

so that $0 \le \zeta \le 1$. Using (9) — (10) and (17) we obtain the following differential equation for ζ:

*The author is indebted to V. L. Pokrovskii for these observations.

$$d^2\zeta/d\tau^2 + \zeta (I_{20} - I_{10}) + \tfrac{3}{2} I_{10}\zeta^2 = \tfrac{1}{2} I_{20}, \qquad (18)$$

where

$$\tau = \varepsilon t\, [2\lambda^2/\mu_1\mu_2 (k_1 - k_2)^2]^{1/2}.$$

Integrating once in (18) and introducing the initial conditions we have

$$(d\zeta/d\tau)^2 + \zeta^2 (I_{20} - I_{10}) + I_{10}\zeta^3 - I_{20} = 0 \qquad (19)$$

The cubic term in the left side of (19) has the following roots

$$0; \quad 1; \quad -I_{20}/I_{10}.$$

Consequently, ζ varies periodically from 0 to 1 with period $2\tau_0$, where

$$\tau_0 = \int_0^1 \frac{d\zeta}{\sqrt{\zeta (1-\zeta) (I_{20} + I_{10}\zeta)}}. \qquad (20)$$

This same period characterizes the oscillations of the energy in wave 1 (E_1) between zero and the initial value and the oscillations of the energy of wave 2 between E_{20} and $E_{20} + \omega_2 E_{10}/\omega_1$. When the frequency of the first wave is close to ω_H ($\omega_H - \omega_1 \ll 1$) its energy increases sharply, $I_{10} \gg I_{20}$ and the modulation period is determined approximately by relation

$$\tau_0 = I_{10}^{-1/2} \ln (4\, I_{10}/I_{20}).$$

However, the applicability condition for Eqs. (9) — (10) imposes definite limitations on how small $\omega_H - \omega$ can be. Specifically, (11) and the requirement $B_\omega \ll A_\omega$ mean that the inequality $\epsilon (\omega_H - \omega)^{-3/2} \ll 1$ must be satisfied.

Using (9) we can easily estimate the width of the resonance interaction region. The "detuning" frequency is given by the relation

$$|1 - \omega_1 + \omega_2| \lesssim \varepsilon.$$

The quadratic terms in u and ρ are of order ϵ^4 far from resonance; at resonance these terms are of order ϵ^2 and the nonlinear inertia term $u\,\partial u/\partial z$ can be of the same order of magnitude as the driving force $\epsilon^2 (v\,\partial A^*/\partial z + \text{c.c.})$. It is easily shown, however, that this term does not contain harmonics that interact. Thus it is valid to neglect the quadratic terms in u and ρ.

All the foregoing considerations are obviously valid to an accuracy of order ϵ for the resonance interaction and ϵ^2 for the nonresonance case. There is no qualitative change in the results if the electron temperature is nonzero. In place of (13) we obtain a resonance condition of the form

$$(\omega_1 - \omega_2)^2 - (c_s/c)^2 (k_1 - k_2)^2 = 1,$$

where c_S is the electron thermal velocity.

If we take $\omega_H = 0$ in the above formulas the interaction of circularly polarized waves in an isotropic plasma can be treated.

In conclusion we wish to thank V. L. Pokrovskii for valuable discussions and comments.

[1] V. L. Ginzburg and A. V. Gurevich, Usp. Fiz. Nauk 70, 201 and 293 (1960), Soviet Phys.-Uspekhi 3, 115 and 175 (1960).

[2] P. A. Sturrock, Proc. Roy. Soc. (London) A242, 277 (1957).

[3] Landau and Lifshitz, Elektrodinamika sploshnykh sred (Electrodynamics of Continuous Media), Gostekhizdat, 1957.

Translated by H. Lashinsky
33

ELECTROMAGNETIC PROPERTIES OF A RELATIVISTIC PLASMA, III

V. P. SILIN and E. P. FETISOV

P. N. Lebedev Physics Institute, Academy of Sciences, U.S.S.R.

Submitted to JETP editor January 4, 1961

J. Exptl. Theoret. Phys. (U.S.S.R.) **41**, 159-170 (July, 1961)

We consider the problem of reflection and absorption of electromagnetic waves striking the plane bounding an electric plasma at an oblique angle. The main difference between oblique incidence and the case of normal incidence previously considered is that longitudinal waves are excited inside the plasma at frequencies close to those for which the longitudinal dielectric constant of the plasma vanishes. In the particular case of nonrelativistic temperatures, the energy spent in exciting the longitudinal waves exceeds the energy lost as a result of collisions between the plasma particles, provided that the condition (44) is satisfied.

1. The theory of electromagnetic properties of a semi-infinite plasma has been the subject of many papers.* At the present time the question of reflection, refraction, and absorption of electromagnetic waves incident perpendicularly to the surface of a sharply delineated plasma can be regarded as relatively well investigated. To the contrary, the case of inclined incidence remains essentially uninvestigated.

We have undertaken to fill this gap in part. We consider here the problem of oblique incidence of electromagnetic waves on the surface of an isotropic plasma (without constant field) with arbitrary particle distribution (in particular, relativistic). Such an analysis will enable us to study not only the question of losses connected with the occurrence of a transverse field in the plasma (called below the transverse losses), but also the question of the excitation of longitudinal waves and losses connected with the occurrence of a longitudinal field (longitudinal losses).

When we consider the semi-infinite plasma, we assume specular or diffuse reflection of the particles from its surface.[1] Both conditions must be regarded as rather approximate. These boundary conditions, however, can explain the role of effects occurring as a result of the presence of the plasma boundary, both in the case of a plasma bounded by a solid surface and in the case of a plasma confined by a magnetic field (under the condition that the transition layer is sufficiently small).

2. To study the electromagnetic properties of an electron plasma (assuming that the ions form a homogeneous background), we use, as is customary, the kinetic equation with self-consistent field. Being interested in the region of larger frequencies (much higher than the collision frequency), we can write here the kinetic equation in the form

$$\frac{\partial \delta f}{\partial t} + \mathrm{v}\frac{\partial \delta f}{\partial \mathrm{r}} + e\mathbf{E}\frac{\partial f_0}{\partial \mathbf{p}} = -\nu\delta f. \qquad (1)$$

Here f_0 is the equilibrium electron distribution function, and δf is the nonequilibrium addition; ν is the collision frequency.

Assuming specular reflection of the electrons from the surface of the plasma, when

$$\delta f(v_z > 0, z = 0) = \rho\delta f(v_z < 0, z = 0) \quad (\rho = 1) \qquad (2)$$

(here $z = 0$ corresponds to the surface of a plasma filling the half-space $z \geq 0$), we obtain the following solution of the kinetic equation for the case of an incident electromagnetic wave with time and space dependence $\exp\{i\omega(-t + z\cos\theta/c + y\sin\theta/c)\}$, where θ is the angle of incidence:

$$\delta f = -\frac{e}{v_z} f_0' \int_z^\infty dz' \exp\left\{-\frac{z-z'}{v_z}\chi\right\} \mathbf{vE}(z'), \qquad v_z < 0,$$

$$\delta f = \frac{e}{v_z} f_0' \int_0^z dz' \exp\left\{-\frac{z-z'}{v_z}\chi\right\} \mathbf{vE}(z') + \frac{e}{v_z} f_0' \int_0^\infty dz' \exp\left\{-\frac{z+z'}{v_z}\chi\right\} \times \{E_x v_x + E_y v_y - E_z v_z\}, \qquad v_z > 0.$$

Here $\chi = \nu - i\omega(1 - v_y\sin\theta/c)$ and f_0' is the derivative of the equilibrium distribution function with respect to the energy.

*For lack of space we cannot discuss these papers in any detail. We refer the reader, for example, to the book,[2] which contains a relatively complete bibliography.

Expressions (3) are used to determine the current density

$$\mathbf{j} = e\int \mathbf{v}\delta f d\mathbf{p},$$

which is contained in the field equations. If we now eliminate from the field equations the magnetic induction, and extend the electric field to include all space (the tangential components E_x and E_y in even fashion, and the normal component E_z in odd fashion), then, as can be readily verified, we obtain for the Fourier components of the electric field

$$E_i(q) = \frac{1}{\sqrt{2\pi}}\int dz e^{-iqz} E_i(z)$$

the following equation

$$k^2 E_i(q) - k_i(\mathbf{kE}(q)) - (\omega^2/c^2)\,\varepsilon_{ij}(\omega, \mathbf{k})\,E_j(q) = -\sqrt{2/\pi}\,a_i;$$

$$\mathbf{k} = (0, \omega\sin\theta/c, q), \quad \mathbf{a} = (E_x'(0), E_y'(0) - i\omega\sin\theta E_z(0)/c, 0). \tag{4}$$

The dielectric permittivity tensor ϵ_{ij} has in our case of isotropic plasma the form

$$\varepsilon_{ij}(\omega, \mathbf{k}) = \varepsilon^t(\omega, k)(\delta_{ij} - k^{-2}k_ik_j) + k^{-2}k_ik_j\varepsilon^l(\omega, k).$$

Here the transverse and longitudinal permittivities are determined by the usual formulas[1]

$$\varepsilon^t(\omega, k) = 1 + \frac{4\pi e^2}{\omega k^2}\int d\mathbf{p}\,\frac{(\mathbf{kv})^2 f_0'}{\omega + i\nu - \mathbf{kv}}, \tag{5}*$$

$$\varepsilon^t(\omega, k) = 1 + \frac{2\pi e^2}{\omega k^2}\int d\mathbf{p}\,\frac{[\mathbf{kv}]^2 f_0'}{\omega + i\nu - \mathbf{kv}}. \tag{6}$$

The equations written out solve the formal aspect of the theory of inclined incidence of radiation on a semi-infinite plasma when the electrons are specularly reflected from the surface. We now proceed to an analysis of the pertinent results.

3. We turn first to the relatively simple case of s-polarization, when the electric vector of the incident wave is perpendicular to the plane of incidence. In this case only the x component differs from zero, and is given by

$$E(z) = \frac{E_x'(0)}{\pi}\int_{-\infty}^{+\infty}\frac{dqe^{iqz}}{(\omega/c)^2\varepsilon^t(\omega, k) - k^2}. \tag{7}$$

The difference between this equation and Eq. (7) of an earlier paper by one of the authors,[2] is that the quantity q in the denominator of the integrand is replaced by k. This corresponds in fact to the result obtained by Reuter and Sondheimer.[3]

The complex coefficient of reflection, in the case of s-polarization, is

$$r_s = \frac{(c/4\pi)\cos\theta\, Z_s - 1}{(c/4\pi)\cos\theta\, Z_s + 1},$$

where $Z_S(\omega) = (4\pi i\omega/c^2)\,[E_x(0)/E_x'(0)]$ is the surface impedance, connected by the relation

$$Z_s(\omega) = -(4\pi i\omega/c^2)\lambda_s$$

with the effective complex depth of penetration

$$\lambda_s^{(3)} = -\frac{1}{\pi}\int_{-\infty}^{+\infty}\frac{dq}{(\omega/c)^2\varepsilon^t(\omega, k) - k^2}. \tag{8}$$

Under conditions when the spatial dispersion is weak, we can represent the transverse permittivity in the form ($\omega \gg \nu$):[1,2]

$$\varepsilon^t(\omega, k) = \varepsilon(\omega) - \alpha^t c^2k^2/\omega^2 = 1 - \omega_0^2/\omega^2 - \alpha^t c^2k^2/\omega^2 + i\nu\omega_0^2/\omega^3;$$

$$\omega_0^2 = -\frac{4\pi e^2}{3}\int d\mathbf{p}v^2 f_0', \qquad \alpha^t = -\frac{4\pi e^2}{15}\int\frac{v^4 f_0'}{c^2\omega^2}d\mathbf{p}. \tag{9}$$

Thereupon we get for the effective depth of penetration

$$\lambda_s = \frac{ic}{\omega}\left[(1 + \alpha^t)(\varepsilon(\omega) - (1 + \alpha^t)\sin^2\theta)\right]^{-1/2}. \tag{10}$$

In the case of a nonrelativistic plasma, the contribution due to a^t is negligibly small. To the contrary, in the relativistic case this is no longer so. Actually, for example, in the ultrarelativistic case $a^t = \omega_0^2/5\omega^2$.

In order for expansion (9) to be valid, the conditions

$$|\varepsilon(\omega)| \ll mc^2/\varkappa T_e \qquad (\omega^2 \gg \omega_{Le}^2\varkappa T_e/mc^2) \tag{11}$$

must be satisfied in the case of nonrelativistic plasma, and

$$|\varepsilon(\omega)| \ll 1 \tag{12}$$

in the relativistic case.

Expression (10) is due to the contribution of the pole of the integrand of (8). Let us consider now the contribution due to the branch point of the dielectric constant. We have

$$\delta\lambda_s^{(3)} = -\frac{2i}{\pi}\frac{c}{\omega}\left(1 + i\frac{\nu}{\omega}\right)\int_1^\infty \frac{dx\, x\,\mathrm{Im}\,\varepsilon_+^t(\omega, x(\omega + i\nu)/c)}{\sqrt{x^2 - \sin^2\theta\,\omega^2/(\omega + i\nu)^2}} \times\left\{\left[\mathrm{Re}\,\varepsilon_+^t\left(\omega, \frac{\omega + i\nu}{c}x\right) - (1 + i\nu/\omega)^2x^2\right]^2 + \left[\mathrm{Im}\,\varepsilon_+^t\left(\omega, \frac{\omega + i\nu}{c}x\right)\right]^2\right\}^{-1}. \tag{13}$$

The expressions for ϵ_+^t were derived earlier (see [2]) for the case of a relativistic Boltzmann particle distribution. In the nonrelativistic case, when the main contribution is made by the values

*$(\mathbf{kv}) = \mathbf{k}\cdot\mathbf{v}$; $[\mathbf{kv}] = \mathbf{k}\times\mathbf{v}$.

$x \sim c/v_T \sim \sqrt{mc^2/\kappa T_e}$, the expression for $\delta\lambda_s^{(3)}$ is independent, accurate to terms $\sim \kappa T_e/mc^2$, of the angle of incidence and agrees with the following expression[2]

$$\delta\lambda_s^{(3)} \approx -\frac{2i\omega^2}{\pi c^2}\int_0^\infty \frac{dk}{k^4}\,\mathrm{Im}\,\varepsilon^t(\omega, k) = 2i\sqrt{\frac{2}{\pi}}\,\frac{c}{\omega}\,\frac{\omega_{Le}^2}{\omega^2}\left(\frac{\kappa T_e}{mc^2}\right)^{3/2}. \tag{14}$$

Here we assume $\omega \gg \nu$ and $(\omega_{Le}^2/\omega^2)(\kappa T_e/mc^2) \ll 1$.

In the ultrarelativistic case, assuming $\omega \gg \nu$, we have

$$\delta\lambda_s^{(3)} = \frac{ic}{\omega}\,\frac{3}{2}\,\frac{\omega_{0p}^2}{\omega^2}\int_1^\infty \frac{dx}{\sqrt{x^2-\sin^2\theta}}\,(1-1/x^2)\left\{\left(1+\frac{\omega_{0p}^2}{\omega^2}\,\frac{3}{4x}\right.\right.$$
$$\times\left[-\frac{2}{x}+(1-1/x^2)\ln\frac{x-1}{x+1}\right]-x^2\Big)^2$$
$$\left.+\left(\frac{3\pi}{4x}\right)^2\frac{\omega_{0p}^2}{\omega^2}(1-1/x^2)^2\right\}^{-1}, \tag{15}$$

where $\omega_{0p}^2 = 4\pi e^2 N_e c^2/3\kappa T_e$.

In order to exhibit the dependence of the latter expression on the angle of incidence θ, we give the values of $\delta\lambda_s^{(3)}(\omega/ic)$ when $\omega = \omega_{0p}$. Thus, when $\theta = 0$, 30, 60, and 90° we have accordingly the values 0.09, 0.10, 0.115, and 0.24.

The formulas obtained permit, in particular, a determination of the absorbing ability of the plasma, $A = 1 - |r|^2$. In the case of nonrelativistic temperature with $\epsilon_0 - \sin^2 < 0$ we have

$$A_{nr}^{(s)} \approx \frac{2\cos\theta}{\sqrt{\sin^2\theta-\varepsilon_0}}\,\frac{\nu}{\omega} + 8\sqrt{\frac{2}{\pi}}\,(\sin^2\theta-\varepsilon_0)\left(\frac{\kappa T_e}{mc^2}\right)^{3/2}\cos\theta. \tag{16}$$

When $\theta = 0$, this formula coincides with equation (38) of [2].

The contribution to the absorbing ability, a contribution not connected with the plasma-particle collisions with each other, can also be determined directly by calculating the energy lost by the electrons on colliding with the plasma surface. In the case when $\epsilon_0 - \sin^2\theta > 0$ this contribution is now equal to

$$\frac{8\sqrt{2/\pi}\,(\omega_{Le}/\omega)^2(\kappa T_e/mc^2)^{3/2}\cos\theta\,(\varepsilon(\omega)-\sin^2\theta)}{(\sqrt{\varepsilon(\omega)-\sin^2\theta}+\cos\theta)^2}. \tag{17}$$

In the case of s-polarization which we are considering, it is easy to obtain the solution also by assuming diffuse reflection of the electrons from the plasma boundary, corresponding to $r = 0$ in Eq. (2). Now we obtain for the field the following expression

$$E_x(z) = \frac{E_x(0)}{2\pi i}\int_{-i\delta-\infty}^{-i\delta+\infty}\frac{dq}{q}\,e^{iqz}\exp\left\{\frac{1}{2\pi i}\int_{-\infty}^{+\infty}\frac{dq'}{q-q'}\right.$$
$$\left.\times\ln\left[1-\frac{\omega^2}{c^2q'^2}\,(\varepsilon^t(\omega, k)-\sin^2\theta)\right]\right\}, \tag{18}$$

and for the complex depth of penetration we have

$$\lambda_s^{(D)} = \left\{\frac{1}{\pi}\int_0^\infty dq\,\ln\left[1-\frac{\omega^2}{c^2q^2}\,(\varepsilon^t(\omega, k)-\sin^2\theta)\right]\right\}^{-1}. \tag{19}$$

Under conditions of weak spatial dispersion, the contribution of the zero of the dispersion equation yields

$$\lambda_s^{(D)} = \frac{ic}{\omega}\left[\frac{1+\alpha^t}{\varepsilon(\omega)-(1+\alpha^t)\sin^2\theta}\right]^{1/2}. \tag{20}$$

The branch point of the dielectric permittivity makes a contribution

$$\{\delta\lambda_s^{(D)}\}^{-1} = \frac{i\omega}{\pi c}\left(1+i\frac{\nu}{\omega}\right)^3$$
$$\times\int_0^1 da\int_1^\infty dx\,x\left[x^2-\left(\frac{\omega}{\omega+i\nu}\right)^2\sin^2\theta\right]^{1/2}\mathrm{Im}\,\varepsilon_+^t$$
$$\times\{[a\,\mathrm{Re}\,\varepsilon_+^t-(1+i\nu/\omega)^2x^2$$
$$+(1-a)\sin^2\theta]^2+(a\,\mathrm{Im}\,\varepsilon_+^t)^2\}. \tag{21}$$

In the nonrelativistic limit, the result for $\delta\lambda$ does not depend on the angle of incidence, accurate to $(\kappa T_e/mc^2)$. In the opposite, ultrarelativistic limit, $\delta\lambda$ depends continuously on θ.

4. We now proceed to the somewhat more cumbersome but more interesting case of p-polarization, when the electric vector of the incident wave lies in the plane of incidence. This case is of special interest because a longitudinal wave, which cannot be excited in the case of s-polarization, can now penetrate into the plasma.

The field produced in the plasma as a result of the incident plane electromagnetic wave can be described in this case by the formulas

$$E_y(z) = E_y^t(z) + E_y^l(z), \tag{22}$$

$$E_y^t(z) = \left\{E_y'(0) - i\frac{\omega}{c}\sin\theta E_z(0)\right\}$$
$$\times\frac{1}{\pi}\int_{-\infty}^{+\infty}\frac{dqq^2e^{iqz}}{[q^2+(\omega/c)^2\sin^2\theta]\,[(\omega/c)^2\varepsilon^t(\omega, k)-(\omega/c)^2\sin^2\theta-q^2]}, \tag{23}$$

$$E_y^l(z) = \left\{E_y'(0) - i\frac{\omega}{c}\sin\theta E_z(0)\right\}$$
$$\times\frac{1}{\pi}\int_{-\infty}^{+\infty}\frac{dq\sin^2\theta\,e^{iqz}}{[q^2+(\omega/c)^2\sin^2\theta]\,\varepsilon^t(\omega, k)}. \tag{24}$$

The complex reflection coefficient is determined by the following formulas:

$$r_p = \frac{\cos\theta - Z_p\,(c/4\pi)}{\cos\theta + Z_p\,(c/4\pi)}, \tag{25}$$

$$Z_p(\omega, \theta) = \frac{4\pi i\omega}{c^2}\,\frac{E_y(0)}{E_y'(0) - i(\omega/c)\sin^2\theta E_z(0)} = -\frac{4\pi i\omega}{c^2}\lambda_p. \tag{26}$$

From (22) – (24) it is clear that the effective depth of penetration is made up, in additive fashion, of the transverse and longitudinal depths, given by the formulas

$$\lambda_p^t = -\frac{1}{\pi} \times \int_{-\infty}^{+\infty} \frac{dqq^2}{[q^2 + (\omega/c)^2 \sin^2\theta]\,[(\omega/c)^2 \varepsilon^t(\omega, k) - (\omega/c)^2 \sin^2\theta - q^2]}, \tag{27}$$

$$\lambda_p^l = -\frac{\sin^2\theta}{\pi} \int_{-\infty}^{+\infty} \frac{dq}{[q^2 + (\omega/c)^2 \sin^2\theta]\,\varepsilon^l(\omega, k)}. \tag{28}$$

We note that in the calculation of these integrals, the contributions of the singularity of the integrands at the point $q^2 + (\omega/c)^2 \sin^2\theta = 0$ cancel each other out in the summary expression for λ_p. The reason for it is that the longitudinal and transverse permittivities are equal to each other when $k = 0$. Consequently we disregard from now on the contribution of this singularity.

Under conditions when the spatial dispersion is weak and we can use expression (9) for the transverse permittivity, the contribution to the right half of (27), due to the zero of the dispersion equation for the transverse oscillations, has the form

$$\lambda_p^t = \frac{ic}{\omega\varepsilon(\omega)} \left[\frac{\varepsilon - (1+\alpha^t)\sin^2\theta}{1+\alpha^t}\right]^{1/2} = \frac{ic}{\omega^2 - \omega_0^2 + \omega_0^2 i\nu/\omega} \times \left[\frac{\omega^2\cos^2\theta - \omega_0^2 + \omega_0^2 i\nu/\omega - \omega^2\alpha^t\sin^2\theta}{1+\alpha^t}\right]^{1/2}. \tag{29}$$

To be able to use expansion (9) here, inequalities (11) and (12) must be satisfied.

Analogously, in the case of weak spatial dispersion we can write for the longitudinal permittivity the following expression:*

$$\varepsilon^l(\omega, k) = \varepsilon(\omega) - \frac{c^2k^2}{\omega^2}\alpha^l, \tag{30}$$

$$\alpha^l = -\frac{4\pi e^2}{5c^2\omega^2}\int dp v^4 f_0'. \tag{31}$$

In particular, in the case of a Boltzmann particle-energy distribution we have

$$\alpha^l = \frac{4\pi e^2 N_e mc^4}{5(\varkappa T_e)^2\omega^2 K_2(mc^2/\varkappa T_e)} \int_1^\infty \frac{dx}{x^3}(x^2-1)^{5/2}\exp\left(-\frac{mc^2}{\varkappa T_e}x\right). \tag{31a}$$

For the case of nonrelativistic ($mc^2 \gg \varkappa T_e$) and in the case of ultrarelativistic temperatures ($mc^2 \ll \varkappa T_e$) we have now, respectively,

$$\alpha_{nr}^l = 3\varkappa T_e\omega_{Le}^2/mc^2\omega^2, \qquad \alpha_{ur}^l = 3\omega_{0p}^2/5\omega^2. \tag{31b}$$

The contribution to the right half of (28), due to the zero of Eq. (30), has the form

$$\lambda_p^l = \frac{ic}{\omega}\frac{\sqrt{\alpha^l}}{\varepsilon(\omega)}\frac{\sin^2\theta}{\sqrt{\varepsilon(\omega) - \alpha^l\sin^2\theta}}. \tag{32}$$

This result, obtained with the aid of the approximate expression (30), will not be valid if the condition $|\epsilon(\omega)| \ll 1$ is violated.

The longitudinal permittivity is also relatively simplified if $kv_T \gg \omega$. Now

$$\varepsilon^l = 1 + (kr_{scr})^{-2}, \tag{33}$$

$$r_{scr}^{-2} = -4\pi e^2\int dp f_0'. \tag{34}$$

In the case of a Boltzmann electron distribution* we have

$$r_{scr}^{-2} = 4\pi e^2 N_e/\varkappa T_e. \tag{34a}$$

Now the pole contribution to formula (28) has the form

$$\lambda_p^l = -\sin^2\theta r_{scr}. \tag{35}$$

Finally, as $kc \to \omega + i\nu$ we obtain in the case of an ultrarelativistic plasma

$$\lambda_p^l = i\frac{8}{3}\frac{\omega^2}{\omega_{0p}^2}\frac{c}{\omega}\frac{\sin^2\theta}{\cos\theta}\exp\left[-\frac{2}{3}\frac{\omega^2}{\omega_{0p}^2} - 2\right].$$

Inasmuch as in this case $\omega \gg \omega_{0p}$, we are dealing with an exponentially small quantity.

Let us turn now to an examination of the contributions to the left halves of (27) and (28), due to the branch point of the permittivity. The integrals along the edges of the cut yield accordingly

$$\delta\lambda_p^t = -\frac{2i}{\pi}\frac{c}{\omega}(1 + i\nu/\omega) \times \int_1^\infty \frac{dx}{x}\left[x^2 - \sin^2\theta\left(\frac{\omega}{\omega + i\nu}\right)^2\right]^{1/2} \operatorname{Im}\varepsilon_+^t\left(\omega, \frac{\omega+i\nu}{c}x\right) \times \left\{\left[\operatorname{Re}\varepsilon_+^t\left(\omega, \frac{\omega+i\nu}{c}x\right) - (1 + i\nu/\omega)^2x^2\right]^2 + \left[\operatorname{Im}\varepsilon_+^t\left(\omega, \frac{\omega+i\nu}{c}x\right)\right]^2\right\}^{-1}, \tag{36}$$

$$\delta\lambda_p^l = -\frac{2i}{\pi}\frac{\sin^2\theta}{(1+i\nu/\omega)}\frac{c}{\omega}\int_1^\infty dx \operatorname{Im}\varepsilon_+^l\left(\omega, \frac{\omega+i\nu}{c}x\right)\Big|\varepsilon_+^l \times \left(\omega, \frac{\omega+i\nu}{c}x\right)\Big|^{-2}\left[x^2 - \sin^2\theta\left(\frac{\omega}{\omega+i\nu}\right)^2\right]^{-1/2}. \tag{37}$$

Formula (36) assumes the form (14) in the nonrelativistic case, when the main contribution to the

*In the transparency region we must take account of the contribution of the Cerenkov effect to the imaginary part of ε^l:

$$\delta\varepsilon^l = -i\frac{4\pi^2e^2\omega}{k^2}\int dp\delta(kv - \omega)f_e'.$$

*We note that allowance for the motion of the ions causes a term $4\pi e_i^2 N_i/\varkappa T_i$ to appear in formula (34a).

integral is made by large values of x. Analogously, the integrand in (37) can be assumed independent* of the angle of incidence

$$\delta\lambda_p^l \approx -\frac{2ic}{\pi\omega}\frac{\sin^2\theta}{1+i\nu/\omega} \times \int_1^\infty \frac{dx}{x^2}\,\mathrm{Im}\,\varepsilon_+^l\left(\omega, \frac{(\omega+i\nu)}{c}x\right)\Bigg/\left|\varepsilon_+^l\left(\omega, \frac{(\omega+i\nu)}{c}x\right)\right|^{-2}. \quad (37a)$$

For the case of Maxwellian electron distribution

$$\delta\lambda_p^l = \frac{ic}{\omega}\sin^2\theta\sqrt{\frac{2}{\pi}}\left(\frac{\varkappa T_e}{mc^2}\right)^{1/2}\frac{\omega_{Le}^2}{\omega^2} \times \int_0^{\beta_{max}} d\beta\beta e^{-\beta^2/2}\left\{\left(1+\frac{\omega_{Le}^2}{\omega^2}\beta^2\,[1-\mathrm{Re}\,J_+(\beta)]\right)^2 + \frac{\pi}{2}\frac{\omega_{Le}^4}{\omega^4}\beta^2 e^{-\beta^2/2}\right\}^{-1},$$

$$\beta_{max}^{-1} = \sqrt{\frac{\varkappa T_e}{mc^2}}\,[(1+i\nu/\omega)^2-\sin^2\theta)^{1/2},$$

$$J_+(\beta) = \beta e^{-\beta^2}\int_{+i\infty}^{\beta} e^{\tau^2/2}\,d\tau.$$

We can put with high degree of accuracy $\beta_{max} = \infty$. The numerical integration yields for $\omega = \omega_{Le}$

$$\delta\lambda_p^l \approx 1.7\frac{ic}{\omega_{Le}}\sin^2\theta\sqrt{\frac{2}{\pi}}\left(\frac{\varkappa T_e}{mc^2}\right)^{1/2}. \quad (38)$$

Below the Langmuir frequency we can use for estimates the formula

$$\delta\lambda_p^l \sim \frac{ic}{\omega}\sin^2\theta\sqrt{\frac{2}{\pi}}\left(\frac{\varkappa T_e}{mc^2}\right)^{1/2}\frac{\omega^2}{\omega_{Le}^2}\left\{\frac{1}{2}\ln\left(1+\frac{\omega_{Le}^2}{\omega^2}\right)-\frac{\omega_{Le}^2}{\omega^2+\omega_{Le}^2}\right\}.$$

In the opposite case of ultrarelativistic temperatures, using Eqs. (11) and (12) of [4], we obtain ($\omega \gg \nu$)

$$\delta\lambda_p^t = -\frac{ic}{\omega}\frac{3}{2}\frac{\omega_{0p}^2}{\omega^2}\int_1^\infty\frac{dx}{x^2}\sqrt{x^2-\sin^2\theta}\left(1-\frac{1}{x^2}\right)\left\{\left(1+\frac{\omega_{0p}^2}{\omega^2}\frac{3}{4x}\times\left[-\frac{2}{x}+\left(1-\frac{1}{x^2}\right)\ln\frac{x-1}{x+1}\right]-x^2\right)^2 + \left(\frac{3\pi}{4x}\right)^2\frac{\omega_{0p}^2}{\omega^2}\left(1-\frac{1}{x^2}\right)^2\right\}^{-1}, \quad (39)$$

$$\delta\lambda_p^l = -\frac{ic}{\omega}3\frac{\omega_{0p}^2}{\omega^2}\sin^2\theta\int_1^\infty\frac{dx}{x^4(x^2-\sin^2\theta)^{1/2}} \times\left\{\left(1+3\frac{\omega_{0p}^2}{\omega^2}\frac{1}{\lambda^2}\left[1+\frac{1}{2x}\ln\frac{x-1}{x+1}\right]\right)^2+\left(\frac{3\pi}{2}\frac{\omega_{0p}^2}{\omega^2}\right)^2\frac{1}{x^6}\right\}^{-1}. \quad (40)$$

In order to display the dependence of these expressions on the angle of incidence θ, we give the following numerical values for $\omega_{0p}^2 = \omega^2$. Thus, for angles $\theta = 0, 30, 60, 90°$ we have for $\delta\lambda^t(\omega_{0p}/ic)$ the values 0.09, 0.088, 0.077, and 0.07 respectively. Analogously we have for $\delta\lambda^l(\omega_{0p}/ic)$ the values $(0, 0.12, 0.15, 0.16)\times\sin^2\theta$.

The results obtained can be used to determine the absorbing ability of a plasma, connected in the case of p-polarization with the effective depth of penetration by the following relation

$$A^{(p)} = \frac{4\cos\theta(\omega/c)\,\mathrm{Im}\,\lambda}{[\cos\theta+(\omega/c)\,\mathrm{Im}\,\lambda]^2+[(\omega/c)\mathrm{Re}\lambda]^2}. \quad (41)$$

At large values of $\epsilon(\omega)$, when, as is well known, the Leontovich boundary conditions are applicable, an analysis of our formulas is of little interest, for in this case we can use directly the results obtained in the analysis of normal incidence (see [2]). We therefore concentrate our attention from now on on the case $|\epsilon(\omega)| \lesssim 1$.

For angles not too close to $\pi/2$, we can neglect the dissipative terms in the denominator of (41). Therefore to determine the effect of various factors on the dissipation of electromagnetic waves it is sufficient to compare the corresponding dissipative contributions to Im λ, contained in the numerator of (41). Thus, in the relativistic case when $\omega \approx \omega_{0p}$, as follows from the estimates given above, the longitudinal and transverse losses are comparable in magnitude when θ is not too small. A comparison of (38) with (14) shows that in the nonrelativistic case, when $\omega \sim \omega_{Le}$, the longitudinal losses connected with the collisions of the particles against the surface of the plasma are $(mc^2/\kappa T_e)$ times greater (at not too small angles θ) than the transverse losses in the case of specular reflection of electrons from the surface.

It must be noted that the indicated longitudinal losses are equal in order of magnitude to the transverse losses in the case of diffuse reflection of the electrons from the plasma boundary.[2] To clarify the role of such losses, we must compare expression (38) with the imaginary parts of formulas (29) and (32) under conditions when the plasma is not transparent, $\epsilon'(\omega) - \alpha^l\sin^2\theta < 0$. If $\omega_0^2 - \omega^2 \sim \omega_0^2$ in this case, then the losses connected with collisions between particles will be negligibly small if the inequality

$$25N_eL^2 \ll T_e^4\sin^4\theta \quad (42)$$

is satisfied, where T_e is in degrees Kelvin, N_e is the number of electrons per cubic centimeter, and L is the Coulomb logarithm. We note that this is similar to the analogous inequality obtained for the case of diffuse reflection of electrons.[2]

Under these conditions we obtain the following expression for the absorbing ability

*The expression for ε_+^l for the case of Boltzmann electron distribution is given in the cited book[1] (see also the Appendix).

$$A^{(p)} \cong \left\{4\sqrt{\frac{2}{\pi}}\,1.7\cos\theta\sin^2\theta\left(\frac{\varkappa T_e}{mc^2}\right)^{1/2}\varepsilon'^2 + \cos\theta\,\frac{\nu}{\omega}\,2\,\frac{\omega_{Le}^2}{\omega^2}\,\frac{2\sin^2\theta-\varepsilon'}{\sqrt{\sin^2\theta-\varepsilon'}}\right\} \times (1-\varepsilon')^{-1}(\sin^2\theta-\varepsilon'\cos^2\theta)^{-1}.$$

Further, in the region where the plasma is opaque to the transverse waves [$\epsilon'(\omega) - \sin^2\theta < 0$] and transparent to the longitudinal waves [$\epsilon'(\omega) - \alpha^l \sin^2\theta > 0$], the imaginary part of (32) makes the following contribution to the numerator of (41), along with $\operatorname{Im}\lambda_p^t$ and $\operatorname{Im}\delta\lambda_p^l$, at not too small values of ϵ' ($|\epsilon'| \gg |\epsilon''|$):

$$\operatorname{Im}\lambda_p^l = \frac{c}{\omega}\frac{\sqrt{\alpha^l}}{\varepsilon'(\omega)}\frac{\sin^2\theta}{\sqrt{\varepsilon'(\omega)-\alpha^l\sin^2\theta}}. \qquad (43)$$

This contribution is not at all connected with the dissipation of electromagnetic waves, and is brought about by the excitation of longitudinal waves in the plasma when a transverse wave is obliquely incident from the vacuum on the surface of the plasma.

In either an ultrarelativistic or a nonrelativistic plasma, the energy converted into longitudinal waves is much greater than the energy lost to collisions between the plasma particles and the surface, provided $\epsilon'(\omega) \ll 1$. To the contrary, when $\epsilon'(\omega) \sim 1$, the corresponding energies become commensurate, and therefore the conditions under which the energy lost to excitation of longitudinal waves is greater than the energy lost by collision between particles will be determined by inequality (42) for the case of a nonrelativistic plasma.

In the case $\alpha^l < \epsilon'(\omega) \ll 1$, the corresponding condition has the form

$$25N_eL^2 \ll T_e^4\sin^2\theta\,(1-\omega_{Le}^2/\omega^2). \qquad (44)$$

The region is narrower here than in the case of (42), owing to the increase in the dissipative losses due to collisions of the particles inside the plasma. This increase is due to an increase in depth of penetration of the transverse field into the plasma with decreasing $\epsilon'(\omega)$, and this naturally increases the fraction of the energy lost by the field in the plasma. We note that formula (32), and consequently also formula (43), were obtained under the condition $|\epsilon'(\omega)| \ll 1$, and therefore we must in fact use formula (44).

Under conditions when the inequality (44) is applicable, we have for the absorbing ability of the plasma the following expression:

$$A^{(p)} = \frac{4\cos\theta\sin^2\theta\sqrt{\alpha^l\varepsilon'^3(\omega)}}{[\varepsilon'^{3/2}\cos\theta+\sqrt{\alpha^l}\sin^2\theta]^2+(-1+\sin^2\theta/\varepsilon')\varepsilon'^2}. \qquad (45)$$

If, in addition, $(\epsilon')^3 \gg \alpha^l$, then

$$A^{(p)} = 4\frac{\sqrt{\alpha^l\varepsilon'(\omega)}}{1-\varepsilon'(\omega)}\,\frac{\cos\theta\sin^2\theta}{\sin^2\theta-\varepsilon(\omega)\cos^2\theta}. \qquad (46)$$

Finally, in the case when the plasma is transparent also to the transverse waves, $\epsilon'(\omega) > (1+\alpha^t)\times\sin^2\theta$, the main fraction of the energy is transferred to the transverse wave in the plasma. The waves formed are absorbed in the plasma, and their energy is converted into heat. As is well known, the corresponding heat is determined by the imaginary part of the dielectric constant, which is brought about by collisions of plasma particles with each other; in the case of longitudinal waves it is also due to the possibility of Cerenkov radiation. For the heat released by absorption of the transverse waves per unit volume at a depth z, we obtain

$$\frac{Q^t}{V} = \frac{\omega}{8\pi}\left(\frac{\nu}{\omega}\frac{\omega_0^2}{\omega^2}\right)|1+r_p|^2\,|H_{xi}(0)|^2 \times \exp\left\{-\frac{z\nu}{c}\frac{\omega_0^2/\omega^2}{[\varepsilon'(\omega)-\sin^2\theta\,(1+\alpha^t)]^{1/2}}\right\}, \qquad (47)$$

where r_p is given by (25).

Analogously we obtain for longitudinal waves (when $k v_T/\omega \ll 1$)

$$\frac{Q^l}{V} = \frac{\omega}{8\pi}\varepsilon^{l\prime\prime}|1+r_p|^2\,|H_{xi}(0)|^2 \times \exp\left\{-\frac{z\omega}{c\sqrt{\alpha^l}}\frac{\varepsilon^{l\prime\prime}}{[\varepsilon'-\alpha^l\sin^2\theta]^{1/2}}\right\},$$

$$\varepsilon^{l\prime\prime} = \frac{\nu_{\text{eff}}\omega_{Le}^2}{\omega^3}+\sqrt{\frac{\pi}{2}}\frac{\omega\omega_{Le}^2}{k^3(\varkappa T_e/m)^{3/2}}\exp\left(-\frac{\omega^2 m}{2k^2\varkappa T_e}\right). \qquad (48)$$

When $1 \gg kr_D \gg 1/\sqrt{\ln \varkappa T_e/e^2N_e^{1/3}}$, the collisions can be neglected, i.e., under these conditions the main contribution is produced by Cerenkov absorption.

We note, finally, that in the opacity region the Cerenkov absorption mechanism makes no contribution to the dissipation.

APPENDIX

ASYMPTOTIC BEHAVIOR OF THE FIELD AT LARGE z

Let us examine briefly the question of the asymptotic value of the field at large distances from the plasma surface. We can say that the asymptotic expression of interest to us is determined by the singularities of the Fourier transforms of the field, which we have obtained above. The presence of poles, obviously, leads here to solutions that depend exponentially on the coordinates. In particular, in the opacity region the field decreases expo-

nentially, and in the transparency region we can speak of waves.

Under conditions when the spatial dispersion of the dielectric permittivity is small, we have for this wave part of the field

$$E_y^t(z) = -\left\{E_y'(0) - i\frac{\omega}{c}\sin\theta\, E_z(0)\right\}\frac{ic}{\omega c(\omega)} \times \left[\frac{\varepsilon(\omega) - \sin^2\theta\,(1+\alpha^t)}{1+\alpha^t}\right]^{-1/2} \times \exp\left\{iz\frac{\omega}{c}\left[\frac{\varepsilon(\omega) - \sin^2\theta\,(1+\alpha^t)}{1+\alpha^t}\right]^{1/2}\right\}, \quad (A.1)$$

$$E_y^l(z) = -\left\{E_y'(0) - i\frac{\omega}{c}\sin\theta E_z(0)\right\}\frac{ic}{\omega}\frac{\sin^2\theta\sqrt{\alpha^t}}{\varepsilon(\omega)[\varepsilon(\omega) - \alpha^t\sin^2\theta]^{1/2}} \times \exp\left\{iz\frac{\omega}{c\sqrt{\alpha^t}}\sqrt{\varepsilon(\omega) - \alpha^t\sin^2\theta}\right\}. \quad (A.2)$$

At frequencies greater than the plasma frequency, we obtain for an ultrarelativistic plasma the following contribution of the pole to the longitudinal field

$$E_y^l(z) = -\left\{E_y'(0) - i\frac{\omega}{c}\sin\theta E_z(0)\right\}\frac{ic}{\omega}\frac{8}{3}\frac{\omega^2}{\omega_{0p}^2} \times \frac{\sin^2\theta}{\cos\theta}\exp\left(-\frac{2\omega^2}{3\omega_{0p}^2} - 2\right)\exp\left\{iz\frac{\omega}{c}\cos\theta\right\}. \quad (A.3)$$

It is clear that the amplitude of the field decreases exponentially with increasing frequency.

We note that formulas (A.1) and (A.2) can be obtained from the differential equations of the field, which apply when the permittivities are given by formulas (9) and (30), and if in addition we use the boundary condition $E_z(0) = 0$.

The branch point of the permittivity causes the field to have a coordinate dependence that cannot be identified with a wave (see [2,5]). The corresponding contribution to the longitudinal and transverse fields has the following form

$$E_y^t(z) = \left\{E_y'(0) - i\frac{\omega}{c}\sin\theta E_z(0)\right\}\frac{2ic}{\pi\omega}(1 + i\nu/\omega) \times \int_1^\infty \frac{dx}{x}\left[x^2 - \sin^2\theta\left(\frac{\omega}{\omega + i\nu}\right)^2\right]^{-1/2} \times \exp\left\{iz\frac{\omega+i\nu}{c}\left[x^2 - \sin^2\theta\left(\frac{\omega}{\omega+i\nu}\right)^2\right]^{1/2}\right\} \times \operatorname{Im}\varepsilon_+^t\left(\omega, \frac{\omega+i\nu}{c}x\right)\left\{\left[\operatorname{Re}\varepsilon_+^t\left(\omega, \frac{\omega+i\nu}{c}x\right) - \left(1 + i\frac{\nu}{\omega}\right)^2x^2\right]^2 + \left[\operatorname{Im}\varepsilon_+^t\left(\omega, \frac{\omega+i\nu}{c}x\right)\right]^2\right\}^{-1}, \quad (A.4)$$

$$E_y^l(z) = \left\{E_y'(0) - i\frac{\omega}{c}\sin\theta E_z(0)\right\}\frac{2ic}{\pi\omega}\left(1 - i\frac{\nu}{\omega}\right) \times \int_1^\infty \frac{dx}{x}\left[x^2 - \sin^2\theta\left(\frac{\omega}{\omega+i\nu}\right)^2\right]^{-1/2} \times \exp\left\{iz\frac{\omega+i\nu}{c}\left[x^2 - \sin^2\theta\left(\frac{\omega}{\omega+i\nu}\right)^2\right]^{1/2}\right\} \times \operatorname{Im}\varepsilon_+^l\left(\omega, \frac{\omega+i\nu}{c}x\right)\Big/\left|\varepsilon_+^l\left(\omega, \frac{\omega+i\nu}{c}x\right)\right|^2; \quad (A.5)$$

$$\operatorname{Re}\varepsilon_+^l\left(\omega, \frac{\omega+i\nu}{c}x\right) = 1 - \frac{2\pi e^2N_ec^2}{\varkappa T_e\omega^2\left(1 + i\frac{\nu}{\omega}\right)}\left[K_2\left(\frac{mc^2}{\varkappa T_e}\right)\right]^{-1}\left(\int_{-\infty}^{-1} + \int_1^\infty\right)\frac{dx'}{x'^3} \times \mathrm{P}\frac{1}{x' - x}\left\{\frac{1}{1 - x'^{-2}} + 2\left(\frac{mc^2}{\varkappa T_e}\right)^{-1}\frac{1}{\sqrt{1 - x'^{-2}}} + 2\left(\frac{mc^2}{\varkappa T_e}\right)^{-2}\right\}\exp\left\{-\frac{mc^2}{\varkappa T_e}\frac{1}{\sqrt{1 - x'^{-2}}}\right\}, \quad (A.6)$$

$$\operatorname{Im}\varepsilon_+^l\left(\omega, \frac{\omega+i\nu}{c}x\right) = \frac{2\pi^2e^2N_ec^2}{\varkappa T_e\omega^2\left(1 + i\frac{\nu}{\omega}\right)}\left[K_2\left(\frac{mc^2}{\varkappa T_e}\right)\right]^{-1}\frac{1}{x'^3} \times \left\{\frac{1}{1 - x'^{-2}} + 2\left(\frac{mc^2}{\varkappa T_e}\right)^{-1}\frac{1}{\sqrt{1 - x'^{-2}}} + 2\left(\frac{mc^2}{\varkappa T_e}\right)^{-2}\right\}\exp\left\{-\frac{mc^2}{\varkappa T_e}\frac{1}{\sqrt{1 - x'^{-2}}}\right\}, \quad (A.7)$$

and $\operatorname{Re}\epsilon_+^t$ and $\operatorname{Im}\epsilon_+^t$ are defined in [2].

In general, the resultant expressions are complicated. In the ultrarelativistic limit we have for the transverse field the following contribution to the asymptotic expression corresponding to formula (A.4):

$$E_y^t(z) \approx -\left\{E_y'(0) - i\frac{\omega}{c}\sin\theta E_z(0)\right\}\frac{3}{2}\left[1 - \left(\frac{\omega}{\omega+i\nu}\right)^2\sin^2\theta\right] \times \frac{\omega_{0p}^2}{(\omega+i\nu)^2}\left(\frac{c}{\omega}\right)^3\left\{-2i\frac{\nu}{\omega} + \left(\frac{\nu}{\omega}\right)^2 - \frac{3}{2}\frac{\omega_{0p}^2}{\omega^2\left(1 + i\frac{\nu}{\omega}\right)}\right\}^{-2}\frac{1}{z^2} \times \exp\left\{i\frac{z}{c}\sqrt{(\omega+i\nu)^2 - \omega^2\sin^2\theta}\right\}. \quad (A.8)$$

In the case of a nonrelativistic plasma, the asymptotic behavior of the field can be determined by the saddle-point method, as was done by Landau[6] and Shafranov. [7] In this case the limits of the integrals in (A.4) and (A.5) are 0 and ∞, while the integrands are assumed to be independent of the angle of incidence θ, in view of the large value of the ratio $mc^2/\varkappa Te$. It should be noted however, that relativistic effects come into play when z is sufficiently large, and the asymptotic expression obtained in this manner does not apply. The corre-

sponding distances are determined from the conditions $z \gtrsim (mc^2/\kappa T_e)(c/\omega)$.

[1] A. A. Rukhadze and V. P. Silin, Elektromagnitnye svoistva plazmy i plazmopodobnykh sred (Electromagnetic Properties of Plasma and Plasma-like Media), Atomizdat, 1961).

[2] V. P. Silin, JETP **40**, 616 (1961). Soviet Phys. JETP **13**, 430 (1961),

[3] G. E. H. Reuter and E. H. Sondheimer, Proc. Roy. Soc. **A195**, 336 (1948).

[4] V. P. Silin, JETP **38**, (1960). Soviet Phys. JETP **11**, 1121 (1960).

[5] V. P. Silin, FMM (Physics of Metals and Metallography) **10**, 942 (1960).

[6] L. D. Landau, JETP **16**, 574 (1946).

[7] V. D. Shafranov, JETP **34**, 1475 (1958), Soviet Phys. JETP **7**, 1019 (1958).

Translated by J. G. Adashko
34

THE SHELL MODEL AND THE SHIFT OF SINGLE-PARTICLE LEVELS IN NUCLEI OF THE "CORE + NUCLEON" TYPE, DUE TO ADDITION OF A PAIR OF NUCLEONS

V. E. ASRIBEKOV

Submitted to JETP editor, January 11, 1961

J. Exptl. Theoret. Phys. (U.S.S.R.) 41, 171-182 (July, 1961)

The shift of single-particle levels in nuclei of the "core + nucleon" type, caused by the addition of a pair of particles (nucleons or holes) of the same type to the nucleus, is investigated within the framework of the shell model. The shifts are estimated quantitatively by perturbation-theory calculation of the change in level spacing due to unequal shifting of the levels when an additional pair is added to the nucleus. Two mechanisms of level shift are examined, one where the shift is due to a change in the core parameters (isotopic and isotonic shifts) and where the shift results from direct interaction between the pair and odd particle, the core remaining unperturbed (in this case the pair enters the nucleus as a system which is autonomous and independent of the core and in which the particles are paired with respect to the angular momentum $J = 0$). An estimate of the isotopic and isotonic shifts for a number of typical nuclei indicates that the first mechanism does not correspond to the experiments. On the other hand, a calculation of the relative level shifts based on the second mechanism, performed for a large number of nuclei of the "core + nucleon" type for which experimental level schemes are available, leads to results which are in good agreement with the experimental data. It is shown that there is a competition between the closely-spaced levels on which the pair is located.

INVESTIGATIONS (particularly quantitative) of nuclear configurations within the framework of the shell model entail considerable difficulties, because the nuclear levels are not identified to the same degree of unambiguity in all nuclei. The clearest picture of nuclear configurations is observed in odd nuclei of the "core + nucleon" type, in which both groups of nucleons (after subtracting the odd nucleon) fill closed shells or subshells and form an inert "core." Single-particle energy levels in these nuclei arise as real excited states of the odd nucleon, which is situated in a certain averaged field of the core. The sequence of levels in nuclei of the "core + nucleon" type is satisfactorily described by a Mayer scheme[1] intermediate between the energy schemes corresponding to idealized potentials (oscillator and well).

As shown by the presently known experimental data on nuclear level schemes,[2] the sequence of excited levels, established for odd nuclei of the "core + nucleon" type, can be regarded as valid also for other odd nuclei, which contain one or several added pairs of like nucleons in an even or odd group of like particles. On going to these nuclei, however, i.e., on adding, for example, one pair of nucleons to the initial "core + nucleon" nucleus, the levels of the latter are subjected to unequal shifts and the distances between the corresponding levels change (to the extent that certain level pairs cross).

A level shift of this kind can be attributed either to a change in the core parameters (depth or radius of the well) when a pair of like nucleons is added (isotopic and isotonic shifts), or to direct interaction (in the form of a perturbation) of a pair with the odd nucleon producing the levels; the core remains unperturbed and the pair forms a certain autonomous system in the nucleus, wherein the nucleons are paired with respect to the angular momentum ($J = 0$).

The purpose of the present article is to establish the character and the main cause of this shift of single-particle levels, and to derive quantitative estimates for the changes in level spacing in nuclei of the "core + nucleon" type when a pair of like nucleons (neutrons or protons) is added.* It is expected that the relative level shift in the two nuclei ("core + nucleon" and "core + nucleon + pair") will indeed be determined by the interaction between the nucleons of the additional pair with the core and the unpaired nucleon, and that a

*This analysis is also valid for nuclei of the "core + hole" type, and for the case when a pair of nucleons is removed (and not added), i.e., when a pair of "holes" is produced. This is implied throughout, and occasionally the single term "particle" will be used.

quantitative analysis of this effect is possible within the framework of the shell model through the use of perturbation theory (in spite of the fact that the shell model does not predict with satisfactory accuracy the level spacings themselves).

1. ISOTOPIC AND ISOTONIC SHIFTS

We examine the level shift of the unpaired nucleon in a "core + nucleon" nucleus, a shift due to the change in the average potential of the core when a pair of neutrons or a pair of protons is added to the nucleus.

Within the framework of the model, the average potential of the core, which characterizes the self-consistent field produced by the nucleons in the closed neutron and proton shells, can be regarded as independent (except for very light nuclei). Consequently, the total self-consistent field is made up of two independent self-consistent fields, the neutron and proton fields, and the average potential of the core can be expressed as a sum of two potentials with corresponding statistical weights, proportional to the number of neutrons and protons in the nucleus. If the unpaired nucleon is a neutron, the average potential of the core can be assumed to have the form[3]

$$V^{(n)} = \frac{N}{A} V_{nn} + \frac{Z}{A} V_{np} = \frac{N_0}{A} V_{nn} + \frac{Z_0}{A} V_{np} + \frac{N - N_0}{A} (V_{nn} - V_{np}), \quad (1)$$

where V_{nn} characterizes the interaction of the neutron with the neutron medium, V_{np} the interaction with the proton medium, and N_0 and Z_0 are the numbers of neutrons and protons corresponding to the stability of the nucleus A. Analogously, for the unpaired proton, the average potential of the core is assumed to be

$$V^{(p)} = \frac{Z}{A} V_{pp} + \frac{N}{A} V_{pn} = \frac{Z_0}{A} V_{pp} + \frac{N_0}{A} V_{pn} - \frac{N - N_0}{A} (V_{pp} - V_{pn}), \quad (2)$$

where V_{pp} and V_{pn} determine the interaction of the proton with the proton and neutron media.

For stable nuclei, the potentials (1) and (2) consist of only the first two terms, which characterize the potential of the stable core V_0. After subtracting the Coulomb interaction, V_0 is identical for the unpaired neutron and proton ($V_0^{(n)} \approx V_0^{(p)} \approx V_0$). On the other hand, in view of the charge independence of the nuclear forces, it is natural to assume $V_{pp} \approx V_{nn}$ and $V_{np} \approx V_{pn}$. As a result we obtain a two-parameter average core potential for the external unpaired neutron and proton*

$$V^{(n)}(Z, N) = V_0 + \frac{N - N_0}{A} V',$$

$$V^{(p)}(Z, N) = V_0 + \frac{Z - Z_0}{A} V' + V_{\text{Coul}}, \quad (3)$$

where

$$Z - Z_0 = -(N - N_0), \qquad V' \approx V_{nn} - V_{np} \approx V_{pp} - V_{pn}$$

and V_{Coul} is the Coulomb energy of the unpaired proton.

In the calculation of the relative shifts of the nuclear levels, potentials (3) were regarded as ordinary rectangular potential wells (without account of the smearing of the potential on the boundary) that depend on the neutron-proton distribution in the nucleus A(Z, N).

We chose for the potentials (3) the parameters $V_0 = 45$ Mev and $V' = -89$ Mev (the nuclear radius is $R = 1.4\,A^{1/3}$ Fermi units). This choice is not an essential limitation, since it can be shown that the results of the calculations vary very little with small changes in the parameters of the potentials in (3), and that any combination of parameters in this range can be used in practice.

The distance between the levels nlj (E_{nlj}) and $n'l'j'$ ($E_{n'l'j'}$) in the nucleus A(Z, N) is given by the following well-known expression:

$$\delta E_{n'l'j', nlj}(Z, N) = E_{n'l'j'}(Z, N) - E_{nlj}(Z, N) = 10.5 \cdot A^{-2/3} \{[x_{n'l'j'}(Z, N)]^2 - [x_{nlj}(Z, N)]^2\} \text{ Mev}; \quad (4)$$

where here x_{nlj} are the roots of the transcendental equation obtained from the condition that the logarithmic derivatives of the external and internal wave functions of the unpaired nucleon be equal on the boundary of the potential well (3). On going from nuclei A(Z, N) of the "core + particle" type to nuclei $A \pm 2$ ($Z, N \pm 2$) and $A \pm 2$ ($Z \pm 2, N$) (i.e., on "adding" or "removing" a pair of like nucleons), the energy levels of the unpaired particle E_{nlj} experience an unequal shift ΔE_{nlj}, as a result of which the distances between levels (4) change. Depending on the type of additional pair of nucleons, the relative level shifts due to the change in the core potential can be classified either as isotopic ($\Delta Z = 0$, $\Delta N = \pm 2$)

$$\Delta_{(\Delta N)}(\delta E_{n'l'j', nlj}) = \delta E_{n'l'j', nlj}(Z, N \pm 2) - \delta E_{n'l'j', nlj}(Z, N) \quad (5)$$

or isotonic ($\Delta N = 0$, $\Delta Z = \pm 2$)

*A potential of this kind, but with smeared edge (with account of the diffuse boundary of the nucleus) was investigated by Sliv and Volchok.[4]

$$\Delta_{(\Delta Z)}(\delta E_{n'l'j', nlj}) = \delta E_{n'l'j', nlj}(Z \pm 2, N) - \delta E_{n'l'j', nlj}(Z, N). \quad (5')$$

Equations (4), (5), and (5′) were used to calculate the change in distances between different levels for the transitions $A \rightarrow A \pm 2$ in a series of typical nuclei with known experimental level schemes. The results of the calculations, together with the experimental values of the change in distance between corresponding levels, are listed in Tables I and II.

As can be seen from these tables, the nuclei considered were those in which the numbers of neutrons N and protons Z corresponded to the filled shells (subshells) in the Mayer scheme. The numbers (+1) or (−1) in the columns marked N and Z indicate the type of odd nucleon (or hole) whose levels are shifted by a change in the potential of a core made up of a combination of nucleons (Z, N) from the closed shells (subshells). In many cases the problem is not single valued: the energy spectrum of the nucleus can be simultaneously regarded as pertaining either to a nucleon or to a hole, but with different core potentials. For example, for the nucleus with 39 protons, we can consider, along with the variant having an unpaired proton Z = 38 (+1), an alternate variant with an unpaired hole Z = 40 (−1) (the filled subshells for Z = 38 and Z = 40 are $1f_{5/2}$ and $2p_{1/2}$ respectively). The core potentials corresponding to these two cases will be different, owing to the dependence of the potential V(Z, N) on Z. Duplicate calculations were carried out for these nuclei (the results of these calculations were not listed in Tables I and II because they did not improve the agreement with experiment).

From a comparison of the theoretical change in level spacing with the experimental data in Tables I and II it follows quite obviously that the proposed mechanism, where the levels are shifted by a change in the core parameters (the isotopic and isotonic potential shifts), does not correspond to reality at all (the discrepancies are both in sign and in order of magnitude); this was expected from preliminary estimates of the effect. In any case, this mechanism could not be the only cause of level shift of an odd particle when a pair is added to a "core + particle" nucleus. Characteristically, the determined isotopic and isotonic relative level shifts are as a rule one order of magnitude smaller (in absolute value) than the corresponding experimental values; this demonstrates that the proposed level-shift mechanism is patently insufficient to explain the real level shifts.

2. PERTURBATION OF SINGLE-PARTICLE LEVELS BY A NUCLEON PAIR ADDED TO THE CORE

We shall assume that when two like nucleons (or holes) are added to a nucleus A of the "core + nucleon" (or "core + hole") type, the added

Table I. Isotopic shift ($\Delta Z = 0$, $\Delta N = \pm 2$)

Level difference $n'l'j' - nlj$	Z	N	Δ N	$\Delta(\delta E)_{theor}$, kev	$\Delta(\delta E)_{exp}$, kev
$1h_{11/2} - 2d_{3/2}$	58	78(+1)	+2	+51	+485
$1g_{9/2} - 2p_{1/2}$	50(−1)	64	+2	−6	+58
$1g_{9/2} - 2p_{1/2}$	50(−1)	66	+2	+1	+23
$1g_{9/2} - 2p_{1/2}$	38(+1)	50	−2	+103	−532
$1g_{9/2} - 2p_{1/2}$	38(+1)	50	+2	+31	−356
$1g_{9/2} - 2p_{1/2}$	50	40(+1)	+2	+76	−286
$1h_{11/2} - 3s_{1/2}$	50	66(+1)	+2	+72	−231
$1f_{5/2} - 2p_{3/2}$	38(−1)	50	−2	+18	−550
$2d_{3/2} - 3s_{1/2}$	50	66(+1)	+2	+4	−137
$2p_{3/2} - 1f_{7/2}$	20	20(+1)	+2	−346	−1359
$2p_{3/2} - 1f_{7/2}$	20(+1)	28	−2	−55	−2590

Table II. Isotonic shifts ($\Delta N = 0$, $\Delta Z = \pm 2$)

Level difference $n'l'j' - nlj$	N	Z	ΔZ	$\Delta(\delta E)_{theor}$, kev	$\Delta(\delta E)_{exp}$, kev
$1h_{11/2} - 2d_{3/2}$	82(−1)	58	−2	+ 9	− 79
$1h_{11/2} - 2d_{3/2}$	78(+1)	58	−2	− 10	+ 13
$1g_{9/2} - 2p_{1/2}$	50(−1)	38	−2	+ 12	+ 83
$1g_{9/2} - 2p_{1/2}$	50(−1)	38	+2	+ 10	− 200
$1g_{9/2} - 2p_{1/2}$	56	40(+1)	+2	− 33	+ 608
$1g_{9/2} - 2p_{1/2}$	50(−1)	40	+2	− 40	− 70
$1g_{9/2} - 2p_{1/2}$	50	38(+1)	+2	+150	−1017
$1g_{9/2} - 2p_{1/2}$	40(+1)	50	+2	− 46	+ 75

pair is not incorporated in the core, but enters autonomously into one of the shells outside the core, in a state "paired" with respect to the angular momentum ($J = 0$). This added pair interacts with the unpaired nucleon, perturbs the states of the latter, and thereby produces unequal shifts of the various single-particle excitation levels of the nucleus. The unequal shifts change the relative distances between the levels.

The relative shift of the single-particle levels nlj and $n'l'j'$, for two corresponding nuclear configurations A and $A \pm 2$, is determined by the expression

$$\Delta_{(\pm 2)}(\delta E^{(A)}_{n'l'j',\, nlj}) = \Delta_{(\pm 2)} E^{(A)}_{n'l'j'} - \Delta_{(\pm 2)} E^{(A)}_{nlj}, \qquad (6)$$

where $\Delta_{(\pm 2)}E^{(A)}_{nlj}$ and $\Delta_{(\pm 2)}E^{(A)}_{n'l'j'}$ are individual shifts of the levels nlj and $n'l'j'$, analogous to isotopic and isotonic shifts. These shifts, however, are no longer due to a change in the core potential upon "addition" of the pair, but to the direct interaction between the pair and the unpaired nucleon V_{1P}. The perturbing potential V_{1P} was chosen in the form of a δ-function two-particle potential with all types of interactions between nucleons (with exception of tensor forces)

$$V_{1P} = 4\pi \sum_{i=1}^{2} \delta(\rho - r_i)\{a(\tau\tau_i)(\sigma\sigma_i) + c + d(\sigma\sigma_i) + e(\tau\tau_i)\} \qquad (7)$$

Within the framework of the single-particle model, the individual level shift $\Delta_{(\pm 2)}E^{(A)}_{nlj}$ was considered, in accordance with perturbation theory, as a first-approximation correction to the eigenvalue of the energy of the unpaired particle in the nucleus, without account of the correlation interaction* between the particles within the pair occupying the level $n_0 l_0 j_0$:

$$\Delta_{(\pm 2)}E_{nlj;\, n_0 l_0 (j_0) J=0} = \langle V_{1P}\rangle = (\Psi_{nlj;\, n_0 l_0 (j_0) J=0} | \hat{V}_{1P} | \Psi_{nlj;\, n_0 l_0 (j_0) J=0}). \qquad (8)$$

We chose for the core potential the two idealized potentials of the shell model—a rectangular well and oscillator potential. In the analysis of the nucleon (or hole) distribution over the levels, however, we used the real level sequence, which is intermediate between the levels corresponding to the two idealized potentials. A characteristic feature of our calculations was that in the case of the rectangular well we used the core potential $V(Z, N)$ defined in (3) and dependent of the number of neutrons N and protons Z in the nucleus (not only on the atomic number A), with a well radius $R = 1.4\, A^{1/3}$ Fermi units. The oscillator potential considered was standard (with the usual dependence on A but not on N or Z), and consequently isotopic and isotonic effects of the core potential were not taken into account.

Substitution of the antisymmetrized wave function of the nucleus into (A) leads to the following final formula for the level shifts (for either the rectangular-well or for the oscillator potential):

$$\Delta_{(\pm 2)}E^{(A)}_{nlj;\, n_0 l_0 (j_0) J=0} = 2(2j+1)\{f + gB(l, l_0; j, j_0)\} D_{nl,\, n_0 l_0}, \qquad (9)$$

where

$$B(l, l_0; j, j_0) = \frac{2}{(2j+1)(2j_0+1)} \sum_L K(l, l_0, L) \frac{(l+L-l_0)!\,(l+l_0-L)!\,(L+l_0-l)!}{(l+l_0+L+1)!}$$
$$\times \left\{\left(\frac{l+l_0+L}{2}\right)! \Big/ \left(\frac{l+l_0+L}{2} - l\right)! \left(\frac{l+l_0+L}{2} - l_0\right)! \left(\frac{l+l_0+L}{2} - L\right)!\right\}^2,$$

$$K(l, l_0, L) = \begin{cases} (L+l_0-l+1)(L-l_0+l), & j = l - \frac{1}{2}, \quad j_0 = l_0 + \frac{1}{2} \\ (L+l_0+l+2)(-L+l_0+l+1), & j = l + \frac{1}{2}, \quad j_0 = l_0 + \frac{1}{2} \\ (L+l_0+l+1)(-L+l_0+l), & j = l - \frac{1}{2}, \quad j_0 = l_0 - \frac{1}{2} \\ (L+l_0-l)(L-l_0+l+1), & j = l + \frac{1}{2}, \quad j_0 = l_0 - \frac{1}{2} \end{cases}$$
$$|l - l_0| \leqslant L \leqslant l + l_0, \qquad l + l_0 + L - \text{even},$$

$$D_{nl,\, n_0 l_0} = \int |R_{nl}(\rho)|^2 |R_{n_0 l_0}(\rho)|^2 \rho^2 d\rho. \qquad (10)$$

The constants f and g (9) are combinations of the constants a, c, d, and e of the perturbing interaction potential (7), and depend on whether unlike particles [n(pp) or p(nn)] or like particles [n(nn) or p(pp)] enter into the interacting "particle–pair" system: in the case of a combination of unlike particles

$$f_u = c - d - e + a, \qquad g_u = d - a; \qquad (11)$$

and in the case of combination of like particles

*The correlation interaction could change the wave function of the nucleus, and this would lead to some new theoretical values of the relative level shifts. We assume this effect too small in the first approximation.

$$f_l = c - d + e - a, \quad g_l = d + a. \qquad (11')$$

The radial integrals D_{nl,n_0l_0} can be calculated only by numerical means. Calculations for an oscillator potential were made by Zeldes,[5] who tabulated all the main radial integrals. For a rectangular well, the tabulation of the integrals becomes impossible, in view of the fact that the integrals are not standard and in view of the explicit dependence on the well radius R and of the isotopic or isotonic properties of the potential V(Z, N), so that an individual calculation is necessary for each specific case.

An analysis was made of practically all nuclei A of the "core + particle" type, and of the corresponding nuclei A ± 2 of the "core + particle + pair" type, for which either the experimental level schemes (or at least one pair of corresponding levels with an established relative shift) were known. The core nuclei chosen had closed shells or subshells, the Mayer scheme serving as a criterion. The constants f and g were chosen from a comparison of the calculated relative level shifts with the experimental values, made simultaneously for all investigated typical nuclei. Nuclei in which the level shift is due to a combination of interacting unlike particles (the constants f_u, g_u) were distinguished from those with a combination of interacting like particles (the constants f_l, g_l).

The constants were chosen such as to obtain satisfactory relative level shift values for the greatest possible number of nuclei. For this purpose, the system of equations in the form $\alpha f + \beta g = \Delta(\delta E)_{exp}$, obtained for the entire group of investigated nuclei with the aid of formulas (6) and (9) for the ground levels (according to the Mayer scheme) and near-lying levels of the pair, was reduced to a system of equations in the form $\alpha' f/g + \beta' = 1/g$. This system was solved by using a wide range of trial values of f/g, in such a way that a constant (1/g) common to all nuclei was obtained from the left half of the corresponding equation for at least one level of each nucleus. We chose in this fashion the following values of the constants for the two basic potentials and for the two types of interacting "particle-pair" combinations:

$f_{u(well)} = +1$, $g_{u(well)} = -0.1$; $f_{u(osc)} = +0.317$, $g_{u(osc)} = -0.033$ and $f_{l(well)} = +0.5$, $g_{l(well)} = -2.5$; $f_{l(osc)} = +2.5$, $g_{l(osc)} = -1.25$,

With these constants the theoretical values of the relative nuclear-level shifts deviated least from the corresponding experimental values. The ratio of the constants f_u/g_u and f_l/g_l was compared with the results of certain energy calculations based on the shell model (in particular, with Flowers' results,[6] where the best values of these constants were determined from a theoretical analysis of the energy scheme of the O^{16} nucleus), and also with the corresponding analysis of experiments on np scattering at high energies. It turned out that when an odd neutron interacts with a pair of protons or an odd proton interacts with a pair of neutrons, the estimated ratio of the constants is $f_u/g_u \sim (+10)/(-1)$ for either the oscillator or the rectangular-well potential. This agrees both with Flowers' data and with the corresponding results of the analysis of np-scattering experiments. To the contrary, when an odd nucleon interacts with a pair of like particles [n(nn) or p(pp)], the ratio f_l/g_l for the oscillator potential differs from that for the rectangular well, namely

$$f_{l(osc)}/g_{l(osc)} \sim (+2)/(-1), \quad f_{l(well)}/g_{l(well)} \sim (+1)/(-5).$$

Whereas in the case of an oscillator potential the ratio of the constants (~ -2) coincides with the np-scattering data (but not with the data obtained by energy calculations based on the shell model), in the case of the rectangular well the ratio obtained for the constants ($-\frac{1}{5}$) has never been encountered before, and agrees neither with Flowers' shell calculations ($-\frac{4}{5}$) nor with the results of the analysis of the np-scattering experiments (-2).

The results of the calculations and their comparison with the experimental data are summarized in Tables III, IIIa (combinations of unlike particles) IV, and IVa (combinations of like particles).* All possible pairs of nuclear levels (of typical nuclei), for which a relative shift has been established experimentally, are considered. Omissions from the tables denote that the corresponding theoretical values greatly deviate from the experimental result; the relative shifts in parentheses are those for which calculations yield only qualitatively correct results. For the levels that the pair added to the nucleus can occupy, Tables IIIa and IVa indicate two or three alternative versions, the first of which (underlined) is the ground level (above the core) within the framework of the Mayer scheme. The latter is the result of the approach used in this investigation, wherein the data on the relative level shifts are distributed among Tables III, IV, IIIa, and IVa.

In each calculation of the relative level shifts of an odd particle, we assumed first that the pair

*$\bar{n}$ and $\bar{p}$ denote in the tables holes in neutron and proton shells respectively.

Table III. Relative shift of single-particle levels $\Delta(\delta E)$ (combinations of unlike interacting particles)

$_ZX_N^A \to {}_{Z'}X_{N'}^{A\pm 2}$	Level difference $n'l'j' - nlj$	$\Delta(\delta E)_{exp}$, kev	Combination of interacting particles	Level of pair $n_0 l_0 j_0$	$\Delta(\delta E)_{well}$, kev	$\Delta(\delta E)_{osc}$, kev
$_{41}Nb_{50}^{91} \to {}_{41}Nb_{52}^{93}$	$1g_{9/2} - 2p_{1/2}$	+ 75	$p\ (nn)$	$2d_{5/2}$	+ 77	(+90)
$_{49}In_{64}^{113} \to {}_{49}In_{66}^{115}$	$1g_{9/2} - 2p_{1/2}$	+ 58	$\bar{p}\ (nn)$	$3s_{1/2}$	+ 61	+60
$_{39}Y_{50}^{89} \to {}_{39}Y_{48}^{87}$	$1g_{9/2} - 2p_{1/2}$	−532	$\bar{p}\ (\bar{n}\bar{n})$	$1g_{9/2}$	−536	
$_{38}Sr_{49}^{87} \to {}_{40}Zr_{49}^{89}$	$1g_{9/2} - 2p_{1/2}$	−200	$\bar{n}(pp)$	$2p_{1/2}$	−182	
$_{28}Ni_{33}^{61} \to {}_{26}Fe_{33}^{59}$	$1f_{5/2} - 2p_{3/2}$	−261	$n\ (\bar{p}\bar{p})$	$1f_{7/2}$	−260	
$_{21}Sc_{28}^{49} \to {}_{21}Sc_{26}^{47}$	$1f_{5/2} - 2p_{3/2}$	−140	$p\ (\bar{n}\bar{n})$	$1f_{7/2}$	(−268)	−133

Table IIIa. Relative shift of single-particle levels $\Delta(\delta E)$ (combinations of unlike interacting particles). Competition of pair levels

$_ZX_N^A \to {}_{Z'}X_{N'}^{A\pm 2}$	Level difference $n'l'j'-nlj$	$\Delta(\delta E)_{exp}$, kev	Combination of interacting particles	Level of pair $n_0 l_0 j_0$	$\Delta(\delta E)_{well}$, kev	$\Delta(\delta E)_{osc}$, kev
$_{38}Sr_{49}^{87} \to {}_{36}Kr_{49}^{85}$	$1g_{9/2} - 2p_{1/2}$	+83	$\bar{n}(\bar{p}\bar{p})$	$1f_{5/2}$		
				$2p_{1/2}$	+78	(+92)
				$2p_{3/2}$		+82
$_{40}Zr_{49}^{89} \to {}_{42}Mo_{49}^{91}$	$1g_{9/2} - 2p_{1/2}$	−70	$\bar{n}(pp)$	$1g_{9/2}$ / $2p_{1/2}$	−69	(−94)
$_{39}Y_{50}^{89} \to {}_{39}Y_{52}^{91}$	$1g_{9/2} - 2p_{1/2}$	−356	$\bar{p}(nn)$	$2d_{5/2}$ / $1g_{7/2}$	−378	
$_{49}In_{66}^{115} \to {}_{49}In_{68}^{117}$	$1g_{9/2} - 2p_{1/2}$	+23	$\bar{p}(nn)$	$1h_{11/2}$ / $3s_{1/2}$	+21,5	(+60)
$_{58}Ce_{81}^{139} \to {}_{56}Ba_{81}^{137}$	$1h_{11/2} - 2d_{3/2}$	−79	$\bar{n}(\bar{p}\bar{p})$	$1g_{7/2}$ / $2d_{5/2}$	−79	
$_{58}Ce_{79}^{137} \to {}_{56}Ba_{79}^{135}$	$1h_{11/2} - 2d_{3/2}$	+13	$n(\bar{p}\bar{p})$	$1g_{7/2}$ / $3s_{1/2}$	+15	
$_{50}Sn_{65}^{115} \to {}_{48}Cd_{65}^{113}$	$1h_{11/2} - 3s_{1/2}$	−247	$\bar{n}(\bar{p}\bar{p})$	$1g_{9/2}$ / $2p_{1/2}$	−240	−241
$_{37}Rb_{50}^{87} \to {}_{37}Rb_{48}^{85}$	$1f_{5/2} - 2p_{3/2}$	−550	$\bar{p}(\bar{n}\bar{n})$	$1g_{9/2}$ / $2p_{1/2}$	−540	

Table IV. Relative shift of single-particle levels $\Delta(\delta E)$ (combinations of like interacting particles)

$_ZX_N^A \to {}_{Z'}X_{N'}^{A\pm 2}$	Level difference $n'l'j'-nlj$	$\Delta(\delta E)_{exp}$, kev	Combination of interacting particles	Level of pair $n_0 l_0 j_0$	$\Delta(\delta E)_{well}$, kev	$\Delta(\delta E)_{osc}$, kev
$_{38}Sr_{49}^{87} \to {}_{38}Sr_{47}^{85}$	$1g_{9/2} - 2p_{1/2}$	+155	$\bar{n}(n\bar{n})$	$1g_{9/2}$	+163	
$_{41}Nb_{50}^{91} \to {}_{43}Tc_{50}^{93}$	$1g_{9/2} - 2p_{1/2}$	−286	$p(pp)$	$1g_{9/2}$	−260	
$_{39}Y_{50}^{89} \to {}_{41}Nb_{50}^{91}$	$1g_{9/2} - 2p_{1/2}$	−1017	$\bar{p}(pp)$	$2p_{1/2}$	(−800)	−1089
$_{50}Sn_{67}^{117} \to {}_{50}Sn_{69}^{119}$	$1h_{11/2} - 2d_{3/2}$	−94	$n(nn)$	$1h_{11/2}$	−100	
$_{58}Ce_{79}^{137} \to {}_{58}Ce_{81}^{139}$	$1h_{11/2} - 2d_{3/2}$	+485	$n(nn)$	$2d_{3/2}$	+470	(+660)
$_{50}Sn_{67}^{117} \to {}_{50}Sn_{69}^{119}$	$1h_{11/2} - 3s_{1/2}$	−231	$n(nn)$	$1h_{11/2}$	−220	

Table IVa. Relative shift of single-particle levels $\Delta(\delta E)$ (combinations of like interacting particles). Competition of pair levels

$_ZX_N^A \rightarrow {}_{Z'}X_{N'}^{A+2}$	Level difference $n'l'j' - nlj$	$\Delta(\delta E)_{exp}$, kev	Combination of interacting particles	Level of pair $n_0 l_0 j_0$	$\Delta(\delta E)_{well}$, kev	$\Delta(\delta E)_{osc}$, kev
$_{41}Nb_{56}^{97} \rightarrow {}_{43}Tc_{56}^{99}$	$1g_{9/2} - 2p_{1/2}$	+608	$p\,(pp)$	$1g_{9/2}$ / $2p_{1/2}$	+608	+633
$_{50}Sn_{65}^{115} \rightarrow {}_{50}Sn_{67}^{117}$	$1h_{11/2} - 3s_{1/2}$	—192	$\bar{n}\,(nn)$	$3s_{1/2}$ / $1g_{7/2}$	—200	
$_{20}Ca_{21}^{41} \rightarrow {}_{20}Ca_{23}^{43}$	$2p_{3/2} - 1f_{7/2}$	—1359	$n\,(nn)$	$1f_{7/2}$ / $2p_{3/2}$	—1369	
				$1f_{5/2}$		—1313
$_{21}Sc_{28}^{49} \rightarrow {}_{23}V_{28}^{51}$	$2p_{3/2} - 1f_{7/2}$	—2142	$p\,(pp)$	$1f_{7/2}$ / $2p_{3/2}$	(—1000)	(—1273)
				$1f_{5/2}$		(—1562)
$_{21}Sc_{28}^{49} \rightarrow {}_{23}V_{28}^{51}$	$1f_{5/2} - 2p_{3/2}$	—1575	$p\,(pp)$	$1f_{7/2}$ / $2p_{3/2}$	(—1000)	(—1036)

added to the nucleus is located in the lowest level above the core (shell or subshell). The favorable cases where the theoretical shifts agreed with the corresponding experimental values are gathered in Tables III and IV. However, along with this ground level of the pair (according to the Mayer scheme), we considered simultaneously a group (3 or 4) of neighboring alternative occupation levels for the pair, and the relative level shifts were determined on the basis of the method developed above (simultaneous solution of a system of equations for all groups of nuclei), with allowance for all possible locations of the pair. Quantitative estimates have shown that when the relative shifts agree with the experimental values the pair is not always at the ground level (above the core) called for by the scheme employed.

In many cases, singled out in Tables IIIa and IVa, the theoretical and experimental values agree if the pair is at some level neighboring with the ground level. These neighboring levels, which the pair entering the nucleus can occupy instead of the ground level indicated by the Mayer scheme, will be called competing levels. It is characteristic that the competing levels encountered in all the foregoing cases are precisely those closest to each other in the Mayer scheme, which can, generally speaking, overlap when the pair is added to the nucleus, i.e., the sequence of two or three neighboring levels can change. This result is all the more worthy of attention, for along with the pair levels that undoubtedly compete with the ground levels, we considered also two or three (and in some cases even more) other levels, which were not close from the point of view of the Mayer scheme. In none of these nuclei, however, did the calculations indicate a possibility that the pair can occupy these levels.

By way of illustration let us describe several characteristic cases of level competition in several nuclei.

For the case of the indium isotopes $_{49}In_{66}^{115} \rightarrow {}_{49}In_{68}^{117}$ ($\Delta N = +2$, Table IIIa), the relative shift of the levels $1g_{9/2}$ and $2p_{1/2}$ is characterized, for different pair locations, by the following values (for a rectangular well):

Pair level	$\Delta(\delta E)_{theor}$, kev
$1\,h_{11/2}$	+262
$3\,s_{1/2}$	+21.5
$2\,d_{3/2}$	+104

$\Delta(\delta E)_{exp} = +23$ kev

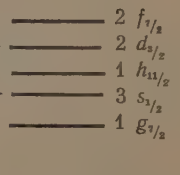

Of the three competing levels, satisfactory results are obtained not with the first level above the core, $1h_{11/2}$, but with the lower level $3s_{1/2}$, (according to the adopted shell scheme) in the direct vicinity of the ground level $1h_{11/2}$.

In the case of a transition from $_{41}Nb_{56}^{97}$ to $_{43}Tc_{56}^{99}$ ($\Delta Z = +2$, Table IVa), the relative shift of the same levels is (for a rectangular well):

Pair level	$\Delta(\delta E)_{theor}$, kev
$1\,g_{9/2}$	—162
$2\,p_{1/2}$	+608

$\Delta(\delta E)_{exp} = +608$ kev

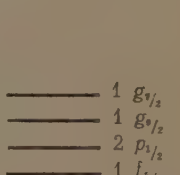

In this case, the competing near-lying levels are $1g_{9/2}$ (ground) and $2p_{1/2}$. Calculations of the relative level shifts, carried out for other possible occupations of non-competing remote levels by the pair, always lead, in the case of the investigated nuclei, to values that deviate from experiment. For example, in the case of the transition $_{41}Nb^{97}_{56} \rightarrow {}_{43}Tc^{99}_{56}$, the results are clearly unsatisfactory for all possible non-competing pair levels: $1f_{5/2}$, $1g_{7/2}$, $2d_{3/2}$, etc; the situation for the transition $_{49}In^{115}_{66} \rightarrow {}_{49}In^{117}_{68}$ is analogous.

In general, for each type of nucleon there exist, as it turned out, definite groups of closely-spaced levels. These compete, in particular, when the number of nucleons of the nucleus is changed. In our case considered the competition between levels manifests itself under level shifts caused by adding an additional pair to a nucleus of the "core + particle" type. On the basis of the analysis of Tables IIIa and IVa, we can single out the following groups of competing levels:

a) for deuterons

$$(1f_{7/2},\ 2p_{3/2},\ 1f_{5/2}),\ (2p_{1/2},\ 1g_{9/2}),\ (2d_{5/2},\ 1g_{7/2},\ 3s_{1/2});$$

b) for protons

$$(1f_{7/2},\ 2p_{3/2},\ 1f_{5/2}),\ (2p_{1/2},\ 1g_{9/2}),\ (1g_{7/2},\ 2d_{5/2}),\ (1h_{11/2},\ 2d_{3/2},\ 3s_{1/2}).$$

We note that in many cases the type of potential (well, oscillator) decides which of the competing levels will predominate when the pair is added to the nucleus (see next to the last line in Table IIIa and last three lines in Table IVa).

3. DISCUSSION OF RESULTS

The theoretical analysis of the relative shifts of single-particle levels in nuclei of the "core + particle" type, when a pair of like particles (nucleons or holes) is added to the nucleus, shows unequivocably that the level shift is due to direct interaction (regarded as a small perturbation) between the pair and the odd particle. As can be seen from Tables III and IV, this mechanism explains satisfactorily the relative level shifts in typical nuclei, if account is taken of the isotopic and isotonic properties of the nuclear potential. In the case of a rectangular well, the agreement with relative level shifts is found to be very good, with the exception of the series of light nuclei for which, as expected, better results are obtained with the oscillator potential (in spite of the neglect of its isotopic and isotonic properties). For the oscillator potential, the results of the calculations frequently disagree with the experiment, this being a natural consequence of neglecting the dependence of the potential on N and Z. The good tabulated results, obtained without account of the correlation interactions inside the pair, offer some evidence that the correlation effects may affect insignificantly the energy values under consideration.

As can be seen from the calculations of the relative level shifts of specific typical nuclei, the number of constants necessary for a satisfactory explanation of these shifts does not exceed the number of constants (f and g) involved in the theoretical formulas (particularly in the case of a rectangular potential well), i.e., the same constants f and g are valid for all the nuclei. The latter circumstance is, in the case of a rectangular potential well, the result of an account of the dependence of the nuclear radius and the depth of the well on the neutrons N and protons Z in the nucleus A(Z, N). As was noted by Nemirovskii,[3] the dependence of the radius of the nucleus and the depth of the well on N and Z can be reduced only to the dependence on N and Z established above [formula (3)] for the depth of the well of the core V(Z, N), with the nuclear radius having the usual form $R = 1.4 \times A^{1/3}$ Fermi units.

In the case of an oscillator potential, the choice of the constants f and g is less successful, but it is much better than that obtained by Zeldes,[5] who used from three to five parameters for each pair of levels, and who did not distinguish between the principal effects of interactions of the odd particle in the nucleus and the secondary effects (in particular, the effect of pair correlation). The result of the oscillator potential can be improved appreciably by taking into account the isotopic and isotonic properties of this potential, i.e., its dependence on N and Z. Critical remarks of this kind were advanced by Peierls (in connection with Zeldes' paper[7]), who noted that the excessive number of parameters used to explain the relative level shifts of even-odd nuclei is the result of failure to account for the dependence of radius of the nucleus (or, what is the same, of the depth of the well) on the number of neutrons and protons in the nucleus.

Peierls' remark does not apply to our work if a rectangular well is used. The choice of just a rectangular potential well as an exact potential dependent on N and Z is connected with the character of the available experimental data: most of the typical nuclei with known experimental schemes can be described by a rectangular well better than by an oscillator potential (the percentage of light nuclei is insignificant).

The competition between pair levels, established through the use of the approach employed here,

needs additional verification by other means, although the effect itself was already discussed in earlier papers on this problem.[5,7] The verification becomes particularly essential if the correlation interactions in the pair are taken into account, particularly their dependence on the position of the pair in the nucleus (as is well known, the pairing energy of nucleons is different at different levels).

In conclusion we note that, within the framework of the shell model, the addition to a "core + particle" nucleus of not one but two, three, or more pairs (all within a single shell) should, if pairing is taken into account, lead to relative level shifts $\Delta(\delta E)$ that vary linearly with the number of pairs "introduced" into the nucleus. This effect was theoretically indicated by Zeldes,[5] and noted in Shpinel's[8] analysis of the experimental level schemes. However, the linear dependence of $\Delta(\delta E)$ on ΔN or ΔZ holds only for a definite number (2 or 3) of supplementary pairs in a given shell, beyond which one cannot regard a new pair entering into the shell as being independent of the remaining pairs; consequently the linear dependence is violated and the correlation of the pair must be taken into account. Nonetheless, the linearity observed when at least the first two pairs are added is evidence that these pairs are autonomous in the nucleus, and thereby demonstrates the possible insignificance of correlation effects in the interacting "particle-pair" system.

I express my deep gratitude to K. A. Ter-Martirosyan for numerous discussions and continuous interest in the work, and also to N. I. Gaĭdukov for help with the numerical calculations.

[1] M. Goeppert-Mayer and J. H. D. Jensen, Elementary Theory of Nuclear Shell Structure, Wiley, New York, 1955.

[2] B. S. Dzhelepov and L. K. Peker, Skhemy raspada radioaktivnykh yader (Decay Schemes of Radioactive Nuclei), AN SSSR, 1958.

[3] P. É. Nemirovskii, JETP **36**, 889 (1959), Soviet Phys. JETP **9**, 627 (1959); Izv. AN SSSR, Ser. Fiz. **23**, 1503 (1959), Columbia Tech. Transl. p. 1486.

[4] L. A. Sliv and B. A. Volchok, JETP **36**, 539 (1959), Soviet Phys. JETP **9**, 374 (1959).

[5] N. Zeldes, Nucl. Phys. **2**, 1 (1956/57).

[6] B. H. Flowers, Proc. of Rehovoth Conference on Nuclear Structure, Amsterdam, 1958.

[7] N. Zeldes, Nucl. Phys. **7**, 27 (1958).

[8] V. S. Shpinel', Izv. AN SSSR, Ser. Fiz. **22**, 995 (1958), Columbia Technical Translation, p. 984.

Translated by J. G. Adashko
35

ROTATION OF THE PLANE OF POLARIZATION OF LIGHT IN THE CASE OF PARITY NONCONSERVATION

A. M. PERELOMOV

Submitted to JETP editor January 19, 1961

J. Exptl. Theoret. Phys. (U.S.S.R.) 41, 183-185 (July, 1961)

Interactions which do not conserve parity are included in a treatment of the rotation of the plane of polarization of light by a system. A concrete calculation is carried out for the hydrogen atom.

THE rotation of the plane of polarization of light by an optically active molecule, i.e., a molecule whose mirror image is not congruent with the original molecule, was first treated from the quantum-mechanical point of view by Rosenfeld[1] (cf. also [2] and [3]). It has been pointed out by Zel'dovich[4] that in the case of parity nonconservation the effect of rotation of the plane of polarization is possible in a substance which does not contain optically active molecules, and an estimate of the effect was given.*

Let us consider this question more fully. We introduce the following notations: $\mathbf{r}$, $\mathbf{p}$ are the coordinate and momentum of the electron, $\mathbf{l}$ and $\sigma/2$ are the orbital angular momentum and the spin, $\mathbf{m} = \mathbf{l} + \sigma$, $\mathbf{A}(\mathbf{r})$ is the vector potential of the light wave, $\mathbf{k}$ and ϵ are the wave vector and and the polarization, $|\mathbf{k}| = \omega/c = 1/\lambda$, ω and λ are the frequency and wavelength of the light, m_i and m_f are the projections of the angular momentum on the z axis before and after the collision, and c_i and c_f are the remaining quantum numbers characterizing the states of the atom before and after the collision.

If the wavelength of the light is much larger than the distance between atoms, the substance can be regarded as continuous and can be characterized by an index of refraction n. In the case of parity conservation the indices of refraction of right and left circularly polarized light are the same for a substance that does not contain optically active molecules. In the case of parity nonconservation, which can be caused, for example, by a direct four-fermion interaction between electron and proton (neutron), or by the existence of an anapole moment of these particles,[6,7] the even states of the atom (or molecule) will contain a small admixture of odd states, and the index of refraction n_+ for right circularly polarized light will not be equal to the index n_- for left circularly polarized light. When plane polarized light passes through the medium its plane of polarization is rotated in unit length through the angle

$$\varphi = (n_+ - n_-)/2\lambda. \tag{1}$$

The index of refraction can be expressed either in terms of the dipole moment $\mathbf{d}$ induced by the electromagnetic field of the light wave, or by the amplitude for scattering of light by the atom through the angle 0°. In [1-3] an expression for the dipole moment has been found,

$$\mathbf{d} = \alpha'\mathbf{E} - \frac{\beta'}{c}\frac{\partial \mathbf{H}}{\partial t} + \gamma'\mathbf{H},$$

which is not invariant under a change of the sign of the time, and becomes invariant only when the last term is absent, i.e., for $\gamma' = 0$. If we express the index of refraction in terms of the scattering amplitude, then as is well known n is connected with the forward-scattering amplitude a_0, averaged over all orientations of the atom (or molecule), in the following way:[8]

$$n^2 = 1 + 4\pi\lambda^2 a_0 N_0,$$

where N_0 is the number of atoms per unit volume. In a theory which is invariant under time reversal we have

$$a(c_f, m_f, \mathbf{k}', \varepsilon'; c_i, m_i, \mathbf{k}, \varepsilon) = a(c_i, -m_i, -\mathbf{k}, -\varepsilon; c_f, -m_f, -\mathbf{k}', -\varepsilon'). \tag{3}$$

Using the Hermitian character of the Hamiltonian, we find in the first nonvanishing approximation

$$a(c_f, m_f, \mathbf{k}', \varepsilon'; c_i, m_i, \mathbf{k}, \varepsilon)^* = a(c_i, m_i, \mathbf{k}, \varepsilon; c_f, m_f, \mathbf{k}', \varepsilon'). \tag{4}$$

In the general case the amplitude

$$a_0 = \frac{1}{2j_i + 1}\sum_{m_i} a(c_i, m_i, \mathbf{k}, \varepsilon'; c_i, m_i, \mathbf{k}, \varepsilon)$$

*There is also a similar estimate in a later paper by Baier and Khriplovich,[5] which deals with parity nonconservation in the interaction between electrons.

can be represented in the form

$$a_0 = \alpha(\varepsilon\varepsilon') + i\beta\frac{k}{|k|}[\varepsilon\varepsilon']. \qquad (5)^*$$

Using the Hermitian character of a_0, we find that α and β are real. We note that only the second term contributes to the rotation of the plane of polarization. The first term contributes to the polarizability of the atom (or molecule). Since $(\epsilon\cdot\epsilon')$ does not change sign under inversion and time reversal, and $\mathbf{k}\cdot[\epsilon\times\epsilon']$ changes sign under inversion but not under time reversal, it follows that the detection of a rotation of the plane of polarization will prove parity nonconservation and violation of charge-conjugation invariance, but can say nothing about conservation or nonconservation of the time parity.

In the nonrelativistic approximation the Hamiltonian of an atom (or molecule) including a part that does not conserve parity can contain terms of the type $\Sigma\mathbf{p}_i\mathbf{b}_i$, where $\mathbf{b}_i$ is an operator which contains no derivatives. These terms give an additional interaction with the electromagnetic field, $(e/c)\Sigma\mathbf{A}(\mathbf{r}_i)\mathbf{b}_i$, but it can be shown that this interaction does not contribute to the rotation of the plane of polarization.

In the dipole approximation we get

$$\alpha = \frac{2e^2\omega^2}{3c^2}\sum_n \frac{\mathbf{r}_{in}\mathbf{r}_{ni}(E_n - E_i)}{(E_i - E_n)^2 - (\hbar\omega)^2},$$

$$\beta = \frac{2e^2}{3\hbar c}\frac{(\hbar\omega)^3}{mc^2}\sum_n \frac{\mathrm{Im}\,\mathbf{r}_{in}\mathbf{m}_{ni}}{(E_i - E_n)^2 - (\hbar\omega)^2}. \qquad (6)$$

Let us consider the hydrogen atom. Suppose there exists an anapole moment of the electron, or else a weak four-fermion interaction between the electron and the proton. Then in nonrelativistic approximation, neglecting the spin of the proton in the latter case, we have

$$\mathcal{H}_0 = \frac{p^2}{2m} - \frac{e^2}{r} + \frac{f}{2m}[\sigma_e\mathbf{p}\,\delta(\mathbf{r}) + \delta(\mathbf{r})\,\sigma_e\mathbf{p}]. \qquad (7)$$

If it is the proton that has the anapole moment, we must replace σ_e by σ_p in this formula.

The only terms of importance for the calculation are the admixture of the $nP_{1/2}$ states in the ground $1S_{1/2}$ state and the admixture of the $1S_{1/2}$ state in the $nP_{1/2}$ state:

$$\psi_i = |1S_{1/2}\rangle + i\sum_n \delta_n |nP_{1/2}\rangle,$$

$$\psi_n = |nP_{1/2}\rangle + i\delta_n|1S_{1/2}\rangle + \ldots,$$

$$\delta_n = -i\frac{\langle 1S_{1/2}|V|nP_{1/2}\rangle}{E_n - E_1} = -\frac{2e^4m^2f}{\pi}\frac{1}{\sqrt{1-n^{-2}}}\frac{1}{n^{3/2}},$$

$$V = (f/2m)\,[\sigma_e\mathbf{p}\;\delta(\mathbf{r}) + \delta(\mathbf{r})\,\sigma_e\mathbf{p}]. \qquad (8)$$

After some simple calculations we get

$$\varphi \approx \frac{8\pi}{9}\frac{\rho}{n_0}\left(\frac{a}{\lambda}\right)^2\frac{1}{a}\sum_n \delta_n r_{n1}\frac{2(E_{nP_{3/2}} - E_{nP_{1/2}})(E_n - E_1)e^4a^{-2}}{[(E_n - E_1)^2 - (\hbar\omega)^2]^2},$$

$$r_{n1} = \frac{1}{a}\int R_{n1}(r)\,R_{10}(r)\,r^3dr, \quad \rho = N_0a^3, \quad f = bG, \qquad (9)$$

where $a = \hbar^2/me^2$ is the Bohr radius, $G = 10^{-5}M_n^{-2}$ is the weak-interaction constant, and $n_0 = (n_+ + n_-)/2$ is the mean index of refraction.

Substituting for r_{n1} the expression

$$r_{n1} = \frac{16n^4\sqrt{n}(n-1)^{n-3}}{(n+1)^{n+3}}\sqrt{1-\frac{1}{n^2}} \qquad (10)$$

(cf., e.g., [9]), we find

$$\varphi \approx 2\cdot 10^{-19}\frac{b\rho}{n_0}\frac{1}{a}\left(\frac{a}{\lambda}\right)^2\sum_n\left(\frac{2}{n}\right)^4\left(\frac{n-1}{n+1}\right)^n\left(1-\frac{1}{n^2}\right)^{-6}. \qquad (11)$$

For $b \approx \rho \approx n_0 \approx 1$, $(a/\lambda) \sim 10^{-3}$, we have $\varphi \approx 10^{-17}$ rad/cm.

Since this expression $\sim 1/Z$ for $\hbar\omega \ll E_n - E_1$, the rotation of the plane of polarization must be largest in hydrogen. It can be seen from Eq. (9) that if we do not take the fine structure into account we get zero rotation of the plane of polarization. This leads to a decrease of the rotation of the plane of polarization by a factor of 10^{-4} in comparison with the value that could be expected from general considerations. Neither inclusion of the electron spin nor inclusion of the proton spin changes this result. The rotation of the plane of polarization of light near resonance, and also the conversion of plane polarized light into elliptically polarized light (the Cotton-Mouton effect) can evidently not be observed on account of the strong absorption. A more exact formula for φ can be obtained by calculating with relativistic functions.

In conclusion I express my gratitude to Academician Ya. B. Zel'dovich for many discussions.

*$\varepsilon\varepsilon' = \varepsilon\cdot\varepsilon'$; $[\varepsilon\varepsilon'] = \varepsilon\times\varepsilon'$.

[1] L. Rosenfeld, Z. Physik **52**, 161 (1928).

[2] E. U. Condon, Revs. Modern Phys. **9**, 432 (1937).

[3] Kausman, Walter, and Eyring, Chem. Revs. **26**, 339 (1940).

[4] Ya. B. Zel'dovich, JETP **36**, 964 (1959), Soviet Phys. JETP **9**, 682 (1959).

[5] V. N. Baĭer and I. B. Khriplovich, JETP **39**, 1374 (1960), Soviet Phys. JETP **12**, 959 (1961).

[6] Ya. B. Zel'dovich, JETP **33**, 1531 (1957), Soviet Phys. JETP **6**, 1184 (1958).

[7] Ya. B. Zel'dovich and A. M. Perelomov, JETP **39**, 1115 (1960), Soviet Phys. JETP **12**, 777 (1961).

[8] M. Lax, Revs. Modern Phys. **23**, 287 (1951).

[9] H. Bethe and E. Salpeter, Quantum Mechanics of One- and Two-electron Systems, Academic Press, New York, 1957.

Translated by W. H. Furry
36

DIAMAGNETIC PERTURBATIONS IN MEDIA CAUSED BY IONIZING RADIATION

G. A. ASKAR'YAN

P. N. Lebedev Physics Institute, Academy of Sciences, U.S.S.R.

Submitted to JETP editor February 14, 1961

J. Exptl. Theoret. Phys. (U.S.S.R.) 41, 186-189 (July, 1961)

Diamagnetic perturbations in media produced by intense ionizing radiation are studied. It is shown that diamagnetism is produced predominantly by fast electrons. Estimates are given of the perturbation in the magnetic field and of the bursts of radio waves accompanying powerful bursts of ionization. It is noted that these effects can be utilized for remote dosimetry and for recording bursts of ionization, for the investigation of the behavior of fast electrons in a medium, for the transmission of force to a medium from an inhomogeneous magnetic field, etc.

REGIONS of media on a laboratory, terrestrial, or astronomical scale are often subjected to ionizing radiation. If an external magnetic field is applied to the medium, then whenever the density and energy of free electrons is sharply increased a diamagnetic moment will appear in a portion of the medium the variations in which will give rise to wavelike and quasistationary electromagnetic perturbations. Such processes can occur in the laboratory when a portion of a medium is irradiated by an intense flux of x rays or γ rays, and in the atmosphere or the ionosphere under the influence of sharp intense bursts of ionizing radiation, in the case of spark discharges in media etc.

1. ARTIFICIAL DIAMAGNETIZATION OF MEDIA

We investigate the diamagnetism of a medium due to the diffusion of free electrons produced by an ionizing agency. This diamagnetism is caused by the transverse drift of the diffusing electrons under the action of the Lorentz force due to the interaction between the external magnetic field and the diffusion velocity. We assume that at each instant of time we have a given electron spectrum $\eta_e(t, \epsilon, \mathbf{r})$, where ϵ is the kinetic energy of the electrons and $\mathbf{r}$ is the position vector of the volume element under consideration. The diamagnetic moment per unit volume of the medium (c.f., for example,[1]) is given by

$$M_1(r,t) = -\int_0^{\epsilon_m} \frac{\eta_e \varepsilon_\perp}{H} \frac{l_s^2}{l_s^2 + \rho_H^2} d\varepsilon,$$

where ρ_H is the radius of curvature of the electron trajectories, $\epsilon_\perp$ is the transverse (with respect to the magnetic field H) fraction of their kinetic energy, and $l_s(\epsilon)$ is the scattering mean free path of the electrons; within a wide range of electron energies $l_s(\epsilon) = C\epsilon^2/Z^2 d$ where d is the density and Z is the atomic number of the material of the medium.

It follows from the nature of the integrand that as the electron energy increases their diamagnetic activity also increases sharply. This enables us in a number of cases of practical interest to neglect the diamagnetic contribution of the slow electrons in spite of the fact that their density can exceed by many orders of magnitude the density of the high energy electrons responsible for the diamagnetism. In particular, in the case of air ionized by γ rays or by hard x rays the greatest diamagnetic effect is due to the energetic Compton electrons, while the secondary electrons produced by them make only a small contribution.

If in the integration we pick out the most effective electron groups of volume density n_e we can distinguish two characteristic cases: for $l_s^2(\epsilon_{eff}) \gg \rho_H^2$ (medium of low density, or a strong magnetic field, or high electron energies) we obtain $M_1 \approx n_e \epsilon_\perp / H$ ($\sim 1/H$); for $l_s^2(\epsilon_{eff}) \ll \rho_H^2$ (medium of high density, or a weak magnetic field, or low electron energies) we obtain $M_1 \approx n_e \epsilon_\perp l_s^2 / H\rho_H^2$ ($\sim H$). For example, in the nonultrarelativistic case $M_1 \approx n_e r_0 H l_s^2$, where r_0 is the classical electron radius.

The effect of artificial diamagnetization of media in a beam of x rays can be established under laboratory conditions. We assume that a volume of the medium, surrounded by a coil for recording the signal and by a metallic shell to screen it from induced effects, is traversed by an x-ray beam. The potential difference appearing between the ends of the coil as the intensity of the x-ray beam is varied is given by

$$\mathcal{E} \approx \frac{\nu}{c}\dot{\mu} H\pi a^2 = \frac{2\pi^2\nu}{c}\dot{n}_e l_s^2 r_0 H a^2 \text{ for } l_s^2 < \rho_H^2.$$

For example, for $\epsilon \approx 50$ kev in air $l_s = 10^{-4}\epsilon^2/P \sim 0.25$ cm for P = 1 atm; for an attainable (using a pulsed current in the tube of the order of several hundred milliamperes) density of such electrons $n_e \sim 10^4$ electrons cm^{-3} (the density $n_e = q_e\tau_e$ does not depend on the pressure, since the number of electrons produced per cm^3 per second is $q_e \sim P$, while their lifetime is $\tau_e = 1/P$) and for $H \sim 10^3$ oe, number of turns $\nu \approx 10^3$ and turn radius $a \approx 10$ cm we obtain $\mathcal{E} \approx 10^{-8}/T$ v/sec $> 10^{-2}$ v if the time during which the intensity of the beam changes is $T < 10^{-6}$ sec. In the case of powerful ionization bursts in the atmosphere[2] changes in local magnetic susceptibility are possible down to values close to the value of the magnetic susceptibility for an ideal diamagnetic substance $\mu = 0$.

2. EMISSION OF RADIO WAVES DUE TO IONIZATION BURSTS IN A MEDIUM SITUATED IN A MAGNETIC FIELD

In those cases when diamagnetic perturbations due to radiation bursts occur sufficiently suddenly they must be accompanied by bursts of radio waves. These bursts can be utilized for remote dosimetry or for recording bursts of ionization in a medium subjected to an external magnetic field. The changes in the total magnetic moment due to the total instantaneous number N_e of high-energy electrons

$$M(t) = \int_V M_1(t)dV = N_e(t)\frac{\varepsilon}{H}\cdot\frac{l_s^2}{l_s^2 + \rho_H^2},$$

will determine the intensity and the spectral distribution of the magnetic dipole radiation for wavelengths exceeding the dimensions of the region subjected to ionization. The intensity of the radiation is given by

$$W_\omega d\omega = (8\pi/3c^3)\,|\ddot{M}_\omega|^2 d\omega,$$

where

$$\ddot{M}_\omega = -i\omega\dot{M}_\omega \text{ for } \dot{M}(\pm\infty) = 0$$

or

$$\ddot{M}_\omega = -\omega^2 M_\omega \text{ for } M(\pm\infty) = 0.$$

For example, in the case of a sudden appearance or disappearance of a magnetic moment M_0 during a time T (the condition for sudden change is $\omega T \ll 1$) we obtain

$$W_\omega d\omega = (2\omega^2/3\pi c^3)\, M_0^2 d\omega.$$

The integrated rate of radiation of energy is given by

$$dW/dt \approx \ddot{M}^2/c^3 \approx M_0^2/c^3T^4.$$

Let us make an estimate of the electromagnetic radiation accompanying a powerful burst of γ radiation[2] which produces relativistic Compton electrons in a volume of dimensions of the order of the mean free path for the quanta (in air the mean free path for absorption is $L_\gamma \approx 3\times10^4 P^{-1}$ cm). The scattering mean free path for electrons in air is $l_s = 10^{-4}\epsilon_{kev}^2/P$, therefore $l_s \approx 10^2$ cm $\ll \rho_H \approx 10^4$ cm for $\epsilon \approx 1$ Mev and for the earth's magnetic field $H \approx 0.3$ oe. The instantaneous total number of Compton electrons in a volume of dimensions of the order of the mean free path for the γ quanta is $N_e \approx N_\gamma\tau_e/T$, where τ_e is the electron lifetime before they lose their energy; $\tau_e \approx 10^{-7}P_{atm}^{-1}$ sec. For $T \sim 3$ μsec the intensity of the burst $dW/dt \approx (N_\gamma 10^{-20})^2$ kw, where N_γ is the total number of γ quanta emitted in the burst.

In order to obtain more definite information with respect to the spectrum of the radiation it is necessary to know the specific form of the function M(t). From the equation for the balance of the number of Compton electrons

$$\dot{N}_e + N_e/\tau_e = \dot{N}_\gamma(t),$$

we obtain on setting $\dot{N}_\gamma(t) = N_{\gamma_0}\exp(-t/T)$

$$N_e \approx \frac{\dot{N}_{\gamma_0}}{1 - 1/T\tau_e}\{e^{-t/T} - e^{-t/\tau_e}\},$$

and consequently

$$M_\omega \approx r_0 l_s^2 H (N_e)_\omega \approx \frac{1}{2\pi} r_0 l_s^2 H\dot{N}_{\gamma_0}\frac{1}{(i\omega - 1/\tau_e)(i\omega - 1/T)},$$

$$W_\omega = \frac{8}{3}\frac{\pi}{c^3}\omega^4 |M_\omega|^2$$

$$\approx \frac{2}{3\pi c^3}\{r_0 l_s^2 H\dot{N}_{\gamma_0}\}^2\frac{1}{1 - (\omega\tau_e)^{-2}}\frac{1}{1 + (\omega T)^{-2}}.$$

We now discuss another case of a burst of diamagnetism which arises when a cluster of accelerated electrons falls on the boundary of a dense medium in the presence of a longitudinal magnetic field. In this case the diamagnetism is associated with the appearance of transverse components of the velocities as a result of Coulomb scattering. For example, if the total number of electrons in the bunch is $N_e \sim 10^{10}$, their energy is given by $\epsilon \approx 1$ Mev, the density of the medium is $d \sim 1$ g/cm^3 ($l_s \approx 0.1$ cm) and the intensity of the field is $H \approx 10^4$ oe ($\rho_H \approx 0.1$ cm $\approx l_s$), we obtain $M_0 \sim 1$ cm^3 oe. The loss of electrons in this case is unimportant since the time during which the electrons lose their energy $\tau_e \sim \epsilon/\epsilon_x' c \sim 3\times10^{-11}$ sec, i.e., it is comparable with the duration of the incidence of the bunch $T \sim a/c \sim 3\times10^{-11}$ sec if the dimensions of the bunch are $a \sim 1$ cm. The total rate of radiation of energy is given by dW/dt

$\approx M_0^2/c^3T^4 \sim M_0^2/a^3T \sim 3$ kw. The ratio of the energy of this radiation to the energy of the bremsstrahlung (or transition radiation) in the portion of the spectrum determined by $\omega T \lesssim 1$ is given by

$$W_{\omega\text{diam}}/W_{\omega\text{brems}} \approx (\varepsilon\omega T)^2/(eHa)^2 \sim 3 \cdot 10^{-2}$$

for the numerical values given above. By reducing the density of the medium and the intensity of the field it is possible to increase the intensity of the burst of radiation due to the diamagnetism. In its nature and in its polarization this magnetic dipole radiation differs from the electric dipole field of the bremsstrahlung or transition radiation from the bunch, and this will facilitate discrimination between bursts of radiation. In some cases it is necessary to take into account the effect on the radiation of the motion of the localized diamagnetization produced. Such effects can occur, in particular, in cosmic ray showers in which the zone of high energy electrons and of high ionization density moves with high velocities.

We note that pulsed diamagnetic perturbations should also be expected from spark discharges in a longitudinal magnetic field. These perturbations must be more rapid and must produce more radiation than perturbations associated with the gas kinetic spreading of the plasma produced by a spark in a magnetic field. (This question is discussed in greater detail in [3].)

3. FORCES EXERTED BY INHOMOGENEOUS MAGNETIC FIELDS

The production of diamagnetism in a portion of a medium by a concentrated ionizing agency can give rise to forces being exerted on such media by inhomogeneous magnetic fields. For example, a dense medium situated in the radiation field of a reactor will experience a volume force

$$F_1 \approx M_1 \frac{\partial H}{\partial Z} = \dot{n}_\gamma \frac{\tau_e}{L_\gamma} \varepsilon \frac{l_s^2}{l_s^2 + \rho_H^2} \frac{1}{H} \frac{\partial H}{\partial Z},$$

tending to expel the medium from the magnetic field ($F_1 \sim 100$ dyne for $\dot{n}_\gamma \sim 10^{18}$ quanta/cm^2 sec, $l_s \sim \rho_H$ and $(1/H)(\partial H/\partial Z) \sim$ cm^{-1}). This effect can be increased by repeating it many times. For example, if in a constant corrugated axially symmetric field the ionizing radiation is increased on those sectors where the field gradient has the same direction, then the expelling effect will be additive. This effect can be utilized for the dosimetry of powerful radiation fluxes, and for the creation of circulation in media. In particular, one can attain high velocities of gas efflux from a constant inhomogeneous or modulated magnetic field by utilizing as a local ionizing agency powerful beams of radio waves, electron beams, etc.

In conclusion we note that the well-known effects restricting the diffusion of electrons and reducing the diamagnetism of an electron gas (for example, the effect of Coulomb fields and the transition to ambipolar diffusion, the reflection of electrons from the boundaries of the volume etc.; with respect to ambipolar diamagnetism cf. [1]) do not play any appreciable role in the majority of processes discussed by us. In these processes the carriers of diamagnetism—high-energy electrons—are continually being produced and are lost, and as a consequence of the dissipation of their energy a large number of slow secondary electrons are formed which hinder the formation of appreciable Coulomb fields capable of affecting the diffusion of energetic electrons. The countercurrent of these secondary electrons gives a small contribution to the diamagnetism due to the low mobility of slow electrons. Indeed, the ratio of the densities of azimuthal currents of slow and fast electrons $J_s/J_f \approx n_{es}u_sk_s(n_{ef}u_fk_f)^{-1} \approx k_s/k_f$, where k are the electron mobilities, and u are the directed radial velocities which are acted upon by the magnetic field and give rise to the appearance of azimuthal diamagnetic currents (in accordance with the condition for the equality of the densities of the countercurrents we have $n_su_s \approx n_fu_f$).

[1] H. Alfvén, Cosmical Electrodynamics, Oxford, 1950, Ch. 3.

[2] M. H. Johnson and B. A. Lipmann, Phys. Rev. 119, No. 3 (1960).

[3] G. A. Askar'yan, J. Tech. Phys. (U.S.S.R.) 31, 781 (1961), Soviet Phys.-Tech. Phys. 6, in press.

Translated by G. Volkoff
37

SPACE AND CHARGE PARITIES AND MANY-MESON ANNIHILATIONS OF THE PROTON-ANTIPROTON SYSTEM

M. I. SHIROKOV

Joint Institute for Nuclear Research

Submitted to JETP editor January 24, 1961

J. Exptl. Theoret. Phys. (U.S.S.R.) **41**, 190-196 (July, 1961)

Experiments on the three- and four-meson annihilations of polarized antiprotons in hydrogen are proposed for the purpose of determining the values of the spatial and charge parities of the proton-antiproton system.

1. A paper by Okonov and the writer[1] has stated the problem of checking whether the spatial and charge parities of the system $p\bar{p}$ are just what they should be for a Dirac particle and antiparticle. Experiments on the two-meson annihilation $p + \bar{p} \to \pi + \pi$ were proposed for this purpose. It is now established that the weight of this channel is very small[2] (evidently there is one two-meson annihilation for each 400 $p\bar{p}$ annihilations*).

In the present paper we show how one can establish the spatial and charge parity types of the $p\bar{p}$ system from experiments on the three- and four-meson annihilation channels, by using polarized antiprotons.[2] In this connection we also discuss a (non-Dirac) choice of the parities which absolutely forbids the two-meson annihilations. This is done because the existence of such annihilations cannot as yet be regarded as firmly established, because of experimental difficulties: it is necessary to exclude cases of annihilation $\bar{p} + p \to \pi^+ + \pi^-$ plus π^0 or a low-energy γ-ray quantum (such annihilations are not forbidden by this choice of parities). On the other hand, the absence of two-meson annihilations would not be conclusive evidence in favor of this choice of the parities (since other explanations are possible).

The proposed experiments also allow a check of a hypothesis of Okonov,[6] which explains the suppression of the two-meson channel by assuming that $p\bar{p}$ annihilation in the singlet state predominates.

*This fact is not in contradiction with the simplest statistical theories of multiple production, which give the correct mean multiplicity on condition that the interaction volume is taken to be ten Fermi volumes, i.e., about $10 \cdot (4\pi/3)(\hbar/m_\pi c)^3$.[3,4] Obviously the agreement is worse with statistical theories that take the interaction volume to be $(4\pi/3)(\hbar/m_\pi c)^3$. By including the $\pi\pi$ interaction and other considerations, these theories give the correct mean multiplicity, but one gets a two-meson channel of the order of several percent (cf., e. g.[5]).

2. As in [1], the various choices for the parities of the system $p\bar{p}$ are denoted by symbols $\{\pi_{p\bar{p}}, c_{p\bar{p}}\}$, where $\pi_{p\bar{p}}$ is the product of the intrinsic parities of p and $\bar{p}$ and $c_{p\bar{p}}$ is the factor $+1$ or -1 in the expression $\pm 1(-1)^{l+s}$ for the charge parity of the system $p\bar{p}$.

In the Appendix it is shown that for the choice $\{-1, -1\}$ (which forbids two-meson annihilation) the angular distribution $\sigma(\vartheta, \varphi, \vartheta')$ of the reaction $\bar{p} + p \to \pi^+ + \pi^- + \pi^0$ must go to zero at the points $\vartheta = \vartheta' = 90°$, $\varphi = 0$ or $180°$, whereas with the other choices $\sigma(90°, 0°, 90°)$ does not have to equal zero. ϑ' is the angle between the direction $\mathbf{p}_a$ of the incident beam and the total momentum $\mathbf{p}'$ of the π^+ and π^- mesons (in the c.m.s. of the reaction); ϑ is the angle between $\mathbf{p}'$ and the momentum $\mathbf{p}$ of the π^+ meson, referred to a Lorentz frame in which the total momentum of π^+ and π^- is zero; φ is the angle between the vectors $\mathbf{p}_a \times \mathbf{p}'$ and $\mathbf{p}' \times \mathbf{p}$. By $\sigma(\vartheta, \varphi, \vartheta')$ we mean the angular distribution integrated over the azimuthal angle of the vector $\mathbf{p}'$ (for this it makes no difference whether or not the p or the $\bar{p}$ is polarized).

If $\sigma(90°, 0°, 90°) = 0$, the integral of $\sigma(\vartheta, \varphi, \vartheta')$ over a neighborhood of the point $(90°, 0°, 90°)$ cannot exceed a certain fraction of the total cross section σ of the three-meson channel.

It can be shown that in this version of the theory the angular distribution $\sigma(\vartheta_-, \varphi_-; \vartheta_+, \varphi_+; \vartheta')$ of the reaction $\bar{p} + p \to \pi^- + \pi^- + \pi^+ + \pi^+$ (integrated over φ') must be zero for φ_-, φ_+ equal to 0 or $180°$ and $\vartheta_- = \vartheta_+$. Since this is true for arbitrary angles ϑ' and ϑ_- $(= \vartheta_+)$, the integral

$$\int_0^\pi d\cos\vartheta' \int_0^\pi d\cos\vartheta_- \sum_{\alpha,\beta=0,\pi} \sigma(\vartheta_-, \alpha; \vartheta_-, \beta; \vartheta') \qquad (1)$$

must also be zero. The definitions of the angles are as follows: ϑ' and φ' are the spherical angles of the sum $\mathbf{p}'$ of the momenta of the two π^- mesons

(in the c.m.s. of the reaction) relative to the set of axes $z_a y_a x_a$ (the z_a axis is parallel to the incident beam, and the y_a axis is, for example, along the polarization vector of p); ϑ_- and φ_- are the spherical angles of the momentum $\mathbf{p}_-$ of one of the π^- mesons (in a Lorentz frame in which the total momentum of the two π^- mesons is zero) relative to axes $z'y'x'$ (the z' axis is parallel to $\mathbf{p}'$ and the y' axis is parallel to $\mathbf{z}_a \times \mathbf{p}'$); ϑ_+ and φ_+ are measured in this same set of axes. The expression for $\mathbf{p}_-$ in terms of the momenta $\mathbf{p}_1^-$ and $\mathbf{p}_2^-$ of the two π^- mesons, measured in the c.m.s. of the reaction, is given in Eq. (A.2) of the Appendix.

3. We note that a study of the angular distribution of the annihilation π mesons makes possible a check as to whether the spatial, charge, and combined parities are conserved in the annihilation process. Namely, from invariance under spatial inversion I and the existence of definite parities of p, $\bar{p}$, and the π mesons it follows that $\sigma(\vartheta, \varphi, \vartheta') = \sigma(\vartheta, -\varphi, \vartheta')$ for three-meson annihilation and

$$\sigma(\vartheta_-, \varphi_-; \vartheta_+, \varphi_+; \vartheta') = \sigma(\vartheta_-, -\varphi_-; \vartheta_+, -\varphi_+; \vartheta') \qquad (2)$$

for four-meson annihilation (cf. [7]). From invariance under the charge conjugation C it follows that

$$\begin{aligned} &\sigma(\vartheta, \varphi, \vartheta') = \sigma(\pi - \vartheta, \varphi, \pi - \vartheta'), \\ &\sigma(\vartheta_-, \varphi_-; \vartheta_+, \varphi_+; \vartheta') = \sigma(\vartheta_+, -\varphi_+; \vartheta_-, -\varphi_-; \vartheta'). \end{aligned} \qquad (3)$$

Finally, from invariance under IC it follows that

$$\begin{aligned} &\sigma(\vartheta, \varphi, \vartheta') = \sigma(\pi - \vartheta, -\varphi, \pi - \vartheta'), \\ &\sigma(\vartheta_-, \varphi_-; \vartheta_+, \varphi_+; \vartheta') = \sigma(\vartheta_+, \varphi_+; \vartheta_-, \varphi_-; \vartheta'). \end{aligned} \qquad (4)$$

The angular distributions have these properties for any choice of the parities.

4. The availability of polarized antiprotons[2] allows us to propose the following simple experiment for the determination of the spatial parity of $\bar{p}p$. One needs to compare the signs of the quantities Δ_1 and Δ_2 (see Appendix), which are defined for the reaction $\bar{p} + p \to \pi^+ + \pi^- + \pi^0$ in the following way:

$$\Delta_1 = \int_0^{\pi/2} d\cos\vartheta' \int_0^{\pi} d\cos\vartheta \left[\int_{-\pi/2}^{\pi/2} d\varphi' H(\vartheta, \vartheta', \varphi') - \int_{\pi/2}^{3\pi/2} d\varphi' H(\vartheta, \vartheta', \varphi') \right],$$

$$\Delta_2 = \int_{\pi/2}^{\pi} d\cos\vartheta' \int_0^{\pi} d\cos\vartheta \left[\int_{-\pi/2}^{\pi/2} d\varphi' H(\vartheta, \vartheta', \varphi') - \int_{\pi/2}^{3\pi/2} d\varphi' H(\vartheta, \vartheta', \varphi') \right]. \qquad (5)$$

Here $H(\vartheta, \vartheta', \varphi') = F(\vartheta, 0°, \vartheta', \varphi') + F(\vartheta, 180°, \vartheta', \varphi')$, where $F(\vartheta, \varphi, \vartheta', \varphi')$ is the angular distribution of the reaction in the case of polarized $\bar{p}$ (or p). Thus one must select cases in which p lies in the plane formed by the vectors $\mathbf{p}_a$ and $\mathbf{p}'$ (i.e., $\varphi = 0$ or 180°), divide them into four classes, and compare the signs of the right-left asymmetry for backward emergence (in the c.m.s.) of the π^0 mesons (Δ_1) and for forward emergence (Δ_2). The amount of allowable spread of the angles φ around 0° and 180° depends on the absolute values of Δ_1 and Δ_2 and on the energy of the $\bar{p}$. It can be seen from Table I that the relative sign of Δ_1 and Δ_2 determines the choice of the spatial parity.

In the case of four-meson annihilation everything that has been stated holds for quantities Δ_1 and Δ_2 defined in the following way:

$$\Delta_1 = \int_0^{\pi} d\cos\vartheta_- \int_0^{\vartheta_-} d\cos\vartheta_+ \int_0^{\pi} d\cos\vartheta' \left[\int_{-\pi/2}^{\pi/2} d\varphi' H - \int_{\pi/2}^{3\pi/2} d\varphi' H \right],$$

$$\Delta_2 = \int_0^{\pi} d\cos\vartheta_- \int_{\vartheta_-}^{\pi} d\cos\vartheta_+ \int_0^{\pi} d\cos\vartheta' \left[\int_{-\pi/2}^{\pi/2} d\varphi' H - \int_{\pi/2}^{3\pi/2} d\varphi' H \right]. \qquad (6)$$

Here H means the sum $\sum_{\alpha,\beta=0,\pi} F(\vartheta_-, \alpha; \vartheta_+, \beta; \vartheta', \varphi')$ [cf. Eq. (1)]; it is understood that $\bar{p}$ (or p) is polarized.

We note that the observation of reliable cases of two-meson annihilation, together with equality of the signs of Δ_1 and Δ_2, would mean that the parities are those given by the Dirac theory.

Table I

Parity type	Relative sign of Δ_1 and Δ_2	(R+L)−(F+B)	I (ϑ, ϑ′)
{−1, +1} Dirac type	+		
{−1, −1}	+	Vanishes at points $\vartheta = \vartheta' = 90°$, $\varphi = 0°, 180°$	$I(90°, 90°) = 0$
{+1, +1}	−		
{+1, −1}	−		$I(90°, 90°) = 0$

5. More difficult experiments—with both the antiprotons and the target protons polarized—would make it possible to establish the choice of the charge parity. One can see whether the quantity

$$(R+L)-(F+B)=\int_{-\pi/4}^{\pi/4}d\varphi' G + \int_{3\pi/4}^{-3\pi/4}d\varphi' G - \int_{\pi/4}^{3\pi/4}d\varphi' G - \int_{-3\pi/4}^{-\pi/4}d\varphi' G, \quad (7)$$

(see Table I) is zero at the points $\vartheta = \vartheta' = 90°$, $\varphi = 0$ or $180°$; here $G(\vartheta, \varphi, \vartheta', \varphi')$ is the angular distribution of $\bar{p} + p \to \pi^+ + \pi^- + \pi^0$ in the case of antiprotons and protons polarized in the same direction perpendicular to the beam.

A distinguishing feature of the choice $c_{\bar{p}p} = -1$ is the vanishing at the point $\vartheta = \vartheta' = 90°$ of the quantity

$$I(\vartheta, \vartheta') = \int_0^{2\pi} d\varphi \left[\int_0^{2\pi} d\varphi' G(\vartheta, \varphi, \vartheta', \varphi') - \int_0^{2\pi} d\varphi' F(\vartheta, \varphi, \vartheta', \varphi')\right] \quad (8)$$

(see Table I). Instead of F one can use the angular distribution from unpolarized $\bar{p}$ and p.

6. For the Dirac choice of the parities it follows from the selection rules for the spatial and charge parities that two-meson annihilation can occur only through the triplet states of the system $\bar{p}p$ (cf. e.g., Table I in reference 1). Okonov[6] has suggested explaining the suppression of two-meson annihilation by the hypothesis that $\bar{p}p$ annihilation is possible only in the singlet state of this system. Then the angular distribution of the annihilation π mesons must not depend on the azimuth φ', even if the antiprotons are polarized. In particular, we must have $\Delta_1 = \Delta_2 = 0$ and $I(\vartheta, \vartheta') = 0$. On this hypothesis there cannot be any dependence of the angular distribution of the annihilation products on the polarization of $\bar{p}$ or p.

In conclusion I express my gratitude to Professor M. A. Markov, V. I. Ogievetskii, and É. O. Okonov for discussions.

APPENDIX

THREE-MESON ANNIHILATION

1. For the reaction $\bar{p} + p \to \pi^+ + \pi^- + \pi^0$ the selection rules for the spatial and charge parities are

$$-\pi_{\bar{p}p}(-1)^{l_a+l+l'} = +1, \qquad c_{\bar{p}p}(-1)^{l_a+s+l} = +1, \quad (A.1)$$

l_a is the orbital angular momentum of the system $\bar{p}p$, l is the orbital angular momentum of $\pi^+\pi^-$, l' is the orbital angular momentum of the system $(\pi^+\pi^-) - (\pi^0)$, and s is the total spin of $\bar{p}p$. From Eq. (A.1) we do not get any simple results (such as that annihilation from the s state is forbidden) of the sort we had in the case of two-meson annihilation, where such results make it possible to distinguish the parity types $\{\pi_{\bar{p}p}, c_{\bar{p}p}\}$ in terms of the energy dependence of the cross section. A determination of the parity type in general requires experiments with polarized $\bar{p}$ and p.

2. Let us get from Eq. (A.1) the resulting relations between the amplitudes $\langle \mathbf{pp'} | R | \mathbf{p}_a m_a m_b \rangle$ for transition from the initial state characterized by the presence of $\bar{p}$ and p with the relative momentum $\mathbf{p}_a$ and spin projections m_a and m_b on the direction of $\mathbf{p}_a$ to a final state with three π mesons in a state described by the momenta $\mathbf{p}$ and $\mathbf{p'}$. $\mathbf{p}$ is the momentum of the π^+ in a Lorentz frame in which the total momentum of π^+ and π^- is zero (the momentum of the π^- in this system is $-\mathbf{p}$). In the c.m.s. of the reaction this total momentum is $\mathbf{p'}$.[7,8] If $\mathbf{p}_1$, $\mathbf{p}_2$, and $\mathbf{p}_3$ denote the momenta of π^+, π^-, and π^0 in the c.m.s. of the reaction, then

$$\mathbf{p} = \mathbf{p}_1 + (\mathbf{p}_1 + \mathbf{p}_2)\left[\frac{(\mathbf{p}_1+\mathbf{p}_2, \mathbf{p}_1)}{(\mathbf{p}_1+\mathbf{p}_2)^2}\left(\frac{E_{12}}{\varkappa_{12}} - 1\right) - \frac{\sqrt{p_1^2+\varkappa^2}}{\varkappa_{12}}\right], \quad \mathbf{p'} = \mathbf{p}_1 + \mathbf{p}_2 = -\mathbf{p}_3, \quad (A.2)$$

where (cf. [7])

$$E_{12} = \sqrt{p_1^2+\varkappa^2} + \sqrt{p_2^2+\varkappa^2}, \quad \varkappa_{12} = \sqrt{E_{12}^2 - (\mathbf{p}_1+\mathbf{p}_2)^2}$$

($\varkappa$ is the mass of the $\pi^\pm$ meson, and the speed of light has been set equal to unity).

The following expression has been obtained in [7]:

$$\langle \mathbf{pp'} | R | \mathbf{p}_a m_a m_b \rangle \equiv R_{m_a, m_b}(\vartheta, \varphi, \vartheta', \varphi') = \sum_{l,s,m} (4\pi)^{-3/2}(2J+1)\sqrt{2l+1}\, D^{l}_{0,m}(-\pi, \vartheta, \pi-\varphi) \times D^{J}_{m, m_a+m_b}(-\pi, \vartheta', \pi-\varphi')\langle lm | R^J | m_a m_b\rangle, \quad (A.3)$$

$$\langle lm | R^J | m_a m_b\rangle = \sum_{l', l_a, s} \sqrt{\frac{2l'+1}{2J+1}} C^{Jm}_{lml'0}\langle ll' | R^J | s l_a\rangle \times \sqrt{\frac{2l_a+1}{2J+1}} C^{sm_a+m_b}_{1/2 m_a 1/2 m_b} C^{Jm_a+m_b}_{sm_a+m_b l_a 0}, \quad (A.4)$$

ϑ' and φ' are the spherical angles of $\mathbf{p'}$ relative to axes with the z_a axis parallel to $\mathbf{p}_a$; ϑ and φ are the spherical angles of $\mathbf{p}$ relative to axes z'y'x' (the z' axis is parallel to $\mathbf{p'}$, and the y' axis is parallel to $[\mathbf{p}_a \times \mathbf{p'}]$). Furthermore,

$$D^{l}_{m,n}(\Phi_2, \theta, \Phi_1) = e^{-im\Phi_2}\mathcal{P}^{l}_{mn}(\cos\theta)\, e^{-in\Phi_1},$$

where the function $\mathcal{P}^{l}_{mn}$ differs from the function

P^l_{mn} defined in [9] by the factor i^{n-m} and is equal to the function $d^l_{m,n}$ defined in [10].

In the right member of Eq. (A.4) let us insert under the summation sign a factor $c_{\bar{p}p}(-1)^{l_a+s+l}$, which is equal to +1 by Eq. (A.1); we then use a property of the Clebsch-Gordan coefficients:

$$C^{Jm_a+m_b}_{sm_a+m_b l_a 0} = (-1)^{J-s-l_a} C^{J,-m_a-m_b}_{s,-m_a-m_b,l_a 0},$$

$$C^{sm_a+m_b}_{1/2 m_a 1/2 m_b} = C^{s,-m_a-m_b}_{1/2,-m_b 1/2,-m_a}. \qquad (A.5)$$

We then can verify that the right member of Eq. (A.4) is the element $\langle lm \,|\, R^J \,|\, -m_b - m_a\rangle$ multiplied by $c_{\bar{p}p}(-1)^{l+J}$; that is,

$$\langle lm \,|\, R^J \,|\, m_a m_b\rangle = c_{\bar{p}p}(-1)^{l+J} \langle lm \,|\, R^J \,|\, -m_b - m_a\rangle. \qquad (A.6)$$

Substituting the right member of Eq. (A.6) for $\langle lm \,|\, R^J \,|\, m_a m_b\rangle$ in the right member of Eq. (A.3), and using the equation (for integer j)

$$D^j_{m,n}(-\pi,\ \theta,\ \pi - \Phi)$$
$$= (-1)^{j-m} D^j_{m,-n}(-\pi, \pi - \theta, \pi + \Phi)$$
$$= (-1)^{j-n} D^j_{-m,n}(-\pi, \pi - \theta, \pi - \Phi), \qquad (A.7)$$

we get the following consequence of invariance under the charge conjugation C:

$$R_{m_a, m_b}(\vartheta, \varphi, \vartheta', \varphi') = c_{\bar{p}p} R_{-m_b, -m_a}(\pi - \vartheta, \varphi; \pi - \vartheta', -\varphi'). \qquad (A.8)$$

Analogously, we can get (cf. [7] and [11]) the consequence of invariance under spatial inversion:

$$R_{m_a, m_b}(\vartheta, \varphi, \vartheta', \varphi')$$
$$= \pi_{\bar{p}p}(-1)^{m_a+m_b} R_{-m_a,-m_b}(\vartheta, -\varphi, \vartheta', -\varphi'). \qquad (A.9)$$

The dependence of $R_{m_a,m_b}(\vartheta, \varphi, \vartheta', \varphi')$ on φ' is known [see Eq. (A.3)]. Therefore we can remove a factor $\exp\{i(m_a + m_b)\varphi'\}$ from the equations (A.8) and (A.9). Hereafter we shall not write the argument φ'.

The relations (A.8) and (A.9) and some combinations of these relations are written out in Table II for the various parity types. The following notations have been used:

$$R_{-1/2,-1/2}(\vartheta, \varphi, \vartheta') = a, \quad R_{-1/2,+1/2} = b,$$
$$R_{+1/2,-1/2} = c, \quad R_{+1/2,+1/2} = d.$$

Then $R_{-1/2,-1/2}(\vartheta, -\varphi, \vartheta') = a'$, and similarly for b, c, and d;

$$R_{-1/2,-1/2}(\pi - \vartheta, \varphi, \pi - \vartheta')$$
$$= \tilde{a};\ R_{-1/2,-1/2}(\pi - \vartheta, -\varphi, \pi - \vartheta') = \tilde{a}'$$

and similarly for b, c, and d.

3. If the beam and the target are polarized in the direction y_a (perpendicular to p_a), the angular distribution of π^+, π^-, π^0 is of the form (cf., e.g., [11])

$$G(\vartheta, \varphi, \vartheta', \varphi') \sim W(\vartheta, \varphi, \vartheta') + \sqrt{2}\,\tilde{P}_y[-\operatorname{Im}\tilde{W}_- \cos\varphi' + \operatorname{Re}\tilde{W}_- \sin\varphi'] + \sqrt{2} P_y[-\operatorname{Im} W_- \cos\varphi' + \operatorname{Re} W_- \sin\varphi'] - \tilde{P}_y P_y[\operatorname{Re} W_{-,-} \cos 2\varphi' + \operatorname{Im} W_{-,-} \sin 2\varphi' + \operatorname{Re} W_{-,+}]. \qquad (A.10)$$

The values of the antiproton polarization $\tilde{P}_y$ and the target proton polarization P_y are defined in the usual way as the average values of the y component of the spin operator, $\sigma_y/2$. The coefficients W that appear in Eq. (A.10) can be expressed in terms of the transition amplitudes a, b, c, d:

$$W(\vartheta, \varphi, \vartheta') = \tfrac{1}{4}[|a|^2 + |b|^2 + |c|^2 + |d|^2],$$
$$\tilde{W}_- = (ac^* + bd^*)/2\sqrt{2}, \qquad W_- = (ab^* + cd^*)/2\sqrt{2},$$
$$W_{-,-} = ad^*/2, \qquad W_{-,+} = -bc^*/2. \qquad (A.11)$$

It can be seen from Table II that $b = +\tilde{b}$ or $b = -\tilde{b}$, depending on the parity type, i.e., b does not (or does) change sign when ϑ and ϑ' are replaced by $\pi - \vartheta$ and $\pi - \vartheta'$, respectively. We shall say that the function b is even (or odd) relative to the point $\vartheta = \vartheta' = 90°$ (for any φ). From Table II and Eq. (A.11) it follows that for $\pi_{\bar{p}p} = -1$ the coefficients $\tilde{W}_-$ and W_- for $\varphi = 0$ and 180° are even functions relative to the point $\vartheta = \vartheta' = 90°$, and for $\pi_{\bar{p}p} = +1$ they are odd functions. The functions $W_{-,-}$ and $W_{-,+}$ are even functions in all parity types; in some types they vanish at the points $\vartheta = \vartheta' = 90°$, $\varphi = 0$ and 180°, or on the line $\vartheta = \vartheta' = 90°$, φ arbitrary. It can also be seen that for the type $\{-1, -1\}$ all of the functions a, b, c, d, and consequently all of the W coefficients are zero at the points $\vartheta = \vartheta' = 90°$, $\varphi = 0$ or 180°. Along with these quantities the integral

Table II

Parity type	I	C	IC
{−1, +1} Dirac type	$a=d'$, $b=-c'$	$a=\tilde{d}$, $b=\tilde{b}$, $c=\tilde{c}$	$a=\tilde{a}'$, $d=\tilde{d}'$
{−1, −1}	$a=d'$, $b=-c'$	$a=-\tilde{d}$, $b=-\tilde{b}$, $c=-\tilde{c}$	$a=-\tilde{a}'$, $d=-\tilde{d}'$
{+1, +1}	$a=-d'$, $b=c'$	$a=\tilde{d}$, $b=\tilde{b}$, $c=\tilde{c}$	$a=-\tilde{a}'$, $d=-\tilde{d}'$
{+1, −1}	$a=-d'$, $b=c'$	$a=-\tilde{d}$, $b=-\tilde{b}$, $c=-\tilde{c}$	$a=\tilde{a}'$, $d=\tilde{d}'$

$$\int_0^{2\pi} d\varphi' G(\vartheta, \varphi, \vartheta', \varphi') \equiv \sigma(\vartheta, \varphi, \vartheta')$$

also vanishes at this point (see Article 2 of the main text).

In processing the experimental data one must obtain from Eq. (A.10) the coefficients of $\cos \varphi'$ and $\cos 2\varphi'$ and that of $\widetilde{P}_y P_y \operatorname{Re} W_{-,+}$. In some cases it is not necessary to study the behavior of these coefficients as functions of ϑ, φ, ϑ'; it is enough to consider certain integrals of the coefficients over these angles. The recipes given here for distinguishing between the parity types correspond precisely to the determination of the coefficients and the subsequent integration (if this is possible).

We note that for the determination of $\pi_{\bar{p}p}$ it would be sufficient in principle to use only the invariance under the inversion I. For such a procedure, however, it is necessary to know the signs of the polarizations of $\bar{p}$ and p (i.e., to know whether $\widetilde{P}_y$ and P_y are positive or negative) (cf. [12]).

Note added in proof (June 15, 1961). At the present time (June, 1961) it has been definitely established that there are two-meson $\bar{p}p$ annihilations [see G. R. Lynch et al., Bull. Am. Phys. Soc. II, 6, 40 (1961)]. Therefore agreement of the signs of Δ_1 and Δ_2 would mean that the parities are those of the Dirac theory.

A. Pais has called the writer's attention to the fact that he had previously [Phys. Rev. Letters 3, 242 (1959)] pointed out certain symmetries of the angular distribution of the products of $\bar{p}p$ annihilation which follow from conservation of the charge and combined parities. It can be shown that the first equations in the relations (3) and (4) of the present paper are equivalent to Pais's relations (5) and (6).

[1] M. I. Shirokov and É. O. Okonov, JETP **39**, 285 (1960), Soviet Phys. JETP **12**, 204 (1961).

[2] O. Chamberlain, Proc. 1960 Int. Conf. on High Energy Physics at Rochester, Univ. of Rochester, 1960, p. 653.

[3] E. Segré, Ann. Rev. Nucl. Sci. **8**, 127 (1958).

[4] B. R. Desai, Phys. Rev. **119**, 1390 (1960).

[5] E. Eberle, Nuovo cimento **8**, 610 (1958).

[6] É. O. Okonov, JETP **39**, 1059 (1960), Soviet Phys. JETP **12**, 738 (1961).

[7] M. I. Shirokov, JETP (in press).

[8] R. H. Dalitz, Phys. Rev. **94**, 1046 (1954).

[9] Gel'fand, Minlos, and Shapiro, Predstavleniya gruppy vrashchenii i gruppy Lorentsa (Representations of the Rotation Group and the Lorentz Group), Fizmatgiz, 1958, Part I, Sec. 7.

[10] M. Jacob and G. C. Wick, Ann. Phys. **7**, 404 (1959).

[11] M. I. Shirokov, JETP **36**, 1524 (1959), Soviet Phys. JETP **12**, 1081 (1961).

[12] S. M. Bilenky, Nuovo cimento **10**, 1049 (1958). R. H. Capps, Phys. Rev. **115**, 736 (1959).

Translated by W. H. Furry
38

DETERMINATION OF THE PION-NUCLEON INTERACTION CONSTANT FROM THE DIFFERENTIAL CROSS-SECTIONS OF ELASTIC pp-SCATTERING

Yu. M. KAZARINOV, V. S. KISELEV, I. N. SILIN, and S. N. SOKOLOV

Joint Institute for Nuclear Research

Submitted to JETP editor January 24, 1961

J. Exptl. Theoret. Phys. (U.S.S.R.) 41, 197-198 (July, 1961)

We have used the p-p scattering cross sections at 147, 330 and 380 Mev to determine the π-N interaction constant f^2. The results obtained from E_p equal to 137 and 380 Mev do not disagree with a value $f^2 = 0.08$. The cross sections for an energy of 330 Mev can not be made to agree satisfactorily with the value $f^2 = 0.08$.

AN analysis of the experimental data on neutron-proton scattering[1] has shown that, within the limits of experimental error, the differential cross section $\sigma_{np}(\vartheta)$ is apparently not in disagreement with a value of the renormalized pion-nucleon interaction constant $f^2 = 0.08$ in a wide energy range from 90 to 630 Mev. As a similar study of the data on proton-proton scattering may give interesting results, we studied $\sigma_{pp}(\vartheta)$ at energies of 147[2], 330[3], and 380[4] Mev by the same method as the one used in [1].

The Coulomb effects were taken into account by a method proposed by Stapp and co-workers.[5] To do this the $\bar{R}$ matrix is written in the form

$$\bar{R} = \bar{S} - 1 = \bar{S} - \bar{S}_c + \bar{S}_c - 1 = \bar{\alpha} + \bar{R}_c,$$

where $\bar{\alpha}$ is the matrix the elements of which can be expressed in terms of the total phase shifts δ_l and the phase shifts due purely to Coulomb scattering, Φ_l, and $\bar{R}_C$ is the R-matrix of the Coulomb scattering alone. The values of the δ_l are taken from [5] and [6].

The corrections to the Coulomb expression which we have obtained were evaluated from the differential cross sections. The errors introduced here were determined from the errors in the phase shifts, assuming these to be independent. This leads, apparently, to an increase in the error of determining the Coulomb effects as one can show that there exists the relation $\bar{\Delta}^2/\bar{\Delta}_C^2 = \bar{k}$ between the weighted mean squares of the error sources $\bar{\Delta}_C^2$ and $\bar{\Delta}^2$ found with and without taking correlations between parameters into account; $\bar{k} = (\Sigma k_i)/m$ is the average correlation factor[1] and m the number of parameters which is varied.

The nuclear part of the p-p scattering cross section was written in the form

$$\sigma_{pp}(\vartheta) = a_1 b^2\left[\frac{1}{(x_0 - x)^2} + \frac{1}{(x_0 + x)^2}\right] + a_2\left[\frac{1}{x_0 - x} + \frac{1}{x_0 + x}\right] + \sum_{n=0}^{n_{max}} A_n x^{2n}, \quad (1)$$

where we used the well-known analytical properties of the p-p scattering amplitude [in the same way as was done in [1] for $\sigma_{np}(\vartheta)$], and where $b = \mu^2/2k^2$, μ is the pion mass, k the momentum of the particle in the center of mass system, $x_0 = 1 + b$, $x = \cos\vartheta$, and a and A_n are undetermined coefficients.

We used the following facts to estimate n_{max} in (1). Using the Mandelstam representation and also the data in a paper by Cini and co-workers[7] one can show that the contribution to the polarization $P(\vartheta)\sigma_{pp}(\vartheta)$ from terms in the amplitude which are singular at $x = \pm x_0$ vanishes, when

$$P(\vartheta)\,\sigma_{pp}(\vartheta) = \sin\vartheta \sum_{n=0}^{n_{max}} c_n x^{2n-1},$$

where n_{max} is the same as the n_{max} in (1).* If one knows the angular dependence of the polarization one can thus establish at which orbital angular momenta the main contribution to the scattering cross section begins to give the pole term contained in the single-meson diagram.

The coefficients a_1 found for energies of 380 and 147 Mev give for f^2 values of 0.066 ± 0.014 and 0.07 ± 0.015 respectively for $v^2 = \chi^2/\overline{\chi^2} = 0.6$, 1.6 and $n_{max} = 1$ and 0. These values agree well with the results obtained from considering in [1] $\sigma_{np}(\vartheta)$ and do not contradict $f^2 = 0.08$. Increasing n_{max} by unity does not change a_1 appreciably in either case. The fast increase of the error with increasing n_{max} makes it, however, impossible to consider data for which n_{max} is larger.

*A similar relation exists also in the neutron-proton scattering case.

The coefficient a_1 obtained for $E_p = 330$ Mev turned out to be approximately one order of magnitude larger than for $E_p = 380$ and 147 Mev, and $f^2 = 0.19 \pm 0.01$ ($n_{max} = 2$). A change in the number of terms in the expression for $\sigma_{pp}(\vartheta)$ does also in this case not influence the magnitude of the first coefficient greatly. The criterion of agreement, $v^2 = \chi^2/\overline{\chi^2}$ remains constant and inadequate when we change n_{max} in (1) from 2 to 4 ($v^2 = 3$). An attempt to satisfy the experimental data with a fixed coefficient $a_1 = f^4 = 0.0064$ increases v^2 to 3.9 and also gives $A_{n_{max}} < 0$. This may all possibly indicate that there is an appreciable error in the experimental data on $\sigma_{pp}(\vartheta)$ at that energy. One should mention, however, that in a discussion of the results obtained with L. I. Lapidus it was noted that this fact may be connected also with the "near-threshold singularities."[8]

[1] Amaglobeli, Kazarinov, Sokolov, and Silin, JETP **39**, 948 (1960), Soviet Phys. JETP **12**, 657 (1961).

[2] Palmer, Cormack, Ramsey, and Wilson, Ann. Phys. **5**, 199 (1958).

[3] N. Hess, Revs. Modern Phys. **30**, 368 (C8, C13, F4) (1958).

[4] Holt, Kluyver, and Moore, Proc. Phys. Soc. (London) **71**, 781 (1958).

[5] Stapp, Ipsilantis, and Metropolis, Phys. Rev. **105**, 302 (1957).

[6] Gel'fand, Grashin, and Ivanova, Inst. Theor. Exptl. Phys. Acad. Sci. U.S.S.R., preprint.

[7] Cini, Fubini, and Stanghellini, Phys. Rev. **114**, 1633 (1959).

[8] L. I. Lapidus and Chou Kuang-Chao, JETP **39**, 112 (1960), Soviet Phys. JETP **12**, 82 (1961).

Translated by D. ter Haar
39

RADIATIVE CORRECTIONS TO BETA DECAY

B. V. GESHKENBEĬN and V. S. POPOV

Submitted to JETP editor January 27, 1961

J. Exptl. Theoret. Phys. (U.S.S.R.) 41, 199-204 (July, 1961)

The problem of radiative corrections to β decay is discussed. A method is indicated for introducing different form-factors for the proton and electron (for the interaction with the photon) without coming into conflict with gauge invariance. An estimate is made of the contribution from diagrams that correspond to the emission of a virtual photon directly from the four-fermion vertex, as renormalized by the strong interactions. This estimate shows that the contribution of these diagrams can decidedly change the size of the radiative correction to β decay and eliminate the discrepancy between the predictions of the theory with a conserved vector current and the experimental results.

1. In recent times there has been a number of papers [1-3] on the calculation of the radiative corrections to β decay and μ decay. This interest in the radiative corrections is due to the fact that if the radiative corrections have been calculated correctly and if the experiments on the lifetimes of the O^{14} nucleus and the μ meson are correct, then the hypothesis of the conservation of a vector current in β decay [4] is untrue. [5] The radiative corrections to μ decay have undoubtedly been calculated correctly, since μ mesons do not take part in the strong interactions, and the result is finite in any order of perturbation theory [6] and does not depend on a "cut-off."

For β decay the situation is different. It has been shown [2,3] that the correction to the lifetimes of the neutron and the O^{14} nucleus is logarithmically divergent in the region of large momenta of the virtual γ-ray quantum. To get finite results, which could be compared with experiment, one has made a "cut-off" in the vertex parts for the interaction of the photon with the proton and electron, using for both the same value of the momentum of the virtual photon, $\Lambda \sim M_p$. The electromagnetic form-factor of the proton is due to the strong interactions and actually cuts off at $\Lambda_p \sim M_p$, but the electron does not take part in the strong interactions, and its form-factor is cut off by the weak interactions at values $\Lambda_e \sim 50$—400 Bev. [7]

If, however, one simply introduces different cut-off limits for the electron and proton, the calculation is not gauge invariant. Since the neutron and proton that take part in the β decay can be replaced by an arbitrary number of virtual π mesons, it is possible for a γ-ray quantum to be emitted directly from the complete four-fermion vertex. These processes, which have not been considered in references 2 and 3, are represented by diagrams 1, 2, 3 (see figure). In the present paper we shall take into account the difference between the form-factors of the proton and electron, without destroying the gauge invariance, and shall estimate the contribution from diagrams 1, 2, and 3, which correspond to the emission of a γ-ray quantum from the four-fermion vertex.

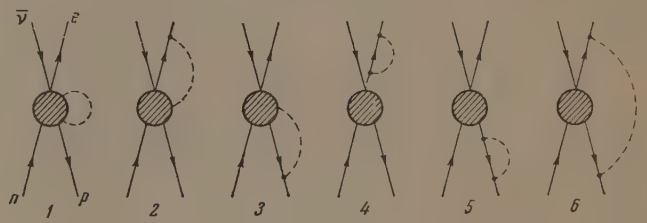

2. We shall prove the gauge invariance of the second-order radiative corrections to β decay. This means that if we take the propagation function of the photon with an arbitrary longitudinal part,

$$D_{\mu\nu}(k) = -ik^{-2}(\delta_{\mu\nu} + C(k^2)k^{-2}k_\mu k_\nu), \qquad (1)$$

the result will not depend on the arbitrary function $C(k^2)$. With effects of a possible renormalization on account of strong interactions included, the matrix element for β decay is of the form

$$2^{-1/2} G \sum_i (\bar{\psi}_p F^{(i)}(q) \psi_n)(\bar{\psi}_e O_i (1 + \gamma_5) \psi_\nu),$$

where $i = 1, \ldots, 5$ numbers the possible types of weak interaction, O_i are the usual local operators of β decay ($O_i = 1$, γ_μ, $\sigma_{\mu\nu}$, $i\gamma_5\gamma_\mu$, γ_5 for $i = 1, \ldots, 5$), and $F^{(i)}(q)$ is the most general form of the operator producing the change of a neutron to a proton in the i-th type of β-decay interaction (including effects of any number of virtual π mesons); $F^{(i)}$ depends only on the total momentum q transferred to the leptons. It is ob-

vious that $F^{(i)}(q)$ is represented by the sum of all diagrams with one vertex O_i for the emission of the lepton pair (e, ν) and any number of virtual π-meson and nucleon-antinucleon lines.

Let us consider one of these diagrams and denote it by $f^{(i)}(p_1, p_2, q)$, where p_1, p_2, q are the four-momenta of the neutron and proton and the total four-momentum of the leptons. Let $f_\lambda^{(i)}(p_1, p_2, q, k)$ be the matrix element for the emission of a photon with momentum k and polarization λ from the diagram $f^{(i)}(p_1, p_2, q)$ (the momentum p_1 of the incoming neutron is fixed). The matrix element $f^{(i)}(p_1, p_2, q, k)$ is represented by the sum of the diagrams corresponding to the emission of the photon (k, λ) from each charged line of the original diagram $f^{(i)}(p_1, p_2, q)$.

In electrodynamics the well known generalized Ward's theorem

$$k_\mu \Gamma_\mu(p, p-k, k) = e\{G^{-1}(p-k) - G^{-1}(p)\} \quad (2)$$

is valid both for fermions and also for bosons.[8] Applying it to the calculation of the quantity $k_\lambda f_\lambda^{(i)}(p_1, p_2, q, k)$, we find the only charged line that contributes is that ending in the proton, and the contributions from the closed charged loops add to zero. The result is that

$$k_\lambda f_\lambda^{(i)}(p_1, p_2, q, k) = e\{f^{(i)}(p_1, p_2, q) - f^{(i)}(p_1, p_2 - k, q + k)\}.$$

Summing this equation over all diagrams, we get

$$k_\lambda F_\lambda^{(i)}(p_1, p_2, q, k) = e\{F^{(i)}(p_1, p_2, q) - F^{(i)}(p_1, p_2 - k, q + k)\}. \quad (3)$$

In all there are six diagrams for the radiative corrections (see figure). (Diagrams with emission of the γ-ray quantum by the neutron are always gauge invariant when summed, since the charge of the neutron is zero.) Let us find the contribution to these diagrams from the longitudinal part of $D_{\mu\nu}(k)$ (we denote it by $\delta F^{(i)}$). Let us consider diagram 1. It is obtained from the original diagram $F^{(i)}(p_1, p_2, q)$ by the successive emission of two photons with momenta k and $-k$; according to Eq. (3), we have the following equation for the emission of photons with arbitrary momenta k and k' from $F^{(i)}(p_1, p_2, q)$:

$$k_\lambda k'_\mu F_{\lambda\mu}(p_1, p_2 - k - k', q; k, k') = e\{k'_\mu F_\mu(p_1, p_2 - k', q; k') - k'_\mu F_\mu(p_1, p_2 - k - k', q + k; k')\} = e^2\{F(p_1, p_2, q) + F(p_1, p_2 - k - k', q + k + k') - F(p_1, p_2 - k, q + k) - F(p_1, p_2 - k', q + k')\}.$$

Setting $k' = -k$, we get

$$k_\lambda k_\mu F_{\lambda\mu}^{(i)}(p_1, p_2, q; k, -k) = e^2\{F^{(i)}(p_1, p_2 - k, q + k) + F^{(i)}(p_1, p_2 + k, q - k) - 2F^{(i)}(p_1, p_2, q)\}. \quad (4)$$

In our treatment each individual diagram with a virtual photon connecting two lines is counted twice, since we have summed independently over the possible points of emission of the first and second photons; therefore the result must be divided by 2.* We get as the result

$$\delta F_1^{(i)} = -\frac{e^2}{(2\pi)^4 i}\int d^4k \frac{C(k^2)}{k^4}[F^{(i)}(p_1, p_2, q) - F^{(i)}(p_1, p_2 - k, q + k)] \quad (4a)$$

(the index 1 indicates that this is the contribution to the matrix element from diagram 1). An analogous treatment can be used for the other diagrams. We give the results:

$$\delta F_2^{(i)} = \delta F_3^{(i)} = \frac{e^2}{(2\pi)^4 i}\int d^4k \frac{C(k^2)}{k^4}[F^{(i)}(p_1, p_2, q) - F^{(i)}(p_1, p_2 - k, q + k)], \quad (4b)$$

$$\delta F_4^{(i)} = \delta F_5^{(i)} = -\frac{e^2}{(2\pi)^4 i}\int d^4k \frac{C(k^2)}{k^4}\frac{1}{2}F^{(i)}(p_1, p_2, q), \quad (4c)$$

$$\delta F_6^{(i)} = \frac{e^2}{(2\pi)^4 i}\int d^4k \frac{C(k^2)}{k^4}F^{(i)}(p_1, p_2 - k, q + k). \quad (4d)$$

Adding, we get †

$$\sum_k \delta F_k^{(i)} = 0.$$

3. Thus the validity of the generalized Ward's identity (2) at each electromagnetic vertex and of the identity (3) at the four-fermion vertex guarantees that the requirements for gauge invariance of the radiative corrections to β decay are satisfied. This means that the result will not depend on the choice of the arbitrary function $C(k^2)$ in the photon propagator $D_{\mu\nu}(k)$. Equations (2) and (3) impose restrictions only on the longitudinal parts of

*Actually this treatment is a simplified one, since the equation (3) does not relate to the case in which the photon is emitted and absorbed by the same virtual line in the diagram $F^{(i)}$. Furthermore, for the π mesons there are double electromagnetic vertices. A rigorous treatment, however, does not change the result.

†It can be seen from these formulas that the sum of diagrams 4, 5, and 6 is not separately gauge invariant if the form factors $F^{(i)}(q)$ of the weak interaction depend on the momentum q. The μ meson has no strong interactions, and therefore for the decay of the μ meson $F^{(i)}(q)$ reduce to the corresponding local operators $\gamma_\mu(1 + \gamma_5)$. The radiative corrections to μ decay are represented by the diagrams 4, 5, and 6 only, and their sum is gauge invariant. With the transverse gauge (1a) each of these diagrams is finite, and consequently the result does not depend on the arbitrary cut-off momenta Λ_μ and Λ_e.

the electromagnetic vertices Γ_μ, $F_\lambda^{(i)}$ and $F_{\lambda\mu}^{(i)}$, and the transverse parts of Γ_μ, $F_\lambda^{(i)}$, $F_{\lambda\mu}^{(i)}$ can be arbitrary.

We shall suppose that the longitudinal parts of Γ_μ, $F_\lambda^{(i)}$, $F_{\lambda\mu}^{(i)}$ are chosen so that Eqs. (2) and (3) are satisfied, and take $C(k^2) = -1$, i.e., we take $D_{\mu\nu}(k)$ in the transverse gauge of Landau and Khalatnikov [9]

$$D_{\mu\nu} = -ik^{-2}(\delta_{\mu\nu} - k^{-2}k_\mu k_\nu). \tag{1a}$$

Then in virtue of the equation $D_{\mu\nu}(k)k_\nu = 0$ the longitudinal parts of Γ_μ, $F_\lambda^{(i)}$, $F_{\lambda\mu}^{(i)}$ do not occur at all in the matrix element, and the result will be gauge invariant for an arbitrary cut-off of the transverse parts of Γ_μ, $F_\lambda^{(i)}$, $F_{\lambda\mu}^{(i)}$.

Let us first examine the case in which the form-factor of the weak interaction does not depend on q, i.e., $F^{(i)}(q) = \gamma_\mu(1 + \gamma_5)$. In this case only the diagrams 4, 5, 6 contribute to the radiative corrections (and only these diagrams have been considered in[1,3]). The exact form of the vertices Γ_μ is not known, and therefore we make the simplest choice

$$\Gamma_\mu^{(p)} = a_p(k^2)\gamma_\mu, \quad \Gamma_\mu^{(e)} = a_e(k^2)\gamma_\mu. \tag{5}$$

It is not hard to verify that with the gauge chosen for the photon propagator $D_{\mu\nu}(k)$ the matrix elements 4 and 5 are finite, and in the matrix element 6 there must be the cut-off factor $a_p a_e$. We take the cut-off function $a(k)$ in the form

$$a(k, n) = [\Lambda^2/(k^2 + \Lambda^2)]^n. \tag{6}$$

For agreement with the experimental data of Hofstadter[10] on the behavior of the electromagnetic form-factor of the proton for small k^2 we must take $\Lambda_p = (6n/\overline{r^2})^{1/2}$, where $(\overline{r^2})^{1/2}$ is the root-mean-square radius of the charge distribution in the proton.

In the paper by Behrends et al.[1] the matrix elements 4, 5, and 6 have been calculated on the assumption $n = \frac{1}{2}$, and the photon propagator was taken in the Feynman gauge: $D_{\mu\nu}(k) = \delta_{\mu\nu}/ik^2$. In our case we must add to the matrix elements 4, 5 from[1] the quantity

$$\Delta M_4 + \Delta M_5 = 2i\pi^2 N\left(-\ln(\Lambda_p/\lambda) + \tfrac{1}{2}\right)M. \tag{7}$$

Here $N = ie^2/4\pi^3$, $e^2 = \alpha = 1/137$, λ is the mass of the photon, and M is the matrix element of β decay without radiative corrections.

The β-decay Hamiltonian of the V − ΛA type is usually written in the form

$$H = 2^{-1/2}G(\bar{\psi}_p\gamma_\mu(1 + \Lambda\gamma_5)\psi_n)(\bar{\psi}_e\gamma_\mu(1 + \gamma_5)\psi_\nu).$$

Then diagram 6 means the exchange of a virtual photon between the charged particles (p, e) which occur in different brackets. To simplify the calculations it is convenient to go over to a way of writing the Hamiltonian in which the charged particles are in the same bracket; to do this we must perform the operation of charge conjugation and the Fierz transformation[11] (i = 0, 1, 2, 3, 4):

$$H = 2^{-1/2}G\sum_{i=0}^{4} c_i(\bar{\psi}_p O_i \psi_{\bar{e}})(\bar{\psi}_{\bar{\nu}}(1 - \gamma_5)O_i\psi_n) = \sum_{i=0}^{4} c_i H_i,$$

$$c_i = \left(1 + \Lambda, \ -\tfrac{1}{2}(1 - \Lambda), \ 0, \ \tfrac{1}{2}(1 - \Lambda), \ -(1 + \Lambda)\right). \tag{8}$$

For the i-th type of β-decay term the change of the matrix element 6 as compared with[1], when the Hamiltonian is written in the form (8), is given by

$$\Delta M_6^{(i)} = NH_i\left\{-\frac{a_i^2}{4}\left[\int\frac{a_p(k, n)a_e(k, n)}{(k^2 + \lambda^2)^2}d^4k - \int\frac{a_p^2(k, 1/2)}{(k^2 + \lambda^2)^2}d^4k\right] + \int\frac{a_p(k, n)a_e(k, n)}{(k^2 + \lambda^2)^2}d^4k\right\}.$$

The quantities a_i are determined from the condition

$$\sum_{\mu=1}^{4}\gamma_\mu O_i\gamma_\mu = a_i O_i.$$

$$a = (4, -2, \ 0, 2, -4) \quad \text{for} \quad i = 0, 1, 2\ 3.\ 4.$$

It can be shown that for $\lambda \to 0$ (λ is the mass of the photon)

$$\int\frac{a_p(k, n)a_e(k, n)}{(k^2 + \lambda^2)^2}d^4k = i\pi^2\begin{cases}2\ln(\Lambda_p/\lambda) - 1 - \psi(2n) - \gamma & \text{for } \Lambda_e = \Lambda_p \\ 2\ln(\Lambda_p/\lambda) - 1 - \psi(n) - \gamma & \text{for } \Lambda_e \gg \Lambda_p\end{cases}. \tag{9}$$

Here $\psi(x) = d\ln\Gamma(x)/dx$ is the logarithmic derivative of the Γ function (cf., e. g.,[12]), and $\gamma = 0.5772$ is the Euler constant. From this we find that the total change in the sum of diagrams 4, 5, 6 is

$$\Delta M = i\pi^2 N\sum_{i=0}^{4} c_i\left\{\frac{a_i^2}{4}[\psi(n) - \psi(1)] + \psi(n) - \gamma\right\}H_i. \tag{10}$$

For the V − A interaction the radiative correction to the lifetime of a nucleus against β decay is of the same form as in Eq. (4.5) of[2], in which we have only to replace the cut-off limit Λ_p by Λ_{eff}:

$$\Lambda_{eff} = \Lambda_p\exp\left\{\tfrac{2}{3}[\psi(1) - \psi(n)] + \tfrac{1}{6}(\psi(n) + \gamma)\right\}. \tag{11}$$

Values of Λ_{eff} are shown in the table. As we see, for $n = \frac{1}{2}$ (cut-off by the Feynman method) choice

n	$\frac{\Lambda_p}{M}$	$\frac{\Lambda_{eff}}{\Lambda_p}$	$\frac{\Lambda_{eff}}{M}$
0.5	0.47	2	0.94
1.0	0.67	1	0.67
1.5	0.82	0.736	0.60

of Λ_p in accordance with the experiments of Hofstadter and use of the fact that $\Lambda_e \gg \Lambda_p$ gives practically the same result as the assumption $\Lambda_p = \Lambda_e = M$ (M is the mass of the nucleon).

4. In the β-decay theory with a conserved vector current the operator $F^{(v)}(q)$ has the form

$$F^{(v)} = f_1(q^2/M^2)\,\gamma_\alpha + \tfrac{1}{2}M^{-1}f_2(q^2/M^2)\,\sigma_{\alpha\beta}q_\beta, \qquad (12)$$

where the form-factors f_1 and f_2 are equal to the isotopic-vector parts of the electric and magnetic form-factors of the nucleon and can be found from the experiments of Hofstadter.[13] In particular,

$$f_1(0) = 1, \qquad f_2(0) = (\mu_p - \mu_n)/e = 3.70$$

(μ_p and μ_n are the anomalous magnetic moments of the proton and neutron).

Since $F^{(v)}$ depends on q^2, it is not only by the proton electromagnetic form-factor a_p that diagram 6 is cut off. For $\Lambda_e \gg \Lambda_p$ the cut-off factor $a_p a_e f_1 \approx a_p^2$, and the result is close to that found in the paper of Behrends and others.[1]

For an estimate of the contribution of diagrams 1, 2, 3 let us find the limiting values of $F_\lambda^{(i)}$ and $F_{\lambda\mu}^{(i)}$ for small k:

$$F_\lambda^{(i)}(k=0) = -e\partial F^{(i)}(q+k)/\partial k_\lambda|_{k=0}$$
$$= -e\partial F^{(i)}(q)/\partial q_\lambda,$$
$$F_{\lambda\mu}^{(i)}(k=0) = e^2\partial^2 F^{(i)}(q+k)/\partial k_\lambda\,\partial k_\mu|_{k=0}$$
$$= e^2\partial^2 F^{(i)}(q)/\partial q_\lambda \partial q_\mu. \qquad (13)$$

It is impossible to determine from Eqs. (3) and (4) the subsequent terms of the expansions of $F_\lambda^{(i)}$ and $F_{\lambda\mu}^{(i)}$ in powers of k, since there can be transverse parts of $F_\lambda^{(i)}$, $F_{\lambda\mu}^{(i)}$ linear in the photon momentum k. Substituting $F^{(v)}(q)$ in the formulas (13) and omitting in the calculations terms of the order m_e/M, we find the limiting values of the operators $F_\lambda^{(v)}$ and $F_{\lambda\mu}^{(v)}$:

$$F_\lambda^{(v)}(k=0) = -(e/2M)\,f_2(0)\,\sigma_{\alpha\lambda},$$
$$F_{\lambda\mu}^{(v)}(k=0) = (2e^2/M^2)\,f_1'(0)\,\delta_{\lambda\mu}\,\gamma_\alpha. \qquad (14)$$

In the calculation of the contribution from diagrams 1, 2, 3 we shall use the expression (14) and cut off the integration over the momentum of the virtual photon at the mass of the nucleon. The use of the values (14) for $F_\lambda^{(v)}$ and $F_{\lambda\mu}^{(v)}$ right up to $k^2 = M^2$ is illegitimate, but we hope that in this way we shall get the correct order of magnitude for the contribution of diagrams 1, 2, 3. With this crude estimate the contribution from these diagrams is almost equal in magnitude to the contribution from diagrams 4, 5, 6, but is opposite in sign. This leads to a great decrease in the size of the radiative correction to the lifetime of a nucleus against β decay, as compared with earlier results,[2,3] and we may suppose that an accurate inclusion of diagrams 1, 2, 3 will remove the discrepancy between the theory of the conserved vector current and experiment.

In all of the foregoing we have used the expression for the electromagnetic vertex of the proton which is valid when the proton is a real particle ($p^2 = M^2$) before and after the emission of a photon. In our case this condition is not satisfied (cf. diagrams 3, 5, 6). Since the "nonreality" of the proton is important only for $k^2 \sim M^2$ we can hope that the "nonreality" of the proton will not change the results very much. The contribution from the anomalous magnetic moments of the neutron and proton has been calculated by Berman,[3] using the data of Hofstadter, and it was found to be small.

In conclusion we express our sincere gratitude to B. L. Ioffe and I. S. Shapiro for their constant interest in this work and for several discussions.

[1] Behrends, Finkelstein, and Sirlin, Phys. Rev. **101**, 866 (1956). T. Kinoshita and A. Sirlin, Phys. Rev. **107**, 593, 638 (1957).

[2] T. Kinoshita and A. Sirlin, Phys. Rev. **113**, 1652 (1959).

[3] S. M. Berman, Phys. Rev. **112**, 267 (1958).

[4] R. P. Feynman and M. Gell-Mann, Phys. Rev. **109**, 193 (1958). S. S. Gershteĭn and Ya. B. Zel'dovich, JETP **29**, 698 (1955), Soviet Phys. JETP **2**, 576 (1956).

[5] R. P. Feynman, Proc. 1960 Int. Conf. on High-Energy Physics at Rochester, Univ. of Rochester, 1960, page 501.

[6] Ya. A. Smorodinskii and Ho Tso-Hsiu, JETP **38**, 1007 (1960), Soviet Phys. JETP **11**, 724 (1960).

[7] B. L. Ioffe, JETP **38**, 1608 (1960), Soviet Phys. JETP **11**, 1158 (1960).

[8] H. S. Green, Proc. Phys. Soc. **A66**, 873 (1953). Y. Takahashi, Nuovo cimento **6**, 371 (1957).

[9] L. D. Landau and I. M. Khalatnikov, JETP **29**, 89 (1955), Soviet Phys. JETP **2**, 69 (1956).

[10] R. Hofstadter, Revs. Mod. Phys. **28**, 214 (1956).

[11] M. Fierz, Z. Physik **104**, 553 (1957).

[12] I. M. Ryzhik and I. S. Gradshteĭn, Tablitsy integralov, summ, ryadov, i proizvedenii (Tables of Integrals, Sums, Series, and Products), Gostekhizdat, 1951.

[13] Hofstadter, Bumiller, and Croissiaux, Phys. Rev. Letters **5**, 263 (1960).

Translated by W. H. Furry
40

A RELATIVISTIC FIELD-THEORY MODEL WITH AN EXACT SOLUTION

D. A. KIRZHNITS and S. A. SMOLYANSKII

P. N. Lebedev Physics Institute, Academy of Sciences, U.S.S.R.

Submitted to JETP editor January 30, 1961

J. Exptl. Theoret. Phys. (U.S.S.R.) **41**, 205-208 (July, 1961)

We have considered a model which is the relativistic generalization of the Ruijgrok-Van Hove-Lee model, and which is free of the difficulties of that model.

1. For the study of the general problems of quantum field theory it is useful to have at one's disposal a relativistically-invariant model which can be solved explicitly. We consider one such model in the present paper. It will be used in the following to analyze the difficulties of a field theory with a point interaction, the singularities of a non-local theory, and so on.

We use as the basis from which to construct such a model the static Ruijgrok-Van Hove model[1] (in short: RVH) which is a generalization of the usual Lee model. As these two, the model proposed here describes the scalar interaction between scalar mesons (θ) and a nucleon field (V, N). The interaction Hamiltonian

$$H' = \sum_u \bar{\psi}_u (\sigma_+ \varphi_+ + \sigma_- \varphi_-) \psi_u \qquad (1)$$

(the meaning of the index u is explained below) corresponds to the processes $V \rightleftarrows N + \theta$ and $N \rightleftarrows V + \theta$ with bare coupling constants g_V and g_N, respectively. In (1)

$$\psi = \begin{pmatrix} \psi_V \\ \psi_N \end{pmatrix}, \qquad \sigma_+ = \begin{pmatrix} 0 & g_N \\ g_V & 0 \end{pmatrix}, \qquad \sigma_- = \begin{pmatrix} 0 & g_V \\ g_N & 0 \end{pmatrix},$$

and $\varphi_\pm$ is the creation and annihilation part of the field φ.

2. To construct a relativistic theory we must give up the static character of the nucleon field.* We shall describe the latter by the Lagrangian (see [2])

$$L_0 = \sum_u \bar{\psi}_u (i (u\nabla) - M) \psi_u. \qquad (2)$$

Here and henceforth the summation is over all values of the four-vector u which satisfy the condition $u_0^2 - \mathbf{u}^2 = 1$, $u_0 > 0$. The vector u which has the meaning of the four-velocity of a particle is not at all connected with its momentum and is together with the momentum characteristic for its state.* The magnitude of u is not changed during the interaction process as the Hamiltonian (1) is diagonal.

The presence of a separate vector u enables us to consider the quantity ψ_u as a two-component spinor without coming into conflict with relativity or with the parity-conservation law. Indeed, a Lorentz transformation corresponding to a velocity $\delta\mathbf{v}$ gives

$$\psi'_u = (1 + \delta\mathbf{v}\mathbf{l})\, \psi_u,$$

where the vector $\mathbf{l} \sim [\sigma \times \mathbf{u}]$ is a polar vector. We remind ourselves of the fact that in the usual theory $\mathbf{l}$ is proportional to the axial spin vector σ because there are not two vectors, and that we have thus a four-component spinor.

We make two remarks concerning the nucleon dispersion law

$$E = (\mathbf{up} + M)/u_0. \qquad (3)$$

First of all, it follows from (3) that sometimes (for instance, when two nucleons with the same u are scattered) the energy and momentum conservation laws are not independent. It is thus necessary to check specially whether the vacuum and single-particle states are stable. From this point of view it is essential that there is no pair creation in our model and that the processes where a θ particle is emitted by a free nucleon are also forbidden. Indeed, the energy conservation law gives for those processes

$$\mathbf{u}\Delta\mathbf{p}/u_0 = \omega, \qquad (4')$$

where $\Delta\mathbf{p}$ is the change in the nucleon momentum. The momentum conservation law $\Delta\mathbf{p} = \mathbf{k}$, or

*The θ-N scattering cross section becomes then different from zero; it vanishes in the RVH model because recoil is neglected.

*The model considered here differs from the Bloch-Nordsieck model[2] in a number of important points; in particular, there is no connection between u and p and the problem is completely isotropic.

$$u\Delta p/u_0 = uk/u_0 \qquad (4'')$$

is easily seen to be incompatible with (4').

It is moreover clear from (3) that the energy of a state is not always positive and can change its sign (when $p^2 < 0$) when the frame of reference changes. On this point there is an essential difference with the usual model where always $p^2 > 0$ and where the sign of the energy is invariant. The natural relativistic generalization of the sign of the energy in the model considered is the sign of the quantity (up) which in the rest frame of the particle (when $\mathbf{p} = 0$) is the same as the sign of the energy and which is always positive. It is essential in this connection that just the quantity (up) and not p^2 determines the characteristics of the excited single-nucleon states (see Sec. 4 below).

To conclude this section we establish the connection between our model and the RVH and Lee models. For $g_N = 0$ we get the relativistic generalization of the Lee model. If we retain in the sums in (1) and (2) only the one term with $\mathbf{u} = 0$, $u_0 = 1$, we get the RVH model. Finally, if we put $g_N = 0$, we come back to the usual Lee model.

3. We turn now to a study of the proposed model. We start with the charge normalization. We note that it is performed exactly as in the RVH model[1] and is reduced to finding the exact Schrödinger wave function for the single-nucleon state. The only difference consists in that it is necessary to replace $\omega^{3/2}$ by $\omega^{1/2}(u_0\omega - \mathbf{u}\cdot\mathbf{k})$ in the corresponding integrals. We give here the final expression for the renormalized charges g_{0V} and g_{0N}:

$$g_{0V} = g_{0N} = (g_V g_N)^{1/2}. \qquad (5)$$

The renormalized charge is thus different from zero in the model considered, as in the RVH model. The vanishing of the charge in the Lee model—both the usual and the relativistic model—is simply connected with the fact that the process $N \rightleftarrows V + \theta$ is forbidden: we see from (5) that g_{0V} tends to zero as $g_N = 0$. This fact indicates once more that the situation in the Lee model is by no means indicative of similar difficulties in real field theories where there is complete symmetry between the emission and absorption of particles.*

4. We turn now to a study of the structure of the renormalized theory. Because of (5) we can at once put $g_V = g_N = g$, $\sigma_V = \sigma_N = g\tau_1$. We shall start from the functional equation for the fermion Green's function[4]

$$[i(u\nabla) - M + g\tau_1\Phi(x)]\, G_{uu'}(x, x'|\varphi) = \delta(x - x')\,\delta_{uu'},$$

$$\Phi(x) = \varphi(x) - i\int d\xi \Delta(x-\xi)\frac{\delta}{\delta\varphi(\xi)}.$$

*A subsequent paper[3] is devoted to this kind of problems.

The boson Green's function is in our model the same as the free function $\Delta(x - x')$.

One solves the equation given here easily as the dependence on the external field φ is at once split off as an exponential

$$\exp\left\{g\tau_1\int d\xi\varphi(\xi)\,[K(x'-\xi) - K(x-\xi)]\right\},$$

$$K(x) = (2\pi)^{-4}\int d^4k\,[(u\,k) + i\varepsilon]^{-1}\exp(-ikx). \qquad (6)$$

Performing in the usual way the mass renormalization and splitting off the Z factor, we get

$$G_c(p) = -i(2\pi)^{-4}\int_0^\infty d\xi\exp\{i\xi((up) - M_0) + \chi(\xi)\},$$

$$\chi(\xi) = ig^2\int_0^\infty d\xi'(\xi' - \xi)\Delta(\xi' u). \qquad (7)$$

This expression has no ghost singularities whatever.

The vertex part is immediately obtained from the relation

$$g\Gamma(x, x', \xi) = (\delta G(x, x')/\delta\varphi(\xi))_{\varphi=0}.$$

Using (6) we get the generalized Ward equation

$$(uk)\,\Gamma(p, k) = \tau_1\{G^{-1}(p) - G^{-1}(p-k)\}, \qquad (8)$$

through which the vertex part is completely determined. Using (7) and (8) we can also verify that the equality $g_0 = g$ holds and also find the asymptotic behavior

$$G(p) \sim p^\alpha/(up), \qquad \Gamma \sim \zeta^{-\alpha},$$

where $\alpha = g^2/4\pi^2$, $\zeta = \max(p, k)$. The decrease in the vertex part is in complete agreement with the well-known Lehmann-Symanzik-Zimmermann theorem.

5. The model constructed here satisfies thus the general requirements of field theory and the simultaneity condition.* One sees easily that the same properties are also possessed by a somewhat modified model with a complex charge

$$\sigma_V = g\tau_1, \qquad \sigma_N = g^*\tau_1.$$

All relations in the foregoing, except (5), remain valid if we perform the substitution

$$g^2 \to |g|^2. \qquad (9)$$

The charge renormalization is now of the form

$$g_0 = g, \qquad (g^*)_0 = g^*.$$

To verify the validity of what we just stated, it is sufficient to note that the contribution from every virtual line is, indeed, connected with the substitution (9).

*We note that the unitarity of the theory follows immediately from the Hermiticity of (1).

[1] T. W. Ruijgrok and L. Van Hove, Physica **22**, 880 (1956).

[2] N. N. Bogolyubov and D. V. Shirkov, Introduction into the Theory of Quantized Fields, Interscience, 1957, Sec. 41.

[3] D. A. Kirzhnits, JETP **41**, 417 (1961), Soviet Phys. JETP **14**, No. 2 (1962).

[4] S. F. Edwards and R. E. Peierls, Proc. Roy. Soc. (London) **A224**, 24 (1954).

Translated by D. ter Haar
41

THE FARADAY EFFECT FOR EXCITONS

I. P. IPATOVA and R. F. KAZARINOV

Leningrad Physico-Technical Institute, Academy of Sciences, U.S.S.R.

Submitted to JETP editor January 31, 1961

J. Exptl. Theoret. Phys. (U.S.S.R.) 41, 209-210 (July, 1961)

The rotation of the plane of polarization near an absorption line of a large-radius exciton is considered. The angle of rotation depends on the effective mass and the exciton radius. An order of magnitude estimate of the angle of rotation near the 2p state of an exciton in a Cu_2O crystal gives a measurable magnitude for this effect.

ONE may expect an appreciable rotation of the plane of polarization (Faraday effect) near exciton absorption lines corresponding to transitions to exciton p states.

For cubic crystals the angle of rotation φ can be expressed in terms of the component of the gyration vector **G** along the direction of the magnetic field **H** (**H** ∥ z)

$$\varphi = (\pi d/\lambda)\, G_z/\varepsilon, \qquad (1)$$

where d is the thickness of the sample, ϵ the dielectric constant when there is no magnetic field, and λ the wavelength of the light.[1] The vector **G**, in turn, is defined as the antisymmetric part of the dielectric constant $\epsilon_{\mu\nu}(\mathbf{H})$:

$$G_\gamma = \delta_{\gamma\mu\nu}\,\varepsilon_{\mu\nu}. \qquad (2)$$

The problem is thus reduced to evaluating the antisymmetric part of the exciton dielectric constant.

It is well known that the transitions to the s states are allowed transitions for Mott excitons.[2-4] Transitions to p states are forbidden; their intensity is $(a/r_0)^2$ times smaller than the intensity of transitions to s states (a: lattice constant, r_0: exciton radius). For Mott excitons $(a/r_0) \ll 1$.

However, the s state does not change in the approximation which is linear in the magnetic field and there is no Faraday effect. It is thus necessary to consider the "forbidden" transitions to p states.

The exciton conductivity connected with the transitions to p states can in the first perturbation-theory approximation in the magnetic field be obtained from the general Eq. (16) of [2]:

$$\sigma_{\mu\nu} = \sum_{n;m=0,\pm1} T^{nm}_{\mu\nu}/[\gamma - i\,(\omega - \omega_n - \Omega m)], \qquad (3)$$

where ω is the light frequency, $\Omega = eH/2Mc$, M the reduced exciton mass, ω_n the hydrogen-like energy level, γ the width of the exciton line, m the magnetic quantum number, and $T^{nm}_{\mu\nu}$ a tensor the real part of which is connected with the oscillator strength of the transition and the imaginary part of which is responsible for the rotation of the polarization plane

$$T^{nm}_{\mu\nu} = \frac{1}{E_0}\sum_i \left(\frac{\partial J^{vc}_\nu}{\partial k_\alpha}\right)_{\mathbf{K}_i}\left(\frac{\partial J^{cv}_\mu}{\partial k_\beta}\right)_{\mathbf{K}_i}\left(\frac{\partial \Psi_{n1m}}{\partial x_\beta}\right)_{\mathbf{x}=0}\left(\frac{\partial \Psi^*_{n1m}}{\partial x_\alpha}\right)_{\mathbf{x}=0}. \qquad (4)$$

Here E_0 is the minimum value of the frequency of the main transition, $\mathbf{K}_i$ is that point in momentum space which corresponds to that transition, Ψ_{n1m} are the hydrogen-like wave functions of the exciton p state

$$J^{vc}_\nu(\mathbf{k}) = J^{vc*}_\nu(\mathbf{k}) = e\int d^3r\, u^*_{vk}(\mathbf{r})\hat{v}_\nu u_{ck}(\mathbf{r})$$

are the interband matrix elements of the current, evaluated using Bloch wave functions.

Apart from the selection rules for the hydrogen-like wave functions, $T^{nm}_{\mu\nu}$ involves also the interband selection rules for $(\partial J^{vc}_\nu/\partial k_\alpha)_{\mathbf{K}_i}$, which must be established in each case from the symmetry properties of the crystal.

Using the relation $\Psi_{n1m}(\mathbf{x}) = \Psi^*_{n1-m}(\mathbf{x})$, we get from (4)

$$T^{nm}_{\mu\nu} = T^{n-m}_{\nu\mu}; \qquad T^{nm}_{\mu\nu} = (T^{nm}_{\nu\mu})^*. \qquad (5)$$

The first of these equations ensures that the Onsager relations are satisfied, the second leads to the antisymmetry of Re $\sigma_{\mu\nu}$ when there is no absorption. Assuming that $|\omega_n - \omega| \gtrsim \nu > \Omega$ we get from (3) and (5)

$$-i\varepsilon^{\text{antis}}_{\mu\nu} = \frac{2\pi}{\omega}(\sigma_{\mu\nu} - \sigma_{\nu\mu}) = -i\frac{4\pi}{\omega}\sum_n \mathrm{Im}\,\{T^{n1}_{\mu\nu}\}\frac{\Omega}{\gamma^2 + (\omega - \omega_n)^2}. \qquad (6)$$

Substituting (6) into (1) and using the explicit form of $(\partial\Psi_{n1m}/\partial x_\alpha)_{\mathbf{x}=0}$ we get for the angle of rotation near the line n = 2

$$\varphi = \frac{\pi}{2}\frac{1}{\varepsilon}\left(\frac{d}{\lambda}\right)\left(\frac{a}{2r_0}\right)^5 \frac{\Omega\omega}{\gamma^2 + (\omega - \omega_n)^2}\,\beta_{xy}, \qquad (7)$$

where $\beta_{xy} \sim 1$ is a component of an antisymmetric tensor.

Obtaining an order of magnitude estimate of φ for the yellow exciton series in a Cu_2O crystal ($\epsilon = 10$) we get $\varphi \gtrsim 0.5°$ for $H = 10^3$ G, $|\omega - \omega_n| \sim \gamma \sim 10\,\Omega$, $r_0 \lesssim 30\,a$, $d = 500\,\mu$. The absorption coefficient in the yellow series is small ($\sim 10^2$ cm^{-1})[5] and the intensity of the incident light will thus only decrease by a factor of a hundred for a thickness of 500 μ. The use of photomultipliers makes it possible to observe intensities decreased by a factor of a thousand.

One can thus estimate from the magnitude of the angle of rotation the exciton radius, if its reduced mass is known. Moreover, the selection rules entering into $T_{\mu\nu}^{nm}$ may turn out to be an important aid for interpreting exciton spectra.

The authors express their deep gratitude to L. É. Gurevich, O. V. Konstantinov, and G. M. Éliashberg for valuable discussions of this paper.

[1] L. D. Landau and E. M. Lifshitz, Elektrodinamika sploshnykh sred (Electrodynamics of Continuous Media) Gostekhizdat, 1957, part II, Sec. 82.

[2] R. F. Kazarinov and O. V. Konstantinov, JETP **40**, 936 (1961), Soviet Phys. JETP **13**, 654 (1961).

[3] R. J. Elliott, Phys. Rev. **108**, 1384 (1957).

[4] D. S. Bulyanitsa, Vestnik LGU, No. 4 (1960).

[5] I. Pastrnyak, Opticheskie svoistva zakisi medi (Optical Properties of Cuprous Oxide) Thesis, Physico-Technical Inst., 1959.

Translated by D. ter Haar
42

POSSIBILITY OF GENERATION AND AMPLIFICATION OF HYPERSOUND IN PARAMAGNETIC CRYSTALS

U. Kh. KOPVILLEM and V. D. KOREPANOV

Kazan' State University

Submitted to JETP editor January 31, 1961

J. Exptl. Theoret. Phys. (U.S.S.R.) **41**, 211-213 (July, 1961)

The interaction between a nonequilibrium paramagnetic spin system and the crystal lattice is studied theoretically. Conditions under which spin-lattice interaction leads to the excitation or amplification of hypersound in crystals are studied. Parameters are introduced characterizing the efficiency of transformation of the energy of magnetic ions into the energy of hypersound. Specific calculations show that in a number of cases it is much easier to create conditions for generation of phonons than for generation of photons at the expense of the spin system energy. It is noted that nonequilibrium spin systems may be used to detect weak acoustic and electromagnetic signals.

IT is well known that the methods of high-frequency acoustic spectroscopy represent a promising tool for the investigations of the properties of solids and irreversible processes taking place in them. One of the difficulties in the way of these methods is the production, transmission, and detection of acoustic vibrations with a frequency of the order of kilomegacycles and even higher. It is therefore natural to seek new means for generating hypersound directly in those materials in which its action is studied. Taking into consideration the analogy which exists between the process of photon production and phonon production at the expense of the energy of magnetic ions in crystals, it is useful to attempt to apply the theoretical and experimental material available from research on paramagnetic quantum photon generators to the development of paramagnetic hypersonic generators. The present research is devoted to the study of this possibility.

According to the theory of Al'tshuler,[1] which is supported by experimental data,[2] the creation and annihilation of phonons take place in paramagnetic crystals under the action of hypersound of frequency $\nu_{ba} = (E_b - E_a)/h \sim 10^{10}$ cps at the expense of the annihilation and creation of magnons—quanta of the Zeeman and Stark energies of the magnetic ions in a static magnetic field and in the crystalline electric field.

Let Q_t, Q_{ext} and Q_A be the figures of merit of the crystalline acoustic resonator, characterizing respectively the ordinary damping of sound in the crystal, damping by coupling with the surrounding medium, and damping as the result of the creation of the magnons. It is known that the configuration of the energy levels E_α of magnetic ions can be chosen in such a fashion that upon saturation of magnetic resonance for a certain pair (E_α, E_β), the difference in the populations Δn_{ab} for the pair (E_a, E_b) is negative. It is easy to see that in this case Q_A becomes negative and an amplification of the hypersound will take place in the crystal, described by the formula

$$G_{ba} = \frac{P_{ref}}{P_{inc}} = \left[\frac{Q_{ext}^{-1} - Q_p^{-1} - Q_A^{-1}}{Q_{ext}^{-1} + Q_p^{-1} + Q_A^{-1}}\right], \quad (1)$$

where the subscripts "ref" and "inc" refer to the reflected and incident intensities of the hypersound. If the transition $E_a \longleftrightarrow E_b$ is forbidden for magnetic dipole transitions, and the condition

$$-Q_A^{-1} > Q_p^{-1} + Q_{ext}^{-1} \quad (2)$$

is satisfied, the crystal will generate hypersound of frequency ν_{ba} under the action of lattice vibrations even in the absence of an external acoustic field. That is, the energy of the variable magnetic field expended in the production of $\Delta n_{ba} < 0$ is converted to the energy of hypersound.

Let

$$\mathcal{H}_1 = \cos(\omega_{ba} t)\, R \sum_{i=1}^{N} [\langle a|\mathcal{P}^i|b\rangle + \langle b|\mathcal{P}^i|a\rangle] \quad (3)$$

be the operator describing the interaction of the magnetic ions i with the variable magnetic (R=H) and acoustic (R=A) fields, where t is the time, R is the amplitude, $R\langle a|\mathcal{P}^i|b\rangle$ is the matrix element of transition of the ion i between the states $|a\rangle$ and $|b\rangle$ under the action of the perturbation $\mathcal{H}_1$. We introduce the imaginary susceptibility and the corresponding Q by the relations

$$\chi_R'' = (2\hbar V)^{-1}\,\Delta n_{ab}\,|\langle a|\mathcal{H}^{i}|b\rangle|^2\,g(\nu_{ba}),$$
$$Q_H = (4\pi\chi_H''\eta)^{-1}, \qquad Q_A = \omega_{ba}^{-1}\,Fc = (2\chi_A''\eta)^{-1}\,\rho\omega_{ba}^2, \qquad (4)$$

where η is the filling factor, F is the coefficient of sound absorption,[1] ρ is the density of the crystal, c is the velocity of sound in the crystal, $g(\nu_{ba})$ is the normalized form factor of the absorption curve of magnetic or acoustic energy of the spin system, and V is the volume of the crystal.

Let us estimate the value of Q_A for the ion Ni^{2+} in $NiSiF_6 \cdot 6H_2O$ for a static field H_0 perpendicular to the symmetry axis of the crystal z. Using data on the change of the constant D of the axial crystalline field as a consequence of an applied static field X_{zz} along the z axis,[3] we obtain

$$Q_A \sim T\,(2S+1)\,k\rho\Delta c_z^2[2\pi\nu_{ba}N^*\alpha_{33}^2|\langle a|S_z^2|b\rangle|^2]^{-1}\,(\partial D/\partial X_{zz})^{-2}$$
$$= 6.38\cdot 10^{11}\,T/\nu_{ba}, \qquad (5)$$

where k is Boltzmann's constant, N* is the number of Ni^{2+} ions in 1 cm^3, S is the spin, Δ is the line width of magnetic resonance, α_{33} is the elastic constant, and T is the temperature which describes the difference of populations in the levels (E_a, E_b). The following constants are used:[3]

$$c_z^2 = 2.5\cdot 10^{11}\ (\text{cm/sec})^2,\quad N^* = 4\cdot 10^{21},\quad \rho = 2.08\ \text{g/cm}^3,$$
$$\alpha_{33} = 0.5\cdot 10^{12}\ \text{dynes/cm}^2,\qquad \Delta = 3.2\cdot 10^{9}\ \text{cps},$$
$$\partial D/\partial X_{zz} = -3.37\cdot 10^{-26}\ \text{erg-cm}^2/\text{dyne},$$
$$|\langle a|S_z^2|b\rangle|^2 = 10^{-1};$$

The distance Ni-Ni is taken to be equal to 6.27 A. For $T = 1°K$ and $\nu_{ba} = 10^{10}$ cps, we get $Q_A \sim 63.8$.

For Cr ions in $NH_4[Al_{0.99} + Cr_{0.01}]\cdot(SO_4)_2\cdot 12H_2O$, the following values are obtained:[3] $\partial D/\partial L = 8.71\times 10^{-22}$ erg-cm^2/dyne, $H_0 \parallel (111)$; in the case of the crystal $K_3[Co_{0.99} + Cr_{0.01}]\cdot(CN)_6$, one obtains $\partial D/\partial L = 1.01\times 10^{-22}$ erg-cm^2/dyne, $\partial E/\partial L = 1.22\times 10^{-23}$ erg-cm^2/dyne, $\partial g_y\beta H_0/\partial L = 1.22\times 10^{-22}\,\beta H_0$ erg-cm^2/dyne, where the y axis is parallel to the c axis of the crystal. Here L is the hydrostatic pressure on the surface of the crystal, E is the constant of a rhombic crystalline field, and β is the Bohr magneton. Substitution of these data in (5) shows that the Cr ions yield a significantly smaller value of Q_A than the Ni ions.

If the acoustic resonator is disconnected from the acoustic wave guide, then the radiation of sound in air is characterized by $Q_{ext} \sim 3\times 10^4$ (see [4]) and $Q_p \sim 5.5\times 10^4$ for $\nu = 10^9$ cps.[2] The numerical estimates that have been carried out show that the condition (2) is satisfied, and paramagnetic crystals can be used as sources of hypersound of frequency $10^{11} - 10^{12}$ cps.

As an illustration, we consider several possible schemes of operation of a generator or amplifier of hypersound, using nickel fluorosilicate with H_0 parallel to the trigonal axis z of the crystal. The spin Hamiltonian for Ni^{2+} has the form[5]

$$\mathcal{H} = \beta\,(g_zH_zS_z + g_xH_xS_x + g_yH_yS_y) + D\,(S^2{}_z - \tfrac{2}{3}),$$

where $S = 1$, g_α are the spectroscopic splitting factors along the α axis, $D = -0.12\ \text{cm}^{-1}$, and $g_z = 2.29$ at 14°K. For $H_0 \parallel z$ the position of the energy levels (E_1, E_2, E_3), corresponding to the states $(|-1\rangle, |0\rangle, |+1\rangle)$, is described by the formulas

$$E_1 = \tfrac{1}{3}D - g_z\beta H_z,\quad E_2 = -\tfrac{2}{3}D,\quad E_3 = \tfrac{1}{3}D + g_z\beta H_z.$$

Since $\langle 1|S_x|-1\rangle = 0$, it is convenient to use the pair of levels (E_1, E_2) for generation and amplification of hypersound. The negative difference in populations between these levels can be obtained by different means. Let $E_1 < E_3 < E_2$, and the pulsed variable magnetic field of frequency $\nu_{kl} = h^{-1}(E_l - E_k)$ and amplitude H be circularly polarized in the xy plane, where the duration of the pulse $\Delta t \ll T_1, T_2$ satisfies the condition $2g_x\beta H\hbar^{-1}\Delta t = \pi$, where T_1 and T_2 are the longitudinal and transverse relaxation times of the spin-system magnetization. To obtain a maximum difference in population between the levels (E_1, E_3), alternation of two pulses with carrier frequencies ν_{21} and ν_{23}, respectively, is necessary. If $E_1 < E_2 < E_3$, three pulses are required with carrier frequencies ν_{21}, ν_{32}, and ν_{21}. Operation of the generator in the continuous state is possible if the difference of populations of the pair of levels (E_1, E_3) becomes negative in saturation of the transitions $|1\rangle \longleftrightarrow |0\rangle$ or $|-1\rangle \longleftrightarrow |0\rangle$.

Let us consider interference effects brought about by interaction of the fields H and A for $\Delta n_{ab} < 0$. Let the relation obtained from (2) by replacing Q_A by Q_H be satisfied for the field H in the resonator. If sound vibrations are excited in a crystal which fills the resonator, then additional losses appear which are brought about by creation of phonons at the expense of the annihilation of magnons, and it is necessary to replace Q_H^{-1} by $Q_H^{-1} - Q_{HA}^{-1}$, which leads to a violation of the condition for cascade production of photons at the expense of $\Delta n_{ab} < 0$, and to a sharp change in the amplitude H. Conversely, cascade production of phonons for $\Delta n_{ab} < 0$ can be stopped as a result of creation of photons from magnons, wherein one must replace Q_A^{-1} in (2) by $Q_A^{-1} - Q_{AH}^{-1}$. Here

$$Q_{HA} = [4\pi\chi_A''A^2]^{-1}H^2, \quad Q_{AH} = [2\chi_H''H^2]^{-1}\rho\omega_{ba}^2A^2.$$

The relations that have been set down show that

the method of double magnetic hypersonic resonance in the presence of a strong variable magnetic field (which brings about inversion of the populations, $\Delta n_{ab} < 0$) can be used for detection of a weak amplitude A (or H) without A (or H) going beyond the limits of the crystal.

The authors are grateful to S. A. Al'tshuler for discussion of results.

[1] S. A. Al'tshuler, JETP **28**, 38, 49 (1955), Soviet Phys. JETP **1**, 29, 37 (1955).

[2] Jacobsen, Shiren, and Tucker, Phys. Rev. Lett. **3**, 81 (1959).

[3] W. M. Walsh, Phys. Rev. **114**, 1473, 1485 (1959).

[4] L. Bergman, Ultrasonics (Russian translation), IIL, 1957, p. 82.

[5] K. D. Bowers and J. Owen, Report Progr. Phys. **18**, 304 (1955).

[6] N. Bloembergen, Phys. Rev. **104**, 324 (1956).

Translated by R. T. Beyer
43

EXCITATION OF NUCLEI IN HEAVY μ-MESIC ATOMS

D. F. ZARETSKII and V. M. NOVIKOV

Submitted to JETP editor February 4, 1961

J. Exptl. Theoret. Phys. (U.S.S.R.) **41**, 214-221 (July, 1961)

We consider the process where nuclei are electromagnetically excited by muons (radiationless excitation) during the 2p-1s transition in a mesonic atom. The ratio of the probability that a γ quantum is emitted by the muon to the probability of a radiationless excitation with subsequent decay of the nucleus through various nuclear channels is evaluated.

1. INTRODUCTION

ONE of the authors has shown earlier[1] that the transition of a muon from the 2p to the 1s state can in heavy mesonic atoms take place by a direct transfer of the whole of the energy of the transition to the nucleus. The probability for the excitation of the nucleus during this transition was evaluated assuming that $\rho\Gamma_{\text{nucl}} \gg 1$ (case of overlapping nuclear levels) where ρ is the density of the nuclear levels at an excitation energy equal to the energy of the transition, and Γ_{nucl} is the average width of the nuclear levels at the same energy. One can in that limiting case interpret the process where the nucleus is excited as the inverse of the internal conversion effect. Such a process was called the effect of a radiationless excitation of the nucleus. The ratio of the probability W_{nucl} of a radiationless excitation of the nucleus to the probability W_γ of the emission of a γ quantum could in that limiting case be written in the form

$$W_{\text{nucl}}/W_\gamma = \Gamma_{\text{n.r.}}/\Gamma_\gamma, \tag{1}$$

where $\Gamma_{\text{n.r.}}$ is the width of the radiationless excitation of the nucleus which is proportional to the photoexcitation cross section and Γ_γ is the width for the emission of a γ quantum by a muon.

There is also interest in the other limiting case when $\rho\Gamma_{\text{nucl}} \ll 1$ (case of non-overlapping levels). In that case the nucleus can disintegrate through one of the nuclear channels but the process of a reverse transfer of energy to the muon is also possible. This leads to the result that the yield of γ quanta for that transition is larger in comparison than the one given by Eq. (1) and that thus W_{nucl}/W_γ in the case of non-overlapping levels must depend not only on Γ_γ and $\Gamma_{\text{n.r.}}$, but also on $\rho\Gamma_{\text{nucl}}$.

We compute in the present paper W_{nucl}/W_γ for the case $\rho\Gamma_{\text{nucl}} \ll 1$ and arbitrary ratio of Γ_γ and $\Gamma_{\text{n.r.}}$. The case $\Gamma_{\text{n.r.}} \gg \Gamma_\gamma$ was considered earlier by us.[2] An estimate of $\Gamma_{\text{n.r.}}/\Gamma_\gamma$ for a number of elements[3] shows, however, that this quantity is of the order of unity. In the case of non-overlapping levels, the effect of the excitation of the nuclei by a muon is important only, if the width of the muon energy level is appreciably larger than the distance between nuclear levels. In heavy mesonic atoms such as thorium and uranium $\Gamma_{\text{n.r.}} \sim 1$ kev, and $1/\rho$ is of the order of several electron volts so that the condition

$$\rho\Gamma_{\text{n.r.}} \gg 1, \tag{2}$$

on which our calculation is based is satisfied with very good accuracy.

We assume for the sake of simplicity in this paper that the transition of the muon from a more highly excited state into the 2p-state is not accompanied by the effect of the radiationless excitation. This is a reasonable assumption, since transitions between higher states have less energy and thus also a smaller probability for a radiationless excitation. On the other hand, such an assumption is not one of principle, since one can easily generalize the calculation to the case of a radiationless excitation at any transition.

2. ANALYSIS OF THE BOUND MUON-NUCLEUS SYSTEM

The Hamiltonian of the muon-nucleus system is of the form

$$H = H_0 + V, \tag{3a}$$

$$H_0 = H_{\text{nucl}} + T_\mu - \left\langle \psi_0 \left| \sum_{i=1}^{Z} \frac{e^2}{|\mathbf{r}_i - \mathbf{r}_\mu|} \right| \psi_0 \right\rangle, \tag{3b}$$

where H_{nucl} is the Hamiltonian of the nucleus, T_μ the kinetic energy operator of the muon, and the third term in (3b) is the potential in which the muon in the mesonic atom moves ($\mathbf{r}_\mu$ is the muon coordinate, $\mathbf{r}_i$ the proton coordinate, and the sum is taken over all protons), ψ_0 is the wave function of

the ground state of the nucleus. V is the dipole part of the operator

$$\left\langle \psi_0 \left| \sum_{i=1}^{Z} \frac{e^2}{|r_i - r_\mu|} \right| \psi_0 \right\rangle - \sum_{i=1}^{Z} \frac{e^2}{|r_i - r_\mu|}. \quad (4)$$

The eigenfunctions of the Hamiltonian H_0 are clearly all possible products of wave functions ψ_i of the nucleus with muon wave functions φ_k. The wave functions of the total Hamiltonian H which satisfy the Schrödinger equation $H\Psi_\lambda = E_\lambda \Psi_\lambda$ will be expanded in terms of the complete set of wave functions of the Hamiltonian H_0:

$$\Psi_\lambda = \sum_{i,k} C_{\lambda;i,k} \psi_i \varphi_k, \quad (5)$$

where the $C_{\lambda;i,k}$ are the expansion coefficients.

Since $\Gamma_{n.r.}$ is much smaller than the distance between the muon levels, but much larger than the distance between the nuclear levels which correspond to the energy of excitation of the nucleus during the 2p-1s transition, one can for energies E_λ of the system which are close to the energy E_p of the 2p-1s transition write the sum (5) in the form

$$\Psi_\lambda = C_{\lambda;0,2p} \psi_0 \varphi_p + \sum_c C_{\lambda;c,1s} \psi_c \varphi_s, \quad (6)$$

where φ_p and φ_s are the muon wave functions for the 2p and the 1s state, respectively; in the following we shall for the sake of simplicity write $C_{\lambda,p}$ instead of $C_{\lambda;0,2p}$ and $C_{\lambda,c}$ instead of $C_{\lambda;c,1s}$. The other terms in (5) are negligibly small and can be omitted.

Substituting (6) into the Schrödinger equation with the Hamiltonian H and using the normalization of the Ψ_λ we get the following set of equations for the coefficients C_λ and the eigenvalues E_λ:

$$C_{\lambda,p} V_c = (E_\lambda - E_c) C_{\lambda,c}, \quad (7)$$

$$\sum_c C_{\lambda,c} V_c^* = (E_\lambda - E_p) C_{\lambda,p}; \quad (8)$$

$$|C_{\lambda,p}|^2 + \sum_c |C_{\lambda,c}|^2 = 1, \quad (9)$$

where $V_c = \langle \psi_c \varphi_s | V | \psi_0 \varphi_p \rangle$. Substituting (7) into (9) we get

$$|C_{\lambda,p}|^2 = \left\{ 1 + \sum_c |V_c|^2 / (E_\lambda - E_c)^2 \right\}^{-1}. \quad (10)$$

From (7) and (8) we find an equation for the eigenvalues:

$$E_\lambda - E_p = \sum_c [|V_c|^2 / (E_\lambda - E_c)]. \quad (11)$$

From (10) we see that a characteristic interval for the sum over c is $|E_\lambda - E_c| \lesssim \Gamma_{n.r.}$. One may assume that $|V_c|^2$ which is proportional to the cross section for the photoexcitation of the nucleus[1] is constant in an interval of $\sim \Gamma_{n.r.}$ and that the levels E_c are distributed equidistantly with a density $\rho = 1/\bar{D}$ where $\bar{D}$ is the average distance between the levels of the nucleus at the given energy E_p. Taking this into account we find

$$\sum_c [|V_c|^2/(E_\lambda - E_c)] = \pi \overline{|V_c|^2}\, \rho \operatorname{ctg} \pi \rho \Delta, \quad (12)^*$$

$$\sum_c [|V_c|^2/(E_\lambda - E_c)^2] = \pi^2 \overline{|V_c|^2}\, \rho^2 / \sin^2 \pi \rho \Delta, \quad (13)$$

where Δ is the distance from E_λ to the nearest level E_c. The details of the calculations leading to (12) and (13) were given in [2].

Eliminating Δ from (12) and (13) we find a connection between the sums over c in (12) and (13)

$$\sum_c \frac{|V_c|^2}{(E_\lambda - E_c)^2} = \frac{1}{\overline{|V_c|^2}} \left[\pi^2 \rho^2 \overline{|V_c|^4} + \left(\sum_c \frac{|V_c|^2}{E_\lambda - E_c} \right)^2 \right]. \quad (14)$$

Substituting (14) into (10) and using (11) we find

$$|C_{\lambda,p}|^2 = \overline{|V_c|^2} / [(E_\lambda - E_p)^2 + \pi^2 \rho^2 \overline{|V_c|^4} + \overline{|V_c|^2}]. \quad (15)$$

Using the condition (2) we can neglect the last term in the denominator in (15) and find finally

$$|C_{\lambda,p}|^2 = (\Gamma_{n.r.}/2\pi\rho)\, [(E_\lambda - E_p)^2 + (\Gamma_{n.r.}/2)^2]^{-1}, \quad (16)$$

where $\Gamma_{n.r.} = 2\pi \overline{|V_c|^2} \rho$.

In the following we shall need to evaluate different sums over the levels E_λ of the bound muon-nucleus system. To find the eigenvalues E_λ it is in principle necessary to solve Eq. (11). However, condition (2) has as a consequence that the levels E_λ are distributed nearly equidistantly up to terms of the order $1/\Gamma_{n.r.} \ll 1$. Indeed, one gets easily from (11) the following expression for the distance between two consecutive levels E_λ and $E_{\lambda'}$:

$$E_\lambda - E_{\lambda'} = \frac{1}{\rho} \left\{ 1 + \frac{\pi}{2\rho\Gamma_{n.r.}} \left[1 + 4 \left(\frac{E_\lambda - E_p}{\Gamma_{n.r.}} \right)^2 \right] \right\}. \quad (17)$$

The second term in (17) is small compared to unity.

3. ACCOUNT OF THE DAMPING OF THE MUON-NUCLEON SYSTEM

We neglect according to our scheme the dipole interaction between the muon and the nucleus in more highly excited muon states so that the wave function of the system is $\psi_0 \varphi_{exc}$, where φ_{exc} is an arbitrary excited muon state from which it can make the transition to the 2p state. During the transition from $\psi_0 \varphi_{exc}$ the level Ψ_λ of the muon-nucleus system is excited. The probability ω_λ for the excitation of level λ is proportional to the square of the matrix element for the transition, i.e.,

*ctg = cot.

$$\omega_\lambda \sim |\langle \Psi_\lambda | H_\gamma | \psi_0 \varphi_{\text{exc}} \rangle|^2 = |C_{\lambda,p}|^2 |\langle \varphi_0 | H_\gamma | \varphi_{\text{exc}} \rangle|^2,$$

where H_γ is the interaction between the muon and the electromagnetic field which leads to this transition. Taking the normalization $\Sigma \omega_\lambda = 1$ into account we get $\omega_\lambda = |C_{\lambda,p}|^2$.

Without loss of generality we can assume that the $C_{\lambda,p}$ are real. Since the probability of finding the system in the state λ after the muon has made the transition from the higher state is equal to $C^2_{\lambda,p}$ the total wave function of the system at $t = 0$ must be written in the form

$$\Psi|_{t=0} = \sum_\lambda C_{\lambda,p} \Psi_\lambda = \sum_\lambda C^2_{\lambda,p} \psi_0 \varphi_p + \sum_{\lambda,c} C_{\lambda,c} C_{\lambda,p} \psi_c \varphi_s = \psi_0 \varphi_p. \quad (18)$$

The sum over λ, c in (18) vanishes because of the orthonormality of the coefficients C_λ.

We consider now transitions from the state Ψ_λ which are accompanied by the emission of a γ quantum by the muon (H_γ is the interaction between the muon and the electromagnetic field) and by the decay of the nucleus through different nuclear channels (the neutron channel, nuclear quanta, fission). We do not know the explicit form of the interaction operator H'_{nucl} corresponding to the nuclear processes, but only the square of the matrix element of this operator enters in the final result and is proportional to the nuclear width. We assume for the sake of simplicity that only one nuclear channel is open. If the decay of the excited nucleus proceeds independently through the different channels (decay of the compound nucleus) we can replace in the final result the partial nuclear width by the total width.

The wave function of the system when the nucleus is in its ground state, the muon in its ground state, and the γ quantum emitted by the muon has an energy E_ν is denoted by Φ_ν; the wave function of the system when the muon is in the ground state while the nucleus after decay and the decay products of the nucleus have a total energy E_k is denoted by Φ_k. We can write the wave function Ψ of the Hamiltonian $\mathcal{H} = H_0 + V + H_\gamma + H'_{\text{nucl}}$ which satisfies the initial condition (18) in the form

$$\Psi = \sum_\lambda b_\lambda(t) \Psi_\lambda e^{-iE_\lambda t/\hbar} + \sum_\nu b_\nu(t) \Phi_\nu e^{-iE_\nu t/\hbar} + \sum_k b_k(t) \Phi_k e^{-iE_k t/\hbar}, \quad (19)$$

where $b_\lambda(0) = C_{\lambda,p}$, $b_\nu(0) = b_k(0) = 0$. Substituting (19) into the Schrödinger equation we get an equation for the coefficients b, which we shall assume to be equal to zero for $t < 0$ (see, for instance,[4]):

$$i\hbar \dot{b}_n(t) = \sum_m \mathcal{H}_{nm} e^{i(E_n - E_m)t/\hbar} b_m(t) + i\hbar\delta(t) \sum_\lambda C_{\lambda p} \delta_{n\lambda}, \quad (20)$$

where n and m stand for all indices λ, ν, and k.

We Fourier-transform the coefficients b:

$$b_\lambda = -\frac{1}{2\pi i} \int_{-\infty}^{+\infty} G_\lambda(E) e^{-i(E_\lambda - E)t/\hbar} dE,$$

$$b_{\nu,k} = -\frac{1}{2\pi i} \int_{-\infty}^{+\infty} G_{\nu,k}(E) \zeta(E - E_{\nu,k}) e^{i(E_{\nu,k} - E)t/\hbar} dE, \quad (21)$$

where

$$\zeta(x) = \lim_{\sigma \to +0} [1/(x + i\sigma)].$$

We are interested in the total probability W_γ that the muon has emitted a γ quantum; it is clearly equal to

$$W_\gamma = \sum_\nu |b_\nu(\infty)|^2,$$

and similarly

$$W_{\text{nucl}} = \sum_k |b_k(\infty)|^2.$$

On the other hand[4]

$$b_\nu(\infty) = G_\nu(E)|_{E=E_\nu}, \qquad b_k(\infty) = G_k(E)|_{E=E_k}.$$

Substituting (21) into (20) we get equations for G_λ, G_ν, and G_k:

$$(E - E_\lambda) G_\lambda = \sum_\nu H^{(\gamma)}_{\lambda\nu} \zeta(E - E_\nu) G_\nu + \sum_k H^{(\text{nucl})}_{\lambda k} \zeta(E - E_k) G_k + C_{\lambda p},$$

$$G_\nu = \sum_\lambda H^{(\gamma)}_{\nu\lambda} G_\lambda, \qquad G_k = \sum_\lambda H^{(\text{nucl})}_{k\lambda} G_\lambda, \quad (22)$$

where

$$H^{(\gamma)}_{\lambda\nu} = \langle \Psi_\lambda | H_\gamma | \Phi_\nu \rangle = C_{\lambda p} \langle \varphi_p | H_\gamma | \varphi_s \rangle = C_{\lambda p} H_\nu,$$

$$H^{(\text{nucl})}_{\lambda k} = \langle \Psi_\lambda | H_{\text{nucl}} | \Phi_k \rangle = \sum_c C_{\lambda c} \langle \psi_c | H_{\text{nucl}} | \Phi_k \rangle = \sum_c C_{\lambda c} H_{ck}.$$

We shall assume that H_ν is independent of the energy E_ν in an interval $\Gamma_\gamma + \Gamma_{\text{n.r.}}$. This assumption is satisfied, since $\Gamma_\gamma + \Gamma_{\text{n.r.}} \ll E_p$. Similarly, $H_{c,k}$ is independent of E_k. G_ν and G_k are then also independent of E_ν and E_k and the indices ν and k are merely indicators of the channel through which the muon-nucleus system has decayed. Using this assumption one can easily evaluate the sums over ν and k in (22). Eliminating G_λ we get a set of equations for G_k and G_ν

$$G_\nu \left[1 + i\frac{\Gamma_\gamma}{2} \sum_\lambda \frac{C^2_{\lambda p}}{E - E_\lambda}\right] + G_k \left[i\pi H^*_\nu \rho_k \sum_{\lambda,c} \frac{C_{\lambda p} C_{\lambda c} H_{ck}}{E - E_\lambda}\right] = H^*_\nu \sum_\lambda \frac{C^2_{\lambda p}}{E - E_\lambda},$$

$$G_\nu \left[i\pi H_\nu \rho_\nu \sum_{\lambda,c} \frac{C_{\lambda p} C^*_{\lambda c} H^*_{ck}}{E - E_\lambda}\right] + G_k \left[1 + i\frac{\Gamma_{\text{nucl}}}{2} \sum_{\lambda,c} \frac{C^2_{\lambda,c}}{E - E_\lambda}\right] = \sum_{\lambda c} \frac{C_{\lambda p} C^*_{\lambda c} H^*_{ck}}{E - E_\lambda}, \quad (23)$$

where $\Gamma_\lambda = 2\pi |H_\nu|^2 \rho_\nu$, $\Gamma_{nucl} = 2\pi \overline{|H_{ck}|^2} \rho_k$; ρ_ν and ρ_k are respectively the densities of the final states ν and k.

When solving Eqs. (23) we meet with double sums over c; to evaluate them we assume that the phases of the matrix elements are random. We get then, for instance,

$$\Big|\sum_c C_{\lambda c} H_{ck}\Big|^2 = \sum_c |C_{\lambda c}|^2 |H_{ck}|^2 = \overline{|H_{ck}|^2} \sum_c |C_{\lambda c}|^2,$$

$$\sum_{cc'} C_{\lambda c} C^*_{\lambda' c'} H_{ck} H_{c'k} = \sum_c |H_{ck}|^2 C_{\lambda c} C_{\lambda' c} = \overline{|H_{ck}|^2} (\delta_{\lambda\lambda'} - C_{\lambda\rho} C_{\lambda'\rho}). \quad (24)$$

Indeed, as

$$C_{\lambda c} H_{ck} = V_c H_{ck} C_{\lambda\rho} / (E_\lambda - E_c),$$

the phase of this product is determined by the phase of the product of the matrix elements $\langle \psi_0 | V | \psi_c \rangle \langle \psi_0 | H_{nucl} | \Phi_k \rangle$. On the other hand, the number of effective terms in the sum over c is of the order $\rho\Gamma_{n.r.} \gg 1$ so that already a small change in phase from one level to the next of the order of $\Delta\varphi \sim 1/\rho\Gamma_{n.r.} \ll 1$ reduces the sum of the cross terms to zero. In that approximation we get, using (24)

$$G_\nu = H_\nu \left[\sum_\lambda \frac{C^2_{\lambda\rho}}{E - E_\lambda} - i \frac{\Gamma_{nucl}}{2} \sum_{\lambda'\lambda} \frac{C^2_{\lambda\rho}}{(E - E_\lambda)(E - E_{\lambda'})} (\delta_{\lambda\lambda'} - 1) \right]$$
$$\times \left[1 + \frac{\Gamma_\nu \Gamma_{nucl}}{4} \sum_{\lambda\lambda'} \frac{C^2_{\lambda\rho}}{(E - E_\lambda)(E - E_{\lambda'})} (\delta_{\lambda\lambda'} - 1) + \frac{i}{2} \sum_\lambda \frac{\Gamma_\gamma C^2_{\lambda\rho} + \Gamma_{nucl}}{E - E_\lambda} \right]^{-1},$$

$$G_k = \left[\sum_{\lambda c} \frac{C_{\lambda\rho} C_{\lambda c} H_{ck}}{E - E_\lambda} \right] \left[1 + \frac{\Gamma_\gamma \Gamma_{nucl}}{4} \sum_{\lambda\lambda'} \frac{C^2_{\lambda\rho}}{(E - E_\lambda)(E - E_{\lambda'})} (\delta_{\lambda\lambda'} - 1) + \frac{i}{2} \sum_\lambda \frac{\Gamma_\gamma C^2_{\lambda\rho} + \Gamma_{nuc}}{E - E_\lambda} \right]^{-1}. \quad (25)$$

We get thus for the probability that the muon-nucleus system decays through nuclear channels

$$W_{nucl} = \frac{\Gamma_{nucl}}{2\pi} \int_{-\infty}^{+\infty} dE \left[\sum_\lambda \frac{C^2_{\lambda\rho}}{(E - E_\lambda)^2} - \left(\sum_\lambda \frac{C^2_{\lambda\rho}}{E - E_\lambda} \right)^2 \right]$$
$$\times \left\{ \left[1 + \frac{\Gamma_\gamma \Gamma_{nucl}}{4} \sum_{\lambda\lambda'} \frac{C^2_{\lambda\rho}}{(E - E_\lambda)(E - E_{\lambda'})} (\delta_{\lambda\lambda'} - 1) \right]^2 + \frac{1}{4} \left(\sum_\lambda \frac{\Gamma_\gamma C^2_{\lambda\rho} + \Gamma_{nucl}}{E - E_\lambda} \right)^2 \right\}^{-1}. \quad (26)$$

We obtain for W_γ a more complicated integral; we evaluate therefore only W_{nucl} and we find W_γ from the normalization condition $W_\gamma = 1 - W_{nucl}$.

One can evaluate the sums over λ occurring in (26), but the integrand we obtain then is too complicated for immediate integration. To evaluate (26) we break up the path of integration into sections about each value E_{λ_0} as shown in Fig. 1.

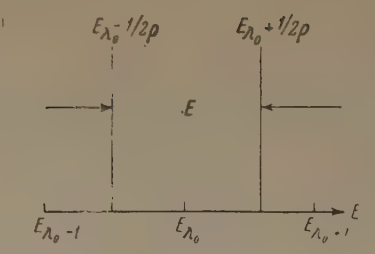

FIG. 1

The integrand in each such section is appreciably simpler than the general expression (26). After first evaluating the integral along this section as a function of E_{λ_0} we sum then over all such sections.

Using (16) we get*

$$\sum_\lambda \frac{C^2_{\lambda\rho}}{E - E_\lambda} = \frac{E - E_\rho + 1/2\,\Gamma_{n.r.} \operatorname{ctg} \pi\rho (E - E_\rho)}{(E - E_\rho)^2 + (1/2\,\Gamma_{n.r.})^2}. \quad (27)$$

Along the above-mentioned interval around E_{λ_0} we write (27) in the form

$$\sum_\lambda \frac{C^2_{\lambda\rho}}{E - E_\lambda} = \frac{2\pi\rho}{\Gamma_{n.r.}} C^2_{\lambda_0\rho} \frac{(E_{\lambda_0} - E_\rho) + (E - E_{\lambda_0}) + 1/2\,\Gamma_{n.r.} \operatorname{ctg} \pi\rho (E - E_{\lambda_0})}{1 + 2\pi\rho C^2_{\lambda_0\rho} [(E - E_{\lambda_0})^2 + 2 (E - E_{\lambda_0})(E_{\lambda_0} - E_\rho)]/\Gamma_{n.r.}}. \quad (28)$$

The second term in the denominator of (28) is less than or of the order of magnitude of $1/\rho\Gamma_{n.r.} \ll 1$. Neglecting that term compared to unity and introducing for the sake of simplicity the notation $x = E_\lambda - E_\rho$, $y = E_{\lambda_0} - E_\rho$, we get

$$\sum_\lambda \frac{C^2_{\lambda\rho}}{E - E_\lambda} = \frac{2\pi\rho}{\Gamma_{n.r.}} C^2_{\lambda_0\rho} \left(x + y + \frac{\Gamma_{n.r.}}{2} \operatorname{ctg} \pi\rho x \right). \quad (29)$$

We similarly evaluate the other sums near $E = E_{\lambda_0}$:

$$\sum_\lambda (E - E_\lambda)^{-1} = \pi\rho \operatorname{ctg} \pi\rho x,$$
$$\sum_\lambda C^2_{\lambda\rho} / (E - E_\lambda)^2 = \pi^2 \rho^2 C^2_{\lambda_0\rho} (1 + \operatorname{ctg}^2 \pi\rho x). \quad (30)$$

We take further into account that $2x/\Gamma_{n.r.} \times \cot \pi\rho x \ll 1$ in the above mentioned interval of integration everywhere except where $x \gtrsim (1/2\rho) \times (1 - 2/\pi\rho\Gamma_{n.r.})$, since the integrand in (26) is essentially positive and has its minimum value in the given interval for $x = \pm 1/2\rho$; we can thus neglect x in (29). The error introduced then is of the order of $1/\rho\Gamma_{n.r.} \ll 1$. Substituting (29) and (30) into (26), we perform the substitution $\xi = \tan \pi\rho x$ and change from a sum over λ_0 to an integral

$$\sum_{\lambda_0} \to \int \rho dE_{\lambda_0} = \frac{1}{2} \rho\Gamma_{n.r.} \int_{-\infty}^{+\infty} dt, \qquad t = 2 \frac{E_{\lambda_0} - E_\rho}{\Gamma_{n.r.}}. \quad (31)$$

We have then

*ctg = cot

$$W_{\text{nucl}} = \frac{\pi\rho\Gamma_{\text{nucl}}}{2}\frac{1}{\pi^2}\int\int_{-\infty}^{+\infty} dt\, d\xi\, (t^2+1)$$

$$\times\left\{\left[\left(1+t^2+\frac{\Gamma_\gamma}{\Gamma_{\text{n.r.}}}\frac{\pi\rho\Gamma_{\text{nucl}}}{2}\right)\xi-\frac{\Gamma_\gamma}{\Gamma_{\text{n.r.}}}\frac{\pi\rho\Gamma_{\text{nucl}}}{2}\,t\right]^2\right.$$

$$\left.+\left[\frac{\Gamma_\gamma}{\Gamma_{\text{n.r.}}}(t\xi+1)+\frac{\pi\rho\Gamma_{\text{nucl}}}{2}(t^2+1)\right]^2\right\}^{-1}. \quad (32)$$

Using the theory of residues one can easily evaluate the integrals in (32). We obtain finally

$$W_{\text{n.r.}} = \left[1+\frac{\Gamma_\gamma}{\Gamma_{\text{n.r.}}}\frac{1+(\pi\rho\Gamma_{\text{nucl}}/2)^2}{\pi\rho\Gamma_{\text{nucl}}/2}+\left(\frac{\Gamma_\gamma}{\Gamma_{\text{n.r.}}}\right)^2\right]^{-1/2}, \quad (33)$$

and for the ratio (1)

$$\frac{W_\gamma}{W_{\text{nucl}}} = \left[1+\frac{\Gamma_\gamma}{\Gamma_{\text{n.r.}}}\frac{1+(\pi\rho\Gamma_{\text{nucl}}/2)^2}{\pi\rho\Gamma_{\text{nucl}}/2}+\left(\frac{\Gamma_\gamma}{\Gamma_{\text{n.r.}}}\right)^2\right]^{1/2}-1. \quad (34)$$

When the condition

$$\Gamma_{\text{n.r.}} \gg \Gamma_\gamma/\rho\Gamma_{\text{n.r.}} \quad (35)$$

is fulfilled we get from (34)

$$W_\gamma/W_{\text{nucl}} = \Gamma_\gamma/\Gamma_{\text{n.r.}}\pi\rho\Gamma_{\text{nucl}}. \quad (36)$$

This result is the same as the result obtained in [2] assuming $\Gamma_{\text{n.r.}} \gg \Gamma_\gamma$. From the calculations given in the foregoing it follows that (35) is a more rigorous criterion for the validity of Eq. (36).

The schematic behavior of the yield of γ quanta from the muon 2p-1s transition as a function of $\rho\Gamma_{\text{nucl}}$ is given in Fig. 2. The behavior of the curve $W_\gamma(\rho\Gamma_{\text{nucl}})$ for $\rho\Gamma_{\text{nucl}} \approx 1$ is interpolated between the values given by (34) for $\rho\Gamma_{\text{nucl}} \ll 1$ and the value $\Gamma_\gamma/(\Gamma_\gamma+\Gamma_{\text{n.r.}})$ for $\rho\Gamma_{\text{nucl}} \gg 1$. It is clear from Fig. 2 that the γ-quanta yield for $\rho\Gamma_{\text{nucl}} \approx 1$ differs little from the case where the overlapping of the nuclear levels is complete, in agreement with reference 1. At very small $\rho\Gamma_{\text{nucl}}$ the decrease in the γ-quanta yield during the 2p-1s transition is proportional to $\sqrt{\rho\Gamma_{\text{nucl}}}$.

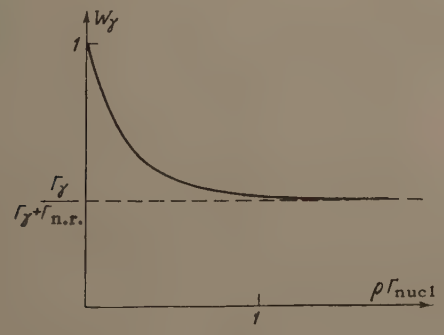

FIG. 2

4. CONCLUSION

Calculations recently performed[3] show that $\Gamma_\gamma \sim \Gamma_{\text{n.r.}}$ for all nuclei in the region Th, U, and Pu. From (34) it is clear that for such a ratio of widths the dependence of the γ-quanta yield on $\rho\Gamma_{\text{nucl}}$ for one muon at rest is weak. For instance, when $\Gamma_\gamma = \Gamma_{\text{n.r.}}$ a change in $\pi\rho\Gamma_{\text{nucl}}/2$ from 0.1 to 0.5 leads to an increase in W_γ from 0.71 to 0.79. The dependence of W_γ on $\rho\Gamma_{\text{nucl}}$ can be more important only in the case when $\Gamma_{\text{n.r.}} \gg \Gamma_\gamma/\rho\Gamma_{\text{nucl}}$.

Experimental results obtained in reference 5 show that W_γ depends weakly upon $\rho\Gamma_{\text{nucl}}$. This result is in qualitative agreement with theory. A quantitative treatment of the experiments to find $\rho\Gamma_{\text{nucl}}$ will be possible once W_γ is measured more accurately for different nuclei.

In conclusion the authors express their gratitude to B. M. Pontecorvo, M. Ya. Balats, L. G. Landsberg, and L. N. Kondrat'ev for discussing the experimental data.

[1] D. F. Zaretskii, Doklady sovetskikh uchenykh na 2-ĭ Mezhdunarodnoĭ konferentsii po mirnomu ispol'zovaniyu atomnoĭ energii (Contributions of Soviet scientists to the second international conference on the peaceful use of atomic energy) AN SSSR, 1958.

[2] D. F. Zaretsky and V. M. Novikov, Nuclear Phys. **14**, 540 (1960).

[3] V. M. Novikov, JETP **41**, 276 (1961), this issue, p. 198

[4] W. Heitler, Quantum Theory of Radiation, Oxford, 1954.

[5] Balats, Kondrat'ev, Landsberg, Lebedev, Obukhov, and Pontecorvo, JETP **39**, 1168 (1960), Soviet Phys. JETP **12**, 813 (1961).

Translated by D. ter Haar
44

NONADIABATIC CORRECTIONS TO THE ROTATIONAL SPECTRUM OF ATOMIC NUCLEI

Yu. T. GRIN'

Submitted to JETP editor February 4, 1961

J. Exptl. Theoret. Phys. (U.S.S.R.) 41, 222-225 (July, 1961)

We have used a consistent microscopic description to evaluate the $BI^2(I+1)^2$ term in the energy of a rotating system of particles, without taking pair correlations into account. The calculated coefficient B agrees qualitatively with the experimental value.

IT is well known that in the regions $150 < A < 190$ and $A > 226$ the atomic nuclei are deformed and possess rotational excitations along with single-particle and "vibrational" excitations.

In that region, the energies E_I of the rotational states are much smaller than the single-particle and vibrational excitation energies and have the simple form

$$E_I = \hbar^2 I(I+1)/2J + E_0 , \quad (1)$$

where I is the spin of the nucleus, J the moment of inertia, and E_0 a constant. Equation (1) corresponds to the energy of a rotating system calculated up to terms of the order Ω^2, where Ω is the angular rotational velocity.

It is of interest to study the corrections to the energy of the system of higher order in the rotational velocity. One usually obtains such corrections by considering phenomenologically the influence of vibrations on the rotation. They are then of the form

$$E_v = -2I^2(I+1)^2/(\hbar\omega_v)^2 J^3 , \quad (2)$$

where $\hbar\omega_V$ is the average vibrational frequency in the nucleus.

In deformed nuclei, however, the collective excitations with energies of $0.7 - 1.2$ Mev can be called vibrational only under very special conditions, for they are not connected with the vibrations of the surface of the nucleus and are, apparently, bound states of two quasi-particles, as is the case in a spherical nucleus. There is thus no sufficient basis for applying Eq. (2) in this case.

It is of interest to calculate the corrections to the rotational energy of the system, using a consistent microscopic description. To do this we consider particles moving in a self-consistent potential. We shall then neglect the residual interaction between the particles which leads to "pairing off."

We can write the Hamiltonian of a rotating nucleus in the form

$$H = H^0 - \mathbf{M}\Omega , \quad (3)$$

where H is the Hamiltonian in a rotating coordinate system, M the angular momentum, and Ω the angular velocity.

To evaluate the energy of the system we need to know the density matrix which one can easily find from the Green function

$$G(x_1, x_2) = -i\langle\Phi_0|\, T\psi(x_1)\psi^+(x_2)\,|\Phi_0\rangle ,$$

where T is the chronological operator, Φ_0 the ground state wave function, and ψ and ψ^+ are annihilation and creation operators for the particles. The equation for the Green's function is of the form

$$(i\partial/\partial t - H)G = \delta(\mathbf{r}_1 - \mathbf{r}_2) . \quad (4)$$

In particular, it is for a rotating system of the form

$$(i\partial/\partial t - H^0 + M^x\Omega)\, G = \delta(\mathbf{r}_1 - \mathbf{r}_2). \quad (5)$$

If we consider $M^x\Omega$ to be a perturbation, we can easily find G in zeroth approximation. The component $G^0_\lambda(\omega)$ of the expansion of the function G in terms of the eigenfunctions of the Hamiltonian H^0 is of the form[1]

$$G^0_\lambda(\omega) = 1/[\omega - \varepsilon_\lambda + i\delta\theta(\varepsilon_\lambda)], \quad (6)$$

where ϵ_λ are the eigenvalues of the Hamiltonian H^0, and

$$\theta(\varepsilon_\lambda) = \begin{cases} +1, \text{ if } \varepsilon_\lambda - \varepsilon_{\lambda_0} > 0 \\ -1, \text{ if } \varepsilon_\lambda - \varepsilon_{\lambda_0} < 0 , \end{cases}$$

where ϵ_0 is the energy of the Fermi surface.

In successive orders of perturbation theory the corrections to the Green function are of the form

$$G'_{\lambda\lambda'} = G^0_\lambda H'_{\lambda\lambda'} G^0_{\lambda'},$$
$$G''_{\lambda\lambda'} = G^0_\lambda H'_{\lambda\lambda_1} G^0_{\lambda_1} H'_{\lambda_1\lambda'} G^0_{\lambda'},$$
$$\cdots\cdots\cdots\cdots\cdots\cdots$$
$$G^{(4)}_{\lambda\lambda'} = G^0_\lambda H'_{\lambda\lambda_1} G^0_{\lambda_1} H'_{\lambda_1\lambda_2} G^0_{\lambda_2} H'_{\lambda_2\lambda_3} G^0_{\lambda_3} H'_{\lambda_3\lambda'} G^0_{\lambda'} \quad (7)$$

(summation is understood to occur over repeated indices and $H' = M^x\Omega$).

The density matrix is obtained from the relation

$$\rho_{\lambda\lambda'} = \int_C G_{\lambda\lambda'} \frac{d\omega}{2\pi i}, \tag{8}$$

where the contour C consists of the real axis and a semicircle in the upper half-plane. Once we know the density matrix we can easily evaluate the energy of the system, using the formula

$$E = \mathrm{Sp}\, H\rho = \sum_{\lambda\lambda'} H_{\lambda\lambda'}\rho_{\lambda'\lambda}. \tag{9}$$

In the expansion of the energy in terms of the perturbation, odd terms in Ω vanish and we get from (9)

$$E = \sum_\lambda \varepsilon_\lambda \rho^0_\lambda + \sum_\lambda \varepsilon_\lambda \rho''_{\lambda\lambda} + \sum_{\lambda\lambda'} \varepsilon'_{\lambda\lambda'}\rho'_{\lambda'\lambda} + \sum_{\lambda\lambda'} \varepsilon'_{\lambda\lambda'}\rho^{(3)}_{\lambda'\lambda} + \sum_\lambda \varepsilon_\lambda \rho^{(4)}_{\lambda\lambda}. \tag{10}$$

Using Eqs. (6), (7), and (8) we get after simple calculations

$$E = E_0 + \frac{\Omega^2}{2}\sum_{\lambda\lambda'} \frac{|M^x_{\lambda\lambda'}|^2 (n_\lambda - n_{\lambda'})}{\varepsilon_\lambda - \varepsilon_{\lambda'}}$$

$$- \Omega^4 \Bigg[\sum_{\lambda,\lambda_1,\lambda'} \frac{M^x_{\lambda\lambda'} M^x_{\lambda'\lambda} M^x_{\lambda\lambda_1} M^x_{\lambda_1\lambda} n_\lambda}{(\varepsilon_\lambda - \varepsilon_{\lambda_1})^2 (\varepsilon_\lambda - \varepsilon_{\lambda'})}$$

$$- \sum_{\substack{\lambda \\ \lambda_1 \neq \lambda'}} \frac{M^x_{\lambda\lambda'} M^x_{\lambda'\lambda} M^x_{\lambda\lambda_1} M^x_{\lambda_1\lambda} n_{\lambda_1}}{(\varepsilon_\lambda - \varepsilon_{\lambda_1})^2 (\varepsilon_{\lambda_1} - \varepsilon_{\lambda'})} \Bigg], \tag{11}$$

where

$$n_\lambda = \begin{cases} 1, & \varepsilon_\lambda - \varepsilon_0 < 0 \\ 0, & \varepsilon_\lambda - \varepsilon_0 > 0 \end{cases}.$$

Equation (11) gives a general expression for the corrections to the energy of the system arising from the rotation. The quantity E_0 is the internal energy which is independent of the rotation. The term proportional to Ω^2 corresponds to the rotational energy of a rigid body, as we have not taken pair correlations into account.

It has been shown by Migdal[2] that the first sum in (11) is equal to the moment of inertia of a rigid body. The term proportional to Ω^4 is the correction we are looking for. To evaluate it we use a simple model of a deformed axially-symmetric oscillating nuclear potential

$$U = \tfrac{1}{2} m [\omega_x^2 (x^2 + y^2) + \omega_z^2 z^2].$$

Then the operator $\dot{M}^x = m(\omega_y^2 - \omega_z^2) yz$. The matrix element $\dot{M}^x_{\lambda\lambda'}$, is different from zero for the transitions $n'_x = n_x \pm 1$, $n'_y = n_y \pm 1$. In the semiclassical approximation all possible values of $\dot{M}^x_{\lambda\lambda'}$, are the same.

One sees easily that

$$\sum_{\lambda\lambda'} |f_{\lambda\lambda'}|^2 \frac{(n_\lambda - n_{\lambda'})}{(\varepsilon_\lambda - \varepsilon_{\lambda'})} = \sum_{\lambda\lambda'} |f_{\lambda\lambda'}|^2 \delta(\varepsilon_\lambda), \tag{12}$$

as long as $|f_{\lambda\lambda'}|^2$ changes little in the interval $(\epsilon_\lambda - \epsilon_{\lambda'})$.

By evaluating the sum over the intermediate states λ_1 and λ' one can then show that in the semiclassical approximation the first sum within the square brackets in (11) is equal to

$$\frac{1}{8d_1^6}\sum_\lambda [(\dot{M}^2)_{\lambda\lambda}]^2 \delta(\varepsilon_\lambda), \tag{13}$$

where $d_1 = \omega_x - \omega_z = \omega_0\beta$, where ω_0 is the average oscillator frequency and β the deformation.

One can show similarly that the second sum within the square brackets in (11) is equal to

$$\frac{1}{16d_1^6}\sum_\lambda [(\dot{M}^2)_{\lambda\lambda}]^2 \delta(\varepsilon_\lambda). \tag{14}$$

One verifies easily by a direct calculation that in the same semiclassical approximation

$$\sum_{\lambda'} (\dot{M}^2)_{\lambda\lambda'} (\dot{M}^2)_{\lambda'\lambda} = (\dot{M}^4)_{\lambda\lambda} = 4(\dot{M}^2)^2_{\lambda\lambda}. \tag{15}$$

Using Eqs. (13), (14), and (15) we get then

$$E^{(4)} = -\frac{\Omega^4}{2^6 d_1^6}\sum_\lambda (\dot{M}^4)_{\lambda\lambda}\delta(\varepsilon_\lambda). \tag{16}$$

On the other hand,

$$\sum_\lambda (\dot{M}^4)_{\lambda\lambda}\delta(\varepsilon_\lambda) = (\omega_x^2 - \omega_z^2)\int \rho(\varepsilon_0, \mathbf{r})(yz)^4\, dV, \tag{17}$$

where

$$\rho(\varepsilon_0, \mathbf{r}) = \sum_\lambda \varphi^*_\lambda(\mathbf{r})\varphi_\lambda(\mathbf{r})\delta(\varepsilon_\lambda)$$

is the density of particles with energy ϵ_0. In the semiclassical approximation the particle density is

$$\rho(\varepsilon_0, \mathbf{r}) = 3mC\sqrt{2m(\varepsilon_0 - U)}, \tag{18}$$

where C is a constant.

We express the sum (17) in terms of the moment of inertia and the total level density at the Fermi surface $\rho_0(\epsilon_0) = \int \rho(\epsilon_0, \mathbf{r})\, dV$. Evaluating the density and the moment of inertia, we get

$$\rho_0 = 3C\pi^2\varepsilon_0^2/\omega_{0s}^3 \qquad J_0 = C\pi^2\varepsilon_0^4/2\omega_0^5, \tag{19}$$

$$\sum_\lambda (\dot{M}^4)_{\lambda\lambda}\delta(\varepsilon_\lambda) = \frac{2^3\cdot 3^3\cdot d_1^4 J_0^2}{5\rho_0}. \tag{20}$$

Substituting Eq. (20) into (16), and taking into account that $\Omega^2 = I(I+1)J_0^2$ we find

$$E^{(4)} = -\frac{9}{40\rho_0 J_0^2 d_1^2} I^2 (I+1)^2. \tag{21}$$

The coefficient in front of $I^2(I+1)^2$ in the expansion of the energy of the system is usually denoted by B. Comparing the coefficient B obtained from Eq. (21) with B_V from (2), we get

$$B/B_v \sim (\hbar\omega_v)^2 J_0/\rho_0 d_1^2. \quad (22)$$

The energy of the "vibrational" levels in a deformed nucleus is about 0.7 — 1 Mev, i.e., of the order of the energy required to break up a pair amounts to $\sim \epsilon_0 A^{-2/3}$. Since $J_0 \sim A^{5/3}/\epsilon_0$, $\rho_0 \sim A/\epsilon_0$, and $d_1 \sim \epsilon_0 A^{-2/3}$, we have $B/B_V \sim A^{2/3}$.

The formula thus yields for the energy correction arising from the coupling of the rotation to the single-particle motion an appreciably larger value than the phenomenological correction connected with the vibrations. Numerically, they turn out to be very close to one another.

When the deformation decreases, B increases, as in this model $B \sim \beta^{-2}$. A similar tendency is observed experimentally. The criterion for the applicability of perturbation theory is the condition $\beta \gg A^{-2/3}$. The theory developed here is thus applicable in the region of stable deformations where $\beta \sim A^{-1/3}$.

Let us estimate the average numerical value of the coefficients B. For the rare-earth region $h^2/J_0 \approx 13$ kev, d = 2 Mev, and $\rho_0 = 3A/2\epsilon_0 \approx 7$ Mev^{-1}. It follows then from Eq. (21) that $B_{theor} \sim 2 \times 10^{-3}$ kev, while $B_{exp} \sim 10 \times 10^{-3}$ kev. For the region of the heavy elements $h^2/J_0 = 7.4$ kev, d = 1.7 Mev, $\rho_0 \approx 10$ Mev^{-1}, and $B_{theor} \sim 0.5 \times 10^{-3}$ kev, $B_{exp} \sim 4 \times 10^{-3}$ kev.

To obtain quantitative agreement between theory and experiment it is necessary to take into account the effects of pair correlation and for small deformation also the presence of collective excitations; this will be done in subsequent papers.

[1] V. M. Galitskii and A. B. Migdal, JETP **34**, 139 (1958), Soviet Phys. JETP **7**, 96 (1958).

[2] A. B. Migdal, JETP **37**, 249 (1959), Soviet Phys. JETP **10**, 176 (1960).

Translated by D. ter Haar
45

REFLECTION OF ELECTROMAGNETIC WAVES IN GYROTROPIC MEDIA FROM A MAGNETIC-FIELD WAVE

G. I. FREĬDMAN

Radiophysics Institute, Gor'kii State University

Submitted to JETP editor February 6, 1961

J. Exptl. Theoret. Phys. (U.S.S.R.) 41, 226-233 (July, 1961)

We consider reflection of electromagnetic waves in a ferrite or in an infinite homogeneous plasma from a magnetic-field wave (moving magnetic "mirror"), and also reflection from a moving plasma and from an ionization wave produced in a stationary plasma. The calculations are made in the geometric optics approximation, and a more exact solution is found near the point at which this approximation becomes invalid. It is shown that in all cases considered the frequency increases upon reflection. The wave amplitude and total energy of the wave packet also increase after reflection; an exception is reflection from an ionization wave, for which the amplitude of the reflected wave is equal to the amplitude of the incident wave and the total energy of the wave packet decreases upon reflection.

INTRODUCTION

THE increase in frequency and amplitude, occurring when electromagnetic waves are reflected from a plasma moving in a medium with dielectric constant $\epsilon > 1$, were discussed by Lampert[1] and by Feĭnberg and Tkalich.[2] Zagorodnov et al[3] reported an experiment in which an increase in frequency was observed when electromagnetic waves were reflected from a plasma moving inside a helical transmission line.

An analogous effect can be obtained by using the dependence of the effective dielectric constant or permeability of certain types of electromagnetic waves, propagating in a plasma or in a ferrite, on the magnetic field intensity. For example, the effective dielectric constant for a right-hand polarized plane wave, propagating in a plasma along the direction of the magnetic field, is

$$\varepsilon_{\text{eff}} = \varepsilon[\omega^2 - (\omega_{\text{pl}}^2 + \omega\omega_H)]/\omega\,(\omega - \omega_H). \qquad (1)$$

Here $\omega_{\text{pl}}^2 = 4\pi e^2 N/\epsilon m$ is the square of the plasma frequency, $\omega_H = eH_0/cm$ the Larmor frequency, N the electron density, H_0 the intensity of the magnetic field, e the absolute value of the electron charge, and ϵ the dielectric constant of the medium in which the plasma is situated. The expression for the effective dielectric constant of waves with left-hand polarization differs in the sign of ω_H from expression (1) for right-hand polarized waves.

It is seen from (1) that ϵ_{eff} can be negative not only in a region with sufficiently high electron density, but also in a region with sufficient magnetic field intensity. Consequently, such a region, like a region with large electron concentration, can serve as a mirror for an electromagnetic wave with right-hand polarization; a "mirror" for left-hand polarized waves will be a region where the magnetic field intensity H_0 decreases.

It is also easy to verify that a region with increasing magnetization field intensity can serve as a mirror for several types of waves propagating in a ferrite. For example, quasi-transverse waves in a two-dimensional waveguide (Fig. 1)

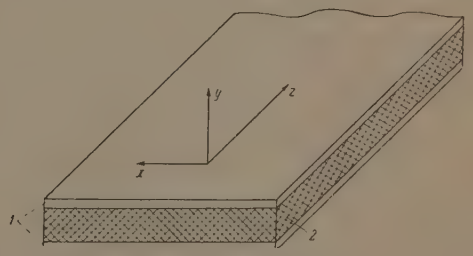

FIG. 1. Two-dimensional waveguide; 1 – perfectly conducting plates, 2 – ferrite.

filled with ferrite and right-hand polarized waves in a homogeneous unbounded ferrite will be reflected from the region where

$$0 < \omega - 4\pi M\gamma < \gamma H_0,$$

for the effective magnetic permeability for these waves will be negative in this region[4] (here γ is the absolute value of the gyromagnetic ratio for the electron spin, and M is the saturation magnetization of the ferrite).

By producing fields that vary in space and in time, it is possible to obtain "mirrors" moving with high velocities, and consequently increase the frequency greatly.* However, reflection from such a moving "mirror" has certain features distinguishing it from reflection from regions where the magnetic field is constant in time. We consider in the present paper the reflection of quasi-transverse waves in a two-dimensional waveguide filled with ferrite, and of right-polarized waves in an unbounded plasma, from the traveling wave of a longitudinal magnetic field. For comparison, we consider the reflection of electromagnetic waves from a plasma moving in a medium with $\epsilon > 1$, and from an ionization wave produced in a stationary plasma.

REFLECTION OF QUASI TRANSVERSE WAVES IN A TWO DIMENSIONAL WAVEGUIDE FILLED WITH A FERRITE, FROM THE WAVE OF THE MAGNETIZATION FIELD

It follows from the results of Suhl and Walker[4] that when a two-dimensional waveguide filled with a ferrite magnetized to saturation is sufficiently thin, the components of the field of the quasi-transverse wave can be regarded as being independent of the transverse coordinates, except when the frequency is close to a certain critical value:†

$$\omega_{cr} = \gamma \sqrt{H_0 (H_0 + 4\pi M)}.$$

This, obviously, remains valid also when the magnetization field H_0 varies sufficiently slowly in time and in the coordinate z along which the wave propagates. In this approximation, the problem of the propagation of quasi-transverse waves is one-dimensional, and Maxwell's equations as well as the equation for the magnetization vector can be readily reduced to the form

$$\frac{\partial^2 h_x}{\partial z^2} = \frac{\varepsilon}{c^2}\left[\frac{\partial^2 h_x}{\partial t^2} - \omega_M \omega_B h_x + \omega_0 \omega_B m_x + \frac{1}{\omega_B}\frac{\partial \omega_B}{\partial t}\frac{\partial m_x}{\partial t}\right],$$

$$h_y = -m_y, \qquad e_x = e_z = 0, \qquad \frac{\partial e_y}{\partial t} = \frac{c}{\varepsilon}\frac{\partial h_x}{\partial z};$$

$$\frac{\partial m_x}{\partial t} = -\omega_B m_y, \qquad \frac{\partial m_y}{\partial t} = -\omega_M h_x + \omega_0 m_x. \tag{2}$$

It is assumed here that the dissipative term in the equation for the magnetization vector vanishes, the magnetization field $\mathbf{H_0}(t, z)$ has only a longitudinal component $H_{0Z} = H_0(t, z)$, and the y axis is perpendicular to the walls of the two-dimensional waveguide (see Fig. 1). In addition, the following notation is used

$$m_x = 4\pi M_x, \qquad m_y = 4\pi M_y, \qquad \omega_0 = \gamma H_0,$$
$$\omega_M = \gamma 4\pi M, \qquad \omega_B = \omega_0 + \omega_M;$$

M is the magnetization vector.

If $H_0(t, z)$ is a sufficiently slow function, the propagation of quasi-transverse waves can be investigated by the method of geometric optics.[8-10] We seek the solution in the form

$$h_x = (h_0 + h_1 + \ldots) e^{i\psi}, \qquad \mathbf{m} = (\mathbf{m}_0 + \mathbf{m}_1 + \ldots) e^{i\psi},$$
$$e_y = (e_0 + e_1 + \ldots) e^{i\psi}, \tag{3}$$

where $h_0 \gg h_1 \gg \ldots$; $|\mathbf{m}_0| \gg |\mathbf{m}_1| \gg \ldots$; $e_0 \gg e_1 \gg \ldots$ and $\partial\psi/\partial t$ and $\partial\psi/\partial z$ are slow functions compared with the eikonal ψ.

The equations obtained from (2) and (3) for the eikonal ψ and for the successive approximations of the field amplitudes can be readily integrated in quadratures, if the magnetization field has the form of a wave traveling at a constant velocity V along the z axis, i.e., if $H_0(t, z)$ depends only on the quantity $\xi = Vt - z$. In this case the field amplitude depends only on ξ, and we have, in particular, in the zeroth approximation

$$h_0 = h_0(-\infty)\left[\psi_z + \beta\frac{\sqrt{\varepsilon}}{c}\psi_t\left(1 + \frac{\omega_0}{\omega_M}\chi^2\right)\right]_{-\infty}^{1/2}$$
$$\times\left[\psi_z + \beta\frac{\sqrt{\varepsilon}}{c}\psi_t\left(1 + \frac{\omega_0}{\omega_M}\chi^2\right)\right]_{\xi}^{-1/2}$$
$$\times\exp\left\{\frac{1}{2}\beta\frac{\sqrt{\varepsilon}}{c}\int_{-\infty}^{\xi}\psi_t\frac{\omega_M(\omega_B^2 + \psi_t^2)}{(\psi_t^2 - \omega_0\omega_B)^2}\right.$$
$$\left.\times\left[\psi_z + \beta\frac{\sqrt{\varepsilon}}{c}\psi_t\left(1 + \frac{\omega_0}{\omega_M}\chi^2\right)\right]^{-1}\frac{d\omega_B}{d\xi}d\xi\right\},$$

$$\beta = V\sqrt{\varepsilon}/c, \quad \chi = m_{x0}/h_0 = -\omega_M\omega_B/(\psi_t^2 - \omega_0\omega_B). \tag{4}$$

The wave number ψ_z and the frequency ψ_t also depend only on ξ, and are determined from the equations

$$\psi_z^2 = \frac{\varepsilon}{c^2}\psi_t^2\frac{\psi_t^2 - \omega_B^2}{\psi_t^2 - \omega_0\omega_B}, \qquad \psi_z = \frac{\psi_{t0} - \psi_t}{V}, \tag{5}$$

while the eikonal ψ is equal to

$$\psi = -\int_{\xi_0}^{\xi}\psi_z(\xi)\,d\xi + \psi_{t0}t. \tag{6}$$

Here ψ_{t0} is an arbitrary integration constant, equal to the frequency at the point where $\psi_z = 0$; ξ_0 is an arbitrary constant.

Let us examine the case when an electromagnetic wave with initial frequency $\psi_{t;1}(-\infty)$, satisfying the condition $\psi_{t;1}(-\infty) > \omega_B(-\infty)$, propagates in a direction opposite to the wave of the

*It can be shown that in a two-dimensional waveguide and in an unbounded ferrite, such a 'mirror' can be a shock electromagnetic wave[5,6] with front duration longer than the period of the incident wave. If the duration of the front of the shock wave is shorter than the period of the incident weak electromagnetic wave, no reflection can take place.[7]

†It should be noted that [4] states erroneously that $\omega_{cr} = \gamma H_0$.

magnetization field, which is a monotonically increasing function of ξ. Analyzing the properties of the solutions of (5), we readily see that the frequency $\psi_{t;1}$ increases with increasing ξ, i.e., with increasing magnetization field, while the wave number $\psi_{z;1}$ decreases, vanishing at a point ξ_1 determined from the condition $\psi_{t;1}(\xi_1) = \psi_{t0} = \omega_B(\xi_1)$.

When $\beta = 0$, i.e., when the magnetization field is independent of the time, the geometric optics is no longer valid in the vicinity of this point. However, if $\beta > 0$ and $H_0(\xi)$ is a sufficiently slow and smooth function, the first approximation in the vicinity of ξ_1 remains much smaller than the zeroth approximation, since $h_1/h_0 \sim (dH_0/d\xi)^2$, $d^2H_0/d\xi^2$, and the proportionality coefficients remain finite in ξ_1 when $\beta > 0$. Consequently, geometric optics still applies at this point,* although the sign of the wave number, and consequently the direction of the phase and group velocities, does change (Fig. 2). The group velocity, however, is smaller than the V. The electromagnetic wave can therefore again be regarded as incident relative to the magnetization-field wave.

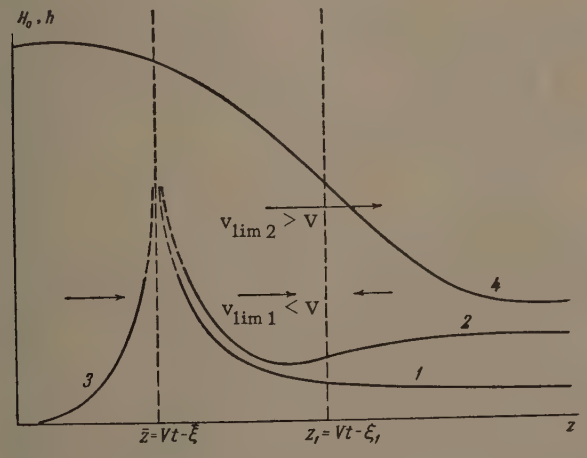

FIG. 2. Amplitudes of the magnetic fields of the incident (1), reflected (2), and refracted (3) waves and of the magnetization field H_0 (4), as functions of z at the instant t. The arrows show the direction of the energy, averaged over the period of the flux, in various regions of space.

When $0 < \beta < 1$, geometric optics does not hold for an arbitrarily slow variation of $H_0(\xi)$ in the vicinity of the point $\bar{\xi}$ where $d\psi_t/d\xi = \infty$, and the group velocity is equal to V. The frequency $\bar{\psi}_t$, the wave number $\bar{\psi}_z$, and the coordinate $\bar{\xi}$ of this point, from which we shall henceforth measure ξ, are determined from (5) and from

$$\bar{\psi}_z + \beta(\sqrt{\varepsilon}/c)\bar{\psi}_t(1 - \omega_0\chi^2/\omega_M) = 0. \qquad (7)$$

The vicinity of $\bar{\xi}$ reflects a wave whose group velocity is greater than the velocity of the magnetization-field wave. We shall henceforth call this the reflected wave. As $\beta \to 1$, the reflected wave appears only when the maximum value of the magnetization field tends to infinity. When $\beta \geq 1$, there can be no reflected wave, and the field at any point is described by formulas (4) — (6), which in this case have for $\omega_{inc} > \omega_B(-\infty)$ only one solution, describing a wave incident with respect to the magnetization-field wave.

To determine the connection between the amplitudes and phases of the incident and reflected waves, we assume, as is usually done,[8,9] that the coefficient of refraction varies linearly in the region where geometric optics is invalid. In the case considered below, it is sufficient for this purpose to put

$$\omega_B = \bar{\omega}_B(1 + 2\alpha\xi). \qquad (8)$$

When $\alpha V \ll \bar{\psi}_t$, a solution of (2) can be sought in the form

$$h_x(t, z) = [h_0(\xi) + h_1(\xi) + \ldots] \exp[i(\bar{\psi}_t t + \bar{\psi}_z z)],$$
$$m(t, z) = [m_0(\xi) + m_1(\xi) + \ldots] \exp[i(\bar{\psi}_t t + \bar{\psi}_z z)],$$
$$e_y(t, z) = [e_0(\xi) + e_1(\xi) + \ldots] \exp[i(\bar{\psi}_t t + \bar{\psi}_z z)]. \qquad (9)$$

Here $|h_0| \gg |h_1| \gg \ldots$; $|m_0| \gg |m_1| \gg \ldots$; $|e_0| \gg |e_1| \gg \ldots$ are slowly varying functions, so that $|\partial m_0/\partial t| \ll |\psi_t m_0|$ and so on, but their second derivatives cannot be regarded as small.

We restrict ourselves to a case when the magnetization-field wave velocity is so high that $0 < (1-\beta) \ll 1$. We then obtain in the zeroth approximation the following equation for the amplitude of the magnetic field

$$d^2h_0/d\eta^2 - (2\alpha\bar{\psi}^2/\beta^2)^{-2}\eta h_0 = 0, \quad \eta = 2\alpha(\psi_z^2\xi/\beta^2 - i\bar{\psi}_z), \qquad (10)$$

the solution of which has the form[8,9]

$$h_0(\xi) = A(2\alpha\bar{\psi}_z^2/\beta^2)^{-1/3}\Phi[(2\alpha\bar{\psi}_z^2/\beta^2)^{-2/3}\eta]. \qquad (11)$$

Here Φ is the Airy function. From the properties of this function[8,9] it is seen that when $\xi > 0$ the amplitude of the refracted wave is a damped function, which for large ξ is proportional to*

$$\exp\left\{-\frac{\sqrt{\varepsilon}}{c}\int_0^{\xi}\left[(1-\beta^2)\omega_M\omega_0 - \psi_{t0}^2\right]^{1/2}\frac{d\xi}{1-\beta^2}\right\}.$$

From a comparison of (11) with the solution (4) — (6), in the approximation of geometric optics, it is seen that when ξ is negative and large in absolute value, the field is a sum of the incident and reflected waves $h_{0;1}$ and $h_{0;2}$ respectively:

*This can be seen also from the fact that the point ξ_1 has no singularities in a coordinate system moving with velocity V.

*The refracted wave is described, apart from a constant factor, by formulas (12) and (14), where the index used is 1.

$$h_{0;\,1,2} = \mp h_{1,2}\left\{\frac{[\psi_{z;\,1,2} + \beta(\sqrt{\varepsilon}/c)\,\psi_{t;\,1,2}(1+\omega_0\chi^2/\omega_B)]_{-\infty}}{[\psi_{z;\,1,2} + \beta(\sqrt{\varepsilon}/c)\,\psi_{t;\,1,2}(1+\omega_0\chi^2/\omega_B)]_{\xi}}\right\}^{1/2}$$

$$\times \exp\left\{\frac{1}{2}\frac{\beta\sqrt{\varepsilon}}{c}\int_{-\infty}^{\xi}\psi_{t;\,1,2}\,\frac{\omega_M(\omega_B^2+\psi_{t;\,1,2}^2)}{(\psi_{t;\,1,2}^2-\omega_0\omega_B)^2}\right.$$

$$\times\left[\psi_{z;\,1,2}+\frac{\beta\sqrt{\varepsilon}}{c}\psi_{t;\,1,2}\left(1+\frac{\omega_0\chi^2}{\omega_B}\right)\right]^{-1}\frac{d\omega_B}{d\xi}\,d\xi$$

$$\left.+\,i\left(\psi_{1,2}\mp\frac{\pi}{4}\right)\right\};$$

$$e_{0;\,1,2} = (c\psi_{z;\,1,2}/\varepsilon\psi_{t;\,1,2})\,h_{0;\,1,2}, \qquad \psi_{1,2} = -\int_0^{\xi}\psi_{z;\,1,2}\,d\xi + \psi_{t0}t. \tag{12}$$

The ratio of the amplitude of the incident wave (h_1) to the amplitude of the reflected wave (h_2) far ahead of the front of the magnetization-field wave is approximately equal to the ratio of the wave frequencies in this region:

$$h_2/h_1 \approx \psi_{t;\,2}(-\infty)/\psi_{t;\,1}(-\infty). \tag{13}$$

The dependence of the frequency and of the wave numbers on ξ is determined from Eq. (5), which in the case $\omega_0 \ll \psi_t$ can be approximately written in a more convenient form:

$$\psi_{t;\,1,2} = \frac{1}{1-\beta^2}\left\{\psi_{t0}\mp\beta\left[\psi_{t0}^2-(1-\beta^2)\,\omega_B^2\right.\right.$$

$$\times\left.\left(1-\frac{\omega_0}{\omega_B}\left(1-\frac{\omega_B^2}{\chi_{t;\,1,2}^2}\right)\right)^{1/2}\right]\Bigg\},$$

$$\psi_{z;\,1,2} = \frac{\sqrt{\varepsilon}}{c(1-\beta^2)}\left\{-\beta\psi_{t0}\pm\left[\psi_{t0}^2-(1-\beta^2)\,\omega_B^2\right.\right.$$

$$\times\left.\left.\left(1-\frac{\omega_0}{\omega_B}\left(1-\frac{\omega_B^2}{\psi_{t;\,1,2}}\right)\right)\right]^{1/2}\right\}. \tag{14}$$

The square bracket in (14) vanishes at the point of reflection $\bar{\xi}$, and consequently the frequencies and wave numbers of the incident and reflected waves are equal to each other. On going further into the region of weaker magnetization field, the frequency of the incident wave decreases, while that of the reflected wave increases. Consequently, an increase in frequency takes place upon reflection, and, as can be readily verified, this increase obeys the usual Doppler formula. According to (13), the amplitude of the reflected wave increases, as does also the total energy of the reflected wave packet, W_2. Indeed, the energy of the wave packet is proportional to the energy flux density averaged over the period and to the duration of the wave packet, which varies upon reflection as the reciprocal of the frequency. It then follows from (12) – (14) that the ratio of W_2 (total energy of the reflected wave packet) to W_1 (total energy of the incident wave packet) is

$$\frac{W_2}{W_1} = \left(\frac{h_2}{h_1}\right)^2\frac{\psi_{t;\,1}^2(-\infty)\,|\,\psi_{z;\,2}(-\infty)\,|}{\psi_{t;\,2}^2(-\infty)\,|\,\psi_{z;\,1}(-\infty)\,|} \tag{15}$$

and is greater than unity.

REFLECTION OF PLANE ELECTROMAGNETIC WAVES IN UNBOUNDED PLASMA FROM A LONGITUDINAL MAGNETIC-FIELD WAVE, FROM A UNIFORMLY MOVING INHOMOGENEOUS PLASMA, AND FROM AN IONIZATION WAVE IN A STATIONARY PLASMA

For all the three cases mentioned in the heading, Maxwell's equations can be readily written in the form

$$\frac{\partial^2\mathbf{e}}{\partial z^2} - \frac{\varepsilon}{c^2}\frac{\partial^2\mathbf{e}}{\partial t^2} - \frac{4\pi}{c^2}\frac{\partial\mathbf{j}}{\partial t} = 0, \quad \operatorname{rot}\mathbf{e} = -\frac{1}{c}\frac{\partial\mathbf{h}}{\partial t}. \tag{16}*$$

We confine ourselves to a very simple plasma model, without pretending to describe fully the processes occurring in the plasma. Namely, we assume that in the case of reflection from a magnetic field that varies in space and in time, and from a moving plasma, the current density $\mathbf{j}$ is

$$\mathbf{j} = -eN\mathbf{v}. \tag{17}$$

In this equation N is the electron density, which is constant in the former case and depends on $\xi = Vt - z$ in the latter (V is the velocity of motion of the plasma); $\mathbf{v}$ is the forced solution of the equation of motion of the electrons:

$$d\mathbf{v}/dt = -(e/m)\,\mathbf{e} - (e/mc)\,[\mathbf{vH}]. \tag{18}‡$$

In the case of reflection from an ionization wave† it is necessary to take into account the alternating current produced by the uniform motion of the electrons, at a velocity determined by the initial conditions at the instant of ionization. Assuming the initial velocity upon ionization to be equal to zero and replacing the summation by integration we find that in an ionization wave

$$\mathbf{j} = -eN\mathbf{v} + e\int_{-\infty}^{t}\mathbf{v}(t)\,\frac{\partial N}{\partial t}\,dt. \tag{19}$$

Investigating the solution of (16) – (19) by the same method as the solution of (2), we find that far in front of the reflecting point the field is equal to the sum of the fields of the incident and reflected waves ($\mathbf{e}_{0;1}$ and $\mathbf{e}_{0;2}$ respectively).

*rot = curl.

†$[\mathbf{vH}] = \mathbf{v}\times\mathbf{H}$.

‡An ionization wave, namely a moving boundary of a region with increased electron concentration, can be obtained by exposing a stationary gas to ionizing radiation of intensity that varies in space and in time. Obviously, no limitations are imposed on the velocity of the ionization wave.

In reflection from a moving plasma, we confine ourselves to the case of nonrelativistic plasma velocity,* $V \ll c$, so that the effect of the magnetic field of the wave on the electrons can be disregarded, and we can assume $d\mathbf{v}/dt = \partial\mathbf{v}/\partial t$. In reflection from a magnetic-field wave, we consider only a right-hand polarized wave, and also assume that $\omega_H \ll \omega_{pl} < \psi_t$ and $\beta^2 \ll 1$. Then the dependence of the frequencies and wave numbers of the incident and reflected waves on ξ will have in all three cases the following explicit form:

$$\psi_{t;1,2} = \frac{1}{1-\beta^2}\{\psi_{t0} \mp \beta[\psi_{t0}^2 - (1-\beta^2)\omega_{pl}^2 - \psi_{t0}\omega_H]^{1/2}\},$$
$$\psi_{z;1,2} = \frac{\sqrt{\varepsilon}}{c(1-\beta^2)}\{-\beta\psi_{t0} \pm [\psi_{t0}^2 - (1-\beta^2)\omega_{pl}^2 - \psi_{t0}\omega_H]^{1/2}\}. \quad (20)$$

From a comparison of (20) with (14) we see that in all three cases the change in frequency and wave number is qualitatively similar to that in reflection from a magnetization-field wave in a ferrite.

The amplitudes of the incident wave and the wave reflected from a magnetic-field wave vary as

$$e_{0;1,2} = e_{1,2}\left\{\left[\psi_{z;1,2} + \frac{\sqrt{\varepsilon}}{c}\beta(\psi_{t;1,2} + \omega_{pl}^2\omega_H/(\psi_t - \omega_H)^2\right]_{-\infty}\right.$$
$$\times\left.\left[\psi_{z;1,2} + \frac{\sqrt{\varepsilon}}{c}\beta(\psi_{t;1,2} + \omega_{pl}^2\omega_H/(\psi_t - \omega_H)^2)\right]_{\xi}^{-1}\right\}^{1/2}$$
$$\times\exp\left\{\beta\frac{\sqrt{\varepsilon}}{c}\frac{\omega_{pl}^2}{4}\int_{-\infty}^{\xi}\frac{d\omega_H}{d\xi}\left[(\psi_{t;1,2} - \omega_H)^2\right.\right.$$
$$\times\left.\left.\left[\psi_{z;1,2} + \frac{\sqrt{\varepsilon}}{c}\beta\left(\psi_{t;1,2} + \frac{\omega_{pl}^2\omega_H}{(\psi_t - \omega_H)^2}\right)\right]\right]^{-1}d\xi\right\}. \quad (21)$$

The ratio of the amplitudes of these waves at infinity $e_{0;1}(-\infty)/e_{0;2}(-\infty) = e_1/e_2$ is equal in this case to the ratio of the corresponding exponential factors in (21) with an upper integration limit equal to zero. This ratio is less than unity, i.e., the amplitude of the wave increases upon reflection, and, as can be readily shown,† in a way as to increase also the energy of the wave packet.

In reflection from a moving plasma (a) and from an ionization wave in a stationary plasma (b), the amplitudes are determined respectively by the equations

$$e_{0;1,2} = e_{1,2}'\{[\psi_{t0}^2 - (1-\beta^2)$$
$$\times\omega_{pl}^2(-\infty)]/[\psi_{t0}^2 - (1-\beta^2)\omega_{pl}^2(\xi)]\}^{1/4}\varphi(\xi);$$
$$e_2/e_1 = \psi_{t;2}(-\infty)/\psi_{t;1}(-\infty),\quad \varphi = \psi_{t;1,2}(\xi)/\psi_{t;1,2}(-\infty);$$
$$e_2/e_1 = 1,\qquad \varphi = 1. \quad (22)$$

It follows from (12), (13), (21), and (22) that reflections from a magnetization-field wave in a two-dimensional waveguide filled with a ferrite, from a magnetic-field wave in a homogeneous moving plasma, and from a moving inhomogeneous plasma all are qualitatively alike; in addition to increasing the frequency, the reflection increases the amplitude of the reflected wave and the energy of the reflected wave packet.

The increase in energy of the reflected wave packet can be attributed in the first two cases to the fact that the magnetic moment per unit volume of the ferrite, deflected by the high-frequency field from the direction of the magnetizing field (or the magnetic moment of the electron produced by the high-frequency field) is situated in an increasing magnetic field. This increases energy of interaction between these moments and the magnetic field,* and therefore more energy is reradiated than was originally expended by the high-frequency field.

In reflection from an ionization wave, the frequency increases in exactly the same way as in reflection from a moving plasma. The amplitude of the reflected wave, however, is equal to the amplitude of the incident wave, and consequently the energy of the wave packet is decreased by reflection. Part of the energy of the incident wave packet goes into the kinetic energy of uniform motion of the electrons.

The author is grateful to A. V. Gaponov for advice and for a discussion of the manuscript.

*From the equation for the adiabatic invariant[11] it is seen that for an electron this increase is equal to the increase in kinetic energy of its rotational motion.

*At relativistic plasma velocities, a solution in the geometrical-optics approximation was obtained by Ostrovskii.[10]

†In the calculation of the ratio of the energies of the reflected and incident wave packet it is necessary to replace the ratio of the squares of the magnetic-field amplitudes in (15) by the ratio of the squares of the electric-field amplitudes.

[1] M. A. Lampert, Phys. Rev. **102**, 299 (1956).

[2] Ya. B. Faĭnberg and V. S. Tkalich, ZhTF **29**, 491 (1959), Soviet Phys.-Tech. Physics **4**, 438 (1959).

[3] Zagorodnov, Faĭnberg, and Egorov, JETP **38**, 7 (1960), Soviet Phys. JETP **11**, 4 (1960).

[4] H. Suhl and L. Walker, Waveguide Propagation of Electromagnetic Waves in Gyrotropic Media (Russ. Transl.) IIL, 1955.

[5] A. V. Gaponov and G. I. Freĭdman, Izv. Vuzov —Radiofizika **3**, 80 (1960).

[6] G. I. Freĭdman, ibid. **3**, 277 (1960).

[7] L. A. Ostrovskii, ibid. **2**, 833 (1959).

[8] L. D. Landau and E. M. Lifshitz, Electrodynamics of Continuous Media, Pergamon, 1961.

[9] Al'pert, Ginzburg, and Feĭnberg, Rasprostranenie radiovoln (Propagation of Radio Waves), GITTL, 1953.

[10] L. A. Ostrovskii, op. cit. [5] **4**, 293 (1961).

[11] L. D. Landau and E. M. Lifshitz, Classical Theory of Fields, Addison-Wesley, 1951.

Translated by J. G. Adashko
46

NUCLEON CORRELATIONS AND PHOTONUCLEAR REACTIONS. I THE PHOTODISINTEGRATION OF He^4

G. M. SHKLYAREVSKII

Leningrad Physico-Technical Institute, Academy of Sciences, U.S.S.R.

Submitted to JETP editor February 6, 1961

J. Exptl. Theoret. Phys. (U.S.S.R.) **41**, 234-238 (July, 1961)

We consider a model in which pair correlations are taken into account and discuss the photodisintegration of the He^4 nucleus. The available experimental data allow us to estimate the range of the pair correlations r_K^S (S: spin of the correlated pair). In triplet states $r_K^1 \approx (1.3 \text{ to } 1.4)\ 10^{-13}$ cm. We obtain an upper limit for the correlation range in singlet states: $r_K^0 \lesssim r_K^1/3$.

1. One of the directions in which the theory of the nucleus has been developed is via an account of nucleon pair correlations. There are a number of papers[1-3] devoted to this problem. On the other hand, Levinger[4] has some time ago indicated the importance of nucleon correlations for the theory of photonuclear reactions in the high energy region.

Gorbunov[5] has obtained experimental data on the reactions

$$He^4(\gamma, np)\,D, \qquad \text{(A)}$$

$$He^4(\gamma, 2n)\,2p, \qquad \text{(B)}$$

and in particular the cross section for the reaction A and the ratio of the number of cases in which reaction B is observed to the number of cases of reaction A (which is approximately equal to $1/8$). We shall show in the present paper that these experimental data enable us to reach some conclusions about the character of the nucleon correlations in the He^4 nucleus. As the correlation is essentially determined by nucleon-nucleon interactions at small distances, these conclusions can apparently also be applied to other nuclei. We can here note beforehand that the small difference between the cross sections for the reactions B and A indicates that the correlations of nucleon pairs in singlet states is appreciably weaker than in triplet states: our calculations corroborate this assumption.

2. We write the He^4 nucleus wave function in the form

$$\Psi = N \sum_S \prod_{ij} (1 + \chi_{ij}^S \hat{Q}^S)\, \Psi_{IPM}, \qquad (1)$$

where Ψ_{IPM} is the independent particle model wave function, $\hat{Q}^S$ the projection operator into a nucleon pair state with total spin S and vanishing total relative orbital angular momentum; χ_{ij}^S are correlators.

We shall assume that the correlators have the following properties: 1) they are functions of $|\mathbf{r}_i - \mathbf{r}_j|$ only and $\chi_{ij}^S(0) = -1$ corresponding to a strong nucleon-nucleon repulsion at small distances while $\chi_{ij}^S \to 0$ as $r \to \infty$; the distance over which the correlation differs appreciably from zero is called the correlation range; 2) the correlation range may depend on the spin of the correlated nucleon pair; 3) the correlators are independent of the third component of the isotopic spin of the pair in virtue of the charge-independence of the nuclear forces. We shall also assume that the correlators are small, and shall neglect their products with one another. The criterion that they are small is expressed by the inequality

$$\sum_{mn}{}' |c_{\alpha\beta}^{mn}|^2 \ll 1,$$

where the $c_{\alpha\beta}^{mn}$ are the expansion coefficients

$$\chi_{ij}^S \varphi_i^\alpha \varphi_j^\beta = \sum_{mn} c_{\alpha\beta}^{mn} \varphi_i^m \varphi_j^n.$$

The φ_i^α are here the single-particle functions out of which Ψ_{IPM} is constructed; i and j are particle numbers; α and β are their individual quantum numbers.

The function Ψ must be normalized using the condition $|\langle \Psi | \Psi_{IPM} \rangle|^2 = 1$. To evaluate the normalizing factor N we write the two-particle function $\psi_\beta^S(ij) = (1 + \chi_{ij}^S \hat{Q}^S)\, \varphi_i^\alpha \varphi_j^\beta$ in the following form

$$\psi_{\alpha\beta}^S(ij) = (z_{\alpha\beta}^S + \hat{q}\chi_{ij}^S \hat{Q}^S)\, \varphi_i^\alpha \varphi_j^\beta,$$
$$z_{\alpha\beta}^S = 1 + \langle \varphi_i^\alpha \varphi_j^\beta | \chi_{ij}^S \hat{Q}^S | \varphi_i^\alpha \varphi_j^\beta \rangle, \qquad (2)$$

where the operator $\hat{q}$ makes the components of

$\chi_{ij}^S \hat{Q}^S \varphi_i^\alpha \varphi_j^\beta$ which belong to Ψ_{IPM} vanish. When writing it in this form the condition* is satisfied.

$$\langle \varphi_i^\alpha \varphi_j^\beta \mid \hat{q} \chi_{ij}^S \hat{Q}^S \mid \varphi_i^\alpha \varphi_j^\beta \rangle = 0$$

Using the fact that the correlators are small we have

$$N = \left\{ \prod_{S\alpha\beta} z_{\alpha\beta}^S \right\}^{-1} \equiv Z^{-1}$$

and

$$\Psi \approx \Psi_{IPM} + \sum_{ij} \{z_{ij}^S\}^{-1} \hat{q} \chi_{ij}^S \hat{Q}^S \Psi_{IPM}. \qquad (3)$$

We note the resemblance of Eq. (3) with the expression for the wave function in the first order of usual perturbation theory.

3. It is convenient to take as the wave function $\Psi^{(-)}$ of the final state an eigenfunction of the Hamiltonian

$$H_f = \sum_{i=1}^{4} T_i + V_{12} + V_{34},$$

where to fix our ideas the numbers 1 and 2 indicate respectively a proton and a neutron with momenta $\hbar k_1$ and $\hbar k_2$, while the numbers 3 and 4 indicate the proton and the neutron which in reaction A form a deuteron and in reaction B move with some energy of the relative motion $E_{rel} = \hbar^2\kappa^2/2\mu$ ($\mu = m/2$ is the reduced mass). Such a choice of H_f is connected with the fact that the interaction V_{34} which leads to the formation of a deuteron must be taken into account exactly. The remaining part of the interaction

$$V' = \sum_{i>j} V_{ij} - V_{12} - V_{34}$$

can be taken into account approximately but we shall not do that as the correction will only be important near the threshold of the reaction.

We only evaluate the total cross section for the reactions, and restrict ourselves therefore in the operator for the electromagnetic transition H_ζ to the electrical dipole term, i.e., we put

$$H_\zeta \sim \frac{e}{2} \sum_i \nabla_i \zeta \tau_3^i,$$

where ζ is the polarization vector of the γ quantum and τ_3^i the third component of the isotopic spin of the i-th nucleon.

If we separate the motion of the center of mass of the nucleon pairs 1-2 and 3-4 from their relative motion, which is possible when we choose oscillator wave functions,† we get the cross section for the $He^4(\gamma, np)D$ reaction in the following form:*

$$d\sigma^A \sim \tfrac{3}{4} \mid G(K)\, g_0 \overline{g_1}\,(k)\, k\zeta \mid^2 d\mathbf{K}\, d\mathbf{k}, \quad g_0 = \int \varphi_d(r)\, \varphi_{rel}(r)\, dr,$$

$$\widetilde{g}_S(k) = (2\pi)^{-3/2} \int e^{-ikr} \hat{q} \chi^S \hat{Q}^S \varphi_{rel}(r)\, dr, \quad S = 0, 1,$$

$$G(K) = (2\pi)^{-3/2} \int e^{-iKR} \Phi(R)\, dR. \qquad (4)$$

Here φ_d is the deuteron wave function, φ_{rel} the wave function of the relative motion of the nucleon pair, $\mathbf{k} = \frac{1}{2}(\mathbf{k}_1 - \mathbf{k}_2)$, $\mathbf{K} = \mathbf{k}_1 + \mathbf{k}_2$, and $\Phi(R)$ is the wave function of the center of mass of one pair of nucleons in the He^4 nucleus with respect to the other pair. In deriving Eq. (4) we have assumed the phase shift in the p state to be equal to zero.

For a given energy E^A of the incident γ quantum the magnitudes of the momenta $\hbar K$ and $\hbar k$ are connected through the energy conservation law. Integrating (4) over the angles of the vectors K and k and over all values of k possible for a given E^A we obtain the cross section for the reaction A as function of the energy E^A. It is, finally, necessary to give the explicit form of the correlators. The most convenient form for calculations is

$$\chi_{ij}^S = -\exp\{-\beta_S r_{ij}^2\}, \qquad (5)$$

and then the correlation range $r_K^S \approx \beta_S^{-1/2}$. A comparison of the calculated and the experimental cross sections for the $He^4(\gamma, np)D$ reaction (see Fig. 1) enables us to choose $\beta_1 \approx (0.5 \text{ to } 0.6) \times 10^{26}$ cm^{-2} corresponding to a correlation range in the triplet state of $r_K^1 \approx (1.4 \text{ to } 1.3) \times 10^{-13}$ cm. This result corroborates the validity of the assumptions made in Sec. 2 involving the smallness of the correlators.

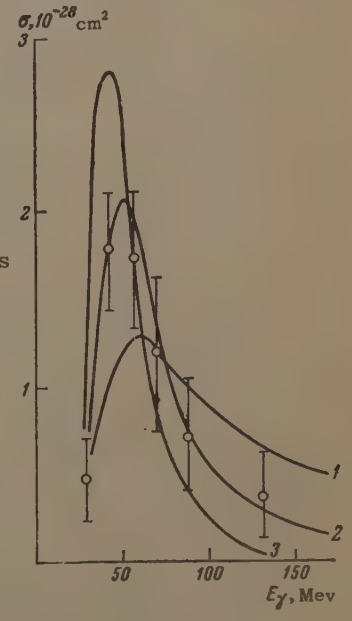

FIG. 1. Total cross section for the $He^4(\gamma, np)D$ reaction. The points are Gorbunov's experimental data[5] and the curves 1, 2, and 3 the theoretical total cross sections for $\beta_1 = 0.7$, 0.5, and 0.3×10^{26} cm^{-2}, respectively.

*One usually puts $\langle \varphi_i^\alpha \varphi_j^\beta \mid \chi_{ij} \mid \varphi_i^\alpha \varphi_j^\beta \rangle = 0$. It is, however, practically impossible to find a function χ_{ij} with arbitrary parameters satisfying this condition.

†The elimination of the center-of-mass motion was performed by the method used by Lipkin.[6]

*For the sake of simplicity we have omitted from Eqs. (4) and (6) the factor $4\{z^S\}^{-2}(e^2/\hbar c)(2\pi)^2\hbar^4 m^{-2} E_\gamma^{-1}$, where E_γ is the energy of the γ quantum.

Indeed, for the above-mentioned values of β we have $\sum_{mn}' |c_{\alpha\beta}^{mn}|^2 \approx 0.048$ and 0.040.

4. We can obtain information about the triplet correlation range only from the data on the $He^4(\gamma, np)D$ reaction. It turns out, that one can determine an upper limit for r_K^0 by comparing the cross sections of the reactions A and B (in practice one compares the number of cases where the reactions A and B are observed under identical circumstances[5]).

We evaluate the cross section for the $He^4(\gamma, 2n)2p$ reaction for the case where $\mathbf{k}_1$ and $\mathbf{k}_2$ are the same as the corresponding momenta in the reaction A and the nucleons 3 and 4 move with a relative momentum κ. The energy necessary for this case is $E^B = E^A + \epsilon_d + \hbar^2\kappa^2/2\mu$, where ϵ_d is the deuteron binding energy. We get

$$d\sigma^B \sim (4\pi)^{-1} \sum_S \frac{3^S}{4} \Big| G(\mathbf{K})\, g_{0S}(\varkappa)\, \tilde{g}_S(\mathbf{k})\, \mathbf{k}\zeta + G(\mathbf{K})\, g_{0S}(k)\, \tilde{g}_S(\varkappa)\, \varkappa\zeta \Big|^2 d\mathbf{K}\, d\mathbf{k}\, d\varkappa,$$

$$\times\ g_{0S}(u) = \sqrt{\frac{2}{\pi}} \int \frac{\sin(ur + \delta^S)}{ur} \varphi_{rel}(r)\, r^2\, dr. \qquad (6)$$

Here, δ^S is the phase of the s wave in the corresponding spin state.

Integrating (4) over the angles of the vector $\mathbf{k}$ and multiplying it by the number of γ quanta in the beam with energy E^A (denoted by n^A) we get for the reaction A the number of reactions for a given momentum $\hbar\mathbf{K}$. On the other hand, integrating (6) over the angles of the vectors $\mathbf{k}$ and κ, multiplying it then by n^B and integrating over κ from zero to its maximum value determined by the end-point energy of the γ spectrum and the energy E^A we obtain the number of reactions B with energies from $E^A + \epsilon_d$ to E^B_{max} (for the same fixed values of $\mathbf{K}$ and $\mathbf{k}$). We denote this quantity by $p^B(E^A, k)$. The ratio p^B/p^A can then be expressed in the form

$$p^B/p^A \equiv C(E^A, k) = [n^A g_0^2 \tilde{g}_1^2(k)]^{-1} \sum_S \left(\tfrac{1}{3}\right)^{1-S} \Big\{ \tilde{g}_S^2(k) \int n^B g_{0S}^2(\varkappa)\varkappa^2\, d\varkappa + k^{-2} g_{0S}^2(k) \int n^B \tilde{g}_S^2(\varkappa)\varkappa^4\, d\varkappa \Big\}. \qquad (7)$$

We note that the momentum $\hbar\mathbf{K}$ has disappeared from this ratio.

The quantity

$$x = \int p^A(E, k)\, C(E^A, k)\, dE dk \Big/ \int p^A(E, k)\, dE\, dk \qquad (E \equiv E^A)$$

in which we are interested can be evaluated for different assumed values of the parameter β_0. The results are given in Fig. 2.

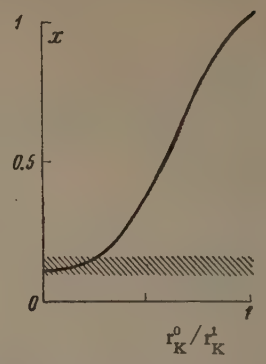

FIG. 2. The results of the calculations of x. The shaded band corresponds to the experimental value $x \approx 1/8$ (see reference 5).

If we take into consideration a certain lack of precision both in the experimental data and in the calculations, we can state that the correlation range in the singlet state of a nucleon pair is not larger than about 1/3 that of the triplet correlation range. This result depends only little on the precise choice of the form of the correlators.

There are at the present no calculations which enable us to find the form of the correlators of the correlation range from a general theory and it is thus difficult to interpret the result obtained here. It is, apparently, connected with the large difference between the nucleon-nucleon forces in the ^3S and the ^1S states at small distances.

I consider it a pleasant duty to express my deep gratitude to M. Ya. Amus'ya for valuable discussions connected with this work.

[1] A. de Shalit and V. F. Weisskopf, Ann. Phys. **5**, 282 (1958).

[2] M. Ya. Amus'ya, JETP **39**, 639 (1960), Soviet Phys. JETP **12**, 449 (1961).

[3] F. Coester and H. Kümmel, Nuclear Phys. **17**, 477 (1960).

[4] J. S. Levinger, Phys. Rev. **84**, 43 (1951).

[5] A. N. Gorbunov, Trudy, Phys. Inst. Acad. Sci. **13**, 174 (1960).

[6] H. J. Lipkin, Phys. Rev. **110**, 1395 (1958).

Translated by D. ter Haar
47

THE NEUTRINO AND THE DENSITY OF MATTER IN THE UNIVERSE

B. PONTECORVO and Ya. SMORODINSKII

Joint Institute for Nuclear Study

Submitted to JETP editor February 7, 1961

J. Exptl. Theoret. Phys. (U.S.S.R.) 41, 239-243 (July, 1961)

The possibility that the energy density of the neutrino and antineutrino in the Universe is comparable to or greater than the energy density due to the rest mass of hydrogen is considered. The assumption of a large neutrino and antineutrino energy density is not inconsistent with the available experimental data. Some methods of verifying this assumption, which arises as a result of discussion of PC-asymmetry of the world together with the hypothesis of existence of anti-worlds, are discussed. The importance of the Fermi $(e\nu)(e\nu)$ interaction which ensures transfer of energy to the $\nu\bar{\nu}$ component is emphasized. It is shown that the small magnitude of the "visible" kinetic energy density (which is much smaller than the energy density due to the rest mass of the nucleons) is not in contradiction with the hypothesis of separation of matter from anti-matter as a result of fluctuations in a charge symmetric universe. The fluctuation hypothesis merely requires that sometime in the past the neutrino and antineutrino energy density exceeded the nucleon energy density by several orders of magnitude.

INTRODUCTION

UP to this time there does not exist a well-founded estimate of the density of neutrinos and antineutrinos in space. Since these particles are hardly at all absorbed by dense matter, and since the manner of their production in the past is unknown, their number could attain large magnitudes. Although it is generally accepted that the matter in the Universe consists in essence of hydrogen a natural question arises: could not the energy contained in the neutrinos and antineutrinos in the Universe be comparable to or even larger than that contained in hydrogen?

CHARGE ASYMMETRY OF THE WORLD AND THE FLUCTUATION HYPOTHESIS

The assumption of a large number of ν and $\bar{\nu}$ in the universe arises, for example, in the discussion of the question of charge (more precisely, PC) asymmetry of the Universe. The possibility of existence of anti-worlds, resulting from fluctuations in a charge symmetric Universe, has been repeatedly discussed in the literature. Although at this time there are no experimental grounds for supposing that anti-worlds really exist, it seems of interest to us to note that the fluctuation hypothesis requires the existence in the Universe (now, or sometime in the past) of a large charge symmetric "background." Such a background should in principle consist to a large extent of ν and $\bar{\nu}$, whose densities are equal. Therefore the fluctuation hypothesis in principle leads to a conclusion which can be verified under "earthly" conditions. We note immediately that should this background exist today a measurement of the flux and energy of ν and $\bar{\nu}$ would give the value of a very important parameter—the average energy density in the Universe. At present the energy density of the Universe is estimated from the "smear-out" of galaxies. All astronomical estimates at this time agree that the average density of such "smeared-out" galaxies does not exceed 10^{-29} g/cm^3 (10^{-2} Mev/cm^3) or is less than 10^{-5} protons in 1 cm^3.[1] *

It follows from the equations of the general theory of relativity, that the average energy of relativistic particles (in our case neutrinos) falls in direct proportion to the curvature of the space a^{-1} (the energy density of such particles falls as a^{-4}). In other words, the average energy

*The question of the matter density in the Universe is particularly important for deciding on a cosmogonic model of the world. The magnitude of the average density coresponding to a flat Universe (passage from a closed to an open model) is $\sim 5 \times 10^{-29}$ g/cm^3.[2] In connection with the fact that recently the scale of cosmic distances was increased by more than a factor of two this number should be decreased to approximately 2×10^{-29} g/cm^3, which is close to the quoted estimate of the density. The size of the neutrino component may, therefore, turn out to be decisive.

of the neutrino in the past should be larger than its present energy by as many times as the curvature was larger in the past. Therefore in the past, when the density of matter was colossal, the neutrino energy density may have been larger than the nucleon energy density by many orders of magnitude. These may have been the conditions under which fluctuations took place. We have nothing to say about the mechanism of the fluctuation, in particular the question of "primordialness" of $\nu\bar{\nu}$ pairs is left open. We shall only remark that from our point of view the presence of anti-matter in our galaxy is by no means excluded.

Obviously the estimate of ν and $\bar{\nu}$ energy density in the Universe depends strongly on the concrete cosmogonic model. Let us emphasize once more that the fluctuation hypothesis requires the existence of a large symmetric background of neutral particles now or sometime in the past.

If today the energy density of ν and $\bar{\nu}$ should turn out to be small in comparison with nucleon energy density (as is quite likely), this would in no way contradict the fluctuation hypothesis.

At the same time the existing experimental data, discussed below, do not exclude the possibility of even large (i.e., in comparison with nucleon energy density) values for the energy density of ν and $\bar{\nu}$, and furthermore large values ($\gtrsim 100$ Mev) for the average energy are not a priori excluded either. It is therefore of importance to verify whether the contribution of neutrinos to the general energy density in the Universe is substantial also at the present time (from a different point of view the importance of this problem was indicated by Kharitonov[3] and Marx and Menyhard[4]).

THE UNIVERSAL WEAK INTERACTION AND THE ENERGY TRANSFER INTO THE $\nu\bar{\nu}$ COMPONENT

If the possibility of existence of energy density of ν and $\bar{\nu}$ comparable to 10^{-2} Mev/cm^3 is seriously considered then one is confronted in a natural way by the question: why are there not in the Universe intense fluxes of γ rays with energy and energy density comparable to the energy of the proposed lepton flux? One can answer right away that the energy of annihilation photons (from the decay of pions) will be naturally degraded under conditions of substantial matter density because of their interaction, and this then explains the absence of high energy photons. However, such "degraded" energy cannot disappear but should, at first glance, appear in the Universe in the form of thermal energy, photonic energy, etc., in quantities no smaller than the energy connected with the nucleon rest mass. It is known, however, that the density of thermal and photonic (i.e., "symmetric") energy in the Universe is small in comparison with the density ("nonsymmetric") of energy connected with rest mass; this is difficult to explain (if the ν and $\bar{\nu}$ density is today comparable with the nucleon density). This objection can be eliminated if neutrino-electron scattering exists (as predicted, for example, in the Fermi universal weak interactions theory). Then it is possible in electromagnetic processes to emit in place of photons $\nu\bar{\nu}$ pairs (via a virtual or real e^+e^- pair[5]). At very high temperatures and densities (and even more so under conditions that now interest us) the emission of $\nu\bar{\nu}$ pairs becomes the sole effective mechanism for radiation of energy by dense bodies.[5-8]

EXISTING INFORMATION ON THE ν AND $\bar{\nu}$ ENERGY DENSITY

Let us discuss now the experimental data on the ν and $\bar{\nu}$ energy density in space. Direct information on maximum densities of ν and $\bar{\nu}$ may be obtained from the assumption that in the experiments of Reines and Cowan[9] and Davis,[10] performed with the help of a reactor, the effect observed with the reactor turned off was due in its entirety to neutral leptons from cosmic space. In the Reines and Cowan experiment antineutrinos of energy 3 — 10 Mev could be registered; it follows from the experiment that the flux of antineutrinos from cosmic space with energies from 3 to 10 Mev cannot be significantly in excess of 10^{13} cm^{-2} sec^{-1}. This corresponds to a maximum value of the order of 10^3 Mev/cm^3 for the energy density of 3 to 10 Mev antineutrinos.

As far as high energy antineutrinos are concerned, no information can be deduced from the Reines and Cowan experiment, in which by selecting events of the type $\bar{\nu} + p \rightarrow n + e^+$ detection of $\bar{\nu}$ with energies $\gg 10$ Mev was made impossible.

In the experiments of Davis it was shown that

$$c\int_0^\infty \rho(E)\sigma(E)\,dE \leqslant 1.1 \cdot 10^{-33}\ \text{sec}^{-1},$$

where $\rho(E)$ is the density of cosmic neutrinos with energy E (including neutrinos from the sun) in units of Mev^{-1} cm^{-3} and $\sigma(E)$ is the cross section for the reaction $\nu + Cl^{37} \rightarrow Ar^{37} + e^-$. Roughly speaking, this cross section is proportional to the neutrino energy squared in the region from several Mev to several tens of Mev. It follows from an analysis of the Davis experiment that the energy density of cosmic space neutrinos with an energy

of a few Mev cannot exceed several tens of Mev per cm^3. About a neutrino whose energy is of the order of 1 Bev, which makes it capable of disintegrating the argon nucleus, the Davis experiment clearly says nothing. An estimate of the energy density of neutrinos with energies up to a 100 Mev can be obtained by assuming that the detector in the Davis experiment was irradiated by monoenergetic neutrinos of energies equal to the maximum energy for which nucleon recoil does not prevent the formation of Ar^{37} (let us say, $E \sim 70$ Mev). Even in this extreme case the maximum (i.e., permissible by the experiment) energy density of these neutrinos is of the order of a few Mev per cm^3 and significantly exceeds W_H^{max}—the maximum hydrogen energy density in the Universe ($W_H^{max} \sim 10^{-2}$ Mev/cm^3).

Let us discuss now the information that could be obtained from experiments carried out underground. At large depths the neutrinos and antineutrinos from cosmic space will produce charged leptons distributed isotropically with an intensity independent of the depth. If their energy is significantly in excess of the rest energy of the muon, then the ν and $\bar{\nu}$ will effectively produce muons. The latter should be slowed down and stopped and under equilibrium conditions the number of muons created and stopped should be equal. It follows from measurements[11] at a depth of 6000 g/cm^2 that the number of muons stopped in emulsions, reaching the emulsion from the lower hemisphere, is $\sim 10^{-8}\,sec^{-1}\,cm^{-3}$. This number can be viewed as the maximum possible number of muons produced by cosmic neutrinos (since muons entering the emulsion from the lower hemisphere could be products of the decay of pions emitted from stars produced by the penetrating component). From here it follows that

$$c\int_0^\infty \rho(E)\,\sigma(E)\,dE \lesssim 10^{-32}\,sec^{-1},$$

where $\sigma(E)$ is the neutrino-nucleon cross section. For neutrinos and antineutrinos with energies of ~ 1 Bev the value of σ lies between the limits $10^{-38} - 10^{-39}$ cm^2,[12] so that underground measurements of slow muon intensity require that the energy density of ~ 1 Bev neutrinos and antineutrinos be $\lesssim 10^{-1}$ Mev/cm^3. This number is rather near to the magnitude of W_H^{max}.

An even lower limit for the possible energy density of 1 Bev neutrinos and antineutrinos is obtained, if one takes as the starting point the results of the experiments performed[13] with the help of telescopic counters at a depth of $\sim 10^5$ g-cm^{-2}. These data, however, are difficult to interpret from our point of view, so that one may only conclude that the maximum energy density of ν and $\bar{\nu}$ with energy equal to or larger than 1 Bev cannot be greatly in excess of W_H^{max}, and is probably less than W_H^{max}. In any event under the existing conditions of experimental techniques it is fully realistic to attempt to detect neutrino and antineutrino fluxes of the order of 10^5 cm^{-2} sec^{-1} and with energies of ~ 1 Bev. This problem is considerably less complicated than the problem of detecting neutrinos from an accelerator; the latter problem has been lately widely discussed (in particular at the conferences on high energy physics at Kiev and Rochester). Such a flux would produce inside the Earth between 10 and a 100 isotropically distributed charged particles (electrons and muons) daily per ton of matter.

It is necessary to emphasize that for ν and $\bar{\nu}$ energies of the order of or less than $m_\mu c^2$ production of muons by neutrinos is impossible; the underground measurements in no way exclude energy densities of ν and $\bar{\nu}$ larger than W_H^{max}.

Experiments on detection of ν and $\bar{\nu}$ in cosmic rays were discussed previously,[14] under the assumption that these particles were produced in collisions of "cosmic-radiation protons" with the earth's atmosphere or with interstellar matter. It is obvious that in that case the number of neutrinos is very small; this can be seen right away from, for example, the extremely low intensity of high-energy γ rays from π^0 decay.

CONCLUSION

It follows from what has been said above, that it is not possible to exclude a priori the possibility that the neutrino and antineutrino energy density in the Universe is comparable to or larger than the average energy density contained in the proton rest mass. This should be tested experimentally.

In conclusion we note that under conditions of very high densities and energies the predominance of the "symmetric" type of energy in the form of $\nu\bar{\nu}$ pairs over other symmetric energy forms is a rather general property, connected with the scattering of neutrinos by electrons, and may be of interest also apart from its connection with the fluctuation hypothesis. In general the mechanism responsible for the "transfer" of energy into the neutrino component could lead to a substantial density of ν and $\bar{\nu}$ in the Universe. The existence of this mechanism will put into doubt estimates of matter density in the Universe, based on "visible" forms of matter only.

It should be emphasized that experimental dis-

proving of the hypothesis on the existence of a given neutrino and antineutrino energy density $\int \rho(E) E dE$ in the Universe becomes more difficult with decreasing average energy. Roughly speaking, the ν and $\bar{\nu}$ energy density that can be experimentally detected is inversely proportional to the square of the energy of the neutral leptons for energies larger than a few Mev. At lower energies the difficulties in detection are colossal. Thus, for example, the hypothesis on the existence of ν and $\bar{\nu}$ density equal to or larger than W_H^{max} can be easily tested experimentally (it has, perhaps, already been disproved by the existing data on underground muon intensity), if the neutrino energy is $\gtrsim 1$ Bev. If, however, the ν and $\bar{\nu}$ have an energy of ~ 100 Mev then a test of the hypothesis is realistic but involves considerable difficulties. For neutrinos with energy of ~ 1 Mev it is difficult to disprove experimentally ν and $\bar{\nu}$ energy densities even many orders of magnitude larger than W_H^{max}.*

The most convenient method for measuring fluxes of neutral leptons of 1 Bev energy consists of detecting the secondary muons produced by the neutrinos.[14,15] For ν and $\bar{\nu}$ energies in the region between several Mev and several hundreds of Mev the Reines-Cowan and Davis experiments are fully applicable. Regarding detection of ν and $\bar{\nu}$ with energies $\lesssim 1$ Mev it seems to us that electron-neutrino scattering provides the sole detection possibility. Unfortunately today this possibility exists in principle only.

The authors express their gratitude to A. G. Masevich and S. B. Pikelner for valuable discussions.

*However, a neutrino density $W \gg H$ is in contradiction with cosmological data.[15]

[1] S. V. Allen, Astrophysical Magnitudes (Russ. Transl.), IIL, 1960.

[2] Ya. A. Smorodinskii, Tr. 7-go soveshchaniya po kosmogonii, (Trans. Seventh Conf. on Cosmogony), Moscow, 1957.

[3] V. M. Kharitonov, Soveshchaniye po fizike elementarnykh chastits, (Conf. on Physics of Elementary Particles.) Erevan, 1960.

[4] G. Marx and N. Menyhárd, Science **131**, 299 (1960).

[5] B. Pontecorvo, JETP **36**, 1615 (1959), Soviet Phys. JETP **9**, 1148 (1959).

[6] G. M. Gandelman and V. S. Pinaev, JETP **37**, 1072 (1959), Soviet Phys. JETP **10**, 764 (1960).

[7] H. Y. Chiu and P. Morrison, Phys. Rev. Lett. **5**, 573 (1960).

[8] H. Y. Chiu and R. Stabler, Neutrino Emission Processes and Stellar Evolution, preprint 1960.

[9] F. Reines and C. L. Cowan, Proc. of the 2-nd Intern. Conf. on the Peaceful Uses of Atomic Energy, Geneva, 1958.

[10] R. Davis and D. S. Harmer, Bull. Amer. Phys. Soc. **4**, 217 (1959).

[11] E. P. George and J. Evans, Proc. Phys. Soc. **A63**, 1248 (1950); **A64**, 193 (1951).

[12] T. D. Lee and C. N. Yang, Phys. Rev. Lett. **4**, 307 (1960). N. Cabbibo and R. Gatto, Nuovo cimento **15**, 304 (1960).

[13] Miesowicz, Jurkiewicz, and Massalski, Phys. Rev. **77**, 380 (1950).

[14] M. A. Markov, Proc. of the 1960 Ann. Int. Conf. on High Energy Physics at Rochester, Univ. of Rochester, 1960, pp. 578, 580, 874.

[15] Ya. B. Zeldovich and Ya. A. Smorodinskii, JETP **41**, 907 (1961), Soviet Phys. JETP **14**, in press.

Translated by A. M. Bincer
48

ON THE $K^+ \to \pi^+ + \pi^0 + e^+ + e^-$ DECAY

I. G. IVANTER

Institute of Scientific Information, Academy of Sciences, U.S.S.R.

Submitted to JETP editor February 11, 1961

J. Exptl. Theoret. Phys. (U.S.S.R.) 41, 244-246 (July, 1961)

The decay $K^+ \to \pi^+ + \pi^0 + e^+ + e^-$ is treated without taking final-state interactions into account. The distribution of effective masses of the pion-pion system is obtained. In the calculation, a new approximation technique is applied to calculate the integrals over phase space of the bremsstrahlung probability density when two of the four particles are very light.

In radiative kaon decay, the γ quantum can be radiated by the kaon or by pions as internal bremsstrahlung or by a block of heavy particles in the decay vertex. We call the radiation emitted by the block of heavy particles vertex radiation. As Good[1] noted, the vertex part of the amplitude plays a relatively greater role in radiative θ^+ decay than in other radiative decays, since the vertex radiation is not forbidden by the $\Delta T = \pm\frac{1}{2}$ rule, while the basic $K^+_{2\pi}$ decay is forbidden by this rule.

In this paper, internal conversion of radiative θ^+ decay is calculated. The amplitude is

$$\mathcal{M} = -i4\pi\alpha\,(2\pi)^4 k^{-2}(8p_0q_0r_0)^{-1/2}\langle \bar{u}_{e^-}\hat{N}u_{e^+}\rangle, \qquad (1)$$

where α is the fine-structure constant; p, q, r, and k are the four-momenta of the K^+, π^+, π^0, and the virtual γ quantum, respectively; and the four-vector N is

$$N_\nu = q_\nu\,[k^2\varphi_1 + (rk)\,\varphi_3 + 2G/[(q+k)^2 - \mu_+^2]$$
$$+ 2G/[(p-k)^2 - M^2]] + r_\nu\,[k^2\varphi_2 - (qk)\,\varphi_3$$
$$+ 2G/[(p-k)^2 - M^2]] + i\varepsilon_{\rho\sigma\mu\nu}q_\rho r_\sigma k_\mu \varphi_{\text{mag}}. \qquad (2)$$

Here φ_1, φ_2, and φ_3 are functions of the invariants, G is the K^+ decay constant, and μ_+ and M are the masses of the π^+ and K^+, respectively.

Internal conversion differs from radiative θ^+ decay in that the vertex part of the amplitude depends not on one unknown function, but on three; however, the terms containing φ_1 and φ_2 give much smaller contributions to the amplitude than the term containing φ_3. We assume that the φ_i are functions of the single invariant $s = (r+q)^2$. In the calculations, we neglect the difference in the masses of π^0 and π^+.

After invariant integrations of the probability density by Dalitz's method[2] (see also Okun' and Shebalin[3]), the probability density will be a function only of

$$y = (r_0 + q_0)/M, \qquad x = [(r+q)^2 M^{-2}]^{1/2},$$

since the integrations over the light-particle phase space, the momentum difference of the π^0 and π^+, and the direction of the total momentum of the two pions have already been performed. The variables x and y vary within the limits

$$a \leqslant x \leqslant 1 - 2m_0,$$
$$x \leqslant y \leqslant \tfrac{1}{2}(1+x^2) - 2m_0, \quad a = \mu/m, \quad m_0 = m/M,$$

where m is the electron mass.

The expression for the probability density is the sum of several terms:

$$W = W_{BB} + W_{3B} + W_{33} + W_{\text{mag}}. \qquad (3)$$

Here, the conversion of internal bremstrahlung of the K^+ and π^+ is given by W_{BB}, the interference of the bremstrahlung and the main term of the vertex radiation is given by W_{3B}, the main term of the electric vertex radiation is given by W_{33}, and the magnetic radiation is given by W_{mag}; the terms corresponding to interference of the bremstrahlung with the smaller terms in the vertex radiation are not written, since they turn out to be negligible.

If W_{33} and W_{mag} are related to the corresponding constants $|\varphi_3|^2$ and $|\varphi_{\text{mag}}|^2$, it turns out that

$$M_{\text{mag}}/|\varphi_{\text{mag}}|^2 = W_{33}/|\varphi_3|^2 + \Delta,$$

where Δ is a small correction of the same order of magnitude as the terms we have neglected. For the probability density of the internal conversion of the K^+ and π^+ bremstrahlung, we obtain

$$W_{BB}\,dx\,dy = \frac{\alpha^2|G|^2M}{6(2\pi)^3}\left(1+\frac{m_0^2}{t-y}\right)\left(1-\frac{2m_0^2}{t-y}\right)^{1/2}$$
$$\times\left\{\frac{x^3\ln[(1+z)/(1-z)]}{w(t-y)}\right.$$
$$-\frac{4a^2(y^2-x^2)^{1/2}(x^2-4a^2)^{1/2}}{[(1-y)^2x^2+(x^2-4a^2)(y^2-x^2)](t-y)}$$
$$\left.-\frac{x^2(y^2-x^2)^{1/2}(x^2-4a^2)^{1/2}}{w^2(t-y)}\right\}dx\,dy + \Delta_1\,dx\,dy, \qquad (4)$$

where

$$t = (1 + x^2)/2, \quad w = (1 - x^2)/2,$$
$$z = (y^2 - x^2)^{1/2}(x^2 - 4a^2)^{1/2}x(1 - y). \qquad (5)$$

and Δ_1 is a correction of the same order of magnitude as the terms dropped above.

For the interference term W_{3B} we obtain

$$W_{3B}\,dx\,dy = \frac{\alpha^2 \operatorname{Re}(G\varphi_3^*)M}{6(2\pi)^3}\left\{-4a^2x\ln\frac{1+z}{1-z} + \frac{x^2(x^2-4a^2)^{1/2}(y^2-x^2)^{1/2}}{t-y} + x(2a^2-x^2)\ln\frac{1+z}{1-z}\right\} \times\left(1+\frac{m_0^2}{t-y}\right)\left(1-\frac{2m_0^2}{t-y}\right)^{1/2}dx\,dy. \qquad (6)$$

For the pure vertex term W_{33} we have

$$W_{33}\,dx\,dy = \frac{|\varphi_3|^2\alpha^2M}{6(2\pi)^3}\left(1+\frac{m_0^2}{t-y}\right)\left(1-\frac{2m_0^2}{t-y}\right)^{1/2}\frac{1}{12}(x^2-4a^2)^{3/2} \times\{-2y\sqrt{y^2-x^2} + (5x^2-1)\sqrt{y^2-x^2} + 2w^2\sqrt{y^2-x^2}/(t-y)\}\,dx\,dy. \qquad (7)$$

In the calculation of the integrals over y, the function $\ln[(1+z)/(1-z)]$ was expanded in a power series; even after this step, elliptic integrals appear. In order to avoid these, the following approximation was used. It is easy to show that if $\epsilon > 0$ is small enough, and if A and t are finite and F(y) is a function without poles, then the relation

$$\int_A^{t-\varepsilon}\left[1+\frac{\varepsilon}{2(t-y)}\right]\left(1-\frac{\varepsilon}{t-y}\right)^{1/2}\frac{F(y)\,dy}{t-y} = \int_A^{t-\varepsilon}\frac{F(y)\,dy}{t-y} + F(t)\left\{\int_A^{t-\varepsilon}\left(1-\frac{\varepsilon}{t-y}\right)^{1/2}\frac{dy}{t-y} - \int_A^{t-\varepsilon}\frac{dy}{t-y} + \frac{\varepsilon}{2}\int_A^{t-\varepsilon}\left(1-\frac{\varepsilon}{t-y}\right)^{1/2}\frac{dy}{(t-y)^2}\right\} \qquad (8)$$

is correct to any desired accuracy.

m_0^2 is a very small quantity in comparison with any of the other parameters of the system. This allows us to use formula (8), after which all the integrals over y can be carried out. The expressions thus obtained are very cumbersome; therefore, we do not give the expressions themselves, but just their graphs.

The figure shows the quantities

$$a_B = W_{BB}\frac{6(2\pi)^3}{|G|^2\alpha^2M}, \qquad a_{3B} = W_{3B}\frac{6(2\pi)^3}{\alpha^2M\operatorname{Re}(G\varphi_3^*)}\left|\frac{G_0}{G}\right|,$$
$$a_{33} = W_{33}\frac{6(2\pi)^3}{\alpha^2M|\varphi_3|^2}\left|\frac{G_0}{G}\right|^2.$$

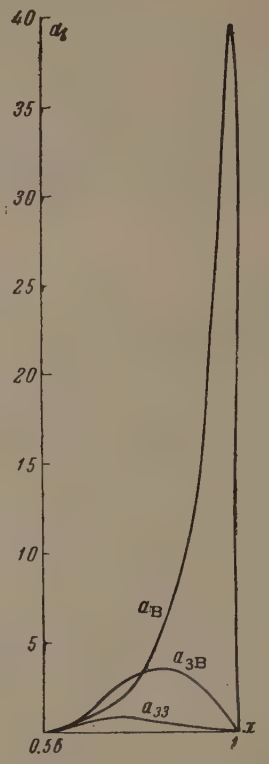

In the figure a_{3B} is multiplied by 20 and a_{33} by 400, which corresponds to a ratio of the square moduli of the θ^0 and θ^+ decay constants of $|G_0/G|^2 = 400$.

The average value of the internal bremstrahlung conversion coefficient is found to be $\bar{\rho}_{BB} = 1/73$.

The author expresses his gratitude to L. B. Okun' for suggesting this problem and to K. A. Ter-Martirosyan, S. G. Matinyan, and R. M. Muradyan for interesting comments.

[1] I. D. Good, Phys. Rev. **113**, 352 (1959).

[2] R. H. Dalitz, Phys. Rev. **99**, 915 (1955).

[3] L. B. Okun' and E. P. Shebalin, JETP **37**, 1775 (1959), Soviet Phys. JETP **10**, 1252 (1960).

Translated by M. Bolsterli
49

A GAUGE INVARIANT FORMULATION OF NEUTRAL VECTOR FIELD THEORY

V. I. OGIEVETSKII and I. V. POLUBARINOV

Joint Institute for Nuclear Research

Submitted to JETP editor February 16, 1961

J. Exptl. Theoret. Phys. (U.S.S.R.) 41, 247-255 (July, 1961)

It is shown that the theory of a neutral vector field with nonzero rest mass admits of a gauge invariant formulation without the introduction of auxiliary fields. In this theory the gauge invariance has a trivial physical meaning: the quanta of zero spin, described by the four-vector A_μ, do not interact with anything. Only the quanta with spin 1 take part in interactions.

1. INTRODUCTION

THERE is a widespread belief[1-10] that the theory of the neutral vector field $A_\mu(x)$ with nonzero rest mass, unlike electrodynamic theory, cannot be formulated in a gauge invariant way without the introduction of auxiliary fields. This is regarded as a serious obstacle to attempts which have been made rather frequently in recent times to carry through an analogy between the baryon charge and the electric charge or between the hyperon charge by the introduction of corresponding vector fields (Lee and Yang, Sakurai, and others[5-7,9,10]).

In the usual formulation of the neutral vector field theory one uses the equation (cf., e.g., [11,12])

$$\Box A_\mu - \partial^2 A_\nu/\partial x_\mu \partial x_\nu - m^2 A_\mu = -j_\mu, \qquad (1)$$

which is equivalent to the equation

$$(\Box - m^2)\, A_\mu = -j_\mu \qquad (2)$$

with the supplementary condition

$$\partial A_\mu/\partial x_\mu = 0. \qquad (3)$$

Neither Eq. (1), nor Eq. (2) with supplementary condition (3), is gauge invariant.

The need for the supplementary condition (3) is motivated by the wish to exclude the spin 0 and assure that the energy is positive definite.

We note that at the price of introducing, in addition to the four-vector $A_\mu(x)$, an auxiliary scalar field $B(x)$ Stueckelberg[3] succeeded in constructing a gauge invariant formalism for the vector field with the supplementary condition.[1,4,8,11] In such a theory, however, the meaning of the gauge invariance is to a large extent obscured.

It will be shown below that the theory of a neutral vector field with nonzero rest mass admits of a gauge invariant formulation without the introduction of any auxiliary fields. For this we must entirely renounce the supplementary condition. In the theory to be considered $A_\mu(x)$ obeys only the gauge-invariant equation (2) (Sec. 2). It turns out that only the part of $A_\mu(x)$ with the spin 0 is subject to the gauge transformation. Here the physical meaning of the gauge invariance is that the vector-field quanta with spin 0 have no interaction with other fields or with each other (Sec. 3). Therefore the use of a supplementary condition to exclude the spin 0 is superfluous. It is also not needed to assure positive definiteness of the energy (Sec. 3). This theory is completely equivalent to the usual theory of the neutral vector field with nonzero mass based on Eq. (1) or on Eqs. (2) and (3) (Sec. 4).

It can be said that in the present case the gauge invariance plays the part that is usually played by supplementary conditions in the theory of higher spins. Unlike the usual supplementary conditions it does not exclude the quanta of the undesired spin, but only "renders them harmless."

2. BASIC EQUATIONS

As is common practice (cf., e.g., [12]) we take the Lagrangian density which describes the neutral vector field A_μ in interaction with a spinor field* ψ in the form

$$L(x) = -\frac{1}{2}\frac{\partial A_\nu}{\partial x_\mu}\frac{\partial A_\nu}{\partial x_\mu} - \frac{m^2}{2} A_\mu A_\mu + j_\mu A_\mu - \bar{\psi}\left(\gamma_\mu \frac{\partial}{\partial x_\mu} + M\right)\psi$$

$$j_\mu = ig\bar{\psi}\gamma_\mu\psi. \qquad (4)$$

The Lagrangian and the equations of motion that follow from it,

*In analogous ways one can write the interaction for cases involving several fields, and also for couplings of the type of an anomalous magnetic moment.

$$(\Box - m^2) A_\mu = -j_\mu, \tag{5}$$

$$(\gamma_\mu \partial / \partial x_\mu + M)\psi = ig\gamma_\mu \psi A_\mu, \tag{6}$$

and also the equal-time ($x_0 = y_0$) commutation relations, which are analogous to those for electrodynamics,*

$$\{\psi(x), \psi(y)\} = 0, \qquad \{\psi(x), \bar{\psi}(y)\} = \gamma_4 \delta(x - y),$$
$$[A_\mu(x), A_\nu(y)] = 0, \qquad \left[A_\mu(x), \frac{\partial A_\nu}{\partial y_4}(y)\right] = \delta_{\mu\nu}\delta(x - y),$$
$$[\psi(x), A_\nu(y)] = 0, \qquad \left[\psi(x), \frac{\partial A_\nu}{\partial y_4}(y)\right] = 0, \tag{7}$$

are invariant† under the gauge transformations

$$\psi'(x) = \exp[ig\Lambda(x)]\psi(x), \tag{8}$$

$$A'_\mu(x) = A_\mu(x) + \partial\Lambda(x)/\partial x_\mu \tag{9}$$

with arbitrary $\Lambda(x)$ satisfying the equation

$$\frac{\partial}{\partial x_\mu}(\Box - m^2)\Lambda = 0. \tag{10}$$

Gauge invariance thus exists for $m \neq 0$ in just the same way as in the case in which one sets $m = 0$ in Eqs. (4), (5), and (10) (quantum electrodynamics).

We note that unlike the treatment in [5-7,9], where the function $\Lambda(x)$ was assumed completely arbitrary, in the transformations (8) and (9) considered here $\Lambda(x)$ is restricted by the condition (10). This same restriction also holds in quantum electrodynamics, unlike the classical theory.

From the gauge invariance of the Lagrangian or of the equations there follows the conservation law:‡

$$\frac{\partial}{\partial x_\mu}\left(-j_\mu\Lambda - \frac{\partial A_\nu}{\partial x_\mu}\frac{\partial\Lambda}{\partial x_\nu} + A_\nu \frac{\partial^2\Lambda}{\partial x_\mu \partial x_\nu}\right) = 0. \tag{11}$$

This equation must hold for any $\Lambda(x)$ that satisfies Eq. (10). In particular, for $\Lambda = \text{const}$ we get

$$\partial j_\mu / \partial x_\mu = 0 \tag{12}$$

the conservation law for the current.

Differentiating Eq. (5) and taking Eq. (12) into account, we get the equation

$$(\Box - m^2)\,\partial A_\mu / \partial x_\mu = 0, \tag{13}$$

which we shall need soon.

*The equal-time commutations can be taken in this form, since no supplementary condition is imposed on the field operators A_μ.

†The Lagrangian density (4) is invariant apart from a divergence, which of course affects no results (cf. Appendix 1).

‡For a derivation of this conservation law and a discussion of the associated operator transforming the state vectors see Appendix 1.

3. THE ABSENCE OF INTERACTIONS WITH THE QUANTA OF SPIN 0

One uses a four-vector $A_\mu(x)$ with a view to the description of particles of spin 1. Within the framework of the homogeneous Lorentz group there are no quantities that describe only particles of spin 1. In accordance with this, along with quanta of spin 1, $A_\mu(x)$ also describes quanta of spin 0. Namely, A_μ can be divided into two parts:

$$A_\mu = \left(A_\mu - \frac{1}{m^2}\frac{\partial}{\partial x_\mu}\frac{\partial A_\nu}{\partial x_\nu}\right) + \frac{1}{m^2}\frac{\partial}{\partial x_\mu}\frac{\partial A_\nu}{\partial x_\nu}, \tag{14}$$

where the first part describes quanta of spin 1 and the second quanta of zero spin. One can verify this by applying the invariant operator of the square of the spin[13-16] for the field $A_\mu(x)$ (cf. Appendix 2):

$$(\Gamma^2)_{\mu\nu} = 2(\delta_{\mu\nu}\Box - \partial^2/\partial x_\mu \partial x_\nu) \tag{15}$$

which has the eigenvalues $s(s+1)\Box$ for spin s. Namely, using Eq. (13), we can easily verify that

$$(\Gamma^2)_{\mu\nu}\left(A_\nu - \frac{1}{m^2}\frac{\partial}{\partial x_\nu}\frac{\partial A_\lambda}{\partial x_\lambda}\right) = 2\Box\left(A_\mu - \frac{1}{m^2}\frac{\partial}{\partial x_\mu}\frac{\partial A_\lambda}{\partial x_\lambda}\right), \tag{16}$$

$$(\Gamma^2)_{\mu\nu}\frac{1}{m^2}\frac{\partial}{\partial x_\nu}\frac{\partial A_\lambda}{\partial x_\lambda} = 0. \tag{17}$$

Naturally these same quanta of zero spin are also described by the scalar $\partial A_\mu / \partial x_\mu$ itself.

It must be emphasized that under the condition (1) the gauge transformation (9) changes only the part of A_μ with the spin 0:

$$\frac{1}{m^2}\frac{\partial}{\partial x_\mu}\frac{\partial A'_\nu}{\partial x_\nu} = \frac{1}{m^2}\frac{\partial}{\partial x_\mu}\frac{\partial A_\nu}{\partial x_\nu} + \frac{\partial\Lambda}{\partial x_\mu}, \tag{18}$$

while the part with the spin 1 remains unchanged:

$$A'_\mu - \frac{1}{m^2}\frac{\partial}{\partial x_\mu}\frac{\partial A'_\nu}{\partial x_\nu} = A_\mu - \frac{1}{m^2}\frac{\partial}{\partial x_\mu}\frac{\partial A_\nu}{\partial x_\nu}. \tag{19}$$

If we want to consider only the quanta with the spin 1, then it would seem to be necessary to take steps to exclude the quanta with zero spin. Our assertion is that in the case of vector quanta of nonzero rest mass no special steps of this sort (for example, imposition of a supplementary condition) are needed. It already follows from the gauge invariant field equations (5) and (6) themselves that the quanta with spin 0 do not interact with other fields nor with each other: the part of A_μ that describes them obeys the free-particle equation

$$(\Box - m^2)\frac{1}{m^2}\frac{\partial}{\partial x_\mu}\frac{\partial A_\nu}{\partial x_\nu} = 0 \tag{20}$$

[a trivial consequence of Eq. (13)]. Consequently,

the equation with interaction, Eq. (5), is obeyed by just the part of A_μ with spin 1:

$$(\Box - m^2)\left(A_\mu - \frac{1}{m^2}\frac{\partial}{\partial x_\mu}\frac{\partial A_\nu}{\partial x_\nu}\right) = -j_\mu. \qquad (21)$$

Thus the quanta with spin 0 do not affect the physics; if any set of such quanta is present in the initial state, precisely this same set is present in the final state. Otherwise the matrix element of the S matrix is equal to zero.

This assertion can be formulated in the language of conservation laws. From the free-particle equation (13) there follow conservation laws for the total four-vector momentum $P_\mu^{(0)}$ and angular momentum $M_{\mu\nu}^{(0)}$ of the scalar field $m^{-1}\partial A_\mu/\partial x_\mu$, and moreover, of the number of quanta with each value of the momentum. Thus the S matrix is diagonal in the quantum numbers of the quanta with spin 0.

The imposition of a supplementary condition of the form

$$\partial A_\mu/\partial x_\mu = 0 \qquad (22)$$

or*

$$\left(\frac{\partial A_\mu}{\partial x_\mu}\right)_- \Phi = 0 \qquad (23)$$

for the exclusion of the spin 0 is superfluous, since it affects only the part of $A_\mu(x)$ that describes the free quanta of spin 0, which do not interact with anything.

As still another, and sometimes the main, argument[1,2] in favor of the necessity of imposing the condition (22), the point has been made that otherwise the operator P_0 for the total energy is not positive-definite. But the energy operator $P_0^{(0)}$ of the always free quanta of spin zero is conserved. Therefore as the physical energy operator we may take the operator†

$$P_0^{\text{phys}} = P_0 - P_0^{(0)}. \qquad (24)$$

This operator is conserved and gauge invariant, and its spectrum is positive definite. Also it is really permissible not to make this subtraction. Then the energy would be reckoned not from zero, but from some gauge-dependent negative level. Thus also from this point of view there is no necessity of the supplementary condition (22).

4. EQUIVALENCE TO THE USUAL THEORY WITH THE SUPPLEMENTARY CONDITION

Although the scalar field $m^{-1}\partial A_\mu/\partial x_\mu$ has turned out to be free, it has not yet been eliminated from the Dirac equation (6). Let us now break up the operator $\psi(x)$ into factors depending on the gauge and independent of the gauge:

$$\psi(x) = \exp\left[ig\frac{1}{m^2}\frac{\partial A_\nu}{\partial x_\nu}\right]\varphi(x),$$

$$\varphi(x) \equiv \exp\left[-ig\frac{1}{m^2}\frac{\partial A_\nu}{\partial x_\nu}\right]\psi(x), \qquad (25)$$

where φ is the part of ψ that does not depend on the gauge.* In the variables φ and apart from a four-dimensional divergence the Lagrangian density (4) can be rewritten in the form

$$L(x) = -\frac{1}{4}F_{\mu\nu}^{(1)}F_{\mu\nu}^{(1)} - \frac{m^2}{2}A_\mu^{(1)}A_\mu^{(1)} + \frac{1}{2}\left(\frac{\partial}{\partial x_\mu}\frac{1}{m}\frac{\partial A_\nu}{\partial x_\nu}\right)^2$$
$$+\frac{m^2}{2}\left(\frac{1}{m}\frac{\partial A_\nu}{\partial x_\nu}\right)^2$$
$$+\frac{ig}{2}\bar{\varphi}\gamma_\mu(\varphi A_\mu^{(1)} + A_\mu^{(1)}\varphi) - \bar{\varphi}\left(\gamma_\mu\frac{\partial}{\partial x_\mu} + M\right)\varphi, \qquad (26)$$

where

$$F_{\mu\nu}^{(1)} \equiv \frac{\partial A_\nu^{(1)}}{\partial x_\mu} - \frac{\partial A_\mu^{(1)}}{\partial x_\nu}, \qquad A_\mu^{(1)} \equiv A_\mu - \frac{1}{m^2}\frac{\partial}{\partial x_\mu}\frac{\partial A_\nu}{\partial x_\nu}. \qquad (27)$$

This Lagrangian corresponds to the usual theory of the interaction of a spinor field φ and a vector field $A_\mu^{(1)}$ with the supplementary condition[17]

$$\partial A_\mu^{(1)}/\partial x_\mu = 0 \qquad (28)$$

and, in addition, describes a free scalar field $m^{-1}\partial A_\nu/\partial x_\nu$, which now does not appear in the Dirac equation.

The commutation relations for the fields φ and $A_\mu^{(1)}$ are the same as in the usual theory with the supplementary condition.† At the same time the interacting fields φ and $A_\mu^{(1)}$ commute with the scalar field $m^{-1}\partial A_\nu/\partial x_\nu$ and with all of its derivatives. Consequently, the scalar field $m^{-1}\partial A_\nu/\partial x_\nu$ is completely dynamically independent. Thus the theory under discussion is entirely equivalent to the usual theory of the neutral vector field with the supplementary condition. The equivalence of the two theories can also be established by a different method, by means of the unitary transformation of Dyson,[18,11] which also "turns off" the vector interaction of the scalar field.

5. CONCLUDING REMARKS

Let us make one remark about the mass renormalization. A gauge transformation affects

*In the theory under consideration this condition fixes the gauge and means that in the physical states Φ there are no quanta with spin 0.

†For the concrete form of the operator P_0^{phys} for a free field A_μ see Appendix 3.

*Apart from a constant phase factor, under the transformations (8)–(10) we have

$$\varphi' = \exp\left[-\frac{ig}{m^2}(\Box - m^2)\Lambda\right]\varphi = \exp\left[-\frac{ig}{m^2}\cdot\text{const}\right]\varphi.$$

†These relations can be obtained from the commutation relations (7) and the equations of motion (5) and (6).

only the part of A_ν that describes the quanta of spin zero. Consequently, it is only for these quanta that we can expect that the mass will not have to be renormalized. And indeed this is so, because they do not interact with anything. As for the quanta with spin 1, their mass is naturally renormalized in the process of the interaction. The equation (5), with the mass renormalization of the quanta of spin 1 taken into account, can be written, for example, in the form

$$(\Box - m^2)A_\mu = -j_\mu - \delta m^2\left(A_\mu - \frac{1}{m^2}\frac{\partial}{\partial x_\mu}\frac{\partial A_\nu}{\partial x_\nu}\right). \qquad (29)$$

Finally we point out that in this theory of a vector field A_ν with nonzero mass the Green's functions obey the same laws of gauge transformation as in electrodynamics.[19-23] These laws connect averages over the same state of products of operators in two different gauges. This state is the vacuum in both gauges for the quanta with spin 1, but contains no quanta with spin 0 from the point of view of only one gauge (Appendix 1). The Ward identity follows from these laws, as in electrodynamics.

The writers heartily thank M. A. Markov and B. N. Valuev for general remarks, and A. A. Logunov and M. I. Shirokov for a discussion of the question of the operator for the square of the spin. We are especially grateful to L. G. Zastavenko, Ya. A. Smorodinskii, and Chou Kuang-Chao for stimulating discussions of a number of points in this work.

APPENDIX 1

THE CONSERVATION LAW THAT FOLLOWS FROM GAUGE INVARIANCE

After a gauge transformation (8) and (9), with Eq. (10) taken into account, the Lagrangian density (4) differs from its original value by a divergence. For an infinitesimal transformation we have

$$\delta L(x) = -\frac{\partial}{\partial x_\mu}\left(A_\nu \frac{\partial^2 \Lambda}{\partial x_\mu \partial x_\nu}\right). \qquad (1.1)$$

Calculating the variation of $L(x)$ in the usual way, using the Euler equations, we arrive at the conservation law (11), which can also be written in the equivalent form

$$\frac{\partial}{\partial x_\mu}\left[\left(\frac{\partial}{\partial x_\mu}\frac{\partial A_\nu}{\partial x_\nu}\right)\Lambda - \frac{\partial A_\nu}{\partial x_\nu}\frac{\partial \Lambda}{\partial x_\mu} + A_\mu(\Box - m^2)\Lambda\right]$$

$$\equiv \frac{\partial}{\partial x_\mu}K_\mu = 0. \qquad (1.2)$$

In Eq. (11) one can substitute any function $\Lambda(x)$, limited only by Eq. (10), and therefore Eq. (11) represents a continuum of conservation laws, corresponding to the continuum of the parameters of the gauge group. It is easy to verify that Eq. (11) is equivalent to Eq. (5).

We can now write the gauge transformation of the eigenvectors, without changing the eigenvalues, and of the field operators, in the form

$$\Psi' = \exp\left(\int dx K_4\right)\Psi \equiv U\Psi, \qquad \psi'(x) = U\psi(x)U^{-1},$$

$$A'_\mu(x) = UA_\mu(x)U^{-1} \qquad (1.3)$$

[the last two relations are a different way of writing Eqs. (8) and (9)].

From the points of view of different gauges the same state has different sets of the noninteracting gauge of spin 0. For example, let us define the vacuum in two different gauges by the relations

$$a^+_\mu p_\mu \Psi_0 = 0, \qquad a'^+_\mu p_\mu \Psi'_0 = 0, \qquad (1.4)$$

where $a^+_\mu p_\mu$ are operators for annihilation of quanta of spin 0, corresponding to $\partial A_\mu/\partial x_\mu$ (see Appendix 3). If $ia_\mu p_\mu$, λ and $-ia_\mu p_\mu$, λ^+ are the amplitudes of the positive and negative frequency parts of the three-dimensional Fourier expansions of $\partial A_\mu/\partial x_\mu$ and $\Lambda(x)$, which hold by Eq. (13) and for the special case of a $\Lambda(x)$ which satisfies the same equation, then

$$\Psi'_0 = U\Psi_0 \equiv \exp\{-i\int d\mathbf{p}\,[a_\mu p_\mu \lambda^+(\mathbf{p}) + a^+_\mu p_\mu \lambda(\mathbf{p})]\}\Psi_0$$

$$= \exp\left\{-\frac{m^2}{2}\int d\mathbf{p}\lambda(\mathbf{p})\,\lambda^+(\mathbf{p}) - i\int d\mathbf{p}\lambda^+(\mathbf{p})\,p_\mu a_\mu\right\}\Psi_0. \qquad (1.5)$$

The last expression gives the expansion of the vacuum of the new gauge, Ψ'_0, in terms of the states of the old gauge, which are produced by the creation operators $p_\mu a_\mu$ from the old vacuum Ψ_0.

Thus the vacuum from the point of view of one gauge is not the vacuum from the point of view of another gauge. This is understandable, since the conditions (1.4), and also the more general condition (23), are not gauge invariant, since they are conditions that establish and fix a gauge.

APPENDIX 2

THE OPERATOR FOR THE SQUARE OF THE SPIN FOR THE FIELD $A_\mu(x)$

The general definition of the operator for the square of the spin (one of the invariants of the inhomogeneous Lorentz group) for arbitrary many-component functions transforming according to representations of the inhomogeneous Lorentz group has been given and discussed in a number of papers.[13-16] This definition is [16]:

$$\Gamma^2 = -p^2_\lambda \tfrac{1}{2} m_{\rho\sigma}m_{\rho\sigma} + m_{\lambda\rho}m_{\lambda\sigma}p_\rho p_\sigma, \qquad (2.1)$$

where

$$p_\lambda = \frac{1}{i}\frac{\partial}{\partial x_\lambda}, \qquad m_{\rho\sigma} = \frac{1}{i}\left(x_\rho \frac{\partial}{\partial x_\sigma} - x_\sigma \frac{\partial}{\partial x_\rho}\right) + s_{\rho\sigma} \tag{2.2}$$

are the infinitesimal operators of displacements and four-dimensional rotations for the given function. The matrices $s_{\rho\sigma}$ are the infinitesimal operators for rotations of the components of the function.

Since for a vector function $A_\mu(x)$

$$(s_{\rho\sigma})_{\mu\nu} = i(\delta_{\rho\mu}\delta_{\sigma\nu} - \delta_{\rho\nu}\delta_{\sigma\mu}), \tag{2.3}$$

substitution of Eqs. (2.2) and (2.3) in Eq. (2.1) at once gives the expression (15).

The law of transformation of the vector function $A_\mu(x)$, and thus also the infinitesimal operators p_λ and $m_{\rho\sigma}$ and the operator (2.1) or (15) for the square of the spin constructed from them, do not depend on whether $A_\mu(x)$ is subjected to any equations or not. Whereas, however, in the case of equations without interaction A_μ can be divided into independent parts with spins 0 and 1, in the case of an interaction this might not be so.

In our case, as we have seen (Sec. 3), even in the presence of the interaction $A_\mu(x)$ breaks up into dynamically independent parts with spins 0 and 1.

APPENDIX 3

THE NORMAL PRODUCT OF OPERATORS OF THE VECTOR FIELD AND THE DEFINITION OF THE PHYSICAL ENERGY OPERATOR IN THE FREE CASE

In the free case it is convenient to define all operators in the form of normal products, i.e., so that all creation operators shall stand to the left of the annihilation operators.

For example, it is in this sense that we would like to understand the operator for the four-momentum

$$P_\mu = \int d\mathbf{p}\, p_\mu : a_\nu^+ a_\nu : \qquad (p_0 = \sqrt{\mathbf{p}^2 + m^2}), \tag{3.1}$$

as we indicate by the colons.

The operators a_ν and a_ν^+ obey the commutation relations

$$[a_\mu(\mathbf{p}_1),\ a_\nu^+(\mathbf{p}_2)] = \delta_{\mu\nu}\delta(\mathbf{p}_1 - \mathbf{p}_2). \tag{3.2}$$

It is clear from these relations that the annihilation operators are a_m and a_0^+, and the creation operators are a_m^+ and a_0. But writing the normal product in Eq. (3.1) in the form

$$: a_\nu^+ a_\nu : = a_m^+ a_m - a_0 a_0^+ \tag{3.3}$$

is not permissible, because of its lack of covariance. We can give a covariant definition if we break up the operators a_μ and a_μ^+ into parts with the spins 0 and 1:

	Annihilation operators	Creation operators
$s = 1$	$a_\mu + m^{-2} a_\nu p_\nu p_\mu$	$a_\mu^+ + m^{-2} a_\nu^+ p_\nu p_\mu$
$s = 0$	$-m^{-2} a_\nu^+ p_\nu p_\mu$	$-m^{-2} a_\nu p_\nu p_\mu$

(here $p^2 = -m^2$). One can establish the spins of these parts by means of the invariant operator for the square of the spin, Eq. (15) (cf. Appendix 2), written in the momentum representation. Their meanings as annihilation and creation operators follow from Eq. (3.2).

The ways of writing normal products are not, for example,

$$:\left(a_\mu^+ + \frac{a^+p}{m^2}p_\mu\right)\left(a_\nu + \frac{ap}{m^2}p_\nu\right): = :\left(a_\nu + \frac{ap}{m^2}p_\nu\right)\left(a_\mu^+ + \frac{a^+p}{m^2}p_\mu\right): = \left(a_\mu^+ + \frac{a^+p}{m^2}p_\mu\right)\left(a_\nu + \frac{ap}{m^2}p_\nu\right), \tag{3.4}$$

$$: \frac{a^+p}{m^2}p_\mu \frac{ap}{m^2}p_\nu : = : \frac{ap}{m^2}p_\nu \frac{a^+p}{m^2}p_\mu : = \frac{ap}{m^2}p_\nu \frac{a^+p}{m^2}p_\mu. \tag{3.5}$$

In mixed products with $s = 1$ and $s = 0$ the order is immaterial because of the commutation.

The normal product in Eq. (3.1) can now be expanded as

$$P_\mu = \int d\mathbf{p}\, p_\mu \left\{\left[a_\nu^+ a_\nu + \frac{(a^+p)(ap)}{m^2}\right] - \frac{(ap)(a^+p)}{m^2}\right\}. \tag{3.6}$$

The first term in the curly brackets is the positive definite operator for the number of quanta of spin 1, and the second is the negative definite operator for the number of quanta of spin 0. Accordingly the energy of the quanta of spin 1 is positive definite, and that of the quanta of spin 0 is negative definite.

If we subtract from P_μ the energy-momentum four-vector of the quanta of spin 0, we get the energy momentum operator of the quanta of spin 1 (the physical quanta), which in the free case is invariant under gauge transformations ($a_\mu \to a_\mu + i\lambda(\mathbf{p})p_\mu$)

$$P_\mu^{\text{phys}} = \int d\mathbf{p}\, p_\mu [a_\nu^+ a_\nu + (a^+p)(ap)/m^2] \tag{3.7}$$

and has the energy positive definite.

---

[1] W. Pauli, Relativistic Theory of Elementary Particles (Russian edition, IIL, 1947; probably based on Revs. Modern Phys. **13**, 203 (1941)).

[2] G. Wentzel, Einführung in die Quantentheorie der Wellenfelder, Vienna, Franz Deuticke, 1943.

[3] E. C. G. Stueckelberg, Helv. Phys. Acta **11**, 225 (1938).

[4] R. J. Glauber, Progr. Theoret. Phys. **9**, 295 (1953).

[5] T. D. Lee and C. N. Yang, Phys. Rev. **98**, 1501 (1955).

[6] R. Utiyama, Phys. Rev. **101**, 1597 (1956).

[7] M. E. Mayer, Preprint R-212, Joint Inst. Nuc. Res. 1958.

[8] Y. Fujii, Progr. Theoret. Phys. **21**, 232 (1959).

[9] H. Nakamura, Progr. Theoret. Phys. **21**, 827 (1959).

[10] J. H. Sakurai, Ann. Phys. **11**, 1 (1960).

[11] H. Umezawa, Quantum Field Theory, North-Holland–Interscience, 1956.

[12] N. N. Bogolyubov and D. V. Shirkov, Introduction to the Theory of Quantized Fields, Interscience, 1959.

[13] M. H. L. Pryce, Proc. Roy. Soc. **A150**, 166 (1935); **A195**, 62 (1948).

[14] W. Pauli, see J. K. Lubański, Physica **9**, 310 (1942).

[15] V. Bargmann and E. P. Wigner, Proc. Natl. Acad. Sci. U. S. **34**, 211 (1948).

[16] Yu. M. Shirokov, JETP **21**, 748 (1951).

[17] C. N. Yang and D. Feldman, Phys. Rev. **79**, 972 (1950).

[18] F. J. Dyson, Phys. Rev. **73**, 929 (1948).

[19] L. D. Landau and I. M. Khalatnikov, JETP **29**, 89 (1955), Soviet Phys. JETP **2**, 69 (1956).

[20] E. S. Fradkin, JETP **29**, 258 (1955), Soviet Phys. JETP **2**, 361 (1956).

[21] S. Okubo, Nuovo cimento **15**, 949 (1960).

[22] Evans, Feldman, and Matthews, Preprint, 1960.

[23] V. I. Ogievetskii and I. V. Polubarinov, Preprint D-618, Joint Inst. Nuc. Res. (1960).

Translated by W. H. Furry
50

INTEGRAL EQUATIONS FOR $\pi\pi$-SCATTERING AND PROBLEMS RELATED TO CONVERGENCE OF THE AMPLITUDE EXPANSION

J. FISCHER* and S. CIULLI†

Joint Institute for Nuclear Research

Submitted to JETP editor February 16, 1961

J. Exptl. Theoret. Phys. (U.S.S.R.) 41, 256-262 (July, 1961)

Convergence of the expansions of the cosine dependence of the amplitude, employed in the deduction of the integral equations from the Mandelstam representation, is investigated in the case of $\pi\pi$ scattering. A system of equations for low energies in presented, in which rapid convergence of the expansion of the real part of the amplitude can be attained by a conformal mapping of the cosine plane. Since any power of the function employed contains an infinite number of partial waves, this approach should be especially convenient in cases when high number waves may be important.

1. QUESTIONS OF CONVERGENCE

MANY authors have recently investigated the derivation of a system of equations for elastic pion-pion scattering.[1-3] A general feature of these investigations is that the singularities of the scattering amplitude are determined by means of the Mandelstam two-dimensional integral representation,[4-6] which discloses explicitly the analytic properties of the amplitude and leads to various one-dimensional dispersion relations.

Chew and Mandelstam[1] obtained dispersion relations for the partial waves. The imaginary part of the amplitude in the nonphysical region is obtained by analytic continuation from the physical region of the crossing reactions by expansion in Legendre polynomials.

However, this continuation leads to principal difficulties[1,3,7] because the Legendre series does not converge in the region of the spectral functions and because, furthermore, it converges very slowly in a sufficiently large region near the boundary of the spectral function, so that high-order waves cannot be neglected.

Hsien, Ho, and Zoellner[3] have proposed a different approach, getting around these difficulties. They use dispersion relations for the forward (or backward) scattering only. The path of integration does not cross the regions of the spectral functions. The path of the left-hand integral coincides with the boundary of the physical region of the second (or third) reactions, so that no analytic continuation is necessary. Only integrals over the positive energies at $\cos^2\theta = 1$ remain after the crossing transformation.

To obtain expressions for the partial amplitudes, Hsien et al use, along with the dispersion relation for A, also its derivative* with respect to t (see also [8]). If the isotopic spin I is 0 or 2, only even waves are present:

$$A_l^{0,2} = \sum_{n=0}^{\infty} \frac{1}{n!} \left(\frac{\partial^n A^{0,2}}{(\partial \cos^2\theta)^n} \right)_{\cos^2\theta=1} c_{ln} \qquad (l \text{ even}), \qquad (1)$$

where

$$c_{ln} = \int_0^1 (\cos^2\theta - 1)^n P_l(\cos\theta)\, d\cos\theta,$$

$$A^{0,2}(\nu, \cos\theta) = A^{0,2}(\nu, \cos\theta).$$

Only the S wave is taken into account in [3] and the first two terms are retained on the right side of expansion (1). These expressions are substituted into the unitarity condition only in the given approximation. Analogously, only the P wave is taken into account in the case of odd l.

The series (1) converges not only for all energies $\nu < 3$, where scattering only is possible, but also up to $\nu = 4.8$. Naturally, the rate of convergence of the series depends in this case on the distance between the nearest singularity and the point $\cos^2\theta = 1$. This can be seen from the fact that unitarity necessitates knowledge of the amplitude in

*Physics Institute, Czechoslovak Academy of Sciences, Prague.

†Institute of Atomic Physics, Bucharest.

*$t = -2\nu(1-\cos\theta)$ is the square of the momentum transfer, and $s = 4(\nu+1)$ is the square of the total energy; both are given in units of μ^2 in the c.m.s. of the first reaction. We also use the symbol $\nu = q^2/\mu^2$.[1]

the entire physical region $0 \le \cos^2\theta \le 1$. Since we continue the amplitude into the entire physical region using its values at the point $\cos^2\theta = 1$ only, the amplitude A can be represented only in the form of a series in powers of $\cos^2\theta - 1$, which has its own radius of convergence. With increasing ν, the radius decreases and the convergence becomes worse;[9] starting with $\nu_{max} = 4.8$, the series in the right half of (1) diverges. From this point of view, we can say that the accuracy of the approximation made in [3] is small in the region $\nu > \nu_{max}/2$.

The system of integral equations for the amplitude of the $\pi\pi$ scattering proposed in the present article differs from the system of Hsien et al[3] in two main points. First, to obtain a better approximation of the amplitude we use not the expansion in powers of $\cos^2\theta - 1$, but the expansion

$$A^{0,2}(\nu, \cos^2\theta) = \sum_{n=0}^{\infty} \frac{1}{n!}\left(\frac{\partial^n A}{\partial w^n}\right)_{w=0} w^n(\cos^2\theta).$$

$$w|_{\cos^2\theta=1} = 0.$$

Here $w(\cos^2\theta)$ is chosen to make the expansion converge as fast as possible. In other words, the function $w(\cos^2\theta)$ is a conformal mapping (see [9]) of the complex plane $\cos^2\theta$, with the aid of which ν_{max} can be shifted as far as desired towards higher energies. We can therefore conclude that our equations take into account the region $\nu > 2$ more accurately, because the corresponding expression for the partial wave

$$A_l^{0,2} = \sum_{n=0}^{\infty} \frac{1}{n!}\left(\frac{\partial^n A}{\partial w^n}\right)_{w=0} \int_0^l w^n(\cos^2\theta)\, P_l(\cos\theta)\, d\cos\theta \qquad (2)$$

(l even) converges for all energies. This may prove important in the case when the expected resonance occurs at $\nu > 2$.

Second, our expansion in powers of $w(\cos^2\theta)$, contains an infinite number of waves even in the first approximation, so that the contributions from the higher waves can be estimated. In order not to lose this advantage, we use everywhere expansion in powers of w only; the unitarity condition, in particular, is also expanded in w^n, since a transition to partial waves would lead to the problem of rearrangement of two infinite series, and thereby to loss of accuracy.

As shown earlier[9] the series in w^n converges most rapidly when $w(\cos^2\theta)$ maps the cut $\cos^2\theta$ plane on a unit circle. The cuts themselves are mapped on the boundary of this circle. Consequently, the expansion in powers of w converges in all the cut plane $\cos^2\theta$, particularly in the physical region $0 \le \cos^2\theta \le 1$. This optimal value of w is

$$w_M(\cos^2\theta, \nu) = 1 + 2\sqrt{\tau^2 - 1}\,(\sqrt{\tau^2 - 1} - \sqrt{\tau^2 - \cos^2\theta})/(1 - \cos^2\theta), \qquad (3)$$

where $\tau(\nu)$ is the cosine of the nearest singularity.

Since the function w_M is rather complicated, we sometimes use for preliminary estimates and calculations that do not influence the final result the simpler function

$$w_P(\cos^2\theta, \nu) = (1 - \cos^2\theta)/(\alpha^2 - \cos^2\theta), \quad \alpha^2 = 2\tau^2 - 1, \qquad (3')$$

which maps the left half plane $\mathrm{Re}(\cos^2\theta) < \tau^2$ on the unit circle.

2. UNITARITY CONDITION

As can be seen from (3) and (3′), the functions w_M and w_P contain contributions from all the partial waves. We therefore write the unitarity conditions not for the partial waves, but directly for the amplitude $A(\nu, \cos\theta)$:

$$\mathrm{Im}\, A(\nu, \cos\theta) = \frac{1}{4\pi}\sqrt{\frac{\nu}{\nu+1}}\int_0^{2\pi}\int_{-1}^{+1} A^*(\nu, \cos\theta_1)\, A(\nu, \cos\theta_2)\, d\cos\theta_1 d\varphi, \qquad (4)$$

$$\cos\theta_2 = \cos\theta\cos\theta_1 - \sin\theta\sin\theta_1\cos\varphi.$$

The amplitude $A(\nu, \cos\theta)$ is expanded in powers of w:

$$A^{0,2}(\nu, \cos\theta) = A_0^{0,2}(\nu) + A_1^{0,2}(\nu)\, w + A_2^{0,2}(\nu)\, w^2 + \ldots,$$

$$A^1(\nu, \cos\theta) = \cos\theta\,(A_0^1(\nu) + A_1^1(\nu)\, w + A_2^1(\nu)\, w^2 + \ldots). \qquad (5)$$

Differentiating (4) with respect to $t = -2\nu(1 - \cos\theta)$ and putting $t = 0$, we obtain*

$$\mathrm{Im}\, A^I(\nu, \cos\theta = 1) = \frac{1}{4\pi}\sqrt{\frac{\nu}{\nu+1}}\sum_{m,n=0}^{\infty} A_m^{I*}(\nu)\, A_n^I(\nu)\, K_{m,n}^I(\nu),$$

$$\left(\frac{\partial^i \mathrm{Im}\, A^I}{\partial t^i}\right)_{t=0} = \frac{1}{4\pi(2\nu)^i}\sqrt{\frac{\nu}{\nu+1}}\sum_{m,n=0}^{\infty} A_m^{I*}(\nu)\, A_n^I(\nu)\, K_{m,n}^{I(i)}(\nu), \qquad (6)$$

where

$$K_{m,n}^{I(i)} = \frac{\partial^i}{\partial\cos\theta^i}\int_0^{2\pi}\int_{-1}^{+1} w^m(\cos\theta_1)\, w^n(\cos\theta_2)\, d\cos\theta_1 d\varphi\,|_{\cos\theta=1} \quad \text{for } I = 0, 2,$$

$$K_{m,n}^{1(i)} = \frac{\partial^i}{\partial\cos\theta^i}\int_0^{2\pi}\int_{-1}^{+1} \cos\theta_1 w^m(\cos\theta_1)\cos\theta_2 w^n(\cos\theta_2)\, d\cos\theta_1 d\varphi\,|_{\cos\theta=1} \quad \text{for } I = 1. \qquad (7)$$

*The dispersion integrals are written for t = const, and not for $\cos\theta$ = const. When t = 0 both formulations are equivalent, but the condition t = const is convenient because differentiation of the dispersion integrals with respect to t corresponds to differentiation with respect to θ with a single subtraction.

In the present article we take into account in (6) only i = 0 and 1. Since w_M is a rather complicated function, it is advantageous to evaluate the integrals $K^{I(i)}_{m,n}$, defined by (7), with the aid of electronic computers. In the cases when explicit closed expressions are necessary for the integrals $K^{I(i)}_{m,n}$ we must forego the optimum w_M and substitute w_P into (7). We then obtain for I = 0 or 2:

$$K^I_{00} = 4\pi,$$

$$K^I_{10} = K^I_{01} = 4\pi - 2\pi\alpha^{-1}(\alpha^2-1)\ln[(\alpha+1)/(\alpha-1)],$$

$$K^I_{11} = -2\pi\alpha^{-2}(3\alpha^2-1) - \pi\alpha^{-3}(3\alpha^2+1) \times (\alpha^2-1)\ln[(\alpha+1)/(\alpha-1)];$$

$$K^{I'}_{00} = K^{I'}_{10} = K^{I'}_{01} = 0,$$

$$K^{I'}_{11} = \tfrac{1}{6}\pi\alpha^{-4}(3\alpha^4-2\alpha^2+3) - \tfrac{1}{4}\pi\alpha^{-5}(\alpha^2+1)(\alpha^2-1)^2\ln[(\alpha+1)/(\alpha-1)] \quad (8a)$$

and for I = 1

$$K^1_{00} = 4\pi/3,$$

$$K^1_{01} = K^1_{10} = 4\pi/3 + 4\pi(\alpha^2-1) - 2\pi(\alpha^2-1)\alpha\ln[(\alpha+1)/(\alpha-1)],$$

$$K^1_{11} = 4\pi/3 + 10\pi(\alpha^2-1) - \pi\alpha^{-1}(\alpha^2-1)(5\alpha^2-1)\ln[(\alpha+1)/(\alpha-1)];$$

$$K^{1'}_{00} = K^1_{00}, \qquad K^{1'}_{10} = K^{1'}_{01} = K^1_{01},$$

$$K^{1'}_{11} = 2\pi - \tfrac{1}{2}\pi\alpha^{-2}(\alpha^2-1)(15\alpha^2+1) - \tfrac{1}{4}\pi\alpha^{-3}(\alpha^2-1)(15\alpha^4+1)\ln[(\alpha+1)/\alpha-1)]. \quad (8b)$$

3. INTEGRAL EQUATIONS

We start from the dispersion relations for constant t:

$$A^I(\nu,t) = \frac{1}{\pi}\int_0^\infty \frac{d\nu'}{\nu'-\nu}\operatorname{Im}A^I(\nu',t) + \sum_{J=0}^{2}\frac{1}{2}\tilde{\alpha}_{IJ}\frac{1}{\pi}\int_0^\infty \frac{d\nu'}{1+\nu+\nu'+t/4}\operatorname{Im}A^J(\nu',t), \quad (9)$$

where $\tilde{\alpha}_{IJ}/2$ denotes the matrix of the crossing transformation in isotopic space:

$$\tilde{\alpha}_{IJ} = \begin{pmatrix} 2/3 & -2 & 10/3 \\ -2/3 & 1 & 5/3 \\ 2/3 & 1 & 1/3 \end{pmatrix}. \quad (10)$$

$\tilde{\alpha}_{IJ}$ is connected with α_{IJ} of [1] by the relations $\tilde{\alpha}_{IJ} = (-1)^{I+J}\alpha_{IJ}$.

Restricting ourselves to two terms in the expansion (5), we must differentiate (9) with respect to t and set t = 0. Using (6), we obtain integral equations (without subtraction) for $A^I_0(\nu)$ and $A^I_1(\nu)$:

$$A^I_0(\nu) = \frac{1}{4\pi^2}\int_0^\infty \frac{d\nu'}{\nu'-\nu}\sqrt{\frac{\nu'}{\nu'+1}}\sum_{m,n=0}^{1} A^{I*}_m A^I_n K^I_{mn} - \sum_{J=0}^{2}\tilde{\alpha}_{IJ}\frac{1}{8\pi^2}\int_0^\infty \frac{d\nu'}{1+\nu+\nu'}\sqrt{\frac{\nu'}{\nu'+1}}\sum_{m,n=0}^{1} A^{J*}_m A^J_n K^J_{mn}, \quad (11a)$$

$$\left(\frac{\partial w}{\partial\cos\theta}\right)_{\cos\theta=1} A^I_1(\nu) = -A^1_0(\nu)\delta_{1I} + \frac{\nu}{4\pi^2}\int_0^\infty \frac{d\nu'}{\nu'-\nu}\frac{1}{\sqrt{\nu'(\nu'+1)}}\sum_{m,n=0}^{1} A^{I*}_m A^I_n K^{I'}_{mn} + \sum_{J=0}^{2}\tilde{\alpha}_{IJ}\frac{\nu}{8\pi^2}\int_0^\infty \frac{d\nu'}{1+\nu+\nu'}\frac{1}{\sqrt{\nu'(\nu'+1)}}\sum_{m,n=0}^{1} A^{J*}_m A^J_n K^{J'}_{mn} - \sum_{J=0}^{2}\tilde{\alpha}_{IJ}\frac{\nu}{16\pi^2}\int_0^\infty \frac{d\nu'}{(1+\nu+\nu')^2}\sqrt{\frac{\nu'}{\nu'+1}}\sum_{m,n=0}^{1} A^{J*}_m A^J_n K^J_{mn}. \quad (11b)$$

The factor $(\partial w/\partial\cos\theta)|_{\cos\theta=1}$ is equal to $-1/2(\tau^2-1)$ when $w \equiv w_M$ and to $-1/(\tau^2-1)$ when $w \equiv w_P$.

As shown in Sec. 2, the subtraction has already been carried out in (11b). It is therefore sufficient to subtract only in (11a). Unlike [1] and, [3] where the subtraction is made at the points $s = \bar{s} = t = 4/3$ and $t = 0$, $s = \bar{s} = 2$, respectively, we choose for the subtraction point the threshold of the first reaction $s = 4$, $\bar{s} = t = 0$.

We introduce the following notation

$$A^0(\nu = 0,\ t = 0) = a^0,$$

$$A^2(\nu = 0,\ t = 0) = a^2 \quad (A^1(\nu = 0,\ t = 0) = 0).$$

Both scattering lengths a^0 and a^2 are related by

$$a^0 = \frac{5}{2}a^2 + \frac{1}{8\pi^2}\int_0^\infty \frac{d\nu'}{\sqrt{\nu'}(\nu'+1)^{3/2}}\left(2\sum_{m,n=0}^{1} A^{0*}_m A^0_n K^0_{mn} + 3\sum_{m,n=0}^{1} A^{1*}_m A^1_n K^1_{mn} - 5\sum_{m,n=0}^{1} A^{2*}_m A^2_n K^2_{mn}\right). \quad (12)$$

After subtraction, (11a) becomes

$$A^I_0(\nu) = a^I + \frac{\nu}{4\pi^2}\int_0^\infty \frac{d\nu'}{\nu'-\nu}\frac{1}{\sqrt{\nu'(\nu'+1)}}\sum_{m,n=0}^{1} A^{I*}_m A^I_n K^I_{mn} - \sum_{J=0}^{2}\tilde{\alpha}_{IJ}\frac{\nu}{8\pi^2}\int_0^\infty \frac{d\nu'}{1+\nu+\nu'}\frac{\sqrt{\nu'}}{(\nu'+1)^{3/2}}\sum_{m,n=0}^{1} A^{J*}_m A^J_n K^J_{mn}. \quad (11a')$$

4. ESTIMATE OF ACCURACY OF THE UNITARITY CONDITION

The rate of convergence of the expansion depends on the position of the nearest singularity of the amplitude A, i.e., on the distance from the line t = 4, which is the first of the lines t = const intersecting (asymptotically) the regions of the spectral functions A_{13} and A_{23}. (In the complex-cosine

plane this corresponds to a cut beginning with $\tau_\infty = 1 + 2/\nu$.) However, according to the main premises of the theory we can expect the influence of the far regions of the spectral functions to be negligibly small at low energies. We can therefore assume for estimating purposes that the cut in t begins with the line $t = 44/7$, which crosses the boundary $s = 16t/(t-4)$ of the spectral function at the point $\nu = 10$ ($s = 44$). In the cosine plane, this corresponds to a branch point at $\tau_{10} = 1 + 22/7\nu$.

We give below estimates made at the threshold of the first inelastic process, i.e., $\nu = 3$, where τ_∞ and τ_{10} are respectively equal to $5/3$ and 2.047. To estimate the upper limit of the errors, we choose as the "amplitude" the function

$$A' = (\tau + \cos\theta)^{-1} + (-1)^l (\tau - \cos\theta)^{-1},$$

the singularities of which are concentrated in the very start of the former cut. For a comparison of the convergence of the series in powers of w and $\cos^2\theta - 1$ we refer the reader to Table 1 of [9], where several partial waves are calculated for I = 0 and 2 in both approximations.

The errors in the unitarity conditions are caused by the fact that we restrict ourselves to the constant linear terms in the expansion of the amplitude in w^n. For w we choose w_P [see (3')] with $\tau = 2.047$. Accordingly, the integrals K_{mn} are determined by the formulas (8).

In the case of even isotopic spin I, the errors in the function $\sum_{m,n=0}^{1} A_m^{I*} A_n^I K_{mn}^I$ and of its derivative, compared with their exact expressions (summation from 0 to ∞), are respectively -4.08 and $+33.2$ percent. Although the second of these errors seems large, the total error in (11) is small. This is brought about by the fact that (11b) contains along with $\Sigma A_m^{I*} A_n^I K_{mn}^{I'}$ also terms with $\Sigma A_m^{I*} A_n^I K_{mn}^I$ which are of much greater order of magnitude (when I = 0 or 2). Therefore the error due to the derivative is only 0.67 percent.

In the case when I = 1, both terms are of the same order of magnitude, but the errors of both are very small (-1.74 and -1.046 percent, respectively).

5. CONCLUSION

The analyticity assumptions implied in the Mandelstam representation, together with the unitarity property of the S matrix, serve as a basis for derivation of integral equations for A.

Naturally, such equations cannot be solved without making certain approximations such as the two-particle approximation in the unitarity condition, or the account of only several terms of the expansion of the amplitude in powers of the scattering-angle cosine.

The Mandelstam representation is frequently used to obtain dispersion relations in one variable only (for example, the energy), and these are simpler in form than the two-dimensional relations. The dependence of A on another variable (the momentum transfer or the cosine) is represented in series form. A series in Legendre polynomials can be used in principle, but it diverges in a large part of the nonphysical region. This circumstance was taken into account in [3], but the approach proposed there calls for knowledge of one or several derivatives ($\partial^n A/\partial \cos\theta^n$) for $\cos\theta = \pm 1$, in terms of which the partial waves are expressed. In other words, it is necessary to use in addition to the Legendre series the Taylor series, which in turn has its own convergence region.

In the present article we have, in accordance with [3], also expanded the dependence of A on the cosine in the vicinity of $\cos\theta = \pm 1$, but in powers of a definite function which has singularities precisely where A has them. This causes, first, the amplitude to be expanded in a power series that converges in the most rapid manner (see [9], Appendix 1). The errors due to the inclusion of the first two terms only, estimated in Sec. 4, confirm this result. Second, we have attained, albeit partly, symmetry in the analysis of the energy and of the momentum transfer.

We are grateful to Prof. Chu Hun-Yuang for continuous interest in the work and for valuable remarks. We are also indebted to all the participants of the Seminar given by Academician N. N. Bogolyubov for useful discussions.

Note added in proof (June 16, 1961): Wolf and Zoellner advised us that they obtain good agreement with experiments on τ decay, choosing $a^0 = 0.3$ and $a^2 = 0.2$. Their article will be published in JETP.

[1] G. Chew and S. Mandelstam, Phys. Rev. **119**, 467 (1960).

[2] G. Chew, Ann. Rev. Nucl. Sci. **9**, 29 (1959).

[3] Hsien, Ho, and Zoellner, JETP **39**, 1660 (1960), Soviet Phys. JETP **12**, 1159 (1961).

[4] S. Mandelstam, Phys. Rev. **112**, 1344 (1958).

[5] S. Mandelstam. Phys. Rev. **115**, 1752 (1959).

[6] S. Mandelstam, Phys. Rev. **115**, 1741 (1959).

[7] Efremov, Meshcheryakov, Chu, and Shirkov, On the Derivation of Equations from the Mandelstam Representation, preprint, Joint Institute for Nuclear Research; Nuclear Physics **22**, 202 (1961).

[8] Chew, Goldberger, Low, and Nambu, Phys. Rev. **106**, 1337 (1957).

[9] S. Ciulli and J. Fischer, Nucl. Phys. **24**, 465 (1961).

Translated by J. G. Adashko
51

DISINTEGRATION OF NONEVOLUTIONAL SHOCK WAVES

R. V. POLOVIN and K. P. CHERKASOVA

Physico-Technical Institute, Academy of Sciences, Ukrainian S.S.R.

Submitted to JETP editor February 17, 1961

J. Exptl. Theoret. Phys. (U.S.S.R.) 41, 263-266 (July, 1961)

Disintegration of a magnetohydrodynamic shock wave with a small density discontinuity is investigated. The initial shock wave is a compression wave for which all boundary conditions are satisfied and the entropy increases. If the initial shock wave is evolutional, it cannot disintegrate. A non-evolutional shock wave can disintegrate into six magnetohydrodynamical waves (shock or self-similar waves, depending on the magnitude and direction of the initial magnetic field).

1. In magnetohydrodynamics, satisfaction of the boundary conditions on the discontinuity surface and an increase in the entropy are not sufficient to ensure existence of a shock wave. It is necessary also that the evolutionarity conditions be satisfied,[1,2] namely that the number of outgoing waves be equal to the number of independent boundary conditions on the discontinuity surface. In the opposite case, the problem of small perturbations of the shock wave has no solution, indicating that the initial shock wave disintegrates into several shock and self-similar waves.

The non-evolutionarity regions apparently coincide with the regions where the initial shock wave can disintegrate. A direct proof of this theorem was given only for the particular case when the velocity of the shock wave is close to the Alfven velocity, and the magnetic field on both sides of the shock wave makes a small angle with the normal to the discontinuity surface.

In the present paper we prove this theorem for another particular case, that of a shock wave with a small density jump. Such a shock wave will be evolutionary if the jumps of all the magnetohydrodynamic quantities are small, or non-evolutionary if it is close to a 180° Alfven discontinuity (these waves were investigated in detail by Bazer and Ericson[3]).

2. We consider first the possibility of disintegration of an evolutionary shock wave in which the jumps of all the magnetohydrodynamic quantities are small.

In this case we can use the results obtained by Lyubarskii and Polovin,[4] who determined the amplitudes of the waves produced as a result of disintegration of a small discontinuity:*

$$\Delta_{\pm}^{(\varepsilon)}v = \pm\frac{1}{2R}\left\{\varepsilon\frac{U_y^2c^2\left[\Delta\rho-(\partial\rho/\partial s)_p\Delta s\right]}{U_{\pm}^2-U^2}-\varepsilon\frac{\Delta H_y^2}{8\pi}\right.$$
$$\left.-\frac{\rho U_x^2}{U_{\pm}}\left[\frac{H_y\Delta v_y}{H_x}+\frac{U_y^2\Delta v_x}{U_{\pm}^2-U_x^2}\right]\right\}. \qquad (1)$$

Here

$$\mathbf{U}\equiv\mathbf{H}/\sqrt{4\pi\rho},\qquad U_{\pm}=\left[(U^2+c^2\pm R)/2\right]^{1/2},$$
$$R=\left[(U^2+c^2)^2-4c^2U_x^2\right]^{1/2};$$

$\Delta\rho$, Δs, Δv, and ΔH_y are the jumps in the density, entropy, velocity, and transverse magnetic field on the initial discontinuity; c is the velocity of sound; the upper symbol in the $\pm$ sign pertains to the rapid magnetoacoustic wave, while the lower one pertains to the slow wave; $\epsilon = +1$ for waves propagating in the direction of positive x relative to the medium, while $\epsilon = -1$ pertains to waves propagating in the opposite direction; the x axis is directed along the normal to the discontinuity. A shock wave corresponds to $\Delta_{\pm}^{(\epsilon)}\rho > 0$, while a self-similar wave corresponds to $\Delta_{\pm}^{(\epsilon)}\rho < 0$.

If the initial discontinuity is a shock wave of low intensity, then the jumps in the magnetohydrodynamic quantities are related by the following equations

$$\Delta v_{\pm}/\Delta\rho = \varepsilon U_{\pm}/\rho,\qquad \Delta v_y/\Delta\rho = -\varepsilon H_xH_yU_{\pm}/4\pi\rho^2(U_{\pm}^2-U_x^2),$$
$$\Delta H_y/\Delta\rho = U_{\pm}^2H_y/\rho(U_{\pm}^2-U_x^2),\qquad \Delta p/\Delta\rho = c^2. \qquad (2)$$

Assuming, for the sake of being definite, that the initial discontinuity moved in the direction of negative x ($\epsilon = -1$) and substituting (2) into (1), we obtain

$$\Delta_{\pm}^{(-)}\rho = \Delta_{\pm}\rho,\qquad \Delta_{\pm}^{(-)}\rho = \Delta_{\pm}^{(+)}\rho = \Delta_{\mp}^{(+)}\rho = 0.$$

This means that an evolutionary shock wave of low intensity cannot disintegrate.

3. We now proceed to investigate the disintegration of a non-evolutionary shock wave with small

*An error has crept into this formula in the papers of Polovin and Lyubarskii.[2,4]

density jump. The jumps in the magnetohydrodynamic quantities in such a wave are related by

$$\Delta v_x = U_{1x}\rho_1^{-1}\Delta\rho, \qquad \Delta p = \left[c_1^2 + (\gamma-1)U_{1y}^2\right]\Delta\rho,$$
$$\Delta H_z = 2H_{1y}\left[1 - \frac{U_{1x}^2 - c_1^2 - (\gamma-1)U_{1y}^2}{2U_{1y}^2}\frac{\Delta\rho}{\rho_1}\right],$$
$$\Delta v_y = 2U_{1y}\left[1 - \frac{U_{1x}^2 - c_1^2 - \left(\gamma-\frac{1}{2}\right)U_{1y}^2}{2U_{1y}^2}\frac{\Delta\rho}{\rho_1}\right]. \qquad (3)$$

The subscript 1 pertains to the region in front of the shock wave. We note that as $\Delta\rho \to 0$, this wave goes into an Alfven discontinuity, which rotates the magnetic field through 180°. We note also that the entropy jump on such a wave is a second-order quantity, $\Delta s = (U_{1y}^2/\rho_1 T_1)\Delta\rho$.

The initial shock wave (3) can break up into seven waves; three waves moves to the right (fast magnetoacoustic, Alfven discontinuity, and slow magnetoacoustic), three waves move to the left (fast, Alfven, and slow), and a contact discontinuity, at rest relative to the medium, in the middle.

Let us examine first the Alfven discontinuity. The jumps in the magnetohydrodynamic quantities on the Alfven discontinuity are related by the equations

$$\Delta_A^{(\varepsilon)}H_y = H_{1y}(\eta_\varepsilon - 1), \qquad \Delta_A^{(\varepsilon)}v_y = \varepsilon U_{1y}(1 - \eta_\varepsilon). \qquad (4)$$

The jumps in the other magnetohydrodynamic quantities are equal to zero; the subscript 1 pertains to the region in front of the discontinuity, ϵ has the same meaning as in (2), $\eta_\epsilon = 1$ if there is no Alfven discontinuity, and $\eta_\epsilon = -1$ if the Alfven discontinuity rotates the magnetic field through 180°.

Expressing ΔH_y and Δv_y in terms of $\Delta_\pm^{(\epsilon)}H_y$, $\Delta_\pm^{(\epsilon)}v_y$, $\Delta_A^{(\epsilon)}H_y$, and $\Delta_A^{(\epsilon)}v_y$, and noting that $\Delta_\pm^{(\epsilon)}H_y$ and $\Delta_\pm^{(\epsilon)}v_y$ tend to zero as $\Delta\rho \to 0$, we obtain $\eta_- = -1$ and $\eta_+ = +1$. This means that disintegration of the initial shock wave results in a 180° Alfven discontiniity moving in the same direction as the initial wave. There is no Alfven discontinuity moving in the opposite direction.

We now proceed to determine the amplitudes of the magnetoacoustic waves and of the contact discontinuity. Each of these five waves is characterized by a single parameter—the density jump. On the other hand, the sum of the jumps of each of the five magnetohydrodynamic quantities (p, ρ, v_x, v_y, and H_y) on the seven resultant waves is equal to the initial jump. Since the number of unknown amplitudes is equal to five ($\Delta_+^-\rho$, $\Delta_-^-\rho$, Δ_k, $\Delta_-^+\rho$, and $\Delta_+^+\rho$), we obtain a system of five equations with five unknowns, the solution of which yields

$$\Delta_k\rho = -(\gamma-1)c_1^{-2}U_{1y}^2\Delta\rho,$$
$$\Delta_+^+\rho = \left[\frac{U_{1x}^2+U_{1-}^2}{2\left(U_{1x}^2-U_{1-}^2\right)} + \frac{U_1^2-c_1^2-\gamma U_{1y}^2}{U_{1y}^2} - b_+\left(\frac{U_{1x}U_{1+}}{U_{1x}^2-U_{1-}^2} + \frac{U_{1+}^2+U_{1x}^2-U_{1+}U_{1x}}{U_{1-}^2-U_{1x}^2}\right)\right]\frac{\Delta\rho}{a},$$
$$\Delta_+^-\rho = \left[\frac{U_{1x}^2+U_{1-}^2}{2\left(U_{1x}^2-U_{1-}^2\right)} + \frac{U_1^2-c_1^2-\gamma U_{1y}^2}{U_{1y}^2} + \frac{U_{1+}Rb_+}{U_{1x}U_{1y}^2}\right]\frac{\Delta\rho}{a},$$
$$\Delta_-^{(\varepsilon)}\rho = \left[\frac{U_{1+}^2}{2\left(U_{1+}-U_{1x}\right)} - \frac{U_{1x}^2}{2\left(U_{1+}+U_{1x}\right)} - \frac{U_{1+}\left(U_1^2-c_1^2-\gamma U_{1y}^2\right)}{U_{1y}^2} + \frac{1}{2}\frac{U_{1+}-U_{1x}}{U_{1+}+U_{1x}}U_{1+}b_+\right]\frac{\Delta\rho}{U_{1-}a} - \frac{\varepsilon b_-}{2}\Delta\rho, \qquad (5)$$

where

$$R = \sqrt{\left(U_1^2+c_1^2\right)^2 - 4c_1^2U_{1x}^2},$$
$$x = \left(U_{1+}^2+U_{1x}^2\right)/\left(U_{1+}^2-U_{1x}^2\right) + 2U_{1x}U_{1+}/\left(U_{1x}^2-U_{1-}^2\right),$$
$$b_\pm = \pm\frac{U_{1y}^2}{R}\left[\frac{U_1^2-c_1^2-\gamma U_{1y}^2}{U_{1y}^2} - \frac{c_1^2+(\gamma-1)U_{1y}^2}{U_{1\mp}^2-U_1^2}\right].$$

The character of the wave (shock or self-similar) is determined by the sign of the quantity $\Delta_\pm^{(\epsilon)}\rho$.

If $U_1 \ll c_1$, then all the waves produced during the disintegration are shock waves.

On the other hand, if $U_1 \gg c_1$, $H_{1x} \ll H_{1y}$, or $H_{1y} \ll H_{1x}$, then the slow wave that moves in the same direction as the initial shock wave will be a shock wave. The remaining waves can be either shock or self-similar, depending on the values of U_1/c_1, H_{1x}/H_{1y}, and γ.

The authors are grateful to A. I. Akhiezer for valuable discussions.

[1] Akhiezer, Lyubarskii, and Polovin, JETP **35**, 731 (1958), Soviet Phys. JETP **8**, 507 (1959).

[2] R. V. Polovin, UFN **72**, 33 (1960), Soviet Phys. Uspekhi **3**, 677 (1961).

[3] J. Bazer and W. B. Ericson, Astrophys. J. **129**, 758 (1959); Phys. Fluids **3**, 631 (1960).

[4] G. Lyubarskii and R. V. Polovin, JETP **35**, 1291 (1958), Soviet Phys. JETP **8**, 901 (1959).

Translated by J. G. Adashko
52

HIGH-FREQUENCY MAGNETIC SUSCEPTIBILITY OF A UNIAXIAL ANTIFERROMAGNET IN A LONGITUDINAL MAGNETIC FIELD

M. I. KAGANOV and V. M. TSUKERNIK

Physico-Technical Institute, Academy of Sciences, Ukrainian S. S.R.

Submitted to JETP editor February 17, 1961

J. Exptl. Theoret. Phys. (U.S.S.R.) **41**, 267-271 (July, 1961)

The high-frequency magnetic susceptibility tensor of an antiferromagnet is calculated for various values of a constant magnetic field applied along the axis of the specimen. The calculation is based on the Landau-Lifshitz equation of motion for the sublattice moments.

THE dispersion of the magnetic susceptibility of an antiferromagnet is fundamentally related to rotation of the magnetic moments of the sublattices in the effective magnetic field (including the external magnetic field). The imaginary part of the magnetic susceptibility has resonance characteristics; the resonance frequencies coincide with the natural frequencies of rotation of the system of moments. The resonance frequencies of an antiferromagnet were calculated for various equilibrium configurations by Kittel[1] and by Turov.[2] The present authors[3] calculated the high-frequency magnetic susceptibility of a uniaxial antiferromagnet in the absence of a constant magnetic field.

We know[4] that a sufficiently strong constant magnetic field can change the equilibrium configuration of the sublattice moments; this naturally produces a change in the nature of the dispersion. The subject of this article is the calculation of the high-frequency magnetic susceptibility of an antiferromagnet for various equilibrium configurations of the moments. The results obtained make it possible to determine the equilibrium structures and the type of transition between them from high-frequency measurements.

We consider a uniaxial antiferromagnet with two sublattices, located in a constant and uniform magnetic field directed along the chosen axis, and also in a weak alternating magnetic field of frequency ω. For calculation of the magnetic susceptibility of the antiferromagnet, it is necessary to consider the forced motion of the magnetic moments of the sublattices under the influence of the alternating field. This motion is known to be describable by the Landau-Lifshitz equation

$$\partial \mathbf{M}_s / \partial t = g\,[\mathbf{M}_s \mathbf{H}_e^{(s)}] - (\gamma / M^2)\,[\mathbf{M}_s\,[\mathbf{M}_s \mathbf{H}_e]], \qquad (1)^*$$

where $\mathbf{M}_s$ is the vector magnetization of the s-th sublattice (s = 1, 2); M is the magnitude of the magnetization of each of the sublattices and is assumed to be constant; g is the gyromagnetic ratio, γ a relaxation constant, and $\mathbf{H}_e^{(s)}$ the effective field acting on the s-th sublattice:

$$\mathbf{H}_e^{(s)} = -\partial \mathcal{H} / \partial \mathbf{M}_s, \qquad (2)$$

κ is the energy density of the antiferromagnet,

$$\mathcal{H} = \alpha \mathbf{M}_1 \mathbf{M}_2 - \tfrac{1}{2}\lambda\,[(\mathbf{M}_1\mathbf{n})^2 + (\mathbf{M}_2\mathbf{n})^2] + \eta\,(\mathbf{M}_1\mathbf{n})\,(\mathbf{M}_2\mathbf{n}) - \mathbf{H}\,(\mathbf{M}_1 + \mathbf{M}_2). \qquad (3)$$

Here α is the exchange interaction constant ($\alpha > 0$), and λ and η are anisotropy constants, which will be assumed to be positive.* Positiveness of the constants λ and η insures that in the absence of an external field, the magnetic moments will be directed antiparallel and along the axis of the antiferromagnet (**n** is a unit vector along this axis).

It is known[1] that if a constant magnetic field of magnitude greater than $H_1 = \sqrt{(\lambda+\eta)(2\alpha-\lambda+\eta)}\,M$ is applied along the axis, then the energetically preferred magnetic state is one in which the vectors $\mathbf{M}_1$ and $\mathbf{M}_2$ are oriented symmetrically with respect to the axis **n**, at an angle θ such that

$$\cos\theta = H/M\,(2\alpha - \lambda + \eta). \qquad (4)$$

The transition to the new ground state involves the surmounting of a potential barrier and is accompanied by evolution of heat (a transition of the first kind). Under these circumstances, of course, there is a range of fields in which the antiparallel orientation of moments is metastable. The upper limit of the metastable states is the field

$$H_2 = \sqrt{(\lambda+\eta)(2\alpha-\lambda+\eta)}\,M$$

*$[\mathbf{MH}] = \mathbf{M} \times \mathbf{H}$; $(\mathbf{MH}) = \mathbf{M} \cdot \mathbf{H}$.

*Since the anisotropy energy is related to relativistic interactions, λ and $\eta \ll \alpha$.

(the lability field). According to Eq. (4) the angle between the magnetic moments depends on the applied field when $H > H_2$ and becomes zero when

$$H = H_3 = (2\alpha - \lambda + \eta) M.$$

Subsequent increase of field does not change the structure of the magnetic state. At $H = H_3$ there occurs a phase transition of the second kind: the longitudinal component χ_{zz} of the magnetic susceptibility (the z axis is chosen along $\mathbf{n}$) changes discontinuously from the value $2/(2\alpha - \lambda + \eta)$ for $H < H_3$ to zero for $H \geq H_3$.* We remark that the components χ_{xx} and χ_{yy} of the magnetic susceptibility are continuous at $H = H_3$.

On decrease of the field from values below H_3, it is possible to carry over into the low-field region the configuration with a symmetrical orientation of the moments with respect to the axis. The lability field in this case is

$$H_4 = [\lambda (2\alpha - \lambda + \eta)^2/(2\alpha + \lambda + \eta)]^{1/2} M.$$

We note that $H_4 < H_1$. The difference $H_2 - H_4$ determines the width of the hysteresis loop in the magnetization of the antiferromagnet.

We shall derive an expression for the high-frequency magnetic susceptibility tensor $\chi_{ik}(\omega)$ for various values of the constant field H. The tensor $\chi_{ik}(\omega)$ is calculated by means of Eq. (1), linearized with respect to the high-frequency field, at the equilibrium configurations considered above.

1. $H < H_1$. In this case, as is usual in gyrotropic media, it is convenient to describe the magnetic susceptibility by giving the values of $\chi_\pm$ in

$$m_\pm = \chi_\pm h_\pm,$$

where $h_\pm = h_x \pm i h_y$, $m_\pm = m_x \pm i m_y$; $\mathbf{h}$ is the high-frequency magnetic field and $\mathbf{m}$ the alternating part of the resultant magnetic moment. With the abbreviations

$$\Omega^2 = (g^2M^2 + \gamma^2)(\lambda + \eta)(2\alpha + \lambda + \eta) - \gamma^2 H^2/M^2,$$
$$\Omega_1^2 = 2(g^2M^2 + \gamma^2)(\lambda + \eta), \qquad (5)$$

the expressions for the components of the tensor χ_{ik} can be written

$$\chi_\perp = \frac{\Omega_1^2 - 2i\omega\gamma}{\Omega^2 - (\omega \mp gH)^2 - 2i\omega\gamma(\alpha + \lambda + \eta)}, \qquad \chi_{zz} = 0. \qquad (6)$$

From (6) it is evident that the role of antiferromagnetic resonance line width is played by the quantity $2\gamma(\alpha + \lambda + \eta)$.[3] At $H = 0$ the values of χ_+ and χ_- are equal:

$$\chi_+ = \chi_- = \chi_{xx} = \chi_{yy}.$$

The off-diagonal components χ_{xy} and χ_{yx} are then zero. This means that at $H = 0$ there is no gyrotropy.[3] It should be mentioned that in reference 3 a mistake was made, in consequence of which an incorrect frequency dependence of the imaginary part of χ_{xx} was obtained.*

2. $H_1 < H < H_3$. Because of the dependence of the angle between the magnetic moments upon the magnetic field, in this case $\chi_{zz} \neq 0$. The calculations lead to the following result:

$$\chi_{zz}(\omega) = \chi_{zz}(0) \frac{\nu^2}{\nu^2 + \omega^2} - i\frac{\nu\omega}{\nu^2 + \omega^2}; \qquad (7)$$

$$\chi_{zz}(0) = 2/(2\alpha - \lambda + \eta),$$

$$\nu = (2\alpha - \lambda + \eta)\gamma \sin^2\theta = \gamma(1 - H^2/H_3^2) H_3/M. \qquad (8)$$

Here the angle θ is determined by formula (4). We notice that for $\omega \neq 0$ the value of χ_{zz} approaches zero as $H \to H_3$, i.e., as $\theta \to 0$.

Formula (7) describes a behavior with relaxation time $\tau = 1/\nu$ in the neighborhood of the phase transition of the second kind (where $H \approx H_3$):

$$\tau = \frac{1}{\gamma} \frac{MH_3}{H_3^2 - H^2}. \qquad (8')$$

The approach of the relaxation time to infinity at $H = H_3$ is in accordance with a result of the general theory of phase transitions of the second kind.[5]

We have assumed that the temperature of the body was fixed. If we take into account that all the parameters on which the tensor χ_{ik} depends are functions of temperature, then the equation $H_3 = H$ at fixed H must be regarded as an equation for determination of the temperature T_c of the phase transition of the second kind. Then formula (8′) determines the relaxation time τ in the neighborhood of T_c:

$$\tau = \frac{G}{T_c - T}, \quad G = M/2\gamma \left|\frac{dH_3}{dT}\right|_{T=T_c} \qquad (8'')$$

Formulas (7), (8), (8′), and (8″) show that at fixed frequency there is a field or a temperature at which the absorption in a high-frequency magnetic field along the z axis reaches a maximum. The height and position of the maximum depend on the frequency ω. The maximum always occurs in that phase in which the angle between the sublattice moments is different from zero (this angle

*Strictly, $\chi_{zz} \neq 0$ for $H \geq H_3$. The value of χ_{zz} is determined by the dependence of the energy of spin waves upon the magnetic field (the "paraprocess"). At $T = 0$, χ_{zz} becomes zero. At any temperature below the Curie-Néel temperature, the value of χ_{zz} takes a finite jump at $H = H_3$.

*Our attention was directed to this fact by E. A. Turov, to whom we are very grateful.

plays the role of the parameter η in the general theory[5]). The transverse components of the magneitc susceptibility tensor in this case are

$$\chi_{xx} = \frac{\omega_1^2 - 2i\omega\gamma}{\omega_0^2 - \omega^2 - 2i\alpha\gamma'\omega}\cos^2\theta,$$
$$\chi_{yy} = \frac{1}{\alpha}\frac{\omega_0^2 - 2i\omega\gamma}{\omega_0^2 - \omega^2 - 2i\alpha\gamma'\omega},$$
$$\chi_{xy} = -\chi_{yx} = \frac{2igM\omega\cos\theta}{\omega_0^2 - \omega^2 - 2i\alpha\gamma'\omega}. \quad (9)$$

Here

$$\omega_0^2 = (g^2M^2 + \gamma^2)(4\alpha^2\cos^2\theta - 2(\lambda + \eta)\alpha\sin^2\theta),$$
$$\omega_1^2 = 4\alpha(g^2M^2 + \gamma^2), \quad (10)$$
$$\gamma' = \gamma\left[1 + \cos^2\theta - \frac{1}{2\alpha}(\lambda + \eta)\sin^2\theta\right].$$

The x axis lies in the plane of the magnetic moments, the y axis perpendicular to this plane.

In contrast to the preceding case ($H < H_1$), here there is a single resonance frequency $\omega = \omega_0$. This is connected with the fact that we have not taken account of anisotropy in the basal plane (the xy plane). Calculation of the spin-wave spectrum in this case leads, it is known,[2] to the result that one of the frequencies of the spectrum goes to zero as the wave vector goes to zero.

3. $H > H_3$. As was pointed out above, for $H > H_3$ the two magnetic moments in the equilibrium state are parallel to each other and are directed along the magnetic field ($\mathbf{H} \parallel \mathbf{n}$). The high-frequency magnetic susceptibility tensor in this case coincides with that of a uniaxial ferromagnet:

$$\chi_{xx}(\omega) = \chi_{yy}(\omega) = \chi_\perp(0)\frac{\omega_f^2 - i\omega\gamma_f}{\omega_f^2 - \omega^2 - 2i\omega\gamma_f},$$
$$\chi_{xy}(\omega) = -\chi_{yx}(\omega) = \frac{2igM\omega}{\omega_f^2 - \omega^2 - 2i\omega\gamma_f},$$
$$\chi_{xz} = \chi_{yz} = \chi_{zz} = 0, \quad (11)$$

where

$$\chi_\perp(0) = 2M/(H + (\lambda - \eta)M),$$
$$\omega_f^2 = g^2[H + (\lambda - \eta)M]^2(1 + \gamma^2/g^2M^2),$$
$$\gamma_f = \gamma(H/M + \lambda - \eta). \quad (12)$$

Comparison of formulas (11) and (12) with formulas (9) and (10) shows that at $H = H_3 = (2\alpha - \lambda + \eta)M$, all components of the tensor $\chi_{ik}(\omega)$ are continuous.

Knowledge of the frequency dependence of the magnetic susceptibility tensor enables us to solve the problem of the dependence of the resonance frequency on the form of an ellipsoidal specimen,[6] and also to calculate the frequencies of nonuniform resonance.[7] Both problems reduce to the finding of the characteristic solutions of the system of equations*

$$\mathrm{rot}\,\mathbf{h} = 0,$$
$$\mathrm{div}\,\mathbf{h} = \begin{cases} -4\pi\,\mathrm{div}\,\hat{\chi}\mathbf{h} & \text{(inside the body)} \\ 0 & \text{(outside the body)} \end{cases}$$

with zero boundary conditions at infinity and with the usual boundary conditions at the surface of the body (here the value $\hat{\chi}$ of the tensor at $\gamma = 0$ is used).

In closing, we take this opportunity to thank A. S. Borovik-Romanov for valuable comment.

[1] F. Keffer and C. Kittel, Phys. Rev. **85**, 329 (1952).

[2] E. A. Turov, JETP **34**, 1009 (1958), Soviet Phys. JETP **34** (7), 696 (1958).

[3] M. I. Kaganov and V. M. Tsukernik, JETP **34**, 524 (1958), Soviet Phys. JETP **7**, 361 (1958).

[4] L. Néel, Ann. phys. **5**, 232 (1936).

[5] L. D. Landau and I. M. Khalatnikov, Doklady Akad. Nauk S.S.S.R. **96**, 469 (1954).

[6] C. Kittel, Phys. Rev. **71**, 270 (1947).

[7] L. Walker, Phys. Rev. **105**, 390 (1957).

Translated by W. F. Brown, Jr.
53

*rot = curl.

ONE-MESON CONTRIBUTION TO PHOTOPRODUCTION OF π^- MESONS ON PROTONS

L. V. LAPERASHVILI and S. G. MATINYAN

Physics Institute, Academy of Sciences, Georgian S.S.R.

Submitted to JETP editor February 17, 1961

J. Exptl. Theoret. Phys. (U.S.S.R.) 41, 272-275 (July, 1961)

Quantitative agreement between Drell's theory and the experiments on photoproduction of negative π mesons on protons can be obtained by taking into account the correction suggested by the Salzmans.

THE role of peripheral interactions of elementary particles caused by the exchange of a single virtual pion[1,2] has recently become of considerable interest. Along with the "pology" approach of Chew and Low,[1] connected with extrapolations of cross sections into the unphysical region of values of the 4-momentum transfer squared ($\Delta^2 = -m_\pi^2$), many authors[3-9] have viewed the one-meson contribution as dominant in the region of small, but physical, values of $\Delta^2 \approx m_\pi^2$.

A similar approach has been recently proposed by Drell[6] for photoproduction by high energy photons. In particular, for the photoproduction of π^- on protons

$$\gamma + p \to \pi^- + \pi^+ + p\,, \qquad (1)$$

one can show, according to Drell, that the diagram shown in Fig. 1 will dominate all contributions to the cross section provided that the energy of the emitted π^-, ω, is comparable with the photon energy k, and the angle θ of emission of the π^- in the barycentric frame of the colliding particles is of the order of m_π/ω:

$$\omega \approx k \gg m_\pi\,, \qquad \theta \lesssim m_\pi/\omega \qquad (\Delta^2 \approx m_\pi^2).$$

The differential cross section for process (1) has then the form

$$d^2\sigma(k,\theta,\omega) = \frac{\alpha}{2\pi}\,\frac{\sin^2\theta}{(1-\beta\cos\theta)^2}\,\frac{d\Omega}{4\pi}\,\frac{\omega(k-\omega)}{k^3}\,d\omega\,\sigma_{\pi^+ p}(Q)\,. \qquad (2)$$

Here $\alpha = 1/137$, β is the velocity of the π^- ($\hbar = c = 1$), $d\Omega$ is the solid angle element into which the π^- is emitted, $\sigma_{\pi^+ p}(Q)$ is the elastic scattering cross section for scattering of real π^+ mesons on protons, which is a function of only Q —the kinetic energy of the final π^+ meson and nucleon in their barycentric frame. Special experiments on photoproduction of π^- mesons in hydrogen were performed to test Eq. (2).[10] The dependence on ω (or Q) of $d^2\sigma(\theta, \omega)/d\Omega\, d\omega$ found at the angles

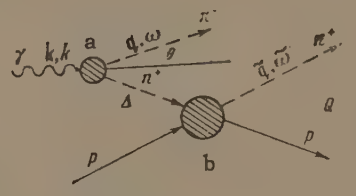

FIG. 1

$\theta = 10.5$, 17.5 and 25° is shown in Figs. 2—4 (k = 1230 Mev in the laboratory frame). [Experimental data at larger angles ($\theta = 38$ and 55°) correspond to $\Delta^2 > 4m_\pi^2$, where Drell's hypothesis does not apply.] The dashed curves appearing in the same figures were constructed using Eq. (2).

It is clear from the figures that Drell's formula correctly reflects the general behavior of the cross section as a function of Q and clearly points to its connection with the $^3/_2$ $^3/_2$ resonance in πN scattering. Quantitatively, however, theory and experiment do not agree—Eq. (2) gives too low a value for the cross section even at $\theta = 17.2°$, where it

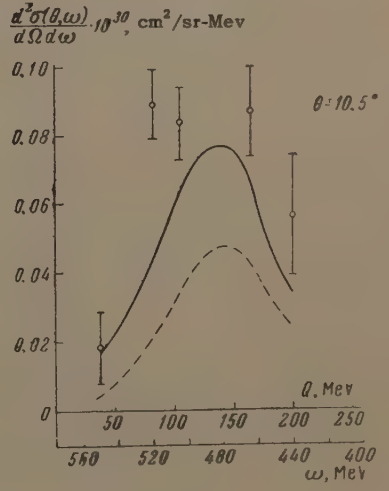

FIG. 2

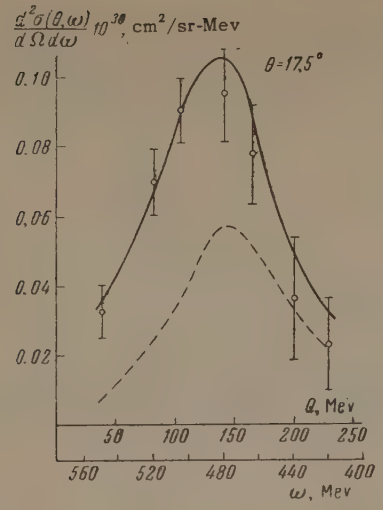

FIG. 3

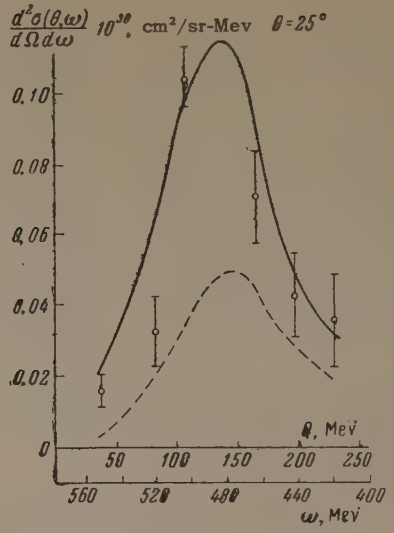

FIG. 4

has a maximum as a function of θ ($\cos\theta_{max} = \beta$) for maximum value of $\sigma_{\pi^+ p}(Q)$.*

It must be further noted that the reproduction of the resonance curve of the πN interaction in process (1) can be obtained to a larger or lesser extent in any isobar model, therefore a real test of Drell's hypothesis requires rigorous quantitative agreement between theory and experiment in that region of angles where the contribution from the diagram of Fig. 1 is supposed to be dominant.

It will be shown below that the discrepancy between theory and experiment is apparent only, and that after an appropriate modification of Eq. (2) quantitative agreement between theory and experiment is obtained.

Indeed, the cross section $\sigma_{\pi^+ p}(Q)$ appearing in Eq. (2) refers to the scattering of a real π^+ meson whereas for physical values of Δ^2 a virtual pion is absorbed in the blob of vertex b (Fig. 1). As was shown by the Salzmans,[8,9] for small physical values of Δ^2 such a meson behaves as an "almost real" incident (in the $\pi^+ + p$ barycentric system) meson. Its energy is approximately equal to the energy $\tilde{\omega}$ of the real π^+ emitted from the blob in the vertex b, while the momenta of these mesons are substantially different—the virtual meson, being off the mass shell, has a three-dimensional momentum Δ significantly larger in magnitude than the momentum $\mathbf{q}$ of the real π^+ meson. As was shown by the Salzmans,[8] this almost trivial circumstance must be taken into account.

In the case under consideration the energies Q are such that one may apply to the blob at the vertex b, where the π^+ meson is absorbed, the statistical model which gives a good description of the $^3/_2$ $^3/_2$ resonance of the πN system.

And so, following the Salzmans,[8] we replace in Eq. (2) the experimental cross section $\sigma_{\pi^+ p}(Q)$ by* $(\Delta^2/\tilde{q}^2)\sigma_{\pi^+ p}(Q)$. The solid curves shown in Figs. 2—4 are obtained when the Salzmans' correction is included in Eq. (2). Figures 3 and 4 show the quantitative agreement between the theory of Drell and experiment for $\theta = 17.5°$ and $\theta = 25°$. Figure 2, apparently, reflects the fact that for $\theta \lesssim 10°$ the referred to previously (see first footnote) circumstance, connected with the decrease of the cross section at small angles, begins to be felt.

*As regards very small angles ($\theta \ll m_\pi/\omega$) where the one-meson approximation is, generally speaking, very good, the hypothesis of the dominant role played by the diagram of Fig. 1 is in all probability false: at small angles the cross section (2) tends to zero and the contribution of other left out diagrams may turn out to be substantial.

*By applying kinematic considerations to the four-legged vertex b we find easily that

$$\Delta^2/\tilde{q}^2 = [(W-M)^2+\Delta^2]/[(W-M)^2-m_\pi^2],$$

where $W = Q + M + m_\pi$ is the total energy of the π^+ and proton in their c.m.s.; M stands for the nucleon mass.

[1] G. F. Chew and F. E. Low, Phys. Rev. **113**, 1640 (1959).

[2] L. B. Okun' and I. Ya. Pomeranchuk, JETP **36**, 300 (1959), Soviet Phys. JETP **9**, 207 (1959).

[3] C. Goebel, Phys. Rev. Lett. **1**, 337 (1958).

[4] F. Bonsignori and F. Selleri, Nuovo cimento **15**, 465 (1960).

[5] V. B. Berestetskii and I. Ya. Pomeranchuk, JETP **39**, 1078 (1960), Soviet Phys. JETP **12**, 752 (1960).

[6] S. D. Drell, Phys. Rev. Lett. **5**, 278 (1960).
[7] S. D. Drell, Phys. Rev. Lett. **5**, 342 (1960).
[8] F. Salzman and G. Salzman, Phys. Rev. **120**, 599 (1960).
[9] F. Salzman and G. Salzman, Phys. Rev. Lett. **5**, 377 (1960).
[10] Kilner, Diebold, and Walker, Phys. Rev. Lett. **5**, 518 (1960).

Translated by A. M. Bircer
54

ON THE EXCITATION OF NUCLEI BY MUONS IN HEAVY MESIC ATOMS

V. M. NOVIKOV

Submitted to JETP editor February 18, 1961

J. Exptl. Theoret. Phys. (U.S.S.R.) 41, 276-280 (July, 1961)

The ratio of the width for nonradiative nuclear excitation to the radiative width is calculated for levels of mu-mesonic atoms and shown to be weakly dependent on the muon matrix elements.

1. After a mesonic atom is formed in a highly excited state ($n \sim 14$), the muon cascades down to the ground state, the final transition of this cascade being the 2p-1s transition.[1] Zaretskii[2] showed that the full 2p-1s transition energy can be transferred to the nucleus (nonradiative excitation process). The ratio of the probability for nonradiative nuclear excitation with subsequent decay of the nucleus through various nuclear channels, W_{nuc}, to the probability for γ emission by the muon, W_γ, is of interest.

If the nuclear levels at an excitation energy equal to the 2p-1s muon transition energy are wide enough so that they can be considered to be overlapping, then this ratio is

$$W_{nuc}/W_\gamma = \Gamma_{nr}/\Gamma_\gamma, \quad (1)$$

where Γ_{nr} and Γ_γ are the nonradiative and radiative widths, respectively, of the 2p muon level.

If the nuclear levels are non-overlapping, the ratio of W_{nuc} to W_γ is determined[3,4] by the quantities $\Gamma_{nr}/\Gamma_\gamma$ and $\rho\Gamma_{nuc}$, where Γ_{nuc} is the average nuclear level width and ρ is the nuclear density at the energy of excitation of the nucleus.

Nonradiative nuclear excitation can also be important in transitions between other muon levels, for example, 3p-1s or the transition from any highly excited s or d state to 2p.

We calculate below the ratio $\Gamma_{nr}/\Gamma_\gamma$ for a dipole transition between arbitrary muon levels. The calculation is performed in the nonrelativistic approximation.

2. The muon-nucleus dipole interaction operator which leads to nonradiative muon transitions with nuclear excitation is

$$V = -\frac{4\pi}{3}e^2 \sum_m \sum_{i=1}^{Z} Y_{1m}(i)\, Y_{1m}^*(\mu) \times \begin{cases} r_i/r_\mu^2 \text{ for } r_\mu \geqslant r_i \\ r_\mu/r_i^2 \text{ for } r_\mu \leqslant r_i \end{cases}, \quad (2)$$

where r_i and r_μ are the position vectors of the protons and the muon, respectively; the summation is over the protons in the nucleus with charge Ze.

In the initial state of the muon-nucleus system, let the muon be in the level with quantum numbers n_1, j_1, and l_1 and let the nucleus be in its ground state with spin I_0. As basis functions for the muon-nucleus system, we choose the eigenfunctions of the total angular momentum of the system, J_{in}, and its projection $M_{J_{in}}$:

$$\Psi^*_{J_{in}M_{J_{in}}} = \sum_{m_{j_1}m_{I_0}} (I_0 j_1 m_{I_0} m_{j_1} | J_{in} M_{J_{in}})\, \psi_{I_0 m_{I_0}} R_{n_1 l_1} \Phi_{j_1 m_{j_1}}, \quad (3)$$

where $\psi_{I_0 m_{I_0}}$ is the wave function of the nucleus in its ground state, $R_{n_1 l_1}\Phi_{j_1 m_{j_1}}$ is the muon wave function, and $(\ldots|\ldots)$ is a Clebsch-Gordan coefficient.

Similarly, we write the wave function of the final state with total angular momentum J_f:

$$\Psi^*_{J_f M_f} = \sum_{m_{j_2} m_{I_f}} (I_f j_2 m_{I_f} m_{j_2} | J_f M_{J_f})\, \psi_{I_f m_{I_f}} R_{n_2 l_2} \Phi_{j_2 m_{j_2}}, \quad (4)$$

where I_f is the spin of the final nuclear state and n_2, j_2, and l_2 are the quantum numbers of the muon final state.

In this representation, the matrix element of the operator (2) is (for brevity, we omit the dependence of the sign of the matrix element on the quantum numbers)

$$\langle J_f M_{J_f} | V | J_{in} M_{J_{in}} \rangle = e^2 \left[\tfrac{4}{3}\pi (2l_1+1)(2j_2+1)\right]^{1/2} (1 l_1 00 | l_2 0) \times W(l_1 l_2 j_1 j_2;\ 1\,{}^1\!/_2) \sum (I_0 j_1 m_{I_0} m_{j_1} | J_{in} M_{J_{in}}) (J_f j_2 m_{I_f} m_{j_2} | J_f M_{J_f}) \times (1 j_2 m m_{j_2} | j_1 m_{j_1}) \left\langle \psi_{I_f m_{I_f}} \left| \sum_{i=1}^{z} r_i f(r_i) Y_{1m}(i) \right| \psi_{I_0 m_{I_0}} \right\rangle, \quad (5)$$

$$f(r_i) = r_i^{-3} \int_0^{r_i} r^3 R_{n_1 l_1} R_{n_2 l_2}\, dr + \int_{r_i}^{\infty} R_{n_1 l_1} R_{n_2 l_2}\, dr, \quad (6)$$

where W is the Racah coefficient and the summation in (5) is over m, m_{j_1}, m_{j_2}, m_{I_0}, and m_{I_f}.

The nuclear matrix element in (5) can be written:

$$\left\langle \psi_{I_f m_{I_f}} \left| \sum_i r_i f(r_i) Y_{1m} \right| \psi_{I_0 m_{I_0}} \right\rangle = (1 I_0 m m_{I_0} | I_f m_{I_f}) \left\langle I_f \left| \sum_i r_i f(r_i) Y_1 \right| I_0 \right\rangle. \quad (7)$$

where the dependence on the magnetic quantum numbers is separated out.

Since we are considering a nonradiative transition of a closed system, the total angular momentum and its projection are conserved. Thus, using (7) and carrying out the summation over magnetic quantum numbers in (5), we obtain

$$\langle J_f M_{J_f} | V | J_{in} M_{J_{in}} \rangle = e^2 \left[\tfrac{4}{3}\pi (2l_1+1)(2j_1+1)(2j_2+1)\right.$$
$$\times (2I_f+1)\left.\right]^{1/2} (1l_1 00 | l_2 0)\, W(I_0 j_1 I_f j_2;\ J_{in} l)$$
$$\left\langle I_f \left| \sum_i q_i f(r_i) \right| I_0 \right\rangle \delta_{J_f J_{in}} \delta_{M_{J_f} M_{J_{in}}} \qquad (8)$$

where we have set $q_i = r_i Y_1(i)$, for brevity.

The nonradiative width is

$$\Gamma_{nr} = 2\pi \overline{|\langle | V | \rangle|^2} \rho. \qquad (9)$$

The bar in (9) denotes summation over the final state quantum numbers J_f, M_{J_f}, j_2, I_f, averaging over the possible values of the total angular momentum of the system J_{in} and $M_{J_{in}}$, and also averaging the absolute square of the nuclear matrix element over those nuclear levels which lie within an energy interval of about Γ_{nr} around the transition energy. Substituting (8) into (9) and using the fact that the probability that the total muon-nucleus angular momentum be J_0 is $(2J_0+1)/(2I_0+1)(2j_1+1)$, we obtain

$$\Gamma_{nr} = \frac{8\pi^2}{9} e^4 (1l_1 00 | l_2 0)^2 \sum_{I_f} \frac{2I_f+1}{2I_0+1} |\langle I_f | q_i f(r_i) | I_0 \rangle|^2_{av} \rho_{I_f}, \qquad (10)$$

where ρ_{I_f} is the density of nuclear levels with spin I_f. The radiative width for the muon transition between the same states is

$$\Gamma_\gamma = \frac{4}{3}\frac{e^2\omega^3}{c^3} (1l_1 00 | l_2 0)^2 \left| \int_0^\infty r^3 R_{n_1 l_1} R_{n_2 l_2} dr \right|^2. \qquad (11)$$

It is convenient to transform the integral in (11) in the following way. We write the equation of motion of the muon in matrix form:

$$m_\mu \langle \ddot{\mathbf{r}} \rangle = -\langle \nabla U \rangle, \qquad (12)$$

where m_μ is the muon mass and U is the potential energy of the muon in the field of the nucleus,

$$U = -Ze^2 \times \begin{cases} 1/r_\mu & \text{for } r_\mu \geqslant R \\ \tfrac{1}{2} R^{-1}[3-(r_\mu/R)^2] & \text{for } r_\mu \leqslant R \end{cases}, \qquad (13)$$

where R is the nuclear radius.

With (12) and (13), we obtain

$$\int_0^\infty r^3 R_{n_1 l_1} R_{n_2 l_2} dr = \frac{Ze^2}{m_\mu \omega^2} \left[\frac{1}{R^3} \int_0^R r^3 R_{n_1 l_1} R_{n_2 l_2} dr \right.$$
$$\left. + \int_R^\infty R_{n_1 l_1} R_{n_2 l_2} dr \right] = \frac{Ze^2}{m_\mu \omega^2} f(R). \qquad (14)$$

$f(x)$ in (14) is the same as that in (6). Thus, the ratio (1) in which we are interested is

$$\frac{\Gamma_{nr}}{\Gamma_\gamma} = \frac{2\pi^2}{3} \frac{m_\mu^2 \omega c^3}{Z^2 e^2} \sum_{I_f} \frac{2I_f+1}{2I_0+1} \left| \left\langle I_f \left| q_i \frac{f(r_i)}{f(R)} \right| I_0 \right\rangle \right|^2_{av} \rho_{I_f}. \qquad (15)$$

The cross section for dipole photoexcitation is[5]

$$\sigma = (8\pi^3/3)(\omega/c)\left[|\langle Q_{1,1} \rangle|^2_{av} + |\langle Q_{1,-1} \rangle|^2_{av} \right] \rho. \qquad (16)$$

We will consider the photoexcitation of the nucleus in the transition $\psi_{I_0} \rightarrow \psi_{I_f}$. We separate out the dependence of the matrix elements in (16) on the magnetic quantum numbers, as we did in (7); then, in the notation introduced previously, we obtain

$$|\langle Q_{1,1} \rangle|^2_{av} = \frac{e^2}{2I_0+1} \sum_{m_{I_0} m_{I_f}} (1 I_0 1 m_{I_0} | I_f m_{I_f})^2 |\langle I_f | q_i | I_0 \rangle|^2_{av}$$
$$= \frac{e^2}{3} \frac{2I_f+1}{2I_0+1} |\langle I_f | q_i | I_0 \rangle|^2_{av}. \qquad (17)$$

Thus, the photoexcitation cross section for the nuclear transition considered above, summed over the final values of the nuclear spin, is

$$\sigma = \frac{16\pi^3}{9} \frac{\omega}{c} e^2 \sum_{I_f} \frac{2I_f+1}{2I_0+1} \left| \left\langle I_f \left| \sum_i{}' q_i \right| I_0 \right\rangle \right|^2_{av} \rho_{I_f}. \qquad (18)$$

Substituting (18) into (15) and letting

$$B = \frac{\sum_{I_f} (2I_f+1) \left| \left\langle I_f \left| \sum_i q_i f(r_i) \right| I_0 \right\rangle \right|^2_{av} \rho_{I_f}}{\sum_{I_f} (2I_f+1) \left| \left\langle I_f \left| \sum_i q_i f(R) \right| I_0 \right\rangle \right|^2_{av} \rho_{I_f}}, \qquad (19)$$

we obtain, finally,

$$\Gamma_{nr}/\Gamma_\gamma = (3/8\pi)(m_\mu c^2/Ze^2)^2 \sigma B. \qquad (20)$$

3. The form factor B takes into account the effect of the finite nuclear size on the ratio (1). For heavy mesonic atoms like uranium, B is of the order of 2. For a point nucleus, B = 1 and the ratio (1) does not depend at all on the muon matrix elements. This is easily understood if one notes that the nonradiative nuclear excitation process can be interpreted as the inverse of internal conversion; then (20) is the inverse internal conversion coefficient. Since the internal conversion coefficient becomes independent of the nuclear matrix elements in the case of a point nucleus, it is natural that the dependence on the muon matrix elements disappears from (20). We note also that (20) depends on the transition energy mainly through the photoexcitation cross section, which is to be taken at the transition energy; B depends rather weakly on the energy.

The magnitude of the form factor B can be estimated as follows. The matrix element in (19) can be written

$$\langle k | \sum_i q_i f(r_i) | 0 \rangle = \sum_{k'} \langle k' | \sum_i q_i | 0 \rangle \langle k | f(r_i) | k' \rangle; \qquad (21)$$

where the summation in (21) is over all intermediate states. In squaring (21) we neglect the cross terms. This is permissible if the phases of the terms in the summation in (21), each of which is the product of essentially different dipole and monopole transition matrix elements, are random. Then

$$\left|\left\langle k\left|\sum_i q_i f(r_i)\right|0\right\rangle\right|^2=\sum_{k'}\left|\left\langle k'\left|\sum_i q_i\right|0\right\rangle\right|^2|\langle k|f(r)|k'\rangle|^2, \tag{22}$$

where $f(r)$ is a very smooth function. For example, for the 2p-1s transition in mesonic uranium, using the numerical muon wave functions given by Pustovalov,[6] we obtain

$$f(r)=1-0.71\,(r/R)^2+0.3\,(r/R)^{7/2}-0.06\,(r/R)^5. \tag{23}$$

The state k is a highly excited nuclear state (in the mesonic uranium 2p-1s transition, $E_K \sim 6$ Mev) and therefore $|\langle k\ f(r)\ k'\rangle|^2$ has a maximum at $k'=k$ and for $k'\neq k$ it is quasiclassically small. On the other hand, the quantity $|\langle k'|\Sigma_i q_i|0\rangle|^2$, proportional to the photoexcitation cross section, is a smooth function of k' and can therefore be taken outside the summation over k':

$$\left|\left\langle k\left|\sum_i q_i f(r_i)\right|0\right\rangle\right|^2\approx\left|\left\langle k\left|\sum_i q_i\right|0\right\rangle\right|^2\sum_{k'}|\langle k|f(r)|k'\rangle|^2$$
$$=\left|\left\langle k\left|\sum_i q_i\right|0\right\rangle\right|^2\langle k|f^2(r)|k\rangle. \tag{24}$$

Substituting (24) into (19), and assuming a uniform charge distribution in the excited state of the nucleus, we obtain

$$B\approx\frac{3}{f^2(1)}\int_0^1 x^2 f^2(x)\,dx,\quad x=\frac{r}{R}. \tag{25}$$

For the 2p-1s transition in U^{238}, $B\approx 1.8$. The photofission cross section for the above-mentioned energy in U^{238} is about 12 mb,[7] and the ratio of the fission width to the sum of fission and neutron widths is about 4.[8] Thus, assuming that the photoexcitation cross section is due to the absorption of electric dipole quanta, we obtain $\sigma\approx 50$ mb. From this

$$(\Gamma_{nr}/\Gamma_\gamma)_{2p-1s}\approx 0.7. \tag{26}$$

The same ratio holds also for Th, since the photoexcitation cross sections for U^{238} and Th are the same.[8]

For the 3p-1s transition in the same elements we obtain $E_{3p-1s}=9.5$ Mev, $B\approx 1.4$, $\sigma\approx 320$ mb, and

$$(\Gamma_{nr}/\Gamma_\gamma)_{3p-1s}\approx 3.5. \tag{27}$$

The results, (26) and (27), can be qualitatively understood by the following argument. The radiation of a γ quantum by the muon is a first order process with a probability of order $e^2/\hbar c$; nonradiative nuclear excitation is a second order process with a probability of order $(e^2/\hbar c)(Ze^2/\hbar c)$. Thus, the ratio of the widths for these two processes is of order $Ze^2/\hbar c$. For the elements mentioned above, $Ze^2/\hbar c\sim 1$. However, for other nuclei and other transitions, the ratio (1) can be much larger or much smaller than $Ze^2/\hbar c$ because of the nuclear matrix elements.

In conclusion, the author expresses his deep gratitude to D. F. Zaretskii for suggesting this problem and for valuable comments.

[1] V. L. Fitch and J. Rainwater, Phys. Rev. **92**, 789 (1953).

[2] D. F. Zaretskii, Reports of Soviet Scientists to the Second International Conference on Peaceful Uses of Atomic Energy, AN SSSR 1959.

[3] D. F. Zaretskii and V. M. Novikov, Nuclear Phys. **14**, 540 (1960).

[4] D. F. Zaretskii and V. M. Novikov, JETP **41**, 214 (1961), this issue, p. 157

[5] J. Blatt and V. Weisskopf, Theoretical Nuclear Physics, Wiley 1951.

[6] G. E. Pustovalov, JETP **36**, 1806 (1959), Soviet Phys. JETP **9**, 1288 (1959).

[7] R. A. Schmidt and R. B. Duffield, Phys. Rev. **105**, 1277 (1957).

[8] Lazareva, Gavrilov, Valuev, Zatsepina, and Stavinskii, USSR Academy of Sciences Session on Peaceful Uses of Atomic Energy, AEC Translation.

Translated by M. Bolsterli
55

CONTRIBUTION TO THE THEORY OF ABSORPTION OF ULTRASONIC WAVES BY METALS IN A MAGNETIC FIELD

G. L. KOTKIN

Moscow State University

Submitted to JETP editor February 20, 1961

J. Exptl. Theoret. Phys. (U.S.S.R.) **41**, 281-287 (July, 1961)

The complex elastic modulus of a metal is computed under conditions when the electron mean free path is much greater than the acoustic wavelength. Some cases are considered when measurement of the sound absorption coefficient permits one to draw certain conclusions regarding the momenta and velocities of the electrons on the Fermi surface.

THE study of ultrasonic absorption in metals at low temperatures in the presence of a magnetic field makes it possible to clarify certain characteristics of the Fermi surface, as was first shown by Pippard.[1] A number of researches have been devoted to a theoretical consideration of this problem.[2-4] In the case in which the electron mean free path l is much greater than the acoustic wavelength λ, the transfer of energy from the lattice to the electrons is not connected with their collisions. A systematic theory of sound absorption under these conditions (without a magnetic field) has been constructed by Silin.[5] In the present work, the case of an infinite mean free path of the electrons is also considered, in contrast with,[2-4] where the length of the free path was essential.

In Sec. 1, general formulas will be obtained for the complex elastic modulus when $l \gg \lambda$. In Sec. 2, sound propagation is considered along the axis of symmetry in a magnetic field and also in the case when the acoustic wave vector $\mathbf{k}$ and the magnetic field $\mathbf{H}$ lie in the plane of symmetry of the Fermi surface. It is shown that in these cases the sound absorption coefficient vanishes in the approximation considered if the field exceeds the value for which the maximum displacement of the electron over the period of its motion in the magnetic field is equal to the acoustic wavelength. In Sec. 3, sound propagation is considered in the case of strong magnetic fields.

1. When the lattice is deformed, the energy of the electron is changed:

$$\varepsilon = \varepsilon_0 + \Lambda_{ik}\, \partial u_l / \partial x_k$$

($\mathbf{u}$ is the lattice displacement vector). The electron distribution function satisfies the equation

$$\frac{\partial f}{\partial t} + \mathbf{v}\frac{\partial f}{\partial \mathbf{r}} + \left(e\mathbf{E} + \frac{e}{c}[\mathbf{vH}] - \frac{\partial}{\partial \mathbf{r}}\Lambda_{ik}\frac{\partial u_l}{\partial x_k}\right)\frac{\partial f}{c\mathbf{p}} = 0. \quad (1.1)^*$$

We assume that $\mathbf{u} \sim \exp i(\mathbf{k}\cdot\mathbf{r} - \omega t)$. Transforming to the variables introduced in the work of I. Lifshitz, Azbel' and Kaganov,[6] we get for the increment δf to the equilibrium distribution function

$$f_0 = 2(2\pi\hbar)^{-3}\,[\exp(\varepsilon_0 - \mu)/T + 1]^{-1}$$

the equation

$$\Omega\frac{\partial \delta f}{\partial \varphi} + ik\mathbf{v}_0\delta f = i\omega\delta f - e\mathbf{v}_0\mathbf{E}\frac{\partial f_0}{\partial \varepsilon} - ik\mathbf{v}_0 u_l k_m \Lambda_{im}\frac{\partial f_0}{\partial \varepsilon} + iu_l k_m \Omega\frac{\partial \Lambda_{im}}{\partial \varphi}\frac{\partial f_0}{\partial \varepsilon}. \quad (1.2)^\dagger$$

Here φ/Ω is the time of motion of an electron with a given energy ϵ_0 and momentum projection in the direction of the magnetic field p_H, Ω is its circular frequency, and $\mathbf{v}_0 = \partial\epsilon_0/\partial\mathbf{p}$.

We restrict ourselves to closed Fermi surfaces. Taking into account the periodicity of $\delta f(\varphi)$, we find

$$\delta f = (iu_l k_m \Lambda_{im} + iek^{-2}\mathbf{kE})\,\partial f_0/\partial\varepsilon - \frac{\Omega^{-1}\int_{\varphi}^{\varphi+2\pi} d\varphi_1\,[eE_\alpha v_\alpha(\varphi_1)\,\partial f_0/\partial\varepsilon - i\omega\delta f(\varphi_1)]\exp\left(ik\int_{\varphi}^{\varphi_1}\mathbf{v}(\varphi')\,d\varphi'/\Omega\right)}{\exp ik\int_0^{2\pi}\mathbf{v}(\varphi)\,d\varphi/\Omega - 1}. \quad (1.3)$$

The indices 0 are omitted on v, while v_α denotes the components of the velocity perpendicular to $\mathbf{k}$.

Adiabatic "switching on" of the interaction at $t = -\infty$ corresponds to a passage about the poles determined by an infinitesimally small imaginary contribution to ω, or by an addition of the opposite

*$[\mathbf{vH}] = \mathbf{v}\times\mathbf{H}$.

†$\mathbf{kv} = \mathbf{k}\cdot\mathbf{v}$.

sign to $\mathbf{k}\cdot\mathbf{v}$. In the case in which $\mathbf{k}\perp\mathbf{H}$, it is shown that $\mathbf{k}\cdot\int_0^{2\pi}\mathbf{v}(\varphi)\,d\varphi\equiv 0$, and it is necessary to take the collisions into account. The condition for the applicability of Eq. (1.3) reduces to $kv\cos\theta \gg \nu$, where ν is the characteristic frequency of collisions for the electrons, and θ is the angle between $\mathbf{k}$ and $\mathbf{H}$.

By making use of Maxwell's equations, we obtain the following equations for the determination of $\mathbf{E}$:

$$\int \delta f\,d\mathbf{p} = -i\mathbf{k}\mathbf{u}N, \tag{1.4}$$

$$e\int v_\alpha \delta f\,d\mathbf{p} = -i\omega eNu_\alpha - \frac{ic^2k^2E_\alpha}{4\pi\omega}. \tag{1.5}$$

Here N is the number of electrons per unit volume.

We introduce the notation

$$-\int d\mathbf{p}A\partial f_0/\partial\varepsilon = \langle A\rangle, \tag{1.6}$$

$$(2\pi)^{-1}\int_0^{2\pi} A(\varphi)\,d\varphi = \widetilde{A}, \tag{1.7}$$

$$\left\langle \frac{A\Omega^{-1}\int_\varphi^{\varphi+2\pi} d\varphi_1 B(\varphi_1)\exp\left(ik\int_\varphi^{\varphi_1}\mathbf{v}(\varphi')\,d\varphi'/\Omega\right)}{\exp 2\pi i\,\mathbf{k}\widetilde{\mathbf{v}}/\Omega - 1}\right\rangle = (A, B). \tag{1.8}$$

Substituting (1.3) in (1.4) and (1.5), we get

$$-iu_ik_m\langle\Lambda_{im}\rangle - ie\mathbf{k}\mathbf{E}k^{-2}\langle 1\rangle - eE_\alpha(1, v_\alpha) + \omega u_ik_m(1, \Lambda_{im}) + \omega e\mathbf{k}\mathbf{E}k^{-2}(1, 1) = -i\mathbf{k}\mathbf{u}N, \tag{1.9}$$

$$-e^2E_\alpha(v_\alpha, v_\beta) + e\omega u_ik_m(v_\beta, \Lambda_{im}) = i\omega eNu_\beta - ic^2k^2E_\beta/4\pi\omega. \tag{1.10}$$

To determine E we use an expansion in powers of v_s/v (v_s is the speed of sound):

$$eE_\alpha = -i\omega e^2u_iB_{\alpha\beta}^{-1}(N\delta_{i\beta} - i(v_\beta, L_i)), \tag{1.11}$$

$$\frac{e\mathbf{k}\mathbf{E}}{k^2} = \frac{u_ik_m}{\langle 1\rangle}(N\delta_{im} - \langle\Lambda_{im}\rangle) - i\omega u_i\frac{(1, L_i)}{\langle 1\rangle} + ieE_\alpha\frac{(1, v_\alpha)}{\langle 1\rangle}; \tag{1.12}$$

$$B_{\alpha\beta} = -e^2(v_\alpha, v_\beta) - i(c^2k^2/4\pi\omega)\delta_{\alpha\beta}, \tag{1.13}$$

$$L_i = k_m(\Lambda_{im} - \langle\Lambda_{im}\rangle\langle 1\rangle^{-1} + N\delta_{im}\langle 1\rangle^{-1}). \tag{1.14}$$

The lattice vibrations are described by the equation[5]

$$\rho\ddot{u}_i = \lambda_{imjl}^{(0)}\frac{\partial u_j}{\partial x_m\partial x_l} - eNE_i - i\frac{e}{c}N\omega[\mathbf{u}\mathbf{H}]_i + \frac{\partial}{\partial x_m}\int\Lambda_{im}f\,d\mathbf{p}, \tag{1.15}$$

where ρ is the density of matter, and $\lambda_{imjl}^{(0)}$ is the tensor of the elastic moduli of the lattice. By using the complex elastic modulus $\lambda_{imjl}(\omega, \mathbf{k})$, introduced by Silin,[5] we transform Eq. (1.5) to

$$\rho\omega^2u_i = k_lk_m\lambda_{imjl}u_j;$$

$$\lambda_{imjl}k_mk_l = \lambda_{imjl}^{(0)}k_mk_l + \delta\lambda_{imjl}k_mk_l, \tag{1.16}$$

$$\delta\lambda_{imjl}k_mk_lu_j = eNE_i - iec^{-1}N\omega H_mu_je_{ijm} - ik_m\int\Lambda_{im}\delta f\,d\mathbf{p}. \tag{1.17}$$

Substituting (1.3), (1.11), and (1.12) in (1.17), we obtain

$$\delta\lambda_{imjl}k_mk_l = -k_mk_l\langle\Lambda_{im}\Lambda_{jl}\rangle - k_mk_l\langle 1\rangle^{-1}(\langle\Lambda_{im}\rangle - N\delta_{im})(\langle\Lambda_{jl}\rangle - N\delta_{jl}) + iec^{-1}N\omega H_me_{ijm} - i\omega(L_i, L_j) - i\omega e^2(N - i(L_i, v_\alpha))B_{\alpha\beta}^{-1}(N\delta_{j\beta} - i(v_\beta, L_j)). \tag{1.18}$$

The first two terms in (1.18) have the same order of magnitude as $\lambda_{imjl}^{(0)}k_mk_l$, and determine the renormalization of the elasticity modulus, brought about by the interaction of the lattice with the electrons. This renormalization is shown not to depend on the magnetic field, and is identical with that obtained by Silin.[5] The remaining terms in (1.18), generally speaking, are much smaller than $\lambda_{imjl}^{(0)}k_mk_l$. They lead to dispersion and sound absorption, determined by the addition of $\delta\omega(\mathbf{k}) = \delta\omega' + i\delta\omega''$ to the normal frequency $\omega_0(\mathbf{k})$ found from (1.16) without account of the small terms in (1.18).

From (1.16), we find

$$\delta\omega' = (\delta\lambda_{imjl} + \delta\lambda_{jlim}^*)k_mk_lu_i^*u_j/\omega_0\rho|u|^2, \tag{1.19}$$

$$\delta\omega'' = -i(\delta\lambda_{imjl} - \delta\lambda_{jlim}^*)k_mk_lu_i^*u_j/\omega_0\rho|u|^2. \tag{1.20}$$

The effect of small additions to the elasticity modulus tensor on the polarization of normal waves is considered in the Appendix.

We now bring (A, B) to a form which is more suitable for investigation. We transform (1.8) by expanding the following function (which is periodic in φ) in a Fourier series:

$$B(\varphi)\exp\left\{ik\int_0^\varphi \mathbf{v}(\varphi')\,d\varphi'/\Omega - i\mathbf{k}\widetilde{\mathbf{v}}\varphi/\Omega\right\}$$

$$(A, B) = -\frac{4\pi i}{(2\pi\hbar)^3}\int m^*\,dp_H\Omega^{-1}\sum_{n=-\infty}^{\infty}\frac{A_n^*B_n}{\mathbf{k}\widetilde{\mathbf{v}}/\Omega + n - i\delta}; \tag{1.21}$$

$$B_n = (2\pi)^{-1}\int_0^{2\pi} d\varphi B(\varphi)\exp\left\{ik\int_0^\varphi \mathbf{v}(\varphi')\,d\varphi'/\Omega - i\mathbf{k}\widetilde{\mathbf{v}}/\Omega - in\varphi\right\}. \tag{1.22}$$

We assume that the Fermi surface has a center of symmetry, so that $B(-\mathbf{p}) = \zeta_BB(\mathbf{p})$, where $\zeta_B = 1$ when $B = 1$, Λ_{ik} and $\zeta_B = -1$ when $B = v_i$. By making the substitutions $\mathbf{p}\to-\mathbf{p}$ and $n\to-n$ in (1.22), we can put (1.22) in the form

$$(A, B) = \frac{2\pi^2}{(2\pi\hbar)^3} m^*\Omega^{-1}$$

$$\times \sum_{|n|<(kv/\Omega)_{max}} \left[(A_n^* B_n + \zeta_{AB} A_n B_n^*) \left| \frac{\partial}{\partial p_H} \frac{k\tilde{v}}{\Omega} \right|^{-1}\right]_{p_{Hn}}$$

$$- \frac{2\pi i}{(2\pi i\hbar)^3} P \int m^* dp_H \Omega^{-1} \sum_{n=-\infty}^{\infty} \frac{A_n^* B_n - \zeta_{AB} A_n B_n^*}{k\tilde{v}/\Omega + n}, \quad (1.23)$$

where p_{Hn} is determined by the condition

$$k\tilde{v}(p_{Hn}) + n\Omega(p_{Hn}) = 0. \quad (1.24)$$

We note that for $\zeta_{AB} = 1$, the quantity (A, B) is real, while for $\zeta_{AB} = -1$, it is imaginary.

With increase in the magnetic field, individual components fall out of the sum in (1.23). This corresponds to jumps in the coefficient of absorption or in its derivative with respect to the field H at $(\mathbf{k}\cdot\tilde{\mathbf{v}}/\Omega)_{max} = n$, as Gurevich has shown.[2] If the Fermi surface differs sharply from elliptic, then $(\partial/\partial p_H)(\mathbf{k}\cdot\tilde{\mathbf{v}}/\Omega)$ can vanish for certain $p_H^{(0)}$. When $\mathbf{k}\cdot\mathbf{v}(p_H^{(0)}) = n\Omega(p_H^{(0)})$, discontinuities also appear,[2] and then analysis of the collision integral close to the discontinuity is essential.

The last term in (1.18) arises from the transverse field E_α. Its role depends, as is well known, on the region of frequencies under consideration. In the region where λ is small in comparison with the skin depth δ in the anomalous skin effect, $B_{\alpha\beta} = -e^2(v_\alpha, v_\beta)$ and the last two components in (1.18) are of the same order. If now $\lambda \ll \delta$, then $B_{\alpha\beta} = -i(c^2k^2/4\pi\omega)\delta_{\alpha\beta}$ and the contribution of the transverse field, generally speaking, is much less than the contribution of the deformation potential.

2. Let z be the axis of symmetry of the Fermi surface of s-th order, and at the same time the axis of symmetry of the crystal, so that sound that is purely longitudinal or purely transverse is possible when $\mathbf{k} \parallel \mathbf{z}$. We consider the case in which the sound is propagated along z, and the magnetic field is directed parallel to this axis. Taking it into account that v_z and L_z do not change upon rotation through an angle $2\pi/s$ about the z axis, we find

$$(L_z)_n = (2\pi)^{-1} \sum_{l=0}^{s-1} e^{-2\pi i n l/s}$$

$$\times \int_0^{2\pi/s} d\varphi L_z(\varphi) \exp\left(ik \int_0^{\varphi} \frac{v_z d\varphi}{\Omega} - \frac{ik\tilde{v}_z\varphi}{\Omega} - in\varphi\right)$$

$$= (2\pi)^{-1} \int_0^{2\pi/s} d\varphi L_z(\varphi) \exp\left(ik \int_0^{\varphi} \frac{v_z d\varphi}{\Omega} - \frac{ik\tilde{v}_z\varphi}{\Omega} - in\varphi\right)$$

$$\times \begin{cases} s & \text{for } n = qs \\ 0 & \text{for } n \neq qs \end{cases} \quad (2.1)$$

(q is an integer).

In place of the transverse components v_α, it is better to make use of the quantities $v_\pm = v_x \pm iv_y$, which satisfy the condition

$$v_\pm(\varphi + 2\pi/s) = \exp(\pm 2\pi i/s)\, v_\pm(\varphi); \quad (2.2)$$

$$(v_\pm)_n = (2\pi)^{-1} \int_0^{2\pi/s} d\varphi v_\pm(\varphi) \exp\left(ik \int_0^{\varphi} \frac{v_z d\varphi}{\Omega} - \frac{ik\tilde{v}_z\varphi}{\Omega} - in\varphi\right)$$

$$\times \begin{cases} s & \text{for } n = qs \pm 1 \\ 0 & \text{for } n \neq qs \pm 1 \end{cases}. \quad (2.3)$$

Consequently, $(v_\alpha)_n = 0$ for $n \neq qs \pm 1$.

Similar equalities are valid for L_i. Thus the components in (1.23) vanish for $n \neq qs$, $qs \pm 1$, and the corresponding discontinuities in the elasticity modulus or its derivative with respect to the field are absent. For example, we have for longitudinal sound in the case $\lambda \gg \delta$

$$k^2\lambda_{zzzz} = -i\omega(L_z, L_z) = -\frac{4\pi^2\omega}{(2\pi\hbar)^3} \sum_{n=0,\ s,\ldots<(kv_z/\Omega)_{max}} m^*\Omega^{-1}$$

$$\times \left[|(L_z)_n|^2 \left| \frac{\partial}{\partial p_H} \frac{k\tilde{v}_z}{\Omega} \right|^{-1}\right]_{p_{Hn}} \quad (2.4)$$

and the discontinuities appear s times less often.

If the magnetic field exceeds the value for which $(k\tilde{v}_z/\Omega)_{max} = 1$, then only the component for $n = 0$ remains in the sum in (1.23). If s is even, then it vanishes for all the (A, B) which are necessary, according to (1.18), for consideration of transverse sound. It is shown that

$$(v_\alpha, v_\beta) = -(v_\beta, v_\alpha), \quad (L_\alpha, L_\beta) = -(L_\beta, L_\alpha),$$

$$(L_i, v_\alpha) = (v_\alpha, L_i). \quad (2.5)$$

In both limiting cases, $\lambda \gg \delta$ and $\lambda \ll \delta$, we obtain $k^2\delta\lambda''_{\alpha z\beta z} = -k^2\delta\lambda''_{\beta z\alpha z}$, so that $\delta\omega''$ vanishes for transverse sound. Thus, in the case of the transverse sound propagation along a symmetry axis of even order of the Fermi surface in a longitudinal magnetic field, the absorption disappears in the approximation considered if the field exceeds

$$H_1 = ck(m^*\tilde{v}_z)_{max}/e.$$

For the free electron model, it was shown by Kjeldaas[7] that the absorption coefficient of transverse sound vanishes for $\mathbf{k} \parallel \mathbf{H}$ if $H > ckmv/e$. We note that the sound absorption coefficient vanishes smoothly or with a discontinuity, depending on whether $(m^*\tilde{v}_z)_{max}$ is achieved for $p_z = p_{z\,max}$, or for $p_z < p_{z\,max}$. If the $\omega(\mathbf{k})$ coincide for the two transverse polarizations, then rotation of the plane of polarization of the sound should be observed for $H > H_1$. The angle of rotation per unit distance is

$$\varkappa = k^3\delta\lambda_{xzyz}/2\rho\omega^2. \qquad (2.6)$$

According to estimate, $\varkappa \sim Nmvk^2/\rho\omega$, which has the same order of magnitude as the angle found by Vlasov[8] for the free electron model.

Let yz be the plane of symmetry of the Fermi surface (and at the same time the plane of symmetry of the crystal). We further consider the case in which **k** and **H** lie in the yz plane. For the substitution $\varphi \to -\varphi$, the values of v_x and L_x change sign, while v_y, v_z, L_y, L_z do not change sign, so that we get

$$(v_x)_n = -(v_x)_{-n}, \qquad (v_y)_n = (v_y)_{-n} \text{ etc.} \qquad (2.7)$$

In view of the assumed symmetry of the crystal a purely transverse wave polarized along the x axis, is possible without the magnetic field. The frequencies of the other two waves with the given **k** will, generally speaking, be different, so that the turning on of the magnetic field produces only a small distortion of the wave under consideration.

Let the frequency be so large that $\lambda \ll \delta$. The sound absorption coefficient is equal to

$$k\delta\omega''/\omega = 2(L_x, L_x)\rho^{-1} \qquad (2.8)$$

and for $H > ck(m^*\tilde{v}_H)_{max}\cos\theta/e$ vanishes. (More accurately, the distortions of the transverse wave lead to an absorption coefficient of the order of $\delta\omega''^2 k/\omega^2$, where $\delta\omega''$ refers to the other polarization.) Thus, in the cases considered, one can determine the value of $(m^*\tilde{v}_H)_{max}$ by measuring the field for which the sound absorption decreases sharply. The completely determined dependence of the absorption limit on the angle θ makes it possible to control the applicability of the theory.

3. In the case of strong fields ($\Omega \gg kv$) we expand (1.8) in powers of kv/Ω:

$$(A, B) = (1+\zeta_{AB})\,2\pi^2(2\pi\hbar)^{-3}\int m^*dp_H\delta(k\tilde{v})\tilde{A}\tilde{B}$$
$$-(1-\zeta_{AB})\,2\pi(2\pi\hbar)^{-3}iP\int m^*dp_H\frac{\tilde{A}\tilde{B}}{k\tilde{v}}$$
$$+(1-\zeta_{AB})(2\pi\hbar)^{-3}i\int m^*dp_H\,\Omega^{-1}\int_0^{2\pi}d\varphi\int_0^{2\pi}d\varphi_1$$
$$\times A(\varphi)B(\varphi_1)\left[\delta(k\tilde{v})\int_{\varphi}^{\varphi_1} kv(\varphi')\,d\varphi' - \sigma(\varphi-\varphi')/2\right]$$
$$+O((kv/\Omega)^2), \qquad (3.1)$$

where

$$\sigma(x) = \begin{cases} -1 & \text{for } x<0 \\ 1 & \text{for } x>0 \end{cases}.$$

For (v_α, v_β) the first terms of the expansion vanish. An estimate shows that the first term in Eq. (1.13) can be neglected for $H \gg (4\pi mNvv_S)^{1/2} \sim 10^5$ oe. The contribution of the transverse field in (1.18) is shown to be equal to

$$4\pi\omega^2e^2N^2c^{-2}k^{-2}(\delta_{ij} - \operatorname{tg}\theta\delta_{y'i}k_jk^{-1}$$
$$-\operatorname{tg}\theta\delta_{y'j}k_ik^{-1} + \operatorname{tg}^2\theta k_ik_jk^{-2}). \qquad (3.2)^*$$

Here y′ is the direction in the plane of **k** and **H** perpendicular to **k**. This leads to dispersion in the sound velocity, which is large for $\omega < 10^8$/sec and falls off with increase in frequency. In the range of fields $\omega vmc/ev \ll H \lesssim 10^5$ oe, both components are important in (1.13). In this region, both large dispersion and sound absorption are observed.

For $\omega > 10^8$/sec, the contribution of the transverse field becomes small, and the sound absorption is determined by the deformation potential. The absorption coefficient is of the same order as for H = 0:

$$\gamma = 2k(L_i, L_j)\,u_i^*u_j/\rho\omega\,|H|^2$$
$$\times\int m^*dp_H\,\delta(v_H)\tilde{L}_iL_j\frac{\operatorname{Re}u_i^*u_j}{|u|^2\pi\hbar^3\rho\omega\cos\theta}. \qquad (3.3)$$

For a given direction of **H** we have $\gamma \sim \cos^{-1}\theta$. The case of degeneration of the frequencies $\omega(\mathbf{k})$ corresponds to that considered in the Appendix. We only note that for small θ the normal vibrations will be elliptically polarized, and for θ close to $\pi/2$, linearly polarized.

In conclusion, I express my deep gratitude to V. P. Silin for suggesting the topic, and for constant assistance in the research.

APPENDIX

We shall regard

$$\rho\delta\gamma_{ij} = iec^{-1}N\omega H_m\,e_{ijm} - i\omega(L_i, L_j)$$
$$-i\omega^2(N\delta_{i\alpha} - i(L_i, v_\alpha))\,B^{-1}_{\alpha\beta}(N\delta_{j\beta} - i(v_\beta, L_j))$$

as a small correction to

$$\rho\gamma_{ij} = \lambda^{(0)}_{imjl}k_mk_l - k_mk_l\langle\Lambda_{im}\Lambda_{jl}\rangle$$
$$+k_mk_l\langle 1\rangle^{-1}(\langle\Lambda_{im}\rangle - N\delta_{im})(\langle\Lambda_{jl}\rangle - N\delta_{jl}).$$

Let all three normal frequencies, corresponding to a given **k** (without account of this correction) be different, and let the normal vibrations be polarized along the ξ, η, ζ axes. Account of $\delta\gamma_{ij}$ in (1.15) leads to a small distortion of the normal vibrations. Instead of a wave polarized along ξ, u = (u, 0, 0), an elliptically polarized wave is obtained:

$$u = (u,\ u\delta\gamma_{\xi\eta}(\gamma_{\xi\xi} - \gamma_{\eta\eta})^{-1},\ u\delta\gamma_{\xi\zeta}(\gamma_{\xi\xi} - \gamma_{\zeta\zeta})^{-1}).$$

*tg = tan.

The ratio of the axes of the ellipse $[\delta\gamma'^2_{\xi\eta}(\gamma_{\xi\xi}-\gamma_{\eta\eta})^{-2} + \delta\gamma''^2_{\xi\xi}(\gamma_{\xi\xi}-\gamma_{\zeta\zeta})^2]^{1/2} \ll 1$, and the direction of the major axis is $[1, \delta\gamma'_{\xi\eta}(\gamma_{\xi\xi}-\gamma_{\eta\eta})^{-1}, \delta\gamma'_{\xi\zeta}(\gamma_{\xi\xi}-\gamma_{\zeta\zeta})^{-1}]$.

Let two normal frequencies $\omega(\mathbf{k})$ corresponding to polarization along ξ, η be the same. The set of equations

$$(\delta\gamma_{\xi\xi} - \delta\omega^2)\, u_\xi + \delta\gamma_{\xi\eta} u_\eta = 0,$$

$$\delta\gamma_{\eta\xi} u_\xi + (\delta\gamma_{\eta\eta} - \delta\omega^2)\, u_\eta = 0$$

serves for the determination of $\delta\omega$ and the polarization of the normal vibrations in this case.

Let us consider in some detail the important case in which $\delta\gamma'_{ij} = 0$. This exists, for example, both for $\lambda \gg \delta$ and for $\lambda \ll \delta$. Depending on the sign of $a^2 = (\delta\gamma''_{\xi\xi} + \delta\gamma''_{\eta\eta})^2 - 4\delta\gamma''_{\xi\eta}\delta\gamma''_{\eta\xi}$, we have two possible cases. For $a^2 > 0$, the normal waves are plane polarized, the direction of polarization lying in the $\xi\eta$ plane and the angles β and $\beta + \pi/2$ coinciding with the ξ axis, where $\tan\beta = (\delta\gamma''_{\xi\xi} - \delta\gamma''_{\eta\eta} + a)/2\delta\gamma''_{\xi\eta}$; their absorption coefficients are $\gamma = k\delta\omega''/\omega = (\delta\gamma''_{\xi\xi} + \delta\gamma''_{\eta\eta} \pm a)/4\omega^2$, and the frequencies are identical.

For $a^2 < 0$, the normal vibrations are elliptically polarized and their absorption coefficients are the same, equal to

$$\gamma = (\delta\gamma''_{\xi\xi} + \delta\gamma''_{\eta\eta})\, k/4\omega^2,$$

while the frequencies are different:

$$\omega = \omega_0 \pm ia/4\omega_0.$$

In particular, if $\delta\gamma''_{ij} = -\delta\gamma''_{ji}$ the absorption is absent and the normal waves are circularly polarized. This leads to a rotation of the direction of the polarization of the plane polarized waves. The angle of rotation per unit distance is equal to $\kappa = k\delta\gamma''_{\xi\eta}/2\rho^2\omega^2$ (see [5]).

[1] A. B. Pippard, Phil. Mag. **2**, 1147 (1957).

[2] V. A. Gurevich, JETP **37**, 71, 1680 (1959), Soviet Phys. JETP **10**, 51, 1190 (1960).

[3] E. A. Kaner, JETP **38**, 212 (1960), **39**, 1071 (1960), Soviet Phys. JETP **11**, 154 (1960), **11**, 747 (1961); Galkin, Kaner, and Korolyuk, JETP **39**, 1517 (1960), Soviet Phys. JETP **12**, 1055 (1961).

[4] A. B. Pippard, Proc. Roy. Soc. (London) **A257**, 165 (1960).

[5] V. P. Silin, JETP **38**, 977 (1960), Soviet Phys. JETP **11**, 703 (1960).

[6] Lifshitz, Azbel', and Kaganov, JETP **31**, 63 (1956), Soviet Phys. JETP **4**, 41 (1957).

[7] T. Kjeldaas, Phys. Rev. **113**, 1473 (1959).

[8] K. B. Vlasov, JETP **36**, 1301 (1959), Soviet Phys. JETP **9**, 921 (1950).

Translated by R. T. Beyer
56

ON THE THEORY OF ELECTROMAGNETIC FLUCTUATIONS IN A NONEQUILIBRIUM PLASMA

F. V. BUNKIN

P. N. Lebedev Physics Institute, Academy of Sciences, U.S.S.R.

Submitted to JETP editor February 25, 1961

J. Exptl. Theoret. Phys. (U.S.S.R.) 41, 288-293 (July, 1961)

The elements of the tensor $\varphi_{\alpha\beta}(\omega)$, which describes the spectral intensity of the fluctuations in electrical current in a nonrelativistic magnetoactive plasma in a strong constant or rapidly varying electric field, are calculated. Expressions are also derived for the elements of the effective-temperature tensor $T^{\alpha\beta}_{\text{eff}}$, which is introduced as a formal extension of the well-known fluctuation-dissipation theorem (Nyquist formula) to the case of a nonequilibrium plasma. Several particular cases are considered.

1. The theory of fluctuation spectra in systems in thermodynamic equilibrium derives chiefly from the so-called fluctuation-dissipation theorem, which establishes the connection between the spectral intensity of the fluctuations of an arbitrary physical quantity and the corresponding (to this quantity) conductivity (which determines the dissipation of energy in the system) and the absolute temperature T.[1-3] In particular, the tensor $\Phi_{\alpha\beta}(\mathbf{r}, \mathbf{r}', \omega)$, which describes the spectral intensity of the fluctuations in electric current density $\mathbf{j}(\mathbf{r}, t)$ in a uniform anisotropic absorbing medium, is given by (only classical fluctuations are taken into account, i.e., $\hbar\omega \ll kT$, and spatial dispersion is neglected)

$$\Phi_{\alpha\beta}(\mathbf{r}, \mathbf{r}', \omega) \equiv \frac{1}{2\pi}\int_{-\infty}^{\infty} \langle j_\alpha(\mathbf{r}, t)\, j_\beta(\mathbf{r}', t+\tau)\rangle e^{i\omega\tau} d\tau = \frac{kT}{\pi}\sigma_{\alpha\beta}(\omega)\,\delta(\mathbf{r}-\mathbf{r}'), \quad (1)$$

where $\sigma_{\alpha\beta}(\omega)$ is the conductivity tensor.* The theorem in (1) makes it possible to formulate and solve the problem of thermal radiation of hot bodies (media) within the framework of macroscopic electrodynamics;[2,4,5] in this case the fluctuation current $\mathbf{j}(\mathbf{r}, t)$ is regarded as a transverse current.

If we now consider media that are not in thermodynamic equilibrium (although they may be stationary in the sense that the conditions do not change in time), obviously there is no universal relation between the tensor $\Phi_{\alpha\beta}$ and $\sigma_{\alpha\beta}$ such as that given by (1) for equilibrium systems. A relation can be obtained between these tensors only by the formal introduction of an additional, (generally, frequency-dependent) Hermitian tensor $T^{\alpha\beta}_{\text{eff}}(\omega)$ (which we call the effective-temperature tensor)*

$$\Phi_{\alpha\beta}(\mathbf{r}, \mathbf{r}', \omega) = (k/\pi)\, T^{\alpha\gamma}_{\text{eff}}(\omega)\, \sigma_{\gamma\beta}(\omega)\, \delta(\mathbf{r}-\mathbf{r}'), \quad (2)$$

where $\sigma_{\alpha\beta}(\omega)$ is the conductivity tensor corresponding to the given nonequilibrium state of the medium.

It is clear that this formal generalization of the fluctuation-dissipation theorem does not yield any advantage as far as determining the tensor $\Phi_{\alpha\beta}$ is concerned; this follows because in general there will be no method of computing the elements of the tensor $T^{\alpha\beta}_{\text{eff}}$ other than independent calculations of the elements of the tensors $\Phi_{\alpha\beta}$ and $\sigma_{\alpha\beta}$ and the expansion of the matrix equation (2) with respect to $T^{\alpha\beta}_{\text{eff}}$. Nevertheless, in certain cases it is convenient to use (2) (cf. below).

One of these cases arises when the tensor $T^{\alpha\beta}_{\text{eff}}(\omega)$ reduces to a frequency-independent scalar T_{eff} (more precisely, when $T^{\alpha\beta}_{\text{eff}} = T^{\alpha\beta}_{\text{eff}}\delta_{\alpha\beta}$). In this case, as in the case of media in thermodynamic equilibrium, $\Phi_{\alpha\beta}$ is determined completely by $\sigma_{\alpha\beta}$ and, as far as electromagnetic fluctuations are concerned, the nonequilibrium medium behaves

*A complex dielectric tensor $\varepsilon'_{\alpha\beta}$ (to take account of absorption) of form $\varepsilon'_{\alpha\beta} = \varepsilon_{\alpha\beta} - i4\pi\sigma_{\alpha\beta}/\omega$ can be defined uniquely, as is well known, if we require that $\varepsilon_{\alpha\beta}$ and $\sigma_{\alpha\beta}$ must be Hermitian tensors. We also note that the tensor $\Phi_{\alpha\beta}(\mathbf{r}, \mathbf{r}', \omega)$ is related to the tensor $\langle j_{\alpha\omega}(\mathbf{r})\, j^*_{\beta\omega'}(\mathbf{r}')\rangle$, where $\mathbf{j}_\omega(\mathbf{r})$ is the Fourier component of the current $\mathbf{j}(\mathbf{r}, t)$, by the relation

$$\langle j_{\alpha\omega}(\mathbf{r})\, j^*_{\beta\omega'}(\mathbf{r})\rangle = \Phi_{\alpha\beta}(\mathbf{r}, \mathbf{r}', \omega)\,\delta(\omega-\omega').$$

*The general approach to the notion of an effective temperature for arbitrary nonequilibrium systems has been given earlier by the author.[6]

like an equilibrium medium at temperature T_{eff}. This case is the situation, for example, in a highly (in particular, in a fully) ionized plasma (cf. below).

In the present paper kinetic theory is used to calculate the elements of the tensor $\Phi_{\alpha\beta}(\mathbf{r}, \mathbf{r}', \omega)$ for a nonrelativistic plasma in a strong, uniform, constant or rapidly varying electric field $\mathbf{E}$ and a fixed uniform magnetic field $\mathbf{H}_0$. By rapidly varying here we mean a field $\mathbf{E}$ characterized by a frequency that satisfies the relation $\Omega \gg \tau_\epsilon^{-1} \sim \delta_{eff}\nu_{eff}$, where τ_ϵ is the relaxation time for the electron energy $\epsilon = mv^2/2$. The quantity δ_{eff} is the mean relative fraction of the energy lost by an electron in a single collision with a heavy particle ($\delta_{eff} \ll 1$); ν_{eff} is the effective frequency of collisions between the electron and heavy particles (more precise definitions of these terms are given, for example, in [7]). If the above condition is satisfied, just as in the case in which $\mathbf{E}$ is constant,* the plasma reaches a stationary state, that is to say, the symmetric part $f_0(v)$ of the electron distribution function

$$f(\mathbf{v}) = f_0(v) + \mathbf{v}f_1(v)/v$$

reaches some average time independent level (the variable part of the function $f_0(v)$ is of order $(\Omega\tau_\epsilon)^{-1}$ and can be neglected). The function $f_0(v)$ will differ appreciably from a Maxwellian distribution $f_{00}(v)$ corresponding to the temperature of the heavy particles T (i.e., thermal equilibrium no longer holds) when the field E becomes sufficiently high:[8]

$$E \gtrsim E_p = [3kTm\delta_{eff}(\Omega^2 + \nu_{eff}^{0\,2})/e^2]^{1/2},$$

where ν_{eff}^0 is the effective collision frequency in the absence of the field E. In further discussion of the nonequilibrium plasma we will keep in mind the fact that the plasma is in a nonequilibrium state due precisely to the presence of such strong fields E.

2. We start by calculating the tensor for the current fluctuations. If spatial dispersion is neglected, in which case the spatial correlation is local (δ-correlation),[9,10] this tensor can be written in the form

$$\langle j_\alpha(\mathbf{r}, t)\, j_\beta(\mathbf{r}+\rho, t+\tau)\rangle = Ne^2\psi_{\alpha\beta}(\tau)\,\delta(\rho), \qquad (3)$$

where N is the electron density, e is the charge of the electron and $\psi_{\alpha\beta}(\tau) = \langle v_\alpha(t)\, v_\beta(t+\tau)\rangle$ is the correlation tensor for velocity fluctuations of a given electron in the plasma: $\langle v_\alpha\rangle = 0$.

If the fluctuations $v_\alpha(t)$ are to be stationary, we require $\psi_{\alpha\beta}(\tau) = \psi_{\beta\alpha}(-\tau)$. Using this property of $\psi_{\alpha\beta}(\tau)$, we obtain from Eqs. (1) and (3) the following expression for the "frequency" part $\varphi_{\alpha\beta}(\omega)$ of the tensor $\Phi_{\alpha\beta}(\mathbf{r}, \mathbf{r}', \omega) = \varphi_{\alpha\beta}(\omega)\times\delta(\mathbf{r}-\mathbf{r}')$:

$$\varphi_{\alpha\beta}(\omega) = \frac{Ne^2}{2\pi}\left\{\int_0^\infty [\psi_{\alpha\beta}(\tau) + \psi_{\beta\alpha}(\tau)]\cos\omega\tau\, d\tau + i\int_0^\infty [\psi_{\alpha\beta}(\tau) - \psi_{\beta\alpha}(\tau)]\sin\omega\tau\, d\tau\right\}. \qquad (4)$$

This expression allows us to compute the tensor $\varphi_{\alpha\beta}(\omega)$ using the velocity tensor $\psi_{\alpha\beta}(\tau)$, which is given only for $\tau > 0$. However, for $\tau > 0$ the elements of $\psi_{\alpha\beta}$ can be determined from the following simple considerations. Let the z axis be along the magnetic field $\mathbf{H}_0$. In the interval between two collisions an electron behaves as though free and moves in a helical path along the magnetic field $\mathbf{H}_0$ with a rotation frequency $\omega_H = |e|H_0/mc$. Hence, for given values of the velocity components v_x, v_y and v_z the nonvanishing second moments at $t = 0$ are

$$\langle v_z(0)\, v_z(\tau)\rangle = v_z^2, \qquad \langle v_x(0)\, v_x(\tau)\rangle = v_x^2\cos\omega_H\tau,$$
$$\langle v_y(0)\, v_y(\tau)\rangle = v_y^2\cos\omega_H\tau,$$
$$\langle v_x(0)\, v_y(\tau)\rangle = -\langle v_y(0)\, v_x(\tau)\rangle = v_x^2\sin\omega_H\tau,$$

if $\tau < \tau_0(v)$, where $\tau_0(v)$ is the time required to travel one mean free path, and zero when $\tau > \tau_0(v)$.

Introducing the step function $p(x)$, which is equal to unity for $x > 0$ and zero for $x < 0$, we can write

$$\begin{aligned}
\psi_{zz}(\tau) &= \langle v_z^2 p(s/v - \tau)\rangle,\\
\psi_{xx}(\tau) &= \langle v_x^2\cos\omega_H\tau\cdot p(s/v-\tau)\rangle,\\
\psi_{yy}(\tau) &= \langle v_y^2\cos\omega_H\tau\cdot p(s/v-\tau)\rangle,\\
\psi_{xy}(\tau) &= \psi_{yx}(-\tau) = \langle v_x^2\sin\omega_H\tau\cdot p(s/v-\tau)\rangle,
\end{aligned} \qquad (5)$$

where the averages are first taken over s, the length of a free path for a given velocity v, by means of the distribution function

$$w(s, v) = \exp[-s/l(v)], \qquad l(v) = v/\nu(v)$$

[$\nu(v)$ is the electron collision frequency], and then with respect to velocity, by means of the electron distribution function $f_0(v)$.*

Substituting (5) in (4) and first carrying out the

*In a highly ionized plasma in a very strong constant field $E > E_c \sim \sqrt{kT_e m}\nu_{eff}(T_e)/e$ (T_e is the electron temperature) the phenomenon of electron "runaway" occurs,[7,8] making it impossible to establish a stationary electron distribution $f(v)$. We assume below that the constant field satisfies the condition $E \ll E_c$.

*The function $f(v)$ is normalized to unity (not to the density N).

integration over τ and then over s, we obtain the following expressions for the nonvanishing elements $\varphi_{\alpha\beta}(\omega)$:

$$\varphi_{zz}(\omega) = \langle\chi_0(v, \omega)\rangle,$$

$$\varphi_{xx}(\omega) = \varphi_{yy}(\omega) = \tfrac{1}{2}\{\langle\chi_{(-)}(v, \omega)\rangle + \langle\chi_{(+)}(v, \omega)\rangle\},$$

$$\varphi_{xy}(\omega) = \varphi^*_{yx}(\omega) = \tfrac{1}{2}\{\langle\chi_{(-)}(v, \omega)\rangle - \langle\chi_{(+)}(v, \omega)\rangle\}, \qquad (6)$$

where the functions χ_0, $\chi_{(-)}$, and $\chi_{(+)}$ are given by

$$\chi_0 = \frac{Ne^2}{3\pi}\frac{\nu v^2}{\omega^2+\nu^2} = \frac{2Ne^2}{3\pi}\frac{\nu\varepsilon}{\omega^2+\nu^2},$$

$$\chi_{(\mp)} = \frac{Ne^2}{3\pi}\frac{\nu v^2}{(\omega\mp\omega_H)^2+\nu^2} = \frac{2Ne^2}{3\pi}\frac{\nu\varepsilon}{(\omega\mp\omega_H)+\nu^2}, \qquad (7)$$

and the brackets $\langle\ \rangle$ denoted averages over the distribution functions $f_0(v)$.

To proceed further in computing the elements of $\varphi_{\alpha\beta}(\omega)$ we must introduce the concrete properties of the plasma and its environment. More precisely, we must assign the type of collisions i.e., the function $\nu(v)$, the nature of the field E (whether $\Omega = 0$ or $\Omega \gg \tau_\epsilon^{-1}$), and its orientation with respect to the field H_0. Introducing these factors uniquely determines the form of the stationary kinetic equation satisfied by the function $f_0(v)$ (cf. [7]) and thus makes it possible, by means of (6), to obtain expressions for $\varphi_{\alpha\beta}(\omega)$ in terms of such parameters as T —the temperature of the heavy plasma particles, N, E, H_0, Ω, and θ, the angle between E and H_0.

Certain particular examples will be considered below. First we compute the components of the tensor $T^{\alpha\beta}_{\text{eff}}(\omega)$, which establishes the general relation between the $\varphi_{\alpha\beta}(\omega)$ and $\sigma_{\alpha\beta}(\omega)$.

3. From (2) and the definition of the tensor $\varphi_{\alpha\beta}(\omega)$ we have

$$kT^{\alpha\beta}_{\text{eff}}(\omega) = \pi\varphi_{\alpha\gamma}(\omega)\,\sigma^{-1}_{\gamma\beta}(\omega), \qquad (8)$$

where $\sigma^{-1}_{\alpha\beta}(\omega)$ is the inverse of the matrix $\sigma_{\alpha\beta}(\omega)$, which characterizes the linear conductivity of the plasma in a given equilibrium state with respect to a small (with respect to the field E) harmonic field $\mathbf{e} = \mathbf{e}_0 e^{i\omega t}$. Expressions for the elements of $\sigma_{\alpha\beta}(\omega)$ in terms of the distribution function $f_0(v)$ are known from the kinetic theory of electrical conductivity (cf. [7]) and can be written as follows ($L \equiv d \ln f_0/d\epsilon$):

$$\sigma_{xz} = \sigma_{zx} = \sigma_{yz} = \sigma_{zy} = 0, \quad \sigma_{zz}(\omega) = -\pi\langle\chi_0(v, \omega)L\rangle,$$

$$\sigma_{xx}(\omega) = \sigma_{yy}(\omega) = -\frac{\pi}{2}\{\langle\chi_{(-)}(v, \omega)L\rangle + \langle\chi_{(+)}(v, \omega)L\rangle\},$$

$$\sigma_{xy}(\omega) = \sigma^*_{yx}(\omega) = -\frac{\pi i}{2}\{\langle\chi_{(-)}(v, \omega)L\rangle - \langle\chi_{(+)}(v, \omega)L\rangle\}. \qquad (9)$$

Calculating the inverse matrix $\sigma^{-1}_{\alpha\beta}$ and using (6) we obtain the following expressions for the nonzero elements of the effective-temperature tensor:

$$kT^{zz}_{\text{eff}} = -\langle\chi_0(v, \omega)\rangle/\langle\chi_0(v, \omega)L\rangle, \qquad (10)$$

$$kT^{xx}_{\text{eff}} = kT^{yy}_{\text{eff}} = -\frac{1}{2}\left\{\frac{\langle\chi_{(-)}(v, \omega)\rangle}{\langle\chi_{(-)}(v, \omega)L\rangle} + \frac{\langle\chi_{(+)}(v, \omega)\rangle}{\langle\chi_{(+)}(v, \omega)L\rangle}\right\}, \qquad (10')$$

$$kT^{xy}_{\text{eff}} = -kT^{yx}_{\text{eff}} = -\frac{i}{2}\left\{\frac{\langle\chi_{(-)}(v, \omega)\rangle}{\langle\chi_{(-)}(v, \omega)L\rangle} - \frac{\langle\chi_{(+)}(v, \omega)\rangle}{\langle\chi_{(+)}(v, \omega)L\rangle}\right\}. \qquad (10'')$$

As expected, at thermodynamic equilibrium $f_0(v) = C\exp(-mv^2/2kT)$ and these formulas give $T^{\alpha\beta}_{\text{eff}} = T\delta_{\alpha\beta}$.

4. We consider other particular examples. Suppose that a plasma is highly (in particular, fully) ionized so that the electron-electron collision frequency $\nu_e \gg \delta\nu$ where $\nu(v)$ is the frequency of electron collisions with heavy particles. Then (cf. [7]), the function $f_0(v)$ is a Maxwellian distribution corresponding to the electron temperature T_e. In the general case the temperature T_e is a monotonically increasing function of E that also depends on the parameters T, N, H_0, Ω, and θ.* In this case Eqs. (10), (10′), and (10″) yield a unique frequency-independent value of the effective temperature:

$$T^{\alpha\beta}_{\text{eff}} = T_e\delta_{\alpha\beta}.$$

Thus, as in the case of an equilibrium medium, the spectral composition of the electromagnetic radiation from a highly ionized plasma is completely determined by the absorptive capacities (the tensor $\sigma_{\alpha\beta}(\omega)$, [7,12]) while the intensity of this radiation is determined by the electron temperature T_e.

We now consider an isotropic plasma ($H_0 = 0$), In this case

$$\sigma_{\alpha\beta}(\omega) = \sigma(\omega)\,\delta_{\alpha\beta}, \qquad T^{\alpha\beta}_{\text{eff}}(\omega) = T_{\text{eff}}(\omega)\,\delta_{\alpha\beta},$$

where $\sigma(\omega)$ and $T_{\text{eff}}(\omega)$ are determined by (9) and (10) respectively. At low frequencies $\omega \ll \nu$ and at high frequencies $\omega \gg \nu$ Eq. (10) yields in accordance with Eq. (7),

$$kT_{\text{eff}}(0) = \frac{\langle\varepsilon/\nu\rangle}{\langle\varepsilon L/\nu\rangle}, \qquad kT_{\text{eff}}(\infty) = \frac{\langle\varepsilon\nu\rangle}{\langle\varepsilon\nu L\rangle}. \qquad (11)$$

The first of these expressions has been given earlier.[6]

Suppose now that the field E is constant and that the plasma is weakly ionized $\nu_e \ll \delta\nu$. Then, if the only collisions of importance are elastic col-

*Expressions for T_e for actual cases are given in [7] and [11].

lisions with neutral particles—solid spheres of radius a,—the function $f_0(v)$ is the well-known Druyvesteyn function[13]

$$f_0(v) = C \exp\left[-3m^2\delta_{el}v^4/8e^2E^2l^2\right], \qquad (12)$$

where $l = v/\nu(v) = (\pi a^2 N_m)^{-1}$, N_m is the density of molecules, $\delta_{el} = 2m/M$, and M is the mass of the molecule. Substitution of (12) in (10) gives the following general expressions for the effective temperature in this case:

$$kT_{eff} = \frac{eEl}{\sqrt{6\delta_{el}}} \int_0^\infty \frac{x^2 e^{-x^2}}{x+\alpha}\,dx \Big/ \int_0^\infty \frac{x^3 e^{-x^2}}{x+\alpha}\,dx,$$

$$\alpha = \sqrt{3\delta_{el}}\, m\omega^2/[2^{3/2}(\pi a^2 N_m)^2\, eEl]. \qquad (13)$$

The dependence of T_{eff} on frequency ω (which is always weak) appears only in the interval $\alpha \lesssim 1$. When $\alpha \gg 1$ we have

$$kT_{eff} = \frac{1}{2} eEl \sqrt{\frac{\pi}{6\delta_{el}}}. \qquad (14)$$

At zero frequency the value of T_{eff} can be only $4/\pi$ times greater at most.

[1] H. B. Callen and T. A. Welton, Phys. Rev. **83**, 24 (1951).

[2] S. M. Rytov, Teoriya elektricheskikh fluktuatsii i teplovovo izlucheniya (Theory of Electrical Fluctuations and Thermal Radiation), AN SSSR 1953; DAN SSSR **110**, 371 (1956), Soviet Phys.-Doklady **1**, 371 (1957).

[3] L. D. Landau and E. M. Lifshitz, Elektrodinamika sploshnykh sred (Electrodynamics of Continuous Media), Gostekhizdat, 1957.

[4] F. V. Bunkin, Dissertation, Phys. Inst. Acad. Sci. 1955; JETP **32**, 811 (1957), Soviet Phys. JETP **5**, 665 (1957).

[5] S. M. Rytov, Usp. Fiz. Nauk **63**, 657 (1957).

[6] F. V. Bunkin, Izv. VUZov, (News of the Colleges), Radiophysics **4**, 3 (1961).

[7] V. L. Ginzburg and A. V. Gurevich, Usp. Fiz. Nauk **70**, 201 (1960), Soviet Phys.-Uspekhi **3**, 115 (1960).

[8] H. Dreicer, Phys. Rev. **115**, 238 (1957).

[9] Yu. L. Klimontovich, JETP **34**, 173 (1958), Soviet Phys. JETP **7**, 119 (1958).

[10] V. P. Silin, Izv. VUZov, (News of the Colleges), Radiophysics **2**, 198 (1959).

[11] B. I. Davydov, JETP **7**, 1069 (1937).

[12] A. V. Gurevich, JETP **30**, 1112 (1956), Soviet Phys. JETP **3**, 895 (1957); Dissertation, Phys. Inst. Acad. Sci. 1957.

[13] M. J. Druyvesteyn, Physica **10**, 69 (1930).

Translated by H. Lashinsky
57

ON THE ROLE OF THE SINGLE-MESON POLE DIAGRAM IN SCATTERING OF GAMMA QUANTA BY PROTONS

L. I. LAPIDUS and CHOU KUANG-CHAO

Joint Institute for Nuclear Research

Submitted to JETP editor February 27, 1961

J. Exptl. Theoret. Phys. (U.S.S.R.) 41, 294-302 (July, 1961)

It is shown that when the sign of the γN-scattering pole diagram connected with π^0-meson decay is correctly chosen, the contribution of the pole to the cross section for the scattering of γ quanta by protons decreases considerably. In order to obtain information on the lifetime of the π^0 meson, the precision of the experiments must be appreciably improved.

1. INTRODUCTION

A few years ago Low[1] called attention to the presence of a pole diagram connected with the decay of the neutral pion, in the amplitude of elastic scattering of γ quanta by protons. An account of this diagram, from the point of view of the double dispersion relations for γN scattering, is equivalent to an examination of the nearest singularity in Q^2. Several interesting considerations in connection with the double dispersion relations for γN scattering are contained in the paper by N. F. Nelipa and L. V. Fil'kov (preprint).* Zhizhin[2] considered a contribution of this amplitude in different states. Recently, Hyman et al[3] and in greater detail Jacob and Mathews[4] noted that the addition of the one-meson pole amplitude greatly improves the agreement between the theoretical and experimental results in the γ-quantum region from 100 to 250 Mev. This problem is considered in detail in a recently published paper by Bernadrini, Yamagata, et al.[5]

It is known that an analysis based on dispersion relations[6,7] leads to scattering cross section values greater than the experimental values in this energy region. In the present paper we wish to call attention to the sign of the pole amplitude, which is very important, since the interference terms play the principal role. From the results of Goldberger and Treiman[8] for the decay of the neutral pion, and from the dispersion relations for forward scattering, which we used previously,[7] it follows that the (relative) sign of the pole diagram differs from that used by Jacob and Mathews. Thus, the addition of the pole diagram does not improve the agreement between the theoretical and experimental results, and the discrepancy calls for a different explanation.

*The authors are grateful to Nelipa and Fil'kov, and also to Dr. Yamagata (see below), for acquainting them with their results prior to publication.

2. SCATTERING AMPLITUDE

We denote by p and p′ the nucleon momentum vectors in the initial and final states, respectively, and by q and q′ the same quantities for the γ quanta. Since they satisfy the conservation law

$$q + p = q' + p', \tag{1}$$

it is convenient to introduce the following four orthogonal vectors:

$$K = \tfrac{1}{2}(q + q'), \qquad Q = \tfrac{1}{2}(q' - q), = \tfrac{1}{2}(p - p'),$$
$$P' = P - K(PK)/K^2, \qquad N_\mu = i\varepsilon_{\mu\nu\sigma\rho} P'_\nu K_\sigma Q_\rho, \tag{2}$$

where $P = (p + p')/2$. From these four vectors we can construct two independent scalars:

$$Q^2, \qquad M\nu = -(PK). \tag{3}$$

The lengths of the vectors introduced in (2) are connected with Q^2 and $M\nu$ by the relations

$$K^2 = -Q^2, \qquad P^2 = -Q^2 - M^2,$$
$$P'^2 = P^2 - (PK)^2/K^2 = Q^{-2}[M^2\nu^2 - Q^2(Q^2 + M^2)],$$
$$N^2 = -P'^2K^2Q^2 = Q^2[M^2\nu^2 - Q^2(Q^2 + M^2)]. \tag{4}$$

The S-matrix element for γN scattering can be represented in the form

$$\langle p'q'|S|pq\rangle = \langle p'q'|pq\rangle + \frac{i}{2\pi}\delta^{(4)}(p' + q' - p - q)\frac{MN}{(p_0p'_0q_0q'_0)^{1/2}}, \tag{5}$$

where

$$N = \bar{u}(p')\, e'_\mu N_{\mu\nu} e_\nu u(p)$$
$$= 2\pi^2 i\left(\frac{p_0p'_0}{M^2}\right)^{1/2}\int d^4z e^{-i(Kz)}\left\langle p'\left|T\left(e'\cdot j\left(\frac{z}{2}\right)\right)\right.\right.$$
$$\left.\left.\times\left(e\cdot j\left(-\frac{z}{2}\right)\right)\right|p\right\rangle. \tag{6}$$

In the center-of-mass system (c.m.s.) the differential cross section is given by the relation

$$\frac{d\sigma}{d\omega} = \sum_{\text{spins}} \left| \frac{M}{W} N \right|^2, \tag{7}$$

where $W^2 = -(P + K)^2$ is the square of the total energy in the c.m.s.

The scattering amplitude N can be written as a sum of six invariant functions ($\hat{K} = \gamma_\mu K_\mu$):

$$e'_\mu N_{\mu\nu} e_\nu = \frac{(e'P')(eP')}{P'^2}[T_1 + i\hat{K}T_2] + \frac{(e'N)(eN)}{N^2}[T_3 + i\hat{K}T_4]$$
$$- \frac{(e'P')(eN) - (e'N)(eP')}{(P'^2N^2)^{1/2}} i\gamma_5 T_5$$
$$+ \frac{(e'P')(eN) + (e'N)(eP')}{(P'^2N^2)^{1/2}} \gamma_5 \hat{K} T_6. \tag{8}$$

In some cases it is also convenient to represent the amplitude as an operator in spin space in terms of six non-covariant functions R_i:

$$\frac{M}{W} e'_\mu N_{\mu\nu} e_\nu = R_1(ee') + R_2(s's) + iR_3(\sigma[e'e]) + iR_4(\sigma[s's])$$
$$+ iR_5[(\sigma k)(s'e) - (\sigma k')(se')]$$
$$+ iR_6[(\sigma k')(s'e) - (\sigma k)(se')], \tag{9}*$$

where $\mathbf{s} = \mathbf{k} \times \mathbf{e}$, $\mathbf{s}' = \mathbf{k}' \times \mathbf{e}'$; $\mathbf{e}$, $\mathbf{k}$ and $\mathbf{e}'$, $\mathbf{k}'$ are the polarization of photon-momentum unit vectors before and after scattering, respectively.

3. MATRIX ELEMENT OF NEUTRAL-PION DECAY

The S matrix for the decay of the neutral pion has the form

$$\langle q'q|S|q_\pi\rangle = \frac{1}{(2\pi)^{3/2}} \frac{1}{\sqrt{2\omega_k}} (2\pi)^4 \delta^{(4)}(q_\pi - q - q')$$
$$\times \langle q'q|J(0)|0\rangle, \tag{10}$$

where q and q′ are the photon momenta; q_π is the 4-momentum of the pion; J(x) is the current of the pion field:

$$J(x) = i\frac{\delta S}{\delta\bar{\psi}(x)} S^+ = ig_0\bar{\psi}(x)\gamma_5\tau_3\psi(x) \tag{11}$$

[$\varphi(x)$ is the meson-field operator, $\psi(x)$ is the nucleon-field operator, and g_0 is the non-renormalized constant of the pion-nucleon interaction]. The Heisenberg equation for the meson field can be written in the form

$$(-\Box^2 + m_\pi^2)\varphi(x) = J(x), \tag{12}$$

and in the notation of Goldberger and Treiman[8]

$$\mathcal{M} \equiv (2\pi)^3 \sqrt{4qq'}\langle q'q|J|0\rangle$$
$$= -i\varepsilon_{\mu\nu\sigma\lambda} e'_\mu e_\nu q_\sigma q'_\lambda F[(q + q')^2], \tag{13}$$

where $F(q^2)$ is the form factor. The expression for the decay S matrix contains $F(-m_\pi^2)$.

*$(ee') = e \cdot e'$ $[ee'] = e \times e'$.

The probability of decay of the neutral pion is

$$w = \sum_{qq'ee'} (2\pi)^3 |\langle qq'|S|q_\pi\rangle|^2/VT$$
$$= \frac{1}{(2\pi)^2}\delta^{(4)}(q_\pi - q - q')\, d^3q\, d^3q' \frac{1}{8q_{\pi 0}q_0q'_0} q^2 q'^2$$
$$\times \sum_{ee'} [(es') + (e's)]^2 |F|^2. \tag{14}$$

Summing over e and e′ and integrating over the angles we obtain in the pion rest system

$$w = (m_\pi^3/64\pi)|F|^2. \tag{15}$$

The pion lifetime τ is

$$\tau = 64\pi/m_\pi^3|F|^2. \tag{16}$$

Using the dispersion technique, Goldberger and Treiman have shown that

$$F(0) = -\frac{ge^2}{4\pi^2 m_n}(1 + \mu_p)\frac{I_0 + \rho I_1}{1 + (g^2/4\pi)I_1}, \tag{17}$$

$$\rho = [2\mu_p - (\mu_p^2 - \mu_n^2)]/(1 + \mu_p), \tag{18}$$

where μ_p and μ_n are the anomalous magnetic moments of the proton and neutron, while I_0 and I_1 are positive integrals. It follows from (17) that

$$F(0)\, g < 0. \tag{19}$$

This sign is of importance for what is to follow.

4. SINGLE-MESON DIAGRAM FOR THE SCATTERING OF GAMMA QUANTA BY PROTONS

The S-matrix element of the pole diagram is

$$\langle p'q'|S - 1|pq\rangle = ig\frac{i}{(2\pi)^3}\bar{u}(p')\gamma_5 u(p)$$
$$\times \delta^{(4)}(p' + q' - p - q)$$
$$\times (2\pi)^4 \frac{1}{(p' - p)^2 + m_\pi^2}\langle q'|J_\pi(0)|q\rangle. \tag{20}$$

It can be shown that

$$\langle q'|J_\pi(0)|q\rangle$$
$$= \frac{1}{(2\pi)^3}\frac{1}{(4q_0q'_0)^{1/2}}(-i)\varepsilon_{\mu\nu\sigma\lambda} e'_\mu e_\nu q'_\sigma q_\lambda F[(q' - q)^2]. \tag{21}$$

Since the matrix element $\langle q'|J_\pi(0)|q\rangle$ is taken for the pole at $(q' - q)^2 = -m_\pi^2$, Eq. (21) contains exactly the value of F encountered in the π^0 decay.

Substituting (21) in (20) and going to the c.m.s., we obtain

$$\langle p'q'|S - 1|pq\rangle = \frac{igF}{(2\pi)^6}\frac{Mq^3}{(4q_0q'_0p_0p'_0)^{1/2}}(2\pi)^4\delta^{(4)}(p' + q'$$
$$- p - q)\frac{1}{2M}[i((\sigma k)(es') - (\sigma k')(e's))$$
$$- i((\sigma k')(es') - (\sigma k)(e's))]. \tag{22}$$

Comparing (22) with (9) we obtain for the contribution of the pole diagram

$$R_{1p} = R_{2p} = R_{3p} = R_{4p} = 0,$$
$$R_{5p} = -R_{6p} = \frac{gF}{8\pi W}\frac{q^3}{(p-p')^2+m_\pi^2}; \quad (23)$$

from this we conclude that the contribution made to the amplitude by the pole diagram due to the exchange and decay of the pseudo-scalar neutral meson reduces to the combination

$$R_{5p} - R_{6p} = \frac{gFm_\pi}{8\pi W}\frac{q}{m_\pi}\frac{1}{1+m_\pi^2/2q^2-\cos\theta}. \quad (24)$$

It is important to note that by virtue of (19)

$$R_{5p} - R_{6p} < 0, \quad (25)$$

if it is assumed that $F(0)$ and $F(-m_\pi^2)$ do not differ greatly.

In the expression for the cross section [formula (16) in [5]] the pole term enters in the combination

$$\tfrac{1}{2}|R_5 - R_6|^2(1-\cos\theta)^3 - \mathrm{Re}\,(R_3 - R_4)^*(R_5 - R_6)(1-\cos\theta)^2. \quad (26)$$

The contribution of one pole diagram has the form

$$I_0^P(\theta) = \tfrac{1}{2}|R_5 - R_6|^2(1-\cos\theta)^3 = \frac{2}{m_\pi\tau}\left(\frac{q}{W}\right)^2\frac{g^2}{4\pi}\left(\frac{1}{m_\pi}\right)^2\frac{(1-\cos\theta)^3}{(1+m_\pi^2/2q^2-\cos\theta)^2} \quad (27)$$

which agrees with the result of Jacob and Mathews.

We can expect the cross section of scattering by 90° to be reduced by addition of the pole term only when the second term in (26) is negative. Since R_4 is large and negative, owing to the large anomalous magnetic moment of the proton, $\mathrm{Re}\,(R_3 - R_4)$ is a positive quantity in the region of energy under consideration. Thus, the second term in (26) is positive if $R_{5p} - R_{6p} < 0$. Consequently, assuming the analysis of Goldberger and Treiman to be correct, the pole diagram does not decrease the theoretical value of the cross section, but increases it.

If we use the results of our own analysis,[7] we find that $\mathrm{Re}\,(R_5 - R_6)$ is determined not only by the limit theorem, but also by the amplitudes of photoproduction of E_2 and M_3. Since in this case the "isotropic" part of the contribution of the pole amplitude is automatically taken into account, it is necessary to add to the previously-obtained amplitude not all of expression (24), but only the contribution of (24) to the higher states, i.e., the difference

$$(R_5 - R_6)_p - \frac{1}{2\pi}\int (R_5 - R_6)_p \sin\theta d\theta.$$

As a result of this procedure, which is necessary in order not to violate the unitarity of the S matrix (when $\theta = 90°$), the quantity y_0^{-1} (where $y_0 = 1 + m_\pi^2/2q^2$) is replaced by

$$y_0^{-1} - \tfrac{1}{2}\ln|(y_0+1)/(y_0-1)|,$$

which leads to replacement of $\frac{2}{3}$ by -0.14 when $q^2 = m_\pi^2$ ($y_0 = \frac{3}{2}$).

Thus, the contribution of the amplitude is decreased by a factor of 5, and the sign of the contribution changes. By virtue of this, a much higher accuracy is necessary before the connection between the amplitude of the neutral-pion decay and the amplitude of the scattering of γ quanta by protons can manifest itself. It was recently shown that the lifetime of the neutral pion is $(2.0 \pm 0.4) \times 10^{-16}$ sec,[9] which also decreases the contribution of the pole diagram.

The indeterminacies in the analysis of the photoproduction cannot influence the conclusion regarding the sign of the interference term in (24), since this sign is determined by the well known theorem for low energies. The scattering amplitude at low frequencies, first obtained by Low[10] and Gell-Mann and Goldberger,[11] is reviewed in the appendix, where it is obtained as the contribution of the single-nucleon terms (see [6]).

We note, in particular, that

$$T_5^0 = \frac{e^2}{M}(1+\lambda)\frac{Q^2}{Q^2/M^2 - \nu^2}. \quad (28)$$

Let us give another, less rigorous but more illustrative proof of the correctness of the determination of the sign of the pole diagram.*

The matrix element $\langle q'|J_\pi(0)|q\rangle$ can be represented in the form

$$\langle q'|J_\pi(0)|q\rangle = i\varepsilon_{\mu\nu\sigma\lambda}e'_\mu e_\nu q_\sigma q'_\lambda \frac{1}{(2\pi)^3}F[(q-q')^2] = -\frac{2Q^2}{(2\pi)^3}F\frac{(e'P')(eN) - (e'N)(eP')}{(P'^2N^2)^{1/2}}, \quad (29)$$

so that

$$\langle p'q'|S-1|pq\rangle = i(2\pi)^{-2}g\delta^{(4)}(p'+q'-p-q) \times i\bar{u}(p')\gamma_5 u(p) \times \frac{2Q^2F}{4Q^2+m_\pi^2}\frac{(e'P')(eN) - (e'N)(eP')}{(P'^2N^2)^{1/2}}; \quad (30)$$

hence

$$T_{5p} = \frac{gF}{\pi}\frac{Q^2}{4Q^2+m_\pi^2}. \quad (31)$$

We now introduce the function

$$f(\nu, Q^2) = T_5(\nu, Q^2)/Q^2. \quad (32)$$

If we regard $f(\nu, Q^2)$ as an analytic function of Q^2 at fixed ν, we obtain from Cauchy's theorem and from (31)

*An analogous approach was used earlier[12] to obtain the Goldberger-Treiman relations.

$$f(\nu, Q^2) = \frac{gF}{\pi}\frac{1}{4Q^2 + m_\pi^2} + J_Q, \quad (33)$$

where J_Q is the dispersion interval, the lower limit of which is $4m_\pi^2$. In the region $Q^2 \ll 4m_\pi^2$, the integral in (33) is small and we can approximate $f(\nu, Q^2)$ by the expression

$$f(\nu, Q^2) \approx \frac{gF}{\pi}\frac{1}{4Q^2 + m_\pi^2}. \quad (34)$$

On the other hand, $f(\nu, Q^2)$ is also an analytic function of ν for fixed Q^2. By Cauchy's theorem with account of (28) we have

$$f(\nu, Q^2) = \frac{e^2(1+\lambda)}{M}\frac{1}{Q^2/M^2 - \nu^2} + J_\nu, \quad (35)$$

where J_ν is a second dispersion integral. In the region $2\nu \lesssim m_\pi$, the pole term will predominate and

$$f(\nu, Q^2) \approx \frac{e^2(1+\lambda)}{M}\frac{1}{Q^2/M^2 - \nu^2}. \quad (36)$$

It is obvious that (34) does not hold near $M^2\nu^2 \approx Q^2$, and (36) does not take place when $4Q^2 = -m_\pi^2$. It is still possible, however, that expressions (34) and (36) are valid simultaneously near certain values of ν and Q^2. Equating these expressions for $2\nu = m_\pi$ and $Q \approx 0$, we obtain

$$F = -4\pi e^2(1+\lambda)/gM, \quad (37)$$

which is very close to the formula of Goldberger and Treiman, obtained by an entirely different method.

Actually, from (17) we obtain for $(g^2/4\pi^2) I_1 \gg 1$

$$F = -4\pi\frac{e^2(1+\lambda)}{g}\frac{I_0 + \rho I_1}{I_1},$$

which coincides with (37), apart for a numerical factor.

The literature reports two different choices of the common phase for the γN scattering amplitude, one with a Thomson limit $+e^2/M$, the other with $-e^2/M$. The error in the published papers lies in the fact that the choice of the common factor in the one-meson amplitude does not correspond to the choice of the sign of the remaining amplitude.

A direct comparison of the amplitude used by Jacob and Mathews[4] with (9) shows that the functions f_i introduced in [4] are related with R_i by the equations

$$-f_1 = R_1 + R_2\cos\theta, \qquad f_2 = R_2,$$
$$f_3 = R_3 + R_4\cos\theta + (R_5 + R_6)(1 + \cos\theta) - (R_5 - R_6)(1 - \cos\theta),$$
$$f_4 = R_4, \qquad f_5 = R_4 + R_5, \qquad f_6 = R_6,$$

where the difference in the common phase factor is taken into account, and from which it is clear that the sign used in [4] for the pole term differs from that proved in the present paper.

APPENDIX

SINGLE-NUCLEON TERMS IN THE DISPERSION RELATIONS

Recognizing that

$$T\left(e'\cdot j\left(\frac{z}{2}\right)\right)\left(e\cdot j\left(-\frac{z}{2}\right)\right) = \theta(z_0)\left[e\cdot j'\left(\frac{z}{2}\right), e\cdot j\left(-\frac{z}{2}\right)\right] + \left(e'\cdot j\left(\frac{z}{2}\right)\right)\left(e\cdot j\left(-\frac{z}{2}\right)\right), \quad (A.1)$$

we determine the retarded and advanced amplitudes:

$$N^{r,a} = \pm 2\pi^2 i\,(p_0 p_0'/M^2)^{1/2} \times \int d^4z e^{\pm i(Kz)}\left\langle p'\left|\theta(\pm z_0)\left[e'\cdot j\left(\frac{z}{2}\right), e\cdot j\left(-\frac{z}{2}\right)\right]\right| p\right\rangle. \quad (A.2)$$

The vertex part of the current has the form

$$\langle p'|ej(0)|p\rangle = \frac{i\varepsilon}{(2\pi)^3}\bar u(p')\left[\hat e + i\frac{\lambda}{4M}(\hat e(\hat p' - \hat p) - (\hat p' - \hat p)\hat e)\right]u(p) = \frac{i\varepsilon}{(2)^3}u(p')\left[(1+\lambda)\hat e + \frac{i\lambda}{M}(eP)\right]u(p), \quad (A.3)$$

where ϵ is the charge of the nucleon.

The pole term has in the region of positive frequencies the form

$$A^0 = -\frac{(2\pi)^6}{4}\sum_n \delta^{(4)}(k - p + p_n)\langle p'|e\cdot j(0)|p_n\rangle \times \langle p_n|e'j(0)|p\rangle = \frac{\varepsilon^2}{4}\int d^3p_n\,\delta^{(4)}(k - p + p_n) \times \bar u(p')\left[(1+\lambda)\hat e + \frac{i\lambda}{M}ep'\right]u(P - K)\,\bar u(P - K) \times \left[(1+\lambda)\hat e' + \frac{i\lambda}{M}e'p\right]u(p). \quad (A.4)$$

Using the relations

$$\sum u(P - K)\bar u(P - K) = \frac{-i(\hat P - \hat K) + M}{2p_{n0}}, \quad (A.5)$$

$$(2p_{n0})^{-1}d^3p_n = d^4p_n\theta(p_{n0})\,\delta(p_n^2 + M^2), \quad (A.6)$$

we obtain

$$A^0 = \frac{\varepsilon^2}{4}\delta(p_n^2 + M^2)\bar u(p')\left[(1+\lambda)\hat e + \frac{i\lambda}{M}(ep')\right] \times [-i(\hat P - \hat K) + M]\left[(1+\lambda)\hat e' + \frac{i\lambda}{M}(e'p)\right]u(p). \quad (A.7)$$

We can express A^0 in terms of the fundamental invariants:

$$A^0 = \frac{(e'P')(eP')}{P'^2}A_1^0 + \frac{(e'N)(eN)}{N^2}A_2^0 + \frac{(e'P')(eN) - (e'N)(eP')}{(P'^2N^2)^{1/2}}A_3^0 + \frac{(e'P')(eN) + (e'N)(eP')}{(P'^2N^2)^{1/2}}A_4^0. \quad (A.8)$$

Comparing (A.7) and (A.8), we obtain

$$A_1^0 P'^2 = \frac{\varepsilon^2}{4}\delta(p_n^2 + M^2)\bar u(p')\left[(1+\lambda)\hat P' + \frac{i\lambda}{M}(P'p')\right] \times [-i(\hat P - \hat K) + M]\left[(1+\lambda)\hat P' + \frac{i\lambda}{M}(P'p)\right]u(p). \quad (A.9)$$

It is easy to verify that

$$(P'p') = (P', P - Q) = (P'p) = P'^2, \tag{A.10}$$

$$\bar{u}(p')\,[\hat{P}'\,(-i(\hat{P}-\hat{K})+M)\,\hat{P}']\,u(p)$$
$$= \bar{u}(p')\left\{-i\hat{K}P'^2+2P'^2M+2i\frac{(PK)}{K^2}\hat{K}P'^2\right\}u(p), \tag{A.11}$$

$$\bar{u}(p')\,\hat{P}'\,[-i(\hat{P}-\hat{K})+M]\,u(p) = \bar{u}(p')\left[M\left(iM-\frac{(PK)}{K^2}\hat{K}\right)\right.$$
$$\left.-i(P^2+(PK))+i\left(\hat{P}\hat{K})+\frac{(PK)}{K^2}\hat{K}\hat{P}\right)\right]u(p), \tag{A.12}$$

$$\bar{u}(p')\,[(-i(\hat{P}-\hat{K})+M)\,\hat{P}']\,u(p)$$
$$= \bar{u}(p')\left[M\left(iM-\frac{(PK)}{K^2}\hat{K}\right)-i(P^2+(PK))\right.$$
$$\left.+i\left(\hat{K}\hat{P}+\frac{(PK)}{K^2}\hat{P}\hat{K}\right)\right]u(p), \tag{A.13}$$

$$\bar{u}(p')\,[-i(\hat{P}-\hat{K})+M]\,u(p) = \bar{u}(p')\,[i\hat{K}+2M]\,u(p). \tag{A.14}$$

Using (A.10) – (A.14) and noting that at the pole we have

$$(P-K)^2 = P^2+K^2-2(PK)$$
$$= 2K^2-2(PK)-M^2 = -M^2$$

or that

$$K^2 = (PK), \tag{A.15}$$

we obtain

$$A_1^0 = \tfrac{1}{4}\varepsilon^2\delta\,(2K^2-2(PK))\,\bar{u}(p')\,(2M+i\hat{K})\,u(p)$$
$$= \frac{\varepsilon^2}{8M}\delta\left(\nu-\frac{Q^2}{M}\right)\bar{u}(p')\,(2M+i\hat{K})\,u(p). \tag{A.16}$$

Analogously,

$$A_2^0 = -\frac{\varepsilon^2}{8M}\delta\left(\nu-\frac{Q^2}{M}\right)\bar{u}(p')\,i\hat{K}\,u(p)\,(1+\lambda)^2, \tag{A.17}$$

$$(A_3^0+A_4^0)\,(P'^2N^2)^{1/2}$$
$$= \frac{\varepsilon^2(1+\lambda)}{8M}\delta\left(\nu-\frac{Q^2}{M}\right)\bar{u}(p')\left[\frac{P'^2}{M}\hat{N}(-iM+\hat{K})\right]u(p), \tag{A.18}$$

$$(A_4^0-A_3^0)\,(P'^2N^2)^{1/2}$$
$$= \frac{\varepsilon^2(1+\lambda)}{8M}\delta\left(\nu-\frac{Q^2}{M}\right)\bar{u}(p')\left[\frac{P'^2}{M}(\hat{K}-iM)\hat{N}\right]u(p). \tag{A.19}$$

From (A.18) and (A.19) we find

$$A_4^0(P'^2N^2)^{1/2} = \frac{\varepsilon^2(1+\lambda)}{8M}\delta\left(\nu-\frac{Q^2}{M}\right)(-iP'^2)\,\bar{u}(p')\,\hat{N}\,u(p),$$
$$A_3^0(P'^2N^2)^{1/2} = \frac{\varepsilon^2(1+\lambda)}{8M}\delta\left(\nu-\frac{Q^2}{M}\right)\frac{P'^2}{M}\,\bar{u}(p')\,\hat{N}\hat{K}u(p). \tag{A.20}$$

It can be shown that

$$\bar{u}(p')\,\hat{N}\hat{K}u(p) = (P'^2N^2)^{1/2}\,i\bar{u}(p')\,\gamma_5 u(p),$$
$$i\bar{u}(p')\,\hat{N}u(p) = K^2\bar{u}(p')\,\gamma_5\hat{K}u(p).$$

If we now take into account the fact that $(P'^2N^2)^{1/2} = P'^2Q^2$ by virtue of (4), we obtain from (A.20)

$$A_3^0 = -\frac{\varepsilon^2(1+\lambda)}{8M}\delta\left(\nu-\frac{Q^2}{M}\right)i\bar{u}(p')\,\gamma_5\,u(p),$$
$$A_4^0 = \frac{\varepsilon^2(1+\lambda)}{8M}\delta(\nu-Q^2/M)\,\bar{u}(p')\,\gamma_5\hat{K}u(p). \tag{A.21}$$

Finally from (A.16), (A.17), and (A.21) we obtain

$$T_1^0 = \frac{\varepsilon^2}{2\pi M}\frac{Q^2}{Q^4/M^2-\nu^2}, \qquad T_2^0 = \frac{\varepsilon^2}{4\pi M}\frac{\nu}{Q^4/M^2-\nu^2},$$
$$T_3^0 = 0, \qquad T_4^0 = -\frac{\varepsilon^2(1+\lambda)^2}{4\pi M}\frac{\nu}{Q^4/M^2-\nu^2},$$
$$T_5^0 = MT_6^0 = \frac{\varepsilon^2(1+\lambda)}{4\pi M}\frac{Q^2}{Q^4/M^2-\nu^2} \qquad \left(\frac{\varepsilon^2}{4\pi}=\frac{1}{137}\right), \tag{A.22}$$

which coincides with the previously-obtained results and has the correct signs.

In all the calculations of the single-nucleon terms it is assumed that parity is conserved in the electromagnetic interactions. The results obtained remain valid also in the presence of CP invariance.

[1] F. E. Low, Proc. 1958 Ann. Intern. Conf. on High Energy Physics at CERN, p. 98.

[2] E. D. Zhizhin, JETP **37**, 994 (1959), Soviet Phys. JETP **10**, 707 (1960).

[3] Hyman, Ely, Frish, and Wahlig, Phys. Rev. Lett. **3**, 93 (1959).

[4] M. Jacob and J. Mathews, Phys. Rev. **117**, 854 (1960).

[5] Bernadrini, Hanson, Odian, Yamagata, Auerbach, and Filosofo, Nuovo cimento **18**, 1203 (1960).

[6] T. Akiba and J. Sato, Progr. Theor. Phys. **19**, 93 (1958).

[7] L. I. Lapidus and Chou Kuang-chao, JETP **37**, 1714 (1959) and **38**, 201 (1960); Soviet Phys. JETP **10**, 1213 (1960) and **11**, 147 (1960).

[8] M. L. Goldberger and S. B. Treiman, Nuovo cimento **9**, 451 (1958).

[9] Glasser, Seeman, and Stiller, Bull. Am. Phys. Soc. **6**, 1 (1961).

[10] F. E. Low, Phys. Rev. **96**, 1428 (1954).

[11] M. Gell-Mann and M. L. Goldberger, Phys. Rev. **96**, 1433 (1954).

[12] Chou Kuang-chao, JETP **39**, 703 (1960), Soviet Phys. JETP **12**, 492 (1961). Bernstein, Fubini, Gell-Mann, and Thirring, Nuovo cimento **17**, 757 (1960).

Translated by J. G. Adashko
58

Letters to the Editor

BETA AND GAMMA SPECTRA OF Te^{117}

N. A. VARTANOV, Yu. A. RYUKHIN, I. P. SELINOV, V. L. CHIKHLADZE, and D. E. KHULELIDZE

Physico-Technical Institute, Academy of Sciences, Georgian S.S.R.

Submitted to JETP editor April 25, 1961

J. Exptl. Theoret. Phys. (U.S.S.R.) **41**, 303 (July, 1961)

AN activity with half-life T = 1.17 hours, attributed to Te^{117}, was obtained when irradiating antimony with high energy protons.[1] Some information about the gamma spectrum of Te^{117} was also obtained during investigation of Te^{115},[2] but was not published owing to its preliminary nature.

The isotope Te^{117} was identified from its daughter isotope Sb^{117} (T = 2.8 hours, E_γ = 0.16 Mev) and obtained from the reaction $Sn^{114}(\alpha, n)Te^{117}$ by irradiating in a cyclotron a target enriched in Sn^{114} (to an abundance of 57%) with alpha particles possessing an energy of about 21 Mev.

The Te^{117} was chromatographically separated from the irradiated target in an anion exchange column containing a 0.1 N solution of ammonium oxalate. The half-life of Te^{117}, measured by a scintillation spectrometer and an end-window counter, was found to be T = 1.1 ± 0.1 hours.

The gamma spectrum of Te^{117} was measured on the scintillation spectrometer and the following gamma lines were found: 0.71, 0.93, 1.10, 1.27, 1.42, 1.70, 1.98, 2.3 Mev, and annihilation radiation. The total intensity of all gamma transitions is about 0.3 of the intensity of the 0.71 Mev gamma line.

The positron spectrum of Te^{117} was studied on a twin-lens spectrometer.[3] The end point of the spectrum is 1.80 ± 0.07 Mev, its Kurie plot is a straight line. Electron lines 0.690 ± 0.003 Mev and 0.719 ± 0.003 Mev were found in the conversion spectrum; these were identified as the K and L conversion lines of the 0.720 ± 0.004 Mev gamma transition. The ratio K/L = 8.3 ± 1.0.

The intensity of the 0.71 Mev gamma line is approximately twice that of the annihilation radiation. If we assume on theoretical grounds that the ratio of the probability of positron decay to that of K capture is on the order of 1, then for the β^+ transition log τf = 4.3 and we may conclude that the β^+ transition is allowed. The internal conversion coefficient for E_γ = 0.72 Mev, calculated under the assumption that the positron decay proceeds to this level, has the value $\alpha_K = 3 \times 10^{-3}$. A comparison with the theoretical value of α_K for this transition at Z = 51 allows us to conclude that the transition multipolarity is M1 or E2.

[1] Kuznetsova, Mekhedov, Rybakov, and Khalkin, Atomnaya énergiya (Atomic Energy) **4**, 583 (1958).

[2] Selinov, Vartanov, Khulelidze, Bliodze, Zaĭtsev, and Khalkin, JETP **38**, 1654 (1960), Soviet Phys. JETP **11**, 1191L (1960)

[3] Selinov, Chikhladze, Khulelidze, and Vartanov, Izv. Akad. Nauk SSSR, Ser. Fiz. **25**, 848 (1961), Columbia Tech. Transl., in press.

Translated by Mrs. Jack D. Ullman
59

POSSIBILITY OF DETECTING GRAVITATIONAL RADIATION UNDER LABORATORY CONDITIONS

V. B. BRAGINSKII and G. I. RUKMAN

Moscow State University

Submitted to JETP editor May 11, 1961

J. Exptl. Theoret. Phys. (U.S.S.R.) **41**, 304-305 (July, 1961)

THE intensity of the gravitational radiation that arises on excitation of the characteristic longitudinal elastic vibrations in a body of cylindrical shape is relatively larger than for other macroscopic mechanical radiators.[1] If one synchronously excites the characteristic longitudinal vibration with amplitude of fractional elongation $\xi = 10^{-5}$ in $n = 2 \times 10^4$ identical cylinders of cross section $S = 10^4$ cm^2, density $\rho = 5.5$ g/cm^2, and speed of sound in the material of the cylinders $v_s = 4 \times 10^5$ cm/sec, the power loss to gravitational radiation is $\sim 10^{-25}$ w.[1,2] For this case it is necessary that the axes of the cylinders, along which the elastic vibrations are excited, be parallel, and that the cylinders be located at distances small in comparison with the wavelength of the radiation (the radiated power is proportional to n^2). The total power losses in the excitation of such a system are $\sim 10^6$ w at frequency 10^6 cps.

We note that to register or measure an electrical or mechanical signal with power 10^{-25} w

under ordinary laboratory conditions is extremely difficult. This is due to the fact that the main obstacle in principle to the registration of weak signals is thermal noise. For a sinusoidal signal of known phase and frequency the minimum power that can be detected with reliability α is given by

$$P_{min} = 2kT\theta^2(\alpha, m)\, M/\tau(m-1). \quad (1)$$

Here T is the absolute temperature of the source of the signal, k is Boltzmann's constant, τ is the time of a single measurement, m is the number of measurements, $\theta(\alpha, m)$ is the tabulated reliability index of the result for a set of m measurements, α is the degree of reliability of the result of the measurements, and M is the "quality factor" of the measuring apparatus as a whole. For an ideal measuring apparatus M = 1. Let us take an example based on experimental data:[3] for α = 0.990, T = 300° K, $\tau m = 6 \times 10^3$ sec one would detect a power of 4×10^{-23} w, which corresponds to $M \approx 5$. Assuming that τm can be increased to 6×10^5 sec (about 8 days) and $M \approx 1$, we get $P_{min} = 10^{-25}$ w. Thus if there should exist an acceptable device that completely absorbed the gravitational radiation, it would be possible to accomplish the detection for the example given above. Owing, however, to the extremely weak interaction of gravitational radiation with matter, it can be shown[1] that to detect the absorption (that is, the conversion into other forms of energy) a power 10^{12} to 10^{15} times the value of 10^{-25} w would be required.

There is a possible type of indirect experiment for the detection of gravitational radiation by the use of the radiating system described above. Let us suppose that we have at our disposal two groups of n identical cylinders, placed close together and with their axes parallel. If we excite vibrations in these groups of cylinders in synchronous phase, then, as has been indicated, the power of the gravitational radiation will be about four times that from one of the groups. If, on the other hand, we excite the vibrations of the two groups with opposite phases, without changing the distances and orientations, then there will be only the octupole radiation, which is much smaller than the quadrupole radiation from a single group. Thus by changing the phase shift of the vibrations in one group of cylinders by π, one can cause synchronous changes of the radiative losses from the second group. For the values of S, n, ξ, ρ, and v_s given above the depth of the modulation of the power expended in the excitation will then be 2×10^{-25} w. Such a direct effect of modulation of the power can be measured. The minimum value of the depth of modulation that can be measured can be calculated by means of the relation (1), since the frequency and phase of the modulation are fixed for the observer.

By changing the mutual orientation of the cylinders one can produce a supplementary control modulation, by using the well known directional pattern of quadrupole radiators.

In arranging the experiment, careful electrostatic and acoustical screening of the two groups of cylinders is necessary.

One can use as the material for the cylinders the ferroelectric substance $BaTiO_3$, and can produce the excitation of the vibrations by means of an alternating voltage, using the inverse piezoelectric effect. If one determines the depth of the modulation of the power associated with the radiation in one group of cylinders by detecting the amplitude of the voltage applied to the cylinders synchronously with changes of phase in the other group, then besides the ordinary thermal noise there are large additional disturbances owing to amplitude fluctuations of the supply generator and the amplifying systems. According to the results of Bershteĭn[4] and Malakhov,[5] for excitation of a system of cylinders at frequency 10^6 cps, with phase modulation at frequency 10^3 cps and power 10^6 w expended in the excitation, one must expect that the spectral density of the power associated with the amplitude fluctuations will be $10^{-9} - 10^{-10}$ w/cps, which is equivalent to a noise temperature $T \approx 3 \times 10^{13}$° K. Therefore it is necessary to use narrow-band symmetrical band-elimination filters at frequencies $10^6 \pm 10^3$ cps with total attenuation of the order of 110 to 130 db. This should lower the noise temperature to ≈ 300° K. The filters must be connected between the amplifier stages and between the amplifiers and the supply generator.

For the values that have been given, radiated power 10^{-25} w, power expended in excitation 10^6 w, at excitation frequency 10^6 cps, and $\xi = 10^{-5}$, the volume of $BaTiO_3$ required is ≈ 40 m^3. Owing to the fact that the power of the gravitational radiation is proportional to $n^2S^2\xi^2$ and the expenditure of power in the excitation of the vibrations in the system is proportional to $nS\xi^2$, one can decrease the amount of power expended for the same radiated power by decreasing ξ and increasing S or n, i.e., at the expense of an increase of the volume of the system.

The writers express their gratitude to Professor V. V. Migulin and S. A. Akhmanov for helpful discussions.

[1] J. Weber, Phys. Rev. 117, 306 (1960).
[2] L. D. Landau and E. M. Lifshitz, Teoriya Polya (Field Theory), 2d Ed., Fizmatgiz, 1960.
[3] V. B. Braginskii and G. I. Rukman, Vestnik MGU, ser. fiz., No. 3 (1961).
[4] I. L. Bershteĭn, Izv. Akad. Nauk SSSR, ser. fiz. 14, 145 (1950).
[5] A. N. Malakhov, Fluktuatsii parametrov nekotorykh kolebatel'nykh sistem (Fluctuations of the Parameters of Some Oscillating Systems), Dissertation, Gor'kii University, 1953.

Translated by W. H. Furry
60

ASYMMETRY IN ANGULAR DISTRIBUTION OF NEUTRONS EMITTED IN THE CAPTURE OF NEGATIVE MUONS IN CALCIUM

V. S. EVSEEV, V. I. KOMAROV, V. Z. KUSH, V. S. ROGANOV, V. A. CHERNOGOROVA, and M. M. SZYMCZAK

Joint Institute for Nuclear Research

Submitted to JETP editor June 4, 1961

J. Exptl. Theoret. Phys. (U.S.S.R.) 41, 306-307 (July, 1961)

FROM a measurement of the asymmetry coefficient of the angular distribution of neutrons from the reaction

$$\mu^- + A \to A' + n + \bar{\nu} \qquad (1)$$

evidence about the nonconservation of parity and about the components of the weak interaction between a μ^--meson and a nucleon can be obtained. For the case of parity nonconservation, the angular distribution of the neutrons emitted by the nucleus in the direct process, bypassing the compound nucleus stage, is of the form[1]

$$N(E_n, \theta) \sim 1 + a\cos\theta, \qquad a = P_\mu \beta(E_n)\tilde{\alpha}, \qquad (2)$$

where $\tilde{\alpha}$ is the asymmetry coefficient of neutron emission on capture of fully polarized μ^- mesons by the nucleus, a coefficient dependent only on the interaction constant of a μ^- meson with a nucleus; P_μ is the residual polarization of the μ^- meson in the K orbit of the mesic atom: $\beta(E_n)$ is a coefficient that takes the nuclear properties into account; E_n is the energy of the emitted neutron and Θ is the angle between the spin direction of the μ^- meson and the direction of emission of the neutron.

In the present note we report on preliminary results of measuring the asymmetry coefficient $\tilde{\alpha}$ on absorbing μ^- mesons in calcium. μ^- mesons with momentum 250 Mev/c (from the synchrocyclotron of the Joint Inst. for Nuc. Res.) were brought to rest in a calcium target of thickness 12 g/cm^2 placed in a magnetic field. The neutrons were recorded for 0.67 μsec, allowing 0.1 μsec after the passage of a μ^- meson, by a threshold scintillation layer detector, insensitive to γ quanta, similar to that described by us previously.[2]

Evaporated neutrons could be excluded from the count by choosing a 7-Mev threshold of neutron counting, and only neutrons from the direct process were detected with sufficient efficiency. The background of chance coincidences was measured simultaneously with the effect, with the same energy threshold.

A telescope of three scintillation counters recorded the disintegration electrons on stopping μ^- mesons in calcium in order to determine P_μ. The asymmetry in the angular distribution of neutrons and disintegration electrons was measured by the method of spin precession of a μ^- meson in a magnetic field, counting for two opposite directions of the magnetic field.

In spite of the four-layer magnetic shielding there was a slight influence of the coil magnetic field in the presence of the leakage field of the accelerator on the amplification coefficient of the photomultipliers of the neutron detector (FÉU-24), which was equivalent to a change in the working threshold by (2.95 ± 0.11)%. The effect of the field was carefully measured, and taking this into account we found

$$A_{Ca} = P_\mu P_\gamma P_n \bar{\beta}\tilde{\alpha}_{Ca} = -(0.067 \pm 0.022), \qquad (3)$$

where $P_\gamma = 0.96$ and $P_n = 0.94$ are coefficients that take account of the recording of an insignificant fraction of γ quanta and evaporated neutrons produced in the capture of a μ^- meson; $\bar{\beta}$ is the mean of the quantity $\beta(E_n)$[1] averaged over the recorded part of the spectrum of primary neutrons and $P_\mu = 0.135 \pm 0.019$. From this $\tilde{\alpha}_{Ca} = -(0.93 \pm 0.33)$.

As a control experiment we measured A_{Al} for μ^--meson capture in aluminum, where there is no asymmetry in view of the complete depolarization of μ^- mesons.[3] The measurements gave $A_{Al} = -(0.015 \pm 0.015)$.

There have recently been reports[4,5] on the measurement of the asymmetry of neutron emission on the capture of μ^- mesons in magnesium and sulfur. The authors limited themselves to presenting the value of A and did not take the re-

sults as far as the calculation of $\tilde{\alpha}$. If a correction is made for the counting of evaporated neutrons in the way which we have used for calcium, then $\tilde{\alpha}$ from all these experiments has roughly the same value, near to unity, with the same (about 35%) statistical error. However, the lower neutron counting threshold (3 — 5 Mev) in these experiments leads to appreciable corrections P_n (0.5 — 0.7), making the value of $\tilde{\alpha}$ derived from [4] and [5] less reliable.

The existence of asymmetry of neutron emission which we have observed confirms the parity nonconservation in μ^- capture.[4,5]

On the basis of the theoretical[1] and measured values of $\tilde{\alpha}$, the presence of a pseudoscalar component of the interaction in process (1) can be deduced, with the sign of the ratio g_P/g_A of the pseudoscalar and pseudovector constants positive.

We must point out that the value of $\tilde{\alpha}$ obtained is appreciably greater than the most probable theoretical value $\tilde{\alpha} = 0.41$, obtained for $g_A/g_V = -1.25$, $g_P/g_A = 8$, $g_T/g_V = 3.7$.[1]

The authors consider it a pleasant duty to thank I. S. Shapiro, É. I. Dolinskii, and L. D. Blokhintsev for discussing the results of the present experiments, and Chang Jun-wa for help with the experiments.

[1] É. I. Dolinskii and L. D. Blokhintsev, JETP **35**, 1488 (1958), Soviet Phys. JETP **8**, 1040 (1959); Akimova, Blokhintsev, and Dolinskii, JETP **39**, 1806 (1960), Soviet Phys. JETP **12**, 1260 (1961).

[2] Evseev, Komarov, Kush, Roganov, Chernogorova, and Shimchak, Prib. i. Tekhn. Eksper. (Instrum. and Exptl. Techniques) No. 1, 68 (1961), Acta Phys. Polonica **19**, 675 (1960).

[3] Ignatenko, Egorov, Khalupa, and Chultém, JETP **35**, 1131 (1958), Soviet Phys. JETP **8**, 792 (1959).

[4] Astbury, Blair, Hussain, Kemp, Muirhead, and Voss, Phys. Rev. Lett. **3**, 476 (1959).

[5] W. L. Telegdi, Proc. Int. Conf. on High Energy Physics, Rochester, 1960.

Translated by R. Berman
61

CORRECTION TO "THE RELATIONSHIP BETWEEN MATRICES OF DIFFERENT TRANSITIONS AND MULTIPLE PROCESSES"

B. T. VAVILOV

Moscow State University

Submitted to JETP editor February 25, 1961

J. Exptl. Theoret. Phys. **41**, 307-308 (July, 1961)

OUR earlier calculation[1] of multiplicity requires the following corrections.

1. Propagation functions in the Bloch-Nordsieck model were replaced incorrectly by $i(2\pi)^{-4}E_p^{-1}$. This approximation was based on the fact that

$$\prod_{i=1}^{n} S^c\left(p_i + \sum_{\alpha=1}^{i} k_\alpha\right) \sim E^{-n}$$

for $|\mathbf{k}_\alpha| \to 0$. Since this approximation is invalid for large $|\mathbf{k}_\alpha|$ the initial system of equations was solved anew for V^{0n},[22] [see Eqs. (9) and (10) in [1]], using a procedure proposed previously.[1,2] In the center-of-mass system we then obtain, instead of Eq. (15) of [1],

$$Q_n = \frac{g^{n+2}m^n\alpha_n(g, E)}{(n!)^{1/2}E_0^n}\prod_{i=1}^{n}\omega_i \Big/ \prod_{i=1}^{n}(\omega_i^2 - k_i^2\cos^2\theta_i), \quad (1)$$

where E_p and ω_i are the energy of the nucleon and of the i-th meson in the final state, $k_i^2 = \omega_i^2 - \mu^2$, and α_n is a function slightly dependent on n and E.

2. It is also necessary to perform a new integration over the final states. This had been done inconsistently in [1] and [2]. When we drop the hypothesis that the mesons are monoenergetic,[1] we must calculate

$$W_n = \int \frac{d^3p_1}{2E_{p_1}}\frac{d^3p_2}{2E_{p_2}}\frac{d^3k_1\ldots d^3k_n}{2\omega_1\ldots 2\omega_n} Q_n^2 \cdot \delta^4\left(q_1 + q_2 - p_1 - p_2 - \sum_{i=1}^{n} k_i\right) \quad (2)$$

where Q_n is given by (1); a factor ensuring correct normalization of the final state[3] is taken into account in Q_n. Using a procedure similar to that proposed in [4] and [5], we can express W_n in terms of Hankel functions. However, multiplicity cannot be calculated for the general case. It must be assumed that the total momentum of the mesons is zero and that the transverse momentum of each meson is conserved ($p_\perp \sim \mu$). We then obtain approximately

$$W_n = (2\pi g m e^4 \mu^{-2})^n E^{2n} n^{-5n}, \quad (3)$$

whence for the most probable number of created mesons in the c.m. system we have

$$\bar{n} = [\pi gm/1{,}4\mu^2]^{6/5}E^{2/5}.$$

[1] B. T. Vavilov and V. I. Grigor'ev, JETP **39**, 794 (1960), Soviet Phys. JETP **12**, 554 (1961).
[2] B. T. Vavilov, Vestnik Moscow State University **6**, 47 (1960).
[3] N. N. Bogolyubov and D. V. Shirkov, Introduction to the Theory of Quantized Fields, Interscience Publ., New York, 1959.
[4] J. V. Lepore and R. N. Stuart, Phys. Rev. **93** [sic!] 1434 (1954); **94**, 1724 (1954).
[5] K. Kobayakawa and T. Imamura, Progr. Theoret. Phys. (Kyoto) **23**, 137 (1960).

Translated by I. Emin
62

Contents of Coming Issues

SOVIET PHYSICS JETP VOLUME 14, NUMBER 2 FEBRUARY, 1962

LETTERS TO THE EDITOR

SOVIET PHYSICS JETP VOLUME 14, NUMBER 3 MARCH, 1962

CONTENTS

LETTERS TO THE EDITOR

SOVIET PHYSICS JOURNALS

Translations of the 1961 Originals—*Published in English by the American Institute of Physics with the cooperation of the National Science Foundation.*

Publication year July, 1961—June, 1962.

Soviet Physics—JETP

A translation, beginning with 1955 issues of *Zhurnal Eksperimental'noi i Teoreticheskoi Fiziki* of the USSR Academy of Sciences. Leading physics journal of Soviet Union. Similar to "The Physical Review" in quality and range of topics. Outstanding new work is most likely to appear in this journal.

Vols. 13 and 14 comprising twelve issues, approx. 4000 pp.
$75 domestic, $79 foreign
Libraries $50 domestic, $54 foreign. Single copies, $8*

Soviet Physics—SOLID STATE

A translation, beginning with 1959 issues of *Fizika Tverdogo Tela* of the USSR Academy of Sciences. Offers results of theoretical and experimental investigations in the physics of semiconductors, dielectrics, and on applied physics associated with these problems. Also publishes papers on electronic processes taking place in the interior and on the surface of solids.

Vol. 3 comprising twelve issues, approx. 3800 pp.
$70 domestic, $74 foreign
Libraries $45 domestic, $49 foreign. Single copies, $8*

Soviet Physics—TECHNICAL PHYSICS

A translation, beginning with 1956 issues of *Zhurnal Tekhnicheskoi Fiziki* of the USSR Academy of Sciences. Contains work on plasma physics and magnetohydrodynamics, aerodynamics, ion and electron optics, and radio physics. Also publishes articles in mathematical physics, the physics of accelerators, and molecular physics.

Vol. 6 comprising twelve issues, approx. 2000 pp.
$55 domestic, $59 foreign
Libraries $35 domestic, $39 foreign. Single copies, $8*

Soviet Physics—ACOUSTICS

A translation, beginning with 1955 issues of *Akusticheskii Zhurnal* of the USSR Academy of Sciences. Devoted principally to physical acoustics but includes electro-, bio-, and psychoacoustics. Mathematical and experimental work with emphasis on pure research.

Vol. 7 comprising four issues, approx. 500 pp.
$12 domestic, $14 foreign
(No library discounts.) Single copies, $4

Soviet Physics—DOKLADY

A translation, beginning with 1956 issues of the physics sections of *Doklady Akademii Nauk SSSR*, the proceedings of the USSR Academy of Sciences. All-science journal offering four-page reports of recent research in physics and borderline subjects.

Vol. 6 comprising twelve issues, approx. 1500 pp.
$35 domestic, $38 foreign
Libraries $25 domestic, $28 foreign*
Single copies Vols. 1 and 2, $5;
Vol. 3 and later issues, $7

Soviet Physics—CRYSTALLOGRAPHY

A translation, beginning with 1957 issues of the journal *Kristallografiya* of the USSR Academy of Sciences. Experimental and theoretical papers on crystal structure, lattice theory, diffraction studies, and other topics of interest to crystallographers, mineralogists, and metallurgists.

Vol. 6 comprising six issues, approx. 1000 pp.
$25 domestic, $27 foreign
Libraries $15 domestic, $17 foreign. Single copies, $5*

SOVIET ASTRONOMY—AJ

A translation, beginning with 1957 issues of *Astronomicheskii Zhurnal* of the USSR Academy of Sciences. Covers various problems of interest to astronomers and astrophysicists including solar activity, stellar studies, spectroscopic investigations of radio astronomy.

Vol. 5 comprising six issues, approx. 1100 pp.
$25 domestic, $27 foreign
Libraries $15 domestic, $17 foreign. Single copies, $5*

Soviet Physics—USPEKHI

A translation, beginning with September, 1958, issue of *Uspekhi Fizicheskikh Nauk* of the USSR Academy of Sciences. Offers reviews of recent developments comparable in scope and treatment to those carried in *Reviews of Modern Physics*. Also contains reports on scientific meetings within the Soviet Union, book reviews, and personalia.

Vol. 4 comprising six issues, approx. 1700 pp.
(Contents limited to material from Soviet sources)
$45 domestic, $48 foreign
Libraries $30 domestic, $33 foreign. Single copies, $9*

**For libraries of nonprofit academic institutions.*